

C 55.404-D 26/2

PROCEEDINGS

Third International Symposium on the North American Vertical Datum

NAVD SYMPOSIUM '85



Rockville, Maryland
April 21-26, 1985



U.S. DEPARTMENT OF COMMERCE
National Oceanic and Atmospheric Administration
National Ocean Service

May 1985



PROCEEDINGS

Third International Symposium on the North American Vertical Datum

NAVD SYMPOSIUM '85

Rockville, Maryland
April 21-26, 1985

David B. Zilkoski
Convenor

Symposium sponsored by:

International Association of Geodesy

U.S. Department of Commerce

National Oceanic and Atmospheric Administration

In cooperation with:

Department of Energy, Mines and Resources, Canada

Pan American Institute of Geography and History

American Geophysical Union

American Congress on Surveying and Mapping

For sale by the
National Geodetic Information Center, NOAA
Rockville, MD 20852

Mention of a commercial company or product does not constitute an endorsement by the National Oceanic and Atmospheric Administration. Use for publicity or advertising purposes of information from this publication concerning proprietary products or the test of such products is not authorized. Any omission of registered trademarks within these proceedings is unintentional.

PREFACE


These proceedings contain the technical papers and national reports presented at the Third International Symposium on the North American Vertical Datum, NAVD Symposium '85, held in Rockville, Maryland, April 21-26, 1985. As the title indicates there were two previous symposia. The first was held at the Defense Mapping Agency's Inter American Geodetic Survey Cartographic School, Fort Clayton, Canal Zone, January 15-18, 1979, and the second in Ottawa, Canada, May 26-30, 1980.

NAVD Symposium '85 was sponsored by the International Association of Geodesy and the United States Department of Commerce/National Oceanic and Atmospheric Administration. In addition, it was supported by the Department of Energy, Mines and Resources, Canada; Pan American Institute of Geography and History; American Geophysical Union; and American Congress on Surveying and Mapping. Their support is gratefully acknowledged.

The symposium addressed topics crucial to the success of the redefinition of the North American Vertical Datum of 1988 (NAVD 88). It focused on crustal motion modeling, vertical datum definition, systematic and random errors in leveling, and new leveling techniques. More than 110 participants from 19 countries convened to discuss the problems confronting the NAVD 88 project. Almost half of the attendees were from outside the United States.

As convenor, I would like to extend my personal thanks to all of the attendees for their participation, which resulted in a successful symposium. I am especially grateful to Doyle G. Frederick, associate director of the U.S. Geological Survey, for his timely keynote address, and to Rear Admiral John D. Bossler, director of NOS Charting and Geodetic Services, who in an entertaining manner gave a serious after-dinner speech on the new adjustment at the Thursday evening banquet. To the NAVD Symposium '85 staff who assisted me in this endeavor--Eleanor Z. Andree, Bernard H. Chovitz, John G. Gergen, Robert H. Hanson, Peggy Morrish, Grace S. Sollers, and Gary M. Young--I express my appreciation.

David B. Zilkoski
Convenor



Digitized by the Internet Archive
in 2012 with funding from
LYRASIS Members and Sloan Foundation

<http://archive.org/details/thirdinternatio00inte>

CONTENTS

Preface.....	iii
--------------	-----

SESSION I: STATUS OF VERTICAL GEODETIC NETWORKS IN NORTH AMERICA

Moderator: C. T. Whalen, National Geodetic
Survey (Ret.), NOAA, Rockville, MD

Status of Vertical Control Networks in Canada J. B. Boal, R. Gareau, and F. W. Young.....	1
Great Lakes Vertical Control H. A. Lippincott.....	11
Status of NGS' North American Vertical Datum (NAVD) Project D. B. Zilkoski and G. M. Young.....	21
Status of the Vertical Control Networks in Mexico R. S. Torres.....	37

SESSION II: NEW LEVELING TECHNIQUES

Moderator: J.-M. Becker, National Land
Survey, Gavle, Sweden

The Swedish Experience with Motorized Leveling -- New Techniques and Tests J.-M. Becker.....	47
Recent Advances in High Precision Trigonometric Motorized Levelling (NIPREMO) in I.G.N. France M. Kasser.....	57
Trigonometric Motorized Leveling at the National Geodetic Survey C. T. Whalen.....	65
Applications and Limitations of Precise Trigonometric Height Traversing A. Chrzanowski, T. Greening, W. Kornacki, J. Second, S. Vamosi, and Y. Q. Chen.....	81

SESSION III: VERTICAL DATUM DEFINITION
(Part 1)

Moderator: R. H. Rapp, Dept. of Geodetic
Science and Surveying, The Ohio State
University, Columbus, OH

Vertical Datum Definitions Discussed in View of European Vertical and Horizontal Networks R. Kelm.....	95
Comparison of Geodetic Leveling to Mean Sea Level Between Portland, Maine, and Atlantic City, New Jersey D. B. Zilkoski and V. Kammula.....	105
Vertical Datum Definition by Integrated Geodesy Adjustment G. W. Hein and B. Eissfeller.....	121
Levelling with the Help of Space Techniques O. L. Colombo.....	137
Accuracy Estimates of Intercontinental Vertical Datum Connections D. P. Hajela.....	145
A Practical Oceanographic Approach to the Problem of Defining a World Vertical Datum D. E. Cartwright.....	155

SESSION IV: VERTICAL DATUM DEFINITION
(Part 2)

Moderator: R. H. Rapp, Dept. of Geodetic
Science and Surveying, The Ohio State
University, Columbus, OH

Impacts of Conversion to the North American Vertical Datum of 1988 on the National Flood Insurance Program M. B. Miller.....	161
The New National Vertical Datum and the National Mapping Program-- A Major Challenge R. B. Southard, Jr.....	167
Report of the Vertical Datum Subcommittee of the Committee on Geodesy R. H. Rapp (Oral presentation of a report submitted to the National Research Council)	

SESSION V: CRUSTAL MOTION AND THE NAVD
Moderator: S. R. Holdahl, National Geodetic
Survey, NOAA, Rockville, MD

A Review of Methods for Predicting Land Subsidence Caused by Withdrawal of Ground Water T. L. Holzer.....	177
On the Effect of Seasonal Variation of Ground Water Level on Geodetic Leveling Y. Baba and M. Kaidzu.....	187
An Update on Rates of Apparent Vertical Movement in the Great Lakes Basin B. J. Tait and P. A. Bolduc.....	193
Vertical Crustal Motion and the North American Vertical Datum L.D. Brown.....	207
A Temporal Homogenization of the Canadian Height Network G. Carrera and P. Vaníček.....	217
Role of the North American Vertical Datum for Earthquake Research and Prediction: An Example from the Great Basin R. S. Stein.....	227
Readjustment of Leveling Networks to Account for Vertical Coseismic Motions S. R. Holdahl.....	237
The Earthquake Deformation Cycle: Implications for the North American Vertical Datum (NAVD) R. Reilinger.....	251

SESSION VI: SYSTEMATIC AND RANDOM EFFECTS IN LEVELING
(Part 1)
Moderator: J. R. Lucas, Nautical Charting Division,
NOAA, Rockville, MD

Minimizing Systematic Errors in Leveling J. H. Richards.....	261
Refraction by Reflection: Test Results P. V. Angus-Leppan.....	275

Refraction and Deflection of the Vertical in Trigonometric Leveling V. Achilli, P. Baldi, and M. Unguendoli.....	287
A Comparison of Approaches to the Levelling Refraction Problem C. E. Calvert and A. H. Dodson.....	301
Field Test Report on the Systematic Effect of Refraction in Precise Levelling P. Heroux, W. Gale, and F. Faucher.....	311
Theoretical Models, Practical Experiments and the Numerical Evaluation of Refraction Effects in Geodetic Leveling R. Heer and W. Niemeier.....	321
Turbulence Effects on a Rapid Precision Leveling System R. J. Lataitis, L. C. Huff, and S. F. Clifford.....	343
On η -Values in Levelling Refraction O. Remmer.....	353
Empirical Determination of Magnetic Corrections for Nil Level Instruments W. E. Strange.....	363
SESSION VII: SYSTEMATIC AND RANDOM EFFECTS IN LEVELING (PART 2)	
Moderator: J. R. Lucas, Nautical Charting Division, NOAA, Rockville, MD	
Estimation of Variance Components in Leveling Using Iterated Almost Unbiased Estimation J. R. Lucas, J. M. Bengston, and D. B. Zilkoski.....	375
Assessment of Levelling Measurements Using the Theory of MINQE Y. Q. Chen and A. Chrzanowski.....	389
Modulated Normal Distribution Study and its Possible Application to Leveling Errors R. Mazaachi.....	401
The Determination of Earth Tidal Parameters Through Geometric Levelling O. Remmer.....	431

An Investigation of Systematic Errors in Canadian Levelling Lines M. Craymer and P. Vaníček.....	441
Accumulation of the Cholesky Square Root in Helmert Blocking D. R. Junkins and R. R. Steeves.....	451
A Summary of Survey Conditions Encountered by NGS L. C. Huff.....	461
Advanced Technology for a New Precise Levelling Rod H. Schlemmer.....	471
SESSION VIII: CRUSTAL MOTION AND OTHER SYSTEMATIC ERRORS	
Moderator:	P. Vaníček, Surveying Engineering Dept. University of New Brunswick, Fredericton, Canada
Panel Discussion (No text available)	
List of Registered Participants.....	477

STATUS OF VERTICAL CONTROL NETWORKS IN CANADA

David Boal, René Gareau, and Fred Young
Geodetic Survey Division
Surveys and Mapping Branch
Energy, Mines and Resources, Canada
615 Booth Street
Ottawa, Canada K1A 0E9

ABSTRACT. Work toward the redefinition of the North American Vertical Datum (NAVD) began in Canada in 1977. A formal agreement of cooperation between EMR and NOAA was signed in 1982. Data automation and relevening are the major activities at present. By the end of 1984, 3600 of 7000 field books had been coded and keypunched. Relevelling has proceeded at a rate of 4000 km per year since 1977 and this rate will increase to 6000 km in 1985. Canada will contribute a basic post-1960 network of 56 000 km to the continental adjustment and later add 60 000 km of densification work which is of slightly lower quality and of older vintage. Several provincial survey agencies are contributing their data to the project. A motorized levelling system has been developed to greatly improve production. EMR is also contributing to the international effort managed by NGS to develop a rapid precision levelling system. In-house research has been concentrated on the modelling of systematic error effects and the implementation of automated data recording systems.

INTRODUCTION

Background

As was reported by (Lachapelle and Gareau 1980), the Geodetic Survey Division of the Surveys and Mapping Branch of EMR has been actively involved in the vertical datum redefinition project in cooperation with USNGS since 1977. In the spring of 1982, a formal Memorandum of Understanding between EMR and NOAA was signed. The Memorandum states in part that "the parties agree to cooperate in the NAVD project and work toward its completion by 1988. . . .the parties agree to coordinate and share research and development related to the project." At EMR, resources for the project are being arranged through reallocations with existing budget levels. When it was defined in 1928, the Canadian (vertical) Geodetic Datum was based on only 30 000 km of levelling. Since that time, over 100 000 km of lines have been added and "force-fitted" to the system without regard to changes of height with time nor to discontinuities along the U.S. border. Computations have been carried out using normal gravity formulations to produce orthometric and dynamic heights for publication.

Current Activities

Automation of data from 7000 field books and other sources will create 1.2 million computer records. To meet the project deadlines, priority has been given to automating a basic network of 56 000 km of levelling observed since 1960. An additional 60 000 km will be automated and adjusted to this framework for densification purposes. The extent of the basic network is shown in figure 1.

Relevelling carried out since 1960 amounts to more than 40 000 km and in 1985 the pace will increase from 4000 to 6000 km annually as a result of adding additional resources to the project and from productivity improvements such as motorized levelling and automated notebooks.

Other developmental activities include the creation of a rod calibration system in the basement of 615 Booth Street and a testing facility at EMR's Magnetic Observatory to determine the effect of the earth's magnetic field on automatic levels. Investigations, either in-house or contracted, include atmospheric refraction effects (H  roux et al 1985), settlement of bench marks and turning points, analysis of tide gauge records and systematic error modelling. Details of some of these activities will be given in the following sections of the paper.

DATA AUTOMATION

System Employed

Levelling data, collected prior to the use of an automated data recording system in the field, are extracted from several sources, including field books, bench mark card files, abstracts, and line histories. Due to the limited availability of equipment and personnel resources, two methods are employed to convert these data to computer-readable form. The data may be compiled by hand directly onto coding forms and sent to the EMR Computer Science Centre (CSC) to be keyed and stored on magnetic tape. Alternatively, the data may be keyed directly from the field books into an intelligent terminal (PDT-11) under software control and then transmitted to CSC for storage. The forms management software (FMS-11) was developed to ensure that data are stored in proper fields and to reduce keying errors by performing character and range checks on the various items as they are entered.

The HP-85 automated data recording system was developed and field-tested in 1981. A more portable computer, the HP-110, is being introduced in 1985. This up-grade also provides IBM PC compatibility and opens the door for the surveyor to a wide range of software tools. Field data are transmitted to CSC for disk storage and later editing and processing.

Rod and level instrument data are stored on computer files to facilitate the application of calibration and collimation corrections to observed data. Other files are created containing historical information for bench marks. A digitizer is used in the determination and verification of geographical coordinates of bench marks. Gravity values are obtained from the National Gravity Data Base which is maintained by the Earth Physics Branch of EMR.

Progress to Date

As of March 1985, 61% of all our first-order data have been compiled for data entry; 48% have been entered and stored on computer files. Also, some first-order data collected by provincial agencies have been automated and processed. At the present rate of production, all of the basic net data will be automated and validated by the end of 1986.

Formats

The Canadian levelling data are automated and stored in formats compatible with those being used by NGS. This is essential to ensure an efficient flow of data from one system to the other when software is being compared and when the adjustment is being performed.

DATA ANALYSIS

Network Design

A basic network of about 56 000 km of first-order level lines is planned. In the south the loop size is compatible with that of the NGS network, while in the north the loops are much larger due to the scarcity of routes that permit first-order procedures to be used. Some lines have been run along river banks and others across frozen tundra. Where feasible, the network is connected to primary tide gauges and water level gauging stations. The level lines generally have been observed since 1960, with adequate check levelling at junctions, and have acceptable rod calibration and instrument collimation data available. Some critical lines are being relevelled to meet these standards.

First-order levelling data not included in the basic net will be automated as resources become available. As much data as possible will be prepared and included in the continental adjustment. Secondary and lower-order vertical data will be adjusted to the redefined network later.

Misclosures

Preliminary loop misclosures have been determined for all basic loops where data are available. These are being revised as some lines are relevelled and corrections are applied for certain systematic effects. Using observed elevation differences and no systematic error corrections, only four of the 106 loops exhibited misclosures greater than $(2\sqrt{k} + 0.2 k)$ mm, where k is the loop perimeter in km.

Validation

Software has been developed to check data values and ranges and to intercompare files created from independent sources for completeness and accuracy.

RELEVELLING

Procedures

The decision to proceed with the redefinition project had a tremendous impact on the amount of levelling that had to be done in the next ten years. Prior to that time, in Canada, the emphasis had been on production rather than great accuracy due to the size of the country and the limited funds available. We still have only about 60% of the country covered with a basic vertical framework. Since our involvement in the NAVD program, the emphasis on accuracy has increased. Our field program is now 90% relevelling and 10% new levelling. The latter is done only in cases where the new line will close an important loop in the basic net or to obtain a new tie to sea level. Before launching the relevelling program, our field procedures were reviewed to ensure that the objective of improved accuracy would be obtained. Errors were analysed to determine their impact on the

accuracy and to develop methods to minimize them in an economical way. To better control some of the errors such as collimation, refraction and settlement, new field procedures were prepared. In 1978, the sight length was reduced from 80 to 60 metres maximum for all work, the requirement to have an even number of set-ups per section was enforced to eliminate differential rod index errors, and the sight imbalance was limited to 5 m per setup and 10 m per section of line between bench marks. In 1984, the imbalance was further reduced to 2 and 4 m respectively, after the in-house work by Héroux and Pellerin confirmed earlier findings by (Poetzschke 1983) and (Stanislaw 1972) that the line of collimation is largely affected by the changes in ambient temperature.

Beginning in 1982, temperature gradients have been measured at every setup to allow for the computation of a refraction correction. Observations are made at 0.5 and 2.5 m above the ground. The probes are attached to the rods for crews on foot or on a T-stick which can be positioned at any of the four corners of the instrument vehicle in the case of motorized levelling, depending on the wind direction.

In 1982, an automated notebook was introduced to replace manual recording of data. An HP-85 microcomputer, installed in a truck, was powered from the battery of the vehicle through a converter. Communication was by means of two-way radios, one in the vehicle and the other carried by the observer. The software was written to allow full alpha-numeric input, thus preserving the flexibility of a field book. Both comments and actual measurements can be entered, see figures 2 and 3 for examples. The system controls the field operations by performing all the necessary checks and computations as the data are entered. It has proved to be one of the best investments for improving the efficiency of our levelling. We have experienced a 50% reduction in the amount of relevening which seems to indicate that booking errors were present in the hand-recorded data. Automation of additional data in the office has been reduced to a minimum. Specifications and procedures can now be controlled rigidly in the field -- an important point since much of the work is done by casuals on our crews or by contractor personnel. In 1985 for example, 95% of our levelling will be carried out under contract. The HP-110 portable microcomputer will be used in 1985 as we begin to phase out the older and less versatile HP-85. Software has been written for the automation of bench mark descriptions in the field using the HP-110 and a minimum of input. Our format for descriptions is very rigid and lends itself to simplified data entry as illustrated in figures 4 and 5.

Motorized Levelling

In 1982, Geodetic Survey decided to develop a motorized levelling unit after learning of the successful experience of other organizations which had employed such systems (Poetzschke 1981, Urban 1980, Becker 1980). A prototype similar to that of NGS was developed and tested before being introduced into production work in 1983. The system consists of three Suzuki 4-wheel drive vehicles, a pair of 3.5 m rods and an HP-85 recording computer. The first year in the field was used to evaluate the limits of the system. It was employed on levelling lines which were not well suited to such a system but it still managed to achieve a 25% increase in production with no loss of accuracy compared to conventional levelling on foot. In 1984 the system was used on levelling lines which were more suitable for it; in fairly flat terrain, along roads with good shoulders, and with nearly uniform bench mark spacing. Production was increased 50% (to 2.5 km/hour) while maintaining the required accuracy. Some further enhancements were made to the system this past winter.

NETWORK INFORMATION

1- NETWORK: N6U84
2- LINE: 105U7284
3- LINE TITLE
CKVL OTTAWA
4- DATE: 19840516 136
5- PROV: U
6- TIME ZONE: Q 7- ORDER: 12
8- AGENCY: 676 9- PARTY CHIEF: JKL
10- CASSETTE: 178 11- CREW: 1
12- RECS: 50

IS INFO OK? (Y/N)
?

KEY CHOICES

K1 - NET INFO. K2 - OBSERVE
K3 - TWO PEG K4 - ENDLINE

EQUIPMENT INFORMATION

1- ROD CODE: 315
2- R1: S#/OF: 183175 30150
3- R2: S#/OF: 183176 30150
4- ROD TYPE/HT: F 3 M
5- INST CODE: 235
6- S#/SC: 460315 100
7- TEMP: T2

ENTER -1 FOR KEY CHOICE/LINE CHG
IS INFO OK? (Y/N)
?

FIGURE 2

SECTION INFORMATION

1- START BM#: D4-16
U#: 83U040
2- END BM#: D4-3
U#: 83U042
LA: 452203
LO: 754023
3- RUN: F
4- TEMP: C,9
5- WIND: 0 SUN: 2
6- OBSERVER: JKL
7- TIME: 14:44

IS INFO OK? (Y/N)
?

OBSERVATIONS

SETUP # 2

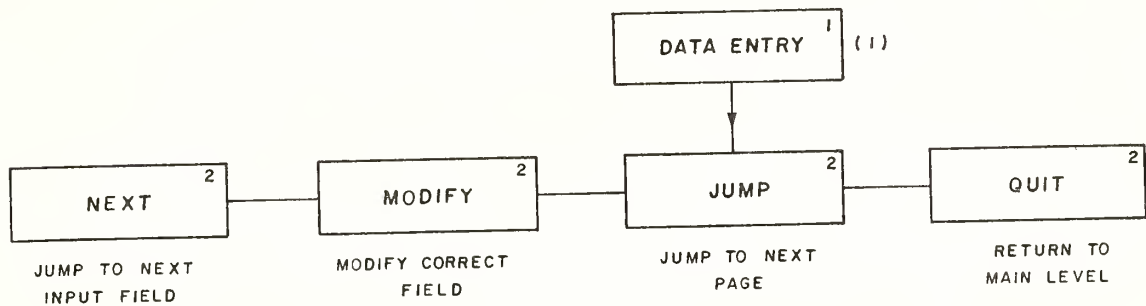
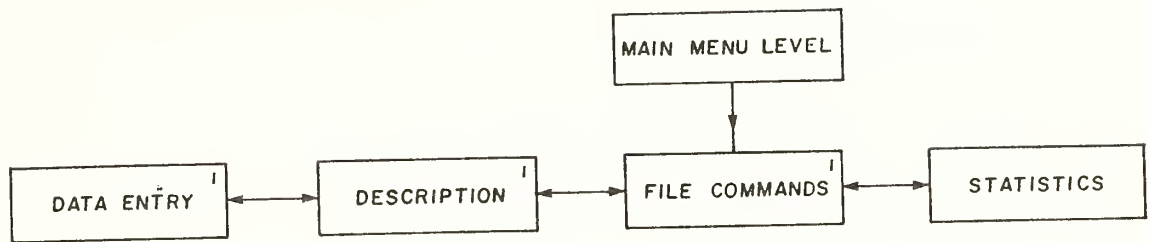
	BACK	FORE	DISCREP
SMALL	11283	10084	
LARGE	41435	40234	- .20 MM
STADIA	1120	1000	- 2 UNITS
STADIA	919	794	

	BS	FS	BAL
DIST	40.2	41.2	1.0 IN F
TOT BAL	0.4 M IN F		

IS SETUP OK? (Y/N)
?

FIGURE 3

FIGURE 4



PAGE 1
BENCH MARK INFO:

STATION NUMBER:

STATION NAME:

MARKER CLASS:

MARKER RECORD:

ESTABLISHING AGY:

PROVINCE CODE:

PAGE 2
REGIONAL DESCRIPTION:

TOWN:

REFERENCE POINT:

ACCESS ROAD:

DISTANCE:

DIRECTION:

PAGE 3
LOCAL DESCRIPTION:

REFERENCE	DISTANCE	DIRECTION
<input type="text"/>	<input type="text"/>	<input type="text"/>
<input type="text"/>	<input type="text"/>	<input type="text"/>
<input type="text"/>	<input type="text"/>	<input type="text"/>

FIGURE 5

55	82A098	BM098	1	2	100 A
57	82A098	N 1 BOYLE			
10	DEEP BENCH MARK IN MANHOLE IN LAWN OF SMITH RESIDENCE, 6.7 KM NORTH OF POST OFFICE ALONG HWY NO. 46, 43.6 KM SOUTH OF DONATVILLE POST OFFICE ALONG HWY NO. 46, 43.6 M SOUTH OF CENTRE LINE OF ROAD ALONG NORTH BOUNDARY OF SECTION 21-65-19, 22.2 M WEST OF CENTRE LINE OF HIGHWAY.				

One-way Levelling

In 1983 and 1984, 1650 km of one-way relevening was done under contract in Nova Scotia to determine its feasibility for this application. Evaluation of the data through comparisons with earlier levelling, is nearly completed and will be reported later.

INVESTIGATIONS AND DEVELOPMENTS

Systematic Error Studies

Investigations of the effects of systematic errors are being conducted. Parts of the basic network with different topographic features are being used to test the changes in loop misclosures and section discrepancies due to the application of various corrections to observed data. Studies are continuing into the development of a model to be used in the application of refraction corrections to historical data for which there are no measured temperature gradients. Preliminary tests indicate that the predicted temperature gradients are not yet suitable for our terrain (Hérault et al 1985).

A recently completed research contract with the University of Toronto included investigations of sea surface topography, temporal homogenization of the network, and the application of regression and autocorrelation techniques in a search for other unaccounted systematic effects which may be present in our data.

Rod Calibration

Until recently level rods had been calibrated by the National Research Council in Ottawa or by Laval University in Quebec City. Last year we developed our own rod calibration system to better check on the quality of the rods being used for our surveys. In the future we will be calibrating all rods both before and after each project on which they are used.

Magnetic Effect

Several of our automatic levels have been tested by NGS personnel at Corbin, Virginia and some compensators exhibit significant response to the earth's magnetic field. Since this is potentially one of the largest sources of systematic error, and because of the large number of different instruments which have been, and are, used in our work, we are developing our own testing facility near Ottawa with the help of the Earth Physics Branch of EMR.

Datum Definition

This involves the selection of a suitable set of tide gauges and the removal of local sea surface topography effects to produce a single equipotential reference surface. Work has been done under contract at the Universities of New Brunswick and Toronto.

Relative Weighting

Investigation of the modulated normal distribution (Mazaachi 1985) for possible application to levelling data has been done in-house. We are also trying the approach suggested by (Remmer 1984) to derive appropriate error estimates for all links in our basic network.

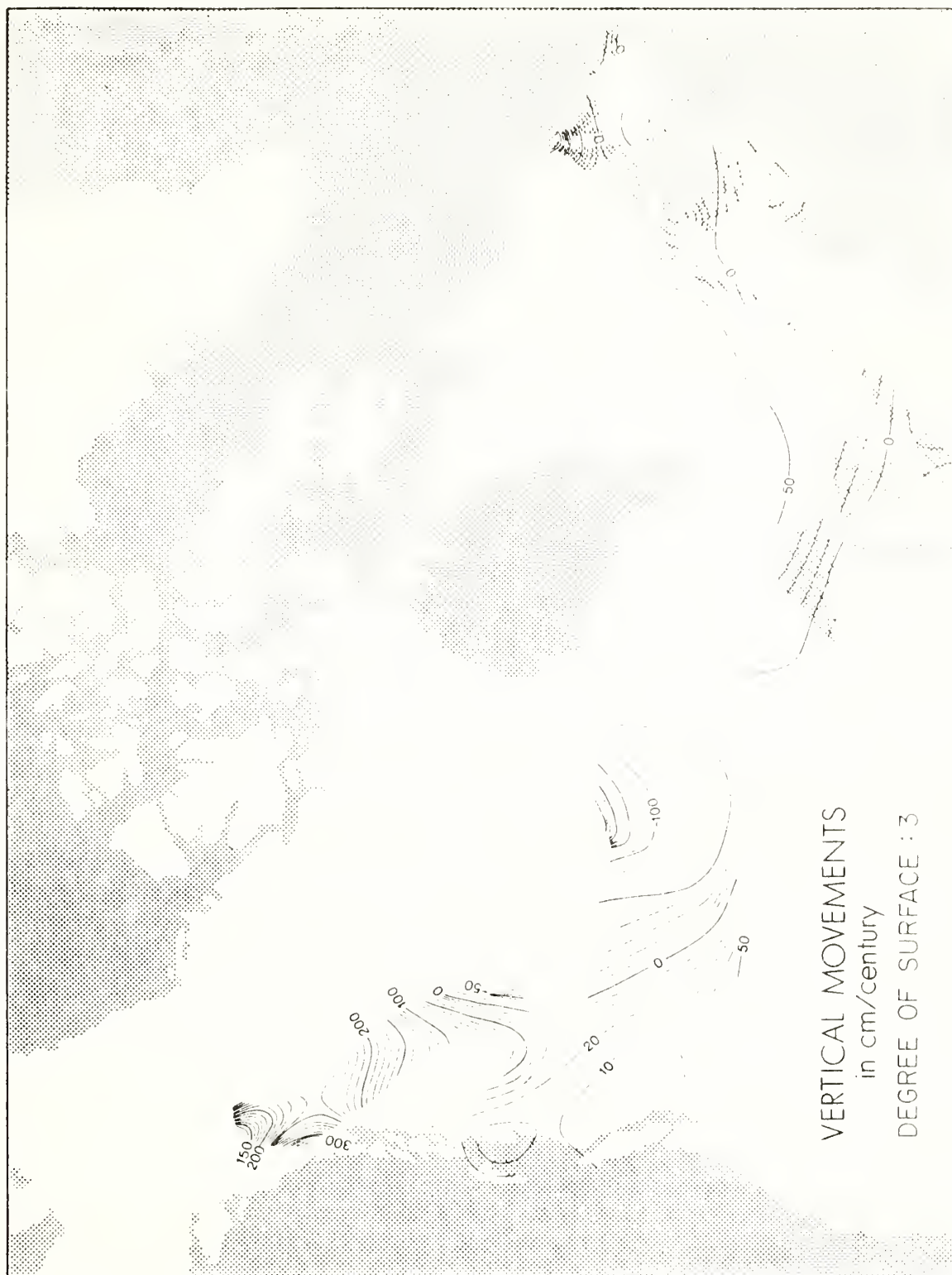


FIGURE 6 VERTICAL CRUSTAL MOVEMENTS IN CANADA DETERMINED FROM RELEVELLED SEGMENTS AND TIDE GAUGES DATA.

Crustal Motion

The temporal homogenization work of (Vaníček et al 1985) determined uplift velocities at tidal bench marks and used the uplift velocities at inland bench marks as given by the map of vertical crustal movements of Canada (Vaníček and Nagy 1981). The map is shown in figure 6. It will be revised to include linear trends from lake level records (Tait 1985) and additional relevelled segments which have become available since 1980. Elimination of presently known sources of systematic error from the relevelled data should improve the reliability of a new map. Corrections to the changes of height with time will be included as parameters in the adjustment of network junction elevations.

GPS satellite surveys will be the most economical means to monitor the network as a whole in future years. GPS determined heights may also play a role in datum definition come 1988.

REFERENCES

- Becker, J.M., 1980: Le nivellement motorisé en Suède, Proceedings of the Second International Symposium on the North American Vertical Datum, pp 847-866, Ottawa, Canadian Institute of Surveying.
- Héroux, P., W. Gale and F. Faucher, 1985: Field Test Report on the Effect of Systematic Refraction in Precise Levelling, Proceedings of the Third International Symposium on the NAVD, Rockville.
- Lachapelle, G. and R. Gareau, 1980: Status of Vertical Geodetic Networks in Canada, Proceedings of the Second International Symposium on the NAVD, Ottawa.
- Mazaachi, R., 1985: Modulated Normal Distribution Study and its Possible Application to Levelling Errors, Proceedings of the Third International Symposium on the NAVD, Rockville.
- Poetzschke, H., 1981: Motorized Levelling in the United States.
- Poetzschke, H., 1983: Variation of the line of sight in the Ni002 Levelling Instrument Due to Temperature Changes, NOAA Technical Memorandum NOS NGS 38, Rockville.
- Remmer, O., 1984: Error Parameters for Levelling Networks, Meddelelse No. 56, Geodaetisk Institut, Kobenhavn, Danmark.
- Stanislaw, S., 1972: Laboratory Investigations of Changes of Position of the Axis of Sight of Automatic Levels Under the Influence of Temperature, Przegląd Geodzyjng, Vol. 44, No. 9.
- Tait, B. and P.A. Bolduc, 1985: An Update on Rates of Apparent Vertical Movement in the Great Lakes Basin, Proceedings of the Third International Symposium on the NAVD, Rockville.
- Vaníček, P. and D. Nagy, 1981: On the Compilation of the Map of Vertical Crustal Movements in Canada, Tectonophysics 71, pp 75-86.
- Vaníček, P., G. Carrera and M. Craymer, 1985: Corrections for Systematic Errors in the Canadian Levelling Network, U of T Technical Report, Toronto.

GREAT LAKES VERTICAL CONTROL

Harry A. Lippincott
Tides and Water Levels Branch
Office of Oceanography and Marine Assessment
National Ocean Service, NOAA
Rockville, MD 20852

ABSTRACT. The Vertical Control Reference System on the Great Lakes is reviewed from its historical beginning over 140 years ago through the establishment of International Great Lakes Datum (IGLD) in 1955. Elevations above mean sea level were determined in 1877, 1903, and 1955. In 1935, differences in elevation between the lakes were determined although no connection was made to sea level. The elevation determination in 1955 was an internationally coordinated effort between the United States and Canada and resulted in the entire Great Lakes-St. Lawrence River system being completely covered by a single uniform vertical control network. The discussion will include the development of the early vertical control system, the concept of water level transfers, the various adjustments which provided bench mark elevations referenced to a common datum, the crustal movement phenomenon, the International Great Lakes Datum (IGLD) 1955, the relationship between IGLD and the National Geodetic Vertical Datum (NGVD) of 1929, and the current status of the IGLD update.

INTRODUCTION

Over one hundred and forty years ago (1841) the U.S. Congress appropriated funds for the "Survey of the Northern and Northwestern Lakes". At that time, the Great Lakes area was the Northern and Northwestern lakes of a rapidly expanding young country. The U.S. Lake Survey was established, under the Corps of Topographical Engineers of the U.S. Army, to carry out the surveys. In the early 1840's, the meager population of the Great Lakes was concentrated in the southern and eastern sections, public transportation was in its infancy, and control for surveys did not exist. One of the first tasks facing this new survey organization was the development of a vertical control reference system. Vertical control, to engineers and surveyors, consists of a network of stable points called "bench marks" whose elevations above or below a reference zero, are known.

EARLY VERTICAL CONTROL

Although surveys were in progress and water level gages were providing data on the relative fluctuations of each of the Great Lakes by 1860, the elevations of the lakes above sea level were not established until 1877. In

1875, levels were run from Greenbush (now Rensselaer), N.Y. on the Hudson River, westerly along the Erie Canal, wagon roads and, the New York and Oswego Midland Railroad to Oswego, N.Y. on Lake Ontario. This leveling established elevations in Oswego Harbor referred to sea level at New York City. Additional leveling in 1875 provided the land connections between Lakes Ontario and Erie and Lakes Erie and Huron. An important concept introduced at this time was a procedure called "water level transfer". Working on the theory that a mean water surface of any body of water will be at an equal elevation throughout, the sea level elevations at Oswego were transferred to the mouth of the Niagara River and using the land level lines mentioned above, and including a water transfer across Lake Erie, a continuous sequence of measurements were provided for basis of assigning a sea level elevation at the Escanaba, Michigan gage on Lake Michigan.

In 1876, the final line of levels, extending from Escanaba on Lake Michigan to Marquette on Lake Superior, for the determination of sea level elevations in the Great Lakes was completed. Adjustment of this leveling resulted in the "Levels of 1877." Further leveling in the Great Lakes includes a 1898 line of levels from Hogansburg, New York to St. Regis and up the St. Lawrence River to Tibbetts Point, a 1898-99 line of levels between Gibraltar and Lexington, 1901 level lines between both Olcott and Buffalo and Detour and Point Iroquois, and a 1902 line of levels rerun between Greenbush and Oswego.

WATER LEVEL TRANSFERS OVER LARGE BODIES OF WATER

Since 1875, the procedure called "Water Level Transfer" has been used to establish vertical datum on each of the Great Lakes. This concept assumes that the mean water surface at any location on each lake will be at an equal elevation during a period of time. A water level transfer (Figure 1) involves a technique where the elevation from a permanent bench mark at one location on a lake is transferred through averaged gage readings to the water level surface and in turn through averaged gage readings at a different location on the same lake to a permanent bench mark at that location. The longer the time period used in the transfers, and the more values averaged, results in greater precision of elevations determined.

Historically, the geodetic community has been reluctant to accept the results based on the concept of water level transfers. However, after familiarity with the concept, many individuals inside and outside the community, past and present, have accepted this procedure as a valuable tool for establishing hydraulically acceptable reference elevations and for monitoring vertical changes in the earth.

The Doctoral Thesis by Herbert W. Stoughten (1980), "Investigation of the Accuracy of Water Level Transfer to Determine Geodetic Elevations in Lake Ontario", further concludes that "From An Engineering Viewpoint, The Water Level Transfer Employing Dynamic Heights Derived From Uncorrected Four Month Mean Lake Level Readings Is At Least As Accurate As First-Order, Class I Geodetic Leveling".

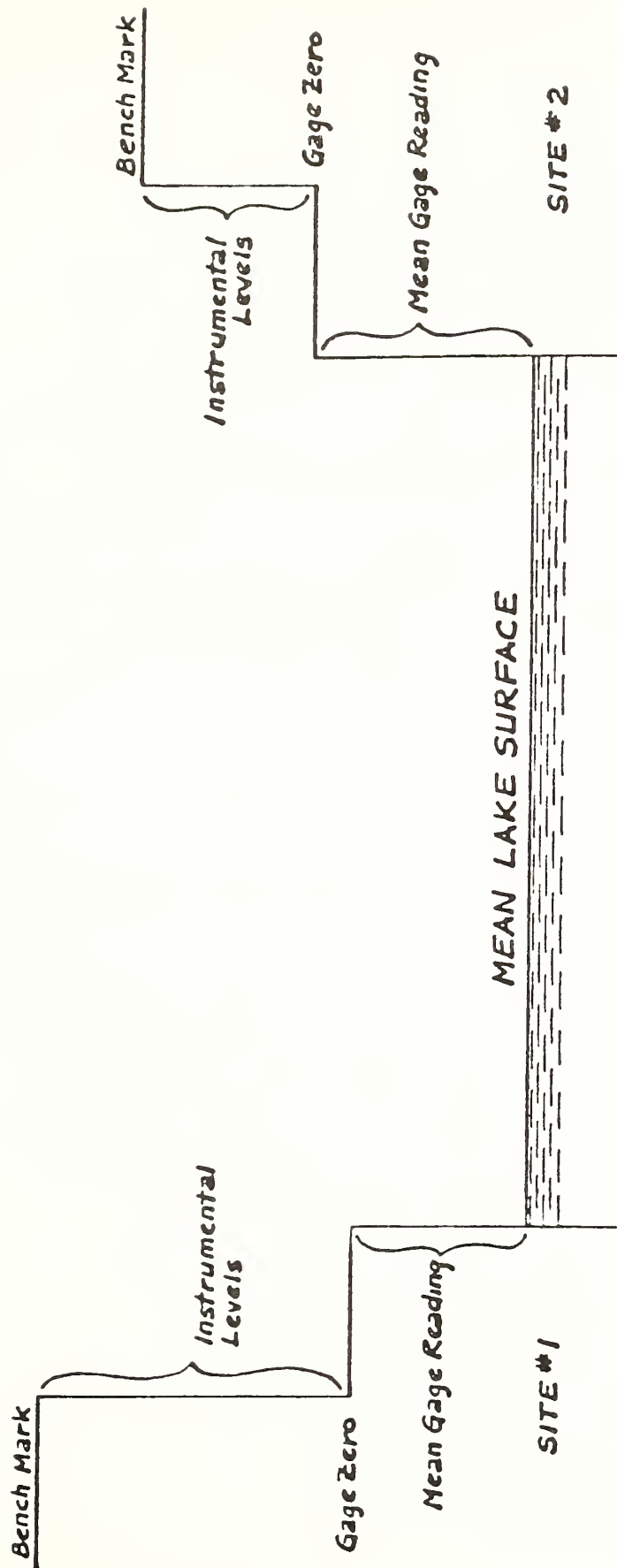


Figure 1 : WATER LEVEL TRANSFER

VARIOUS ADJUSTMENTS REFERENCED TO COMMON DATUMS

Adjusted Levels of 1903

By 1902 all level lines between the lakes had been rerun, and the U.S. Coast and Geodetic Survey had extended its level network westward past the Mississippi River. As the Coast and Geodetic Survey work progressed through the Great Lakes area, the U.S. Lake Survey level lines were incorporated into the national system, and in 1903, these lines were included in the adjustment of all leveling east of the Mississippi. This 1903 adjustment of levels incorporated several series of U.S. Lake Survey water level transfers.

Elevations resulting from this adjustment, which were known as the "Adjusted Levels of 1903", were adopted by the U.S. Lake Survey. Through additional instrumental leveling and water level transfers, elevations on the new datum were determined for all remaining bench marks in the Great Lakes network. This new network soon became known as U.S. Lake Survey 1903 Datum or simply "The 1903 Datum".

Adjustment of 1935

By 1930 it was obvious from the increasing differences in water surface elevations that a reevaluation of bench mark elevations would soon be necessary. In 1933 water level gages were installed in practically every U.S. harbor on the Great Lakes. In view of the new information available from water level transfers and the releveled land connections between lakes, an adjustment of all U.S. Lake Survey elevations was approved early in 1936. This adjustment was to be called the "Adjustment of 1935" or simply "The 1935 Datum".

Since a new sea level connection had not been made, it was decided for this adjustment to hold existing elevations, based on the 1903 adjustment, for the bench marks at one control harbor on each lake and compute new elevations for marks at all other harbors on the lake by water level transfers. Therefore, at Oswego, Cleveland and Harbor Beach, bench mark elevations were held fixed and were adopted as 1935 Datum elevations. The exception to the above were elevations on Lake Superior, which were determined by water level transfer from Harbor Beach to DeTour and instrumental leveling to Point Iroquois. Then, new elevations for the bench marks in all other Lake Superior harbors were computed from 1935 gage records. Therefore, elevations of all bench marks in the Great Lakes area were in harmony as related to the 1935 Datum.

CRUSTAL MOVEMENT PHENOMENON

Through knowledge obtained from measurement of the crustal movement phenomenon during the 1903-1935 period, it was realized at the time of the establishment of 1935 Datum, that future adjustment of elevations would be necessary. It was clear that releveled between the lakes and additional adjustments of elevations would be required, approximately every 20-30 years in the Great Lakes basin. This was because of the natural phenomenon, termed in the Great Lakes area, "crustal movement". As time progressed, computations of mean lake levels from records of gages that had been set in 1903 to record

the same elevations showed different values. These values differed by increasing amounts with time and it was first thought to be the result of differential vertical movement occurring at one or more of the gage sites. Leveling between gage zeros and nearby bench marks showed stability for the immediate area surrounding the gage. This indicated the movement was not of the gage itself, but of some other reason, possibly movement in the earth's crust or overburden. Comparisons for other gage readings showed the phenomenon to be present on all the lakes, being the greatest on Lakes Superior and Michigan.

Mr. G. K. Gilbert of the U.S. Geological Survey proposed in 1898 to use a three gage network on Lakes Michigan and Huron to check the premise of crustal tilt in the Great Lakes Basin. Subsequent investigators as; (Gutenberg 1941), (Moore 1948), and (MacLean 1961) have provided credulity to Gilbert's proposal.

A recent report "Apparent Vertical Movement Over the Great Lakes", prepared by the Coordinating Committee on Great Lakes Basic Hydraulic and Hydrologic Data (1977), lists results of crustal tilt based on the water level transfer procedure.

INTERNATIONAL GREAT LAKES DATUM (IGLD)

A brief examination of vertical control in Canada is introduced to provide a background of the international coordination entailed in the establishment of the International Great Lakes Datum.

In 1935, Canadian government agencies were operating approximately a dozen water level gages along the Canadian shore of the Great Lakes. These gages had been set to record water surface elevations based on the 1903 Datum by making water level transfers from the nearest United States gages. When the 1935 Datum was adopted by the Corps of Engineers, the Canadian government decided to continue using the 1903 Datum values. As a result, lake level data published by agencies of the two governments were not identical for the same lakes and rivers.

These differences were not great and considered insignificant until the advent of international power development on the St. Lawrence River. At this time it became very important for basic hydraulic and hydrologic data pertaining to the Great Lakes System be the same in both countries.

In 1953 the U.S. Lake Survey and its counterpart agencies in Canada began a program of coordinating basic hydraulic and hydrologic data, and one of the many results of this coordination and a high point of U.S.-Canadian cooperation, was the development and establishment of International Great Lakes Datum (1955) or simply IGLD (1955).

In establishing this new international datum, it was necessary to meet certain basic requirements:

- 1) The datum had to be acceptable to both governments, so that previous, uncoordinated datum references could be abandoned. This requirement

meant the new datum had to include bench marks along the entire St. Lawrence River, thus the requirement for the reference zero somewhere in the Gulf of St. Lawrence.

- 2) It had to incorporate an adjustment of all elevations to compensate for changes caused by differential vertical earth movement to the date of datum establishment, and to correct any errors that may have existed because of inconsistencies in the original work. Therefore, it was necessary to make a timely and complete new elevation determination throughout the Great Lakes area by rerunning the first-order lines between the lakes and operating many special water level gages to obtain data for water level transfers across the lakes since resources were not available to run the additional hundreds of miles of first-order level lines around the lakes.
- 3) It had to provide elevations suitable for use in resolving the many involved hydraulic and hydrologic problems existing on the Great Lakes System. The prime reason for adopting dynamic elevations for the new datum was to provide a means of accurate measure of potential hydraulic head between points.

The new datum was established during the period 1952-1958 by first-order leveling along the St. Lawrence River from Point-au-Pere (Father Point), Quebec in the Gulf of St. Lawrence to Kingston, Ontario at the easterly end of Lake Ontario. A parallel line along the United States side of the river was connected with the main Canadian level line at Cornwall, Ontario, at the St. Lawrence Power Dam, at the Iroquios Dam, and at the Thousand Islands Bridge. Water level transfers were made from Kingston to all gage sites on Lake Ontario, where sufficient water level data for the period 1952-1958 were available, and the new datum was established at other locations by using first-order level lines between transfer points.

The new datum was extended to the easterly end of Lake Erie by first-order levels run along the Welland Canal in Canada and along the Niagara River in the United States, and to other sites on Lake Erie by water level transfer supplemented with some short first-order leveling ties. This same procedure extended elevations to Lake Superior. Figure 2 shows the network of level lines and water level transfers used in establishing International Great Lakes Datum (1955).

THE RELATIONSHIP BETWEEN IGLD AND NGVD

International Great Lakes Datum (IGLD), 1955 is the present vertical control reference system in the Great Lakes Basin. An international study between agencies for the development and acceptance of identical elevation data for the Great Lakes and the St. Lawrence River System was completed in 1961. IGLD was the outgrowth of that study. A report prepared by the Coordinating Committee on Great Lakes Hydraulic and Hydrologic data on the "Establishment of International Great Lakes Datum (1955). Second Edition, December 1979, describes the datum establishment and the reader is referred there for an in-depth explanation.

GREAT LAKES-ST. LAWRENCE RIVER

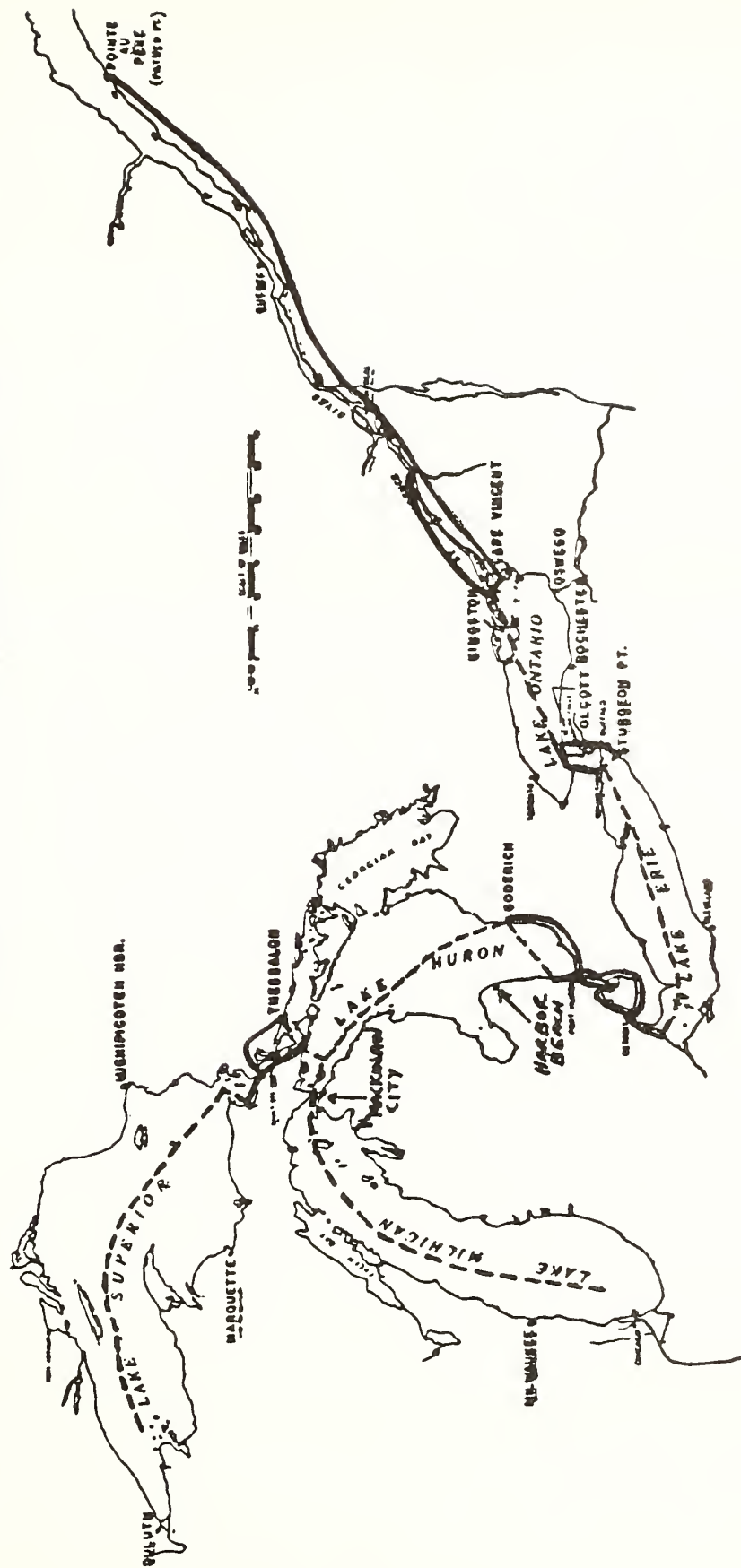


Figure 2 : LEVEL NETWORK, INTERNATIONAL GREAT LAKES DATUM

As previously stated, the new datum has its reference zero based on mean water level surface at Point-au-Pere (Fathers Point), Quebec, with land leveling determining elevations at Kingston, Ontario on Lake Ontario, then by water level transfer to other points on Lake Ontario. A combination of land leveling and water level transfer then extends elevations throughout the remainder of the system to Lake Superior.

The National Vertical Control Network (NVCN) consists of a hierarchy of interrelated nets which span the Nation. Adjustments for each level net of the hierarchy provide bench mark elevations having equal or higher order accuracy. These primary and secondary nets provide a common reference system for user's needs. Bench mark elevations of the NVCN are currently being published as normal orthometric heights. These elevations are referenced to the National Geodetic Vertical Datum (NGVD) of 1929". The 1929 Datum was established by constraining the combined United States and Canada first-order leveling nets to conform to Mean Sea Level as determined at 26 long-term tide stations (21 in the United States and 5 in Canada).

Elevations on IGLD are adjusted in the dynamic number system in that the dynamic value of a bench mark is not a true linear elevation, but a serial number given to the level surface on which the mark lies, and it represents the work required to raise a mass of one pound against the force of gravity from the geoid to the level surface in question in foot-pounds. Some advantages of dynamic elevations are: 1) in vertical earth change or crustal movement studies, differences in the dynamic elevation of bench marks from lake to lake may be compared regardless of the route along which the leveling is done, 2) differences in dynamic elevations give an accurate measure of the potential hydraulic head between the points, and 3) if the mean surfaces of the lakes are indeed level, every point on that particular lake surface will have the same dynamic elevation. If the lake surfaces are sloped, the use of dynamic elevations make it easier to detect their departure from level. For these reasons it was decided to adopt dynamic elevations in establishing IGLD (1955) for use in the Great Lakes Basin.

Elevations referenced to NGVD 1929 are unacceptable for use in resolving the involved hydraulic and hydrologic problems of the Great Lakes system. Primarily, the reasons are; 1) the reference zeros are not located within the system, and 2) that orthometric elevations are not a satisfactory solution for large bodies of water such as the Great Lakes. Orthometric elevations only represent heights above mean sea level. Gravitational forces are not considered and on account of this, no large body of water can be presented as an equipotential surface. Therefore, water level measurements obtained at both ends of a Lake and connected to the NGVD 1929 network would show some magnitude of a permanent northerly slope.

INTERNATIONAL GREAT LAKES DATUM UPDATE

While the subject matter of this text has been primarily a discussion on the historical vertical control system in the Great Lakes up to and including the present vertical control datum it also has shown the need for periodic reevaluation of any vertical control datum used in the Great Lakes. In 1976

the Coordinating Committee on Basic Hydraulic and Hydrologic Data approved a plan for reevaluation of IGLD. Field work to obtain the required data began in 1977 and was completed in December 1983. Field parties of both the National Geodetic Survey, NOS and the Geodetic Survey of Canada, Department of Energy, Mines and Resources completed over 2,000 kilometers of leveling for the update program. During the leveling, ties were made to water level stations operated by NOS and the Canadian Hydrographic Service. At present, the leveling results are being evaluated and placed in automated format, and gage data records are being evaluated for use in the water level transfer procedure. Once these evaluations are completed, the data will be merged to compute new bench mark elevations. These bench marks elevations will be adjusted and referred to the new vertical control datum, International Great Lakes Datum 1980. The target date for publication and distribution of adjusted elevations is October 1986.

REFERENCES

1. Annual Report upon the Survey of the Northern and Northwestern Lakes, Appendix FFF, Annual Report of the Chief of Engineers, 1903, Washington, D.C.
2. Berry, R. M., 1976, "History of Geodetic Leveling in the United States", Surveying and Mapping Quarterly Journal, Vol. XXXVI, No. 2, 137-153, Falls Church, VA., American Congress on Surveying and Mapping.
3. Berry, R. M., 1980, "Uses of Geodetic Vertical Datum in the Great Lakes", Second International Symposium on Problems Related to the Redefinition of North American Vertical Geodetic Networks, 229-241, Ottawa Canada, Canadian Institute of Surveying.
4. Coordinating Committee on Great Lakes Basic Hydraulic and Hydrologic Data, 1977, "Apparent Vertical Movement Over the Great Lakes", Detroit, MI.
5. Coordination Committee on Great Lakes Basic Hydraulic and Hydrologic Data 1979, "Establishment of International Great Lakes Datum (1955)", Second Edition, Detroit, MI.
6. Federal Geodetic Control Committee, 1980, "Specifications to Support Classification, Standards of Accuracy, and General Specifications of Geodetic Control Surveys", Rockville, MD., National Ocean Survey, NOAA.
7. Gilbert, G. K., 1898, "Recent Earth Movement in the Great Lakes Region", Eighteenth Annual Report of the U. S. Geological Survey, Part II, 595-647, Washington, DC.
8. Gutenberg, B., 1941, "Change in Sea Level, Postglacial Uplift, and Mobility of the Earth's Interior", Geodetical Society of America Bulletin 52, 721-772, Boulder, CO.
9. MacLean, W. F., 1961, "Postglacial Uplift in the Great Lakes Region", Doctoral Thesis, Ann Arbor, MI., University of Michigan, Great Lakes Research Division, Special Report No. 14.
10. Moore, Sherman, 1948, "Crustal Movement in the Great Lakes Area", Geodetical Society of America Bulletin 57, 697-710, Boulder, CO.
11. Rappleye, H.S., 1948, "Manual of Leveling Computation and Adjustment", Special Publication 240, Washington, DC., U. S. Coast and Geodetic Survey.
12. Stoughten, H. W., 1980, "Investigation of the Accuracy of Water Level Transfer to Determine Geodetic Elevations In Lake Ontario", Doctoral Thesis, Ann Arbor, MI., University of Michigan.
13. Whalen, C. T., 1978, "Control Leveling", NOAA Technical Report NOS 73 NGS 8, Rockville, MD., National Ocean Survey, NOAA.

STATUS OF NGS' NORTH AMERICAN VERTICAL DATUM (NAVD) PROJECT

David B. Zilkoski and Gary M. Young
Vertical Network Branch
National Geodetic Survey
Charting and Geodetic Services
National Ocean Service, NOAA
Rockville, MD 20852

ABSTRACT. This report provides a brief history of the vertical control portion of the National Geodetic Reference System (NGRS) and presents an update of the progress by the National Geodetic Survey (NGS) on the new adjustment of the North American Vertical Datum of 1988 (NAVD 88). This project, scheduled for completion in 1988, has dominated Vertical Network Branch activities since the project received approval and funding in fiscal year (FY) 1978. The most important production and research efforts are described in this report.

BACKGROUND

The first leveling route in the United States that can be considered to be of geodetic quality was performed in 1856-57 under the direction of G. B. Vose, U.S. Coast Survey (now designated the National Ocean Service). The leveling survey was required to support currents and tides studies in the New York Bay and Hudson River areas. The first leveling line that was officially designated "geodesic leveling" by the Coast and Geodetic Survey followed an arc of triangulation along the 39th parallel. This leveling survey began in 1887, at bench mark A in Hagerstown, Maryland.

By 1900, the vertical control network had grown to 21,095 km of leveling that could be considered "geodetic". These data included work performed by the Coast and Geodetic Survey, various components of the Corps of Engineers, the U.S. Geological Survey, and the Pennsylvania Railroad. A "mean sea level" reference surface was determined in 1900 by holding elevations fixed at five tide stations. Two other tide stations participated indirectly. Subsequent readjustments of the leveling network were performed by the Coast and Geodetic Survey in 1903 (a total of 31,789 km of leveling; eight tide stations were used); 1907 (a total of 38,359 km of leveling; eight tide stations were used); and 1912 (46,462 km of leveling; nine tide stations were used) (Berry 1976).

The next general adjustment of the vertical control network did not occur until 1929. By then the international nature of geodetic networks was well understood and Canada provided its first-order vertical network which was combined with the U.S. net. The U.S. network had

grown to 75,159 km of leveling. Canada provided an additional 31,565 km. The two networks were connected at 24 vertical control points (bench marks) that extended from Maine/New Brunswick to Washington/British Columbia. Mean sea level was held fixed at 21 tide stations in the United States and five in Canada. Although Canada did not adopt the "Sea Level Datum of 1929" determined by the United States, Canadian - U.S. cooperation in the general readjustment strengthened both networks.

INACCURACIES INTRODUCED IN THE 1929 DATUM RESULTS

At the time of the 1929 General Adjustment it was known that local mean sea level at the various tide stations held fixed (at 0.0 elevation) during the adjustment could not, in reality, be considered to be on the same equipotential surface. This is due to sea-surface topography effects, currents, water temperature and salinity, barometric pressure, and other considerations. It was thought at that time, however, that the errors introduced by this approach were not significant, being of the same order of magnitude as terrestrial leveling observational errors. We now know that significant errors were introduced into the 1929 General Adjustment by considering each of the tide stations to be on the same equipotential surface. The error is estimated to be as much as 0.7 m from coast to coast.

Recognition of this distortion and the confusion concerning the proper definition of local mean sea level resulted, in 1976, in a change in designation of the official height system from "Sea Level Datum of 1929" to "National Geodetic Vertical Datum of 1929" (NGVD 29) (Federal Register 1976). The change was in name only; the same geodetic height system continues in the United States from 1929 to the present.

There are several other distortions in the present NGVD 29 system. Some will be discussed later in this paper.

NEW ADJUSTMENT OF THE NORTH AMERICAN VERTICAL DATUM OF 1988

Approximately 625,000 km of leveling have been added to NGRS since the 1929 adjustment. In the intervening years, numerous discussions were held to determine the proper time for the inevitable new general adjustment. In the early 1970's, NGS conducted an extensive inventory of the vertical control network. The inventory identified thousands of bench marks that had been destroyed, due primarily to post-World War II highway construction, as well as other causes. Many existing bench marks had become unusable due to crustal motion associated with earthquake activity, post-glacial rebound (uplift), and subsidence caused by the withdrawal of underground liquids. Other problems were caused by forcing the 625,000 km of leveling to fit previously determined NAVD 29 height values. These distortions, amounting to as much as 9 m, are itemized in Table 1:

Table 1. Distortions in Present NGVD 29 System.

<u>Source of Distortion</u>	<u>Approximate Amount (Meters)</u>
"Patching" 625K km to Old 75K km Net	0.3
Constraining Tide Gage Heights in NGVD 29	0.7
Ignoring True Gravity in NGVD 29	1.5
Refraction Errors	2.0
Post-Glacial Uplift; (Minnesota, Wisconsin, etc.)	0.6
Subsidence Caused by Withdrawal of Underground Fluids	9.0
Crustal Motions From Earthquakes	2.0
Bench Mark Frost Heave	0.5

In 1973, the "Report of the Federal Mapping Task Force on Mapping, Charting, Geodesy and Surveying," Office of Management and Budget (1973), stated, in part:

"The fundamental geodetic networks have become incomplete through obsolescence and need new surveys and a National Adjustment to meet modern demands. ...based on our requirements study, we conclude the vertical control program is falling short of meeting national needs, and, therefore, must be expanded... We recommend doubling the National vertical control program."

A position paper, prepared by the National Geodetic Survey (NGS), soon followed, specifying the tasks and amount of effort required to modernize the vertical control network (National Ocean Survey, 1976). In 1978, the National Research Council's National Academy of Science's Committee on Geodesy (1978) stated in Geodesy: Trends and Prospects:

"We recommend that the computations and additional observations for the new adjustments of the North American Horizontal and Vertical Control Networks by the National Geodetic Survey be given the support necessary to bring about their completion in an orderly way.

"We endorse for scientific, as well as practical reasons, the adjustment of the North American vertical control network...

"The committee endorses the efforts of the National Geodetic Survey to systematize, update and adjust the national horizontal and vertical control networks. ...these data constitute a valuable framework for decades to come."

NGS prepared a budgetary initiative for fiscal year 1977 to finance this project, a revision of which was later approved and the general adjustment program formally began at the beginning of FY 1978. The program called for the completion of several tasks. These tasks will be discussed in more detail later in this paper.

INTERNATIONAL COOPERATION

Early in 1982, Canada and the United States reached agreement on many of their cooperative efforts for the new adjustment and signed a formal Memorandum of Understanding concerning the NAVD 88 readjustment project. The agreement, which was signed by officials of the Canadian Surveys and Mapping Branch and the National Oceanic and Atmospheric Administration, stated:

Adoption of a Common North American Vertical Datum (NAVD 88)

Purpose and Participants

The National Oceanic and Atmospheric Administration, an agency of the Government of the United States of America, and the Surveys and Mapping Branch, an agency of the Government of Canada (hereinafter the "parties"), both having responsibilities in the geodetic field and both desirous of ensuring the adoption and implementation of a common geodetic vertical datum by the two agencies, agree as follows:

1. The parties agree to cooperate in the 1988 North American Vertical Datum (NAVD 88) project and work toward its completion by the end of 1988.
2. The parties agree to coordinate and share research and development related to the project.
3. The same reference surface, as near the geoid as practicable, will be used by both parties as the common datum.
4. The practical or technical realization of a common NAVD will be defined by both parties and will be determined and adopted in a mutually agreeable manner.
5. Both parties agree to adopt the same system of heights and to use compatible mathematical models of corrections to account for systematic errors in the observation of height differences and compatible procedures to incorporate tidal, gravitational, and atmospheric loading effects.

6. For the common adjustment, both parties agree to provide potential differences, based on observed gravity and elevation differences, corrected for systematic error.

7. The parties will agree on the "border junction points" to be used in the adjustment and will confer on the other details associated with the adjustment. For this purpose, their representatives shall meet at least once each year until the completion of the project.

8. The parties agree to utilize NAVD 88 upon completion of the project or as soon as practical thereafter.

9. The rate at which new maps and charts will incorporate NAVD 88 will vary between the parties and will be determined in each case by practical and economic considerations.

10. Costs incurred under this agreement shall be borne by the party incurring such costs.

11. It is understood that the ability of the parties to implement this agreement is subject to the availability of appropriated funds.

12. This agreement may be amended at any time by the mutual consent of the parties concerned.

13. This agreement will become effective upon the signatures of both parties and will remain in effect until terminated by mutual agreement or upon 30 days written notice by either party to the other.

14. Nothing herein is intended to conflict with respective laws and regulations applicable to each of the parties. If the terms of this agreement are found inconsistent with existing regulations or laws applicable to each of the parties, then those portions of the agreement which are determined to be inconsistent shall be invalid, but the remaining terms and conditions of this agreement not affected by any inconsistencies, shall remain in full force and effect.

Similar cooperation will lead to the incorporation of leveling data from Mexico and the Central American countries, making the new vertical datum a truly international one. As reported in the Federal Register (1983), the designation of the new reference for the vertical control network will be the "North American Vertical Datum of 1988," which will also be referred to as "NAVD of 1988" and "NAVD 88," to acknowledge the international scope of the cooperation in the project, and the consistency of the results. The improved geodetic heights are scheduled for distribution in 1989.

TASKS REQUIRED BY THE NAVD 88 PROJECT

Conversion of Data (Descriptive and Archival Observational Leveling Data) to Computer-Readable Form

The first major NAVD task to be completed was the conversion to computer-readable form of descriptive data (bench mark descriptions) from paper copy (primarily field records) under the direction of NGS' National Geodetic Information Branch personnel. In early 1975, NGS applied for and received 1 year of funding under an amendment to the Public Works and Economic Development Act of 1965. The legislation required the funds be spent in an area of high unemployment. Detroit, Michigan, was selected as the potential contract site and the Department of Commerce solicited bids on the project. By January 1976, the contract was awarded.

Preliminary NGS preparation included finalizing formats, preparing conversion instructions, and selecting an on-site technical representative. Descriptions were organized into areas based upon their geographic location within blocks of 1-by-2 degrees of latitude and longitude. The descriptions were sequenced by line numbers in the order desired for publication, updated with recent recovery reports, edited for data omissions or obvious errors, and assigned unique identifiers (designated archival cross reference numbers). This identifier was to serve as the link between bench mark data stored in various computer files.

Acceptable error rates were stipulated to be less than 0.3 percent per data set. All data were key-verified and copied to magnetic tape by contract personnel for shipment to NGS. Agency personnel proofread a sample of submitted data sets. Software was developed to read each data set and check for format errors or data omissions. Despite lost data shipments, a parcel delivery service strike, and tornado damage to the contractor's plant, this contract was successfully completed in March 1977 with a minimum of data-set rejections.

Approximately 60 percent of the active descriptions contained in agency files were automated at a cost of \$330,000. In October 1977, a similar contract was awarded to a Rockville, Maryland, firm. Work proceeded smoothly, and by January 1980, the entire file had been automated. A total of 457,000 bench mark descriptions had been automated over the 4-year period at an approximate contract cost of \$600,000 (Day 1983).

Today all new bench mark descriptions and recovery notes are automated by NGS field personnel as standard operating procedure for new field projects. This information is merged into existing files with software programmed to adhere to specifications as stated in the Federal Geodetic Control Committee's publication "Input Formats and Specifications of the National Geodetic Survey Data Base, Volume II: Vertical Control Data," commonly referred to as the Blue Book. The descriptions reside on five off-line disk packs and can be retrieved by archival cross reference number, state, quadrangle, or county.

The second major task to be completed for the NAVD project was the

conversion of archival (historic) observational leveling data to computer-readable form (Till 1983). In 1975 NGS began retrieving all its original leveling records held in the National Archives and the Washington Federal Records Center. Because of the large volume of data (approximately 50,000 field books), it was necessary to acquire the data over a period of several years.

The retrieval of data was accomplished on a state-by-state basis, following the manner in which the data were stored in the archives. Because this undertaking involved a large volume of data, it was decided that instead of keying individual leveling-rod readings, as is presently done with new NGS surveys, only the stadia intervals, section elevation difference, date, time, "sun code," "wind code," temperature, and number of setups would be converted to computer-readable form.

This conversion was initiated using personnel of the Vertical Projects Section, Vertical Network Branch (VNB). After a period of 1 year, it was decided that these personnel would not be able to convert the observations within the time frame set for the readjustment. Subsequently, in July 1976, a private contract was awarded to convert and validate the archival leveling data. In April 1978, this contract was replaced by one which was responsible for key punching only. (It was learned from the original contract that data validation was best accomplished by NGS.) Beginning with the second contractor, the VNB provided direct technical supervision of the conversion to computer-readable form, and was solely responsible for the validation and review processes. This proved to be very successful. In January 1982, the conversion of all NGS archival observational leveling data to computer-readable form was completed.

The data were processed through a series of computer programs which included "range" checks on individual data fields to ensure the data were "reasonable." Verification of the leveling observations was accomplished by computer recomputation of the leveling lines. The resulting computations were compared against abstracts of the original field computations. Comparisons between individual section lengths and between individual section elevation differences were two of many checks the programs accomplished. The programs also indicated excessive corrections for instrument collimation. When a leveling line was double run, additional comparisons were made. The editing, validation, and review of all archival leveling data were completed in November 1982.

Geographic Positions for Bench Marks

In order to provide automated retrieval capability and apply position-dependent corrections to the observations, a geographic position (latitude, longitude) has been determined for each of the 515,000 bench marks. For those monuments not part of the horizontal control network, the effort involved plotting bench marks on appropriate maps (using the descriptive data mentioned previously) and then determining a "scaled" position using digitizing equipment. This task, which began in 1975, and completed in May 1984, involved a joint effort of personnel from the Vertical Network Branch, Operations

Branch, National Geodetic Information Branch, and the Pacific Marine Center of NOS. Approximately 100,000 of these geographic positions were determined under contract to a private firm in Long Beach, California.

Releveling in Support of the NAVD 88

An important feature of the NAVD 88 program is the releveling of much of the first-order vertical control network in the United States. The dynamic nature of the vertical control network requires a framework of newly observed elevation differences in order to obtain realistic contemporary height values from the readjustment. To accomplish this, NGS has identified 83,000 km of the network for releveling. Replacement of disturbed or destroyed monuments precedes the actual leveling. This effort also includes the establishment of highly stable "deep-rod" bench marks, which will provide reference points for future "traditional" or "satellite" leveling systems. Field leveling is being accomplished to first-order, class II specifications, using the "double-simultaneous" method.

An increase in leveling progress (while maintaining acceptable accuracy) has been accomplished by equipping NGS field leveling units with specially modified subcompact trucks for rodman as well as observers. This form of "motorized" leveling has increased production by at least 20 percent as compared to former leveling procedures. Alternate approaches, including high-accuracy trigonometric leveling, are also being evaluated (Whalen 1984a).

An internationally funded effort to develop a state-of-the-art "rapid precision leveling system" is underway (Huff et al. 1985). To date, 57,000 km of leveling have been accomplished. Completion of field leveling is scheduled for September 1987. Older data which are consistent with the newly observed data will be included in the final framework for the readjustment.

Processing of New Leveling Data

This activity, being performed in the Geodetic Leveling Section, VNB, processes both NGS and non-NGS new leveling projects. The proposed goal is to process 106,000 km of new leveling by September 1987. The tasks consist of validating data fields, applying appropriate corrections, and loading the data into the Vertical Data Base (Balazs 1984 cv). As of April 1985, 82,000 km of leveling have been processed (78 percent complete).

REDUC4 Processing

This procedure consists of converting files from the input format (Koepsell and Ward 1984) to the vertical observation library file format, checking the fields for valid entries, calculating and applying corrections to leveling observations, and loading data into the VNB Data Base. The National Geodetic Vertical Control Network consists of 16,000 leveling lines. This task was completed in January 1985.

Block Validation

Block validation is a process where all observed elevation differences in a predefined area are combined together and analyzed. There are many steps performed during block validation. During the analysis, a first-order primary network, consisting of the latest data, is selected, analyzed, and documented. Appropriate remaining leveling data are then incorporated into the first-order network. Leveling lines which do not fit (statistically) with the network will not be included in the primary network and will be documented in the report.

During the analysis, profiles, loop closures (primary and secondary), section misclosures, date of data, survey order and class, bench mark stability, previous adjustment reports, and past studies are all utilized to make decisions about the data. As of April 1985, 135,000 bench marks have been processed (22 percent complete). The current goal is to process all bench marks by September 1987.

Magnetic Error Modeling

Approximately 50,000 km of NGS leveling lines were observed with compensator-type leveling instruments. In 1981, it was widely publicized that the "horizontal" line of sight of certain compensator (automatic) leveling instruments was influenced by magnetic fields (Rumpf and Meurish, 1981). Professor Rumpf, invited to join forces with NGS, and Charles Whalen, then Chief of VNB, now retired, designed a magnetic calibration facility at NGS' Instrumentation and Equipment Section located in Corbin, Virginia (Whalen 1984b).

The total task includes: (1) identifying factors which cause compensator leveling instruments to deviate from the calibrations performed in the laboratory; (2) estimating the corrections independent of the calibrations, e.g., through profiles and adjustment; (3) estimating factors for instruments which cannot be calibrated; and (4) developing and implementing a procedure to check and apply the correction.

Strange (1985) has begun comparing certain lines of leveling in order to determine empirical magnetic values. These values are determined by comparing repeat leveling over the same line for which at least one of the surveys used instruments that were not significantly influenced by magnetic fields, e.g. spirit-leveling and certain "non-magnetic" compensator instruments. By comparing these surveys with other surveys that used magnetically influenced instruments, an empirical value of the magnetic effect can be determined.

These values provide an independent validation of the laboratory calibrations determined at Corbin, Virginia. Note that laboratory calibrations could not be performed for the majority of NGS' magnetically influenced instruments due to compensator replacement or repair prior to the discovery of the error. For lines surveyed with these instruments, empirically derived correction values provide the only means of reducing the magnetic errors contained in the data.

Obviously the best (and most expensive) solution is to relevel affected lines with "non-magnetic" instruments. NGS intends to keep such releveling to a minimum by judicious application of the laboratory and/or empirical magnetic values.

Appropriate A priori Estimates of Standard Errors

When different types of data are combined and adjusted, it is essential to impose a correct relative weighting scheme. This means that a priori standard errors of observations must be estimated for each group of data. This task includes identifying the different groups of leveling observations, and establishing and implementing a procedure to determine the appropriate a priori standard error of observations in each group.

Groups of data (according to instrumentation, field procedures, etc.) have been identified, but may be modified after additional analysis (Lucas et al. 1985). Different methods for estimating variance components in least-square adjustments are being considered. The Iterative Almost Unbiased Estimation (IAUE) technique (Lucas 1984) has been implemented on NGS' HP1000 minicomputer. Other analyses include: (1) comparing old and new section and loop statistics, (2) profiles, and (3) formal error studies of past field techniques. Some problems anticipated with estimated variance components of leveling data are (1) too small a data sample for a particular group, (2) undetected systematic errors present in the data, and (3) inadequate network design to estimate the internal consistency of groups.

Water-Level Transfers and Tidal Information

This task includes defining the data formats for water-level transfer and tidal data, loading the data, and estimating their observational accuracies.

The 1977-83 water-level transfers and current primary National Tidal Observation Network tidal data (monthly means) have been keyed and placed in computer-readable form by the Tides and Water Level Branch, Office of Oceanography and Marine Services. The data need to be reformatted and placed in the Vertical Network Data Base. Studies have been performed which estimated the accuracies of these data (Stoughton 1980). Additional analysis will be needed to determine how they should be weighted in the NAVD final adjustment.

Interpolate Gravity Values for Bench Marks

The new adjustment will be performed using geopotential numbers. This requires estimating gravity values for all bench marks involved in the readjustment. Phase 1 of this task consists of interpolating gravity values and their corresponding estimates of accuracy for all bench marks in the Vertical Synoptic file. The last of the gravity values were loaded in March 1985.

The second phase of this task is to perform a study to determine if all gravity values are accurate enough for NAVD 88 purposes. A

procedure is being developed in block validation which will examine elevation differences, and determine if the gravity value estimates are accurate enough. If additional gravity values are required, then an observation plan for an area will be developed and implemented. It is not anticipated that many areas of the country will need additional observations.

Development of NAVD Software

The Vertical Network Branch has identified that 3 staff-years of software development effort is required in support of the NAVD 88 project. The programs are needed to increase productivity without sacrificing quality. They mostly include graphics routines; some management tools have also been identified. Some examples of the programs include plotting profiles, junction details, loops, residuals, and networks. Having graphics capabilities is extremely important to the timely success of the project. The specifications and algorithms for each program are being documented. Then they will need to be coded, debugged, and implemented.

In addition to the programs mentioned previously, the programs to perform the Helmert blocking process need to be designed, coded, debugged, and implemented. VNB is currently studying all programs involved with the NAD 83 Helmert blocking system. A majority of the programs can be utilized as they exist today. However, programs that create or modify lowest-level Helmert blocks will have to be rewritten because they are specific to horizontal data. An analysis of these programs is being performed. The "guts" of the Helmert blocking system is currently being converted to a PRIME minicomputer. This will be most helpful in testing the capabilities of the PRIME.

NAVD 88 Crustal Movement Studies and Procedures

This task includes identifying areas of the network which are influenced by crustal motion, and establishing and implementing a procedure to account for these movements.

During the past few years, VNB has been analyzing different numerical techniques in an attempt to model crustal movement. This would enable the NAVD 88 project to include most data and bench marks in one adjustment. The studies, performed mainly in the Houston-Galveston, Texas, area have been successful in identifying the data required to model movements precisely. The lack of required geologic and hydrologic information, along with inadequate network design, makes modeling many areas for precise movements very questionable.

Areas of the networks most likely influenced by crustal movement are fairly obvious, e.g., California, Texas Coast, sections along the East coast, and sections of the U.S. Northern border. Other areas will be identified as block validation continues and additional research material is obtained. It may be possible to modify some observations for crustal motion effects, but it is more likely that most areas will be constrained to the framework network surrounding the area in question after the readjustment. A plan defining the technique to be implemented in these "moving" areas will be developed

and documented for each specific area.

A plan defining the technique to be implemented in California has been developed and documented. The plan includes defining a primary network in California which is consistent within itself, and then making modifications to accommodate crustal motion.

Framework Adjustments

This task will include designing and analyzing framework networks (regional and national). The analyses will be helpful in determining the effects of various datum constraints, magnitudes of height changes from the NGVD 29 datum, influences of systematic errors, deficiencies in network design, and additional releveled requirements.

A plan of action has been developed for designing and analyzing a national primary framework network. This study should be completed within 1 year. Studies comparing local mean sea level to geodetic leveling along the East and West coasts have been performed (Balazs 1984, Zilkoski 1984, Zilkoski and Kammula 1985). A major analysis was also performed in the Gulf Coast region from Texas to Florida. All leveling observations have been processed through program REDUC4. All areas of the country are being analyzed for network deficiencies and the releveled schedule has been made more optimum.

Data Base Design, Entry, and Retrieval

This task includes defining data elements and developing routines to load, edit, and retrieve data from the NGS integrated data base (IDB). VNB and the Systems Development Branch performed a systems analysis study of all VNB activities. The Systems Development Branch is currently identifying all data elements needed for IDB. Once IDB is operational, routines will need to be developed to load, edit, and retrieve data from IDB.

GPS and NAVD 88

Global Positioning System-derived heights cannot be used in their present form as observations in the NAVD readjustment project, however height differences and geoid undulation differences should be helpful in detecting and providing an upper limit on systematic errors in leveling data and for strengthening the network.

Studies have been performed estimating orthometric heights using GPS and gravity (Engelis et al. 1984, Hothem et al. 1985) and estimating subsidence using GPS-derived heights (Strange 1984). NGS is performing many GPS surveys and always ties into the Vertical Control Network. GRDL is currently looking into what GPS surveys offer the NAVD 88 project.

Datum Definition

Datum definition is one of the last tasks which will be performed in the NAVD 88 project. There are many factors which need to be considered before a decision can be made. It may be as simple as

fixing the height of a tidal bench mark and performing a block shift to minimize differences between NAVD 88 heights and the latest Local Mean Sea Level epoch heights. However, there are still some unanswered questions: How do we incorporate tidal heights and water-level transfers? Can we estimate the effects of sea surface topography (SST) at tidal stations? Can satellite information help control datum distortions?

These tasks are currently being analyzed and a specific plan of action is being developed and documented.

Helmert Blocking

This task consists of partitioning 1.5 million unknowns and associated observations into manageable blocks and solving a least-squares adjustment of the entire data set.

The blocking strategy of NAVD will be easier to define than for other large adjustments such as the North American Datum (NAD) readjustment (McKay and Vogel 1984). After the first-level blocks, it is anticipated that 90 percent of the unknowns will be "interior". A blocking strategy needs to be developed which includes boundaries and the unknowns that are to be carried to the higher levels. The Helmert blocking technique for adjustment of data has been documented by others (Dillinger 1978, Isner 1978, Wolf 1978).

Exchange of Data with Canada, Mexico, and Central America

This task includes identifying junction stations and associated information, along with their formats, which will be required at the countries' borders for the final solution. The corrections and methods of applying corrections will also be addressed. There is time before the junction stations are actually needed, but annual meetings are being held to discuss research studies, to establish preliminary formats, and to determine the procedures which will be used to apply the corrections, as well as which corrections are going to be applied.

Publication

This task includes reviewing descriptions on a random basis, and publishing final adjustment heights in 30 minute quads. However, it is planned to have NAVD 88 adjusted heights available to the public immediately following the adjustment. They will be loaded into NGS' IDB and the public will be able to access the IDB directly. It is hoped that most people will access the NGS IDB when requesting data. With the price of computers decreasing and their sophistication increasing, this is not an unrealistic goal. In any event, they will also be available in hard copy and microform, at a higher cost.

Progress and Final Reports

Detailed progress reports addressing each task and their status are prepared every 6 months.

The final report is not scheduled for completion until September 1989. This report will give the history of the network and readjustment project; technical decisions made about weights imposed, observations used, adjustment technique, and crustal motion information. Previously published reports will be the main source for the final report.

CONCLUSIONS

It is obvious that the NAVD 88 project requires an enormous amount of effort. The project, scheduled for completion in 1988, has dominated Vertical Network Branch activities since it received approval and funding, beginning in FY 1978.

The benefits of NAVD 88 make this effort worthwhile. A vertical control network containing a consistent, accurate set of adjusted heights has been needed for several years. Other products and services resulting from the project will be used by people for decades to come. For example, the observed elevation differences, which are now in computer-readable form, are available for future crustal motion studies and regional readjustments. The real benefits will become more apparent when the multitude of users begin using the results of the new adjustment.

REFERENCES

- Balazs, E. I., 1984a: "Preliminary Vertical Data Reduction Procedures," ACSM Bulletin, No. 93, pp. 25-26.
- Balazs, E. I., 1984b: "Comparison of Geodetic Levelings, Corrected for Magnetic Errors, to Mean Sea Level between San Francisco and San Pedro, California," presented at the Chapman Conference on Vertical Crustal Motion: Measurement and Modeling, Harpers Ferry, West Virginia, October 22-26, 1984.
- Berry, R. M., 1976: "History of Geodetic Leveling in the United States", Surveying and Mapping, 36(2), pp. 137-153.
- Day, M. W., 1983: "The processing of Descriptive Leveling Data," ACSM Bulletin, No. 84, p. 31.
- Dillinger, W. H., 1978: "Helmert Block Higher Level System," Proceedings of the Second International Symposium on Problems Related to the Redefinition of North American Geodetic Networks, Arlington, Virginia, April 24-28, 1978. National Geodetic Information Center, NOAA, Rockville, MD.
- Engelis, T., R. H. Rapp, and Y. Bock, 1984: "Measuring Orthometric Height Differences with GPS and Gravity Data," presented at the Chapman Conference on Vertical Crustal Motion: Measurement and Modeling, Harpers Ferry, West Virginia, October 22-26, 1984.
- Federal Register, 1976: 41 (96), p. 20202.

- Federal Register, 1983: 48 (214), p. 50784.
- Hothem, L. D., R. J. Fury, and D. B. Zilkoski, 1984: "Determination of Geoid Slopes using GPS," presented at the Chapman Conference on Vertical Crustal Motion: Measurement and Modeling, Harpers Ferry, West Virginia, October 22-26, 1984.
- Hothem, L. D., R. J. Fury, and D. B. Zilkoski, 1985: "Orthometric Height Determination with GPS Satellite Surveys," Technical Papers, 45th Annual Meeting, ASP-ACSM Convention, Washington, D.C., March 10-15, 1985, p. 528.
- Huff, L. C., S. F. Clifford and R. J. Lataitus, 1985: "Turbulence Effects on the Rapid Precision Leveling System," Proceedings of the Third International Symposium on the North American Vertical Datum, Rockville, Maryland, April 21-26, 1985. National Geodetic Information Center, NOAA, Rockville, MD.
- Isner, J. F., 1978. "Helmert Block Initial Level System," Proceedings of the Second International Symposium on Problems Related to the Redefinition of North American Geodetic Networks, Arlington, Virginia, April 24-28, 1978. National Geodetic Information Center, NOAA, Rockville, MD.
- Koepsell K. S. and R. B. Ward, 1984: "NGS Input Formats and Specifications for Vertical Control Data," ACSM Bulletin, No. 92, pp. 35-36.
- Lucas, J. R., 1984: "A Variance Component Estimation Method for Sparse Matrix Applications," NOAA Technical Report NOS 111 NGS 33 (in press). National Geodetic Information Center, NOAA, Rockville, MD.
- Lucas, J. R., J. M. Bengston, and D. B. Zilkoski, 1985: "Estimation of Variance Components in Leveling using IAUE," Proceedings of the Third International Symposium on the North American Vertical Datum, Rockville, Maryland, April 21-26, 1985. National Geodetic Information Center, NOAA, Rockville, MD.
- McKay, E. J. and S. A. Vogel, 1984: "The North American Datum of 1983: Necessity, Status, and Impact," presented at the ASP-ACSM fall convention, San Antonio, Texas, Sept. 9-14, 1984.
- National Academy of Science, 1978: Geodesy, Trends and Prospects, Committee on Geodesy, National Research Council, Washington, D.C.
- National Ocean Survey, 1976: "Releveling of the Vertical Network," issue paper (unpublished), 68 p.
- National Ocean Survey, 1982: Geodetic Surveys and Services Program Plan 1980-1990, 26 p. National Geodetic Information Center, NOAA, Rockville, MD.
- Office of Management and Budget, 1973: Report of the Federal

Mapping Task Force on Mapping, Charting, Geodesy and Surveying,
Executive Office of the President.

- Rumpf W. E. and H. Meurish, 1981: Systematische aunderungen der ziellinie eines präzisions kompensator-nivelliers--insbesondere des Zeiss N1 1 -- durch magnetische gleich - und wechselfelder. XVI International FIG Congress, Montreux, Switzerland.
- Stoughton, H. W., 1980: "Investigation of the Accuracy of Water Level Transfer to Determine Geodetic Elevations in Lake Ontario," Ph.D. dissertation, University of Michigan, Ann Arbor, Michigan, (published by University Microfilms International, Ann Arbor, Michigan).
- Strange, W. E., 1984: "Accuracy of GPS for Monitoring Vertical Motions," presented at the Chapman Conference on Vertical Crustal Motion: Measurement and Modeling, Harpers Ferry, West Virginia, October 22-26, 1984.
- Strange, W. E., 1985: "Empirical Determination of Magnetic Corrections for N1 1 Level Instruments," Proceedings of the Third International Symposium on the North American Vertical Datum, Rockville, Maryland, April 21-26, 1985. National Geodetic Information Center, NOAA, Rockville, MD.
- Till, J. H., 1983: "The Processing of Archival (Historic) Leveling Data," ACSM Bulletin, No. 82, February 1983, pp. 27-28.
- Whalen, C. T., 1984a: "Precise Trigonometric Leveling," presented at the Chapman Conference on Vertical Crustal Motion: Measurement and Modeling, Harpers Ferry, West Virginia, October 22-26, 1984.
- Whalen, C. T., 1984b: "Magnetic Field Effects on Leveling Instruments," presented at the Chapman Conference on Vertical Crustal Motion: Measurement and Modeling, Harpers Ferry, West Virginia, October 22-26, 1984.
- Wolf, H., 1978: "The Helmert Block Method - Its Origin and Development," Proceedings of the Second International Symposium on Problems Related to the Redefinition of North American Geodetic Networks, Arlington, Virginia, April 24-28, 1978. National Geodetic Information Center, NOAA, Rockville, MD.
- Zilkoski, D. B., 1984: "Geodetic Leveling and Mean Sea Level Along the East Coast of the United States," presented at the Chapman Conference on Vertical Crustal Motion: Measurement and Modeling, Harpers Ferry, West Virginia, October 22-26, 1984.
- Zilkoski, D. B. and V. Kammula, 1985: "Comparison of Geodetic Leveling to Mean Sea Level Between Portland, Maine, and Atlantic City, New Jersey," Proceedings of the Third International Symposium on Problems Related to the Redefinition of North American Vertical Datum, Rockville, Maryland, April 21-26, 1985. National Geodetic Information Center, NOAA, Rockville, MD.

STATUS OF THE VERTICAL CONTROL NETWORKS IN MEXICO

Rafael Sosa Torres
D.G.G.-I.N.E.G.I.-S.P.P.
Departamento de Geodesia Fisica
México, D.F. C.P. 06820

ABSTRACT. The status of the Readjustmen of the Mexican Vertical Control Network is presented. It shows the advances made in the last four years on data inventory, surveying of new lines, technical and processing of vertical and gravimetric data.

Some considerations are made on the future of this Project vis-à-vis the economical crisis suffered by Mexico.

INTRODUCTION

One of the main characteristics of the developing countries as Mexico is its effort for acting in a sistematic way inside of technical frameworks which allow it to take advantage in the best way of the information related to the physical features, resources and socio-economical conditions for a better knowledge of the country in complete and global senses.

The Readjustment of the Vertical Control Network, VCN, is a response to the requeriments of precise geodetic information coming from different social sectors, in particular, from those sectors related with the planning of the social and economical development, although no less import are the requeriments for vertical control in high density coming from private users involved in specific projects, for example, urban equipment, cartography for urban control, cadastral surveys, engineering applications, etc. or the needs of vertical control in scientific applications like the monitoring of earth movements in sismic or fault regions.

The results of the readjustment of the VCN will give us the opportunity to have reliable vertical information with known accuracy compatible with the new procedures and equipments available for vertical surveys. Also it will be a technical and economical profit when the new surveys link with the adjusted VCN: Permanent vertical positions; correlation with others surveys carried out in the same reference system; inicial position easily established; ways for a quick checking of the accuracy and the precision of the survey, and finally, results in agreement with the VCN.

HISTORICAL BACKGROUND

Basically, until 1968, the VCN is the result from surveys made for the Dirección de Geografía y Meteorología and The Departamento Cartográfico Militar, both agencies are overried already.

In fact, from 1968 so far, the Dirección General de Geografía, D.G.G., has take over the responsability of this network.

During 1959 - 1960 a preliminar adjustment of some vertical loops was performed,

referenced it to mean sea level given in 3 tide gauges in the Pacific Ocean and one in the Atlantic Ocean and closing with 4 B.M. of the U.S.A. Control Network.

SPECIFICATIONS

The D.G.G. took over the task to produce Technical Manuals with the Methodologies and Norms and Specifications with the objective to stir up the refinement and the uniformity in methods and specifications required in Vertical Control to keep in high the quality and the utility of the Network. These Manuals contribute to the economy and efficiency when planning or executing specific projects.

So far, the technical manuals for field work in Horizontal, Vertical and Gravity Observations are available including a manual for the processing of gravity data. Similar manuals for the processing of Horizontal and Vertical data have an advance of 25% each.

DATA INVENTORY

The Mexican VCN - (Fig. 1) is given by 24 000 Kms of Control Network, 20 000 Bench Marks and 120 000 Kms of Second Order Network with 15 000 Bench Marks. D.G.G. has surveyed about 5 500 Bench Marks along 10 000 Kms of First Order Levelling Lines and the total Network of Second Order'

In particular, from 1980 to 1984, D.G.G. added 1 635 First Order Bench Marks and 2 491 Second Order Bench Marks along 20 000 Kms of levelling lines. 52 First Order Bench Marks were surveyed to link with the U.S.A. and Guatemala levelling lines to close loops of levelling along the respective border lines.

The linking points with the U.S.A. levelling lines are (Fig. 2) :

Ciudad Juárez	-	El Paso
Ojinaga	-	Presidio
Piedras Negras	-	Eagle Pass
Nuevo Laredo	-	Laredo
Cd. Miguel Hidalgo	-	Roma
Reynosa	-	Hidalgo
Matamoros	-	Brownsville

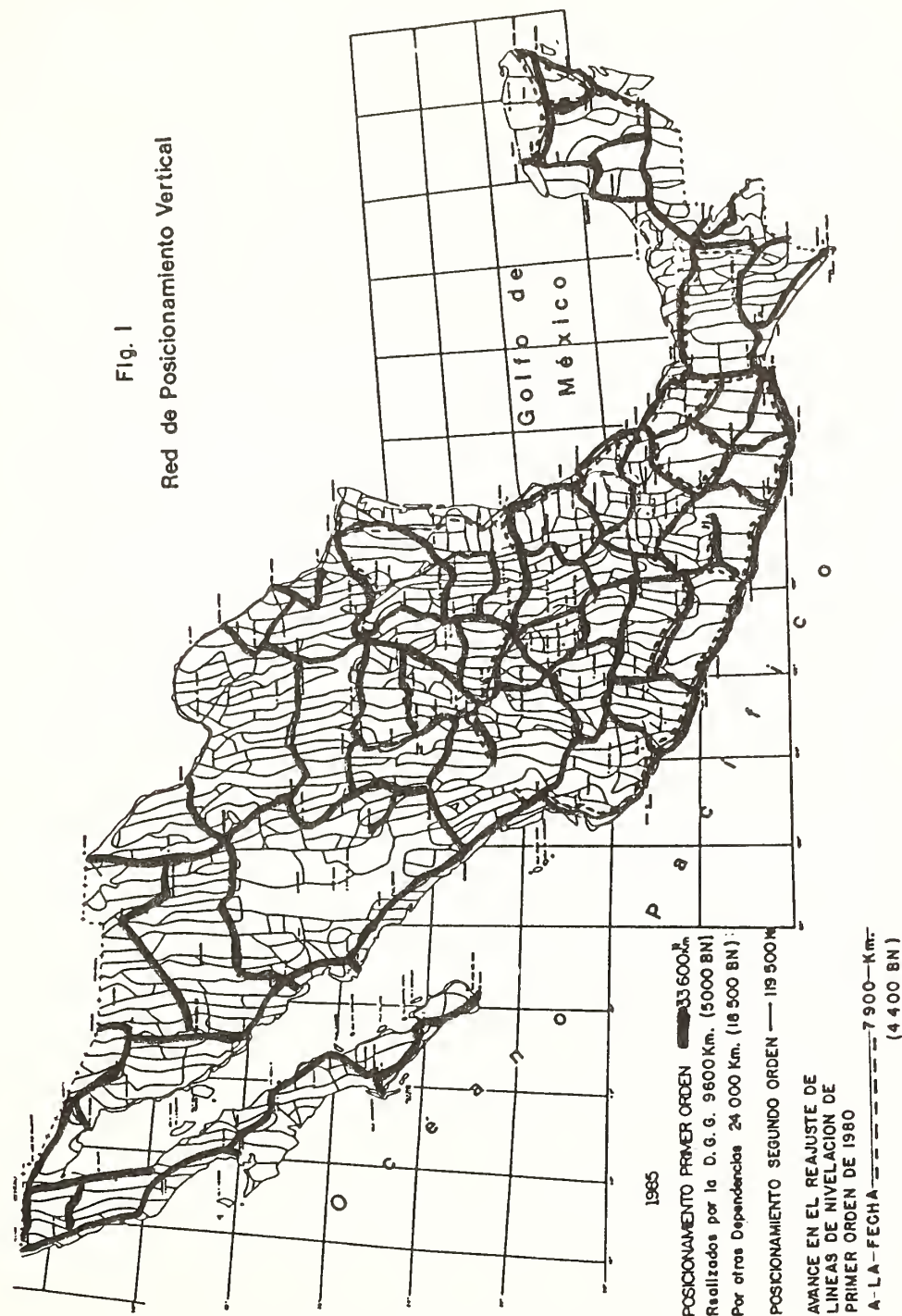
There are projects for:

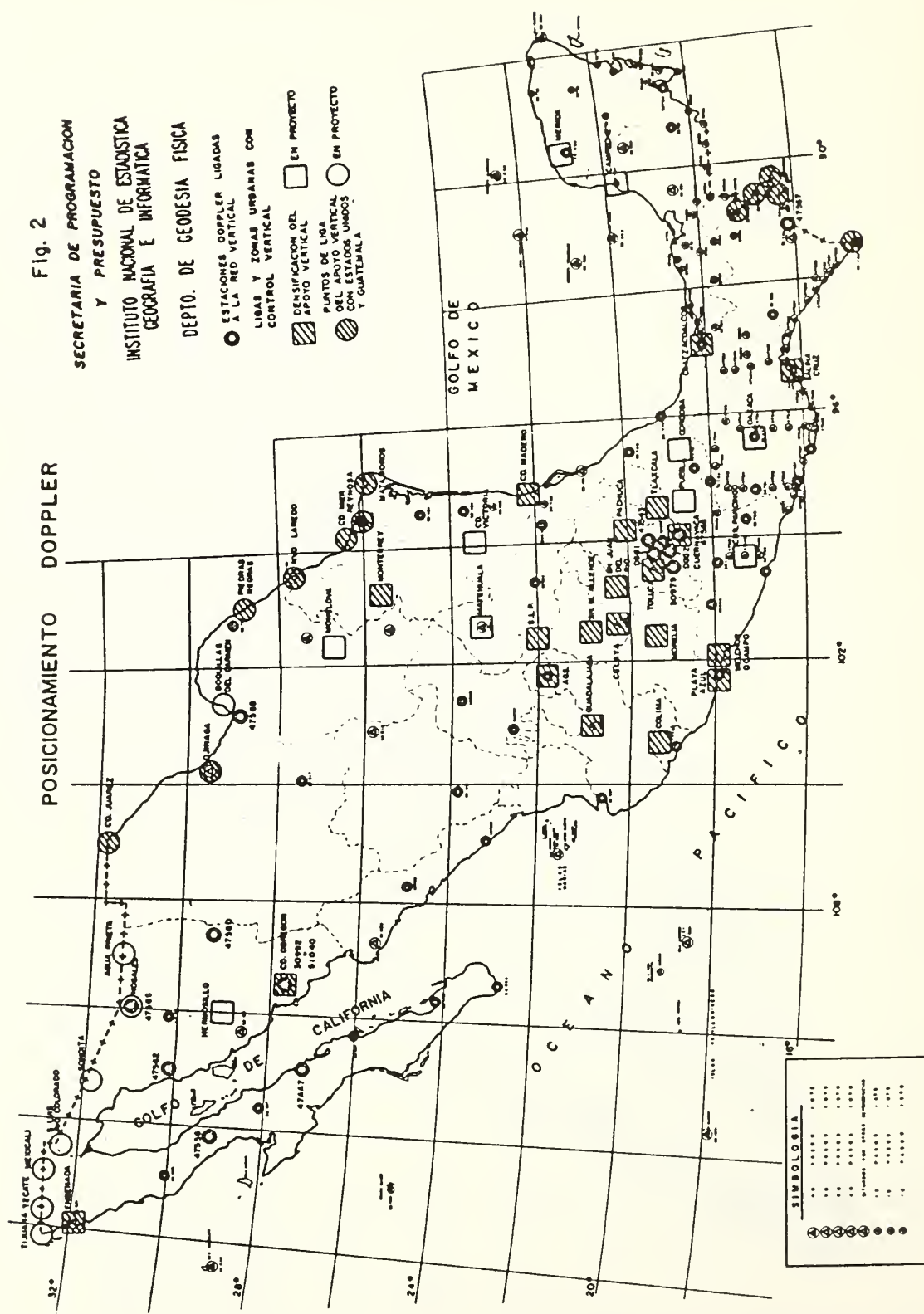
Mexicali	-	Calexico
Sonoita	-	Luckeville
Nogales	-	Nogales
Agua Prieta	-	Douglas .

All those points were selected in common agreement with the Vertical Geodetic Section of NGS - NOAA.

The linking points in our south border line are:

Nuevo Progreso	-	El Ceibo
Frontera Echeverría	-	La Técnica
Benemérito	-	Pipiles
Aforo El Tigre	-	La Bella
Ciudad Hidalgo	-	Ciudad Tecun





On the other hand, 600 Second Order Bench Marks across 3 100 Kms levelled in a area of 900 km^2 (Fig. 2) were surveyed as a part for the densification of vertical control in 21 urban areas with top priority for urban control. Also, 66 Second Order Bench Marks were used to link vertically 58 Doppler Stations for comparison studies and geoidal determinations (Fig.2).

Fig. 3 shows the status of tide gauges stations.

A process of substitution of the old Standard Type Tide Gauge for digital ones is on the way.

Since tide gauge stations are under the responsability of the Universidad Nacional Autónoma de México, U.N.A.M., an agreement for technical cooperation between U.N.A.M. and D.G.G. has been signed in order D.G.G. re-level periodically the micro loops with the Master Bench Marks directly linked to the tide gauges and to have the high differences between the Bench Mark and the corresponding tide gauge.

The gravimetric works have had a significative impulse. They started in june 1980 and so far 10642 gravity observations has been done through levelling lines existing up 24° paralel of latitude north with a coverage of $940\,000 \text{ Km}^2$ which represents the 47% of the Mexican Territory. Fig. 3. For a complete processing of this information it was necessary to create the computer programs PROGRAV, AJUSTGRAV and AJUSTBASE; all them in Fortran Language, double precision and - implemented in the Operative System UNIVAC 1108. PROGRAV gives as results the differences of gravity corrected for static and dynamic drifts and earth tide including Honkasalo's correction, The other two programs perform a Parametric Least Squares Adjustment with the loops of corrected differences of gravity integrating them to the Base Stations of the International Gravity Standardization Network 1971 (IGSN-71). The print out of these programs are the absolute values for gravity stations; free air anomalies and simple Bouguer anomalies (Table 1). An algorithm is in preparation which will allow us the practical determination of Complete Bouguer anomalies.

Those 70 Thousand historical gravity data existing prior to 1980 gravity surveys have been used to obtain point and mean free air anomalies. Mean anomalies were computed from $1^\circ \times 1^\circ$ and $1/3^\circ \times 1/3^\circ$ blocks and the idea is to compare them with mean values derived with 1980 data in order to be able to classify their quality. The obtained results have been unsatisfactory. These data also was used in - combination with astronomic data and geoidal heights derived from Doppler Stations with known orthometric heights and the GEM 8 Geopotencial Model to prove the Surface Fitting Technique and derive a first version of the geoidal shape in the mexican area.

READJUSTMENT OF THE VERTICAL CONTROL NETWORK

The Proyect is carrying out among the normal activities of the D.G.G. in harmony with the programs of priorities defined by the Federal Government. The realization of the Proyect hasn't a dead line since no special funds are available for it. - However the Proyect is undergoing through the following steps:

Human Resources

A full time working group of 5 people is responsible to succeed in the Project. Obviously, there are supporting personnel devoted to data inventory, gravimetric

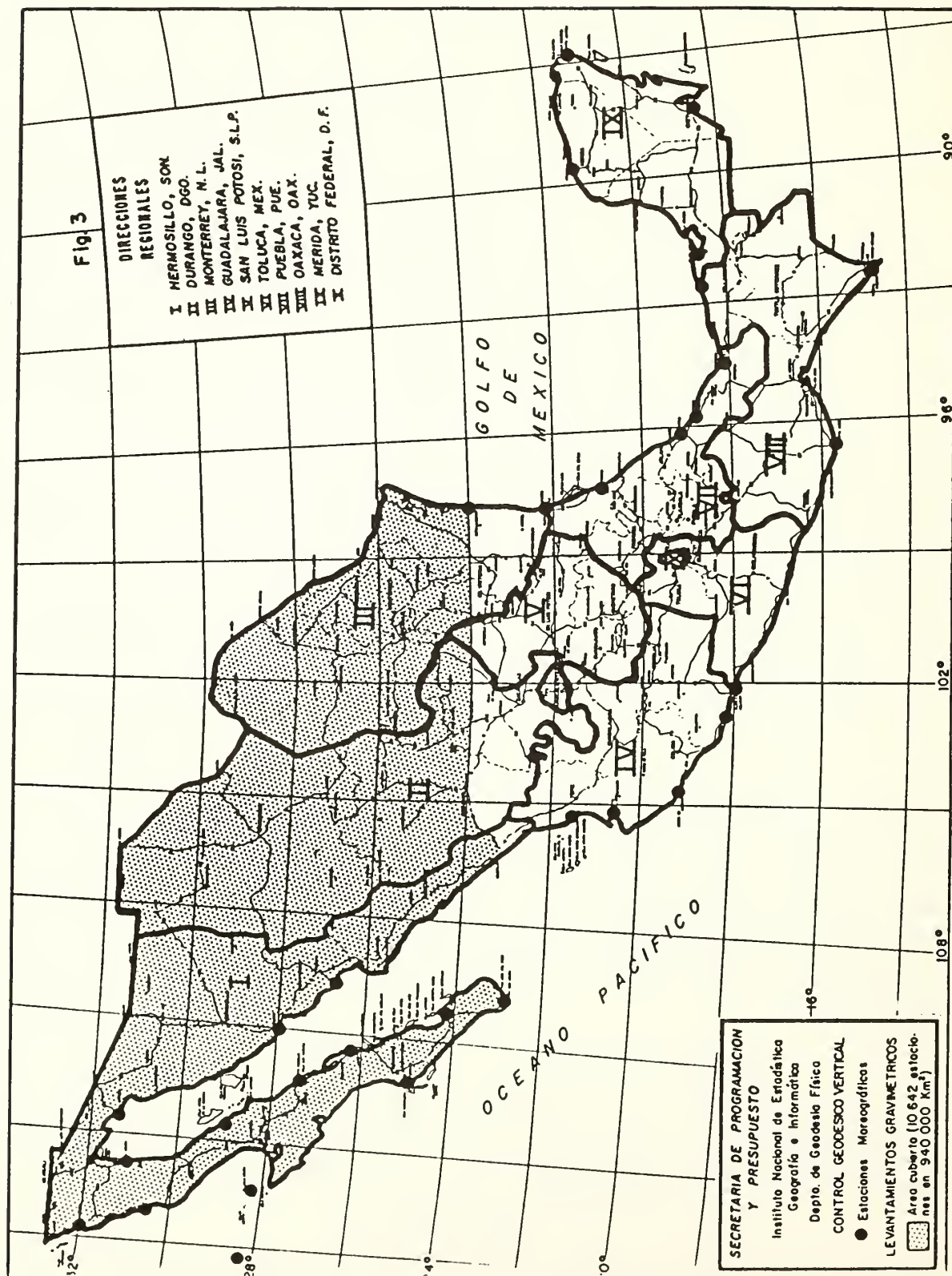


TABLA N° 1

LEVANTAMIENTO REGIONAL CIRCUITO: 21-05 FECHA: 16 02 1984 GRAVIMETRO: LRG050

OBSERVADOR:

REVISOR:

DATOS DE ENTRADA

ESTACION	ϕ	λ	C.P.	h	C.P. FECHA	HORA LECTURA	
						1 ^a	2 ^a
MATAMOROS 9685-62	25 4622	97 318522M		781116	2841010251700610112517005		0
BNP H 264	25 5268	97 302522M		1341016	2841037252726810382527267		0
BNP H 265	25 5296	97 302722M		1111016	2841047252735910482527359		0
BNT 912	25 5120	97 379622M		1331016	2841128251377811292513777		0
BNT 913 A	25 5187	97 342822M		1371116	2841150251923511512519234		0
BNT 911	25 5355	97 412722M		1451016	284121025 6954121125 6954		0
BNT 910	25 4763	97 416322M		1371016	28413 925 2850131025 2859		0
BNT 908	25 4646	97 429322M		1211016	284133525 421133625 420		0
BNT 909 A	25 4648	97 429322M		1121116	284134825 296135025 295		0
BNT 912	25 5120	97 379622M		1331016	28414232513381142425133809E08		0
MATAMOROS 9685-62	25 4622	97 318522M		781116	28415 4251697615 52516975		0

AJUSTE DE REDES GRAVIMETRICAS

LEVANTAMIENTO REGIONAL

CIRCUITO: 21-05

FECHA: 16 02 1984

GRAVIMETRO: LRG050

OBSERVADOR:

REVISOR:

ESTACION	LATITUD [° ' "]	LONGITUD [° ' "]	C.P.	ALTURA [M]	C.P.	GRAVEDAD [MGAL]	O.E. [MGAL]	ANOMALIAS	
								A. L19RE [MGAL]	BOUGUER [MGAL]
BNP H 264	25 52 40.8	97 30 15.1	22	10.400	10	979022.052	.155	9.134	7.970
BNP H 265	25 52 57.7	97 30 16.2	22	11.100	10	979021.975	.179	8.940	7.698
BNT 912	25 51 11.9	97 37 57.7	22	10.300	10	979007.685	.142	-3.513	-4.666
BNT 913 A	25 51 52.2	97 34 16.7	22	10.700	11	979013.490	.222	1.622	.424
BNT 911	25 50 33.0	97 41 16.1	22	14.500	10	979000.694	.258	-8.443	-10.066
BNT 910	25 47 37.7	97 41 37.7	22	13.700	10	978996.452	.265	-9.485	-11.018
BNT 908	25 46 27.5	97 42 55.8	22	12.100	10	978993.955	.260	-11.097	-12.451
BNT 909 A	25 46 28.9	97 42 55.8	22	11.200	11	978993.922	.208	-11.437	-12.690

surveying, etc.

Data Inventory

This was a difficult, laborious and extensive step. About 4 years were consumed in this task. Much of this time was spent to convince the different agencies to allow the transference of their Vertical Data to the D.G.G. data banks. Also, it was laborious and time consuming the process for revision and preliminar analisis to evaluate and classify the compiled vertical data.

Data Bank

At the same time the above activities took place, it was created the necessary technical background for archives, handle and control of vertical information.

There are 3 different data banks. The Physical Bank concentrate the notebook with the original field data.

This information is supported by a Bank of Microfilmes. The filmes are 16-35 mm. Finally, there is a Automatized Bank with two main files INVENTARIO 01 and INVENTARIO 02. The programs and formats employed to operate these files allow a large flexibility in the handing of the data. The data can be classified by level lines, by geographic blocks; by provinces, etc. Considering global figures, there are 30 000 Bench Marks in the Bank, from which 16 000 are First Order Bench Marks.

Standardization Process

The below process (Fig.4) is applied to the levelling lines with the objective to standard the quality of the networks:

- a.- General analisis for data verification and preliminar classification.
- b.- Codification and digitalization of the data.
- c.- Adjustment of each level line. Program LEVEL.
- d.- Adjustment of levelling loops. Program CIRCUIT.
- e.- Analisis and evaluation of the results.

The computer programs LEVEL and CIRCUIT are modified versions adapted to our requeriments from original programs developed by Defense Mapping Agency. Their documentation is in spanish language.

The program LEVEL performs the computations and parametric least squares adjustment of levelling lines. It can process up to 1000 stations; CIRCUIT adjusts levelling loops.

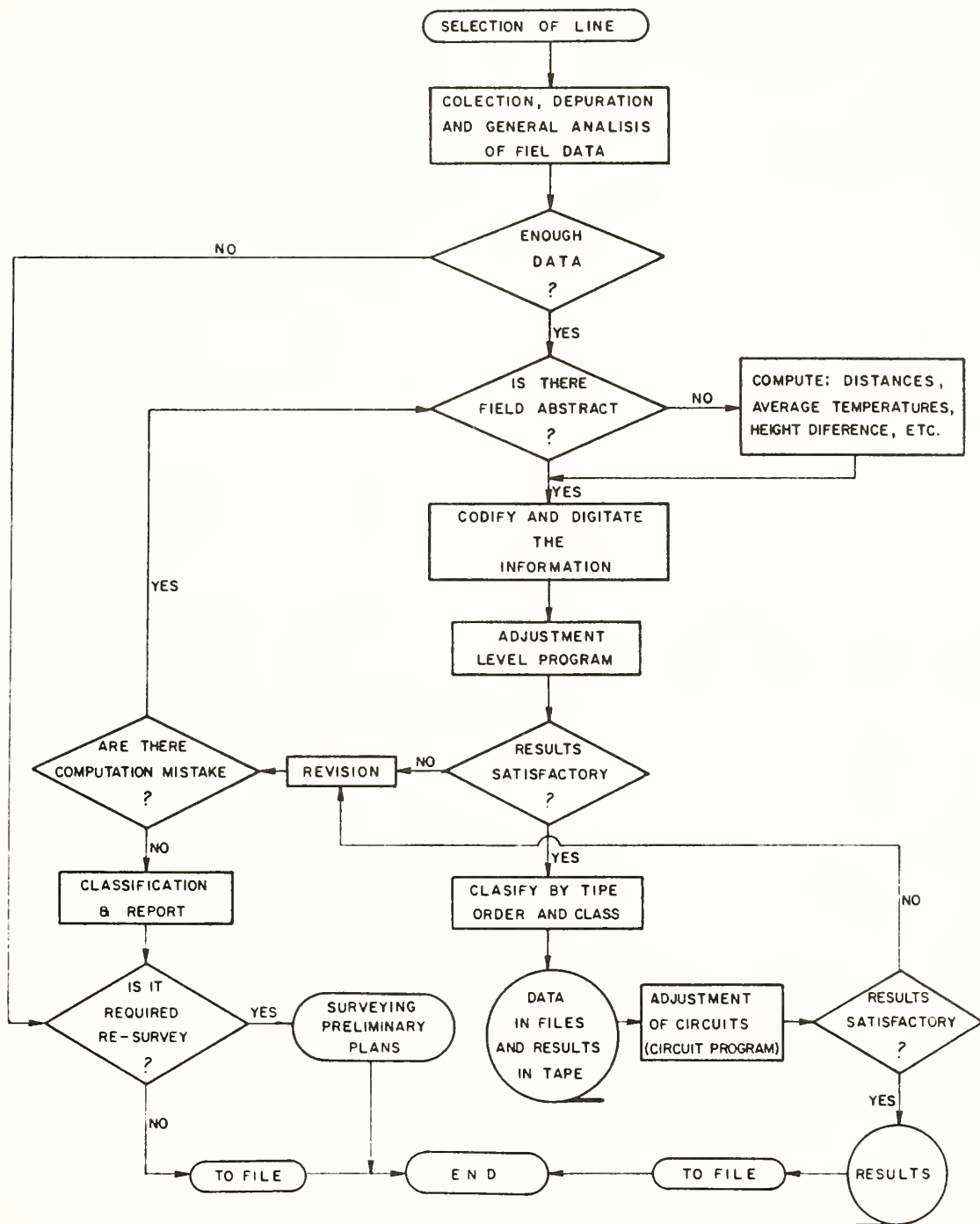
The Fig. 1 gives the advances in this process.

Remaining Steps

After the standardization process would be completed, the next will be:

- a.- Definition of the New Vertical Reference System.
- b.- Readjustment of the Vertical Control Network in a test area.
- c.- Readjustment of the whole Vertical Control Network.
- d.- Readjustment of the Second Order Network.
- e.- Densification and Maintenance of the Net as a permanent activity.

Fig. 4. STANDARDIZATION PROCESS OF LEVEL LINES



CONCLUSIONS

An integral adjustment of the Vertical Control Network requires an uniform and persistent effort. From 1980, D.G.G. had take over this task.

Among the factors limiting the development of these activities, on one hand, is the severe economical crisis suffered by our nation; the crisis has forced us to rationalize the public expenses giving the top priority to those projects tending to satisfy basic or essential needs of the population. On the other hand, as a part of the administrative desconcentration process performed by the federal government to favor a more harmonic development of the nation, the D.G.G. is dividing in regions its geographical activities. Fig. 3. One of the first desconcentrated activities is that related with geodetic control networks.

The progress of this Project can be summarized in:

Formation of Human Resources.

Creation of a Data Bank.

Technical Background for the computations of the readjustment.

Increasing the vertical networks in 20 000 kms of levelling lines with 3126 -
-Bench Marks.

Link points with the control networks of our bordering neighbours which will not only allow to close levelling loops but also an eventual adjustment of all the levelling lines in North America.

The 10642 gravity observations represents a coverage of 47% of the Mexican -
Territory. The gravimetric data, among other purposes, will give us the opportunity to make gravity corrections and to derive orthometric heights from the -
levelling lines.

The standardization of the quality of the data is 20% of the BM'S.

All these activities required norms and specifications and methodologies for their realization, likewise the formation of a background in computation by electronic method: Data Bank, computer programs to operate the Bank and to process and adjust the vertical data.

Although, we consider the realizations are significant, we recognize the fact that there are a lot of activities to come to. Sincerely, we desire the papers and discussions which take place in this Symposium would help us to crown successfully this noble task.

D.G.F.-D.G.G.
April 1985

THE SWEDISH EXPERIENCE WITH MOTORIZED LEVELLING NEW TECHNIQUES AND TESTS

Jean-Marie Becker
National Land Survey of Sweden
Geodetic section
S-801 12 GÄVLE
SWEDEN

1 INTRODUCTION

At the National Land Survey of Sweden a great deal of attention is paid to studying ways and methods to rationalize geodetic activities.

An example of the result of the rationalization process is the development of rapid, efficient and accurate methods for triangulation and trilateration using laser Geodimeters and light-weight portable towers. Using these methods the whole of the Swedish network has been remeasured. The on-going third national precise levelling programme is being carried out using a fully automated system built up around motorized levelling techniques and a fully computerised handling of data from the field to the archives. The programme was initiated in 1974 and has been continually updated to keep abreast of modern technological developments.

Our experiences of modern levelling techniques is based on the levelling of over 37 000 km carried out under a wide variety of physical conditions, and with a large number of different field crews working with different types of equipment.

The results can be summarised as follows:

- a daily production of 12 km for a 5,5 hr working day;
- a releveling rate which is less than 5 %;
- a field season from spring to autumn with a standard working day without stops in the middle of the day.

At the same time tests are in progress which hopefully will result in for example, new methods for trigonometric heighting and traversing.

This report will deal with motorized levelling and, thereafter, the development of new techniques.

2 THE SWEDISH MOTORIZED LEVELLING TECHNIQUE (ML)

With the fully motorized levelling technique, all work is performed directly from the vehicles. The operators do not leave their seats. The only exception to this rule is when connecting to bench marks.

The complete motorization of levelling techniques was made possible not only by the development of the specially designed Zeiss Jena Ni002 reversible compensator level; but also required modification of vehicles and the construction of special accessories.

This technique has been described in several publications (Becker 1977,1984). Therefore, we will only mention its essential characteristics.

2.1 Equipment and personnel

A motorized levelling party consists of four persons: (two surveyors-operators acting alternatively as observer and booker and two assistants staff men) and three vehicles (one vehicle carrying the instrument and two vehicles carrying the staffs).

The three vehicles are equipped with:

- a precision electronic trip meter, Digitrip;
- a hand-held field computer, Micronic 445;
- a set of warning signs;
- some spare parts.

The specially constructed accessories and modifications on the vehicle carrying the instrument are:

- holes in the rear-platform for the legs of the tripod (set-up without contact with the vehicle);
- a lifting device to lift up or lower the tripod and instrument;
- a removable linen roof for protection against wind, rain and sun;
- a radio communication system (interphone);
- a special tripod with long adjustable legs and special feet;
- a quick-setting device;
- an additional tripod of the classical type;
- an electric thermometer for the registration of air t° ;
- a desk;
- a printer coupled to the Micronic for the simultaneous print-out of all data (doubling and control).

The vehicles carrying the staffs were specially equipped with:

- a specially modified door to facilitate the movements of the staff-holder;
- a mounting system allowing movement of the staff during set-up and transport;
- a special, heavy base plate;
- a (3,5 m long) precise levelling staff with an invar inset with double graduations in centimeters starting at 0,5 m;
- a centring arrangement on the base of the staff;
- three bull's eye levels with viewing mirrors;
- electronic sensors coupled to the invar band for recording the band temperature;
- an additional staff for the difficult connections;
- classical foot plates, iron pins.

The ZEISS JENA Ni002 level is a high precision automatic level, specially designed for motorized levelling. Thanks to innovations in its design, this instrument has played a decisive roll in the full motorization of levelling. The elbowjoint eyepiece permits pointing of the instrument and the observation of fore- and backsights from one fixed observing position. Moreover, the reversible pendulum eliminates the problems related to the necessity of having equal fore- and backsights (difficult to realize with vehicles).

2.2 The work method

All operations are performed from the vehicles. For this reason we design working methods so as to minimize observing time and optimize the quality of the results.

- To conciliate both aims, we use the following routine:
- the movement of the vehicles always occurs in the same chronological order;
 - the Ni002 is set up according to the principle of the "red trousers" method;
 - the observations are the whole time carried out as follows (1) to (6).

Position I, left scale

backsight Stadia line (1) - levell. line (2)
foresight " " (3) " " (4)

Position II, right scale

foresight " " (6)
backsight " " (5)

As a rule, the forward and reverse levellings are executed at different times (day, hour) and under different meteorological conditions and by different observers.

All instrument are checked once a week. All staffs are calibrated at least twice a year (every graduation on the invarband) with laser interferometer komparator.

2.3 The observations and their registration

The data are collected simultaneously in the three vehicles, according to a fixed schedule, preprogrammed in the data stacks. Recording routines are not the same for instrument and staff vehicles.

During the registration process, simple computations and checks against given tolerances are done automatically in the data log. The information stored in the data stacks is transferred on to magnetic tapes for transfer into the data bank.

3 RESULTS

To better illustrate the results yielded by the motorized levelling technique, a comparison with standard techniques is made below. The following criteria has been chosen for the comparative study: efficiency quality and working conditions.

3.1 Efficiency

The efficiency of a levelling technique can be illustrated on the one hand by the average (daily or hourly) production and total season production, and on the other hand by the cost per levelled kilometer.

TABLE 1

LEVELLING STATISTICS FOR PERIOD 820501 TO 821027

PARTY	KM TOTAL	KM CHECK	KM REPAY	EFF HRS	NO. BMS	NO. SET-UPS	SET-UPS PR.HR	DIFFERENT BM	BM	BM	BM	BM	AVSIGHT LGTH	AV. LGTH	KM PR.HR	NO. WORK DAYS
1	1,293.6	0.0	18.7	586.4	1387	16004	27.3	1307	12	10	47	40.4	932,7	2,21	100	
2	1,101.3	216.3	0.0	589.9	1183	16496	28.0	1104	35	68	22	33,4	930,9	1,87	112	
3	1,493.6	5.6	12.1	603.2	1623	18551	30.8	1304	91	67	90	40,3	920,3	2,48	112	
4	1,358.7	33.4	27.0	622.2	1599	17217	27.7	1169	94	73	115	39,5	849,7	2,18	109	
5	1,328.1	169.8	0.0	572.4	1400	17990	31.4	1140	165	45	50	36,9	948,6	2,32	107	
=====	=====	=====	=====	=====	=====	=====	=====	=====	=====	=====	=====	=====	=====	=====	=====	=====
	6,575.3	425.1	57.8	2974.1	7192	86,258	29.0	6024	397	263	324	38,1	916,4	2,21	540	

TABLE 2

PRODUCTION STATISTICS FOR PERIOD 1976-1984 WITH MOTORIZED LEVELLING

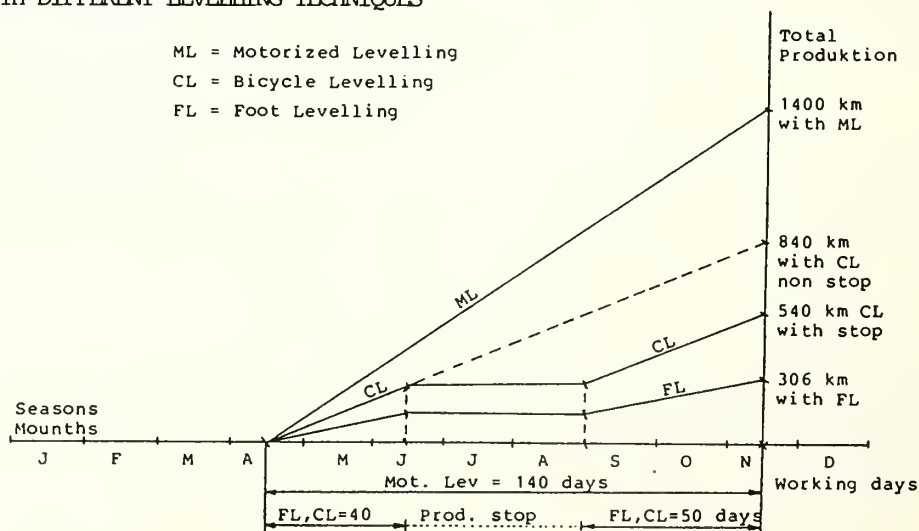
YEAR	NUMBERS OF PARTY	FIELD WORK DAYS	TOTAL PRODUCTION IN KM			DAILY PRODUCTION KM			RELEVELLING %
			ACCEPTED	RELEVELLED	TOTAL	ACCEPTED	RELEVELLED	TOTAL	
1976-1981	1-5	2 023	18 374	1 186	19 560	9,1	0,6	9,7	6,0
1982-1984*	4-6	1 520	17 420	759	18 179	11,5	0,5	12,0	4,2
Total	-	3 362	33 900	1 945	35 845	10,1	0,6	10,7	5,2

*) Measurement with 3,5 m invarstaff.

Table 1 and Table 2 shows the result obtained in Sweden:

- We can see that the average hourly production for a motorized levelling party is about 2,2 km;
- The average daily production under the last 3 years (when using 3,5 m invar-staff) is about 12,0 km;
- The effective working time during a normal 8 hours day is only on an average about 5,5 hours;
- The complete time needed to perform all operations relating to one set-up of the instrument, including the transport time, is on an average between 1,6 to 2,4 minutes;
- In Scandinavian countries our experience shows that it is possible to use motorized levelling without interruption during the whole fieldseason: for Sweden during about 140 days. In the same period the foot (FL) and bicycle (CL) levelling techniques can only be used during 90 days (spring and autumn). Moreover, using standard methods special precautions must be taken and the observations must be interrupted in the middle of the day (shimmer, refraction).

Figure 1 PRODUCTION POSSIBILITIES DURING FIELD SEASON WITH DIFFERENT LEVELLING TECHNIQUES



- Figure 1 also shows that with (ML) motorized levelling technique the total production per season is increased by at least a factor of 2,5 compared to (CL) bicycle levelling and a factor 4 for (FL) foot levelling.

When analysing the cost for a levelled kilometer, we discover that in the industrialized countries, and especially in Sweden, the part representing the wages are relatively high and represent about 90 %. The capital cost (for equipment and cars) are less than 7 % of the total cost. To reduce costs, it is therefore important to reduce the number of operators to a minimum while maintaining an optimal

production rate. The ML used only 4 persons while FL and CL require 4 to 5 and even more persons.

In comparative studies we have as a principle only dealt with the factors related to production in the field. A better comparison is obtained if data processing and works which follows the field work are also included. The Swedish system is fully computerized from data collection in the field (Micronic) through processing (computer PR1ME), to the storage and output of the results (height data bank).

3.2 Quality of the results: accuracy

In order to be able to correctly judge of the quality of the results, we should keep in mind the conditions (regulations and tolerances) which have steered the execution of the field work.

The permitted difference between the forward and reverse levelling of a line is $2 \sqrt{L}$ mm/km (L = distance in km) for the first order network.

Field work is in progress during the whole season without interruption under the most varying working conditions and by a variety of staff.

The average percentage of relevening for all levelling carried out up to the present time with motorized techniques is 5,2 % (see table 2).

In his studies and analysis of our work in the years 1977-78 (Remmer 1979) notes that:

- the optimal non-acceptance limit is about $2,3 \sqrt{L}$ mm/km between a forward and reverse levelling;
- in this case, the number of undetected gross errors only amounts to 2 o/oo.

However, the best criterion to judge of the quality of the measurements is the mean error per kilometer, which can be calculated either from the circuit closures, or from the deviations of the runs. In both cases we note that these mean errors remain under ± 1 mm/km, which complies with the norms for precise levelling.

We think it is worth mentioning here some of the factors which make these results possible with motorized techniques. Among these we can note:

- a higher speed of operation: reduction of the settlement and heaving effects linked to the time factor (staff, tripod);
- a higher line of sight: the instrument is more than 2 m above the ground: almost total elimination of the refraction effects and of shimmer effects;
- perfect stability of the staffs under all operating time;
- permanent check of verticality with the help of the 3 bull's eye levels;
- greater stability of the foot plates;
- no movement around the tripod: sinking effect reduced;
- greater stability of the tripod thanks to the modified feet;
- less fatigue because of the regular change of observers;
- fore- and back sights always over the same surfaces (roads or backs) = identical symmetrical refraction.

3.3 The working conditions

The introduction of motorized techniques has greatly improved the field working environment since nearly all operations are performed from the vehicles. The purely physical part of levelling has been considerably lightened:

- no more long and tiring walks with heavy and cumbersome equipment;
- no need to manually hold the staffs in a vertical position;
- work in seated position for the staff men and the booker;
- special desk facilitating the bookers work;
- preprogrammed automatic registration with the help of the Micronic data logs;
- protection against rain, wind etc.

The weight, volume and quantity of the equipment used need not be limited. Currently, working conditions are such that nearly half of the personnel is female. The safety during the day has been strongly improved because of the numerous warning signs and signals which are mounted on the vehicles. Road users have more respect for the levelling parties. No incident has occurred in the ten past years.

3.4 Conclusions

The Swedish experience with motorized levelling (more than 37 000 km) has confirmed that this technique at the moment is the most appropriate one for largescale precise levelling work.

The obtained results are:

- average daily production about 12 km (by only 5,5 working hours);
- cost per levelled km reduced by about 50 %;
- uninterrupted working throughout the season and during normal working hours;
- improved working environment;
- accuracy as good or even higher as with classical methods even under unfavourable conditions;
- several countries have successfully adopted the Swedish motorized levelling; system (Danmark, Holland, Norway, France, USA, Zambia a s o).

4 NEW TECHNIQUES AND TESTS

During the coming field season experimental work will be carried out to test a number of new techniques. Some of this work will be concerned with the evaluation of methods which have already been introduced in other countries; other parts will be related to the further development of these techniques.

Of particular interest are: indirect levelling and motorized traversing to determine X, Y and Z coordinates.

4.1 Double Motorized Levelling (DML)

This technique is based on the use of only two vehicles as opposed to the now well-known three vehicle technique. DML can be used for simultaneous single levelling. The two vehicle are identically equiped and are basically the same as the instrument vehicle used for the classical motorized levelling (ML) with the exception of the levelling staff which is mounted on both vehicles on a support close to the instrument so that it can be manipulated by the observer.

Each car is crewed by two surveyors with the combined roles of driver, booker, observer and staffmen. Each vehicle is equipped with short-wave radio equipment for inter-car communication and booking is done with the help of electronic data logs. In addition to base plates and temperature recording equipment, a third staff is carried for making connections to bench marks.

FIGURE 2 : DOUBLE MOTORIZED LEVELLING

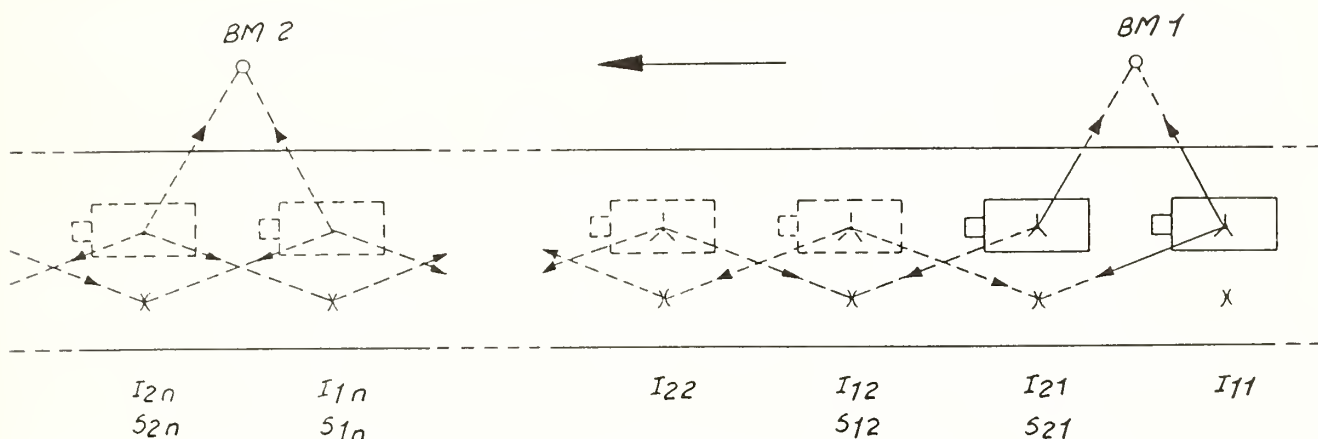


Figure 2 illustrates a possible measuring routine. Each observer records his observations in his own data log. A run between two bench marks results in two independent height determinations measured simultaneously and in the same direction.

The use of this technique appears to offer a number of advantages since investment costs will be reduced by about 20% and the increase in productivity has been estimated to about 15%.

This technique will result in sets of reciprocal observations at the same time, in addition to losing the Δh check, the observations are correlated both in time and with respect to environmental conditions. The overall simplicity of this technique make further investigations interesting. Of particular interest will be the accuracy which can be attained.

4.2 Trigonometric Levelling (TL)

In the early 1970's a number of experiments were carried in the north of Sweden using this technique with transporting crews and equipment by both car and helicopter. Distances were measured using an AGA model 6 Geodimeter and angles observed reciprocally with standard second order theodolites. A modified version of height traversing was also used in the national retriangulation programme.

The results achieved in broken mountainous terrain were very promising. Using the method only along the roads did not result in any significant improvements when compared with "cycle" levelling which was the method in use at that time for second order levelling. In the mountains it was possible to produce results with an accuracy of 10 mm.

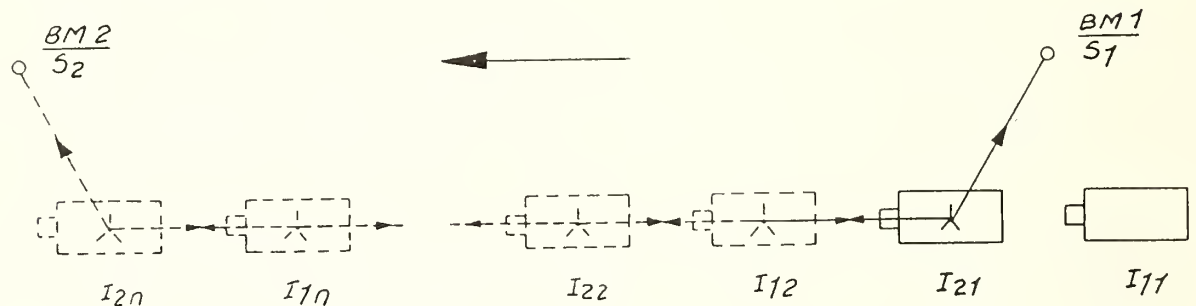
The new generation of total stations has made it possible to develop new and improved methods. In 1981 Bahnert in East Germany reported results of the order of 4 mm/km.

4.21 Motorized Trigonometric Levelling (MTL)

In the USA (Whalen 1984), France (Kasser 1984) and in Canada very promising results have been reported using this technique. The technique has been well documented and is based on the use of total stations to carry out reciprocal observations.

To speed up and improve the accuracy, the total stations will be equipped with a specially designed adapter on which both a reflector and target can be fitted. All observations will be collected using data logs and will be checked and computed during the actual field operations.

FIGURE 3: MOTORIZED TRIGONOMETRIC LEVELLING (MTL)



The tests will be begun using two vehicles and thereafter a series of tests using three vehicles will also be carried out. With three vehicles we feel that productivity will be significantly increased and observing times will be decreased which should improve accuracy: decreased settling.

4.22 Double Motorized Trigonometric Levelling (DMTL)

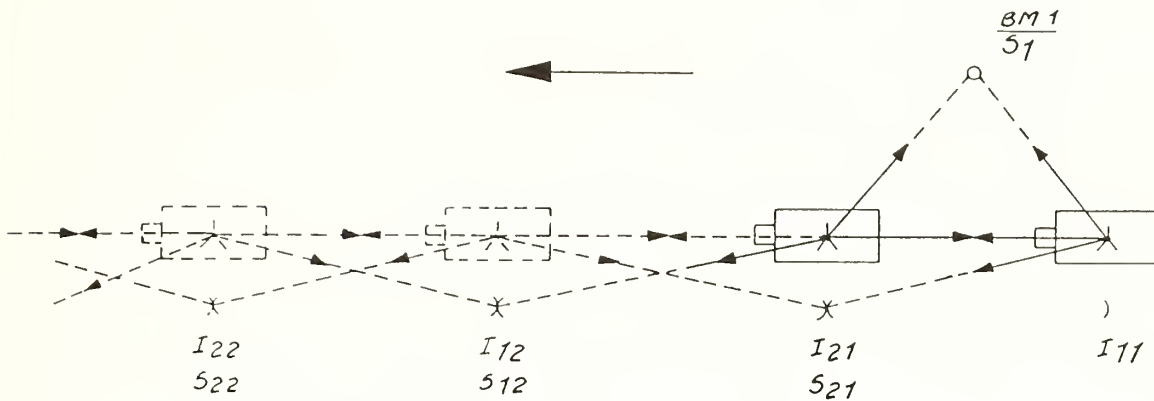
We plan to study the feasibility of combining both methods 4.1 and 4.21. The same vehicles as will be used for DML will also be used for this series of tests. The Ni002 instruments will be replaced with total stations (AGA 142, Kern a s o). On the eccentrically mounted levelling staves a twin set of reflectors and targets will be mounted to form a fixed base on the staves with a centre point approximately 2,5 m above ground level.

A proposed measuring routine is as follows:

- a set of reciprocal distance and vertical angle observations as for MTL followed by observations to the targets and reflectors which are mounted on the levelling staves.

Measurements will be done according to the leap-frog method, see figure 4. Connections will be made to bench marks using a third staff.

FIGURE 4: THE DOUBLE MOTORIZED TRIGONOMETRIC LEVELLING (DMTL)



The combined results will give four separate height traverses i.e. two reciprocally observed height traverses instrument to instrument and two separate traverses instrument to staff.

Possible advantages of this method are:

- improved accuracy from the combined technique;
- decrease of refractive effects: reciprocal observations;
- increased speed: long lines of sight simultaneous forward and reverse observations;
- better productivity in hilly areas;
- lower production costs.

Foreseeable disadvantages are:

- high capital costs: total stations;
- longer set-up times;
- need for better planning and reconnaissance;
- connections two bench marks can be time-consuming;
- data capture routines must be very care-full defined.

It is possible to operate using 3 vehicles but the logistics of the operations would be relatively complicated and disadvantages will presumably outweigh the advantages of such a configuration: handling the observation data would be particularly complicated.

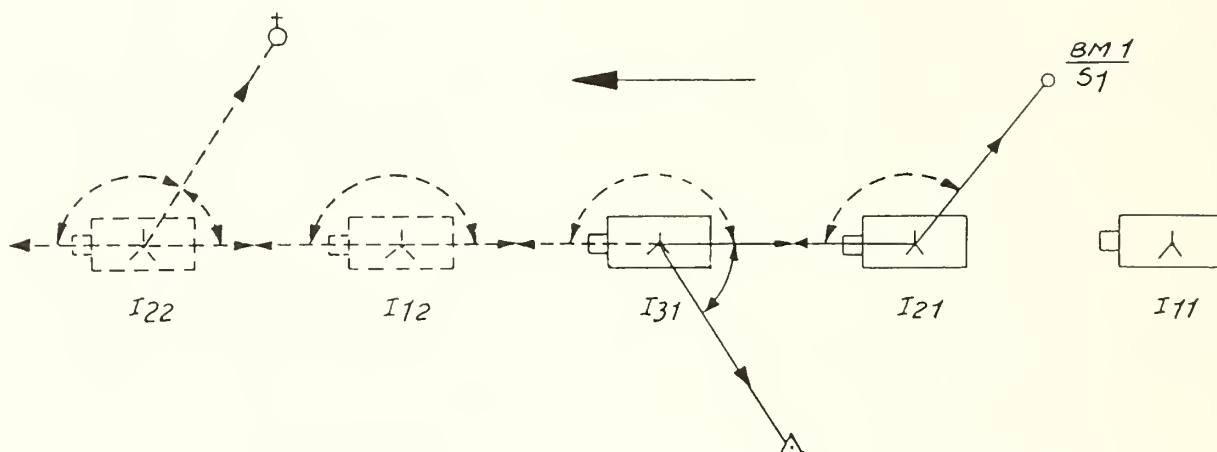
4.3 The Motorized XYZ Technique (MXYZ)

National networks normally comprise separate layouts for the height and planimetric nets each with its own demarcation system. Field observations are carried out as completely separate activities, often by separate sections within the organisation. There is a need for coordinate information for the computation and documentation of height networks. The increasing interest for digital mapping techniques is a further argument for an XYZ determination of bench marks.

The method described in section 4.2 can possibly be adapted to make it possible also to determine station coordinates. Tests will be carried out to test this concept.

It is planned to use three vehicles, each equipped with a total station on which a reflector and target is mounted. Connections to bench marks will be made using the same type of staff as will be used for MTL. The staves will be fitted a specially constructed centring arrangement to make possible an exact set-up both over bench marks and traverse and triangulation points. The observation programme will be the following (see figure 5).

FIGURE 5: THE MOTORIZED XYZ TECHNIQUE (MXYZ)



The instrument vehicle I11 starts from the bench mark BM1 on which the staff S1 is placed.

1. Determination of height difference: I21-BM1
2. Horizontal angle: BM1-I21-I31

The instrument vehicle I1 moves from I11 to I12.

3. Determination of height difference: I21-I31
4. Horizontal angle: I21-I31-I12

The instrument vehicle I2 moves from I21 to I22.

5. Determination of height difference.....

Connections to coordinated points will be made as soon as visibility permits the observation of directions and/or distances. The type and number of connections will depend on accuracy requirements.

There is an opinion at the National Land Survey of Sweden that this method has considerable potential for second and third order networks both in Sweden and in developing countries. Particular attention will be concentrated on accuracy and economy.

References

- BAHNERT G (1981) Einige Erfahrungen mit trigonometrischen Nivellementsnetzen - Vermessungstechnik Heft 4 (1981) pp 126-128.
- BECKER J-M (1977) Experiences using Motorized Levelling Techniques in Sweden - IFS. Stockholm - Com. 5.
- BECKER J-M (1984) The Motorized Levelling Technique. The Swedish Experience - Gävle. LMV-Rapport 1984:15.
- KASSER M (1984) Une méthode d'avenir, le Nivellement Indirect de Précision Motorisé (NIPREMO) - Bulletin d'Information de l'IGN No 2 - pp 45-46.
- WHALEN C T (1984) Preliminary test results of Precise Trig-Leveling with the Wild T2000 - D15 System - ACSM-Bulletin Dec. pp 15-18.

RECENT ADVANCES IN HIGH PRECISION TRIGONOMETRIC MOTORIZED LEVELLING (NIPREMO) IN I.G.N. FRANCE

Michel KASSER

Institut Géographique National
2, Avenue Pasteur - 94160 St-MANDE
FRANCE

ABSTRACT. The need for decreasing the costs of high precision levelling observations have led the IGN-France in a first period to use the Motorized Levelling (as defined by J.M. Becker in Sweden), then to set up the first operational equipment of High Precision Trigonometric Motorized Levelling (in French : NIPREMO). The first experiments conducted in 1981 proved the validity of the concept. The aim was at that time to get a cheap low-precision levelling (5 mm/km) for overseas networks. As we reached easily 3 mm/km without special care, it was decided to try to reach the maximum precision possible while keeping an interesting speed. After that, some new experiments were made in 1983 with Kern E2 and Wild T 2000 Instruments and a commercial use of Nipremo began in Africa with Kern DKM2A & DM502 theodolites and EDM'S. It appears that Nipremo is the best way to level in mountainous areas, even with first order requirements, provided the density of benchmarks is not too high, as in France e.g. (2 benchmarks by km).

HISTORICAL BACKGROUND

We shall refer to the excellent review of the published experiments made by Rüeger and Brunner (1982). It appears that the principle of observing vertical angles to get the altitude of the target is perhaps as old as the geodesy itself ; but in no case it has been considered as a rival for high precision levelling, especially because of the incertitude of the value of the refraction. Geodesists commonly use so long distances in trigonometric heighting that, of course, the quality of denivelation measurement is quite low. At the beginning of the 70es, the increasing diffusion of good and cheap EDM'S let some people to reconsider this question, and various experiments were made and published here and there (e.g. Kratzsch, 1979). Anyway all of them seemed to look for a better precision, and not specially for a strong decrease of the costs.

So the experiments begun in 1981 at French-IGN were devoted to set up a new sort of levelling equipment, able to measure in a quicker way than classical motorized levelling and a particular attention was paid to get a much cheaper low-precision levelling method for overseas surveys. Often we have to level with a 5 or 7 mm/km precision required and classical methods hardly may be degraded to such values with a significant decrease of costs.

Spatial methods, of course, are useless, even if very interesting qualities of relative positionning are proposed using GPS in differential mode.

It is due to the fact that they can provide only geometric values and not geopotential ones, and because the geoid will not be known at the cm-level up to a certain time.

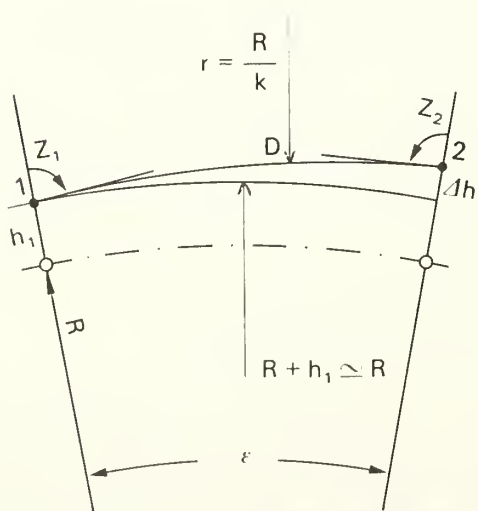
So we made some investigations in Trigonometric Levelling with the goal of going the more fastly possible. By using simultaneous reciprocal vertical angles observation, together with measurement of slope distances, we could get very promising results (Kasser, 1982) as well in speed (4,5 km/h) as in costs (half the cost of classical levelling) and in precision (3 mm/km). So we decided to set up a commercial equipment in Africa, where it has worked several times since 1983 ; and we tried to reach better accuracies, to eventually compete with high precision surveys in France.

The next tests were performed in 1983, with the opportunity of checking the new high-precision electronic theodolites of Wild (T 2000) and Kern (E 2). In spite of minor technical problems, the precision appeared as really excellent (1 mm/km), and in any case good enough for secondary order traverses. So we prepare and expect for late 1985 a fully operational equipment using electronic theodolites destined to French Levelling Network.

THEORY OF OPERATION

The theory is quite classical and need not to be explained in long details. From various discussions and trials it was obvious that the best solution was neither leap-frog nor reciprocal EDM traversing with just one theodolite, but that preferably we had to use simultaneous reciprocal EDM traversing (see Fig. 1) with two instruments.

Fig. 1



- Δh = Denivelation between stations.
- D = Slope distance between stations.
- ϵ = Angle between verticals at stations.
- R = Radius of the earth.
- h_1 = Altitude of station 1.
- k = Coefficient of refraction.
- r = Radius of curvature of ray path.

If we neglect the difference of deviation of the vertical between the two stations 1 and 2, and if we suppose that the coefficient of refraction is constant along the line of sight (i.e. the radius of curvature r of the path is constant), the height difference Δh is calculated as :

$$D h = D \sin \frac{Z_1 - Z_2}{2} \cos \xi/2 \quad (1)$$

which may be expressed as :

$$D h = \frac{1}{2} (D \cos Z_1 - D \cos Z_2) \cos \xi/2$$

i.e. the mean between the denivelations computed separately by each of the two stations 1 and 2, using their own data, provided they have both an EDM.

PRACTICAL ORGANISATION

The team is composed of two cars almost similarly equipped. Each of them is a pick-up. The tripod used is crossing the floor through holes and may rest directly on the road ; a lever system lets the operator to leave the station very quickly by rising the whole tripod + instrument in a well-secured position. The optical axis is 2,1 m above the ground. The instruments chosen were Kern ones because the DM 502 EDM gives the unique feature of not hindering the reversibility of theodolites telescopes. For the overseas equipment, DKM 2A was chosen as a good classical theodolite with probably less risks of failure than an electronic one. For France, E 2 was preferred. The Wild T 2000 (or T 2) + D 14 system is certainly at the same excellent quality level, but D 14 does not authorize important downwards slope sighting for one position of the circle when mounted on the theodolite, and this may be annoying in mountainous areas.

The theodolite with its EDM is fixed by a Zeiss fast set-up head on the tribrach. A direct link is established with the computer (Epson HX-20) that may be operated either by the secretary-driver of the car or preferably by the observer. A full duplex line is used between the two crewmen in order they can discuss easily even in noisy areas. A 3 m invar rod is fixed along the car and may be quickly set up on a benchmark by the secretary-driver. The driver uses a metric counter displaying the distance run by the car with 1 meter accuracy, and has a radio link with the other car. The telescopes of theodolites are framed with targets of a correct size allowing a good pointing by the other observer, and an EDM-reflector is fixed over the theodolite, which permits the measurement of the distance to be performed as fast as possible.

OPERATIONAL PROCEDURE

A lot of solutions may be used. Ours are the following ones :

- At the departure from a benchmark, the secretary-driver puts the 3-meter rod in vertical position on it. Three readings are made : the graduation, the closest to the horizontal, then two others to + and - 50 cm from this one, then again the central graduation with the opposite circle, after reversing of the

telescope. So the optical axis is levelled in respect to the benchmark at $\pm 0,1\text{mm}$. During this period, the other car's operator has chosen his station and at the same instant in the two vehicles (thanks to the radio) the observers begin to measure at each other, one of them (always the same) measures the distance first, and the other measures it at the end of the sequence (if operated simultaneously, the EDM interfere). Between that, two complete sets of readings ("Right circle", "Left circle") are made, and more if an internal discrepancy is noticed by the computer's checks. Then, station 1 sends to the other one (2) his observed denivelation and distance, which are compared with station 2's measurements while taking in account a model of refraction. Every computer conserves its own logs and prints them in order to save the data in case of failure of the magnetic recorder (cassette type).

The temperature and pressure are measured from time to time, depending on the value of the slopes. When the slope is important, a big care must be paid to meteorological data. We use classical barometers and thermometers, but it is easy to imagine automatic readings of electronic probes for this purpose.

It should be emphasized that distance measurements are quite critical data, and that in my opinion two EDM s are not a mere calculation ease, but a real necessity, as an error of distance is impossible to detect.

An other solution which may be possibly used is to send all the data of one station to the other, either by radio manually (but it is quite tedious and long), or automatically by a radio link via a modem, or via the infrared modulated light of the EDM, which is probably more sure. Commercial equipment using this facility exist but we did not test it.

RESULTS

The formula to compute precision we use is Vignal's formula : the probable kilometric error e.p.k is given (in mm) by :

$$\text{e.p.k.} = 2/3 \left[(\text{sum } (f^2 / K) / n) \right]^{1/2}$$

f = closure, n = number of closures, K = length of the loop or section in km.

1) We found that the e.p.k. is fairly modulable, depending on the maximum authorized distance between stations. For $D < 1500 \text{ m}$, $\text{e.p.k.} \approx 3 \text{ mm}$. For $D < 400 \text{ m}$, $\text{e.p.k.} \approx 1 \text{ mm}$. So we can optimize the cost by adjusting this maximum distance, which is quite interesting.

2) The speed is very dependant of the topography, but seems to be never really slower than Motorized Levelling 's one. It is very dependant of the density of benchmarks too. In France, we have commonly around 2 benchmarks by kilometer, so the operations are considerably slowered. In Africa (2 to 5 km between benchmarks) it is much more interesting, as well as in France in mountainous areas where the gains of time may be quite noticeable.

3) Our experiments of Nipremo have not been sufficient to prove it, but it seems that we have not to fear important systematism.

Up to now we could not detect any errors of this type and we have different reasons (Bahnert, 1980) to think that it is normal. The gradient of refraction index is in nearly all circumstances dominated by thermal gradients, and this is one of the principal sources of troubles in geometric levelling, as the thermal layers are generally parallel to the ground and not at all horizontal. In such a case of figure, which is very common, we find that the trigonometric levelling encounters a stable refractivity along the optical path, which is statistically in a single layer. So the radius of curvature of this ray has good chances to be constant, as stated in Eq.1, and the precision is limited by instruments only : The hypothesis necessary to get a proper precision is only that the light ray has a constant radius. We can notice the necessity for the same hypothesis for the validity of the "refraction-by-reflection" method (Angus-Leppan, 1983) imagined also to correct for the effect of refraction, so that it is not clear whether such a method can afford anything more compared to trigonometric levelling using reciprocal simultaneous zenithal measurements, for which some excellent instruments already exist.

4) The existence of fully electronic theodolites have opened the way to the realisation of a very exciting perspective : a completely impersonal manipulation of numeric values during all the different processings of the data observed. The observer has only the interesting job, the choice of the set-up sites, and the charge of aiming at the targets, and the electronics make automatically all the data readings, checks and storages which are, in classical methods, time consuming, tedious, and sources of plenty of mistakes. By conserving the methodology of geometric levelling, it appears as extremely hazardous to find a commercial solution permitting impersonal readings. Here, with trigonometric heighting, this can be made almost completely. The only data to be still read and manually introduced in the computer are the readings on the invar rod, but it seems mostly advisable to help the observer by using a vocal decoder able to understand numerical values and to drive the program.

5) With the two types of electronic stations we used, we experienced severe problems of static electricity that perturbed the links between the micro-computer and the theodolite. Sometimes this link was completely blocked, and serious attention must be paid to the earthings or groundings of cables, because the cars are not the ideal receptacles for high-impedance low-consuming electronic circuitry.

6) For overseas work it appears as extremely suitable to have a complete available equipment in case of failure of one of the components: topographic staffs have scarcely such problems with classical levelling. Here the technical sophistication is considerably higher than previously, and in my opinion a complementary complete electronic spare equipment must be considered as a necessity and taken in account when estimating the costs.

CONCLUSION

Methods like Nipremo have proved to be extremely suitable for modern levelling. If they need a correctly trained staff to work properly, as the technicity required has increased, the counterparts are the followings :

- Very interesting costs of production, modulable in consideration of the quality required.

- A precision compatible, if needed, with first-order requirements.

- The possibility of quasi-complete automatization of data transfers.

- An excellent security while working along the roads.

But some problems remain :

- All sorts of topographies are not equally suitable.

- The roads must be large enough to let two vehicles circulate easily.

- The equipment is complex and failures may be critical.

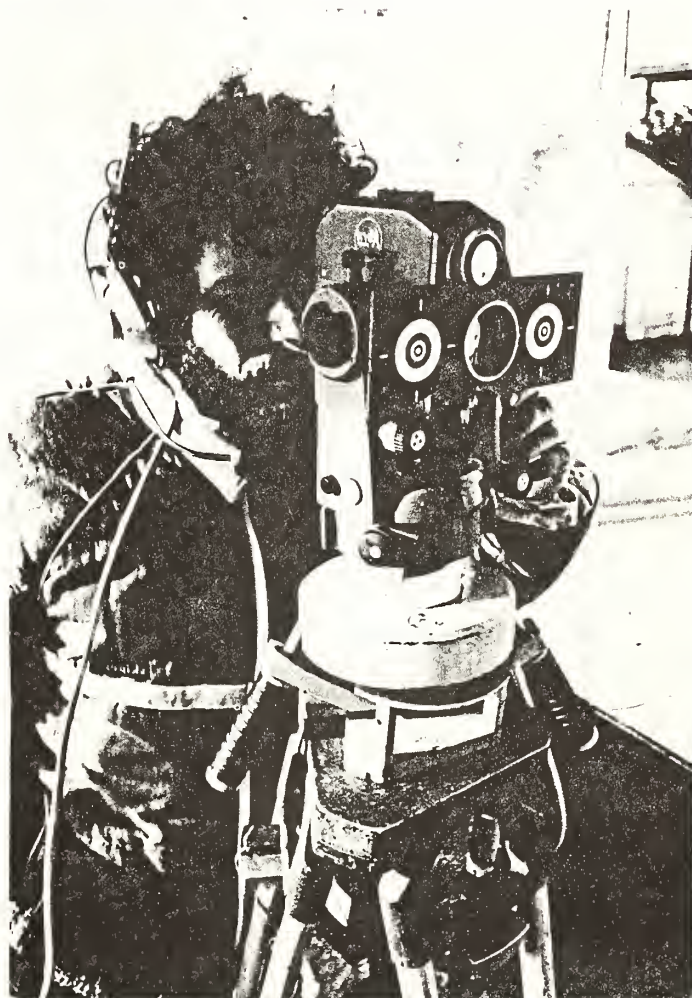
- The car used receives a very particular equipment and it is not easy to change the model, spare parts being not available everywhere in the world. But the equipped car may be used for classical Motorized Levelling too, if necessary.

It appears to us that Nipremo could be an excellent complement of Motorized Levelling, in mountains especially ; and we have tested the possibility of using it to get some data for profiling roads (in X.Y.Z) with a good success, which may signify that such a sophisticated equipment is anyway very versatile and multi-purposes !



Fig. 2 & 3

Showing the Kern equipment (E 1 and D M 502), the targets, the Zeiss fast set-up head, and the car fully equipped, during an intermediate station observation sequence. One can notice the quickly removable protections against wind and rain ; they let the team to operate even with rather bad weathers.



Bibliography :

- ANGUS-LEPPAN (1983). Preliminary study for a new levelling system, Aust. J. Geod. Photo. Surv. n° 39, pp. 69-81.
- BANHERT, G (1980). Die Genauigkeit langseitiger trigonometrischer Nivellements. Vermessungstechnik, Vol. 28, p. 312-314.
- KASSER M. (1982). Expérience de Nivellement trigonométrique Motorisé de Précision. Bulletin KERN n° 34 p. 8-10.
- KRATZCH (1979). Motorisierte Höhenzugmessung mit elektrooptischen Tachymetern. Vermessungswesen und Raumordnung, Vol. 41, p. 139-150.
- RUEGGER, J.M., BRUNNER, F.K. (1982) EDM-Height traversing versus geodetic levelling. The Canadian Surveyor, Vol 36, n° 1 p. 69-88.

TRIGONOMETRIC MOTORIZED LEVELING AT THE NATIONAL GEODETIC SURVEY

Charles T. Whalen
National Geodetic Survey
Charting and Geodetic Services
National Ocean Service, NOAA
Rockville, MD 20852

ABSTRACT. The National Geodetic Survey tested precise trigonometric motorized leveling in 1984-1985 for National Geodetic Vertical Network surveys. Two types of surveys were tested. The first survey used a single Wild T2000-DI5 system and a pair of leveling rods, each equipped with two targets and two small retroreflectors. Motorized leveling instrument/rod vehicles were used to transport the leveling rods for the November-December 1984 first-order, class I tests. The second survey used height transfers between a pair of Wild T2000 theodolites by simultaneous reciprocal zenith angles and slope distances measured with a Wild DI5. Motorized leveling instrument vehicles provided transport for the theodolites. Height transfers between bench marks and theodolites were made using zenith angles and slope distances measured from the instrument to two targets and reflectors on a leveling rod. Trigonometric motorized leveling with the T2000-DI5 met first-order standards for section and loop closures for vertical control surveys.

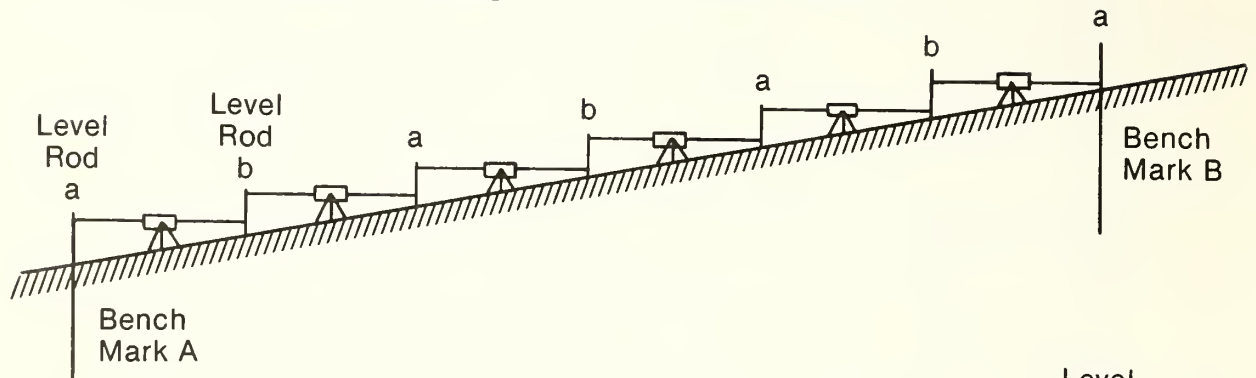
BACKGROUND

Compensator leveling surveys are plagued by systematic errors caused by refraction (Strange 1981, Holdahl 1982, Whalen and Strange 1983), magnetic effects (Rumpf and Meurisch 1981, Whalen 1984a) and by other errors. Survey progress is limited by horizontal sights, although production increases have been achieved by using motorized leveling techniques (Peschel 1974, Becker 1980, Poetzschke 1980, Whalen 1982). The ravages of inflation in the late 1970s and early 1980s spurred plans to decrease leveling costs, increase accuracy, and increase production by developing new leveling systems (Angus-Leppan 1983, Huff 1984). Developmental work has been done to increase production and reduce systematic error effects on leveling, using state-of-the-art equipment and trigonometric leveling by Rueger and Brunner (1981, 1982), Chrzanowski (1983), Kasser (1983, 1984). The advent of new theodolites with capabilities of measuring precise vertical angles produced by Wild Heerbrugg and Kern in Switzerland have increased interest in trigonometric leveling. Results of preliminary trigonometric leveling tests by the National Geodetic Survey (NGS) using the Wild T2000-DI5 system are reported in Whalen (1984b). Conventional and trigonometric leveling procedures used by NGS are shown in figure 1. This report covers first-order trigonometric leveling tests of the same system.

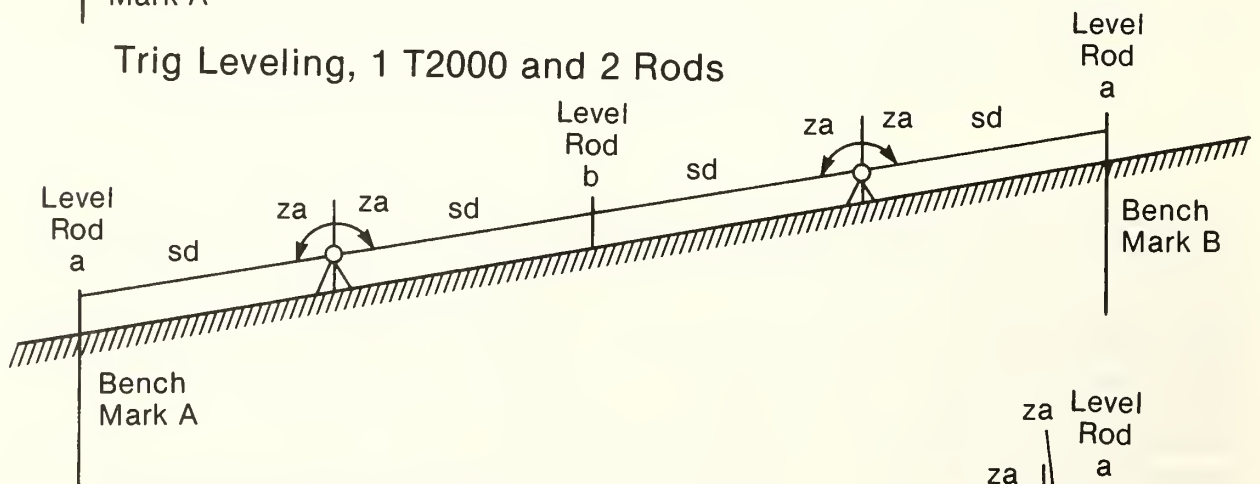
EQUIPMENT

NGS tested two types of first-order leveling surveys. The first survey used one Wild T2000-DI5 system (figs. 1 and 2) with three motorized leveling instrument/rod vehicles and two Kern 1/2-cm leveling rods (fig. 3). The instrument was mounted on a 2-meter tripod in the back of the observing vehicle.

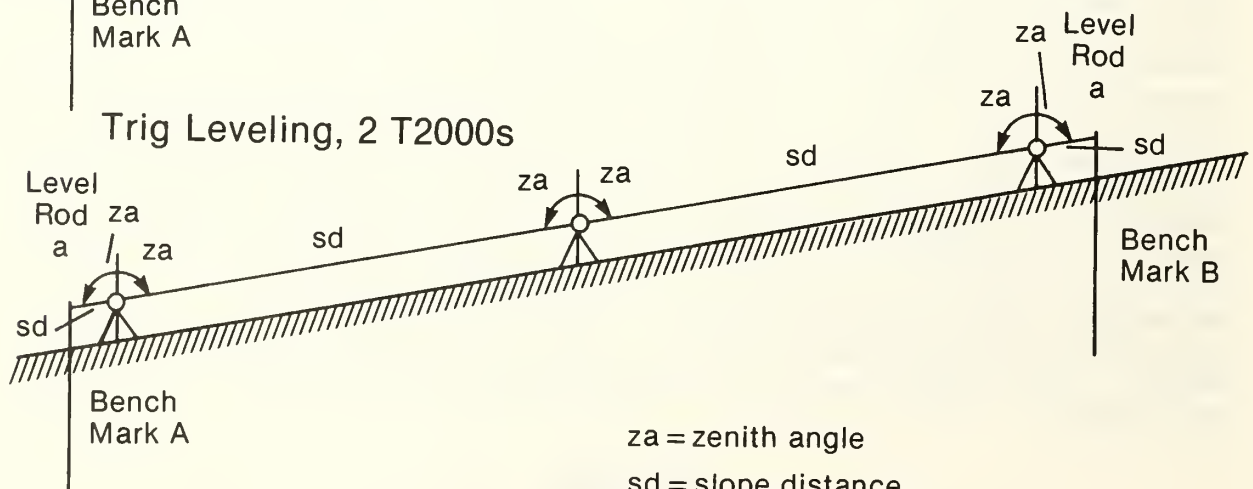
Conventional Leveling, 1 NI002 and 2 Rods



Trig Leveling, 1 T2000 and 2 Rods



Trig Leveling, 2 T2000s



za = zenith angle
sd = slope distance

Figure 1.--NGS conventional and trigonometric leveling.

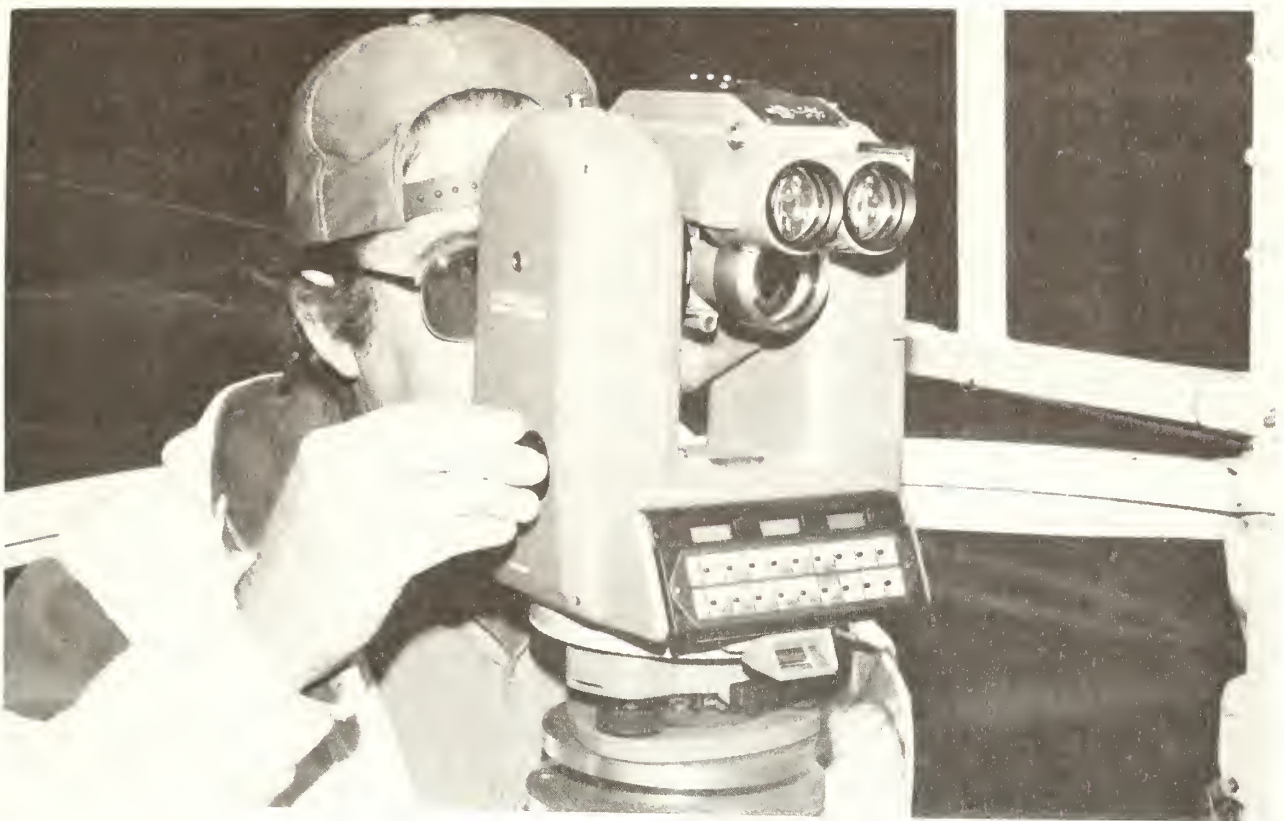


Figure 2.--Wild T2000-DI5 system.

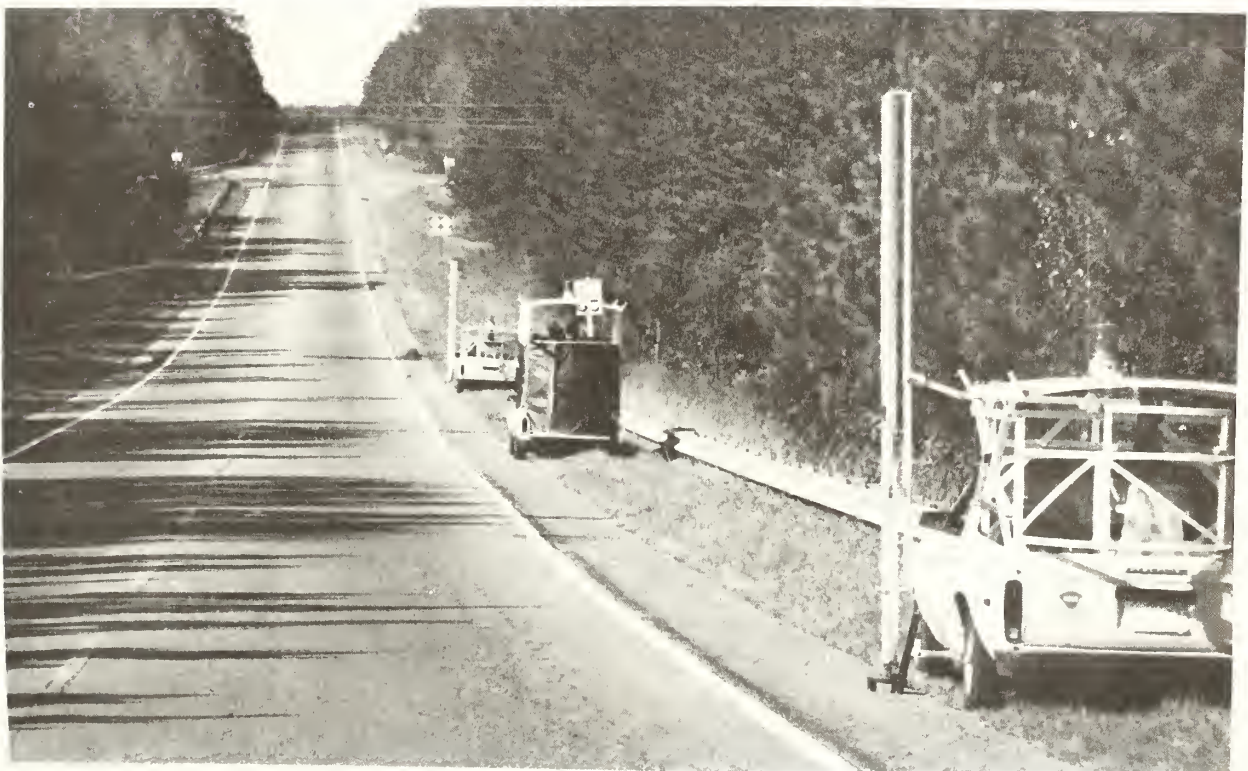


Figure 3.--Motorized trigonometric leveling with 1 T2000-DI5 system and 2 Kern $\frac{1}{2}$ -cm leveling rods.

The tripod legs passed through the floor of the vehicle to the ground. The vehicle is equipped with an electric powered hoist to raise the tripod and instrument for travel between instrument stations. Each rod was equipped with two peanut prisms (retroreflectors) attached to the rod frame, and two targets which were attached to the Invar band (figs. 4 and 5). A Radio Shack Model 100 computer was connected to the T2000-DI5 system via a Wild GIF2 RS232 unit and GIF7 logic adapter (fig. 6). An aspirated temperature probe was used to measure air temperature at the height of instrument at the beginning and end of each section, and a Wallace and Tiernan altimeter was used to measure altitude for air pressure calculations.

The second survey used a pair of Wild T2000-DI5 systems equipped with a target for measuring vertical angles and a peanut prism for measuring slope distance between instruments (figs. 1 and 7). The instruments were mounted on 2-meter tripods and transported between stations in the back of motorized leveling vehicles, as on the first survey. Recording equipment, temperature probes, and altimeters were the same as those used on the first survey.

SURVEYS

The survey test area is shown in figure 8. The cross line on route 636 was not leveled for this test. The loop passes from east to west through Fredericksburg, south along highway 1A, east on 17 bypass to highway 2, then northwest along highway 2 to Fredericksburg. Approximately one-third of the loop is located in urban and suburban Fredericksburg.

A four-man team conducted the first survey using one T2000-DI5 system and two leveling rods. The survey began on November 8 and was completed on December 6, 1984. The weather was generally favorable for surveying, with temperatures varying from -2 to 19 degrees Celsius. The second survey was made by a two-man team observing simultaneous reciprocal zenith angles and distances between a pair of T2000-DI5s. The survey started on December 12, 1984 and ended on February 25, 1985. Temperatures varied from -4 to 22 degrees Celsius. Observing conditions were generally less favorable than on the first survey because of snow and sleet.

SURVEY PROCEDURES

One Instrument and Two Rods

Start of Day

The observer turns on the GIF2 RS232 interface unit and enters the file name, height of instrument, and time zone into the computer. The computer records the date, time, and initializes the T2000 to turn off automatically after recording each set, sets decimal degree mode, DI5 mode, zero prism additive constant, and zero prism scale correction. These last two items are applied by the computer instead of by the T2000.

Start of Section

The observer's initials, wind code, sun code, air temperature at height of instrument, elevation from the altimeter, bench mark survey point serial number (SPSN), bench mark stamping or name, and rod at the bench mark (1 or 2) are keyed into the computer. The computer records the time.

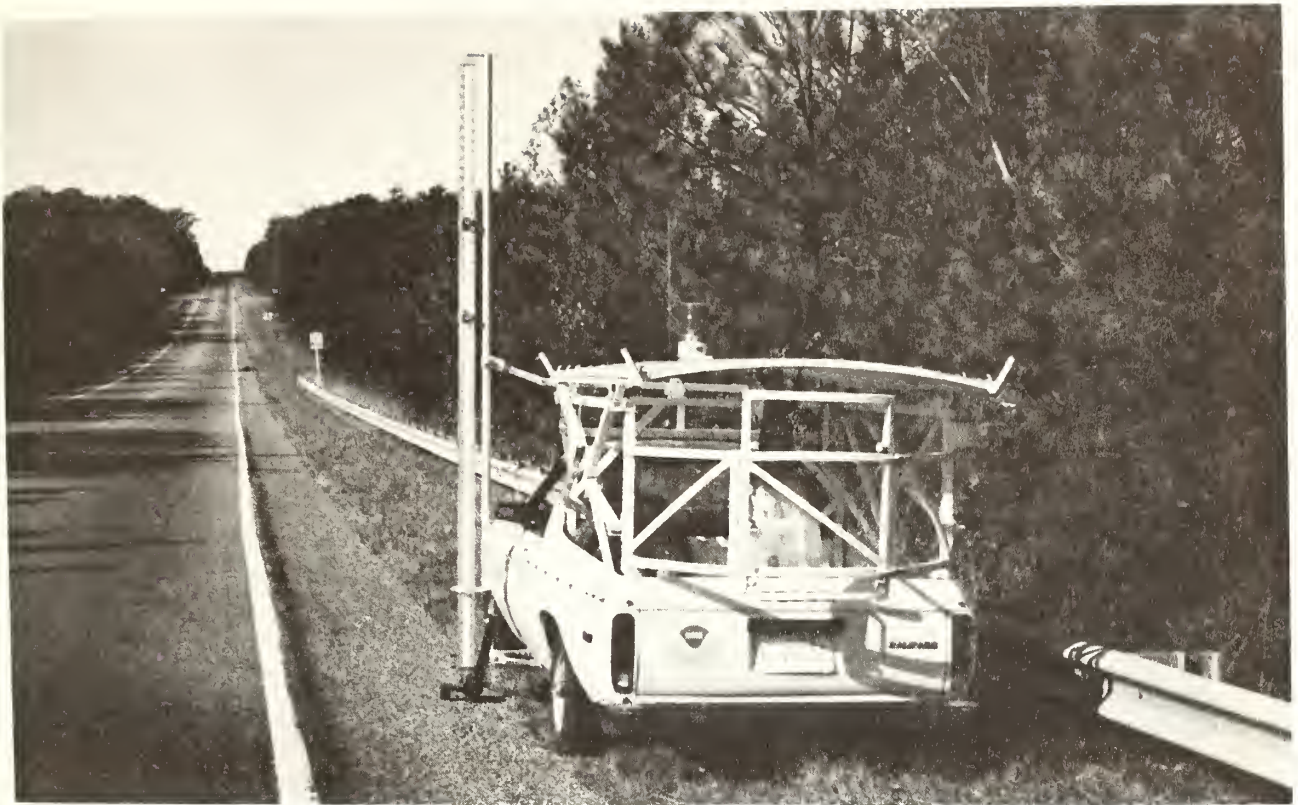


Figure 4.--Kern $\frac{1}{2}$ -cm leveling rod with 2 peanut prisms and targets.



Figure 5.--Peanut prism and rod target.



Figure 6.--Radio Shack Model 100 computer, temperature display with switches for temperature probes and tripod lift, and Wild GIF2 RS232 interface unit with GIF7 logic adapter.



Figure 7.--Wild T2000-DI5 system with vertical angle target, and peanut prism (below telescope).

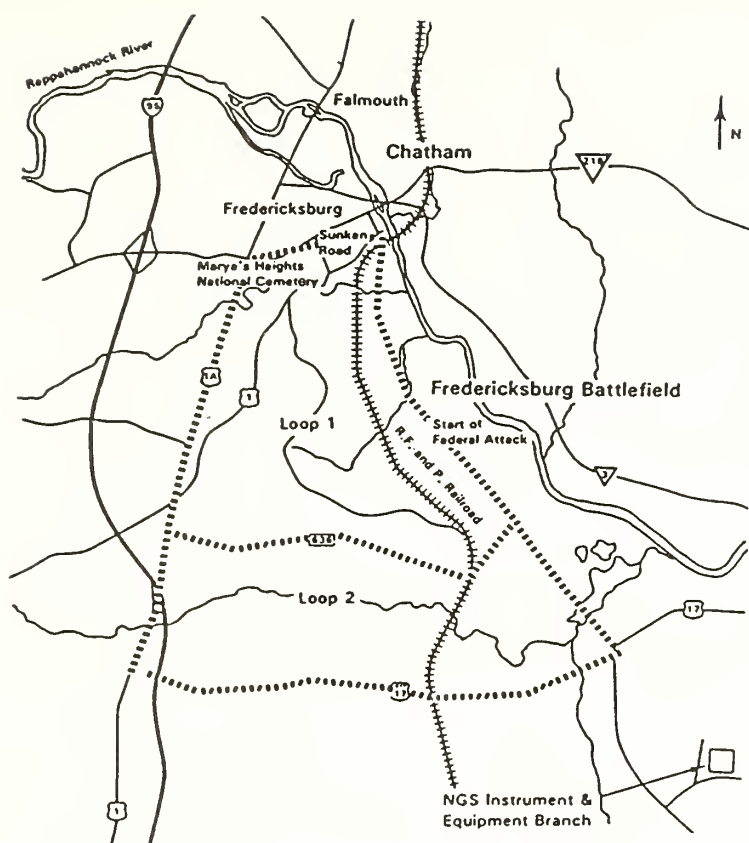


Figure 8.--Motorized leveling test area, Fredericksburg, Virginia.

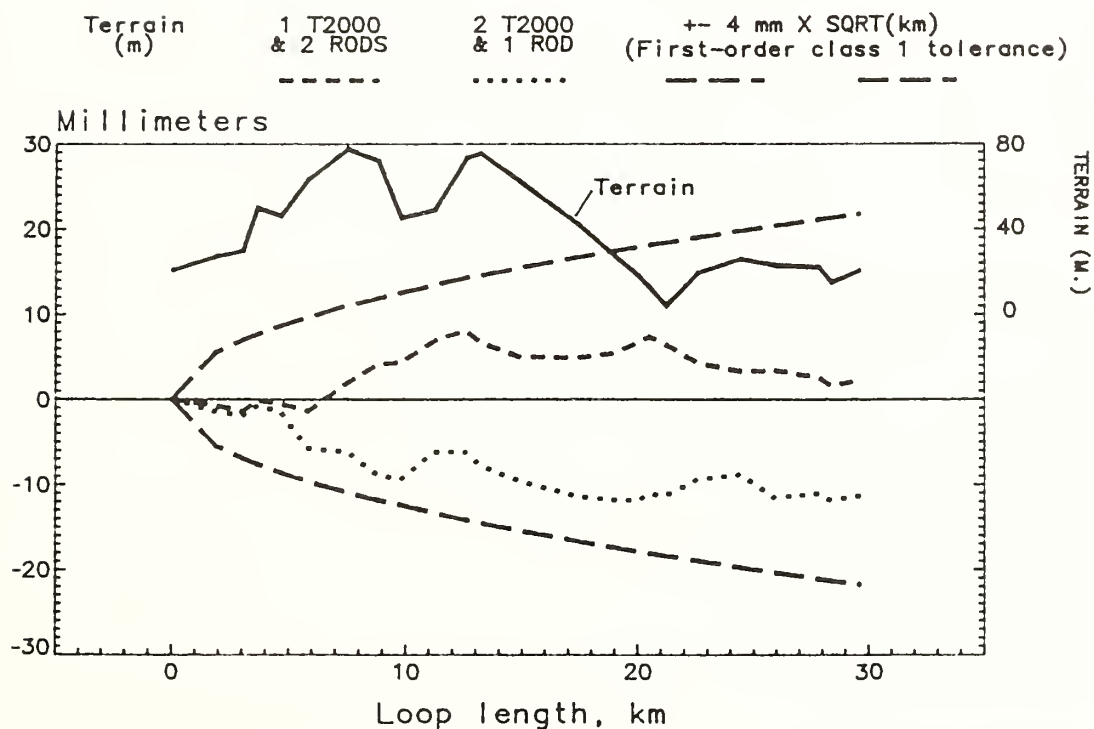


Figure 9.--Profile of trigonometric leveling elevations minus mean elevations from three NI002 surveys, with elevations and first-order, class I loop closure tolerances.

Instrument Station Observations

The observer aligns the instrument horizontal crosshair with a vertical rod target and the vertical crosshair with the center of the peanut prism, then presses the record key on the computer. The computer turns on the T2000-DI5, tells it to record the zenith angle and slope distance and downloads these items. The instrument turns itself off. The observing sequence is: back-sight, top prism and target, direct; foresight, top prism and target, direct (if sight distances and sight distance imbalance are within tolerances, continue, otherwise move instrument or forward rod to adjust distances and restart observations); foresight, bottom prism and target, reverse; and back-sight, bottom prism and target, reverse.

Two elevation differences are computed between rod supports, one from direct and one from reverse observations (appendix). If the difference between the elevation differences is within the tolerance limit, the instrument is moved to the next station. Otherwise, the station is reobserved.

End of Section

The observer enters the temperature, bench mark survey point serial number (SPSN), and bench mark name or stamping into the computer. The computer records the time and displays the section elevation difference and length.

Double Simultaneous Reciprocal Zenith Angles and Slope Distances

The start of day and start of section procedures are as above (one instrument and two rods.)

Bench Mark Tie

Pointing and recording are made as above. The observing sequence is: top (rod prism and target, direct; bottom prism and target, direct; top prism and target, reverse; and bottom prism and target, reverse. Two elevation differences are computed between the bench mark and the horizontal crosshair of the instrument from the two observations to the top and bottom prisms and targets (appendix). If the two elevation differences agree within 0.75 mm they are accepted. Otherwise, they are rejected and the observations are repeated.

Reciprocal Observations Between Instruments

Each observer aligns the horizontal crosshair of his instrument with the vertical target on the side of the other instrument and the vertical cross hair with the peanut prism on the other instrument and presses a computer key to record. The computer turns on the T2000-DI5, tells it to record the zenith angle and slope distance (direct only) and downloads the data. The instrument turns itself off. The observing sequence for each set of observations is: instrument 1 direct, instrument 2 reverse; instrument 1 reverse, instrument 2 direct. The peanut prism is attached below the telescope, opposite the DI5 (fig. 7). By observing with one instrument direct and the other reverse, the DI5 of the direct instrument is aligned with the peanut prism of the other instrument when the telescopes are mutually aligned. The slope distance is observed with the instrument in direct only, to avoid interference between DI5 signals from the two instruments. When one DI5 observes slope distance, the

optics of the other DI5 are covered to avoid reflecting the EDM signal.

On completion of the first distance measurement, the computer calculates and displays the number of observations required based on the distance, and Federal Geodetic Control Committee (FGCC) section misclosure tolerance for the order, and class of survey (appendix, eq. 14). After sufficient observations have been made the computer starts an iterative rejection routine which computes the mean elevation difference, checks the maximum (unrejected) residual from the mean against a tolerance limit and rejects the corresponding observation if the residual exceeds the tolerance. The tolerance limit is based on the number of observations in the sample, the standard error (from previous tests), and a five percent test level using procedures given in Halperin et al, (1955) and in Whalen (1977). The special case is used where the standard error is known, but the mean is not known. If sufficient (unrejected) observations remain, a new mean is computed and the next largest residual is checked against the tolerance. The cycle is repeated until either a sufficient number of observations remain and there are no more rejections, or until too few observations remain and the computer displays a message asking for another set of observations.

When the next bench mark is reached, a bench mark tie is made, as above, and the end of section items (see one instrument and two rods above) are recorded.

DATA PROCESSING

Trigonometric leveling observations were transferred from the Radio Shack Model 100 computer to a cassette at the end of each work day. Periodically, the data were reloaded into a Model 100 computer, transferred to an Osborne Model 1 computer, and stored on floppy disks. Field book pages were generated on the Osborne computer and listed on a Hewlett Packard Thinkjet printer. Vertical control records in prescribed format (Pfeifer and Morrison 1982) were assembled with the Osborne for the NGS data base stored on floppy disks, and transferred to the data base on completion of the tests.

Test software was written in Microsoft BASIC for the Model 100 computer, and in Microsoft BASIC or CBASIC (compiled BASIC) for the Osborne Model 1. The Model 100 Microsoft BASIC uses double precision computations (14 significant digits), as does the CBASIC used on the Osborne. The Osborne Microsoft BASIC uses single precision computations (7 digits internally, and 6 significant digits for listings). The Model 100 computer has a built-in clock with day, date, and time functions, a built-in modem, and a text editing system which can be used to modify BASIC programs.

TEST RESULTS

The two motorized trigonometric leveling surveys are compared with earlier motorized NI002 surveys of the test loop in table 1. The trigonometric survey that used simultaneous reciprocal zenith angles and slope distances between a pair of T2000-DI5 systems gave the highest average production rate in kilometers per staffhour. The survey which used one T2000-DI5 system and two leveling rods gave the lowest production rate.

The standard error of the mean of a forward and a backward running between bench marks separated by 1 kilometer is 0.76 mm for first-order, class I surveys and 1.02 mm for first-order, class II surveys, assuming the FGCC

(1984) tolerances for the differences between such runnings, ± 3 mm and ± 4 mm respectively, are based on a five percent test level (1.96 sigma). The standard errors of the mean of a forward and backward run section, shown in table 1, were determined from least squares adjustments of the surveys. The standard errors of the mean from two Swedish surveys, the NGS NI002 survey, and the NGS survey with one T2000-DI5 and two rods were all within the ± 0.76 mm value for first-order, class I surveys given above. The NGS NI002 survey was run with first-order, class II specifications. The NGS survey, which used two T2000-DI5 systems, had a standard error that was within the first-order, class II value. The survey failed to meet the first-order, class I standard because the writer inadvertently omitted the -22.66 constant in equation 14 (appendix) when writing the recording program. The constants corrects for the uncertainty in the bench mark ties, ± 0.2 mm. Thus the number of observations required to meet first-order, class I specifications was underestimated. Note that the survey had nine rejects. The large number of rejections is believed to be associated with observations on icy roads with positive temperature gradients.

Table 1. Comparison of first-order trigonometric and conventional motorized leveling surveys on the Fredericksburg, Virginia, test loop.

	Swedes NI002 1981 No. 1	Swedes NI002 1981 No. 2	NGS NI002 1983	NGS 1 T2000 -DI5 2 rods	NGS 2 T2000 -DI5 1 rod
Averages:					
km/manhour	0.47	0.47	0.38	0.24	0.50
sets/manhour	6.59	7.03	5.29	2.82	3.35
sets/km	14.1	14.9	13.8	11.8	6.8
meters/set	71	67	73	85	148
minutes/set	2.3	2.1	2.8	5.3	8.9
Standard error of mean					
double run, \pm mm/km	0.42	0.73	0.75	0.66	1.00
degrees of freedom	25	29	24	23	24
number of rejects	0	0	0	1	9
Vertical movement, mm/hour	+0.55	+0.18	-0.35	-0.20	-0.10
standard error, \pm mm/hour	0.14	0.24	0.11	0.11	0.18
30 km loop closure, mm	0.09	1.96	-1.59	-2.10	11.48

The least squares adjustments solved for corrections to preliminary elevations, and for the vertical movement rates shown near the bottom of table 1. The movement rate for the first Swedish survey, which is 3.9 times its standard error, is significant at the 1 percent test level using a Student's t-test. None of the movement rates for the other surveys can be considered significant. Sleet, snow, rain, and high winds occurred during the first Swedish survey and may have contributed to the vertical movement rate for that survey. In spite of the bad survey conditions, that survey had the smallest standard error of the mean of the five surveys.

The first-order, class I loop closure tolerance for the 30-kilometer loop is 22 mm. All of the five surveys closed within the tolerance.

Differences between elevations from the two first-order, NGS trigonometric

leveling surveys and mean elevations from the three NIO02 surveys are shown versus survey distance in figure 9. First-order, class I tolerances for loop closures, $4 \text{ mm} \times \sqrt{\text{loop distance in kilometers}}$, and elevations are also shown. Elevation differences for both both surveys remain within the tolerance limits.

SUMMARY

NGS conducted first-order, motorized trigonometric leveling tests over a 30-km test loop in the vicinity of Fredericksburg, Virginia, between November 8, 1984 and February 25, 1985. Two types of surveys were tested. The first survey used a four-man team with one Wild T2000-DI5 theodolite-EDM system and two leveling rods, each equipped with two peanut prisms and two targets mounted on the Invar band. Sight distances were limited to 54.5 meters and sight imbalances to 2 meters. The survey met first-order, class I tolerances for section and loop closures. Survey progress was 0.24 km per man-hour.

The second survey used one of the above mentioned leveling rods for height transfers between the instrument and bench marks. The two-man team observed simultaneous reciprocal zenith angles and slope distances between a pair of Wild T2000-DI5 systems. Each instrument was equipped with a target for zenith angles measurements and a peanut prism for slope distance measurements. Survey results failed to meet first-order, class I standards, and were classified as first-order, class II, because the number of observations required was underestimated (see TEST RESULTS). Survey progress was 0.50 km per manhour, the highest of all first-order surveys of the test loop. The system is capable of meeting first-order, class I standards with a slight increase in the number of observations between instruments.

A two-man motorized team observing reciprocal zenith angles and slope distances between a pair of T2000-DI5 systems can achieve production rates in kilometers per manhour, which are comparable to those from motorized NIO02 leveling surveys over relatively flat terrain. The production rates for this system should remain constant in rolling and mountainous terrain where NIO02 motorized production rates would substantially decrease because of shortened sight distances.

RECOMMENDATIONS

The recording program for observations with one T2000-DI5 and two rods should be modified to calculate the number of elevation differences needed versus sight distance. The modification would give the observer more flexibility on sight distances. The Halperin rejection routine should be added to the program. The rod targets should be increased in size to permit longer sight distances for lower-order surveys.

Both systems should be tested in the mountains using double-run, first-order, class II surveys. The system which uses observations between a pair of T2000-DI5s should also be tested for river crossings. The temperature gradient should be calculated from air temperatures observed 1 meter above and 1 meter below the height of instrument, at least at the start of each section, for both types of surveys. Observations should be avoided when positive temperature gradients occur with no wind. Air "bubbles" associated with such conditions can cause large apparent vertical offsets of the target which result in large systematic errors in leveling, for long sight distances.

REFERENCES

- Angus-Leppan, P. V. 1983: Preliminary study for a new levelling system. Australian Journal of Geodesy, Photogrammetry, and Surveying, No. 39, pp. 69-81.
- Becker, J. M. 1980: Le nivellement motorise en Suede, Techniques et resultats a ce jour. Proceedings of the Second International Symposium on Problems Related to the Redefinition of the North American Vertical Geodetic Networks, Canadian Institute of Surveying, Ottawa, pp. 847-866.
- Chrzanowski, A. 1983: Economization of vertical control surveys in hilly areas by using modified trigonometric levelling. Technical Papers, 43rd ACSM Spring Convention, pp. 635-644.
- Federal Geodetic Control Committee (FGCC) 1984: Standards and Specifications for Geodetic Control Networks. National Oceanic and Atmospheric Administration, NOS/National Geodetic Information Center, Rockville, MD. 20852, 46 pp.
- Fronczek, C. J. 1977: Use of calibration base lines. NOAA Technical Memorandum NOS NGS-10, National Oceanic and Atmospheric Administration, NOS/National Geodetic Information Center, Rockville, Md. 20852, 38 pp.
- Halperin, M., S. W. Greenhouse, J. Cornfield and J. Zalokar 1955: Tables of percentage points for the Studentized maximum absolute deviate in normal samples. J. Amer. Stat. Assoc. No. 50, pp. 185-195.
- Holdahl, S. R. 1982: Recomputation of vertical crustal motions near Palmdale, California, 1959-1975. J. Geophys. Res., Vol. 87, No. B11, pp. 9374-9388.
- Huff, L. C. 1984: A new rapid precision leveling system. EOS Vol. 65, No. 45.
- Kasser, M. 1983: Essais de nivellement indirect de précision motorisé (NIPREMO). Bulletin d'Information, Institut Geographique National, Paris, No. 47, pp. 21-25.
- Kasser, M. 1984: Une méthode d'avenir, le Nivellement Indirect de Précision Motorisé (NIPREMO). Bulletin d'Information, Institut Geographique National, Paris, No. 84/2, pp. 45-46.
- Peschel, H. 1974: Das motorisierte prazisionsnivellement leistungsfahigstes verfahren genauer hohennmessungen. Vermessungstechnik, Berlin, pp. 57-64.
- Pfeifer, L. and N. L. Morrison 1982: Input formats and specifications of the National Geodetic Survey data base, volume II, vertical control data. Federal Geodetic Control Committee (FGCC) National Oceanic and Atmospheric Administration, NOS/National Geodetic Information Center, Rockville, MD. 20852, 46 pp.
- Poetzschke, H. 1980: Motorized leveling at the National Geodetic Survey. NOAA Technical Memorandum NOS NGS-26, National Oceanic and Atmospheric Administration, NOS/National Geodetic Information Center, Rockville, Md. 20852, 17 pp.

- Rueger, J. M. and F. K. Brunner 1982: EDM-height traversing versus geodetic leveling. The Canadian Surveyor, Vol. 36, No. 1, pp. 69-88.
- Rueger, J. M. and F. K. Brunner 1981: Practical results of EDM-height traversing. The Australian Surveyor, Vol. 30, No. 6, pp. 363-372.
- Rumpf, W. E. and H. Meurisch 1981: Systematische anderungen der ziellinie eines prazisions Kompensator nivelliers - insbesondere des Zeiss Ni 1 durch magnetische gleich und wechselfelder. XVI International FIG Congress, Montreux, Switzerland.
- Strange, W. E. 1981: The impact of refraction corrections on leveling interpretations in California. J. Geophys. Res., Vol 86, No. B4, pp. 2809-
- Whalen, C. T. 1984a: Preliminary test results: Automatic level affected by magnetic fields. ACSM Bulletin, No. 89, pp. 17, 31.
- Whalen, C. T. 1984b: Preliminary test results of precise trig-leveling with the Wild T2000-DI5 system. ACSM Bulletin, No. 93, pp. 15-18.
- Whalen, C. T. and W. E. Strange 1983: The 1981 Saugus to Palmdale, California, leveling refraction test. NOAA Technical Report NOS 98 NGS 27, National Oceanic and Atmospheric Administration, NOS/National Geodetic Information Center, Rockville, Md. 20852, 13 pp.
- Whalen, C. T. 1982: A United States test of the Swedish motorized leveling system. Proceedings of the Second Technology Exchange Week, ASP - Panama and Central American Region, Drawer 934, APO Miami 34004, pp. 292-304.
- Whalen, C. T. 1977: Analysis of rejection procedures. Unpub. report DO-72-02, Defense Mapping Agency H/TC Geodetic Survey Squadron, Francis E. Warren AFB, Wyoming 82001, 44 pp.

Mention of a commercial company or product does not constitute an endorsement by the National Oceanic and Atmospheric Administration. Use for publicity or advertising purposes of information from this publication concerning proprietary products or the tests of such products is not authorized.

APPENDIX -- Equations

Bench Mark Ties or Leveling With One Instrument and Two Rods.

Corrected slope distance (length units in meters), S

$$S = L(1+\text{ppm}) - SP/\tan(Z) + OC + PC/\sin(Z) \quad (1)$$

where L is the observed slope distance, ppm (see below) is the parts per million scale correction from the EDM calibration, SP is the separation between EDM and theodolite sight paths, Z is the mean zenith angle to the target, OC is the EDM offset correction and PC is the horizontal prism offset from the target surface.

Horizontal distance from the instrument to the target, X

$$X = S \sin(Z) \quad (2)$$

Elevation difference from instrument to target, Y

$$Y = S \cos(Z) \quad (3)$$

Elevation difference between instrument and bench mark or turning point, H

$$H = RT - (Y + (1-K)X^2/2R) \quad (4)$$

where RT is the meter value of the rod target height, K is the coefficient of refraction (0.13 assumed), X is from (2), and R is the earth's radius (6,371,000 meters assumed).

Reciprocal Zenith Angles and Slope Distances.

Corrected slope distance (length units in meters), S

$$S = (L^2 - (SM-SP)^2)^{\frac{1}{2}} (1+\text{ppm}) + OC + PC \quad (5)$$

where S, L, SP, ppm, OC and PC are as above and SM is the separation between the prism and crosshairs of the theodolite.

Horizontal distance between theodolite and target, (2) above.

Elevation difference between instrument and target, H

$$H = Y + (1-K)X^2/2R \quad (6)$$

with terms as described above.

Mean elevation difference between instruments, H'

$$H' = (H_f - H_b)/2 \quad (7)$$

where H_f is the foresight elevation difference and H_b is the backsight elevation difference, from (6) above.

Scale Correction, ppm. (Fronczek 1977)

$$\text{ppm} = (282.94 - (105.67/(273.15 + \text{TE}))P - \text{WV} - \text{RS})10^{-6} \quad (8)$$

where TE is the air temperature at height of instrument in degrees celsius, P is the pressure in mm of Hg, WV is the water vapor correction in ppm (assumed 0.4), and RS is the prism scale correction, and

$$P = 25.4e^{(3.3978 - (\text{AL} - \text{SL})3.6792 \times 10^{-5})} \quad (9)$$

where AL is the altimeter reading in feet at the start of the section and SL is the altimeter reading at sea level, in feet (1000 for the altimeter used).

Variance of ddh, mm.

The variance of the difference between two elevation differences (ddh) observed between two rods (A) using one theodolite and two leveling rods with targets and prisms, or between two instruments (B) with simultaneous reciprocal zenith angles (direct and reverse pointings) and slope distances is:

$$\text{Variance of ddh} = aX^b \quad (10)$$

where "a" and "b" are constants determined from earlier trigonometric leveling observations on the Fredericksburg test loop and on a leveling line from Fredericksburg to Orange, Virginia. For observations with one instrument and two rods (A) and for simultaneous reciprocal zenith angles and slope distances between instruments (B) the constants are:

$$a_A = 8.085 \times 10^{-6}$$

$$b_A = 2.2073$$

$$a_B = 6.723 \times 10^{-6}$$

$$b_B = 2.2926$$

The standard error of the mean of two elevation differences determined between an instrument and a bench mark is 0.2 mm, for the surveys with two instruments. The "a" constants were increased by 5 percent to allow for other error sources, and used to derive the equations given below.

Maximum Observing Distance, X.

$$X_A = (30.66nF^2)^{0.828} \quad (11)$$

Where X is the maximum observing distance between leveling rods (A), n is the number of observed elevation differences, and F is the FGCC tolerance on disagreement between forward and backward runnings between bench marks in mm, per kilometer. An elevation difference is based on the mean of direct and reverse pointings, and a slope distance measurement, to a foresight and a backsight rod target.

$$X_B = [n(36.87F^2 - 22.66)]^{0.774} \quad (12)$$

where X is the maximum observing distance between instruments (B), from simultaneous reciprocal observations, n and F as in (11) above. An observed elevation difference is based on the mean of elevation differences observed from each instrument, to the other instrument, using a direct and reverse pointing and a slope distance.

Number of Acceptable Observations Required, n.

$$n_A = X^{1.208} / (30.66F^2) \quad (13)$$

$$n_B = X^{1.292} / (36.87F^2 - 22.66) \quad (14)$$

where A, B, X and F are as above.

APPLICATIONS AND LIMITATIONS OF PRECISE
TRIGONOMETRIC HEIGHT TRAVERSING

A. Chrzanowski, T. Greening, W. Kornacki,
J. Secord, S. Vamosi* and Y.Q. Chen**

Department of Surveying Engineering
University of New Brunswick
Fredericton, N.B., E3B 5A3 CANADA

* Geodetic Survey of Canada, 615 Booth St., Ottawa K1A 0E9

** on leave from the Wuhan Technical Univ. of Surveying and Mapping, Wuhan,
P.R. China

ABSTRACT. Three years of test surveys at the University of New Brunswick with trigonometric height traversing have led to the conclusion that a standard deviation $\sigma \leq 2 \text{ mm}/\sqrt{\text{km}}$ can be achieved at an easily attainable speed of at least 10 km per day regardless of the inclination of the terrain when using precision electronic theodolites such as Kern E2 or Wild T2000 and limiting the lines of sight to not exceed 200 m for the leap-frog method and 250 m for the simultaneous reciprocal measurements. A computer simulated height determination along a 80 km long undulating highway subjected to simulated effects of refraction indicated that the cumulative influence of refraction becomes random after long distances.

INTRODUCTION

As already discussed by many authors, the low speed and systematic errors of geometric levelling with its horizontal lines of sight are reason enough for trying to replace geometric levelling by a trigonometric method with measured slope distances and vertical angles using either a reciprocal or leap-frog (balanced sights to targetted rods) mode of field operation. The targets in trigonometric height traversing can always be placed at the same height above the ground. Thus, the lengths of sight are not limited by the inclination of the terrain and the systematic errors from refraction are expected to become random because the back- and fore-sight lines pass through the same or similar layers of air when traversing along long slopes. By extending the lengths of sight to a few hundred metres, the number of set-ups per kilometre is minimized. This reduces the accumulation of errors due to the sinking of the instrumentation - another significant source of systematic error in geometric levelling.

Until 1982, most of the studies on the replacement of geometric levelling by trigonometric height traversing reported standard errors larger than $4 \text{ mm}/\sqrt{\text{km}}$, thus placing it in the realm of third-order or lower accuracy. For example, Overton [1974] reported $16 \text{ mm}/\sqrt{\text{km}}$ with lengths of sight between 200 m and 830 m; Blasek and Hradilek [1979] obtained a standard error of about $5 \text{ mm}/\sqrt{\text{km}}$, with leg lengths between 200 m and 300 m; and Rueger and Brunner [1981] reported $4.3 \text{ mm}/\sqrt{\text{km}}$, with average sighting distances of 310 m. Kratzsch [1979] at the Technical University in West Berlin reported use of the Kern DKM2-A/DM500 system in two modes of operation: with reciprocal zenith angle measurement and with a leap-frog method. In both cases standard deviations between $3.7 \text{ mm}/\sqrt{\text{km}}$ and $4.2 \text{ mm}/\sqrt{\text{km}}$ were obtained on a 6 km test line using 200 m long lines of sight with

a claimed 1.7 km/h speed for the leap-frog method.

In the last three years extensive tests on trigonometric height traversing have been carried out at the National Geographic Institute (IGN) in Paris. Their tests included about 160 km of traversing and utilized a fully motorized reciprocal method with Kern DKM2-A/DM502 instruments. They reported [Kasser 1983] a 5 mm/ $\sqrt{\text{km}}$ standard deviation with lengths of sight averaging 600 m at a speed of about 4.5 km/h. Their latest tests [personal communication, Kasser, 1984] have included electronic theodolites Kern E2 and Wild T2000 and claim a standard deviation of 2 mm/ $\sqrt{\text{km}}$ with lengths of sight up to 700 m and speed up to 6 km/h - under the optimal conditions of flat terrain under overcast skies in winter.

Very recently, the U.S. National Geodetic Survey has also become involved with trigonometric height traversing. No details on their studies have been available to the authors except in an abstract of a paper by Whalen [1984] in which the second order, class I (U.S. specifications) accuracy was claimed on a 38 km test line using the Wild T2000/DI5 system in both reciprocal and leap-frog modes of operation.

In 1982 the Department of Surveying Engineering at the University of New Brunswick (UNB) initiated research activity in precision trigonometric height traversing under sponsorship by the Natural Sciences and Engineering Research Council of Canada and the Department of Energy, Mines and Resources. The programme concentrates on randomization of systematic errors, particularly of the effects of refraction, with a study on achieving the first order accuracy ($\sigma \leq 1.4 \text{ mm}/\sqrt{\text{km}}$) without the accumulation of systematic errors at a speed higher than the present geometric levelling techniques. A full automation of the field procedures is being investigated.

Field tests of trigonometric height traversing have included both the multi-target leap-frog [Chrzanowski, 1983] and reciprocal methods with the Kern DKM2A/DM502, Kern E2/DM503 and Wild T2000/DI5 measuring systems.

Preliminary results of the first two years of the investigations have been discussed in detail in Chrzanowski [1984] and Greening [1985].

Due to the limited space only a summary and conclusions of current results are given in this paper.

THE THEORETICALLY ACHIEVABLE ACCURACY OF TRIGONOMETRIC HEIGHT TRAVERSING

Two basic types of trigonometric height traversing have been distinguished in the accuracy analysis:

- Traversing with reciprocal measurement of vertical angles
- Leap-frog traversing with balanced backward and forward lengths of sight.

For the purposes of error analysis, the same basic mathematical model for the calculation of the height differences between the theodolite and the target can be used in both cases:

$$\Delta h = s \tan \alpha + c \quad (1)$$

where s is the reduced horizontal distance

α is the vertical angle

c is a term encompassing all the geometrical, refraction, and calibration corrections.

In order to make the leap-frog method compatible with the reciprocal traversing it is assumed that the same distance s between the theodolite and the targets and between two theodolites is used in both cases and that the total number of sets of angle measurements is also the same. This way, the results of the analysis which follows will be applicable for both modes of trigonometric traversing without any further differentiation between the two methods, as far as the influence of random errors is concerned.

Applying the rules of the propagation of variances into equation (1) and assuming that the observations at each station are uncorrelated we can write:

$$\sigma_{\Delta h}^2 = \sigma_s^2 \tan^2 \alpha + \sigma_\alpha^2 \frac{s^2}{\cos^4 \alpha} + \sigma_c^2 . \quad (2)$$

For a traverse consisting of n lines the variance of the total height difference Δh will be:

$$\sigma_{\Delta H}^2 = n \sigma_{\Delta h}^2 \quad (3)$$

thus assuming a random influence of all sources of errors. A possible systematic accumulation of some errors, particularly from refraction is discussed in the next section.

A detailed evaluation of the three basic sources of errors in eqn. (2) is discussed in Chrzanowski [1984] and Greening [1985]. The discussion led to the conclusions which follow.

Standard deviations of $\sigma_s = \pm 4$ mm could be attributed to the measurements of distances to a few hundred metres using the short range EDM such as the DM502, DM503 or DI4 or DI5, with proper calibration of the instruments.

Use of a single second optical theodolite with vertical circle compensation and appropriately designed targets and with lengths of sight to a few hundred metres would allow the vertical angle measurements to have standard deviations of $\sigma_\alpha = \pm 0.7''$ if 9 sets were taken. Precision electronic theodolites, such as the E2 or T2000, would attain $\sigma_\alpha = \pm 0.5''$ in 4 sets.

In the errors associated with the c component of eqn. (1) the following sources were considered: residual effects of refraction, sinking of tripods and/or rods, thermal expansion corrections and verticality of the rods (leap-frog method), and offset corrections for the targets and reflectors. Assuming that the major part of the influence of refraction is removed by the trigonometric method itself, only 0.2 mm allowance per each line of sight was given for the residual error of refraction over distances of few hundred metres with a total $\sigma_c = 0.3$ mm assuming that the offset corrections, verticality of rods and other geometrical corrections can be controlled to about 0.1 mm each.

By placing the above basic error components into eqns. (2) and (3) the theoretically estimated standard deviations of trigonometric height traversing per one kilometre distance were obtained as listed in Table 1 for various inclinations of the traverse routes and for two groups of instrumentation: a) when using the optical 1" theodolites and b) when using the precision electronic theodolites.

TABLE 1. Theoretically Achievable Accuracy of Trigonometric Height Traversing (standard deviations in mm/ $\sqrt{\text{km}}$)

α°	$S[\text{m}]$	150	200	250	300	400	600
a) $\sigma_\alpha = 0.7''$, $\sigma_s = 4 \text{ mm}$, $\sigma_c = 0.3 \text{ mm}$							
0°		1.5	1.7	1.8	2.0	2.2	2.7
4°		1.7	1.8	1.9	2.0	2.2	2.7
8°		2.1	2.1	2.2	2.2	2.4	2.8
12°		2.7	2.6	2.5	2.5	2.7	3.0
b) $\sigma_\alpha = 0.5''$, $\sigma_s = 4 \text{ mm}$, $\sigma_c = 0.3 \text{ mm}$							
0°		1.2	1.3	1.4	1.4	1.6	1.9
4°		1.3	1.4	1.5	1.5	1.7	2.0
8°		1.9	1.8	1.8	1.8	1.9	2.1
12°		2.5	2.3	2.2	2.2	2.1	2.3

The results indicate that, theoretically, even first order accuracy ($\sigma \leq 1.4 \text{ mm}/\sqrt{\text{km}}$) could be attained with the trigonometric methods when using electronic theodolites along routes with inclinations smaller than 4° and lengths of sight shorter than 250 m. However, these tabulated accuracies represent only the influence of random errors with a rather very optimistic value of $\sigma_c = 0.3 \text{ mm}$. There might still be some other sources of error such as changes in the deflection of the vertical, or the influence of the magnetic field and thermal effects on the new electronic instruments which have not yet been adequately tested. In addition, the cumulative effects of any possible systematic errors have been ignored; nonetheless, special attention at UNB has been given to the effects of the atmospheric refraction which is briefly discussed below.

INFLUENCE OF THE ATMOSPHERIC REFRACTION

For clarity, a brief review of the well known basic formulae is given first. Due to refraction, a pointing error τ to a target at a distance S can be expressed as a function of known coefficients of refraction k_1, k_2, \dots, k_n in sub-sections s_1, s_2, \dots, s_n (where $s_1 + s_2 + \dots + s_n = S$) of the line of sight. An approximation by Greening [1985] gives the same results as an approximate expression given earlier by Angus-Leppan [1979]:

$$\tau = \frac{1}{2R} \{ s_1 [k_1 S + k_2 (S - s_1)] + s_2 [k_2 (S - s_1) + k_3 (S - s_1 - s_2)] + s_n [k_n (S - s_1 - \dots - s_{n-1}) + 0] \} \quad (4)$$

In the simple case when the coefficient of refraction is constant along the whole line of sight (circular refracted path), the pointing error is:

$$\tau = \frac{S^2 k}{2R} \quad (5)$$

If a vertical gradient of temperature dT/dz is known at a point along a moderately inclined line of sight then the coefficient of refraction can be calculated at that point from:

$$k = 502(0.0342 + dt/dz)/T^2 \quad (6)$$

where P - barometric pressure in [mb] and T absolute temperature in [K].

The gradient dT/dz at a height z above the ground can be either directly measured or determined from the empirical formula [Kukkamaki, 1938] for the temperature profile:

$$T = a + bz^c \quad (7)$$

from which

$$dT/dz = bcz^{(c-1)} \quad (8)$$

The coefficients a , b , c , can be determined either empirically from temperature measurements at three or more different heights along a vertical line perpendicular to the line of sight or from the free convection theory of heat transfer [Priestley, 1954] from which $c = -0.33$ for turbulent air conditions and b is a function of the sensible heat flux and other meteorological parameters [Holdahl, 1980] which can be measured.

Figure 1 shows typical values of the coefficient of refraction for a sunny summer day in mid-latitudes through the first few metres above the ground. These plots have been constructed using equations (6) and (8) and measurements of temperature published by Banger [1982]. Similar results have been obtained from measurements at UNB on a sunny day (25°C) over a concrete surface.

From equations (5) and (6), in order to limit the refraction error of pointing to be within the aforementioned value of 0.2 mm over a distance of 250 m, the coefficient of refraction would have to be determined with an accuracy of 0.04 which corresponds to an accuracy in dT/dz of 0.007°C/m for $P = 1000$ mb and $T = 300$ K. With presently available instrumentation, the gradients of temperature in turbulent air cannot be determined with an accuracy better than about 0.1°C/m which corresponds to a pointing error of about $\tau = 2.8$ mm at $s = 250$ m assuming a constant gradient of temperature along the entire line of sight. An additional problem in developing a possible correction technique comes from the uncertainty in the temperature profile of model (7). Very recent and on-going investigations at UNB indicate failure of model (7) at heights of 3 m to 4 m above the ground where gradient inversion occurred under certain conditions on both sunny and overcast days. Also the value of $c = -0.33$ has been found to agree with the experimental values only in very unstable conditions (midday, sunny) at heights up to only about 1.5 m above the ground.

Considering the above difficulties, the short term fluctuations of dT/dz and height accuracy requirements, the authors are very skeptical that any practical method for correcting the refraction errors over individual lines can be developed. This skepticism includes the multi-wavelength dispersive methods or any reflective or refractometric methods as suggested by some authors. The only practical remedy is to try to randomize the influence of refraction through a proper field survey method. The trigonometric method itself offers already at least a partial randomization by having the forward and backward lines of sight

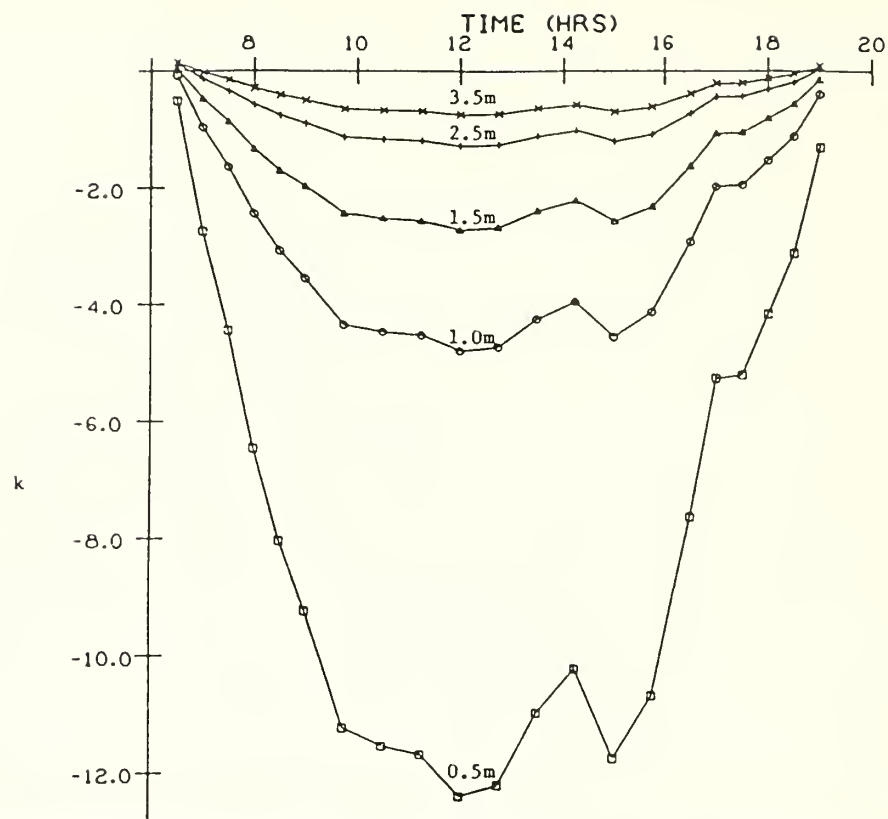


Figure 1. Diurnal Variation of "k" (from data published by Banger [1982]).



Figure 3. Prototype Multi-target Rod

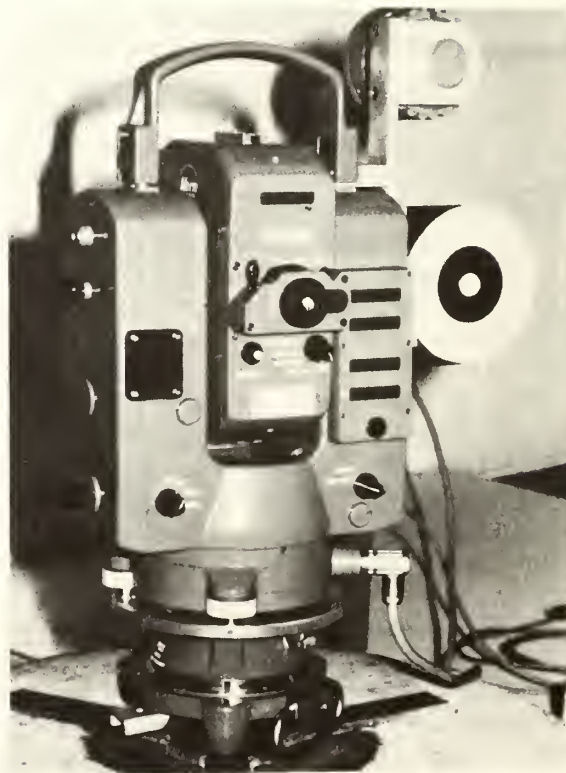


Figure 4. Kern E2 adapted

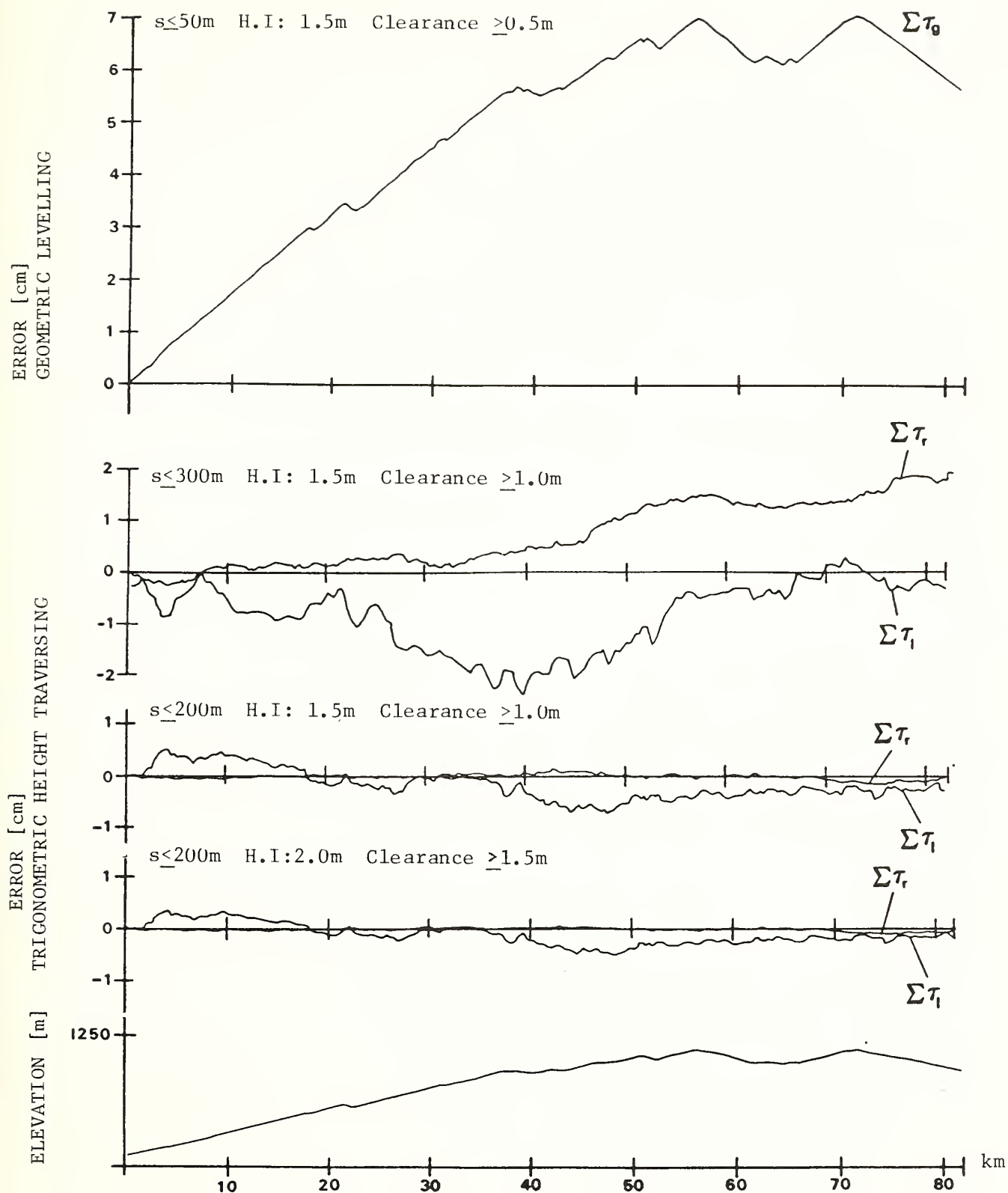


FIGURE 2. Simulation of Height Determination Affected by Refraction

more or less at the same height above the ground. Here, the reciprocal mode of operation should, theoretically, offer a better randomization effect than the leap-frog method. However, in the leap-frog method the observations over the back and forward lines is spread over a time twice longer than in the reciprocal method thus randomizing more the short term changes in the refraction error. The leap-frog method allows for an additional randomization of the refraction errors by using two or more targets at different heights as practiced in the UNB surveys [Chrzanowski, 1983]. This would be rather difficult to introduce in the reciprocal method. It is likely because of this randomizing that no obvious difference in accuracy has been noticed in the test results obtained from both methods as shown in the next section.

In order to see the cumulative influence of the refractive errors in long trigonometric traversing, influence of refraction has been simulated in an 82 km long trigonometric traverse along a slightly inclined (1%) route with random maximum grade changes of 3%.

Details are given in Greening [1985]. The computer generated route profile was divided into 10 m segments for simulating the refraction errors. Kukkamaki's model (8) of the temperature gradient and equations (4) and (6) were used in the simulation accepting $c = -0.33$ and taking a randomly changing value of b with mean value of 1.5 ± 0.2 , corresponding to rather moderate refraction conditions. Figure 2 shows partial results of the accumulation of the refraction errors Σ_{τ_r} and Σ_{τ_ℓ} for the reciprocal and leap-frog traversing respectively over the total route of 82 km with a total elevation difference of about 800 m. Different values of maximum lengths of sight, S , and different heights of instrument, H.I. were used in the simulation for minimum clearances of the lines of sight above the ground ranging from 1.0 m to 1.5 m. For a comparison, the influence of refraction was applied also to a simulated geometrical levelling along the same route which resulted in a total systematic error of about 70 mm. These results demonstrate that reciprocal height traversing is practically free of any systematic refraction errors - when $S \leq 200$ m. The leap-frog method for the same S has a negligibly small total error of refraction but it shows that over shorter routes refraction errors may accumulate up to about 1 mm/km if the minimum ground clearance is 1.5 m. For $S = 300$ m both methods may show significant accumulation of the refraction error although still about 1/3 smaller than in geometric levelling.

Some additional UNB investigations and field tests on the influence of refraction are reported in Chrzanowski [1984]. They included two continuous height determinations for 19 hours over a 500 m long test line with different heights of targets ranging from 1.5 m to 4.5 m above the ground and unfavorable refraction conditions. The results would indicate that the best observation period for the randomization of refraction error is at mid-day between 10 a.m. and 4 p.m. No definite conclusions could be reached on the optimal heights of the targets and of the instrument in the leap-frog method when changing them from 1.5 m to 4.5 m and from 1.5 m to 2.2 m respectively.

FIELD TESTS WITH THE DKM2-A/DM502 SYSTEM

The optical theodolite Kern DKM2-A and EDM instrument DM502 were used in the first field tests using the leap-frog method with 3 or 4 targets at heights up to 5 m and, later on, with only two targets at 2.0 m and 3.5 m above the ground. In order to achieve the accuracy of 0.7" in angle measurement as listed in Table 1, a total of 8 to 12 sets of measurements were taken on each forward and

backward traverse line in various sequences of pointings in order to devise an optimal field procedure. The test surveys were performed along undulating highways and city streets with inclinations of up to 6° . Evaluation of the trigonometric results which are listed in Table 2 is based only on internal misclosures of double or loop surveys with more detail and a comparison with geometric levelling given in Chrzanowski [1984] and Greening [1985]. The lengths of sight of these results ranged from 200 m to 300 m. Most of the surveys were performed on sunny summer days with the height of the instrument about 1.5 m and minimum ground clearances of 1.0 m. The estimated standard deviation of 2.2 mm/ $\sqrt{\text{km}}$ from Table 2 is statistically compatible with the predicted value in Table 1 for the given conditions. Even better results were obtained with the same equipment in measurements of a network of 18 lines for monitoring a hydro-electric power dam near Fredericton. The least squares adjustments of two measurements of the network gave estimated standard deviations for one way levelling of 1.3 mm/ $\sqrt{\text{km}}$ and 1.9 mm/ $\sqrt{\text{km}}$ using lengths of sight averaging 250 m. This comparatively high accuracy could be, perhaps, attributed to the rugged topography of the area in which most portions of the lines of sight were several metres clear of the ground.

The measurements of the 18 lines of the monitoring network took about 3 days while the geometric levelling of the same network required over two weeks.

Along the undulating highways the speed of the trigonometric traversing was about 1 km/h using only one vehicle.

Figure 3 shows a prototype multi-target rod as used in the test measurements.



Fig. 5. Height Traversing Instrument Vehicle

FIELD TEST WITH THE E2/DM503 AND T2000/DI5 SYSTEMS

Towards the end of the summer of 1984 two electronic theodolites Kern E2 and Wild T2000 with EDM instruments DM503 and DI5 respectively became available. They were adapted (Fig. 4) for motorized reciprocal traversing using two small pick-up trucks (Fig. 5) with mechanically elevated tripods constructed at UNB in a manner similar to that of IGN in Paris [1982]. Provided with each of the systems was the facility for RS232C interfacing. Control of the system, as in the T2000/DI5, and the capture of data by a microcomputer, e.g. Epson HX-20 or Sharp PC1500 in this project, became merely the sending and receiving of character strings. Because of its system of operation [Katowski and Salzmann, 1983], the T2000/DI5 was quite versatile since both the measurement and sending of data could be controlled by commands corresponding to the keyboard operations; however, the interfacing consumed much power and required an auxiliary source in the field. In contrast, the E2/DM503 [Munch, 1983], could only be interrogated for the transmission of data with interfacing through a single cable from the converter and 10Ah power supply which was easily sufficient for a full working day. With these external computational means along with hardcopy and cassette storage in the field, the gathering of data and field checking and reduction were greatly simplified, facilitated, and hastened. The economics of the survey were enhanced by increasing speed and ensuring accuracy.

Experiences during the 1984 measurements have emphasized the attention that must be paid to observation procedures and handling of the instruments in the field under variable environment conditions. The index error was found to vary appreciably over several setups and even during a single setup. This is suspected as being a temperature dependence by the compensator and has been confirmed for both instruments in investigations still in progress.

Each of the two systems was used in the leap-frog method in the same test areas as above with targets at only the 2.0 m and 3.5 m heights. The two systems were used together in the reciprocal method with the T2000/DI5 as the master station interfaced to an Epson HX-20. It was apparent that a telemetric link between the two stations would provide proper real-time processing of the measurements, especially with regard to checking the consistency of results and detecting any abnormalities, e.g. from refraction.

Four sets of vertical angle measurements, two to each target in the leap-frog and two from each instrument in the reciprocal method, were taken with lengths of sight to 250 m and inclinations of the terrain to 4.5° .

Generally, the field and laboratory tests of both instruments confirmed the expected accuracy of vertical angle measurements as given in Table 1 except the aforementioned changes in the index error which require further investigation.

Table 2 summarises results of the preliminary tests in the form of misclosures obtained from double or loop traversing. In the analysis, no distinction has been made between the leap-frog and reciprocal results because no obvious differences could be detected from the small sample of field tests. An overall estimated standard deviation of 2.1 mm/ $\sqrt{\text{km}}$ was obtained.

Although the standard deviation estimated from such a small sample was statistically compatible with the 1.5 mm/ $\sqrt{\text{km}}$ value from Table 1 for the given observing conditions, it may indicate an influence of some additional sources of error, perhaps refraction, which would have been expected from the simulation for

such long lines of sight and short traversing routes.

TABLE 2. Misclosures in Trigonometric Height Traversing.

DKM2-A/DM502 (leap-frog)			E2/DM503 and T2000/DI5 (leap-frog and reciprocal)		
Total length L [km]	Misclosure ϵ [mm]		Total length L [km]	Misclosure ϵ [mm]	
1.6	2.7	Urban loop	4.8	3.2	highway 1.-f. route
3.2	2.8	highway route	4.8	4.2	" 1.-f.
3.4	8.9	" "	4.8	5.3	" recipr.
5.0	0.5	" "	3.4	7.7	" 1.-f.
6.8	3.8	" "	3.4	2.8	" 1.-f.
5.0	4.6	" "	3.4	1.5	" recipr.
1.6	1.2	network	4.4	1.4	" 1.-f.
1.3	2.9	"	4.4	0.4	" 1.-f.
1.4	0.9	"	4.4	1.7	" recipr.
1.7	2.8	"	2.9	0.2	Urban 1.-f. loop
2.3	2.6	"	2.9	7.4	" 1.-f.
			2.9	1.8	" recipr.

$$\hat{\sigma} = \left(\frac{\sum_{i=1}^n \frac{\epsilon_i^2}{L_i}}{n} \right)^{\frac{1}{2}} = 2.2 \text{ mm}/\sqrt{\text{km}}$$

$$\hat{\sigma} = \left(\frac{\sum_{i=1}^n \frac{\epsilon_i^2}{L_i}}{n} \right)^{\frac{1}{2}} = 2.1 \text{ mm}/\sqrt{\text{km}}$$

A daily progress of about 8 km was obtained by an inexperienced survey crew using prototype motorized system and lengths of sight to 250 m. Due to economical reasons only two vehicles were used in both the leap-frog and reciprocal tests. With some small refinements to the system a speed of at least 1.5 km/h could be obtained - compatible with motorized geometrical levelling in flat terrain. However, in the hilly terrain of the test surveys, the progress of first order geometrical levelling was only about 3 km/day. A further increase in the speed of trigonometric surveys could perhaps be achieved but at a cost of the decreased accuracy. Due to the influence of the aforementioned short term refraction changes, the observing time along each line should be spread over at least 10 minutes when sighting from 200 m to 250 m in order to randomize the influence.

GENERAL CONCLUSIONS AND RECOMMENDATIONS

the results of the field test surveys and the simulation of the refraction influence have led the authors to conclude that:

- i) the standard deviation of no more than 2 mm/ $\sqrt{\text{km}}$ without a systematic accumulation of refraction error is achievable in trigonometric height traversing even along inclined routes at a speed of 10 km/day when using sights no greater than 200 m for the leap-frog and 250 m for the reciprocal method. By further decreasing the lengths of sight, the influence of refraction can be ignored and the theoretical accuracies as listed in Table 1 can be achieved.

For extremely short sights, for example 60 m, in flat terrain, the accuracy as high as 0.6 mm/ $\sqrt{\text{km}}$ is feasible but at the cost of very slow speed.

- ii. Each of the reciprocal and leap-frog methods has its advantages and disadvantages. In levelling methods with a large density of benchmarks, the reciprocal method is slowed by the necessity of performing separate connecting surveys to the benchmarks. On the other hand, the leap-frog method requires a time consuming reconnaissance for balancing the forward and backward lengths of sight. The reciprocal method is less affected by the cumulative effects of refraction when lines of sight are 200 m or longer. Because there is a single instrument station in the leap-frog method, its real-time processing of data is less complicated than in the reciprocal method in which data is gathered at two separate stations. Since several telemetry systems are available on the market, including a sophisticated system developed at UNB (Chrzanowski and Kurz, 1982), the latter drawback of the reciprocal method can be easily remedied.

As far as the future use of the trigonometric height traversing is concerned, the authors recommend:

- i. Additional automation of the field surveys by using a laser and self centering integrating targets or a laser scanning system for multiple pointing to the targets. Some systems were constructed at UNB (Chrzanowski and Janssen, 1972) already 15 years ago and with the present technology, they could be constructed even more easily.
- ii. Following the first conclusion regarding the randomization of the refraction effects, the specifications for the accuracy of vertical control surveys should be revised to reflect the overall accuracy of trigonometric height traversing as being slightly worse than the present requirements for geometric levelling but without hidden systematic components.

ACKNOWLEDGMENTS

The authors are grateful to the firms of Kern Aarau and Wild Heerbrugg for providing the instrumentation. The assistance of A. Kharaghani, P. Romero, and Z. Shi is appreciated.

REFERENCES

- Angus-Leppan, P. (1979): Refraction in Levelling - its variation with ground slope and meteorological conditions, Aust. J. Geod. Photogramm. Surv. 31. 51-64.
- Angus-Leppan, P.V. (1980): Refraction in Levelling: Extension to Stable and Neutral Atmospheric Conditions: Second International Symposium on Problems Related to the Redefinition of North American Vertical Geodetic Networks, Ottawa.
- Banger, G. (1982): Magnitude of Refraction in Levelling and its Parameters, Austr. J. Geod. Photo. Surv. No. 37.
- Blasek, R. and Hradilek, L.: (1979): Investigation on Refraction in Trigonometrical Levelling Traverses: In: Tengstrom, E. and Teleki, G. (eds), Refractional Influences in Astronomy and Geodesy, Reidel, Dordrecht, pp. 195-201.

- Bomford, G. (1980): Geodesy, 4th Edition, Clarendon Press, Oxford.
- Chrzanowski, A., D. Janssen (1972): Use of Laser in Precision Levelling, The Canadian Surveyor, Vol. 26, No. 4, pp. 369-383.
- Chrzanowski, A., B. Kurz (1982): A Telemetric System for Monitoring Deformations in Difficult Terrain and Climate Conditions, 3rd (FIG) Intern. Symp. on Deformation Measurements by Geodetic Methods, Budapest, August 25-27, Proceedings, Vol. 3, pp. 3-19.
- Chrzanowski, A. (1983): Economization of Vertical Control Surveys in Hilly Areas by Using Modified Trigonometric Levelling, Proceedings of the ACSM Annual Meeting, March, Washington, D.C.
- Chrzanowski, A. (1984): Feasibility Study on the Implementation of the Motorized Trigonometric Height Traversing for Precise Levelling, Report to the Geodetic Survey Division, EMR, Ottawa, DSS Contract No.: OST83-00387.
- Greening, T. (1985): Evaluation of Precision Trigonometric Levelling Methods, M.Sc. Thesis, University of New Brunswick.
- Holdahl, S.R. (1981): A Model of Temperature Stratification for Correction of Levelling Refraction: NOAA Technical Memorandum NOS NGS 31.
- IGN (1982): Nivellement indirect de precision motorise (NIPREMO) - Internal Report of the IGN Department of Levelling on the activity January-February 1982, Paris.
- Kasser, M. (1983): Essais de Nivellement Indirect de Precision Motorise (NIPREMO), Paper No. 508.3, FIG Congress, Sofia.
- Katowski, O, W. Salzmann (1983): "The Angle-measurement System in the Wild THEOMAT T2000", Wild Heerbrugg Ltd., 9 pp.
- Kratzsch, H. (1979): Motorisierte Hohenzugmessung mit electrooptischen Tachymetern, Vermessung-Rundschau. 41 No. 3.
- Kukkamaki, T.J. (1983): Uber die nivellitsche Refraktion, Publ. 25, Finn. Geod. Inst., Helsinki.
- Munch, K.H. (1983): "The Kern E2 Electronic Precision Theodolite: Mechanics-Electronics - System Configuration", F.I.G. XVII International Congress, Sofia, 1983, Kern & Co., Ltd., Aarau, reprint 322e, 1983 08, 22 pp.
- Overton, P.G. (1974): Height Measurements with Distomat Wild DI-10: Wild Reporter No. 7.
- Rueger, J.M. and Brunner, F.K. (1981): Practical Results of EDM-Height Traversing: The Australian Surveyor, Vol 30, No. 6, pp. 363-372.
- Whalen, C.T. (1984a). "Preliminary test results of precise trig-levelling with the Wild T2000-DI5 system". ACSM Bulletin, 93, pp. 15-18.

VERTICAL DATUM DEFINITIONS DISCUSSED IN VIEW OF EUROPEAN VERTICAL AND HORIZONTAL NETWORKS

R. Kelm

Deutsches Geodätisches Forschungsinstitut (DGFI), Abteilung I
Marstallplatz 8, 8000 München 22, FRG

ABSTRACT. The first adjustment of the United European Levelling Network (UELN) resulted in geopotential numbers which are related to one arbitrary, but fixed number of a point marked on the earth surface near Normal Amsterdam Peil (NAP). That means that UELN is defined as a minimally constrained vertical network on a local datum. General and particular problems are discussed with respect to two definitions of a global vertical datum: The oceanographic and the continental definition. The results are: A global vertical datum by continental definition would create less problems in Western Europe because

1. A connection of UELN to the European Horizontal Network (RETrig), in which high accurate geocentric positions will be available soon, is partly existing and may be enlarged without principal problems,
2. Information on the earth gravity field measured on the continental surface, especially at and near the points defining the global vertical datum, is available or can be measured at low expense. Some ideas for the realisation of a global vertical datum by continental definition are presented.

INTRODUCTION

A vertical datum relates a closed physical height information system uniquely to a reference surface. Physical height information is defined here as potential differences of the earth gravity field referred to the earth surface or between the earth surface and an equipotential reference surface, the latter ones being generally called potential numbers. Derived metric quantities of the potential differences are e. g. orthometric or normal heights. A closed system is understood as an independent vertical network the potential differences or heights of which are estimated with net interval data only. The vertical datum of such an independent network is called local vertical datum (LVD).

Two methods are commonly used for the realisation of an LVD:

1. A minimally constrained adjustment of the net by fixing an arbitrary geopotential number of one net point (classically near the ocean surface), e. g. as done in UELN (Ehrnsperger etc. 1982).
2. An overconstrained adjustment by fixing more than one net point, e. g. as done in the National Geodetic Vertical Datum of 1929 in USA, cf. e. g. (Lippold 1980).

The problem which will be analysed here is: What is the best way to refer an LVD to a global vertical datum (GVD)?

The GVD may be defined as a datum which relates the physical height information of the whole earth to the same equipotential reference frame.

At present, there are two methods in discussion for the realisation of the GVD: The oceanographic and the continental datum.

Roughly seen, the oceanographic GVD refers to the physical surface of the ocean. It is known that in the past the geoid had been assumed to coincide with the mean sea level (MSL) of the oceans. During the last decades, it was noted that this assumption was only satisfactory within an accuracy range of ± 1.5 m. Meanwhile, much research work has been performed to model the differences between the sea surface and the geoid, cf. e.g. the review of (Rizos 1980). Nevertheless, problems in the realisation of an oceanographic GVD gave rise to a different definition: The continental GVD. The basic idea was introduced by (Colombo 1980) and means that the GVD is referred to the earth gravity potentials of one or several fundamental sites on continents the accurate coordinates of which in a geocentric system can be obtained.

Both methods will be discussed here by regarding the current situation of vertical and horizontal geodetic networks in Western Europe and in view of the aim to reach a dm accuracy for physical heights with respect to the GVD.

GENERAL CONSIDERATIONS

Let us start with the results of an independent vertical network adjustment: The adjusted potential differences ${}^L W_P$ between the LVD of point L and the net points P, (Fig. 1).

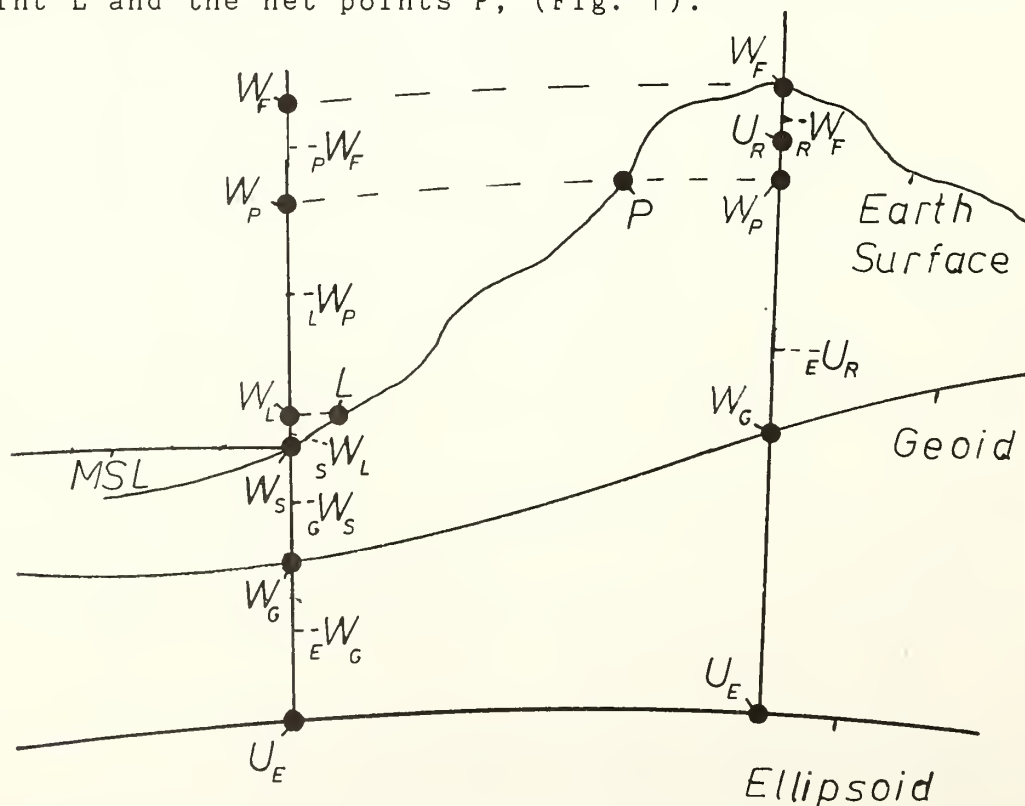


Fig. 1: Potentials and Potential Differences

We shall not discuss here the problems of precisions and accuracies within L^{WP} or its representations, the geopotential numbers L^{CP} ($10 \text{ m}^2/\text{sec}^2$), orthometric heights L^{HP} (m) or normal heights $L^{\bar{H}P}$ (m), but the connections of LVD values L^{WP} to GVD values W_P .

The classical way of connection is the oceanographic one:

$$W_P = U_E + E^{WG} + G^{WS} + S^{WL} + L^{WP}$$

with:

W_P : Potential of net point P in a GVD

U_E : Equipotential of reference level ellipsoid

E^{WG} : Equipotential difference between level ellipsoid and a global geoid

G^{WS} : Potential difference between geoid and mean sea level (MSL)

S^{WL} : Potential difference between MSL and LVD reference point L

Note that for the oceanographic approach no geometrical height information (e. g. ellipsoidal heights) is required.

For the estimation of S^{WL} we need accurate and reliable tide gauge recordings of high frequency. The problems of determining G^{WS} are discussed in detail e. g. by (Rizos 1980). The precision and accuracy results are strongly correlated with the estimation of E^{WG} , the potential disturbance between the level ellipsoid and the actual earth gravity potential (here represented by the geoid) - one of the main tasks of Physical Geodesy and broadly discussed in recent geodetic literature. For our purpose we need only mention a few important accuracy estimations:

$E^{WG} + G^{WS}$ can be estimated with metric accuracy of $\pm 1 \text{ m}$ at present. In future, by applying the results of oceanographic measurements (e. g. steric and geostrophic levelling) and of satellite altimetry, it may be possible to reach an overall accuracy of $\pm 0.5 \text{ m}$.

The continental GVD can be represented by:

$$W_P = U_E + E^{WF} + F^{WP}$$

with

E^{WF} : Potential difference between ellipsoid and a fundamental site F on the continents

F^{WP} : Potential differences between F and net points P

$W_F = U_E + E^{WF} = \text{const}$ then defines the equipotential reference surface of the GVD.

The main idea of the continental approach is that E^{WF} can be estimated very accurately by using knowledge of geocentric site coordinates (with cm accuracy) as well as up-to-date information on the earth gravity field globally for low and medium frequencies and locally (at or near fundamental sites) for high resolution.

Two methods for the continental approach are reported by (Rapp 1983):

1. Definition through orthometric heights L^{H_F} :

Define a LVD with W_L , compute the orthometric height L^{H_F} to a fundamental site F on the continent with known geocentric coordinates by means of levelling observations and estimate an average value of gravity g between L and F as accurately as possible to obtain

$$L^{W_F} = g L^{H_F}$$

The equipotential surface $W_F = W_L + L^{W_F} = \text{const.}$ now becomes the reference surface of the GVD.

2. Definition through Geocentric Positions:

With a given ellipsoidal height E^h_F of a fundamental site F and a known geoidal undulation E^{H_G} compute the orthometric height

$$G^{H_F} = E^h_F - E^{H_G}$$

and the potential difference

$$G^{W_F} = g G^{H_F}$$

with g defined above.

Then the equipotential surface

$$W_F = U_E + E^{W_G} + G^{W_F} = \text{const}$$

defines the reference surface of the GVD.

The realisation of both definitions will be obtained by applying appropriate adjustment procedures for several fundamental sites on different continents.

Accuracy estimations for these approaches are not known. But there are model studies between the connections of two LVD applying the continental datum approach, performed by (Colombo 1980) and (Hajela 1983). For the connection of Europe and USA a metric accuracy between the differences W_L (Europe) - W_L (USA) of ± 45 cm is estimated according to (Hajela 1983).

It is hoped that this accuracy which may also be representative for the continental GVD can be raised by refining the methods and using more recent observations.

PARTICULAR SITUATION IN WESTERN EUROPE

In Western Europe the United European Levelling Net (UELN) has been adjusted several times, the latest, in 1981, called UELN-73, adjustment 1981 (Ehrnsperger etc. 1982), cf. also Fig. 2. The net was adjusted with minimal constraints in a LVD referring to the Normal Amsterdam Peil (NAP) with $W_L = 7.02590 \text{ m}^2/\text{sec}^2$ arbitrarily fixed. It has been decided in phase II to obtain the connection to MSL by measuring and estimating S^{W_L} between tide gauges (Fig. 2) and nearest net points. However, many practical problems have arisen concerning the mareograph recordings and the definition and estimation of MSL in the coastal area of Western Europe. This means

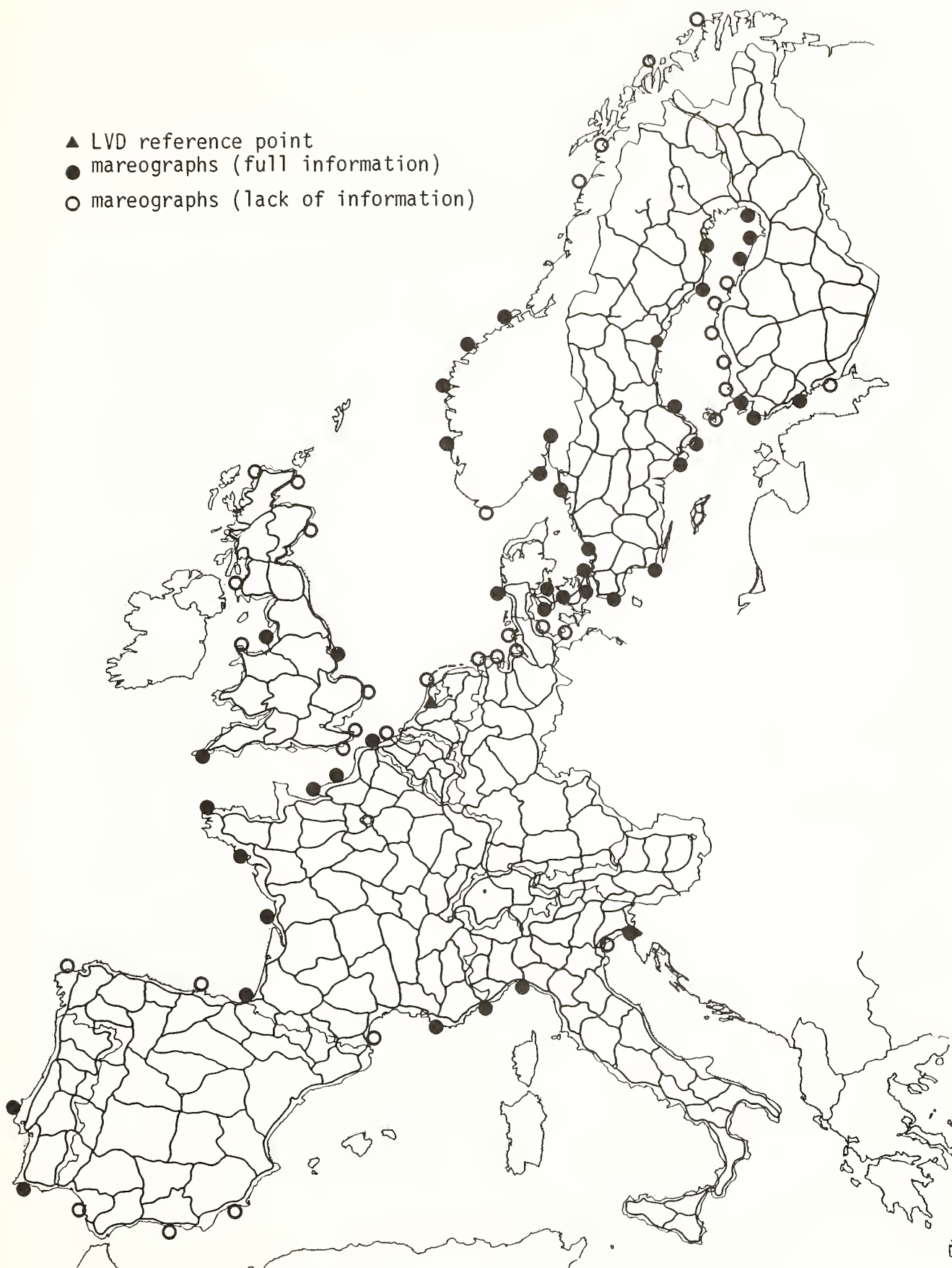


Fig. 2: UELN and Mareographs

that it will be difficult to obtain reliable and accurate estimates for G^W_S and S^W_L in Europe. It is hoped that satellite altimetry results over that area may improve the situation in future.

In view of these problems, it is worth considering the continental GVD definition for Western Europe.

For the continental datum, precise geocentric coordinates of the fundamental sites are required. There are several laser tracking stations in Europe (Fig. 3) for which high-accurate geocentric coordinate solutions are available. Additionally, a large set of net points with geocentric coordinates will be estimated in the near future within the project of the readjustment of horizontal networks called RETrig. In the final phase III the combination of RETrig net points with DOPPLER, LASER, VLBI and recent GPS measurements is considered (Kelm 1984). The collection and analysis of coordinate solutions of the many satellite and VLBI campaign in Europe will be taken over by the European Space Location Data Base (ESL-DB) which is in development (Boucher 1984). A connection of UELN to Laser tracking stations in Europe is already partly available and may be completely available in the near future. Consequently, F^W_P may be computed without major difficulties.

Concerning L^W_F of the definitions through orthometric height and G^W_F of the definition through geocentric positions, the most accurate estimation of g by borehole gravimetry may be extremely difficult due to the simple fact that no boreholes at Laser tracking stations exist, (as far as is known to the author).

This is one reason for a further proposal being given here for a definition of a continental GVD which is related more to the procedure of datum connection, as introduced by (Colombo 1980).

PROPOSAL FOR THE REALISATION OF A CONTINENTAL GLOBAL VERTICAL DATUM

This approach is characterised by the following ideas:

- To use the wealth of information on geocentric coordinates and earth gravity data which is available in Europe at present or will be in the near future (e.g. UELN, RETrig, ESL-DB, several gravity and topography data bases, European Longitudinal Network). It is assumed that this kind of information is also available in other continents.
- To take as a stationary reference gravity model an earth model, as e.g. at present GRIM3-L1 (Reigber etc. 1985).
- To model the potential disturbance pointwise for fundamental sites by using earth surface information of the earth gravity field (e.g. absolute and relative gravity observations, levelled potential differences, astronomical longitudes and latitudes or their differences in the vicinity of fundamental sites).

Note that to each earth surface point the geocentric coordinates have to be determined.

European Triangulation Networks

1 : 4 000 000

- MEDOC Station
- MERITDOC Station
- RETDOC Station

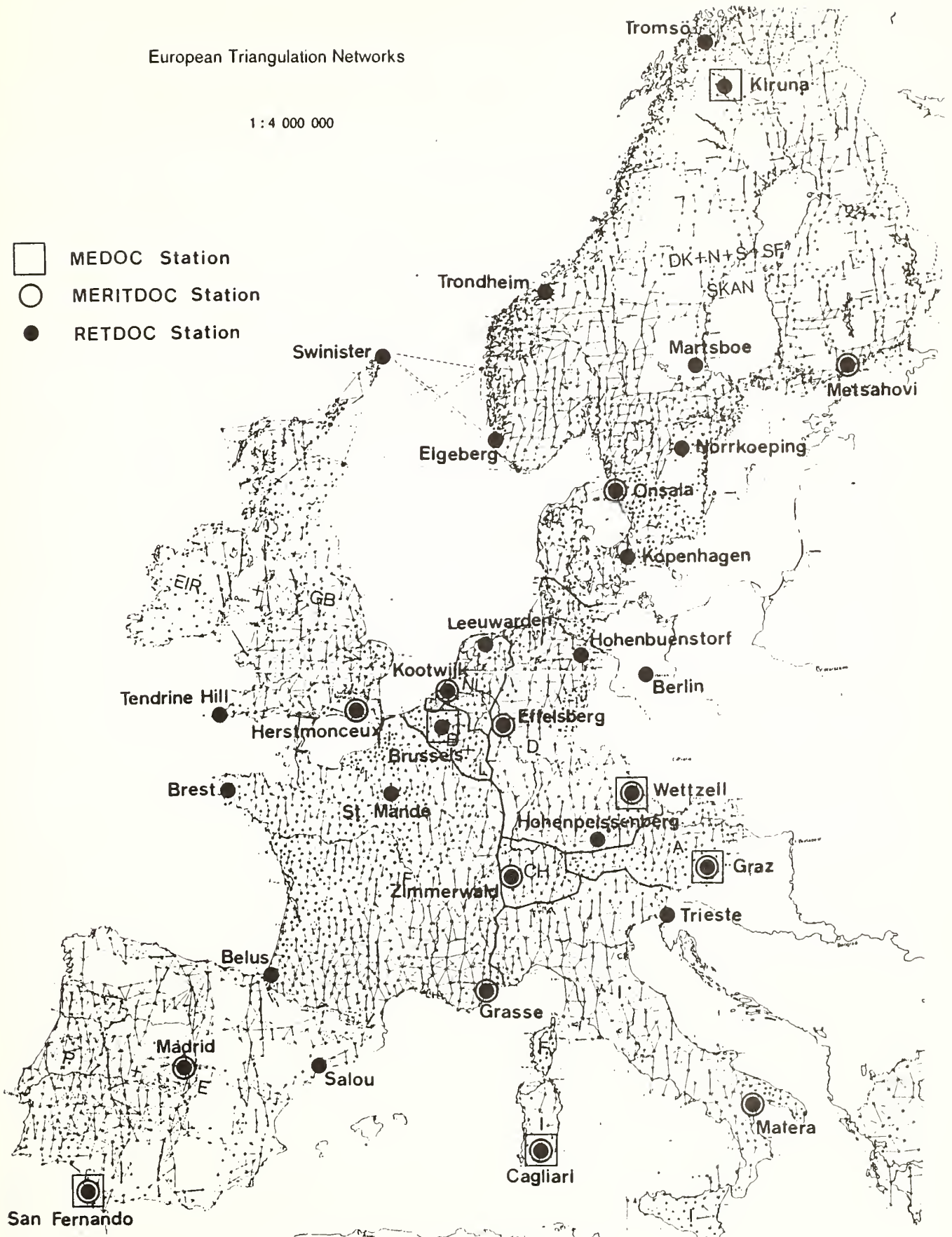


Fig. 3: RETrig and Satellite Sites

The basic equation of this approach is (Fig. 1):

$$W_F = U_E + E_{UR} + R_{WF}$$

with

E_{UR} : Potential difference between ellipsoid and earth model
(i.e.: $U_R = U_E + E_{UR}$ reference potential given by earth model)

R_{WF} : Potential disturbance

The remaining problem is how to model pointwise R_{WF} with earth surface point information as mentioned above. Of course, the topography of the vicinity of F has to be considered as well.

We started simulation and estimation studies for this problem by using the locality characteristics of buried masses as approximation method. For each point information of or near the fundamental site F, an observation equation is constructed with point mass anomalies as unknowns. As a result, W_F of all fundamental sites of the continents are predicted with respect to the same reference frame, i.e. in the same GVD. The estimation procedure can be performed stepwise by using the locality characteristics of buried masses in order to reach a practicable solution.

CONCLUSION

It is relevant in view of the situation in Western Europe to examine the feasibility of a continental GVD. For the realisation of such a GVD a modified approach is proposed which takes over principles of integrated geodesy: Modelling of earth surface point information without reduction of the observations of the geoid. The reference frame of the GVD is given by a stationary highly resolving earth model and by modelling pointwise the potential disturbances using earth surface point information. By remeasuring this point information at suitable intervals of time, time-dependent effects may also be modelled. This raises the accuracy of estimated physical height information within the Global Vertical Datum.

REFERENCES

- Boucher, C., 1984: ESL Reference Manual, CSTG Bulletin, SCS Publication No. 5
- Colombo, O., 1980: A World Vertical Network, Report 296, Dep. of Geodetic Science, The Ohio State University, Columbus
- Ehrnsperger, W., Kok, J., van Mierlo J., 1982: Status and Provisional Results of the 1981 Adjustment of the United European Levelling Network - UELN-73-, DGK/B/No. 258/II, 25-50
- Hajela, D., 1983: Accuracy Estimates of Gravity Potential Differences between Western Europe and United States Through Lageos Satellite Laser Ranging Network, Report 345, The Dep. of Geodetic Science and Surveying, The Ohio State University, Columbus
- Kelm, R., 1984: Activities of the International Computing Centre Munich from 1981 to 1984, Meeting of the Subcommission for the Readjustment of the European Triangulation Network (RETrig), Copenhagen
- Lippold, H., 1980: Readjustment of the National Geodetic Vertical Datum, EOS, vol. 61, No. 24, June 10, 30-35
- Rapp R., 1983: The Need and Prospects for a World Vertical Datum, Proceedings of the INT. Ass. of Geodesy (IAG) Symposia, vol. 2
- Reigber, Ch., Balmino, G., Bosch, W., Moynot, B., Müller, H., 1985: GRIM Gravity Model Improvement Using Lageos (GRIM3-L1), submitted to Journal of Geophysical Research
- Rizos, C., 1980: The Role of the Gravity Field in Sea Surface Topography Studies, Unisurv. S-17, School of Surveying, University of N. S. W., Sidney, Australia

COMPARISON OF GEODETIC LEVELING TO LOCAL MEAN SEA LEVEL BETWEEN PORTLAND, MAINE, AND ATLANTIC CITY, NEW JERSEY

David B. Zilkoski and Vasanthi Kammula
Vertical Network Branch
National Geodetic Survey
Charting and Geodetic Services
National Ocean Service, NOAA
Rockville, MD 20852

ABSTRACT. Datum definition is an important task in the new adjustment of the North American Vertical Datum, named NAVD 88. Heights of tidal bench marks above local mean sea level are usually employed when defining a reference surface for orthometric heights. The definition of the datum should be based on an equipotential surface, or at least a surface which closely approximates an equipotential surface. It is well known that local mean sea level values measured at different tidal stations do not lie on the same equipotential surface. The difference between the measured local mean sea level and a global equipotential surface, coincident with mean sea level at one point, is due to sea surface topography (SST) effects. Comparisons between tidal bench marks, assuming zero elevation difference between local mean sea level values, and observed geodetic leveling height differences are given for five tidal stations between Portland, Maine, and Atlantic City, New Jersey. Three of four of the differences are less than 50 mm. If we assume the leveling data are errorless, then these differences are estimates of SST effects between tidal stations. Of course, assuming the leveling data are errorless is not valid. The analysis described in this report indicates that significant systematic errors are still present in the leveling data and/or in the crustal movement estimates at the tidal bench marks. In order to determine the proper relationship between the two types of data, additional research is required to estimate the remaining systematic errors in leveling data, the SST effects at tidal stations, and the crustal movements at tidal bench marks.

INTRODUCTION

Datum definition is an important task of the new adjustment of the North American Vertical Datum which is called NAVD 88. In the past, heights of tidal bench marks referenced above local mean sea level at selected tidal stations were rigidly constrained to define a reference surface for orthometric heights. A "mean sea level" reference surface was determined for the National Geodetic Vertical Datum of 1929 (NGVD 29) by assuming the heights of local mean sea level (LMSL) at 26 tidal stations to be zero. The

definition of the new 1988 datum should be based on an equipotential surface, or a surface which closely approximates an equipotential surface. It is a known fact that local mean sea level heights determined by tidal data at different sites do not lie on the same equipotential surface. The difference between the measured local mean sea levels and a global equipotential surface, coincident with MSL at one point, is due to sea surface topography (SST) effects.

Heights of tidal bench marks referenced to local mean sea level, or local mean sea level height differences between tidal bench marks, should be incorporated into NAVD 88. However, there are still some unanswered questions: How do we best incorporate and assign weights to tidal height observations? Can we properly estimate the effects of SST at tidal stations? Can satellite information help control datum distortions? The answer to the first question depends largely on the answer to the second question.

Research is underway to estimate SST effects at tidal stations (Merry and Vaníček, 1983). Their results were incomplete because some effects were not accounted for, e.g., the influence of ocean currents and the slope of the seabed. However, their results did indicate a systematic improvement between geodetic leveling differences and local mean sea level differences corrected for partial sea surface topography effects. Galo Carrera, University of Toronto, Toronto, and Petr Vaníček, University of New Brunswick, are currently working on a project to estimate the SST effects at tidal stations located between Portland, Maine, and Atlantic City, New Jersey. This paper presents the comparisons between primary tidal bench marks referenced above local mean sea level (epoch: 1960-78) and observed leveling height differences for five tidal stations from Portland, Maine, to Atlantic City, New Jersey.

LEVELING and LOCAL MEAN SEA LEVEL DATA

Five stations were selected for this analysis; Portland, Maine; Boston, Massachusetts; New York City (Battery), New York; Sandy Hook, New Jersey; and Atlantic City, New Jersey. All leveling data were observed using first-order procedures and were corrected for known systematic errors as described in Balazs and Young (1982). The dates and kilometers of leveling involved are listed in table 1. The leveling data used in epoch 1 are mutually exclusive of the other two epochs. However, this is not the case for epochs 2 and 3 (see table 1); therefore results of epochs 2 and 3 are highly correlated.

Leveling lines were linked together to estimate the height differences between primary tidal bench marks. To compare the relevelings, the height differences for each epoch were corrected for assumed crustal movements which occurred at the tidal bench marks. No attempt was made to estimate movements between surveys in the same epoch. Due to the lack of information, the junction bench marks between leveling lines of the same epoch were assumed stable. If any of these bench marks moved during the time interval between levelings, these results will change accordingly. Movement at the tidal bench marks was estimated using local mean sea level (LMSL) linear trends documented by Hicks et al. (1983) (see table 2). The LMSL linear trends were separated into two components, one accounting for eustatic rise of sea level, and the other for crustal movements of the tide staff. It was assumed that the rate of movement of the primary tidal bench mark was equal to the tide

Table 1. Leveling Data Information

Station - Station	Epoch	Years Leveling Performed (Tidal Station to Tidal Station)	Length (km)
Portland - Boston	1	1923,1943	221.529
	2	1966,1965	269.605
	3	1966*,1965*,1978	278.109
Boston - New York	1	1943,1923,1922,1955	393.344
	2	1965	456.640
	3	1978,1965*	576.882
New York - Sandy Hook	1	1955,1934,1933,1952	98.062
	2	1965,1964	100.314
	3	1965*,1980	102.160
Sandy Hook - Atlantic City	1	1952,1930,1924	176.511
	2	1964	169.005
	3	1980	175.604

* Same data used in epoch 2.

Table 2. Local Mean Sea Level (LMSL) Information

Station	Primary Bench Mark Height above LMSL (1960-78) (m)	LMSL Linear Trend* (mm/yr)	Standard Error of Linear Trend* (mm/yr)
Portland	4.3099	2.3	0.4
Boston	3.3680	0.9	0.3
New York	3.8679	2.5	0.3
Sandy Hook	3.5631	4.0	0.4
Atlantic City	2.9840	3.9	0.4

* Based on 1940-1980 data series (Hicks, et al., 1983).

Note: Movement of Tidal BM i = $(1969.5 - \text{Year of Leveling to Tidal BM i})$
 $\times (- (\text{LMSL Linear Trend} - \text{Eustatic Rise}))$
 Eustatic Rise = 1.0 mm per year

staff rate of movement (see table 2) and, for this study, that the eustatic rise of sea level was 1.0 mm per year (Hicks et. al, 1983). To compare the leveling height differences to the LMSL differences, the leveling height differences were reduced to the year 1969.5, the mean epoch of the latest LMSL datum.

The primary tidal bench mark heights referenced to the latest local mean sea level epoch (1960-78) were obtained from the Tides and Water Levels Branch, NOAA. Table 2 lists the bench mark's height above LMSL, LMSL linear trends, and their estimated standard errors (Hicks et al. 1983).

RESULTS

Table 3 lists the leveling height differences between tidal bench marks for the three epochs of data. There are a few interesting items to point out in this table. First, after correcting for bench mark movements at tidal stations, most of the repeat levelings agreed within twice their estimated standard errors. This was very encouraging. It should be noted that the standard error of the LMSL linear trends were used to estimate the uncertainty in primary bench mark movements. These standard errors, along with the standard error of the leveling data, were used to estimate the standard error of the difference in height difference (Ddh). The second item to note, however, is that most of the Ddh (new minus old) values were positive. Third, the majority of epoch 3-minus-epoch 1 differences are greater than epoch 2-minus-epoch 1 differences. Fourth, results for Sandy Hook to Atlantic City seem out-of-line compared to the others; e.g., the epoch 3 height difference disagrees by more than 90 mm with the other two epochs.

Since the leveling data between Sandy Hook (SH) and Atlantic City (AC) disagreed by such a large amount, the data were plotted to investigate possible data outliers (see figures 1 and 2). Figures 1 and 2 indicate that a systematic error may be present in a portion of the 1964 and/or 1980 data, and a terrain-dependent error may exist in the 1930 data. Looking at figure 1, the 1964 and 1980 data agree for the first 50 km, then during the next 25 km, the 1980 line departs from the 1964 line. Finally, over the last 65 km they seem to agree with each other again. For the majority of the profile the 1964 and 1980 data tend to agree, but they do seem to have a terrain-dependent pattern. This close agreement between 1964 and 1980 could indicate a systematic error in the 1930 data. Since these leveling lines are located along the New Jersey coast, differential subsidence could have occurred between bench marks. However, according to tidal data, SH and AC stations are subsiding at approximately the same rate, 3 mm per year. Considering that epoch 2 data were all observed during 1964 and epoch 3 data all during 1980, and that the two stations are subsiding at the same rate, their relative height differences should not change by 90 mm from 1964 to 1980. Significant errors must exist in one or all three surveys.

An initial investigation of the leveling data between Sandy Hook and Atlantic City did not detect any obvious problems. The 1980 data were observed with one instrument and two rods using the double-simultaneous, single-run technique. There were two observers who alternated observing throughout the entire leveling line. The 1964 survey was double-run, using two instruments and two sets of rods. The observer and equipment were

Table 3. Comparison of Height Differences from leveling Data

Station - Station	Epoch	Observed height difference (m)	Movement (m)	Corrected height difference (m)	Differences (Standard Errors) (mm)		
					Epoch 2 - Epoch 1	Epoch 3 - Epoch 1	Epoch 3 - Epoch 2
Portland - Boston	1	-0.9870	0.0631	-0.9239			
	2	-0.9369	0.0050	-0.9319	-8.0 (30.1)		
	3	-0.9298	0.0037	-0.9261	-2.2 (30.5)	5.8 (23.9)	
Boston - New York	1	0.4996	-0.0244	0.4752			
	2	0.5415	-0.0072	0.5343	59.1 (30.6)		
	3	0.5527	-0.0059	0.5468	71.6 (35.2)	12.5 (35.0)	
New York - Sandy Hook	1	-0.3141	-0.0308	-0.3449			
	2	-0.2903	-0.0098	-0.3001	44.8 (16.5)		
	3	-0.3090	0.0383	-0.2707	74.2 (18.2)	29.4 (16.5)	
Sandy Hook - Atlantic City	1	-0.6544	-0.0795	-0.7339			
	2	-0.7088	0.0006	-0.7082	25.7 (27.1)		
	3	-0.6162	-0.0011	-0.6173	116.6 (30.6)	90.9 (23.6)	

Note: Movement reduced to 1969.5

Standard Error of Difference computed using $1.0 \text{ mm per SQRT(km)}$ for double-run surveys, $1.4 \text{ mm per SQRT(km)}$ for single-run surveys, and the standard error of the linear trend (assuming all data uncorrelated).

Movement at Tidal BM $i = (1969.5 - \text{Year of Leveling to Tidal BM } i) \times (-(\text{LMSL Linear Trend} - \text{Eustatic Rise}))$

Eustatic Rise = 1.0 mm per year

Observed height difference = $h_2 - h_1$

Corrected height difference = $(h_2 + \text{Movement at Tidal BM } 2) - (h_1 + \text{Movement at Tidal BM } 1)$
 $= (h_2 - h_1) + (\text{Movement at Tidal BM } 2 - \text{Movement at Tidal BM } 1)$

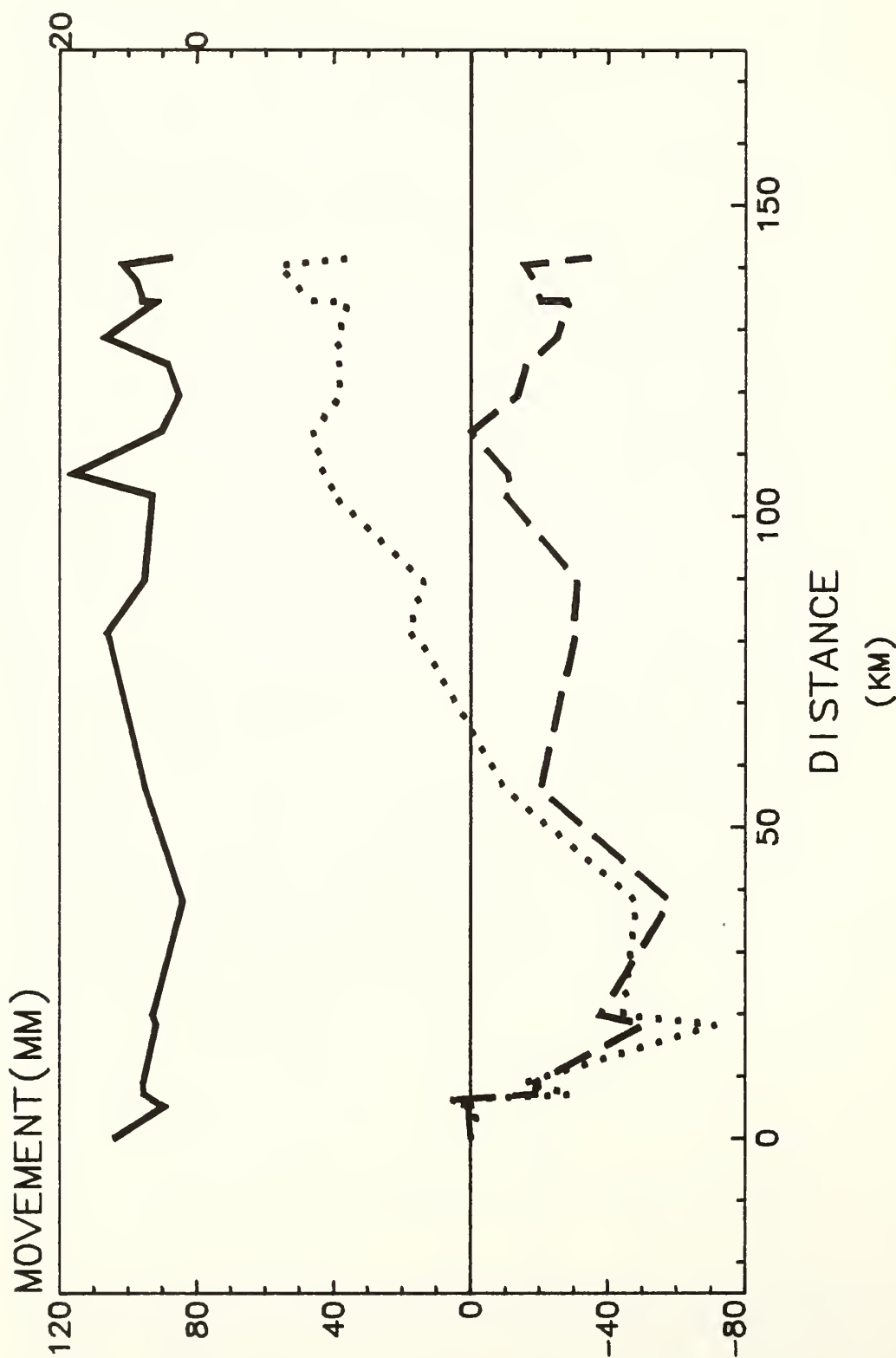


Figure 1 -- Profile from Sandy Hook to Atlantic City, NJ
L243833-L130 L20017-L130

1980-
1930

1964-
1930

TERRAIN(M)

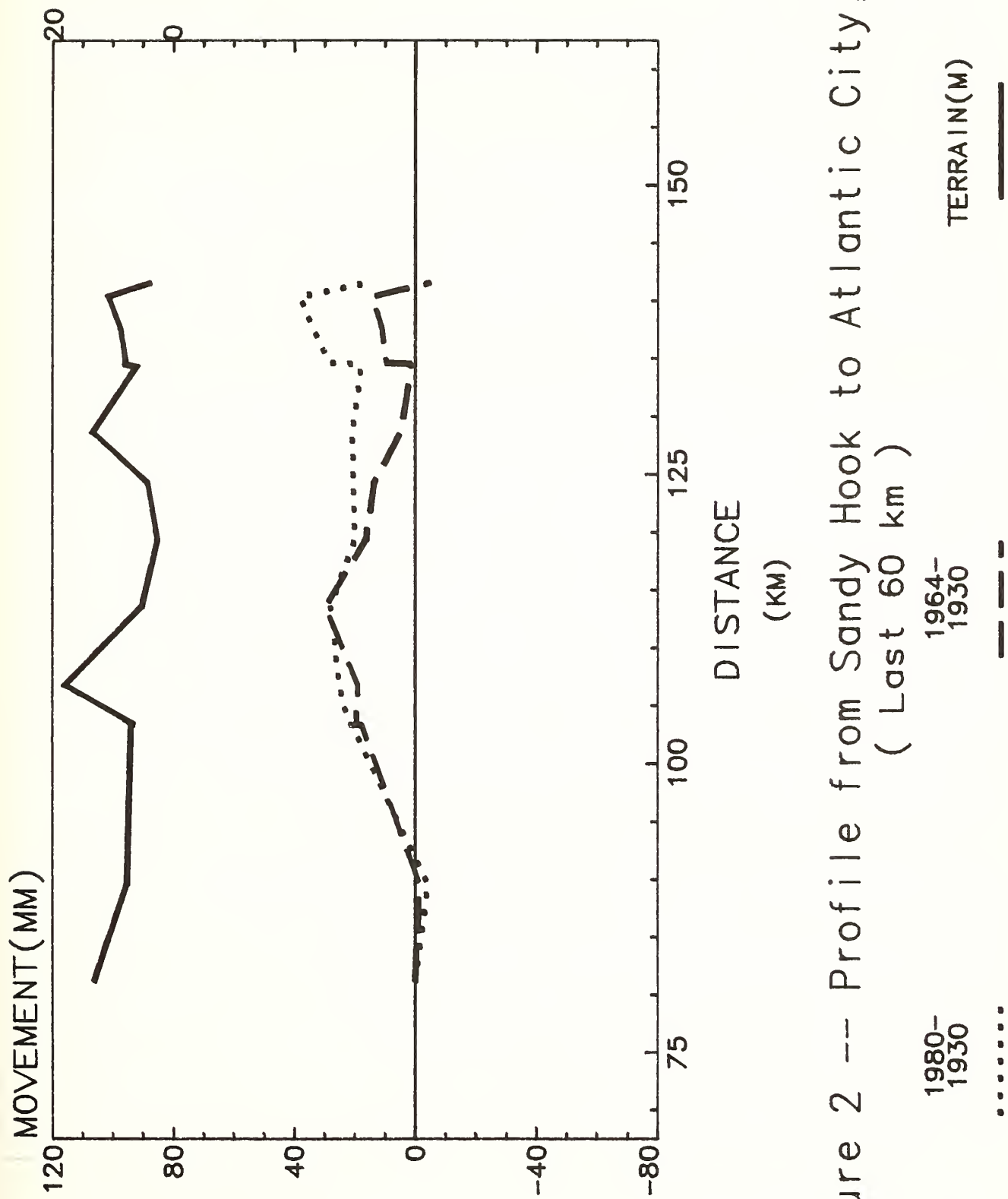


Figure 2 -- Profile from Sandy Hook to Atlantic City, NJ
(Last 60 km)

switched during the 25 km section where the 1980 line departs from the 1964 line (see figure 1). There were, however, other sections observed by that observer using the same equipment. The equipment and observer in question performed approximately 25 percent of the leveling. Figure 2 indicates that a systematic error may be present in another portion of the 1964 and/or 1980 data, i.e., the last 20 km. This portion of the 1964 survey was performed by a different observer using different equipment. More research is required before any conclusions can be made.

To determine which data may be in error, loops were formed using the 1930 (epoch 1), 1964 (epoch 2), and 1980 (epoch 3) data. Figure 3 depicts the leveling lines and their distances used in the analysis. The loop misclosure using the 1930 data was 20.83 mm in 401.96 km. The estimated standard error of the misclosure was 20 mm. The loop misclosure using the 1964 data was -45.31 mm in 388.86 km. Its estimated standard error of the misclosure was 19.7 mm. The loop misclosure using the 1980 data was 33.03 mm in 418.24 kilometers, and its estimated standard error was 25 mm. From loop analyses, all levelings appear reasonable.

Since the 1964 data between Sandy Hook and Atlantic City may be in error, another set of data of about the same epoch, but leveled inland, via South Amboy and Camden to Atlantic City, was included in the study. Table 4 lists the height differences obtained using sets of both data. The data leveled inland follow the same pattern as the rest of the differences listed in table 3; i.e., the new-minus-old differences in height differences are positive. This still doesn't determine which data, the 1964 or 1980, are in error, since coastal data for epoch 2 agree with epoch 1, and inland data for epoch 2 agree with epoch 3. However, it does have some significance because all new-minus-old differences are positive. This could be evidence of a small systematic error present in all three epochs of data. But, due to different procedures, the effect of the error is slightly different, e.g., maximum sight lengths were reduced in the late 50's and again in the 60's. Looking at figures 1 and 2, the profile seems to follow the terrain, except where the 1964 data depart from the 1980 data between the 55 and 80 km points in figure 1. This elevation correlation could be due to a small systematic error remaining in the 1930 data. This warrants additional investigation of our current corrections.

Another factor which influences the computed height differences, and could cause the differences to be positive, are the crustal movement rates estimated from local mean sea level data. Using different estimates for eustatic rise of sea level would change the estimated movement of the tidal bench mark and, therefore, the computed height differences. For this analysis, data (see figure 4) from Camden, New Jersey, to Atlantic City, New Jersey, were used to estimate the movement rate at Atlantic City assuming stability at Camden. The rate estimated from the leveling data was approximately -2.2 mm per year. This is a reasonable estimate, since the movement rate estimated from tidal data was -2.9 mm per year (assuming 1.0 mm per year eustatic rise). However, a 0.7 mm per year difference in movement rates can make a considerable difference in the results when the number of years between epochs is large.

Table 5 lists the height differences for Sandy Hook to Atlantic City using both movement rates. Using -2.2 mm per year, the differences in height differences were reduced and, once again, the majority of the differences

Table 4. Comparison of Height Differences from Sandy Hook to Atlantic City using Coastal and Inland levelings

Station - Station	Epoch	Observed height difference (m)	Movement (m)	Corrected height difference (m)	Differences (Standard Errors)		
					Epoch 2 - Epoch 1	Epoch 3 - Epoch 1	Epoch 3 - Epoch 2
Sandy Hook - Atlantic City	1	-0.6544	-0.0795	-0.7339			
	* 2	-0.7088	0.0006	-0.7082	25.7 (27.1)		
	3	-0.6162	-0.0011	-0.6173	116.6 (30.6)	90.9 (23.6)	
	1	-0.6544	-0.0795	-0.7339			
	** 2	-0.6600	0.0006	-0.6594	74.5 (28.8)		
	3	-0.6162	-0.0011	-0.6173	116.6 (30.6)	42.1 (25.6)	

* Coastal Leveling
** Inland Leveling

Note: Movement reduced to 1969.5
Standard Error of Difference computed using 1.0 mm per SQRT(km) for double-run surveys, 1.4 mm per SQRT(km) for single-run surveys, and the standard error of the linear trend (assuming all data uncorrelated).

Movement at Tidal BM i = (1969.5 - Year of Leveling to Tidal BM i)
X (- (LMSL Linear Trend - Eustatic Rise))

Eustatic Rise = 1.0 mm per year

Observed height difference = h2 - h1

Corrected height difference = (h2 + Movement at Tidal BM 2) - (h1 + Movement at Tidal BM 1)
= (h2 - h1) + (Movement at Tidal BM 2 - Movement at Tidal BM 1)

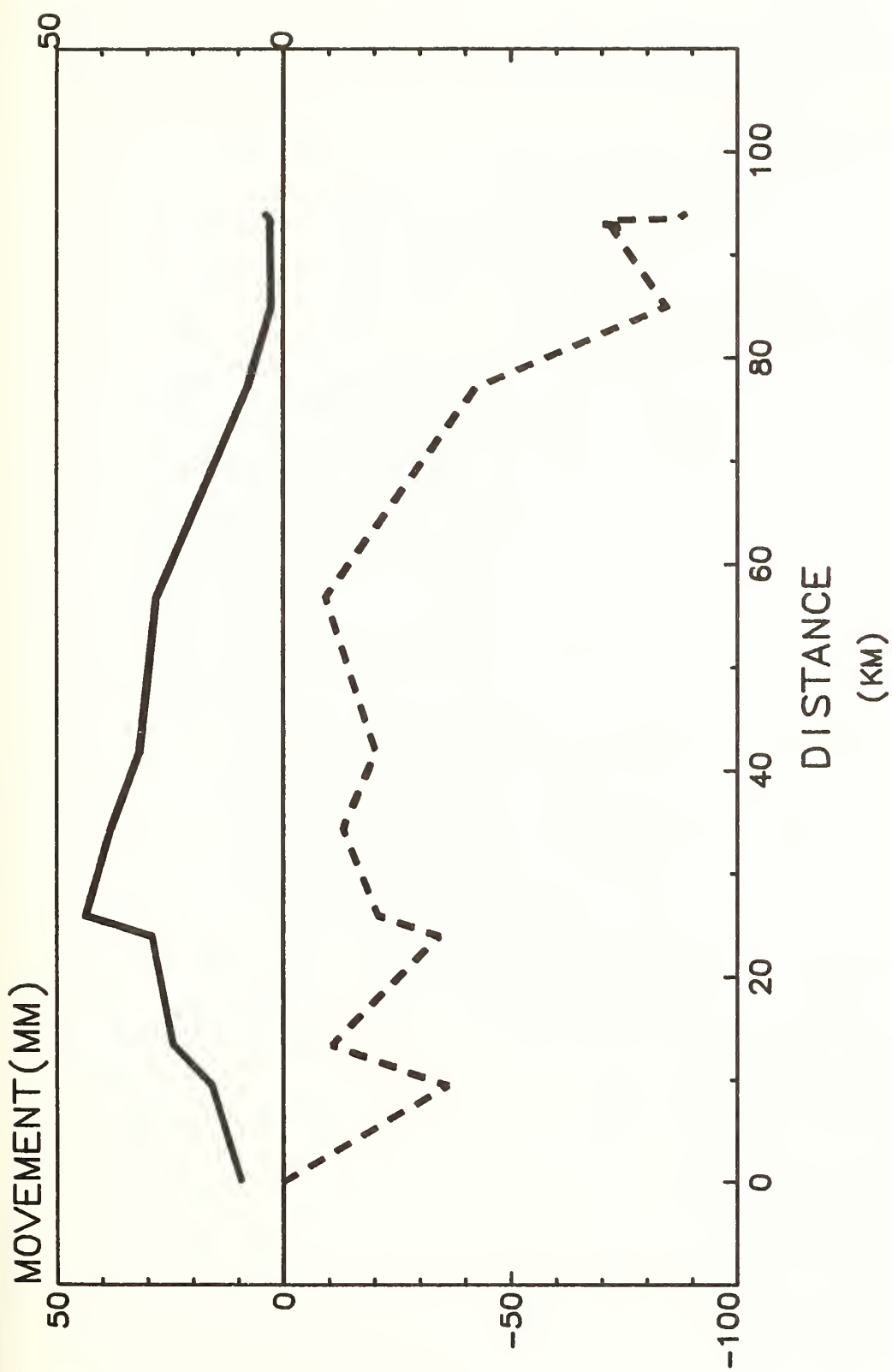


Figure 4 -- Profile from Camden to Atlantic City, New Jersey
L19880-X82467

1964-
1924
TERRAIN(M)

Table 5. Comparison of Height Differences from Sandy Hook to Atlantic City using Subsidence Rate of 2.2 mm per Year

Station - Station	Epoch	Observed height difference (m)	Movement (m)	Corrected height difference (m)	Differences (mm)		
					Epoch 2 - Epoch 1	Epoch 3 - Epoch 1	Epoch 3 - Epoch 2
Sandy Hook - Atlantic City	1	-0.6544	-0.0476	-0.7020			
	* 2	-0.7088	0.0044	-0.7044	-2.4		
	3	-0.6162	-0.0084	-0.6246	77.4		79.8
	1	-0.6544	-0.0476	-0.7020			
	** 2	-0.6600	0.0044	-0.6556	46.4		
	3	-0.6162	-0.0084	-0.6246	77.4		31.0

* Coastal Leveling

** Inland Leveling

Note: Movement reduced to 1969.5

Standard Error of Difference computed using 1.0 mm per SQRT(km) for double-run surveys, 1.4 mm per SQRT(km) for single-run surveys, and the standard error of the linear trend (assuming all data uncorrelated).

Movement at Tidal BM i = (1969.5 - Year of Leveling to Tidal BM i)

X (- (LMSL Linear Trend - Eustatic Rise))

Eustatic Rise = 1.0 mm per year

Observed height difference = h2 - h1

Corrected height difference = (h2 + Movement at Tidal BM 2) - (h1 + Movement at Tidal BM 1)

= (h2 - h1) + (Movement at Tidal BM 2 - Movement at Tidal BM 1)

were positive. Also, using -2.2 mm per year, both of the epoch 2 height differences, inland and coastal, agreed with the epoch 1 height difference within twice their estimated standard error. The differences between epoch 3 and the other two epochs are still large, indicating the error could be in the 1980 data. From this analysis, it is easy to understand why the movement rates and systematic errors in leveling must be better determined if height differences are going to be estimated accurately.

Having analyzed leveling height differences, we can now compare them to height differences derived from tide gauge data assuming zero difference between LMSL values. Table 6 lists the differences between the corrected leveling height differences and height differences estimated from tidal data. Except for Sandy Hook to Atlantic City which contain data outliers, all of the differences are less than 5 cm. The question is, what do these results mean?

It is difficult to say what the results indicate because the SST effects at the tidal stations are not well known. It is not known by how much the leveling differences should agree or disagree with height differences estimated from tidal data. In most cases, the leveling differences and tidal differences agree within 4 cm. This could indicate that the total SST effect between the tidal stations used in this study is less than 4 cm, except for Sandy Hook to Atlantic City. As stated in the Introduction, Petr Vaníček and Galo Carrera are currently performing a study estimating the partial SST effects at the five stations used in this analysis. When this study is completed, these differences will be compared to the leveling differences. Since the leveling results indicated that significant systematic errors may exist in the leveling data, possibly due to unknown error sources and incorrect estimates of crustal movements of tidal bench marks, it may still be difficult to evaluate the SST results.

To evaluate the SST results, the leveling data will require further research to reduce the differences between epochs. Leveling over short distances is very precise, and probably very accurate, but over long distances systematic errors still seem to be present. This makes the stated estimated accuracy of height differences based on random error assumptions questionable. In addition, estimating bench mark movement at the tidal stations needs to be investigated. Repeat levelings from "stable" areas to tidal bench marks may indicate different rates than those determined from tide gauge data. A more economical, and possibly better method, would be to use satellites of the Global Positioning System (GPS) to estimate these movements.

CONCLUSION

Datum definition is an important task of the NAVD 88 project. Depending on how the datum is defined, it can either distort the leveling network or help to control the remaining systematic errors in the leveling data.

The majority of the repeat levelings along the Atlantic coast between Portland, Maine, and Atlantic City, New Jersey, agree within twice their estimated standard errors. However, most of the differences are positive, indicating possible systematic errors in the leveling data and/or in the crustal movements estimates of the tidal bench marks. A profile of the data

Table 6. Comparison of Leveling Differences and Differences from Tidal Data

Station - Station	Epoch	Corrected height difference (m)	Height difference from tidal data (m)	Differences (mm)
Portland - Boston	1	-0.9239		18.0
	2	-0.9319	-0.9419	10.0
	3	-0.9261		15.8
Boston - New York	1	0.4752		-24.7
	2	0.5343	0.4999	34.4
	3	0.5468		46.9
New York - Sandy Hook	1	-0.3449		-40.1
	2	-0.3001	-0.3048	4.7
	3	-0.2707		34.1
Sandy Hook - Atlantic City	1	-0.7339		-154.8
	* 2	-0.7082	-0.5791	-129.1
	3	-0.6173		- 38.2
	** 2	-0.6594		-80.3

* Coastal Leveling

** Inland Leveling

Note: 1960-78 Local Mean Sea Level Epoch

Difference = Corrected height difference - LMSL height difference

between Sandy Hook and Atlantic City also indicates possible systematic errors in the leveling data. Most of the differences between leveling height differences and tidal height differences are less than 4 cm, indicating that the SST effects between tidal stations, which are located close to each other, may be small. Before a definite conclusion can be made, additional research is required to account for the remaining systematic errors in leveling, to estimate crustal movements at tidal bench marks and at junction marks between leveling lines of the same epoch, and to calculate the SST effects at tidal stations.

Due to the short time frame remaining for the completion of this project, the following is one possible scenario for incorporating tidal data in NAVD 88. First, choose four or five tidal stations on each of the three coasts: Atlantic, Pacific, and Gulf. These stations should be located where oceanographers feel they could estimate SST effects between tidal stations within 5 to 10 cm. These stations should also be located where crustal movements are small. Otherwise, repeat leveling surveys and/or GPS will be needed to estimate the movements. These movement rates should be compared to the tidal data estimates.

Second, the leveling data connecting these tidal stations should be analyzed in detail, and additional research performed to refine the corrections currently being applied. Then the tidal height differences and leveling height differences, corrected for crustal movement, should be included in the final NAVD 88 adjustment as observations and weighted according to their estimated accuracies.

The time frame for these studies is critical. If GPS is going to estimate the crustal movements at tidal stations, the first surveys need to be performed in the near future. These movements are small and a long span of time may be needed to estimate the movements. It will also take a considerable amount of time to estimate SST effects and determine the remaining systematic errors in leveling data. This will require an enormous amount of coordination and effort on the part of geodesists and oceanographers. This is not an impossible task, but we must start the analysis now in order to complete it on time for NAVD 88.

REFERENCES

- Balazs, E. I., and G. M. Young, 1982. "Corrections applied by the National Geodetic Survey to precise leveling observations," NOAA Technical Memorandum NOS NGS 34, National Geodetic Information Center, NOAA, Rockville, MD 12 pp.
- Hicks, S. D., H. A. Debaugh, Jr., and L. E. Hickman, Jr., 1983. "Sea level variations for the United States 1855-1980," Department of Commerce, NOAA, NOS, Rockville, Md 170 pp.
- Merry, C. and P. Vaníček, 1983. "Investigation of local variations of sea surface topography," Marine Geodesy, 7, 1-4, pp. 1-126.

VERTICAL DATUM DEFINITION BY INTEGRATED GEODESY ADJUSTMENT

Günter W. Hein and Bernd Eissfeller
Institute of Astronomical and Physical Geodesy
University FAF Munich
Werner-Heisenberg-Weg 39
D-8014 Neubiberg, F.R. Germany

ABSTRACT. For the readjustment of North American leveling networks it is necessary to determine mean sea level as vertical reference for orthometric heights. In the past different tide gauges were fixed which, however, show considerable discrepancies among them due to local phenomena of the sea near the gauges (e.g. different equipotential surfaces, sea surface topography, tides, ocean currents) which lead to distortions in a leveling network. The unique determination of the vertical reference is therefore an important requirement for the final definition of heights.

Let us assume that the following data are available: satellite altimeter data on sea near tide gauges, potential differences derived from geodetic leveling in combination with gravity observations, gravity (anomalies) and deflections of the vertical in a cap around it and tide gauge records. All of those data contribute to the abovementioned problem and guarantee an optimal solution if all the information can be taken into account. For that purpose is the integrated geodesy adjustment the best possible model.

Starting with the observation equations of satellite altimetry and using the already derived equations for the other geodetic quantities involved in such computations the integrated geodesy adjustment is presented for the solution of the vertical datum of a leveling network.

1. INTRODUCTION

For the final publication of heights of a country it is necessary to determine the vertical datum carefully. Assuming orthometric heights, the vertical reference is defined to be the geoid. This time-variable equipotential surface was in the past represented in the form of a tide gauge determined by recording the mean sea surface at this site for several years. Geodetic leveling observations could use these tide gauges then as fixed points. Due to local phenomena, however, like sea surface topography, tides, ocean currents, etc. can the so-determined mean sea level differ significantly from the geoid. Consequently, leveling lines connecting different tide gauges show discrepancies which lead to distortions in a leveling network. A simultaneous adjustment of tide gauges and leveling observations could only result in the determination of a mean surface minimizing the corresponding residuals at the gauges. Thereby it is by no means guaranteed that this mean surface is an equipotential surface nor the geoid.

The definition of a unified vertical datum is not only a necessary and important tool for a country but all over the world. Considering that, e.g., gravity data have

to be referred or reduced with respect to a certain height worldwide in order to compute satellite orbits, the importance is obvious. Unification of a vertical datum means here that the potential differences between different tide gauges should be determined with sufficient accuracy.

With the availability of precise satellite altimeter data (SEASAT; ERS-1 to be launched in 1989/90) a new observation type was found which can significantly contribute to this problem (Mather et al 1978). On the other hand a promising approach was presented by Colombo (1980) where he used gravimetric and leveling data together with a low degree reference gravity field model in a simulation study to compute the potential differences between transoceanic leveling bench marks.

The presented approach here goes one step further. It combines all available geodetic data to solve the vertical datum problem. Moreover, since the quality of satellite altimeter data depend mainly on a precise orbit its determination is included. This enables the user to correct also for errors of given orbit information in a physical model using the true covariance propagation through the observation equation. The underlying theoretical approximation model is the so-called "integrated geodesy adjustment" (Eeg and Krarup 1973, Hein 1982). In particular, the form of the observation equation of satellite altimetry leads to a new concept in treating altimeter data. Since the orbit determination is outlined only briefly in the appendix, the reader is referred to (Eissfeller and Hein 1985) for more details with that respect.

2. THE OBSERVATION EQUATIONS

2.1 Data

Let us assume that the following data are available (demonstrated in Fig. 1):

- satellite altimeter data near tide gauges
- observed potential differences (leveling data combined with gravity observations) between tide gauges
- absolute gravity observations at tide gauges (the absolute gravity data can be determined by relative measurements)
- gravity anomalies and deflections of the vertical in a cap, say 50 to 100 km, around the tide gauges.

It should be pointed out, that it is not necessary for the approach presented here that all kind of data have to be considered in the adjustment model. For example, satellite altimetry data can solve the problem alone. However, for the sake of obtaining the highest accuracy it is advisable to use all available information. The model is also suited for transoceanic connections.

2.2 The observation equation of satellite altimetry

The basic observable of a satellite altimeter is given by

$$H(t) = h(t) - \tau(t) \quad (2-1)$$

where $H(t)$ is the altimeter reading, $h(t)$ the distance between satellite and geoid and $\tau(t)$ is the separation between sea surface and the geoid (see Fig. 2). All quantities refer to time t . The quantity $\tau(t)$ is the sum of several effects like ocean tides, wind, ocean currents, atmospheric pressure and salinity. It can range in the meter level. We assume further, that the satellite Q is

INTEGRATED GEODESY ADJUSTMENT FOR VERTICAL DATUM DEFINITION



SATELLITE ALTIMETRY + LEVELING + GRAVITY ANOMALIES

IAPG

UNIVERSITY FAF MUNICH

NAVD '85 - 2

stabilized in the sense that the measuring direction coincides with the local gravity vector in Q .

For the linearization of (2-1) we introduce approximate values $\tau^0(t)$ and $h^0(t)$. If available, $\tau^0(t)$ can be defined by an oceanic tide model and/or additional oceanographic information. Otherwise $\tau^0(t) = 0$ is certainly justified for linearizing (2-1).

For $h^0(t)$ we have to compute the intersection of the straight line in the measuring direction of the altimeter, approximated by the normal gravity vector \underline{j} at \underline{x}_Q , and the reference potential surface $U = W_0$ where W_0 is the gravity potential at the geoid. Thus, the position vector $\underline{x}_0(t)$ of the corresponding point in an inertial reference frame at the geoid is given by

$$\underline{x}_0(t) = \underline{x}_Q(t) + h(t) \underline{n}_Q^*(t) \quad (2-2)$$

where the normal vector at Q is

$$\underline{n}_Q^*(t) = \underline{g}_Q^*(t) / |\underline{g}_Q^*(t)| \quad (2-3)$$

and (2-2) is subject to

$$W(\underline{x}_0(t)) = W_0(\underline{x}_0^0(t) + \delta \underline{x}_0(t)) = \text{const} . \quad (2-4)$$

By $\underline{g}_Q^*(t)$ we denote the gravity vector at the satellite Q .

Some remarks on the introduction of a reference gravity potential U^* . In order to have a good approximation of the gravity potential we propose to introduce a low-order spherical harmonic expansion of the geopotential (e.g. GEM 10C) whose reference surface is close to the sea surface and the geoid, respectively. Due to the orbit consideration in our concept is the introduction of an ellipsoidal normal potential no longer justified. By $*$ we denote all quantities referring to the inertial system considered in the orbit computations. Consequently, for quantities at the earth's surface the centrifugal potential has to be added,

$$U = U^* + 0.5 \omega^2 r^2 \cos^2 b \quad (2-5)$$

where ω is the angular velocity of the earth's rotation, r is the radius and b the spherical latitude of the considered point.

For the linear variation of (2-1),

$$\delta H(t) = \delta h(t) - \delta \tau(t) \quad (2-6)$$

where

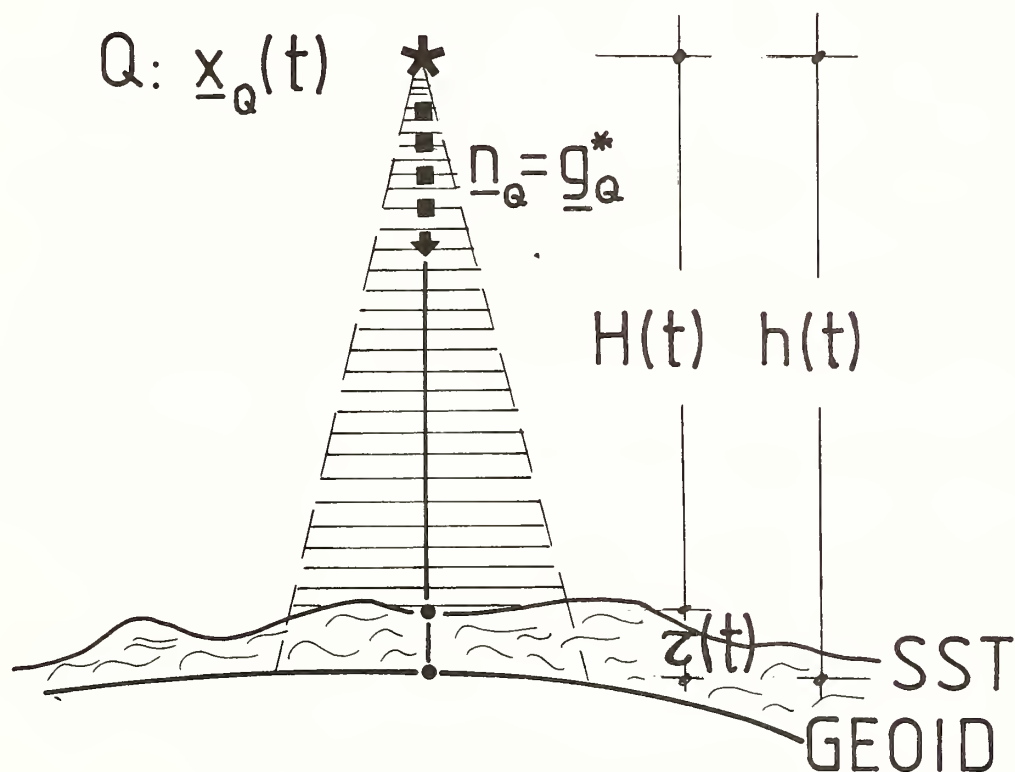
$$\delta h(t) = h(t) - h^0(t) \quad (2-7)$$

$$\delta \tau(t) = \tau(t) - \tau^0(t) \quad (2-8)$$

$$\text{and } h^0(t) = |\underline{x}_Q^0 - \underline{x}_0^0| \quad (2-9)$$

we need the linearized form of (2-2)

GEOMETRY OF SATELLITE ALTIMETRY



$H(t)$... altimeter reading

$h(t)$... distance satellite – geoid ($W=W_0$)

$z(t)$... sea–surface topography

IAPG

UNIVERSITY FAF MUNICH

NAVD '85 – 6

$$\delta \underline{x}_0(t) = \delta \underline{x}_Q(t) + h^0(t) \delta \underline{n}_Q^{**}(t) + \delta h(t) \underline{n}_Q^{0**}(t) \quad (2-10)$$

$\delta \underline{x}_Q$ is the variation of the satellite position derived in the appendix, see eq. (A-16). In other words: Here enters the orbit computation into the observation equation of satellite altimetry. If the orbit is considered to be given without any error, then

$$\begin{aligned} \delta \underline{x}_Q &= 0 \\ \underline{x}_Q^0 &= \underline{x}_Q \end{aligned} \quad (2-11)$$

In order to find the $\delta h(t)$, see (2-7), we have to eliminate the variation $\delta \underline{x}_0(t)$ at the geoid in (2-10) by considering the linear condition (2-4). Denoting by $\underline{y} = [y_1 \ y_2 \ y_3]^T$ the position vector in our earth-fixed reference frame, and introducing the corresponding approximate vector \underline{y}^0 near the geoid (intersection point of approximate altimeter measuring direction and $U = W_0$) the linear condition (2-4) reads (neglecting second order terms $O_2(T \cdot \delta \underline{y}, \dots)$)

$$U(\underline{y}^0) + \left. \frac{\partial U}{\partial \underline{y}} \right|_{\underline{y}=\underline{y}^0} \delta \underline{y} + T(\underline{y}^0) = W_0 \quad (2-12)$$

or, using

$$\frac{\partial U}{\partial \underline{y}} = \underline{j}^T \quad (2-13)$$

and upper indices 0 (indicating that the corresponding quantities have to be evaluated at $\underline{y}^0 = \underline{y}^0(t)$) we get

$$U^0 + \underline{j}^T \delta \underline{y} + T = W_0 \quad (2-14)$$

T is the disturbing potential referring to the introduced spherical harmonic expansion of the geopotential. The still to defining quantities $\delta \underline{n}_Q^{**}(t)$ and $\underline{n}_Q^{0**}(t)$ in (2-10) can be found from (2-3). Further, \underline{g}_Q^{**} has to be linearized using the decomposition

$$\underline{g}_Q^{**} = \underline{j}_Q^{**} + \delta \underline{g}_Q^{**} \quad (2-15)$$

where $\delta \underline{g}_Q^{**}$ is given by (Hein 1982)

$$\delta \underline{g}_Q^{**} = \underline{R}(t) \begin{bmatrix} \cos b \cos l & -\sin b \cos l/r & -\sin l/r \cos b \\ \cos b \sin l & -\sin b \sin l/r & \cos l/r \cos b \\ \sin b & \cos b/r & 0 \end{bmatrix} \begin{bmatrix} \partial T / \partial r \\ \partial T / \partial b \\ \partial T / \partial l \end{bmatrix}_Q \quad (2-16)$$

$\underline{R}(t)$ is a rotation matrix due to nutation, precession, earth-rotation and polar motion referring to an instantaneous time t . It is explicitly defined in (Eissfeller and Hein 1985). r, b, l are spherical coordinates (radius, latitude, longitude). Applying a Taylor expansion we get

$$\begin{aligned}
\underline{n}_Q^*(t) &= \frac{\underline{j}_Q^*}{|\underline{j}_Q^*|} + \frac{1}{|\underline{j}_Q^*|} \left(\underline{I} - \frac{\underline{j}_Q^* \underline{j}_Q^{*T}}{|\underline{j}_Q^*|^2} \right) \frac{\partial \underline{j}_Q^*}{\partial \underline{x}_Q} \delta \underline{x}_Q \\
&\quad + \frac{1}{|\underline{j}_Q^*|} \left(\underline{I} - \frac{\underline{j}_Q^* \underline{j}_Q^{*T}}{|\underline{j}_Q^*|^2} \right) \delta \underline{g}_Q^* + 0_2(\delta \underline{g}_Q^*, \delta \underline{x}_Q)
\end{aligned} \tag{2-17}$$

where $\underline{j}_Q^* = \underline{j}_Q^*(\underline{x}_Q^0)$ and all quantities refer to the inertial system. \underline{I} is the identity matrix. Thus,

$$\underline{j}_Q^* = \underline{R}(t) \underline{j}_Q \tag{2-18}$$

$$|\underline{j}_Q^*| = [\underline{j}_Q^T \underline{R}^T(t) \underline{R}(t) \underline{j}_Q]^{0.5} = |\underline{j}_Q| \tag{2-19}$$

$$\delta \underline{g}_Q^* = \underline{R}(t) \delta \underline{g}_Q \tag{2-20}$$

$$\frac{\partial \underline{j}_Q^*}{\partial \underline{x}_Q} = \underline{R}(t) \left. \frac{\partial \underline{j}}{\partial \underline{y}} \right|_Q \underline{R}^T(t) \tag{2-21}$$

$$\underline{j}_Q^* \underline{j}_Q^{*T} = \underline{R}(t) \underline{j}_Q \underline{j}_Q^T \underline{R}^T(t) \tag{2-22}$$

The approximation value $\underline{n}_Q^{0*}(t)$ of the vector in measuring direction of the altimeter (gravity vector in \underline{Q}) and its variation $\delta \underline{n}_Q^*(t)$ is found from (2-17).

$$\underline{n}_Q^{0*}(t) = \frac{\underline{j}_Q^*}{|\underline{j}_Q^*|} \tag{2-23}$$

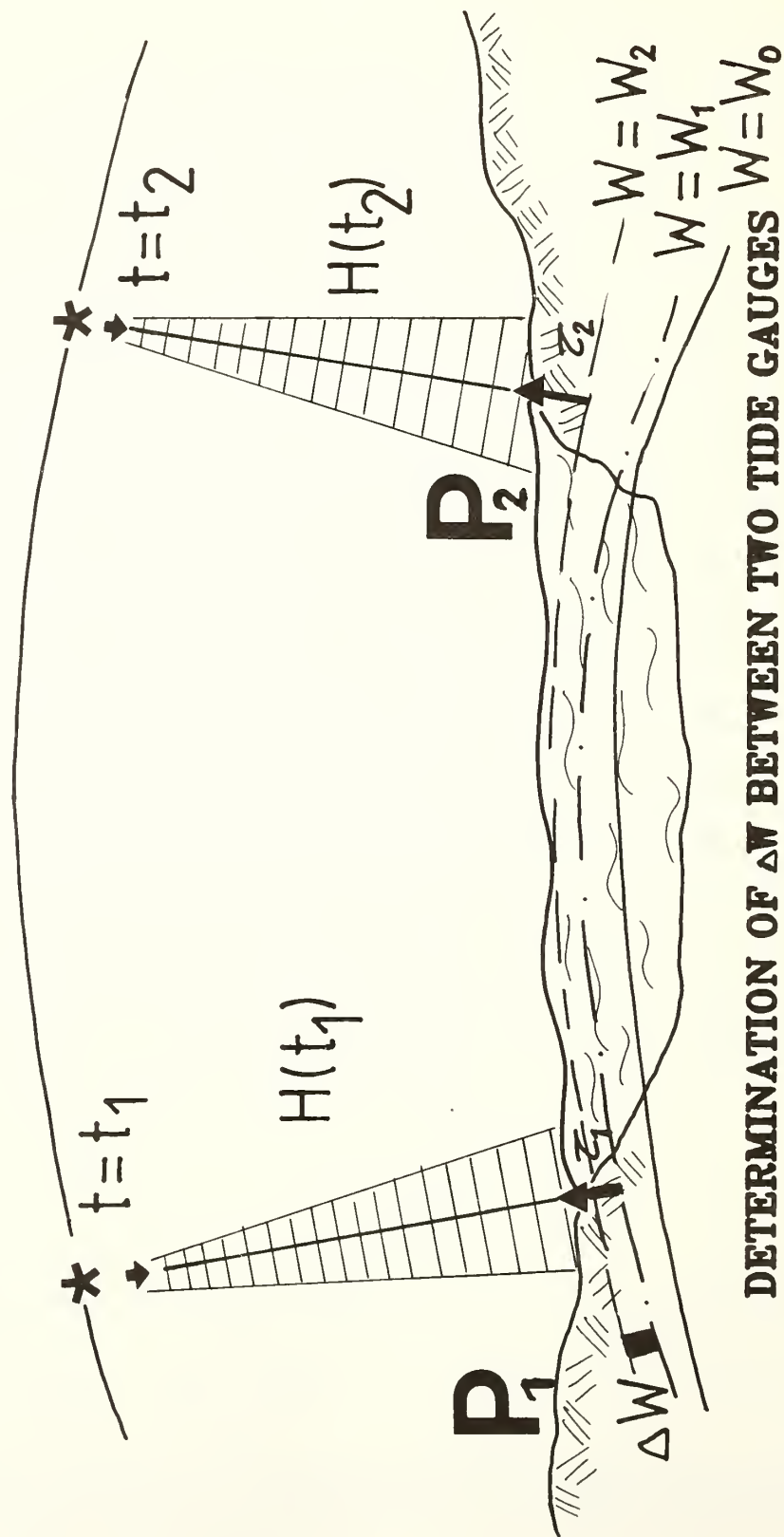
$$\begin{aligned}
\delta \underline{n}_Q^*(t) &= \frac{1}{|\underline{j}_Q^*|} \left(\underline{I} - \frac{\underline{j}_Q^* \underline{j}_Q^{*T}}{|\underline{j}_Q^*|^2} \right) \frac{\partial \underline{j}_Q^*}{\partial \underline{x}_Q} \delta \underline{x}_Q \\
&\quad + \frac{1}{|\underline{j}_Q^*|} \left(\underline{I} - \frac{\underline{j}_Q^* \underline{j}_Q^{*T}}{|\underline{j}_Q^*|^2} \right) \delta \underline{g}_Q^*
\end{aligned} \tag{2-24}$$

For the final linearized observation equation of altimetry we have to transform (2-10) from the inertial system into an earth-fixed reference frame by

$$\delta \underline{y}_0(t) = \underline{R}^T(t) \delta \underline{x}_Q(t) + h^0(t) \underline{R}(t) \delta \underline{n}_Q^*(t) + \delta h(t) \underline{R}^T(t) \underline{n}_Q^{0*}(t) \tag{2-25}$$

and to insert it in (2-14) using (2-23), (2-24) and the orbit variation $\delta \underline{x}_Q(t)$, see (A-16). After having done this we get

THE OBSERVATION EQUATION OF SATELLITE ALTIMETRY: DIFFERENCE MODE



DETERMINATION OF ΔW BETWEEN TWO TIDE GAUGES

$$\begin{aligned}
\underline{j}^T(t) \underline{n}_Q^0(t) \delta h(t) &= W_0 - U(t) \\
&- \underline{j}^T(t) \underline{N}_1(t) \frac{\partial \underline{x}_Q^0(t)}{\partial \underline{u}(t)} \frac{\partial \underline{u}(t)}{\partial \underline{p}} \delta \underline{p} \\
&- T(t) \\
&- \underline{j}^T(t) \underline{N}_1(t) \frac{\partial \underline{x}_Q^0(t)}{\partial \underline{u}(t)} \int_{t_0}^t \frac{\partial \underline{u}(t)}{\partial \dot{\underline{x}}_Q^0(t)} \underline{R}(t) \delta \underline{g}_Q(t) dt \\
&- \underline{j}^T(t) \underline{N}_2(t) \delta \underline{g}_Q(t)
\end{aligned} \tag{2-25}$$

where

$$\underline{N}_1(t) = \underline{R}(t) - \frac{h^0(t)}{|\underline{j}_Q(t)|} \left[\underline{I} - \frac{\underline{j}_Q(t) \underline{j}_Q^T(t)}{|\underline{j}_Q(t)|^2} \right] \frac{\partial \underline{j}}{\partial \underline{y}} \underline{R}^T(t) \tag{2-26}$$

$$\underline{N}_2(t) = \frac{h^0(t)}{|\underline{j}_Q(t)|} \left[\underline{I} - \frac{\underline{j}_Q(t) \underline{j}_Q^T(t)}{|\underline{j}_Q(t)|^2} \right] \tag{2-27}$$

The linearized observation equation of altimetry (2-25) has certain similarities with the one of geodetic leveling. The fourth line of the right hand side of (2-25) can be considered as a path-dependent expression along the instrument - here the satellite - moves.

In order to get a direct relation for the potential difference between two tide gauges P_1, P_2 we use the difference of altimeter readings at times t_1, t_2 converted to geopotential units, as observation. Thus, the altimeter observation equation in difference mode reads

$$\begin{aligned}
P(t_2, t_1) &= \underline{j}^T(t_2) \underline{n}_Q^0(t_2) h(t_2) - \underline{j}^T(t_1) \underline{n}_Q^0(t_1) h(t_1) \\
&+ \underline{j}^T(t_1) \underline{n}_Q^0(t_1) \tau(t_1) - \underline{j}^T(t_2) \underline{n}_Q^0(t_2) \tau(t_2)
\end{aligned} \tag{2-28}$$

where the approximate value is given by

$$\begin{aligned}
P^0(t_2, t_1) &= \underline{j}^T(t_2) \underline{n}_Q^0(t_2) h^0(t_2) - \underline{j}^T(t_1) \underline{n}_Q^0(t_1) h^0(t_1) \\
&+ \underline{j}^T(t_1) \underline{n}_Q^0(t_1) \tau^0(t_1) - \underline{j}^T(t_2) \underline{n}_Q^0(t_2) \tau^0(t_2)
\end{aligned} \tag{2-29}$$

and the variation $\delta P(t_2, t_1)$ is derived from the corresponding expressions (2-25).

$$\begin{aligned}
\delta P(t_2, t_1) &= U(P_1, t_1) - U(P_2, t_2) \\
&+ \left[\underline{j}^T(t_1) \underline{N}_1(t_1) \frac{\partial \underline{x}_Q^0(t_1)}{\partial \underline{u}(t_1)} \frac{\partial \underline{u}(t_1)}{\partial \underline{p}} - \underline{j}^T(t_2) \underline{N}_1(t_2) \frac{\partial \underline{x}_Q^0(t_2)}{\partial \underline{u}(t_2)} \frac{\partial \underline{u}(t_2)}{\partial \underline{p}} \right] \delta \underline{p} \\
&+ T(P_2, t_2) - T(P_1, t_1)
\end{aligned}$$

$$\begin{aligned}
& + \underline{j}^T(t_1) \underline{N}_1(t_1) \frac{\partial \underline{x}_Q(t_1)}{\partial \underline{u}(t_1)} \frac{t_1}{t_0} \frac{\partial \underline{u}(t)}{\partial \dot{\underline{x}}_Q(t)} \underline{R}(t) \delta \underline{g}_Q(t) dt \\
& - \underline{j}^T(t_2) \underline{N}_1(t_2) \frac{\partial \underline{x}_Q^0(t_2)}{\partial \underline{u}(t_2)} \frac{t_2}{t_0} \frac{\partial \underline{u}(t)}{\partial \dot{\underline{x}}_Q(t)} \underline{R}(t) \delta \underline{g}_Q(t) dt \\
& + \underline{j}^T(t_1) \underline{N}_2(t_1) \delta \underline{g}_Q(t_1) - \underline{j}_Q^T(t_2) \underline{N}_2(t_2) \delta \underline{g}_Q(t_2) \\
& + \underline{j}^T(t_1) \underline{n}_Q^0(t_1) \delta \tau(t_1) - \underline{j}^T(t_2) \underline{n}_Q^0(t_2) \delta \tau(t_2)
\end{aligned} \tag{2-30}$$

By (2-30) we have now an expression for the potential difference between two tide gauges determined by altimeter observations.

2.3 Observation equation for potential differences

Assume that leveling combined with gravity measurements was carried out over land between two tide gauges so that we know the quantity

$$W_j - W_i = \int_{P_i}^{P_j} g dz \quad . \tag{2-31}$$

After linearizing it (see Hein 1982, p. 49) we get the linear observation equation for potential differences (in vectorial form)

$$W_j - W_i = U_j - U_i + \underline{j}_j^T \delta \underline{y}_j - \underline{j}_i^T \delta \underline{y}_i + \tau_j - \tau_i \quad . \tag{2-32}$$

Since we are only interested in the vertical dimension it might be preferable to introduce coordinates $\{\varphi, \lambda, z(U)\}$ instead of (y_1, y_2, y_3) where the directions φ, λ of the normal gravity vector \underline{j} are given by

$$\varphi = \arctan \left\{ \frac{\partial U}{\partial y_3} / \left[\left(\frac{\partial U}{\partial y_1} \right)^2 + \left(\frac{\partial U}{\partial y_2} \right)^2 \right]^{0.5} \right\} \tag{2-33}$$

$$\lambda = \arctan \left(\frac{\partial U}{\partial y_2} / \frac{\partial U}{\partial y_1} \right)$$

and z is a normal height measured along the normal plumb line. Thus, the transformation between the two triples is

$$\delta \underline{y} = \begin{bmatrix} \underline{j}^T \\ \partial \varphi / \partial \underline{y} \\ \partial \lambda / \partial \underline{y} \end{bmatrix}^{-1} \begin{bmatrix} \delta U \\ \delta \varphi \\ \delta \lambda \end{bmatrix} = \begin{bmatrix} \underline{j}^T \\ \partial \varphi / \partial \underline{y} \\ \partial \lambda / \partial \underline{y} \end{bmatrix}^{-1} \begin{bmatrix} -j \delta z \\ \delta \varphi \\ \delta \lambda \end{bmatrix} \tag{2-34}$$

The gradients in the Jacobi matrix (2-34) are analytical functions of the reference gravity potential U , and therefore, easy to compute. The same holds for the inverse Jacobi matrices of the order three.

We are assuming further, that the horizontal coordinates φ, λ are given with

sufficient accuracy. Small changes in those coordinates will not reflect the results. Therefore we set $\delta\varphi = \delta\lambda = 0$ in (2-34)

$$\delta \underline{y} = \begin{bmatrix} \underline{j}^T \\ \partial\varphi/\partial \underline{y} \\ \partial\lambda/\partial \underline{y} \end{bmatrix}^{-1} \begin{bmatrix} -j\delta z \\ 0 \\ 0 \end{bmatrix} \quad (2-35)$$

and insert (2-35) in (2-32). Since δz is a small quantity (< 1 m) there might be no difference in considering it as normal or orthometric height variation.

2.4 Observation equation for absolute gravity

If gravity information is available at the tide gauge we can use the already derived observation equation in (Hein 1982, p. 43).

$$g = |\underline{g}| = (\underline{g}^T \underline{g})^{0.5} \quad (2-36)$$

$$g - j = \frac{\partial j}{\partial \underline{y}} \delta \underline{y} + \frac{j^T}{j} \delta \underline{g} \quad (2-37)$$

For $\delta \underline{y}$ we insert again the expression (2-35). For the gravity values in the cap around the tide gauge we may fix the position $\delta \underline{y}$.

2.5 Observation equations for deflections of the vertical (better: for astronomic latitude and longitude)

Deflections of the vertical can give additional information about the slope of the equipotential surface. We therefore take the linear observation equations of astronomic latitude and longitude from (Hein 1982, p. 39-40) and fix the position again.

3. SOLUTION

All linear observation equation presented in section 2 form a linear system of equations of type

$$\underline{l} = \underline{A} \underline{x} + \underline{R} \underline{t} + \underline{n} \quad (3-1)$$

where

$$\underline{l} = [\delta P(t_i, t_j), \delta W_{ij}, \delta g_i, \delta \phi_i, \delta \Lambda_i, \dots]^T \quad (3-2)$$

$$\underline{x} = [\delta \underline{p}^T, \delta \tau(t_i), \delta z_i, \dots]^T \quad (3-3)$$

$$\underline{t} = [T_i, (\partial T / \partial r)_i, \dots]^T \quad (3-4)$$

\underline{A} , \underline{R} are known coefficient matrices of the deterministic unknown vector and the stochastic vector \underline{t} , respectively. \underline{n} is the vector of observational noise.

Considering (3-1) as a general least-squares collocation model (Eeg and Krarup 1973 Moritz 1980; p. 221 f.) we get the solution for \underline{x} and \underline{t} by minimizing the hybrid norm

$$\underline{n}^T \underline{C}_{nn}^{-1} \underline{n} + \underline{t}^T \underline{K}_{tt}^{-1} \underline{t} = \min \quad (3-5)$$

where \underline{C}_{nn} and \underline{K}_{tt} are appropriate covariance matrices of \underline{n} and \underline{t} , respectively. By

$$\hat{\underline{x}} = (\underline{A}^T \underline{D}^{-1} \underline{A})^{-1} \underline{A}^T \underline{D}^{-1} \underline{l} \quad (3-6)$$

where

$$\underline{D} = \underline{C}_{nn} + \underline{R} \underline{K}_{tt} \underline{R}^T \quad (3-7)$$

we solve for the height offsets δz_i of the tide gauges from the geoid, the sea surface topography ($\delta \tau_i$) and - if it is not given - the orbit of the altimeter satellite. In order to minimize the number of unknowns, it might be possible to expand $\delta \tau_i$ in a series with a few coefficients as function of horizontal position. This would also help to solve the interpolation problem which can occur if satellite altimeter data are not directly available at tide gauges but near to them.

By the stochastic unknown vector \underline{t}

$$\hat{\underline{t}} = \underline{K}_{tt} \underline{R}^T \underline{D}^{-1} (\underline{l} - \underline{A} \hat{\underline{x}}) \quad (3-8)$$

we solve for the residual or disturbing potential (and its functionals) at tide gauges. The error estimates of $\hat{\underline{x}}$ and $\hat{\underline{t}}$ are given by

$$\begin{aligned} \underline{E}_{xx} &= (\underline{A}^T \underline{D}^{-1} \underline{A})^{-1} \\ \underline{E}_{tt} &= \underline{K}_{tt} - \underline{K}_{tt} \underline{R}^T \underline{D}^{-1} (\underline{I} - \underline{A} \underline{E}_{xx} \underline{A}^T \underline{D}^{-1}) \underline{R} \underline{K}_{tt} \end{aligned} \quad (3-9)$$

Stepwise collocation procedures can be applied to get small systems of equations.

4. SUMMARY

By the integrated geodesy adjustment and the new type of treatment of satellite altimeter data together with leveling results, gravity information and deflections of the vertical an optimal solution can be found for the vertical datum problem worldwide. Observations to the Global Positioning System (GPS) - in addition to the discussed measurements - might help to determine the geometrical offset unknowns δz_i . For the corresponding observation equations in the integrated model see (Hein and Eissfeller 1985).

APPENDIX.

Satellite motion and linearization of the position vector $\underline{x}_Q(t)$

If the orbit in the observation equation of satellite altimetry is considered to be unknown, the position vector $\underline{x}_Q(t)$ of the satellite has to be linearized and to inserted in (2-24). Thus, orbit integration enters into our model at that stage.

In the following we summarize briefly the derivations. For the reader who is more interested in the details, we refer to (Eissfeller and Hein 1985, Eissfeller 1985).

The basic vector differential equation of satellite motion in an inertial reference frame is given by

$$\ddot{\underline{x}} = \underline{a}(\underline{x}, \dot{\underline{x}}, t) \quad (\text{A-1})$$

where

\underline{x} is the position vector

$\dot{\underline{x}} = \frac{d\underline{x}}{dt}$ is the velocity vector

$\ddot{\underline{x}} = \frac{d^2\underline{x}}{dt^2}$ is the acceleration vector

and

\underline{a} is the vector of resulting accelerations

It is known from classical perturbation theory, that the position and the velocity vector of a satellite are of the form

$$\underline{x} = \underline{x}(\underline{u}(t), t) \quad (\text{A-2})$$

$$\dot{\underline{x}} = \dot{\underline{x}}(\underline{u}(t), t) \quad (\text{A-3})$$

where the vector $\underline{u}(t)$ usually consists of six time dependent Kepler elements

$$\underline{u}(t) = [\Omega(t), i(t), \omega(t), a(t), \epsilon(t), t_p(t)]^T \quad (\text{A-4})$$

The vector $\underline{u}(t)$ in (A-4) is a solution of the following nonlinear vector differential equation

$$\dot{\underline{u}}(t) = \frac{\partial \underline{u}(t)}{\partial \dot{\underline{x}}(t)} \underline{a}_1(t) \quad (\text{A-5})$$

The Jacobi matrix $\partial \underline{u}(t) / \partial \dot{\underline{x}}(t)$ is a 6×3 matrix defined by the partial derivatives of the Kepler elements with respect to velocity coordinates. For the explicit form see (Eissfeller 1985). $\underline{a}_1(t)$ in (A-5) is the vector of disturbing acceleration, which is obtained from the original acceleration vector $\underline{a}(t)$ by subtracting the radial symmetrical term $\underline{a}_0(t)$ of the earth's gravity field. Thus,

$$\underline{a}_1(t) = \underline{a}(t) - \underline{a}_0(t) \quad (\text{A-6})$$

$$\underline{a}_0(t) = \frac{GM}{r} \underline{x} \quad (\text{A-7})$$

For the following linearization procedure it is useful to write (A-5) as an integral equation

$$\underline{u}(t) = \underline{u}_0 + \int_{t_0}^t \frac{\partial \underline{u}(t)}{\partial \dot{\underline{x}}(t)} \underline{a}_1(t) dt \quad (\text{A-8})$$

where \underline{u}_0 is the initial state vector of (A-4).

In order to find a linear variation of the position vector we decompose $\underline{a}_1(t)$.

$$\underline{a}_1(t) = \underline{g}_1^*(t) + \underline{f}(t) \quad ^1) \quad (A-9)$$

$\underline{g}_1^*(t)$ is the gravity vector (without the radial symmetrical part \underline{a}_0). \underline{f} is the vector of remaining disturbing accelerations.

More precisely, we have to consider, that the vectors \underline{g}_1^* and \underline{f} depend on the Kepler elements and on a vector \underline{p} of unknown dynamical parameters.

$$\underline{g}_1^*(t) = \underline{g}_1^*(\underline{u}(\underline{p}, t), t) \quad (A-10)$$

$$\underline{f}(t) = \underline{f}(\underline{u}(\underline{p}, t), \underline{p}, t) \quad (A-11)$$

Since the spherical harmonic coefficients and the earth rotation parameters enter in principle (A-11) and treated as known constants in this approach, \underline{g}_1^* (A-10) is not explicitly dependent of \underline{p} , such as \underline{f} (A-11) is.

The vector of Kepler elements \underline{u} depends of the dynamical parameters \underline{p} , since \underline{u} is a solution of (A-5).

Applying now the following two linearization steps

$$(i) \quad \underline{g}_1^* = \underline{j}_1^* + \delta \underline{g}_1^* \quad (A-12)$$

$$(ii) \quad \underline{p} = \underline{p}^0 + \delta \underline{p} \quad (A-13)$$

leads to the linear variation $\delta \underline{u}(t)$ of Kepler elements

$$\delta \underline{u}(t) = \frac{\partial \underline{u}(t)}{\partial \underline{p}} \delta \underline{p} + \int_{t_0}^t \frac{\partial \underline{u}(t)}{\partial \dot{\underline{x}}(t)} \delta \underline{g}_1^*(t) dt \quad (A-14)$$

The Jacobi matrix $\partial \underline{u}(t)/\partial \underline{p}$ is a solution of the inhomogeneous matrix differential equation (A-14).

$$\begin{aligned} \frac{\partial \dot{\underline{u}}}{\partial \underline{p}} = & \left[\frac{\partial}{\partial \Omega} \left(\frac{\partial \underline{u}}{\partial \dot{\underline{x}}} \right) \underline{a}_1, \frac{\partial}{\partial i} \left(\frac{\partial \underline{u}}{\partial \dot{\underline{x}}} \right) \underline{a}_1, \dots, \frac{\partial}{\partial t_p} \left(\frac{\partial \underline{u}}{\partial \dot{\underline{x}}} \right) \underline{a}_1 \right] \frac{\partial \underline{u}}{\partial \underline{p}} \\ & + \frac{\partial \underline{u}}{\partial \dot{\underline{x}}} \frac{\partial \underline{a}_1}{\partial \underline{u}} \frac{\partial \underline{u}}{\partial \underline{p}} + \frac{\partial \underline{u}}{\partial \dot{\underline{x}}} \frac{\partial \underline{a}_1}{\partial \underline{p}} \end{aligned} \quad (A-15)$$

This can be deduced from applying the gradient operator $\frac{\partial}{\partial \underline{p}}$ on both sides of (A-5).

With $\delta \underline{u}(t)$ (A-14) we find the variation $\delta \underline{x}_Q$ of the position vector $\underline{x}_Q(t)$ of the altimeter satellite Q

$$\delta \underline{x}_Q(t) = \frac{\partial \underline{x}_Q(t)}{\partial \underline{u}(t)} \frac{\partial \underline{u}(t)}{\partial \underline{p}} \delta \underline{p} + \frac{\partial \underline{x}_Q(t)}{\partial \underline{u}(t)} \int_{t_0}^t \frac{\partial \underline{u}(t)}{\partial \dot{\underline{x}}_Q(t)} \delta \underline{g}_Q^*(t) dt \quad (A-16)$$

¹⁾ Quantities of the gravity field with an asterisk refer to the inertial system.

Since the gravity disturbing vector $\delta \ddot{g}_Q$ in (A-16) refers to the inertial system, but is usually referred to an earth-fixed CIO system in spherical coordinates (r, b, l) , we have to use the following transformation

$$\delta \ddot{g}_Q = \underline{R}(t) \begin{bmatrix} \cos b \cos l & -\sin b \cos l/r & -\sin l/r \cos b \\ \cos b \sin l & -\sin b \sin l/r & \cos l/r \cos b \\ \sin b & \cos b/r & 0 \end{bmatrix} \begin{bmatrix} \frac{\partial T}{\partial r} \\ \frac{\partial T}{\partial b} \\ \frac{\partial T}{\partial l} \end{bmatrix}_Q \quad (A-17)$$

The detailed matrix $\underline{R}(t)$ is given in (Eissfeller and Hein 1985). It consists of

$$\underline{R}(t) = \underline{N}(t_0) \underline{P}(t_0) \underline{P}^T(t) \underline{N}^T(t) \underline{R}_3(-\theta(t)) \underline{S}(t) \quad (A-18)$$

where

\underline{N} is the nutation matrix
 \underline{P} is the precession matrix
 \underline{R}_3 is an earth-rotation matrix
 \underline{S} is the matrix of pole coordinates
 θ is the siderial time of Greenwich
 t is the time variable

and t_0 is the initial time of orbit integration .

REFERENCES

- Colombo, O.L., 1980: A world vertical network. Department of Geodetic Science, The Ohio State University, Report No. 296, Columbus, Ohio
- Eeg, J. and T. Krarup, 1973: Integrated geodesy. The Danish Geodetic Institute, Internal Report No. 7, Copenhagen
- Eissfeller, B., 1985: Orbit improvement using local gravity field information and least-squares prediction. Manuscripta Geodaetica 10(2), in print
- Eissfeller, B. and G.W. Hein, 1985: A contribution to 3d-operational geodesy. Part 4: The observation equations of satellite geodesy in the model of integrated geodesy. Report of the University FAF Munich, in print
- Hein, G.W., 1982: A contribution to 3d-operational geodesy. Part 1: Principle and observation equations of terrestrial type. Deutsche Geodätische Kommission, Reihe B, Nr. 258/VII, 31-64, München
- Hein, G.W. and B. Eissfeller, 1985: Integrated modelling of GPS-orbits and multi-baseline components. Proceedings of the First International Symposium on Precise Positioning with the Global Positioning System, Rockville, Maryland, April 15-19, 1985
- Mather, R.S., C. Rizos and T. Morrison, 1978: On the unification of geodetic leveling datums using satellite altimetry. NASA Technical Memorandum 79533
- Moritz, H., 1980: Advanced Physical Geodesy. Herbert Wichmann Verlag, Karlsruhe

LEVELLING WITH THE HELP OF SPACE TECHNIQUES

Oscar L. Colombo
EG&G WASCI
5000 Philadelphia Way, Suite J
Lanham, MD 20706

ABSTRACT. Geodetic levelling, the precise measurement of geopotential differences, has two main applications: finding the vertical coordinates of stations, and determining slopes with respect to a horizontal surface. The first is relevant to establishing geometric positions, and the second is needed sometimes in hydraulic engineering and in science. An example of a scientific application is the study of the departure of the sea surface from a true equipotential surface along the shore. The increasing accuracy and the decreasing cost of space techniques is continuously diminishing the importance of levelling for position determination. In fact, space methods are getting better at estimating not only relative coordinates, but absolute (geocentric) ones as well. But even if these new tools for finding geometric position make the old ones obsolete, some form of levelling will still be needed to measure physical slopes, though sometimes this may be done in ways quite different from those of today. It is conceivable that geodesists, having found station coordinates with space techniques, may then use them to calculate geopotential differences worldwide. This they might do by combining those coordinates with various measurements of the gravity field. Furthermore, for as long as conventional levelling nets remain in use, such combinations can provide vertical control points that are not tide gauges and that can be placed inland. This will have particular interest for those dealing with an area of continental dimensions, like North America, where there are many stations located far from the sea and from each other. The technology needed for this may very well exist already, although the current knowledge of the gravity field seems insufficient. This knowledge could be improved using data from satellites to make better models of that field. In a number of ways, levelling can benefit from the achievements in space geodesy, and play a complementary role in the study of the earth.

SATELLITE GEODESY AND LEVELLING

Over the last three decades, the accuracies of position fixes based on observations of orbiting spacecraft have increased to the point where some laser tracking systems seem close to giving absolute position to better than 0.1 m in all three coordinates. Relative positions inside areas 1000 km or so across are, for some systems, already well below 0.1 m. In addition, the last decade has brought to maturity a new space technique based on the radio waves emitted by distant quasy stellar objects: the method known as very long baseline interferometry, or VLBI. This method is particularly good for measuring distances between points separated by thousands of kilometers and also for observing earth

orientation and rotation. Satellite laser ranging (SLR) is at present catching up with VLBI in accuracy, and both can eventually provide an excellent reference frame and a universal first order net of station coordinates and interstation baselines. Because of the operating costs and logistic problems associated with these techniques, it looks as if (for the next decade at least) their main use may be confined to providing the basic geodetic "skeleton": the reference system and first order global network, whose densification may be done, to an ever increasing extent, by the use of GPS or similar space systems that already may give relative positions at the subdecimeter level for stations less than 500 Km apart. The absolute position then comes from tying the local net to one of the first order points of the SLR/VLBI network. Therefore, in the near future (and perhaps even right now) space geodesy seems likely to exceed by a generous margin the demands of traditional geodetic mapping. In fact, the main reason for achieving subdecimeter accuracies is now the geophysical rather than the purely geodetic use of position determination, particularly the study of crustal movements, plate tectonics, and earth rotation (including precession nutation and polar motion).

Unless some unforeseen difficulties arise with the use of the space techniques, they seem destined to achieve most of the goals of traditional geodetic methods, and also to go a long way beyond that. This means that leveling (in the sense of determining potential differences), except for some local applications mostly related to the construction of waterways, hydroelectric dams and the like, may one day become a redundant and uneconomical way of determining heights for topographic mapping and similar classical purposes.

At this point I would like to repeat that the space methods that seem likely to phase out the older "terrestrial" ones for classical geodetic work, will do so because of their ever increasing accuracy, both local and global, and that the driving force behind the push for greater accuracy is mostly science rather than map-making. Potential differences, which classically have been more of a means to an end (mapping geometric heights), than an end in themselves, have a physical meaning that complements purely geometric fixes. By comparing the relative geometric heights of two points with their potential difference, it is possible to estimate the tilt of the line between them with respect to the horizontal (if the line is relatively short), and by re-surveying both positions and potentials, to estimate the change in that tilt.

In this context, the largely theoretical work done on solving simultaneously for position in three dimensions using both "geometrical" (i.e., satellite fixes) and "gravity" (i.e., measurements of first order gradients of gravity, etc.) may acquire a new and more practical interest in the near future. The main reason is that any method that truly "integrates" geometric data with gravity can give more than three dimensional geometric coordinates, it can give also (if so desired) potential differences. So one might use the most accurate position measurements with the best terrestrial gravity data and with the most accurate field model derived from space techniques, to get what could be a very good set of estimates of both position and of potential differences over the same set of stations: a unified, high quality network containing two complementary and scientifically important kinds of information on the earth's surface. Finally, some of the benchmarks of this "integrated" network could be used to control the adjustment of conventional levelling nets. Since their set up requires only position and gravity, two things that can be measured on land, these control points can be placed anywhere inside a country or a continent, without the restrictions presented by tide gauges that have to be put along a coast, sometimes very far

from the interior. Finally, such a net does not have to be restricted to the confines of a country or a continent, but can span the whole world, just as satellite position nets do.

It is the steady and independent improvement of the various systems that could be "integrated" or brought together in this way, and the high accuracy already reached by them, that makes this idea of "integration" both interesting and, perhaps, ripe for experimental investigation.

THE DEFINITION OF THE VERTICAL DATUM

As this paper is presented in a symposium on the determination of the vertical datum, I would like to say that, having benchmarks where both position and potential are known to a high accuracy, it is possible to choose any of them as the point of "zero height" or datum, the heights of the others being the accurately known potential differences with respect to that datum. At present, this is actually what is done, except that it is always a tide gauge that is chosen as having "zero height". Because of dynamic oceanographic effects (sea surface topography) the sea surface does not lie on the same equipotential at all tide gauges. It is current practice to assume, by so constraining the adjustment, that all the gauges are on an equipotential: this may result in a systematic warping of the adjusted heights that is probably worst in those parts of the net farthest from the gauges. The "accuracy" of the tide gauge (i.e., the uncertainty due to the sea surface topography) is about 1 kgal m (or 1.5 kgal m for the potential difference between two tide gauges). This is pretty far from the goal of tenth of kgal m accuracies mentioned so far. Assume now that an "integrated" position plus levelling net were to achieve such accuracy and its control points were used to establish height everywhere. This would cause the novel problem that even if a tide gauge (connected to this net) were chosen as the datum, some points along the coast would turn out to be below, and some above, the sea level as defined by that gauge, because of the sea surface topography. It has been pointed out that "below sea level" land shown in the chart of a coastal region might confuse some, and be bad for local business generally. If true, this problem may be avoided by using a "local mean sea level" for the region, based on a local tide gauge, when producing regional maps. With at least one station connected both to this gauge and also to the larger (national, international) net, both sets of heights may be converted unambiguously to each other, when necessary. In any event, this is a cadastral problem, while the main reason for setting up very accurate, large, "integrated" nets is likely to be a scientific one, at least in the long run.

THE "INTEGRATED" APPROACH: A MOST INCOMPLETE HISTORIC OUTLINE

The idea of an "integrated" determination of position (and potential) goes such a long way back, and has been pursued by so many, in so many ways, over the years, that I would be unable, out of sheer ignorance of the topic and lack of space, to give credit to even all the main contributors. Instead, I am going to tell here the story of a particular approach, developed by myself several years ago (mostly as a means of estimating the possible accuracy of integrated solutions, rather than as a prescription for practical work), and then to say something about how this idea fits with others, more general and better developed than mine. This discussion will also allow me to give a rudimentary introduction to the principles behind "integration", and a concrete set of ideas for discussing accuracy, as well as what things may influence most the error budget.

In the late Seventies I proposed (Colombo, 1980a and 1980b) using accurate position fixes and some global (i.e., satellite) field model to compute the potential differences between pairs of benchmarks forming a world vertical net. These calculated values would be in error mostly because of the deficiencies of the field model used, supposing that the position fixes from, say, SLR, were very accurate. The global accuracy in field models stood then (and has not improved much since) at about 3 m for point values, so the potential differences could be wrong by about $\sqrt{2} \times 3 = 4.5$ m (or kgal m). These are globally averaged root mean square values (r.m.s.). Compared to that a few decimeters' error in station position is quite negligible. Undeniably, 4.5 kgal m is no improvement over the 1.5 kgal m already offered by tide gauges, but here is where the "integration" of position with local gravity measurements comes along. The error in potential due to the field model is the same as the error in geoid height times the local acceleration of gravity. To obtain accurate geoid heights, the usual procedure these days is to calculate such heights first at a known position using a field model, and then to correct the result by using local gravity measurements around the point in question to estimate the "anomalous" part of the geoid (i.e., that not represented in the model). What has changed from the days before space geodesy is mostly how the positions are determined, and also the nature of the field model, while the "geoid" has graduated from a mere ellipsoid to a more complex figure departing from the former not only with latitude, but also with longitude. As for the way in which the rough values calculated with the model can be refined with local data, the most conventional way would be to use slightly modified gravity anomalies (not referred to a datum based on a tide gauge, but to the benchmark where the "refining" will be done, as in (Colombo, 1b.)) and an appropriately modified form of Stokes' integral formula to estimate the part of the geoid missing from the model. Because of practical considerations, gravity has to be confined to a region near the point of computation (the benchmark). In most theoretical papers such regions are shown as neatly drawn circles, but they need not be so. Instead of Stokes' formula, I used that of least squares collocation for my error analysis, because this method can provide reasonable estimates of the uncertainties due to field model and data errors, as well as of the lack of data outside the circle and the sparsity of the data within. For understanding the idea of collocation, the best introductory text probably remains Heiskanen and Moritz (1967). The experience of recent years seems to indicate that any reasonably executed estimate of the anomalous potential, regardless of technique, is just about as good as any other, but in the case of my study (an error analysis) collocation was particularly suitable for getting a feeling for the problem. What emerged was that the main cause of error could be the field model used, with (random) position and gravity data errors coming a very distant second. Recently, this study has been carried considerably further by Hajela (1983), who not only confirmed my main conclusions, but came up with information that allows me now to put down on paper some numbers that are more relevant to the present situation. Before getting into details, I should explain that my idea for "integrating" geometric and gravity data in a "collocation" adjustment has turned out to be part of a much larger one developed by Eeg and Krarup (1975), Hein (1982), and others, what one might call the "collocation brand" of integrated geodesy. As this paper is an essay on ideas, (which are formulated rigorously in the references) the reader will continue to find his vision unobtruded by equations right to the very end.

THE LIKELY ACCURACY OF AN "INTEGRATED" NETWORK

The accuracy of station coordinates' determination using satellites seems likely to reach the subdecimeter level soon; that of potential differences should depend mostly (according to the studies mentioned before) on the quality of the field model. Particularly important is the amount of error in the spherical harmonics of such models below degree and order 30. Hajela (1983) has shown that, with a cap of 5° around a benchmark containing 3000 measurements of gravity at about 20 km intervals, the benchmark potential could be estimated to within 0.1 kgal m (i.e., about 0.1 m). But this result assumes that all harmonics up to degree 30 are known perfectly and that the rest of the field model, complete up to degree and order 180, has the same accuracy as the one described in (Rapp, 1981). With the full, present-day error in those low degrees, the accuracy worsens to about 0.3 kgal m. Hajela assumed an accuracy of the gravity measurements of 2 mgal, but found that there would be virtually no improvement if better measurements were used. Therefore, one may conclude that some 2/3 of the total r.m.s. error would come from that in the low degree and order part of the field model. The task of getting better low degree models using tracking data of satellites continues quite independently of improvements in levelling techniques, as does position determination itself. Present efforts carried out jointly by faculty and graduate students from the University of Texas at Austin and by scientists from NASA's Goddard Space Flight Center have the stated goal of improving four times the accuracy of the models at low degrees, sometime within the next four years. If this is accomplished, even without further improvement at higher degrees, the accuracy of the estimated potential at a benchmark could come close to 0.15 kgal m. For potential differences, the correlation between errors in the field at nearby benchmarks would be greater the closer these are, and positive, so the error will be in general less than $\sqrt{2}$ of a single point error; once the separation is larger than the shortest wavelength well-modelled in the reference field, the measurements can be treated as uncorrelated and, thus, about 50% higher for a difference than for a single value. This would occur, with present model accuracies, at separations larger than 1000 km. Accordingly, one may estimate (rather conservatively) that the error with the best and most complete fields available at present, the best positioning techniques, and reasonably good gravity, would be about 0.45 kgal m, while improvements in field modelling expected to occur within the next four years may bring this further down, to 0.22 kgal m. Beyond that, the high resolution, dedicated gravity mapping missions of the future, like GRM, may decrease the error (without any use of terrestrial gravity to correct it) to below 0.15 kgal m, on the basis of an expected point accuracy for the geoid of some 0.1 kgal m. With added local gravity information, the accuracy of the estimated difference may get easily below the 0.1 kgalm mark. There is one more reason why the numbers given here may be conservative: these errors are global (world-wide) r.m.s. values, because it is in the nature of collocation to provide global accuracies when given (as in the Colombo and Hajela studies) global statistics for the various sources of error. A global r.m.s. can be very different from the error at an isolated point. In general, the main contributor, the field model, will be best in those regions where the best data (tracking, gravimetry, etc.) used to make this model come from. In this regard, North America and Western Europe are likely to be better places than Central Asia. Moreover, the actual error will tend to be largest where the terrain and/or the field are rougher, and smaller where these are smoother. Even if the topography itself is irregular, it can be smoothed out to a considerable degree by careful terrain corrections. So if the sites chosen for the benchmarks are (a) within smooth areas where (b) the model is likely to fit better because much of

the data for it came from around there, the actual errors could be substantially less than the global r.m.s. on the error analysis mentioned here, and reach the 0.1 kgal m or better, with some luck. In any case, accuracies of 0.2 kgal m are already quite interesting; with them, potential differences (over arbitrarily long distances) would be known some seven times better than with tide gauges (on average), unless effective corrections for the sea surface topography can be made at the latter, which is still an open question.

TESTING BY EXPERIMENT

A 0.2 kgal m accuracy over distances of 1000 km or more can be tested by comparing the potential difference estimated between two carefully placed benchmarks and the corresponding value obtained from a spirit-levelling traverse between them. Part of the "careful placing" could involve the choosing of two sites already connected by a traverse that is thought to be of high quality.

In the original version of the idea and in the more recent work of Hajela, the local gravity data were, basically, in the form of gravity anomalies whose determination required levelling between gravity stations in addition to the gravity readings. The former is a lengthy and expensive task that might be obviated altogether by formulating the problem in terms of gravity disturbances. A gravity disturbance is the difference between the acceleration of gravity at a given point and that acceleration according to the reference field (i.e., the field model) at the same point. To reduce gravimetry to this form and get useful values, one needs to know the position of the station to better than a decimeter. This could be done by first finding the coordinates of the central point, or benchmark, by SLR, and then getting the relative positions of the stations about this point from translocations between the benchmark and each gravity station in turn (using two GPS receivers simultaneously). If the "circular" region is no more than 5° in radius, the GPS position error is unlikely to exceed 0.1 m, which probably is quite acceptable (0.1 m in height translates into 30 μ gal of gravity disturbance error). Most of this error is due to poor determination of the orbits caused by complicated non-gravitational forces acting upon the spacecraft. Such forces are hard to model (radiation pressure, for example) because they depend on the intricate shape and on the attitude of the satellite. The work towards improving the GPS ephemerides is a continuing one, so eventually larger areas may be surveyed in this way to 0.1 m accuracy. Nevertheless, a 5° circle about a benchmark is probably quite adequate already. To keep the quality of the "integrated" network within the 0.1 m/0.1 kgal m range, changes in position and gravity due to various natural and artificial phenomena would require constant monitoring and regular re-surveying. Eventually, the field model itself would have to be updated, particularly at long wavelengths. Fortunately, field modelling is a task with no end in sight, and one that is likely to become accurate enough to pick up any significant changes in gravity below degree and order 30.

Finally, as with any large geodetic system of extreme accuracy, there are all manner of potential sources of systematic error that previous studies have either ignored or dealt with only briefly. Errors in the definition of the coordinate system of the VLBI/SLR stations (i.e., in orientation, position of the geocenter with respect to the origin, etc.), effects of the topography, of local variations of the field caused by changes in water-table height, etc., are just a few that come to mind. Some may be "absorbed" with a few additional parameters to solve for in the adjustment, if the configuration of stations is favorable; still others

may be eliminated by appropriate corrections to the data. Others may go unnoticed until the idea is tried out in full. If these unsuspected sources do not overwhelm the results beyond redemption, their discovery and subsequent study may very well contribute to the further development of geodesy as a scientific discipline. It is the hard problems presented by well-thought out experiments that drive much of what is good and interesting in science.

REFERENCES

- Colombo, O.L., 1980a, A world vertical network, Report No. 296, Department of Geodetic Science, The Ohio State University, Columbus, Ohio.
- Colombo, O.L., 1980b, Transoceanic vertical connections, Proceedings of the second international symposium on problems related to the redefinition of the North American vertical geodetic network, pp. 87-104.
- Eeg, J., and Krarup, T., 1975, Integrated geodesy, in Brosowski and Martin eds., Vol. 13, pp. 77-123.
- Hajela, D.P., 1983, Accuracy of estimates of gravity potential differences between western Europe and the United States through the Lageos satellite laser ranging network, Report No. 345, Department of Geodetic Science and Surveying, The Ohio State University, Columbus, Ohio.
- Hein, G., 1982, A contribution to 3-D operational geodesy: Part I, Principle and observation equations of terrestrial type; Part 2: Principles of solution. Proceedings of the international symposium on geodetic networks and computations organized by the IAG, Munich, German Geodetic Commission, Series B, No. 258/VII, pp. 31-64 and 65-85.
- Heiskanen, W.A., and Moritz, H., 1967, Physical geodesy, W.H. Freeman Company, San Francisco.
- Rapp, R.H., 1981, The earth's gravity field to degree and order 180, using SEASAT altimeter data, terrestrial gravity data, and other data, Report No. 322, Department of Geodetic Science, The Ohio State University, Columbus, Ohio.

ACCURACY ESTIMATES OF INTERCONTINENTAL VERTICAL DATUM CONNECTIONS

D. P. Hajela
Department of Geodetic Science and Surveying
The Ohio State University
Columbus, Ohio 43210

ABSTRACT. The accuracy of connecting the vertical datums of regions, which are separated by oceans, has been investigated. The vertical datum connections are established through geocentric positions of satellite laser ranging (SLR) stations and estimating the geopotential differences between stations in each region obtained through leveling. Different accuracy estimates for the SLR station positions, and any displacement of the SLR coordinate system origin from the geocenter, were considered. It was however found that the accuracy of vertical datum connection primarily depends on the number of SLR stations in each region. A conservative accuracy estimate of leveling was considered for determining geopotential differences over intra-continental distances of several hundred kilometers. Even if the leveling accuracy was further reduced by one-half, the vertical datum connection accuracy was affected only slightly.

The accuracy estimates of the potential coefficients describing the earth's gravity field were considered, along with gravity anomalies in a small area around each SLR station. The accuracy of low degree potential coefficients had the most pronounced effect on the accuracy of the vertical datum connection.

Various anomaly spacing, data cap size, and anomaly accuracy were tried to determine the effect on the accuracy of the vertical datum connection. It was found that anomaly spacing need not be more dense than 10', and a data cap as small as 30' spherical radius would be adequate for establishing the vertical datum connection, if there are a sufficient number of SLR stations. The vertical datum connection was not very sensitive to anomaly accuracy.

VERTICAL DATUM CONNECTIONS

It is well recognized, e.g. see Rapp (1980), that the departure of mean sea level surface from the geoid, i.e., the sea surface topography, is of the order of 1 meter root mean square. The vertical geodetic networks in different continents, which are respectively referenced to mean sea level determinations at coastal tide gages, therefore refer to different equipotential surfaces.

Colombo (1980 a) proposed that a "World Vertical Network" may be defined by "a set of estimated potential differences among benchmarks situated in various continents." If we have several benchmarks P_i and Q_j respectively in two different vertical datums, and if the potential differences $\Delta W_\ell(BMA, P_i)$ and $\Delta W_\ell(BMB, Q_j)$ have been obtained by leveling separately in each region, then

the vertical datum connection, i.e. the potential difference $\Delta W_\ell(\text{BMA}, \text{BMB})$ may be estimated by:

$$\begin{aligned} \Delta W(\text{BMA}, \text{BMB}) = & U(P_i) + T(P_i) + \Phi(P_i) + \Delta W_\ell(\text{BMA}, P_i) \\ & - [U(Q_j) + T(Q_j) + \Phi(Q_j) + \Delta W_\ell(\text{BMB}, Q_j)] + v_{ij} \end{aligned} \quad (1)$$

$$\text{with} \quad v_{ij} = \varepsilon U(P_i) - \varepsilon U(Q_j) + \varepsilon T(P_i) - \varepsilon T(Q_j) + \varepsilon \Delta W_\ell(\text{BMA}, P_i) - \varepsilon \Delta W_\ell(\text{BMB}, Q_j) \quad (2)$$

where the gravity potential W is the sum of normal gravitational potential U , the rotational potential Φ , and the disturbing potential T , and the errors are denoted by ε . The terms $\varepsilon\Phi$ have been omitted in (2) as these are negligibly small ($\approx 0.3\%$) as compared to εU .

It is clear, by a simple consideration, that the number, N_e , of linearly independent equations (1) between pairs of benchmarks P_i, Q_j for establishing the vertical datum correction is one less than the total number of benchmarks. The accuracy estimate $\sigma \Delta W(\text{BMA}, \text{BMB})$ is then obtained from this overdetermined system by:

$$\sigma \Delta W(\text{BMA}, \text{BMB}) = [\underline{a}^T V^{-1} \underline{a}]^{-1/2} = \left[\sum_k \sum_\ell \left(V^{-1} \right)_{k\ell} \right]^{-1/2} \quad (3)$$

where all components of the design vector \underline{a} are equal to 1, and V is the variance-covariance matrix of the "observed" potential differences:

$$V = V(\varepsilon \Delta U) + V(\varepsilon \Delta T) + V(\varepsilon \Delta \Delta W_\ell) \quad (4)$$

where the right hand side terms are the variance-covariance matrices of the errors in $U(P_i) - U(Q_j)$, $T(P_i) - T(Q_j)$, and $\Delta W_\ell(\text{BMA}, P_i) - \Delta W_\ell(\text{BMB}, Q_j)$ respectively.

We consider the benchmarks to be the satellite laser ranging (SLR) stations with positions precisely defined in the Lageos SLR system SL4 (Smith et al., 1982). For example, the SLR station sites in USA and Western Europe are shown in Figures 1 and 2, with a region of 1° spherical radius marked around each site. The normal gravitational field was modeled by the potential coefficients developed by Rapp (1981). The disturbing potential at a SLR station was computed from modified gravity anomalies in a small region around the station referenced to the normal gravitational potential at the SLR station. As the gravity anomalies are not referenced to the geoid potential, a precise definition of the geoid or the sea surface topography is no longer required (Colombo, 1980 a).

The normal gravitational potential U at a SLR station with geocentric coordinates (r, ϕ', λ) is given by:

$$U(r, \phi', \lambda) = \frac{GM}{r} \left[1 + \sum_{n=2}^N (a/r)^n \sum_{m=0}^n \bar{P}_{nm}(\sin \phi') \{ \bar{C}_{nm} \cos m\lambda + \bar{S}_{nm} \sin m\lambda \} \right] \quad (5)$$

where GM is the gravitational constant times the mass of the earth; N is the

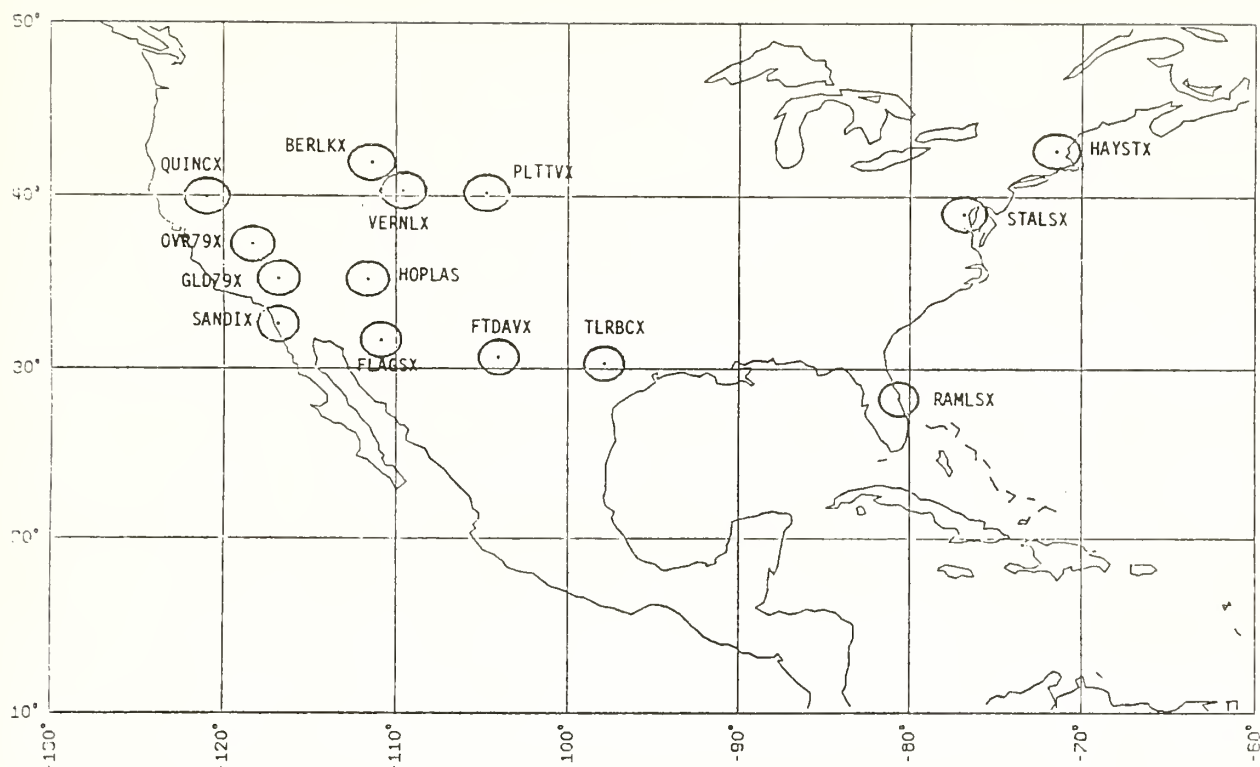


Figure 1: SLR Stations in USA in the SL4 System (Smith et al., 1982).

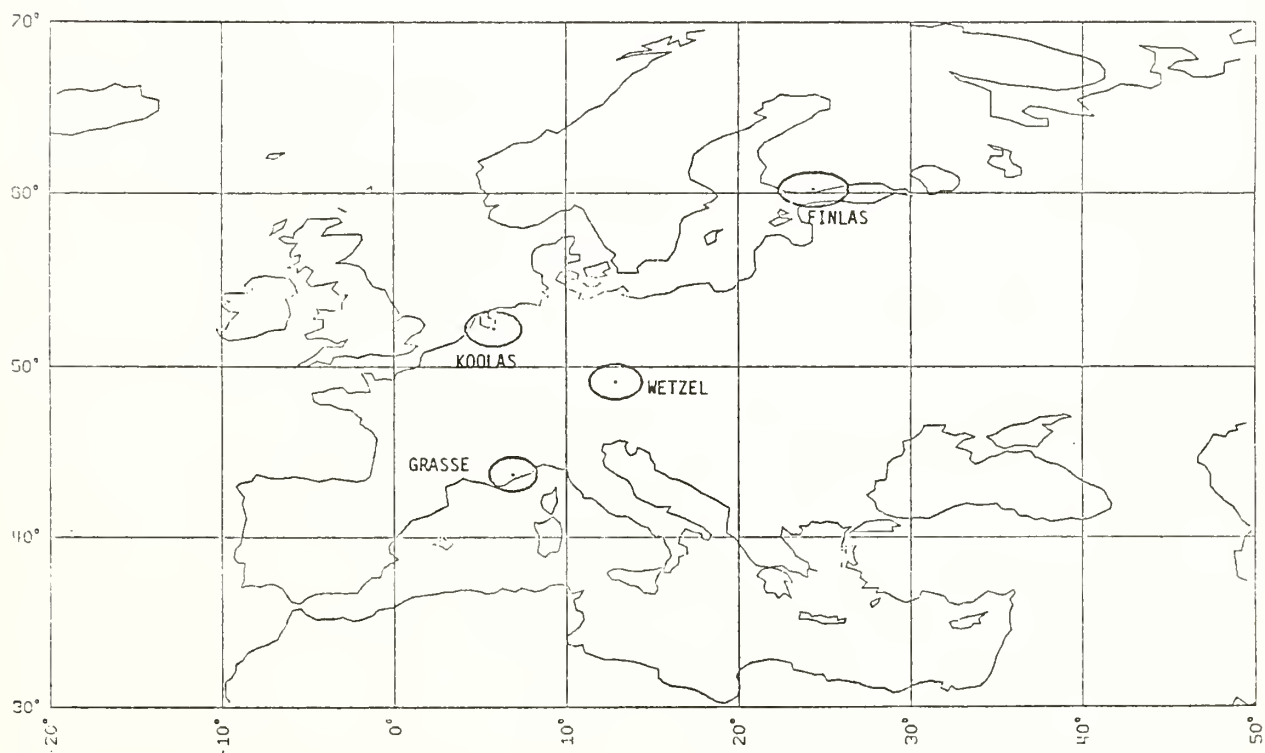


Figure 2: SLR Stations in W. Europe in the SL4 System (Smith et al., 1982).

highest degree of the spherical harmonic expansion; a here is the equatorial radius; \bar{P}_{nm} , \bar{C}_{nm} , \bar{S}_{nm} are respectively the fully normalized Legendre's functions and the potential coefficients of degree n and order m .

The effect of $\varepsilon GM/r$ is negligible on $\varepsilon \Delta U$, as such errors cancel in the differencing. The entire effect of errors $\varepsilon \bar{C}_{nm}$, $\varepsilon \bar{S}_{nm}$ will be considered in evaluating $\varepsilon \Delta T$. εU is predominantly dependent on the radial error εr in the SLR station position, and with uncorrelated εr for SLR stations, the diagonal terms in $V(\varepsilon \Delta U)$ are easily computed from the estimates of $\sigma \varepsilon r$. We will later consider, e.g. in Table 1, the effect of $\sigma \varepsilon r$ being 0, 10, 20,...cm. The shift, εs , of SLR coordinate origin from the geocenter causes correlated errors in station positions, and the off-diagonal elements in $V(\varepsilon \Delta U)$ may be computed under some simplifying assumptions (Colombo, 1980 b) for different estimates of $\sigma \varepsilon s$ like 0, 10, 30,...cm.

The standard deviation of first order class I leveling is usually estimated as $0.5 \sqrt{\ell}$ mm, ℓ in km. However, a more realistic estimate for $\sigma \varepsilon \Delta W_\ell$ over intra-continental distances of several hundred kilometres may be $2 \cdot 10^{-3} \sqrt{\ell}$ kgal.m, ℓ in km; which is equivalent to $0.06 \sqrt{\ell}$ kgal.m, ℓ in 10^3 km. We will consider the effect of different error estimates of intra-continental leveling with:

$$\sigma \varepsilon \Delta W_\ell = k \cdot (0.1 \sqrt{\ell}) \text{ kgal.m, } \ell \text{ in } 10^3 \text{ km; } k = 0, 1, 2, \dots \quad (6)$$

Various tests for the extent, density, and error estimate of gravity anomalies on the accuracy of inter-continental vertical datum connections will now be discussed briefly. For a detailed discussion, See Hajela (1983).

PREDICTED DISTURBING POTENTIAL DIFFERENCES

The predicted value of T , and its error estimate $\sigma \varepsilon T$, at a station P (P_i or Q_j) may be computed by least squares collocation (Moritz, 1980, Sec. 14) from the gravity anomaly vector $\underline{\Delta g}$ as:

$$T(P) = \underline{C}_{T, \Delta g}^T (\underline{C}_{\Delta g, \Delta g} + \underline{D})^{-1} \underline{\Delta g} \quad (7)$$

$$\sigma^2 \varepsilon T(P) = C_{T, T} - \underline{C}_{T, \Delta g}^T (\underline{C}_{\Delta g, \Delta g} + \underline{D})^{-1} \underline{C}_{T, \Delta g} \quad (8)$$

which requires the computation of covariances C of T and $\underline{\Delta g}$; and anomaly error estimate, $\sigma \varepsilon \Delta g$, for computing the noise matrix \underline{D} . We consider effect of $\sigma \varepsilon \Delta g$ as 0, 2, 4,... mgals, and also the effect of different cap size (spherical radius $\psi = 1^\circ, 2^\circ, \dots$) of anomaly data around each SLR station, and the anomaly spacing $\Delta \psi = 5', 10', 15', \dots$

We may also explicitly write T in a series similar to (5) as:

$$T(r, \phi', \lambda) = \frac{GM}{r} \left\{ \sum_{n=2}^N (a/r)^n \sum_{m=0}^n \bar{P}_{nm}(\sin \phi') \left[\varepsilon \bar{C}_{nm} \cos m\lambda + \varepsilon \bar{S}_{nm} \sin m\lambda \right] \right. \\ \left. + \sum_{n=N+1}^{\infty} (a/r)^n \sum_{m=0}^n \bar{P}_{nm}(\sin \phi') \left[\bar{C}_{nm} \cos m\lambda + \bar{S}_{nm} \sin m\lambda \right] \right\} \quad (9)$$

where we have now considered the errors $\varepsilon \bar{C}_{nm}$, $\varepsilon \bar{S}_{nm}$ in the potential

coefficients of the normal gravitational field up to degree N. By also considering a similar expression for $\Delta g(r, \phi', \lambda)$, the required covariances C in (7) and (8) may be computed, which involve ε_n^2 up to degree N, and σ_n^2 from degree N+1 to ∞ :

$$\varepsilon_n^2 = \sum_{m=0}^n \left(\varepsilon^2 \bar{C}_{nm} + \varepsilon^2 \bar{S}_{nm} \right) / (2n + 1) \quad (10)$$

$$\sigma_n^2 = \sum_{m=0}^n \left(\bar{C}_{nm}^2 + \bar{S}_{nm}^2 \right) / (2n + 1) \quad (11)$$

The unknown $\varepsilon^2 \bar{C}_{nm}$, $\varepsilon^2 \bar{S}_{nm}$ are approximated by the estimated variances of the potential coefficients, and the effect of better knowledge of the gravitational field may be tested by equating the estimated variances to zero up to degree 10, 20, σ_n^2 for degrees higher than N are estimated from anomaly degree variance model.

We note from Figures 3 and 4 that improvements in accuracy estimate $\sigma_{\varepsilon} T$ will primarily come from better knowledge of low degree potential coefficients; larger data caps ($\psi \geq 3^\circ$) or greater data density ($\Delta\psi < 1/6^\circ$) will not significantly contribute to improved $\sigma_{\varepsilon} T$. It is obviously preferable to have a smaller ψ , as we need the estimates of $\Delta W_{\ell}(P_i, P')$ for all anomalies in a data cap P_i to reference the anomalies to the normal gravitation potential at the respective SLR stations. To obtain conservative accuracy estimates for the vertical datum connections, we assume the estimated variances of potential coefficients is as in Rapp (1981); and the anomaly spacing $\Delta\psi$ will be considered to be $10'$ apart.

We also note from Figure 5 that for any particular accuracy estimate of the normal gravitational field, and a particular data cap size ψ , the estimated $\sigma_{\varepsilon} T$ is not very sensitive to estimated anomaly accuracy $\sigma_{\varepsilon} \Delta g$. This result is very helpful in answering the concern about the accuracy requirement of gravity anomalies over marine areas around SLR station sites in coastal areas.

Finally, the elements in $V(\varepsilon \Delta T)$ are computed by propagation of covariances through $\sigma^2 \varepsilon T(P_i)$, $\sigma^2 \varepsilon T(Q_j)$ and $\text{cov}[\varepsilon T(P_i), \varepsilon T(Q_j)]$.

ACCURACY ESTIMATES OF SOME VERTICAL DATUM CONNECTIONS

We have 14 SLR station sites in USA and 4 in W. Europe, with $\psi = 1^\circ$ in Figures 1 and 2, which yield $N_g = 17$ independent equations (1) for establishing this vertical datum connection. To ensure that these equations are linearly independent, and to ensure numerical stability in the solution of $\Delta W(\text{BMA}, \text{BMB})$, the data caps should not be overlapping so that different sets of gravity anomalies are used to predict T at each cap center. Hence, as we

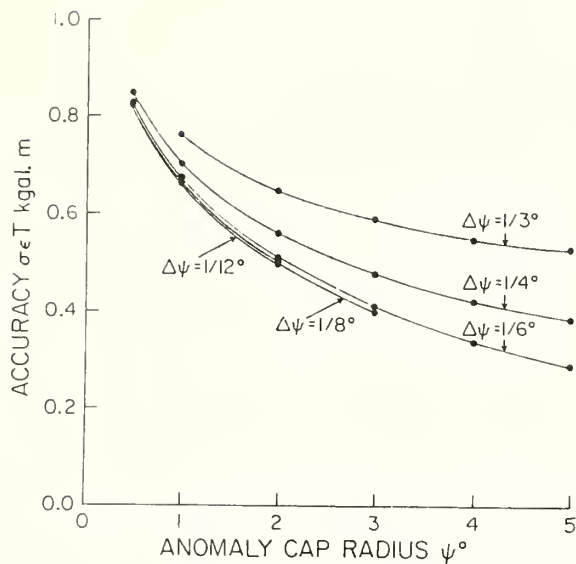


Figure 3: Variation of Accuracy Estimate $\sigma_{\epsilon}T$ of Disturbing Potential with Anomaly Cap Radius ψ and Anomaly Density $\Delta\psi$.

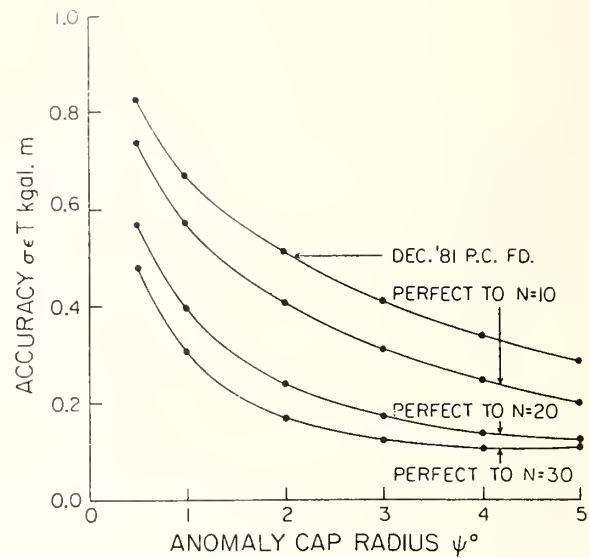


Figure 4: Variation of Accuracy Estimate $\sigma_{\epsilon}T$ of Disturbing Potential with Accuracy of Low Degree Normal Gravitational Field.

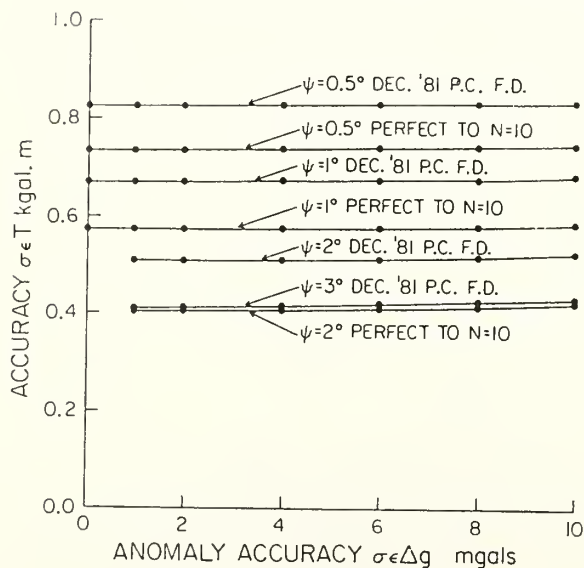


Figure 5: Variation of Accuracy Estimate $\sigma_{\epsilon}T$ of Disturbing Potential with Accuracy of Gravity Anomalies.

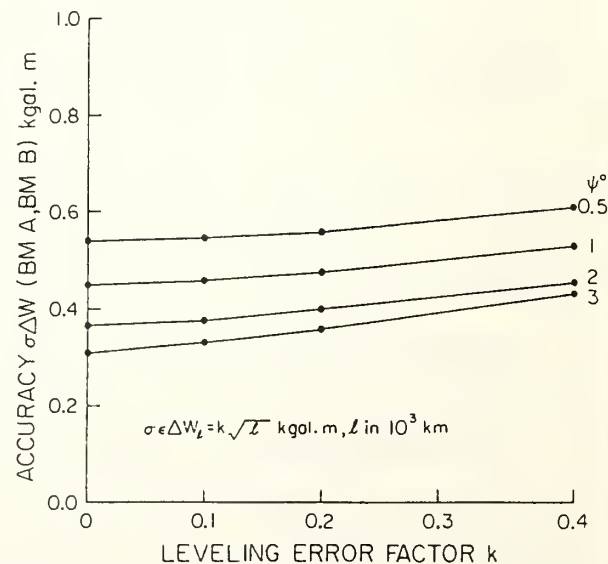


Figure 6: Accuracy Estimate $\sigma\Delta W$ (BMA,BMB) of USA-W. Europe Vertical Datum Connection. Variation Due to Leveling Errors.

increase ψ from 1° to 2° , N_e decreases to 13, and is further reduced to 9 if ψ is 3° .

The variation of accuracy estimate $\sigma\Delta W(\text{BMA}, \text{BMB})$ for the USA - W. Europe vertical datum connection for different accuracy estimates of leveling over intra-continental distances is shown in Figure 6. $\sigma\Delta W(\text{BMA}, \text{BMB})$ is not very sensitive to conservative estimates of leveling errors in (6), even when these are doubled with $k=2$.

The variation of U.S. - W. Europe datum connection accuracy is also given in Table 1 for shift in coordinate origin, and station position radial errors, where we also note the lack of critical sensitivity to station position errors. A reduction in the number of anomalies per cap from $\psi = 2^\circ$ to $\psi = 1^\circ$ would require less field work for estimating $\Delta W_i(P_i, P')$ for the anomalies needed to compute $T(P_i)$, and similarly for $T(Q_j)$. The larger uncertainty, $\sigma_{\epsilon T}$, with $\psi = 1^\circ$ is compensated by a greater redundancy in the number of equations N_e in (1).

The accuracy estimate $\sigma\Delta W$ for vertical datum connections is strongly dependent on the number of SLR stations available for establishing the connection. This is seen in Table 2 where accuracy estimate of vertical datum connections of USA is given with that of W. Europe, Australia, Bermuda, respectively, with the number of stations Q_j being changed from 4 to 2, and to 1. The large uncertainty, $\sigma\Delta W$, in U.S. - Bermuda connection is also repeated for U.S. connection with other cases of $Q_j = 1$, e.g. Bahamas, Hawaii, Peru (South America).

The variation in $\sigma\Delta W(\text{BMA}, \text{BMB})$ with the number of SLR stations available for connection is further seen in Table 3 for the U.S. - W. Europe datum connection. A comparison of Tables 2 and 3 shows that we have similar accuracy estimate of 0.49 kgal.m with $Q_j = 7$ and $\psi = 0.5$, as of 0.50 kgal.m with $Q_j = 4$ and $\psi = 1^\circ$. As the number of SLR stations increases with the use of transportable laser ranging stations, we would have a very modest requirement of field work for gravity anomalies in a data cap with spherical radius $\psi = 0.5$.

CONCLUSIONS

- The accuracy of vertical datum connections is predominantly influenced by the total number of SLR stations available for establishing the connection.

- It is adequate to consider anomalies to a spherical distance of 1° around each SLR station. This may be further reduced to 0.5 if the number of SLR stations exceeds 20.

- Anomaly spacing of about 15 km is sufficient. Easily attained anomaly accuracy of a few mgals is adequate. The anomalies have to be connected to the respective SLR stations by leveling.

- Even very conservative estimates of random errors in leveling over intra-continental distances of several hundred kilometers are not a source of concern.

Table 1: Variation in Accuracy Estimate $\sigma\Delta W(\text{BMA}, \text{BMB})$ for USA-W.Europe Vertical Datum Connection due to:

- (a) s.d. (σ_s) of shift of origin of SLR stations from Goecenter;
 (b) s.d. ($\sigma_{\epsilon r}$) of radial position error in SLR stations; and
 (c) accuracy estimate ($\sigma_{\epsilon\Delta W_\ell}$) of potential difference by leveling between cap centers: $\sigma_{\epsilon\Delta W_\ell} = k(0.1 \sqrt{\ell})$ kgal.m, ℓ in 10^3 km.

Capsize ψ°			2°	1°	0.5°
P _i : # Caps in USA			10	14	14
Q _j : # Caps in W. Europe			4	4	4
# Anomalies per data cap			475	139	43
$\sigma_{\epsilon T}$ in kgal.m			.51	.67	.82
Shift $\sigma_s(\text{cm})$	Position $\sigma_{\epsilon r}(\text{cm})$	Leveling k	Accuracy Estimate $\sigma\Delta W(\text{BMA}, \text{BMB})$ kgal.m		
0	0	0	.37	.45	.54
10	0	0	.37	.46	.54
30	0	0	.41	.49	.57
50	0	0	.49	.56	.63
0	10	0	.37	.46	.54
0	20	0	.38	.46	.54
0	30	0	.39	.47	.55
0	0	1	.38	.46	.54
0	0	2	.40	.48	.56

Table 2: Accuracy Estimate of U.S. and Other Vertical Datum Connections.

Vertical Datum Connections →	U.S.-W.Europe	U.S.- Australia	U.S.-Bermuda
No. of Caps in U.S.	14	14	14
No. of Caps in Other Datum	4	2	1
Anomaly Data Capsize $\psi = 0.5^\circ$ Accuracy Estimate $\sigma\Delta W(\text{BMA}, \text{BMB})$ kgal.m			
$\sigma_S = \sigma_{\epsilon r} = \sigma_{\epsilon \Delta W_\ell} = 0$.54	.65	.88
$\sigma_S = 30$ cm, $\sigma_{\epsilon r} = 10$ cm, and $\sigma_{\epsilon \Delta W_\ell} = 0.1 \sqrt{\ell}$ kgal.m, ℓ in 10^3 km	.58	.73	.89
Anomaly Data Capsize $\psi = 1^\circ$ Accuracy Estimate $\sigma\Delta W(\text{BMA}, \text{BMB})$ kgal.m			
$\sigma_S = \sigma_{\epsilon r} = \sigma_{\epsilon \Delta W_\ell} = 0$.45	.53	.72
$\sigma_S = 30$ cm, $\sigma_{\epsilon r} = 10$ cm, and $\sigma_{\epsilon \Delta W_\ell} = 0.1 \sqrt{\ell}$ kgal.m, ℓ in 10^3 km	.50	.62	.73

Table 3: Accuracy Estimate of U.S. - W. Europe Vertical Datum Connection.
Variation Due to Number of SLR Stations in W. Europe.

No. of Caps in U.S.	14	14	14
No. of Caps in W. Europe	7	4	2
Anomaly Data Capsize $\psi = 0.5^\circ$ Accuracy Estimate $\sigma\Delta W(\text{BMA}, \text{BMB})$ kgal.m			
$\sigma_S = 30$ cm, $\sigma_{\epsilon r} = 10$ cm, and $\sigma_{\epsilon \Delta W_\ell} = 0.1 \sqrt{\ell}$ kgal.m, ℓ in 10^3 km	.49	.58	.74

- Current accuracies of SLR station coordinates are adequate.
- Vertical datum connection between USA and Western Europe is presently feasible. A very conservative accuracy estimate of this connection is about 50 kgal.cm.
- Near-time improved estimates of the gravitation field will yield accuracies better than 40 kgal.cm for this vertical datum connection. An improved accuracy estimate of low degree potential coefficients will have the greatest effect.

REFERENCES

- Colombo, O.L., 1980 a: A World Vertical Network, Report No. 296, Department of Geodetic Science and Surveying, The Ohio State University, Columbus.
- Colombo, O.L., 1980 b: Transoceanic Vertical Datum Connections, Proceedings Second International Symposium on Problems Related to the Redefinition of North American Vertical Geodetic Networks, Ottawa, pp. 87-104.
- Hajela, D.P., 1983: Accuracy Estimates of Gravity Potential Differences Between Western Europe and United States Through Lageos Satellite Laser Ranging Network, Report No. 345, Department of Geodetic Science and Surveying, The Ohio State University, Columbus.
- Moritz, H., 1980: Advanced Physical Geodesy, Abacus Press, Kent.
- Rapp, R.H., 1980: Precise Definition of the Geoid and Its Realization for Vertical Datum Applications, Proceedings Second International Symposium on Problems Related to the Redefinition of North American Vertical Geodetic Networks, Ottawa, pp. 73-86.
- Rapp, R.H., 1981: The Earth's Gravity Field to Degree and Order 180 Using Seasat Altimeter Data, Terrestrial Gravity Data, and Other Data, Report No. 322, Department of Geodetic Science and Surveying, The Ohio State University, Columbus.
- Smith, D.E., P.J. Dunn, D. Christodoulidis and M. Torrence, 1982: Global Baselines from Laser Ranging, Fourth Conference on NASA Geodynamics Program, Goddard Space Flight Center, Greenbelt, Maryland.

A PRACTICAL OCEANOGRAPHIC APPROACH TO THE PROBLEM
OF DEFINING A WORLD VERTICAL DATUM

David E. Cartwright
Institute of Oceanographic Sciences
Bidston Observatory
Birkenhead, L43 7RA
United Kingdom

ABSTRACT. In the context of the IAG Special Study Group on a World Vertical Datum, a traditional oceanographic approach is recommended, making use of the approximately (0.1m accuracy) level property of an isobaric surface at 2000 Decibars (20 MPa). The recommended datum surface is at a fixed geopotential number above this surface, corresponding to an arbitrary density about which the actual sea water density profile is referred. For Worldwide use, a simultaneity of both density profiles and cross-shelf slope measurements by current meter arrays is essential. This will be best achieved by measurements under repeated satellite altimeter tracks, effectively providing a local geoidal estimate from which long term average slopes can be assessed from the altimetry alone. An International Geodetic Levelling Year might be envisaged during the next precise-tracking altimetry mission.

There seems to be general agreement among the IAG Special Study Group that a World Datum must be a geopotentially level surface, or an acceptable approximation to one. At epoch 1990, "acceptable approximation" means better than decimetric accuracy in ellipsoidal heights. In earlier times, the mean sea surface topography (SST) was assumed by geodesists to be an equipotential surface, with coastal tide-gauges as convenient points of reference for all land surveys. This is now agreed between oceanographers and geodesists to be unacceptable in accuracy, although the wording of much geodetic literature still suggests implicitly that the Geoid may be identified with SST after some sort of adjustment. In fact, the concept of a geopotential surface whose mean departure from the SST on a spatial average over all major oceans is zero still seems quite a good ideal to aim for as a Geoid definition, despite the fact that the spatially mean SST rises by an order of a decimetre per century due to changes in global temperature. The difficulty is of course how to access this surface at any given epoch and relate tide-gauge elevations to it. (After all, the geoidal parameter J_2 itself has been shown to be sensibly changing, so any gravitational datum would have to be revised periodically).

The promise of time-averaged global SST from satellite altimetry within the next decade, exciting though it is, does not directly help to define a level datum because it refers the topography at best to the Ellipsoid, so that the steric and dynamic variations of SST are superimposed on the much greater geoidal undulations. Ideally, a suitable geoid N at latitude θ , longitude λ and epoch t_e should be derivable from geocentric SST by a formula of type

$$N(\theta, \lambda, t_e) = SST - \zeta(\theta, \lambda, t_e) - \delta\zeta(\theta, \lambda, t) \quad (1)$$

where ζ is the quasi-permanent deformation of the ocean surface, with zero spatial average over the oceans, and $\delta\zeta$ is the time-dependent deformation due to dynamic forces varying in time scales t much shorter (say 10^{-1} to 10 years) than t_e (half-century or so). Time-averages over one or a few years with adjustment for atmospheric pressure reduces $\delta\zeta$ to centimetric levels, and longer-term changes can be monitored by coastal tide-gauges, but ζ varies spatially by more than 2 metres.

Some oceanographers have computed maps of ζ from recorded hydrographic data and their results are well known. Their broad features seem to be in fair accord with results of geodetic levelling between tide-gauges, for example the 0.6m rise from the east to the west coast of USA, but there are notorious discrepancies from north to south in various parts of the world, about which it seems difficult to decide between possible sources of error. The chief disadvantages of current oceanographic maps of SST are

- (a) they are compounded of hydrographic data recorded at different times and places, so that ζ may be contaminated by aliased $\delta\zeta$
- (b) they may not be reliably extended over wide continental shelves between the deep ocean and the coastline without additional local fieldwork.
- (c) the maps are fundamentally computed in units of gravitational potential, from which conversion to orthometric units is uncertain at sub-decimetre level.

Nevertheless, it seems to me that, failing an absolute measure of geopotential at the Earth's surface, a World Vertical Datum must make some reference to the ocean surface, with reasonable adjustments based on modern methods combined with well tried older methods. The older method which I would advocate is based on the wellknown oceanographic principle of steric levelling, as described for example in Lizitzin's book (1974), but with a more careful interpretation. (My basis is similar to that proposed by R B Montgomery at the IAG/IAPSO Symposium on Marine and Coastal Geodesy at the 1975 General Assembly of IUGG). Essentially, the reference surface to be aimed for is defined as being at a fixed geopotential number above an isobaric surface, 2000 decibars (i.e. 20 Megapascals) below the the annual mean sea surface at epoch t_e . The fixed geopotential number w_0 would be defined in the manner of

$$w_0 = \int_0^{20} \alpha(35, 0, p) dp \quad (2)$$

where $\alpha(s, t, p)$ is the accurately known specific volume of a hypothetical column of sea water of salinity s , temperature t at pressure p MPa. Choice of standards for s and t may be altered on further discussion and calculation, but (35,0) are classical and give a surface which is near a spatial average of the actual sea surface, without being rigidly defined as such an average. 20 Mpa is again arbitrary, a compromise between 10 MPa (eg Wyrteki) which is disturbed by currents, and 40 MPa (Lizitzin) which is too broken up by bottom topography,

The implicit assumption is of course that the specified isobaric surface is also close (within a few centimetres) to being a geopotentially level surface. This assumption is identical to that of a 'level of no motion'. It is certainly controversial, but it is equally certain that very little steady motion exists at ocean depths of order 2km, and that it is hard to account theoretically for more than a few centimetres' departure between such isobaric and equipotential surfaces across oceanic dimensions. I suggest in brief that the assumption be adopted with reservation until a better geopotential measure becomes available, when comparisons will be interesting, and beneficial to science.

Reference of a continental geodetic network to the surface defined above would be through a carefully planned series of hydrographic measurements extending over a year between a few coastal tide-gauges and suitable deep ocean sites, linked to satellite altimetry, possibly with SLR. The general plan is sketched in the attached Figure. T in the upper sketch represents a permanent tide gauge installation, linked to the local geodetic network. A and A' are the ground tracks beneath an altimetric satellite orbit, the ground tracks necessarily repeated at intervals of N days where for TOPEX, N will probably be about 10. A shallow bottom pressure gauge would be installed at B near where path A intersects the coast, and a deep station D would be identified near where A passes over the shelf break in a depth of more than 2km. Density profiles to 20 MPa would be monitored at D periodically, partly by standard ship-based soundings, partly by moored thermistor/conductivity chain. Current meters would be moored at C, ...C_n between B and D, sufficient in number to monitor any spatial variation in the mean (non-tidal) current normal to the path. (If the mean current is known to be weak, then n may be as small as 2 or 3.) The density profile between B and D would also be monitored by XBT each time station D is visited, and barometric pressure and wind would be monitored continuously at a nearby shore station.

The density profile at D, which is commonly measured to about 1 part in 10⁵, gives precise measure of the geopotential difference between the sea surface and the reference surface :

$$\delta w = \int_0^{20} \alpha(s, t, p) dp - w_0 \quad (3)$$

Less precision in measuring p as a function of depth is of no consequence, because the density varies only slightly with depth at 20 MPa. We do not attempt to measure the orthometric depth of the isobaric surface with high precision. Since δw will normally be less than about 1 dynamic metre; it can be converted to orthometric height units by dividing by surface gravity at an ordinary level of precision.

The orthometric height difference in the SST relative to W₀ between D and B is measured in terms of the currents V normal to A by the geostrophic relation:

$$\delta z = \frac{f}{g} \int_B^D V dx \quad (4)$$

where f is the Coriolis parameter, and small adjustments are made for the vertical profiles of current and density, wind stress and barometric pressure. δz would be typically only of order 0.1m, except where major currents are involved. Conversion of shallow bottom pressure at B to surface elevation relative to a nearby land datum is straightforward, and the level difference between that datum and the tide gauge at T is standard geodetic practice.

The point of placing BD along the satellite track A is that current meter moorings are difficult to maintain in shelf seas for long periods, for practical reasons, whereas altimetry is promised over fixed tracks for a few years. The altimetry of BD, with orbital errors ideally reduced to a minimum by means of a Satellite Laser Ranging station (S), gives the ellipsoidal heights of B and D, or at least their relative difference. Adjustment by simultaneous measurements of δZ as described above converts this to the difference of the ellipsoidal heights of the assumed reference surface at B and D. After a month or two of current measurements the altimetric height differences may then be used to monitor variations in δZ for the duration of the altimeter mission. The altimeter could also in principle monitor changes in $\delta w/g$, but repeated density profiles at D would be easy to repeat sufficiently for a yearly average. Long-term variations in the sea level recorded at T would add useful redundancy.

A further refinement would be to choose D at the intersection of A and A' and to instrument both tracks simultaneously, but not if this makes the distances BD and the corresponding B'D' too long for available instrumental resources. In any case, a full geodetic exercise for a given continental area would refer several coastal tide gauges to my assumed reference surface, with final least-squares adjustment. The overall point is of course that other continental networks referred similarly to the w_0 surface should be using the same geopotential datum to better than 0.1m.

There are some oceanographic restrictions to the choice of coastal sites for the above type of exercise. Obviously, T must be close to open sea water, not affected by river water or strong currents. Horizontal distances BD must be as short as possible and should not intersect shoaling banks. The deep station D should not have strong surface currents or any appreciably steady motion at 2km depth. Coastlines with narrow continental shelves such as the west coasts of North and South America and much of the African coast are clearly the best. Equatorial and upwelling areas present special difficulties of strong vertical density gradients and strong surface currents. Western boundary jets are also to be avoided, so a relevant exercise on the eastern coast of USA, for example would preferably be well north of Cape Hatteras. The best area in western Europe would be the north coast of Spain, being very close to deep Biscay water. The coast of Portugal is also close to deep Atlantic water. Great Britain is not well placed because of its wide continental shelf and indented coastline, but its geodetic network has been effectively linked to the European continent by tide-gauge comparisons across the English Channel. Use of the Mediterranean Sea would not be possible without an independent study of the relation between its 20 MPa surface and that of the northeast Atlantic which are not physically connected. In general, each continental state has its own problems which would need joint study by the local geodesists and oceanographers.

Finally, it is fairly obvious that hydrographic links such as are described above should be conducted more or less simultaneously by all countries wishing to refer to the same datum. This is partly implied by the use of rare satellite altimetry missions, but there may be a case for promoting an 'International Year of Geodetic Levelling' on the lines of the 1957-58 IGY.

IOS-Bidston, January 1985

Reference:

Lisitzin E. (1974) Sea-Level Changes. Elsevier, 286pp.

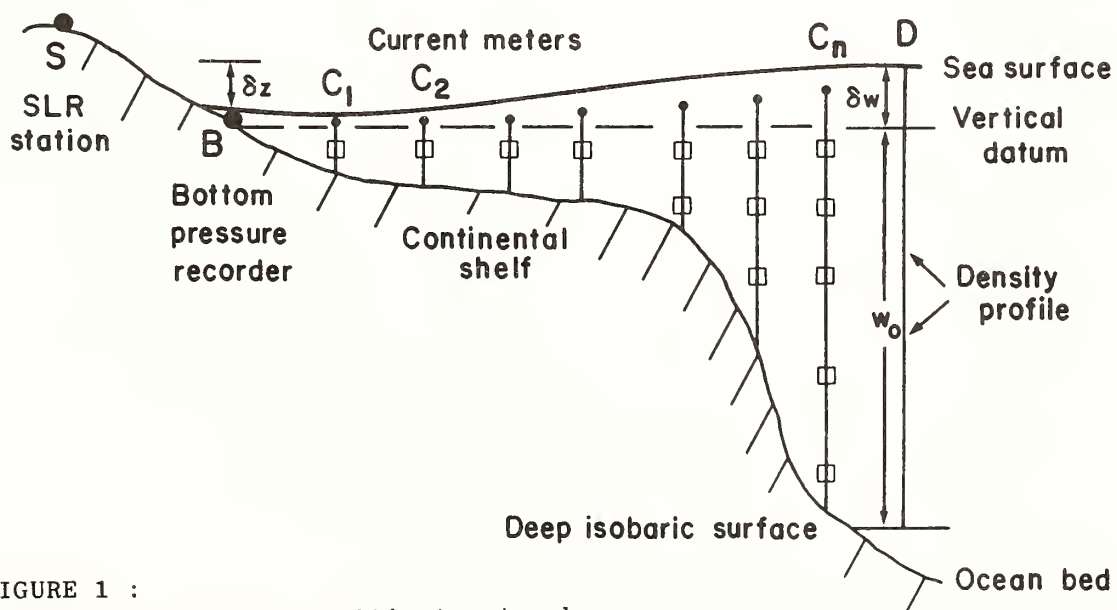
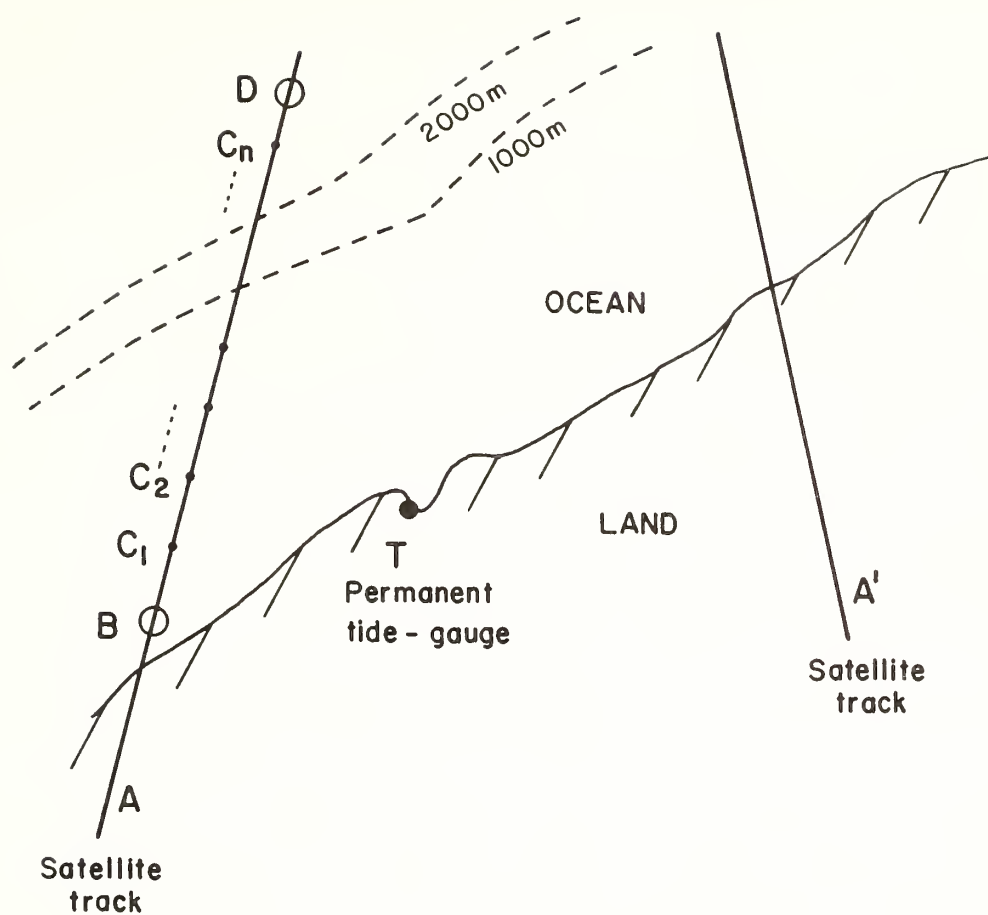


FIGURE 1 :
Recording array under altimeter track
for relating land levels to deep-ocean Datum.

IMPACTS OF CONVERSION TO THE NORTH AMERICAN VERTICAL DATUM
OF 1988 ON THE NATIONAL FLOOD INSURANCE PROGRAM

Matthew B. Miller
Risk Studies Division
Federal Insurance Administration
Federal Emergency Management Agency
500 C Street, SW
Washington, DC 20472

ABSTRACT. The National Flood Insurance Program is a Federal program designed to reduce the escalating costs of property damage caused by floods and to transfer such costs from the general taxpayer to floodplain occupants. The program is based on an agreement that when a community implements programs to reduce future flood losses, the Federal Government makes flood insurance available within the community. A Flood Insurance Study prepared by the Federal Emergency Management Agency (FEMA) provides the data upon which flood insurance premiums and local floodplain management programs are based. The Flood Insurance Study provides maps showing the boundary and elevation of the one percent annual chance (100-year) flood for all significant flooding sources. Insurance rates are set by structure elevation relative to the 100-year flood, and all new construction is required by the community to be protected to or above that flood elevation. Approximately 17,500 communities are currently participating in the National Flood Insurance Program. All flood maps for these communities are referenced to the National Geodetic Vertical Datum (NGVD) of 1929. Conversion to the North American Vertical Datum (NAVD) of 1988 will impact many aspects of the National Flood Insurance Program, including the establishment of vertical control for new flood maps and the utilization of published flood elevations for determining elevation requirements and insurance premium rates for new construction. Activities involved in converting from NGVD of 1929 to NAVD of 1988 include the referencing of all new Flood Insurance Studies to NAVD of 1988 as soon as the new vertical datum is available, converting existing Flood Insurance Studies to NAVD of 1988 when periodic revisions are made, and educating users of Flood Insurance Studies of the nature of the vertical datum adjustment and procedures for converting from NGVD of 1929 to NAVD of 1988. FEMA encourages the National Geodetic Survey to assist in this effort through preparation of publications and conversion tables.

INTRODUCTION

The National Flood Insurance Program is a Federal program under the jurisdiction of the Federal Emergency Management Agency (FEMA) that enables property owners to purchase flood insurance, which is generally not available from private-sector companies. The program is designed to reduce escalating costs of property damage caused by floods and to transfer these costs from the general taxpayer to floodplain occupants. The program is based on agreements with communities throughout the United States that if the community will implement programs to reduce flood losses, the Federal Government, through the National Flood Insurance Program, will make flood insurance available within the community as financial protection against flood losses that do occur.

DOCUMENTS PRODUCED BY FEMA FOR IMPLEMENTING THE NATIONAL FLOOD INSURANCE PROGRAM

The technical data base of the National Flood Insurance Program is the Flood Insurance Study and Flood Insurance Rate Map prepared by FEMA for flood-prone communities. The Flood Insurance Study is the document prepared by FEMA to assist a community in enforcing floodplain management programs to reduce flood losses. The Flood Insurance Rate Map is the document prepared by FEMA for use by insurance agents to establish the applicable flood insurance premium rate for a structure. The Flood Insurance Study contains a Flood Boundary and Floodway Map, which shows the 100-year flood boundary for all significant flooding sources within the community. The 100-year flood is the flood that has a 1 percent chance of exceedence in a given year; it occurs on the average once every hundred years. The 100-year flood is also referred to as the base flood. As a condition of community participation in the National Flood Insurance Program, all new construction must be elevated to or above the base flood elevation. The 100-year flood elevation, or base flood elevation, is also used for insurance rating purposes. The Flood Boundary and Floodway Map also shows the 500-year flood boundary. This is the flood that has a 0.2 percent chance of occurring each year, and occurs on the average once every 500 years. The floodway boundary is also shown on the Flood Boundary and Floodway Map. The floodway is defined as the channel of a river and the adjacent flood plain which must be reserved from development in order to discharge the 100-year flood without cumulatively increasing the water-surface elevation of that flood by a given amount, usually not more than one foot. The floodway is intended to prevent increased flood hazards due to fill and other encroachments into this portion of the 100-year floodplain. It is the community's responsibility to prohibit development in the floodway that would cause an increase in the 100-year flood elevation. The Flood Insurance Study also includes a report which contains a written description of the analysis used to determine the flooding potential within the community and specifically describes areas of flood hazard within the community. It also contains plotted flood profiles (flood elevation versus distance) for the 10-, 50-, 100-, and 500-year flooding events.

The Flood Insurance Rate Map, the document used by insurance agents for determining actuarial risk of flooding, shows the 100- and 500-year boundaries. It also shows lettered zones for flood insurance rating purposes and 100-year flood elevation lines, or base flood elevations, as previously defined.

FEMA's flood maps or the Flood Insurance Study text also document the elevation reference marks used in computing the flood elevations shown on the Flood Insurance Rate Map and in the Flood Insurance Study.

GENERAL NATURE OF IMPACT ON THE NATIONAL FLOOD INSURANCE PROGRAM OF CONVERSION FROM NGVD OF 1929 TO NAVD OF 1988

- By 1988, approximately 10,000 detailed Flood Insurance Rate Maps and Flood Insurance Studies will have been prepared by FEMA. This represents approximately 50,000 individual map panels.
- Every year, FEMA distributes approximately six to eight million map panels to users.
- FEMA policy requires that the most recently adjusted National Geodetic Survey (NGS) bench mark elevations be used for flood insurance and flood plain management purposes. NGS bench marks may be used directly in determining elevation requirements, or communities may use local monumentation tied to NGS bench marks.

Coupling the above with the fact that almost every flood elevation ever determined or mapped by FEMA is referenced to the National Geodetic Vertical Datum (NGVD) of 1929 gives some indication of the magnitude of the conversion from NGVD of 1929 to the North American Vertical Datum (NAVD) of 1988 on the National Flood Insurance Program.

SIGNIFICANT USERS OF VERTICAL CONTROL DATA IN RELATION TO THE NATIONAL FLOOD INSURANCE PROGRAM

- There are approximately 17,500 community officials throughout the United States who utilize FEMA flood maps in administering their communities' participation in the National Flood Insurance Program. These floodplain administrators require that all new construction in their communities be elevated above the base flood elevation. They also use Flood Insurance Studies to require that no construction be permitted in a designated floodway that would cause any increase in a base flood elevation.
- There are approximately 150,000 insurance agents throughout the United States who sell flood insurance under the National Flood Insurance Program. These insurance agents use the Flood Insurance Rate Map to determine the relationship between the elevation of the lowest floor of a structure and the base flood elevation for determining insurance rates.

- There are approximately two million flood insurance policy holders and about 360,000 property owners a year who buy new flood insurance policies under the National Flood Insurance Program. These property owners are required to supply the elevation of their lowest floor to an insurance agent for determination of the appropriate actuarial rate.
- Architects and engineers throughout the nation may consult available Flood Insurance Studies and Flood Insurance Rate Maps to determine proximity of proposed construction to the floodplain. All proposed structure elevations relative to flood elevation are carefully examined, and final structure elevations are set accordingly.
- FEMA's employees and contractors nationwide will be impacted by conversion from NGVD of 1929 to NAVD of 1988. It will be their job to ensure that the National Flood Insurance Program converts in an orderly manner to the new datum and to ensure that flood insurance premiums are accurately assessed in the face of the new datum adjustment.
- Perhaps the most profoundly affected group in the United States will be land surveyors. In theory, the surveyors' responsibilities with regard to the National Flood Insurance Program should only be to determine the precise elevation of specific locations in and around a structure. In practice, surveyors are often requested to interpret a floodplain map and to make determinations for homeowners and floodplain administrators regarding the base flood elevation affecting a particular property.

In summary, there are about 22 million persons at risk because they reside in one of the nation's floodplains. These persons nationwide will be directly or indirectly affected by conversion from NGVD of 1929 to NAVD of 1988 with regard to the National Flood Insurance Program.

IMPLICATIONS OF CONVERSION FROM NGVD OF 1929 TO NAVD OF 1988 ON ACCURACY OF PREDICTED FLOOD ELEVATIONS

A major point to be considered with regard to the conversion from NGVD to NAVD with regard to the National Flood Insurance Program is the potential for change in hydrographic relationships. Floodplain maps relate the relative elevations of water surfaces of floods to land surfaces at a given location. The planimetric configuration of a floodplain and the depth of flooding are most important. There are three general categories of impacts on such hydrographic relationships due to the conversion from NGVD to NAVD.

The first case occurs when relative differences between bench marks remain fairly constant over a given geographic area. This case will be the least difficult for FEMA to address because the relative hydrographic conditions shown on FEMA maps will still be correct. FEMA will only have to ensure that consistent data are used when comparing flood elevations to structure elevations.

The second case involves changes in the relative elevations between bench marks over a given geographic area as a result of improved surveying capabilities or other causes. This will mean that the relative hydrographic features shown on the map are in error to some degree due to changes in hydrologic and hydraulic conditions that are attributable to changes in stream slope and topography. If the errors in water-surface elevation of a flood are minor, say less than 0.5 feet, they will be ignored until a restudy of the community for another reason is initiated. If significant errors in water-surface elevations are present, a restudy of the community's flood hazards will be initiated as FEMA funding permits.

The third case involves changes in the relative elevations between bench marks over a given geographic area as a result of subsidence or uplift of the earth's surface. This will mean, as in the previous case, that the relative hydrographic features shown on the FEMA maps are in error to some degree. As in the previous case, minor errors in flood elevations will be ignored. Otherwise, a restudy of a community's flood hazard areas will be initiated, as funding permits.

MECHANISMS ENVISIONED BY FEMA FOR CONVERTING THE NATIONAL FLOOD INSURANCE PROGRAM FROM NGVD OF 1929 to NAVD OF 1988

- All new Flood Insurance Studies and Flood Insurance Rate Maps will be referenced to NAVD of 1988 as soon as the new vertical datum is available.
- As periodic revisions are made to existing Flood Insurance Studies, they will be converted to NAVD of 1988.

MECHANISMS ENVISIONED BY FEMA FOR EDUCATING FLOOD INSURANCE STUDY AND FLOOD INSURANCE RATE MAP USERS

Both before and after FEMA maps are converted to NAVD, education of users will be necessary. Before conversion of FEMA maps to NAVD, FEMA will have the need for separate reports aimed at different groups of users. A technical treatment of the NAVD conversion should be written with the engineer, surveyor, and floodplain administrator in mind. This report should address technical implications of conversion from NGVD to NAVD on the utilization of flood elevations. It should give specific details for converting from one datum to the other.

A nontechnical treatment of the NAVD conversion should be written with the non-technical Flood Insurance Study and Flood Insurance Rate Map user in mind. This group includes insurance agents and community officials. It will basically tell the user to compare apples to apples and oranges to oranges by comparing flood elevations to land elevations utilizing a consistent datum.

After conversion of a Flood Insurance Study and Flood Insurance Rate Map to NAVD, both the maps and the accompanying report will emphasize the datum used and explain discrepancies with contiguous Flood Insurance Studies and Flood Insurance Rate Maps referenced to NGVD of 1929.

MECHANISMS THROUGH WHICH NGS COULD ASSIST
FEMA IN CONVERSION OF NATIONAL FLOOD INSURANCE PROGRAM TO NAVD

The NGS has exhibited a very real commitment to FEMA in assisting in conversion of the National Flood Insurance Program from NGVD to NAVD. This willingness on NGS's part to work with FEMA in this effort is very much appreciated. There are two specific actions that NGS could take with regard to this conversion that would be of great benefit to FEMA. The first would be preparation of a publication aimed not at the geodesist and crustal motion expert, but rather at the local community engineer and surveyor, which explains the basis of the conversion. The second would be publication of the new bench mark elevations in a format containing at least the following information:

- NGS bench mark designation.
- NGVD elevation value last assigned to that bench mark.
- NAVD elevation value presently assigned to that bench mark.
- The magnitude of the change in value due solely to the datum adjustment.
- The magnitude of the change due to systematic errors and actual changes in the earth's surface.

SUMMARY

The conversion to the NAVD of 1988 will significantly impact the National Flood Insurance Program because all flood elevations shown on the approximately 50,000 maps which will have been produced by FEMA as of 1988 will be referenced to the NGVD of 1929. Where changes in bench mark elevations are relatively consistent over a given geographic area, the technical accuracy of the maps will not be seriously impacted. However, where real changes in ground elevations are reflected in the new bench mark elevations, the accuracy of predicted flood elevations will be in question.

THE NEW NATIONAL VERTICAL DATUM AND
THE NATIONAL MAPPING PROGRAM--A MAJOR CHALLENGE

Rupert B. Southard, Jr.
Chief, National Mapping Division
U.S. Geological Survey
Reston, Virginia 22092

ABSTRACT. The U.S. Geological Survey is responsible for the development and maintenance of the National Mapping Program (NMP). Currently, this program encompasses more than 60,000 different map products, of which over 7 million map copies are distributed annually.

The impact of a change in the national geodetic reference datums on the NMP ranges from negligible to major. Changes in the horizontal datum can be accommodated by shifts in the graticule with respect to the map detail or by labeling new datum values on the latitude and longitude lines.

Vertical datum changes are much more difficult to accommodate. Techniques for interpolating between existing contours have been tried and the results are not always satisfactory. With the cost of recontouring one of the almost 55,000 7.5-minute maps in the NMP ranging from \$3,000 to \$5,000, the manner in which the North American Vertical Datum 1988 is defined is critical. The impact on the NMP and map users must be considered during the process of defining the datum.

INTRODUCTION

Ten years ago, at the 1975 annual ACSM meeting, a panel was held titled "New Horizontal Datum and the Surveyor," and representatives of U.S. and Canadian Federal agencies and the private surveying community presented ideas on the impact of a new horizontal datum on their areas of interest. During the discussion, it was pointed out that U.S. Geological Survey (USGS) cartographers were aware of the impacts of the datum shift. Examples of datum shift statements and treatment of corner graticule ticks were presented that had been used to extend the life of maps that were made obsolete by the adoption of the North American Datum 1927 (NAD-27). It was stated that with this method of accommodating datum changes on the USGS maps, the conversion of all maps in the National Mapping Program (NMP) to the new datum could be accomplished in a reasonable time period. Therefore, a datum that best fits the needs of everyone could be selected, and the old datum, NAD-27, could be abandoned.

Conversion to the new vertical datum in the NMP requires resolution of many of the same issues that are being studied in implementing the new horizontal datum. The paramount issue concerns the conversion of the 60,000 different maps of the

NMP. Can they be altered to agree with a new vertical datum at a reasonable cost and within a reasonable time? If they can, we can look forward to the use of a single vertical datum for the country. If not, we may have to maintain reference to two vertical datums, the North American Vertical Datum of 1929 (NAVD-29) and the new North American Vertical Datum of 1988 (NAVD-88).

NATIONAL MAPPING PROGRAM

The NMP includes more than 60,000 different map products, of which over 7 million map copies are distributed annually. Of the 60,000 maps, about 55,000 are in the 7.5-minute, 1:24,000-scale, primary quadrangle map series. Complete coverage of the lower 49 States by this series is expected by 1989, probably before the NAVD-88 is formally accepted. Since 7.5-minute series maps are the largest scale in the NMP and contain the greatest detail and elevation accuracy, they will be affected most by the vertical datum change. Accordingly, the following discussion will be limited to this series.

Most 7.5-series maps have been produced since the end of World War II, when photogrammetric methods became common practice. The procedures used today for producing a map were established in the early 1950's and with the exception of some evolutionary changes due advances in instrumentation and technology, they have remained essentially the same to this day.

BASIC VERTICAL CONTROL

In preparation for the production of 7.5-minute maps, a third-order level network was established which resulted in few places being more than 5 miles from basic vertical control. These lines were usually established along farm roads, railroads, desert track roads, and mountain trails. The density of lines was less in remote mountainous areas where access was difficult and where there were few roads and trails. As the National Network was developed by the Department of Commerce, the requirement for establishing level lines by the USGS field parties became less. The U.S. Geological Survey field surveyors established over 500,000 benchmarks in support of the 7.5-minute mapping program, and as a result, geodetic control records and descriptions were published and distributed by the USGS. Methods for transfer of these records to the NGS are presently under consideration.

SUPPLEMENTAL VERTICAL CONTROL

The elevation network was further densified in the mapping area to control the aerial photography. Several different survey methods and types of equipment were used; fly levels, stadia traverse, vertical angles, and the elevation meter. The method used to establish the supplemental control was based on the ruggedness of the country (contour interval) and the road network (logistics). The primary purpose of these surveys was to establish elevations at selected image points to control the stereomodels. As the photogrammetric equipment and techniques improved, less field control was necessary and some elevations were established by aerotriangulation methods. Elevations were also established at road intersections, public land survey systems, section corners, stream gaging stations, airports, and at other map feature points. These elevations would appear on the finished map as spot elevations.

The maps were compiled by photogrammetric methods using a variety of stereo-plotters. In the 1950's and 1960's, most maps were compiled on optical projection plotters, such as the ER-55 and the Kelsh. Since then, most maps have been compiled using optical-mechanical projection instruments such as Wild B-8 and Kern PG-2's. Essentially all contouring has been established by photogrammetric methods. In a few areas where the contouring could not be done accurately due to flatness of the ground surface, lack of image detail, or impenetrable ground cover, the contouring was by plane-table survey.

VERTICAL ACCURACY

The contour intervals of the 7.5-minute map series are selected to best express the topography of the area. Contour intervals range from 5 feet to 80 feet depending upon the terrain. In between these two limits are 10-, 20-, and 40-foot intervals. Some maps, in recent years, have been compiled with metric value contours. The distribution of the various contour intervals in the country is depicted in figure 1. In the lower 48 States, 14 percent of the 7.5-minute maps contain 5-foot contours, 34 percent contain 10-foot, 29 percent contain 20-foot, 18 percent contain 40-foot, and 5 percent contain 80-foot.

USGS production processes were designed to produce maps which meet National Map Accuracy Standards (NMAS). The national standard for vertical accuracy requires that 90 percent of the points tested will be accurate to within one-half the contour interval (allowing for the appropriate horizontal shift). Field survey methods are generally used to test the maps, and the map elevation is obtained by interpolation between contours. Statistical sampling is used to select maps to be tested.

Early photogrammetric tests determined that vertical accuracy was a direct function of the flying height of the aerial photography. The "C" factor was developed to calculate the flying height required, given the contour interval and the operational characteristics of the photogrammetric instrument. Other specifications were developed in the production processes so that the finished maps would meet NMAS. The survey closures on supplemental-vertical control lines were required to be within one-tenth of the contour interval and spot elevations were within an accuracy of one-fourth the contour interval. The leveling surveys were done with instruments and procedures which would result in control which met the geodetic control specifications for third-order leveling originally established by the Bureau of the Budget.

THE FINISHED MAP

The topographic variations in USGS maps are considerable. Some examples are given in figures 2, 3, and 4. The topography can be intricate, such as displayed by the contours in figure 2; or very flat and smooth as in figure 3; or steep and rugged as in figure 4. Considering only the contours and the requirements of the NMAS, a limited amount of change in the vertical datum can be allowable without recontouring a map. It is suggested that one-tenth of the contour interval would be a reasonable amount. In flat country a change of less than 1 foot and up to 8 feet in mountainous regions might be allowable.

However, other ways of showing elevation data on a map, i.e. the spot elevations, are affected, and since they are shown to the nearest foot, present a different problem. Spot elevations appear frequently on USGS maps as



Figure 1.--Distribution of topographic maps by contour interval.

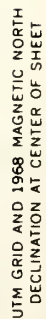
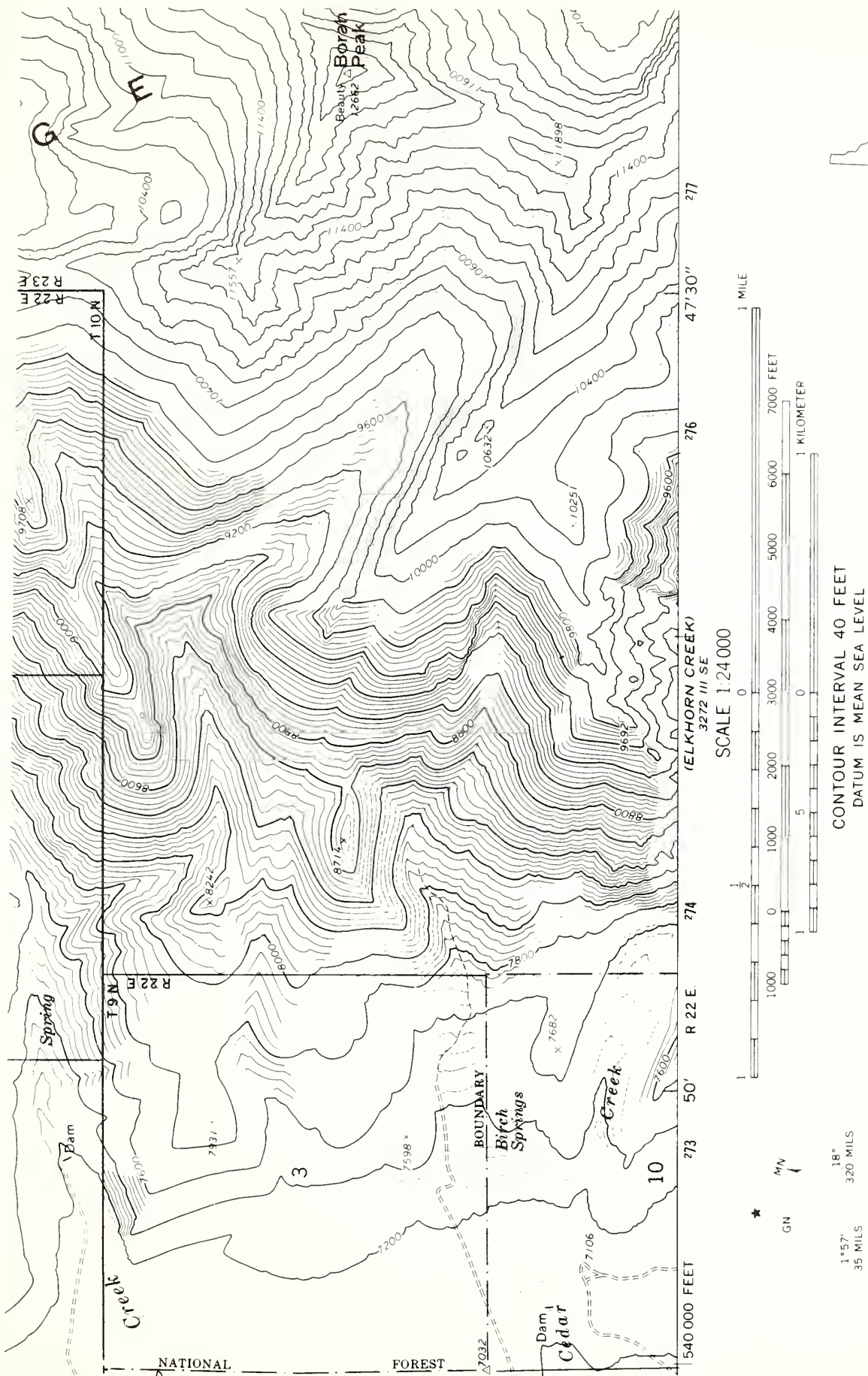


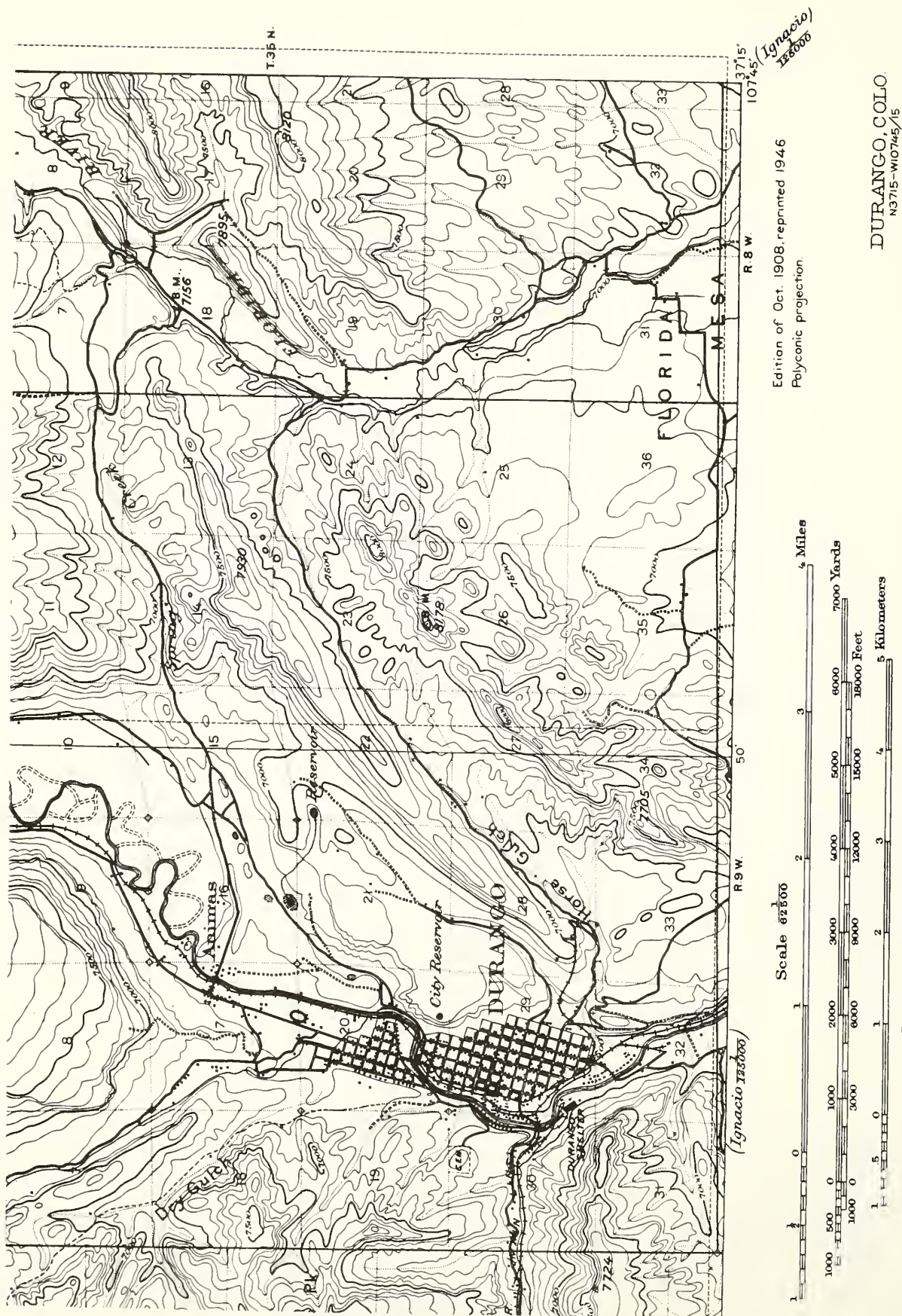
Figure 3.--Part of Meade NW, Kansas, 7.5-minute map (example of midwest farmland topography).



UTM GRID AND 1967 MAGNETIC NORTH
DECLINATION AT CENTER OF SHEET



Figure 4.--Part of Borah Peak, Idaho, 7.5-minute map (example of mountainous topography).



demonstrated in figures 2, 3, and 4. They are usually spaced two points per square mile or about 100 per 7.5-minute map. Redetermining and changing all these values on the maps of the NMP would be a significant undertaking.

DATUM CHANGE STATEMENT

Early in this century cartographers developed a method for extending the life of a topographic map that was made obsolete by a vertical datum change. The 1928 edition of the Topographic Instructions suggests the statement "readjustment indicates that elevations on this map should be increased (decreased) by ___ feet" be added to the map. The contouring of some topographic maps made early in this century was based on a local datum which probably was established by altimeter readings. When the National Vertical Network was later extended into the map area, this statement was applied to the reprinted map to allow the user to correct the elevations. An example of the use of this statement is displayed in figure 5.

CONCLUSIONS

A program for conversion of all maps of the NMP to the NAVD-88 would be prohibitively expensive. Adapting a new vertical datum to the NMP can however be accommodated by use of a datum change statement. This statement could be added at the time of reprinting, after the amount of the elevation change is known. A suitable statement could read "To correct elevations on this map to the NAVD-88, add (subtract) ___ feet."

When considering the NAVD-88 concurrently with NAD-83, the only solution to convert NMP map products is the preparation of a second edition of the series for the total country to convert NMP map products. The conversion of the 60,000 different maps of the National Mapping Program to the NAVD-88 appears to be an expensive (estimated \$45 million) undertaking at this time, given the present state of technology. Developments in the digital cartography technology over the next decade could make the task economically more feasible and reasonable. However, for the near-term, we believe that correction statements regarding the elevation change be added to existing maps. There seems little doubt that the combinations of the adaption of the NAD 83 and NAVD 88 and the development of improved mapping capabilities will lead to a new edition of large-scale coverage of the United States, starting in this century.

A REVIEW OF METHODS FOR PREDICTING LAND SUBSIDENCE CAUSED BY WITHDRAWAL OF GROUND WATER

Thomas L. Holzer
U.S. Geological Survey, MS 977
345 Middlefield Road
Menlo Park, CA 94025

ABSTRACT. Rates of land subsidence caused by withdrawal of ground water commonly are greater than 20 mm/yr and thus can rapidly compromise the accuracy of vertical geodetic control networks. Several methods are available to predict subsidence, but none are consistently accurate enough to provide an alternative to releveling for readjusting these networks. A numerical model developed by Helm (1975) offers some promise, but data required for calibration of the model may preclude its use in most areas.

INTRODUCTION

More than 22,000 km² of land underlain by unconsolidated sediment in the United States have subsided at least 0.3 m because of withdrawal of ground water. The total area that has experienced at least some subsidence is more than 26,000 km². Approximately 80 percent of this subsided area is in the San Joaquin Valley, California, and Houston-Galveston, Texas. The remainder is distributed among 23 different areas. The maximum magnitude of subsidence reported is 9.0 m, which was observed in the San Joaquin Valley from 1926 to 1970. Maximum magnitudes in each area more typically range from 0.5 to 2 m. Annual rates of subsidence commonly exceed 20 mm/yr. Such large losses of elevation have had major economic impact. In low-lying coastal areas, inundation may occur and the potential for flooding is increased in adjacent areas. Inland, differential subsidence may diminish the carrying capacity of canals.

This article is concerned with prediction of subsidence for the purpose of maintaining the accuracy of vertical geodetic control networks in subsidence areas. Accuracies of elevation-differences determined by First-order, class I, and Second-order, class II, leveling between bench marks 50 km apart, the distance between the margin and center of the largest subsidence areas, are approximately 4 and 9 mm, respectively (Federal Geodetic Control Committee, 1984). Thus, subsidence can rapidly reduce the accuracy of vertical geodetic control networks. In small subsidence areas, of course, networks are even more rapidly compromised. If subsidence could be accurately predicted, the frequency of relevelings required to maintain the accuracy of these networks could be reduced.

Several methods are available to predict subsidence. Figueroa Vega and Yamamoto (1984) have classified the methods into three categories: empirical, semi-theoretical, and theoretical. Empirical methods are based on curve fitting of historical subsidence trends; semi-theoretical methods are based on observed relations between subsidence and measurable quantities such as water-level change; and theoretical methods are based on idealizations of the aquifer system. In general, most methods were developed for application to areas where subsidence was ongoing. A few methods, however, are applicable to areas where water levels have not started to decline and there is no subsidence. The accuracy of each of these methods varies from site to site, and, in general, is not comparable to the standards of vertical geodetic

control networks (Federal Geodetic Control Committee, 1984). This report reviews these methods.

CONCEPTUAL BASIS OF LAND SUBSIDENCE

The physical process of land subsidence is conceptually simple and thoroughly documented by many field and laboratory investigations. As ground water is pumped from aquifers, the water level or head declines. This causes pore-water pressure to decrease. This decrease in turn causes the effective stress, the difference between total stress and pore-water pressure, to increase. Because deformation of porous media is controlled by changes of effective stress, pore volume is reduced. In geology and soils engineering, this process is known as compaction and consolidation, respectively. Because the width of aquifer systems typically is large relative to their thickness, all of the compaction is manifested at the land surface as subsidence. Thus, prediction of subsidence is equivalent to prediction of compaction.

Despite a general understanding of the physical process, prediction of subsidence under field conditions and based on physical concepts is confronted by two major obstacles--the heterogeneity of aquifer systems and the rheology of natural sediment. Most aquifer systems consist of interbedded coarse- and fine-grained strata. Pumping and water-level or head measurements are done in the coarse-grained strata, but most of the compaction occurs in the fine-grained strata. In general, compaction does not occur instantaneously with the head declines in the coarse-grained strata because time is required for the head declines to migrate into the fine-grained strata. Thus, compaction may be time dependent simply because pore pressures are not equilibrated within the aquifer system. The time delay is controlled by thickness, compressibility, and permeability of individual beds of the fine-grained strata. If the aquifer system is very heterogenous, detection of all of the fine-grained strata and determination of their physical parameters may be difficult if not impossible. The second obstacle to physically-based prediction methods is the rheology, i.e., response to stress, of fine-grained deposits. Deformation of many clayey deposits under stress is nonlinear and time dependent. Thus, theoretically based predictions at a site may require more data on material properties than are feasible to obtain.

PREDICTIVE METHODS

As was previously noted, predictive methods can be classified into three categories--empirical, semi-theoretical, and theoretical. Many of the methods were developed to analyze the characteristics of aquifer systems within a given subsidence area rather than for specific predictive purposes. Thus, the literature for evaluating the success of predictions is limited. The number of cases in which prediction can be compared with observation is further limited because subsidence commonly was arrested by man-induced water-level recoveries once local subsidence became great enough to warrant serious investigation and mitigation. Thus, published predictions and analyses are frequently hypothetical and have not been tested in realistic situations.

Empirical Methods

Extrapolation of a subsidence record by fitting a smooth geometric curve to leveling data for a period of observation is the simplest method of prediction. Although such curve-fitting may be performed without regard for water-level trends, it is inadvisable to do so since trends may change abruptly in response to many factors including weather, availability of alternative surface water, and economic conditions. In areas where water levels are declining at constant rates, the observed long-term relation between subsidence and time most commonly is linear. Where annual ground-water demand changes significantly, a constant rate of water-level decline and hence subsidence would not be expected. Figueroa-Vega and Yamamoto (1984) published examples of quadratic, exponential, and log-log relations of subsidence with time. They did not specify the nature of the water-level trends during the period of record. Caution should be exercised, however, in extrapolating even linear relations exhibited over long time periods. Some aquifer systems behave bilinearly in response to water levels that decline at a constant rate; that is, the rate of subsidence increases to a new constant value when water-level declines exceed a threshold value (Holzer, 1981). This behavior is probably caused by a change of compressibility as effective stresses in the aquifer system increase. Empirical methods based on curve fitting are deceptively simple and must include analysis of water-level data.

Semi-theoretical Methods

Semi-theoretical methods are based on observed relations between subsidence and related phenomena or parameters. The relations may have a theoretical basis, but it is not a prerequisite for the method. These methods have the advantage over empirical methods that they can accommodate changes of water-level trends to a limited degree.

The ratio of subsidence to head decline is commonly computed by subsidence investigators and is potentially very useful for prediction. The ratio represents the change of aquifer system thickness per unit change in pore pressure, and is therefore proportional to the compressibility of the aquifer system. This ratio when divided by the thickness of the compacting strata determined from boreholes is called the specific unit compaction (Poland and others, 1972). Instantaneous values of specific unit compaction usually are minimum estimates of compressibility because water-level declines are measured in the coarse-grained strata and are greater than the instantaneous values in the slowly draining fine-grained strata. If drainage of the fine-grained strata is complete, specific unit compaction equals the gross compressibility of the system. It has also been demonstrated that if drainage from the fine-grained strata is incomplete, but water-level declines and subsidence are occurring at constant rates, a dynamic equilibrium is achieved and unit specific compaction equals gross compressibility (Holzer, 1981).

As was noted in the discussion of empirical methods, investigations in several areas have indicated that the rates of subsidence may increase when head declines exceed a threshold value unique to a particular area. Therefore, ratios of subsidence to head decline may depend on the magnitude of head decline as well as the completeness of drainage from the fine-grained strata.

The ratio of subsidence to the volume of water withdrawn also has potential application for subsidence prediction. Most of the published correlations, however, are between subsidence volume and the volume of pumped water and thus are unsuitable for prediction of subsidence of individual bench marks. A few examples have been published that describe linear relations between subsidence of individual bench marks and the volume of fluid withdrawn. The most detailed investigation is of several oil fields in California (Castle and others, 1969). This type of subsidence is phenomenologically similar to that from withdrawal of ground water (Poland and Davis, 1969). The authors suggested that the reason for the linear relation was that the volume of liquid production was a better index of average pore-pressure decline than estimates obtained from borehole pressure measurements.

Gabrysch (1969) documented a relation in Houston, Texas, between the ratio of subsidence to head decline and the percentage of clay in the aquifer system. He found that ratio increased in direct proportion to the clay content of the aquifer system. His method has the advantage that it can be used for predictions at sites lacking subsidence data, but having lithologic and head or water-level data. The method suffers, however, from the same potential shortcoming as the ratio of subsidence to head-decline method; the ratio may be time dependent if there are slowly-draining fine-grained strata in the aquifer system.

Theoretical Methods

Most theoretically-based analyses of land subsidence are based on Terzaghi's theory of consolidation (e.g., Lambe and Whitman, 1969). These methods involve analytical or numerical solutions to a boundary value problem based on a one-dimensional equation of vertical flow in the compacting layers. The boundary conditions are pore pressures based on head changes specified at the boundaries of the compacting layers. Domenico and Mifflin (1965) provide an excellent review of this approach as it is applied to land subsidence. In this approach, computation of head declines in the aquifer usually are decoupled or separated from the computation of deformation. Although this decoupling is for analytical convenience, in most field cases it is a reasonable approximation of the physical processes involved in subsidence because of the typically large permeability contrast between fine and coarse-grained strata. A large contrast causes flow in the fine-grained beds to be predominantly vertical (Neuman and Witherspoon, 1969). In the decoupled approach, ground-water flow models are applied to the coarse-grained strata to yield predictions of head changes within these strata, although some of the sophisticated flow models consider flow through the fine-grained strata (e.g., Bredehoeft and Pinder, 1970). The computed head changes are then applied to the boundaries of the fine-grained strata to predict compaction. Three examples of decoupled models that have been applied in specific areas include those developed by Gambolati and Freeze (1973), Helm (1975, 1976), and Narasimham and Witherspoon (1977).

A few investigators have coupled deformation and flow by applying Biot's theory of three-dimensional consolidation (Biot, 1941). As Gambolati and Freeze (1973) recognized, the elegance and rigor of the Biot system of equations is not in doubt, but the practicality of its applicability to geologically realistic situations of subsidence from withdrawal of ground water is. The number of required parameters is larger than for decoupled

approaches and solutions are harder to obtain. For an example of the coupled approach, the reader is referred to Safai and Pinder (1980).

Even with decoupled methods, obtaining representative physical properties of the aquifer system is difficult. Use of laboratory-based parameters from borehole samples has yielded mixed results, with experience in the United States being particularly discouraging (Helm, 1984). Christian and Hirschfield's (1974) example of repeatedly revised predictions of subsidence in the Wilmington oil field is also illustrative of the ground-water experience (Fig. 1).

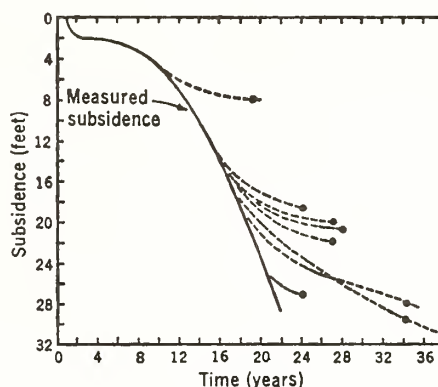


Figure 1. Predicted and observed maximum subsidence at Long Beach, California, associated with pumping of oil from the Wilmington oil field. Time is measured from the beginning of pumping. Solid line is observed subsidence. Dashed lines are subsidence histories predicted by different investigators. Predictions were made at different times after subsidence began (from Christian and Hirschfield, 1974).

The only theoretical model that has been geographically widely applied is Helm's (1975, 1976) field-based decoupled model. The model has been used to simulate subsidence in the San Joaquin and Santa Clara Valleys, California, the Houston-Galveston area, Texas, and the Latrobe Valley, Australia. Input for Helm's model consists of thicknesses of compressible strata, pore-pressure distributions in these strata at the beginning of the calibration period, and observed water levels and associated compaction or subsidence for a multi-year calibration period. Nonunique physical parameters are estimated by trial and error during the calibration period. If water-level recoveries are anticipated during the prediction period, the calibration period must include periods of water-level recovery because aquifer systems respond differently to decreasing effective stress than they do increasing effective stress.

An advantage of theoretical models over empirical and semi-theoretical models is that theoretical models are potentially more accurate if water-level trends change. Because ground-water pumping and water levels can be significantly affected by weather, economic conditions, and local water management practices, this aspect of theoretical models may favor their use where accuracy is an important consideration such as in geodetic applications.

APPLICATION TO GEODETIC CONTROL NETWORKS

Historically, vertical geodetic control networks in subsidence areas have been maintained by repeated levelings to stable bench marks outside of the subsidence area. Because subsidence rates greater than 20 mm/yr are common, even annual relevelings often are unable to maintain the accuracy of these networks which, as was noted, is approximately 4 mm for marks 50 km apart that are leveled to First-order, class I, standards. Thus, subsidence prediction methods offer an approach for improving the accuracy of these networks during the intervals between relevelings. This is, however, a new application of subsidence prediction methods. This section discusses the accuracy of the most popular method in each of the three categories. In general the accuracy required of these methods has not been comparable to that required by geodetic control networks.

The accuracy of predictions based on both linear extrapolation of subsidence records and subsidence to head ratios is strongly dependent on the uniformity of water-level declines. Linear extrapolation of subsidence records will be most accurate where water levels decline at a constant rate. Under this hydrologic condition, predictions to within a few centimeters may be achieved for time periods greater than a decade. Constant-rate water-level declines are rarely observed in practice. In general, water levels fluctuate both annually in response to seasonal ground-water demands and over multiyear periods in response to changes of weather, economic conditions, and water management practices. As a result, the accuracy of linear extrapolations will more commonly be measured in decimeters over periods even as short as a few years.

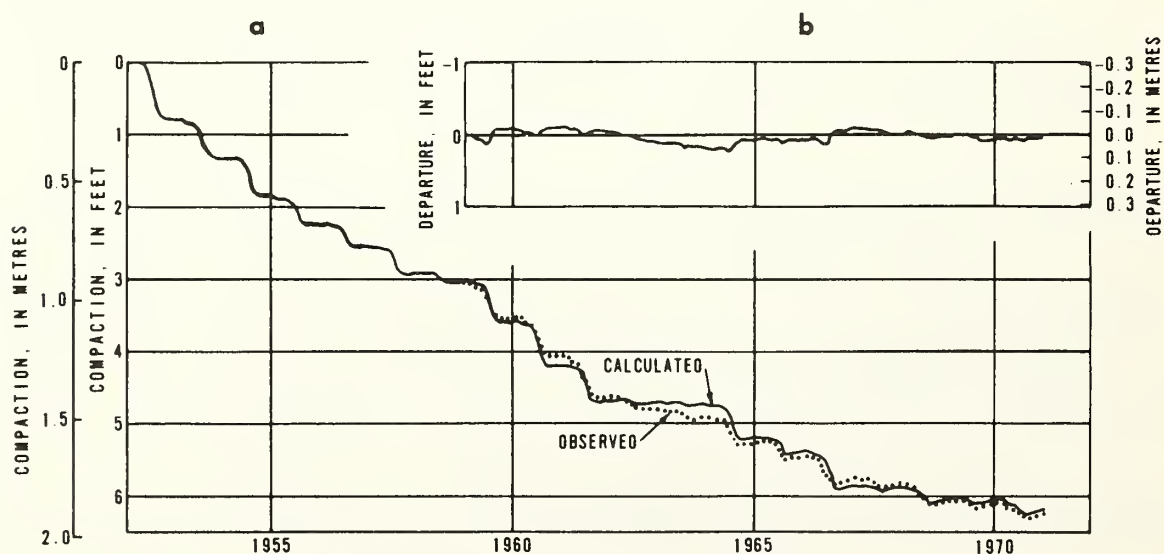


Figure 2. A. Comparison of Helm's (1975) calculated compaction, 1959-1970, based on water-level data for well in San Joaquin Valley, California, with observed compaction. B. Difference (departure) between observed and calculated values. Period 1952-58 was used to calibrate model (from Helm, 1975).

Subsidence-to-head ratios may be used in some situations to compensate for the effect of variations of water-level changes. Ratios are particularly applicable where migration of head declines in coarse-grained strata into the compressible fine-grained strata is rapid. Under this condition, it may be possible to predict subsidence to within a decimeter.

The third method, Helm's (1975, 1976) numerical model, is more flexible than either of the empirical or semi-theoretical methods just reviewed. It can accommodate more complex patterns of water-level change. To obtain accurate results, however, more data are required than for the first two methods. First, the thicknesses of the compressible strata in the aquifer system must be known. Second, the distribution of the pore pressures in the fine-grained strata at the beginning of the calibration period is required. And third, documentation of the historical relation between subsidence and water-level change is needed for model calibration. Helm (1977) demonstrated the sensitivity of the model to amount of subsidence and water-level data available for calibration. For example, at a site in the Santa Clara Valley, California, Helm (1977) found that errors of prediction would be greater than 6 cm if only two calibration points, i.e., two relevelings with contemporaneous water-level data, 3-1/2 years apart were available. The accuracy was improved by using continuous records for calibration. On the basis of 7-year continuous records of water levels and compaction at a site in the San Joaquin Valley, California, compaction predicted with observed water levels agreed with observed compaction to within 7 cm over a 12 year period (Fig. 2).

CONCLUSIONS

Rates of subsidence caused by withdrawal of ground water commonly are high enough to compromise the accuracy of geodetic control networks in subsidence areas. Many methods have been developed that can be used to predict subsidence, but none of them consistently achieve the accuracy required for vertical geodetic control networks. Achievable accuracies range from a few centimeters to decimeter. To achieve maximum accuracy, all of the methods require data on and analysis of past water-level changes.

REFERENCES

- Biot, M. A., 1941: General theory of three-dimensional consolidation, *Journal of Applied Physics*, v. 12, no. 2, pp. 155-164.
- Bredehoeft, J. D., and Pinder, G. F., 1970: Digital analysis of areal flow in multiaquifer ground-water systems: A quasi-three-dimensional model, *Water Resources Research*, v. 6, no. 3, pp. 883-888.
- Castle, R. O., Yerkes, R. F., and Riley, F. S., 1969: A linear relationship between liquid production and oil field subsidence, *International Association of Scientific Hydrology Publication 88*, pp. 162-171.
- Christian, J. T., and Hirschfield, R. C., 1974: Subsidence of Venice: Predictive difficulties, *Science*, v. 185, p. 1185.

- Domenico, P. A., and Mifflin, M. D., 1965: Water from low permeability sediments and land subsidence, *Water Resources Research*, v. 1, pp. 563-576.
- Federal Geodetic Control Committee, 1984: Standards and specifications for geodetic control networks, National Geodetic Information System, Rockville, MD, pp. 2-2.
- Figueroa Vega, G. E., and Yamamoto, S., 1984: Techniques for subsidence in J. F. Poland (ed.), *Guidebook to studies of subsidence due to ground-water withdrawal*, Unesco, pp. 89-106.
- Gabrysch, R. K., 1969: Land-surface subsidence in the Houston region, Texas, *International Association of Scientific Hydrology Publication* 88, pp. 43-54.
- Gambolati, G., and Freeze, R. A., 1973: Mathematical simulation of subsidence of Venice: 1. Theory, *Water Resources Research*, v. 9, pp. 721-733.
- Helm, D. C., 1975: One-dimensional simulation of aquifer system near Pixley, California: 1. Constant parameters, *Water Resources Research*, v. 11, no. 3, pp. 465-478.
- 1976: One-dimensional simulation of aquifer system compacting near Pixley, California: 2. Stress-dependent parameters, *Water Resources Research*, v. 12, no. 3, pp. 375-391.
- 1977: Estimating parameters of compacting fine-grained interbedded confined aquifer system by a one-dimensional simulation of observations: *International Association of Scientific Hydrology Publication* 121, pp. 145-156.
- 1984: Field-based computational techniques for predicting subsidence due to fluid withdrawal, *Geological Society of America, Review of Engineering Geology*, v. VI, pp. 1-22.
- Holzer, T. L., 1981: Preconsolidation stress of aquifer system and induced land subsidence, *Water Resources Research*, v. 17, pp. 693-704.
- Lambe, T. W., and Whitman, R. V., 1969: *Soil mechanics*, pp. 41-42, New York, John Wiley.
- Narasimhan, T. N., and Witherspoon, P. A., 1977: Numerical models of subsidence in shallow ground-water systems, *International Association of Scientific Hydrology Publication* 121, pp. 133-143.
- Neuman, S. P., and Witherspoon, P. A., 1969: Application of concepts of flow in leaky aquifers, *Water Resources Research*, v. 5, pp. 817-829.

Poland, J. F., and Davis, G. H., 1969: Land subsidence due to withdrawal of fluids, Geological Society of America, Reviews in Engineering Geology, v. II, pp. 187-268.

Poland, J. F., Lofgren, B. E., and Riley, F. S., 1972: Glossary of selected terms useful in studies of the mechanics of aquifer systems and land subsidence due to fluid withdrawal: U.S. Geological Survey Water-supply Paper 2025, p. 3.

Safai, N. M., and Pinder, G. F., 1980: Vertical and horizontal land deformation due to fluid withdrawal, International Journal for Numerical and Analytical Methods in Geomechanics, v. 4, pp. 131-142.

ON THE EFFECT OF SEASONAL VARIATION OF GROUND WATER LEVEL ON GEODETIC LEVELING

Yoshio Baba and Masaru Kaidzu
Geographical Survey Institute
Ministry of Construction, Kitazato-1, Yatabe-Machi
Tsukuba-Gun, Ibaraki-Ken, 305 JAPAN

ABSTRACT. In land subsidence areas in Japan, ground water level and ground shrinkage are usually monitored to prevent further subsidence. In such areas, it is often observed that the amount of ground shrinkage varies with changes of season. In such an area, if precise leveling were carried out without regard to this phenomenon, the results would be contaminated. In this paper, an example is given and a numeric simulation on the effect of disregarding such periodic ground shrinkage on the result of a leveling network adjustment is shown.

INTRODUCTION

Since it became clear that most rapid land subsidence is caused by over-pumping groundwater, groundwater levels and ground shrinkage are monitored to prevent further subsidence. In areas where the rate of subsidence decreased to negligibly small values, it was often observed that the amount of ground shrinkage showed some seasonal change corresponding to the seasonal change of the ground water level. The amplitude of such periodic change amounts to as much as 1 to 2 cm. If we carried out a precise leveling survey in such an area without regarding these effects, the result would be contaminated by this unmodeled vertical movement. Because such an area is usually densely populated and seismicity is high throughout Japan, crustal motion is monitored in such areas to decrease earthquake hazard. Therefore, systematic bias in the results of precise leveling is undesirable.

To see the effect of this unmodeled vertical motion on adjusted precise leveling results, a numeric simulation on a simple model network was carried out. The possibility of modeling the phenomenon using observed ground water heights in deep wells is discussed.

AN EXAMPLE OF SEASONAL CHANGE ON GROUND SHRINKAGE

Niigata prefecture, Japan, is known for heavy snowfall in winter. To help clear streets for traffic, warm ground water is pumped and sprinkled on the main streets. Because of this, the amount of pumped ground water increases in the winter time and the ground water level shows large seasonal change. In a year of heavy snowfall, the decrease in ground water level is very large. To monitor the ground water level, the Niigata prefectural government maintains observation wells. At these wells, ground water level and the amount of ground shrinkage are observed continuously throughout the year.

In figure 1, the results of recent observations at the Takada G-2 well are shown. The amplitude of the seasonal change has good correlation with the groundwater level and the amount of snowfall. The ground shrinkage shown in this figure corresponds to the shrinkage of the layer between the surface and 136 m under the ground surface. When we have a heavy snowfall, as in the

winter of 1981, the ground shrinkage in the winter time exceeds more than 2 cm and cannot recover even by the end of the next autumn. In such a case, even if leveling is carried out in the same season of the year, there remains a discrepancy between the height differences leveled in one year and another year.

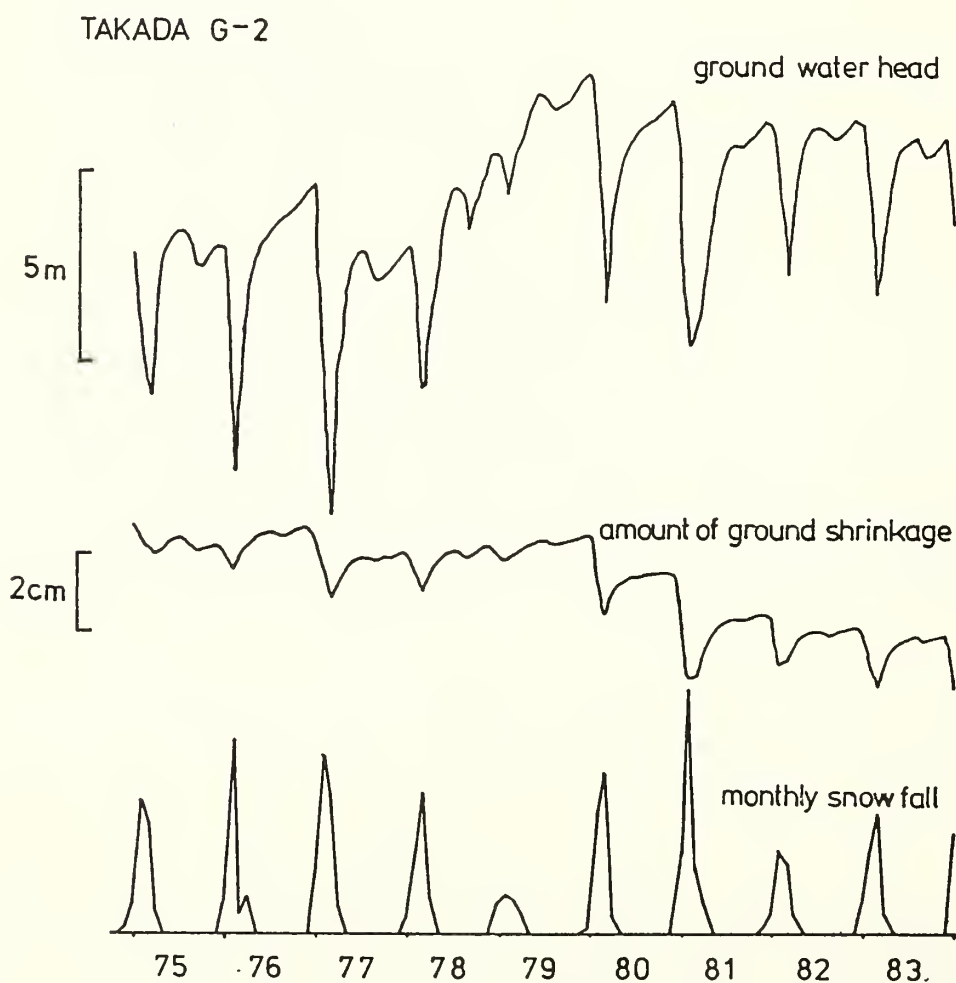


Figure 1.-- Seasonal change of ground water head and ground shrinkage observed at Takada G-2 observation well (Niigata prefectural government, 1984).

SIMULATION OF THE EFFECT OF UNMODELED VERTICAL MOVEMENT

To see the effect of unmodeled seasonal vertical motion, a numerical simulation was carried out using a simple model network.

The model network used for simulation is shown in figure 2. The simulation was carried out by adjusting data in which the height differences are not consistent at the junction bench marks in the assumed subsidence area. Only the elevations of junctions are adjusted in the simulation.

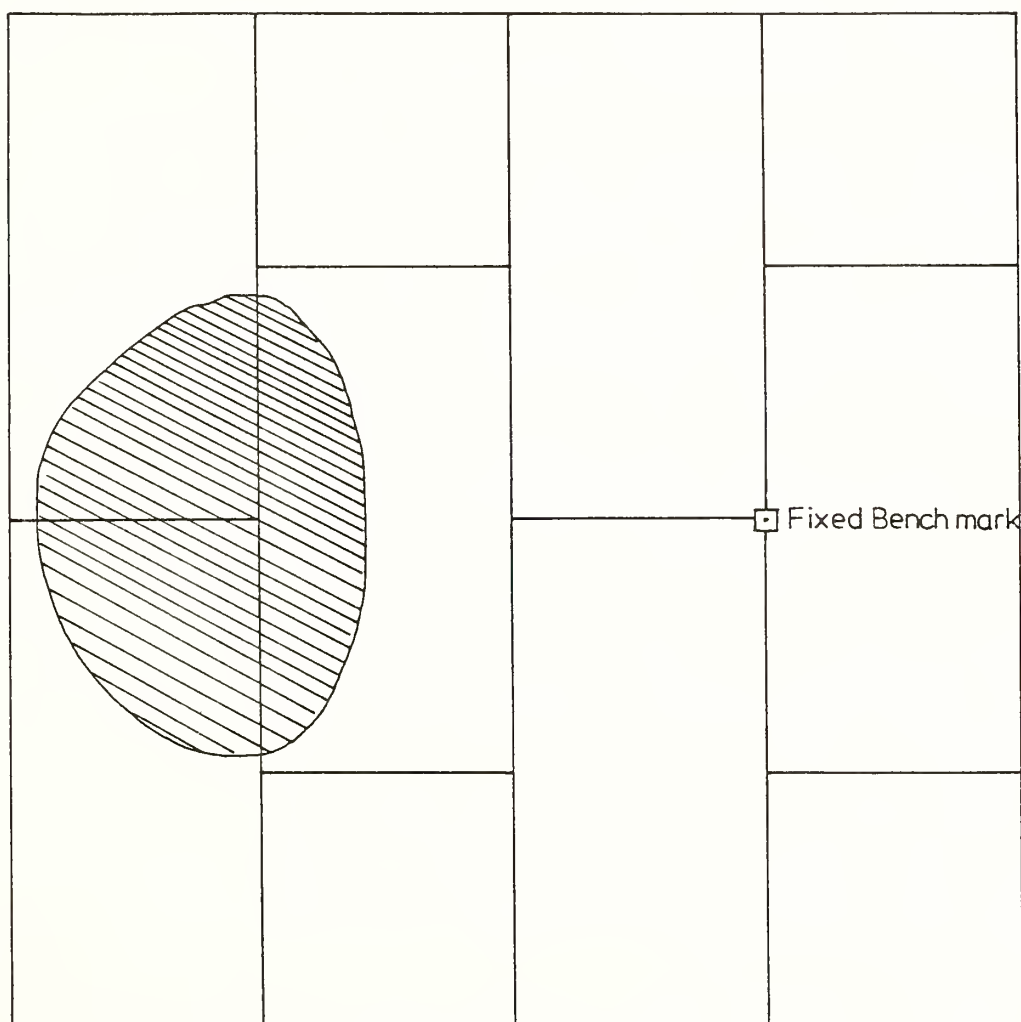


Figure 2.-- Model network for the simulation

The result of the simulation is shown in figure 3. Open arrows show the assumed path of the survey crew through the subsidence area. Along an arrow, the height differences are consistent, but in the direction of different arrows, height differences have 2 cm of discrepancy. It is interesting that in both cases the center of the bias caused by unmodeled vertical motion is not located at the center of the subsidence area. Although the bias is not more than 1 cm, its systematic pattern and the shift of the center from the center of the subsidence area could possibly cause misinterpretation of the results of the leveling survey.

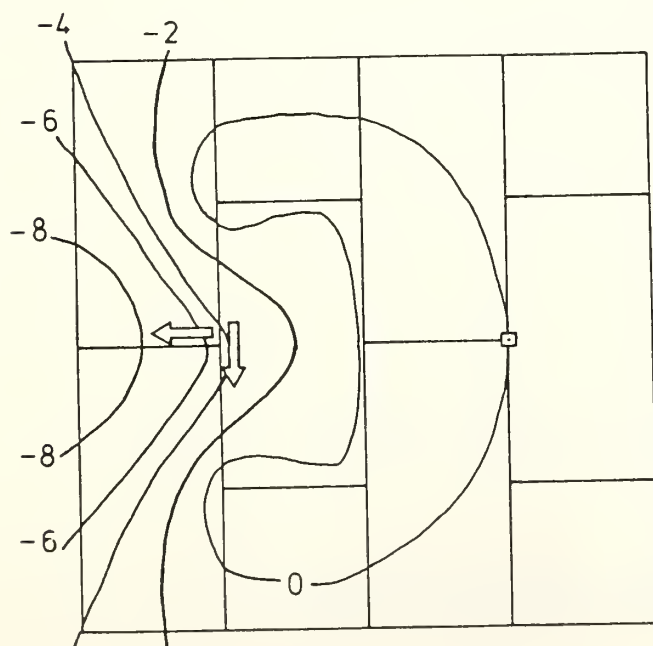
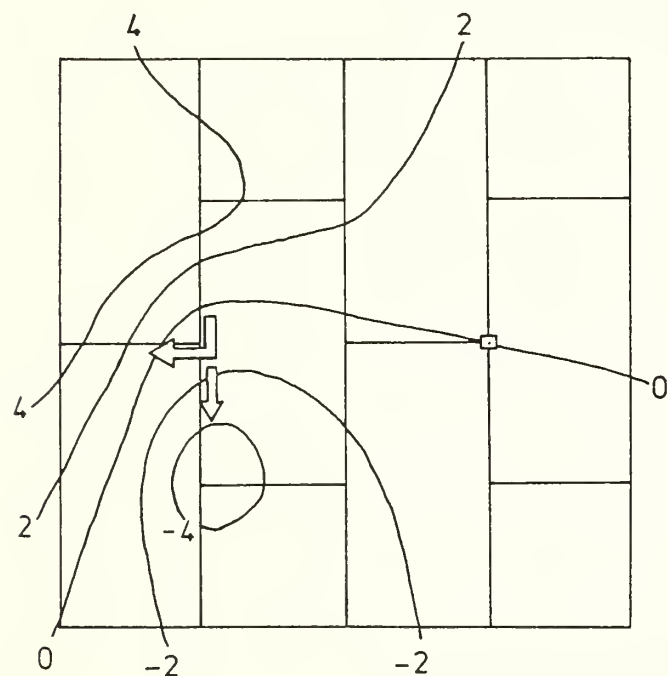


Figure 3.-- Effect of unmodeled vertical motion on the adjusted leveling results, in millimeters.

OTHER SIMILAR PHENOMENA

Besides the phenomena discussed above, we have examples of similar seasonal vertical motion in the Japanese peninsulas. Inouchi (1973) reported the seasonal tilt of Miura peninsula near Tokyo, detected by frequent leveling surveys. In figure 4, the seasonal vertical motion of Omaezaki peninsula is shown. These seasonal vertical motions of the peninsulas seem to have a good correlation with changes in sea level.

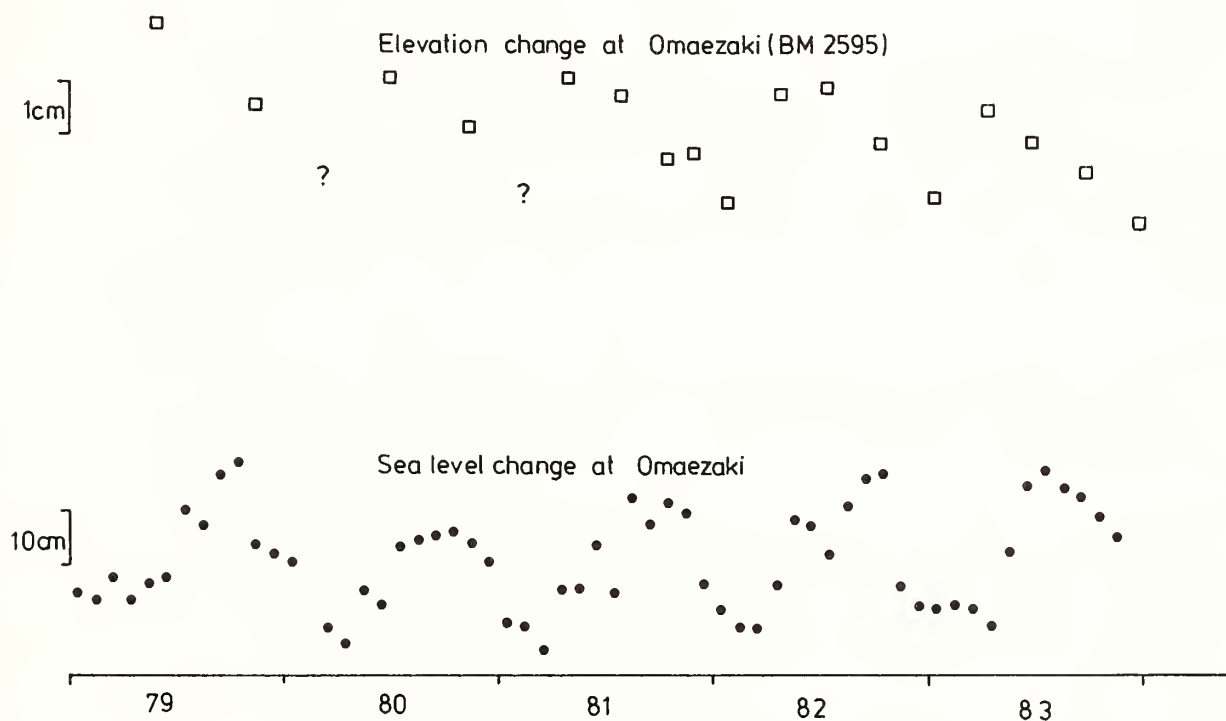


Figure 4.-- Seasonal elevation changes at Omaezaki (Tazima et al., 1984). Omaezaki is the peninsula on the south coast of Japan in the area where the Tokai earthquake is expected to occur in the near future.

The best way to eliminate the effect of this phenomenon is to model the seasonal vertical motion and correct the height differences. However, seasonal vertical motion is not quite periodic as shown in figure 1. Therefore, we need to possess at least the information of groundwater level and the mathematical relation between the groundwater level and the elevation of the bench marks concerned.

If modeling is not practical, we can limit the effect in a certain area. When the network is redundant enough, we can bypass the land subsidence area or down-weight the observed values in such an area. If not, we should survey through the land subsidence area as quickly as possible, so that the unmodeled vertical motion does not amount to a significant quantity before the survey in the area is completed. Doing that, we can limit the effect of the unmodeled vertical motion in the land subsidence area. That is because the height differences measured in such a way are internally consistent and no bias is caused by network adjustment procedure.

CONCLUSION

It is shown that the seasonal vertical motion of the ground caused by the change of the ground water level or similar seasonal vertical motion of the Japanese peninsulas, may cause systematic bias in the adjusted elevation of the bench marks. Because the center of the pseudo-vertical-motion may not be at the center of the real vertical motion, misinterpretation of the leveling results may occur. To limit the effect of such seasonal vertical motion in a certain area, the area should be thoroughly surveyed as quickly as possible.

REFERENCES

- Niigata prefectural government (1984): Jouetsu chiku no kansoku kiroku (Record of the monitoring in Jouetsu), in Japanese.
- Inouchi, Noboru (1973): Astronomical effect on precise levelling for land tilt measurement in the Miura Peninsula, J. Geod. Soc. Japan, 19, pp. 50-52.
- Tazima, M., N. Matsumoto, and M. Kaizumi (1984): Relation between seasonal variation of the Omaezaki Peninsula and sea level change, J. Geod. Soc. Japan, 30, pp. 107-113.

AN UPDATE ON RATES OF APPARENT VERTICAL MOVEMENT IN THE GREAT LAKES BASIN

B.J. Tait and P.A. Bolduc
Ocean Science and Surveys
Department of Fisheries and Oceans
Ottawa, Canada K1A 0E6

ABSTRACT

Numerous researchers have used long period water level data from permanent gauging stations located on the shores of the Great Lakes to determine rates of relative movement in this area. A report published in 1977 by the Coordinating Committee on Great Lakes Basic Hydraulic and Hydrologic Data provided rates of movement based on data from 1974 as far back as 1916. The rates of apparent vertical movement are computed in this paper using data up to 1983. Significant differences between these rates and those reported in previous studies are examined.

INTRODUCTION

Crustal movement in the Great Lakes basin is a phenomenon which has been studied by a variety of researchers and is generally conceded to be an ongoing process. The method most frequently used to determine the rates of movement employs long period records of the water levels measured at numerous gauging stations on the Great Lakes and assumes that the lake surface is a level surface once short period disturbing influences have been averaged out of the water level data. If the differences in water levels recorded at two stations on the same lake show a trend over the years rather than remaining constant then, in the absence of other factors such as bench mark instability or operator errors, a differential movement of the land mass between the station sites is assumed to have occurred.

The Coordinating Committee for Great Lakes Hydraulic and Hydrologic Data was formed in 1953 by interested federal government agencies in the United States and Canada as a focal point for the development of mutually acceptable data bases. A number of reports on apparent vertical movement over the Great Lakes have been published under the auspices of this committee, the most recent one in 1977 utilized data up to 1974. The purpose of the present study is to compute rates of movement based on the procedure used by the Coordinating Committee (1977) but including water levels recorded to 1983. The rates so obtained will be compared with results from earlier studies and any significant differences will be examined.

PREVIOUS STUDIES

The comparison of water level records at pairs of stations located on the same lake for hydraulic studies is not a recent innovation. Moore (1948) reports that the U.S. Lake Survey used the principle of the water level transfer as early as 1875 to establish elevations over long distances.

Studies of crustal movement based on Great Lakes water level data have been carried out by Moore (1948), Price (1954), the Vertical Control Subcommittee of the Coordinating Committee on Great Lakes Basic Hydraulic and Hydrologic Data (May, October, November and December, 1957), Kite (1972) and the Coordinating Committee on Great Lakes Basic Hydraulic and Hydrologic Data (1977). These studies have employed a variety of techniques and data sets.

Moore (1948) used all available records in the lakes, including data from as far back as 1836 in the case of Milwaukee, Wisc. Prior to the installation of self-registering gauges in the early 1900's the observations were based on daily or tri-daily staff readings. Means of the months June to October inclusive were used for all lakes except Lake Erie, in which case May to September were used. The differences for pairs of stations were plotted, straight lines drawn through the points, and "the rates of movement ... adjusted for harmony by the method of Least Squares". (Moore, 1948). The rates computed at selected sites are shown in Table 1, column (a).

Price (1954) carried out a study of Lake Ontario movement rates using the data from five stations. The water levels used for 3 of the stations date to the 1860's. The yearly mean values are based on the four months June to September in order to eliminate possible discrepancies arising from staff reading taken during less than ideal conditions such as spring run-off, ice or gales. Price computed differences between pairs of gauging stations based on yearly means as well as on five year moving means. Differences were also computed between the individual stations and the mean of all five stations. Selected results based on the yearly differences between pairs of individual stations are presented in column (b) of Table 1.

The Vertical Control Subcommittee (1957) used water levels recorded in the four months June to September for the full period of record. Differences in water levels for pairs of stations were computed and a straight line fitted to the data by least squares. The rates so determined were adjusted by balancing the sums of rates within groups of three stations. Only the unadjusted rates are reported in this paper and may be found in column (c) of Table 1. In the case of Lake Ontario rates were computed for the period 1916 to 1956 as well as for the full period of record.

Kite (1972) computed relative rates of movement for pairs of stations based on a linear least squares fit to the differences between yearly mean water levels computed from all 12 months of data. These rates were adjusted using a least squares triangulation technique. Again only the unadjusted rates are reported on this paper (column (d), Table 1). The complete length of record available for each station was employed by Kite.

The Coordinating Committee on Great Lakes Basic Hydraulic and Hydrologic Data (1977) published a second study on apparent vertical movement over the Great Lakes. This study utilized means of June to September water levels for stations with a minimum of 40 years of reliable data prior to 1970. In no case did this include data collected prior to 1916. The rates of apparent vertical movement between pairs of stations were computed by linear regression of the difference in the four-month means (Table 1, column (e)). One of the recommendations coming from this study was that the rates of movement should be updated in about 10 to 12 years.

TABLE 1. APPARENT VERTICAL MOVEMENT AROUND THE
GREAT LAKES COMPUTED BY VARIOUS AUTHORS
(Rates in millimeters per century)

Gauging Station Pair	(a) MOORE	(b) PRICE	(c) Vertical Control Subcomm. (1957)	(d) KITE	(e) Coord. Comm.	(f) TAIT & BOLDUC
<u>Lake Ontario</u>						
Toronto Kingston		+201	+216 (1894-1956) +177 (1916-1956)	+203	+174	+164
Oswego Kingston	+ 70	+ 64	+ 37 (1896-1956) + 73 (1916-1956)	+ 22	+ 79	+76
Oswego Toronto	-177	-137	-189 (1861-1956) -104 (1916-1956)	-180	- 94	-88
<u>Lake Erie</u>						
Cleveland Port Colborne	+101		+131	+139	- 6	+ 3
Port Stanley Port Colborne			+ 21	+ 82	- 61	- 46
Port Stanley Cleveland	- 24		+ 34	- 97	- 55	- 49
<u>Lakes Huron and Michigan</u>						
Thessalon Goderich			-213		-207	-215
Goderich Milwaukee			-140	+ 89	-149	-131
Goderich Collingwood			-162		+204	+206
Goderich Harbor Beach	+ 12		- 3	+ 55	+ 15	+ 37
Goderich Mackinaw City			+113		+ 94	+117
<u>Lake Superior</u>						
Michipicoten Thunder Bay			- 85		-232	-210
Michipicoten Marquette	-168		-308	-302	-408	-394
Michipicoten Duluth			-408	-437	-521	-509
Thunder Bay Marquette	-207		-183	-216	-177	-175
Thunder Bay Duluth			-280	-355	-290	-299

BASIC DATA AND COMPUTATIONS

The water level data used to compute the rates of apparent vertical movement reported on in this paper are those recorded at selected permanent gauging stations on the Great Lakes. These stations are the responsibility of the National Ocean Service of the Department of Commerce in the United States and the Canadian Hydrographic Service of the Department of Fisheries and Oceans in Canada. The stations used are shown in Figure 1 and the period of record employed for each station is listed in Table 2.

The monthly mean water levels for the four months June to September recorded at each station were meaned to provide a time series of yearly values for each station. Differences between the yearly values were determined for the pairs of stations listed in Table 3 and the rate of apparent vertical movement computed by linear regression analysis of the differences.

RESULTS

Sample plots of the differences and the linear equation fitted to the data are shown for one pair of stations on each lake in Figures 2 to 6. Also plotted are the 95% confidence intervals for the data points and for the regression coefficient (trend).

The rates of apparent vertical movement in millimeters per century between stations on Lakes Ontario, Erie, Michigan, Huron, and Superior are given in Table 3 along with the standard error of the regression coefficient. The rates from the Coordinating Committee report of 1977 are provided in this table for comparison.

DISCUSSION

The rates of apparent vertical movement computed in this report for Lakes Ontario, Erie, Huron-Michigan and Superior are shown in Table 3 and indicate no significant changes from those reported by the Coordinating Committee (1977). The differences between the two data sets are of the order of the standard error for the rates computed in this report.

The largest magnitudes for the rates occur on Lake Superior, where a value of 509 mm/century for the Michipicoten-Duluth gauging station pair is reported, and on Lakes Huron and Michigan. The rates on Lakes Ontario and Erie are generally smaller in magnitude.

A comparison of the rates computed by previous authors and those reported in this study is given in Table 1. An examination of this table indicates reasonably consistent results in view of the various techniques and record lengths used. Notable exceptions are the results for the Cleveland-Port Colborne station pair on Lake Erie. The rates determined by earlier studies (+100 to +140 mm/century) vary markedly from the results of the Coordinating Committee (1977) and this paper (-6 and +3 mm/century respectively).

A study of the documentation for the Pt. Colborne gauging station indicates that two separate adjustments were made to the historical data records. One adjustment, reduced the water level data for the years 1951 to 1959 inclusive by approximately 0.12 feet; a second adjustment, made in 1975, reduced the water level data for the years 1911 to 1950 inclusive by 0.15 feet. These adjustments

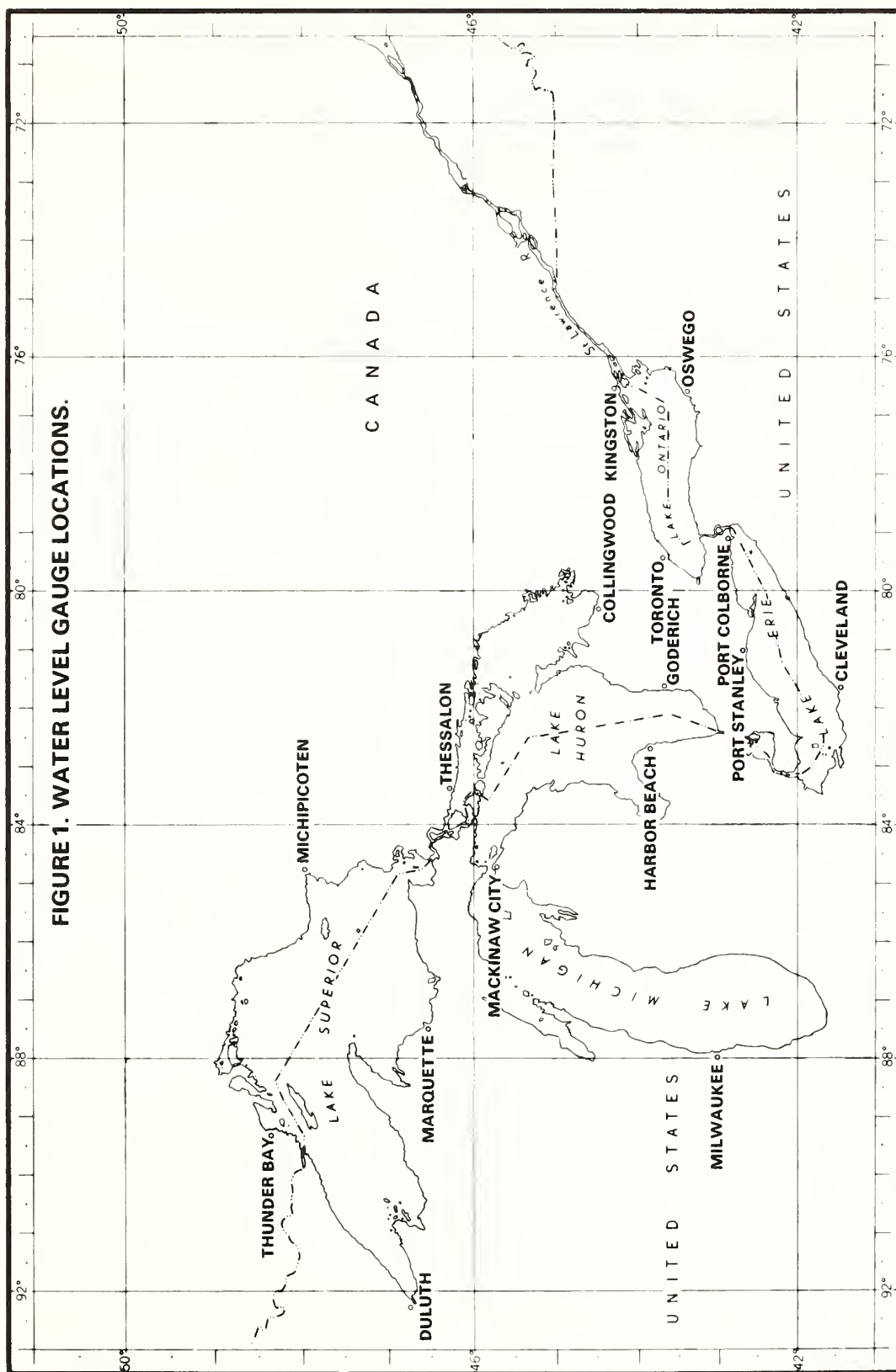


FIGURE 1. WATER LEVEL GAUGE LOCATIONS.

TABLE 2. LIST OF GAUGING STATIONS AND
PERIODS OF RECORDS USED

<u>LAKE</u>	<u>STATION</u>	<u>PERIOD OF RECORD</u>
Ontario	Kingston, Ontario	1916-1983
	Toronto, Ontario	1916-1983
	Oswego, N.Y.	1916-1983
Erie	Port Colborne, Ontario	1926-1983
	Port Stanley, Ontario	1926-1983
	Cleveland, Ohio	1926-1983
Huron-Michigan	Goderich, Ontario	1927-1983
	Collingwood, Ontario	1927-1983
	Thessalon, Ontario	1927-1983
	Harbor Beach, Michigan	1927-1983
	Mackinaw City, Michigan	1927-1983
	Milwaukee, Wisconsin	1927-1983
Superior	Thunder Bay, Ontario	1931-1983
	Michipicoten, Ontario	1931-1983
	Duluth, Minn.	1931-1983
	Marquette, Michigan	1931-1980

TABLE 3. APPARENT VERTICAL MOVEMENT RATES
(Rates in millimeters per century)

<u>First Station</u>	<u>Second Station</u>	<u>Rate*</u>	<u>Standard Error</u>	<u>Previous** Rate</u>
<u>Lake Ontario</u>				
Toronto	Kingston	+ 164	6	+ 174
Oswego	Kingston	+ 76	4	+ 79
Oswego	Toronto	- 88	7	- 94
<u>Lake Erie</u>				
Cleveland	Port Colborne	+ 3	9	- 6
Port Stanley	Port Colborne	- 46	12	- 61
Port Stanley	Cleveland	- 49	11	- 55
<u>Lakes Huron and Michigan</u>				
Thessalon	Goderich	-2 15	16	-207
Goderich	Milwaukee	- 131	16	- 149
Goderich	Collingwood	+206	16	+204
Goderich	Harbor Beach	+ 37	14	+ 15
Goderich	Mackinaw City	+117	15	+ 94
<u>Lake Superior</u>				
Michipicoten	Thunder Bay	-2 10	12	-232
Michipicoten	Marquette	-394	8	-408
Michipicoten	Duluth	-509	10	-521
Thunder Bay	Marquette	-175	11	-177
Thunder Bay	Duluth	-299	9	-290

* Rate is the apparent vertical movement per century. Positive value indicate that second station is rising with respect to first station.

**From Co-ordinating Committee on Great Lakes Basic Hydraulic and Hydrologic Data (1977).

FIGURE 2. RATE OF CHANGE OF WATER LEVEL DIFFERENCES FOR
OSWEGO MINUS KINGSTON

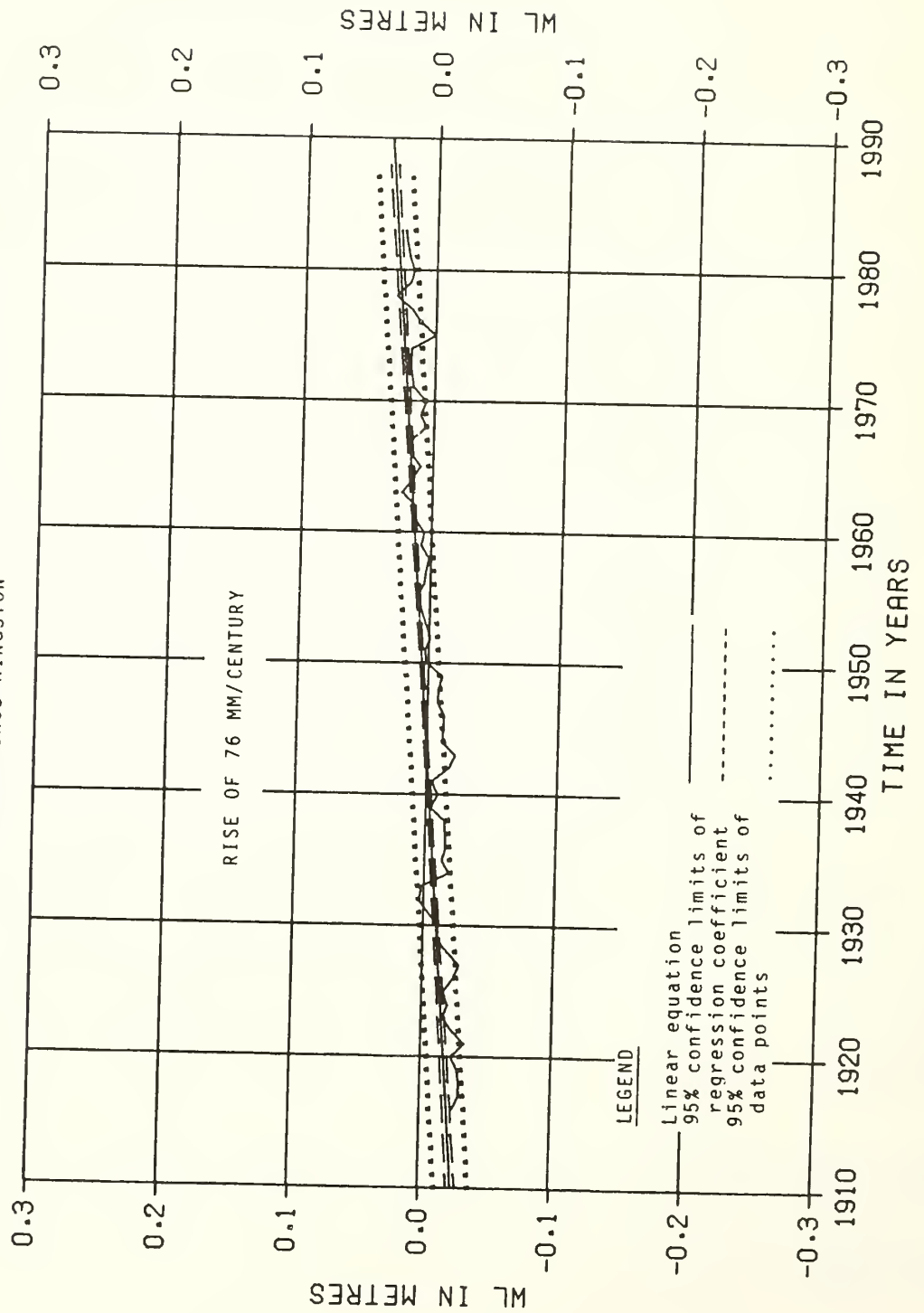


FIGURE 3. RATE OF CHANGE OF WATER LEVEL DIFFERENCES FOR CLEVELAND MINUS PORT COLBORNE

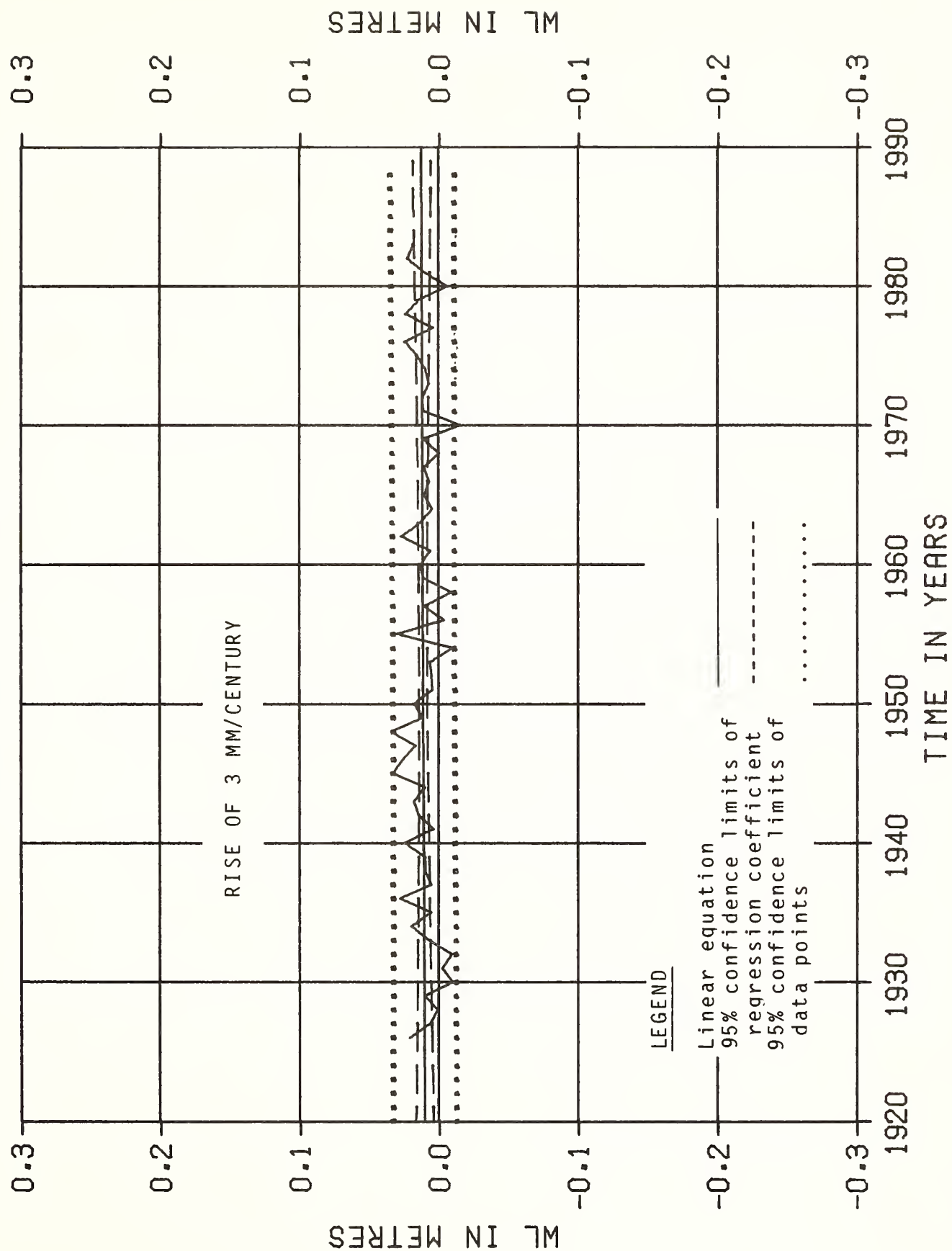


FIGURE 4. RATE OF CHANGE OF WATER LEVEL DIFFERENCES FOR
GODERICH MINUS HARBOR BEACH

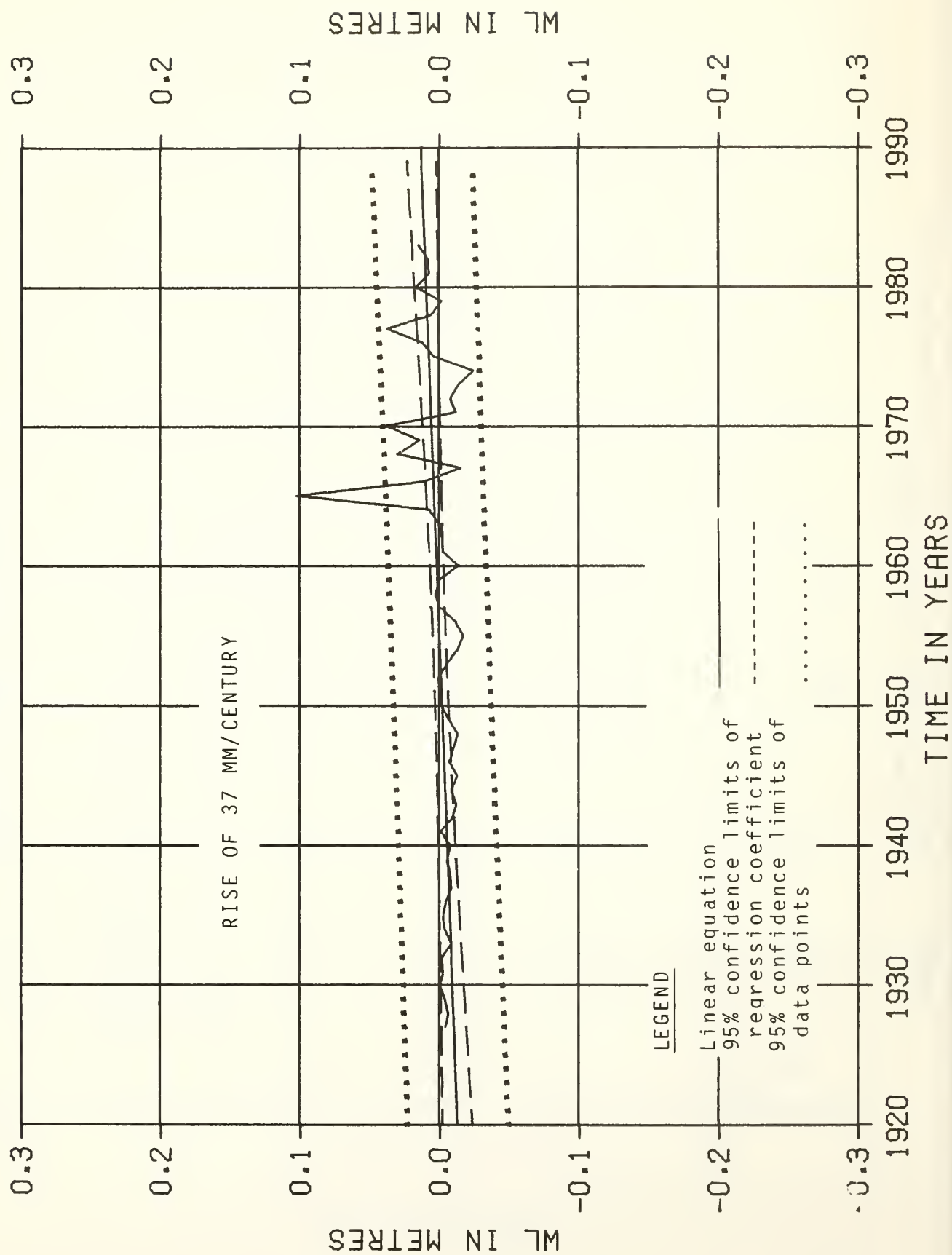


FIGURE 5. RATE OF CHANGE OF WATER LEVEL DIFFERENCES FOR
GODERICH MINUS MILWAUKEE

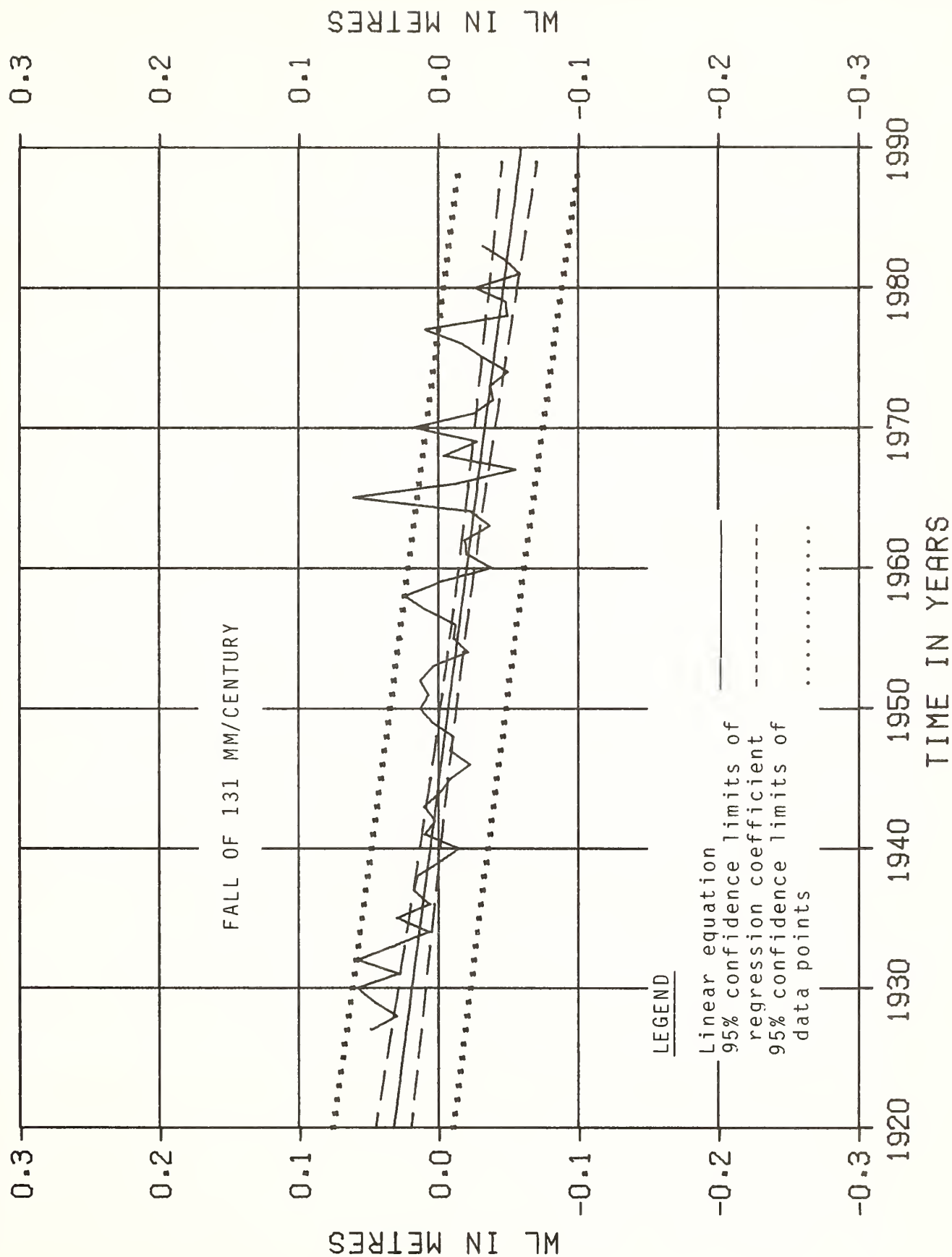
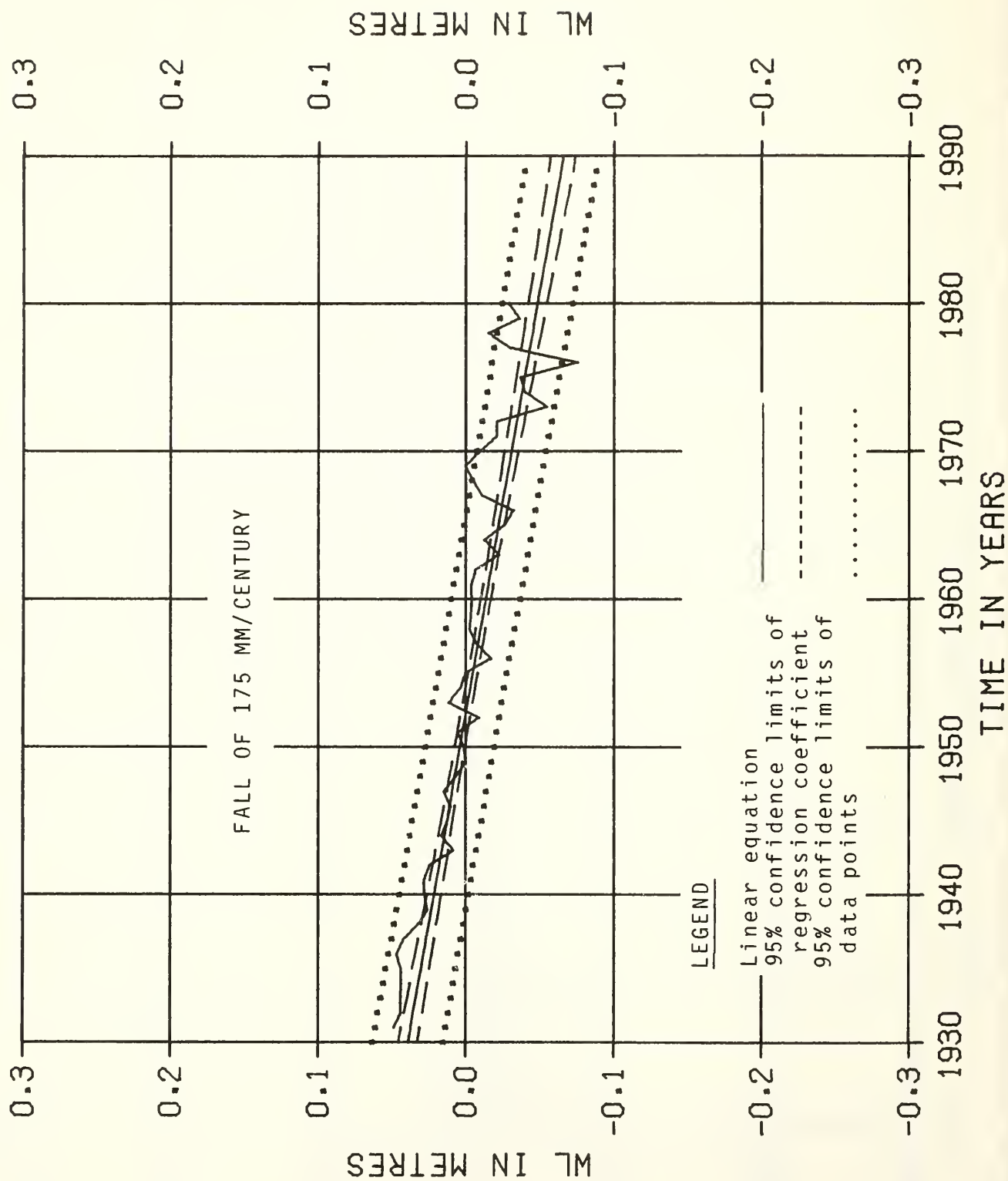


FIGURE 6. RATE OF CHANGE OF WATER LEVEL DIFFERENCES FOR THUNDER BAY MINUS MARQUETTE



were made to compensate for bench mark instabilities that had occurred over the years and that had gone undetected. Moore (1948), the Vertical Control Subcommittee (1957) and Kite (1972) would have worked with Pt. Colborne data for which either one or both of the above adjustments had not been applied. To assess the affect of the adjustment on their results the rates for the Cleveland-Pt. Colborne station pair have been computed using Port Colborne data for the years 1926 to 1959 both with and without the adjustments applied. The rate computed without the adjustments applied is +38 millimeters per century and with the adjustments applied is +6 millimeters per century. The difference of 32 millimeters per century is significant, but not sufficient to explain all of the variation seen in Table 1.

The reports by Moore (1948), Kite (1972) and the Vertical Control Subcommittee (1957) differ from the present study in that they all use Port Colborne water levels dating back to 1860. The effect of using varying lengths of record on the computed rate of movement is discussed and illustrated by the Vertical Control Subcommittee (1957) in their report on Lake Ontario. This report concludes by advising the use of data for Lake Ontario only from 1916 onwards because of improved equipment and control, and by cautioning that the use of data prior to this period results in more erratic results. This is illustrated in column (c) of Table 1 where the rates for Lake Ontario computed from records beginning in 1916 differ by between 36 and 85 millimeters per century from those computed for the entire period of record.

The Vertical Control Subcommittee (1957) report on Lake Erie gives a rate of movement for the Cleveland - Port Colborne gauge pair of +131 millimeters per century based on water levels dating from 1860 to 1955. By comparison the rate computed above using the unadjusted data for the period 1926 to 1959 is +38 millimeters per century, a difference of 93 millimeters per century. The Port Colborne station documentation indicates that the data prior to 1911 are based on once daily staff readings taken at the head of a narrow channel leading from the lake to the entrance lock for the Welland Canal. These data exhibit much more variability than those recorded after the installation of a continuous, self-registering gauge in 1911. In addition, the gauge was relocated in 1925 from the entrance lock to a site outside of the channel. Additional investigation into the characteristics of the data sets collected before and after 1911 and 1925 appears warranted and may explain the large differences in rates for this station pair.

Other factors can, of course, contribute to the variability of the results. MacLean (1961) and Forrester (1980) have shown that water level fluctuations caused by meteorological conditions result in lake surfaces which do not conform to level surfaces, even when seasonal averaging of the data are carried out. MacLean (1961) also refers to a variety of other possible sources of error. A complete investigation of individual factors contributing to errors in the water level data is not, however, within the scope of this paper.

CONCLUSIONS

The Coordinating Committee for Great Lakes Hydraulic and Hydrologic Data (1977) used June through September mean water levels for periods of record dating no earlier than 1916 to compute the rate of apparent vertical movement between gauging station pairs on all of the Great Lakes. For a selected number of pairs of stations the rates of movement were recomputed in the present study

using identical procedures to those used in the above study but with the period of record updated to 1983. The results, shown in Table 3, indicate continuing rates of differential movement between stations which are essentially unchanged from those provided by the Coordinating Committee (1977).

The results from this study also show reasonable agreement with the rates reported by earlier researchers. However, exceptions such as those involving Port Colborne on Lake Erie point out the importance, when computing rates of apparent vertical movement, of examining the history of the establishment and maintenance of the gauging stations to ensure stability of the reference datum and continuity in data collection procedures.

ACKNOWLEDGEMENTS

Data from the gauging stations in the United States of America were supplied by Mr. H. Lippincott of the National Ocean Service, U.S. Department of Commerce, Rockville, Maryland. The authors wish to thank Mr. Lippincott for his generous and timely assistance.

REFERENCES

Coordinating Committee on Great Lakes Basic Hydraulic and Hydrologic Data, 1977: Apparent Vertical Movement Over the Great Lakes, Chicago, Illinois and Cornwall, Ontario.

Forrester, W.D., 1980: Accuracy of Water Level Transfers, Proceedings of the Second International Symposium on Problems Related to the Redefinition of North American Vertical Geodetic Networks, Ottawa, Canada.

Kite, G.W., 1972: An Engineering Study of Crustal Movement Around the Great Lakes, Technical Bulletin No. 63, Inland Waters Branch, Department of the Environment, Ottawa, Ontario.

MacLean, W.F., 1961: Postglacial Uplift in the Great Lakes Region, Special Report No. 14, Great Lakes Research Division, University of Michigan, Ann Arbor, Michigan.

Moore, S., 1948: Crustal Movement in the Great Lakes Area, Bulletin of the Geological Society of America, Vol. 59, No. 7, pp.697-710.

Price, C.A., 1954: Crustal Movement in the Lake Ontario - Upper St. Lawrence River Basin, Surveys and Mapping Branch, Department of Mines and Technical Surveys, Ottawa, Ontario.

Vertical Control Subcommittee, Coordinating Committee on Great Lakes Basic Hydraulic and Hydrologic Data, May 1957: Crustal Movement in the Great Lakes Area, First Interim Report - Lake Ontario.

....., October, 1957: First Interim Report - Lake Erie.

....., November, 1957: First Interim Report - Lake Michigan - Huron.

....., December, 1957: First Interim Report - Lake Superior.

VERTICAL CRUSTAL MOTION
AND THE
NORTH AMERICAN VERTICAL DATUM

Larry D. Brown
Institute for the Study of the Continents
Snee Hall, Cornell University
Ithaca, N.Y. 14853

ABSTRACT. Many parts of North America have demonstrably undergone vertical motions on contemporary time scales. Most dramatic are earthquake deformations: co-seismic dislocation from large events may induce meters of elevation change over thousands of square miles. Other parts of the earthquake cycle may also correspond to geodetically significant motion: post-seismic strains, for example, may accrue in exponentially decaying fashion for years after an earthquake. Subsurface magma movement can induce spectacular (e.g. volcanic eruptions) as well as subtle vertical motions: repeated leveling has now detected uplift inferred to be due to inflation of deep magma chambers in a number of areas, including California, New Mexico and Wyoming. Vertical motion is not restricted to the more "active" western North America: decimeters of uplift observed by releveled in the southern U.S. have been attributed to sedimentary loading in the adjacent Mississippi delta, and water levels in the Great Lakes attest to continued rebound of the Canadian Shield following retreat of the glacial ice sheets. Other parts of the east exhibit more enigmatic "motions": continued "uplift" of the Appalachians may represent some as yet unrecognized epeirogenic force. However, in cases of subtle elevation change, the issue of crustal motion is often intimately related to the problem of systematic leveling error. Geodetically, it is important to identify where crustal motions are sufficiently large to warrant their incorporation into the definition of the NAVD, and to determine temporal variations well enough that realistic time variations can be modeled in the datum adjustment. Conversely it is also important that geodynamic needs for accuracy and spatial coverage be recognized in the development of the NAVD, as it lays the ground work for all future crustal motion study.

INTRODUCTION

To the geologist, the earth's surface seems to be in constant motion: mountain ranges being thrown up or worn down, basins subsiding beneath ever-increasing loads of sediments, and crustal blocks wrenching past one another. This activity results from the interacting motions of lithospheric plates, thin shells which mechanically define the outermost layer of the earth. Earthquakes, volcanoes and less dramatic forms of deformation are contemporary expressions of this global pattern of tectonic activity. Evidence is abundant that many regions of the world, and North America in particular, have undergone, or are presently experiencing,

vertical and horizontal crustal motion at measurable rates.

Thus from the geological perspective it is clear that height is a function of time as well as space. The practical task facing the geodesist in defining a vertical datum is to determine where vertical crustal motion can be large enough to impact network adjustments at the scale of accuracy demanded by the user community. Where vertical motions are significant, the geodesist must further know their time behavior so that he can 1) design cost-effective observation programs to monitor the motion, and 2) realistically model it in adjustment algorithms.

Although geological and geophysical observations and principles are important clues, much of our knowledge of the nature of contemporary vertical motions comes from the very geodetic measurements being used to define the datum. For this reason, making the aforementioned determinations is often intimately intertwined with the problem of discriminating true ground motion from systematic leveling errors.

The question of how to treat vertical motions in defining the NAVD is not an easy one: our understanding of some of their causes is incomplete, spatial coverage of releveling surveys is still perhaps insufficient to identify all areas of ongoing deformation, we cannot predict in detail where episodic motions may occur in the future, and there remains substantial uncertainty whether some of the more subtle patterns of apparent vertical motion are artifacts of systematic leveling errors.

Some of the above uncertainties may soon be resolved: new corrections for systematic leveling errors are being developed and applied, and selected resurveys in areas of suspected ground motion are always possible. Yet enough is now known of vertical motions to suggest that they should be, and reasonably can be, incorporated in any redefinition of the North American Vertical Datum.

This report is an attempt to illustrate the significance of vertical motion to the NAVD with documented examples from across North America of deformations due to a variety of tectonic processes. These examples demonstrate not only that vertical motions can be large, but that they are relatively widespread. Furthermore, the more subtle forms of apparent crustal motion- or systematic error, as the case may turn out to be- are an issue relevant to virtually the entire geodetic network.

SEISMIC DEFORMATION

On March 27, 1964, south-central Alaska experienced a magnitude 8.4 earthquake centered on Prince William Sound. Crustal deformation accompanying this earthquake probably affected over 280,000 square kilometers, with up to 30 meters of differential vertical and 19 meters of horizontal motion (Plafker, 1969). Co-seismic motions such as these are a striking example of tectonically-induced movement which clearly impact local measurements of the vertical datum. Other earthquakes which have demonstrably distorted vertical control in the U.S. include those the 1971 San Fernando, Cal. event, the 1954 Dixie Valley, Nev., events the 1959 Hebgen Lake, Mont., event and more recently the 1981 Borah Peak, Idaho, event to name a few (e.g. Reillinger and Brown, 1981; Stein and Barrientos, 1984). For the most part, dislocation theory (Savage and Hastie, 1966) seems to provide an adequate basis for modeling co-seismic deformations, though one might argue that surface observations are rarely dense enough to test its limitations.

Though co-seismic deformations are the largest and most dramatic motions associated with earthquakes, they represent only part of the earthquake cycle of strain build-up and release (Figure 1; Thatcher, 1981).

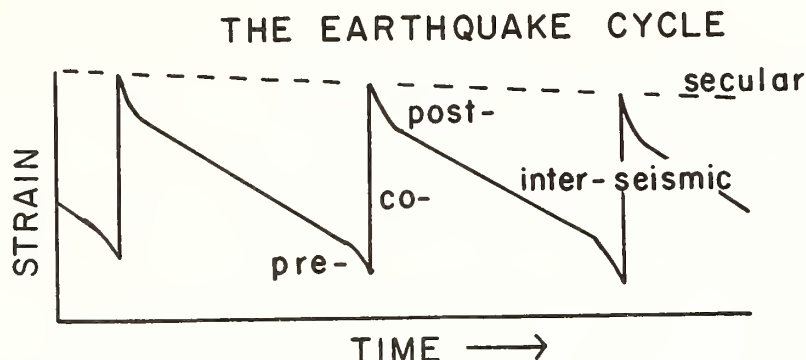


Figure 1. The earthquake cycle. Earthquakes release strain that has slowly accumulated between seismic events. Viscoelastic relaxation of earthquake stresses may induce exponentially decaying post-seismic motions. As stresses approach the failure strength of rock, it is suspected, though rarely observed in the field, that premonitory strains may be induced. These elusive pre-seismic motions are of obvious interest in earthquake prediction.

For some major earthquakes there has been clear evidence of vertical movement continuing years after the seismic event itself. These post-seismic motions are believed to be related to relaxation of earthquake induced stresses deep in the crust or upper mantle (Nur and Mavko, 1974). Though usually much smaller than co-seismic motion, post-seismic rebound can be significant for geodetic networks: uplift following the 1964 Alaska earthquake accumulated to over 50 cm within ten years (Figure 2; Brown et al., 1977). Post-seismic strains appear to decay exponentially with time after the main event, making them relatively predictable.

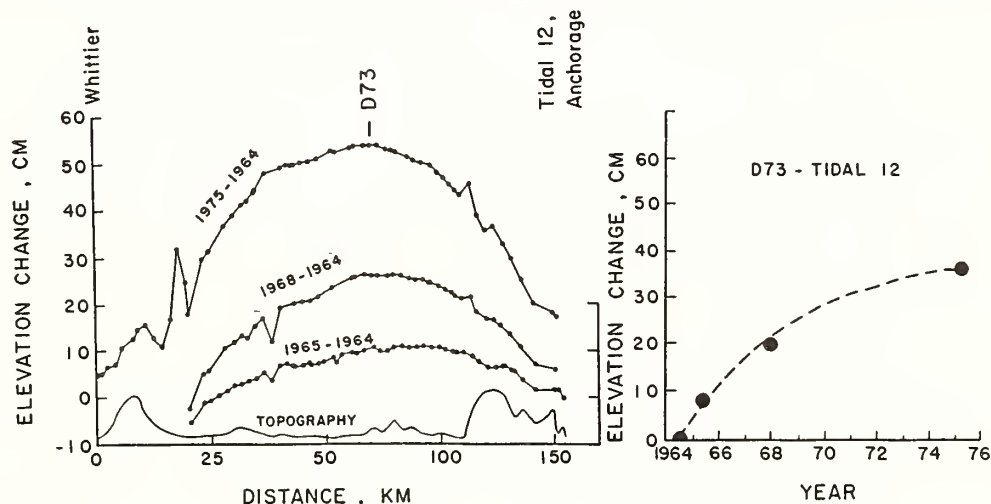


Figure 2. Post-seismic uplift south of Anchorage, Alaska, following the 1964 Prince William Sound earthquake. During the earthquake this area subsided as much as 2 meters. The exponential time behavior is clearly exhibited in this case. (After Brown et al., 1977)

Unlike co-seismic and post-seismic deformations, pre-seismic and inter-seismic strain accumulation has been more difficult to document. Identifying the latter is complicated by the small rates involved and the difficulty of discriminating

earthquake-related strain buildup from secular motions due to other causes. Most difficult of all to capture are pre-seismic motions: since the location and time of a future earthquake cannot (yet) be confidently predicted, it is impossible to know when and where to survey for premonitory motion. Sometimes frequent resurveys in an earthquake prone region can catch pre-seismic motion (Castle et al., 1974). Geophysical techniques, such as tilt or strain monitoring, may be more cost-effective in monitoring for pre-seismic deformation, though these methods suffer from lack of long term stability. In any event, pre-seismic motions, though clearly important for the earthquake prediction problem, may be too small and too infrequent to be of concern in the definition of the NAVD, except in so far as their study benefits from the existence of an accurate reference.

Earthquakes tend to cluster in well-defined belts around the world, generally defining the active boundaries between lithospheric plates. In southern Alaska, western Canada and the northwestern U.S., earthquakes are generated as the Pacific oceanic plate is pushed beneath the North American continent. In California earthquakes are largely associated with the San Andreas fault system, along which the Pacific plate is sliding northward past the North American plate. Between California and the Rocky Mountains, many earthquakes are associated with the continent itself being pulled apart. These seismically active regions are obviously the most likely to have an impact on the NAVD and require first attention. However, it is important to remember that earthquakes have occurred in most areas of North America (Figure 3). The eastern U.S., for example, which seems to have been geologically "stable" compared to the west, has experienced a number

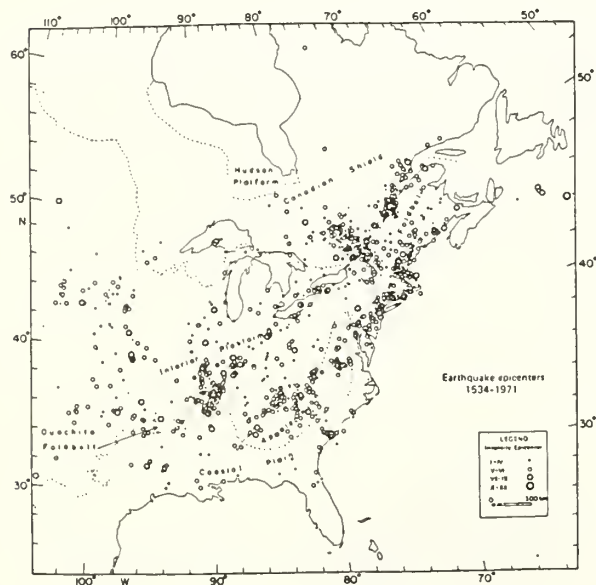


Figure 3. Seismicity of the eastern U.S. (York and Oliver, 1976). Although earthquakes are most common in the seismic belts of the western U.S., important events have also occurred in the more "stable" east.

of major, damaging earthquakes in the past, including the 1811-12 New Madrid, Mo., series and the 1886 Charleston earthquake. Though less frequent than their western counterparts, these "intraplate" events are nonetheless of considerable seismological concern in view of the proximity of population centers and the propensity of eastern earthquakes to be more damaging than equivalently sized events in the west. Though it is possible that inter-seismic strain accumulation might be geodetically measurable in the east, it is unlikely to be large enough to impact the datum directly. More importantly, the NAVD should establish an

accurate reference for measurements of possible future earthquake deformations since measurement of co-seismic and post-seismic motions would be a major contribution to the relatively meager information we now have about intraplate seismicity.

MAGMA INFLATION

The 1980 eruptions of Mt. St. Helens brought home in dramatic fashion the existence of, and hazards associated with, active volcanism in North America. Yet magma induced deformation can be significant even in the absence of contemporary surface volcanism. An excellent example of magma inflation has been documented from precise releveing measurements in central New Mexico (Figure 4). Local uplift and peripheral subsidence north of Socorro, N.M., between about 1912 and 1951 has been associated with a mid-crustal magma chamber detected beneath the rift by seismological measurements (Reilinger and Oliver, 1976). The magnitude of relative uplift is over 10 cm during this time interval, and recent resurveys indicate that such motion has continued at about the same rate (ca. 20 mm/yr). Even larger motions, up to 40 cm, have been measured in the Long Valley caldera of eastern California, a geologically recent volcanic structure. A striking aspect of the Long Valley motion is that it began after 1975, clear evidence that such motions may be episodic (Castle et al., 1984). Though surface deformation due to deep magma inflation can be modeled by static finite element methods (e.g. Dieterich and Decker, 1975), the time behavior is more problematical. Effective incorporation into the NAVD of vertical motions due to such magma inflation may require an ongoing field monitoring program at selected sites. Other areas in the U.S. where magma inflation has been inferred from leveling observations include northern New Mexico and west Texas (Reilinger et al., 1979) and Yellowstone National Park (Pelton and Smith, 1982).

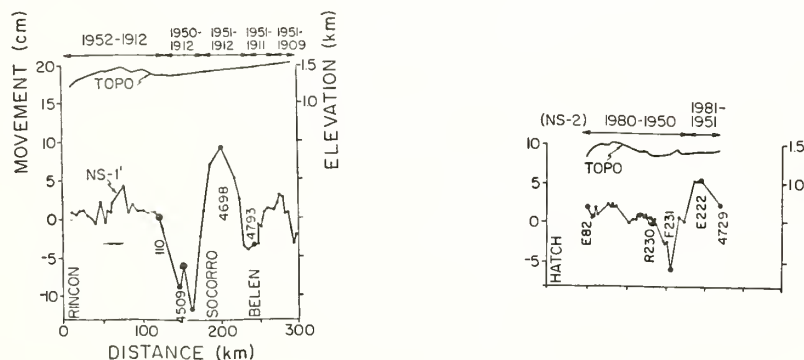


Figure 4. Vertical motion indicated by releveing in central New Mexico. The uplift north of Socorro is inferred to result from inflation of a magma chamber at a depth of about 20 km. New leveling in 1980 suggests that the uplift may have accumulated at a constant rate. (After Larsen et al., 1985).

CRUSTAL LOADING

Volcanism and earthquakes are prime manifestations of the tectonically active nature of much of the western U.S. In contrast, central and eastern North America represent the classic "stable" continental interior, where geologic evidence suggests that the last major tectonic events ceased millions, or even billions, of years ago. Thus it is tempting to treat the east as a "fixed" base for geodetic control. However the evidence suggests that this is not the case, and that parts

of the continental craton and its periphery may be undergoing vertical movement at rates that may impact definition of the NAVD.

The best-known example of vertical motion in the North American interior is that due to post-glacial rebound. Documented both in the geological record (e.g. Walcott, 1972) and by contemporary geodetic measurements (e.g. Vanicek and Nagy, 1980). Such uplift, with present rates of up to a cm/yr, is generally attributed to isostatic recovery following retreat of the great continental ice sheets which began some 15-18,000 years ago (Flint, 1971). Although contemporary post-glacial rebound is most obvious in Fennoscandia, the northern U.S. and Canada, the full response to unloading is global (e.g. Clark, 1980).

Vertical motions due to loading phenomena is not restricted to post-glacial rebound. Filling of reservoirs (Longwell, 1960), draining of aquifers (Holzer, 1979), and shrinking of Holocene lakes (Crittenden, 1963) have all been associated with rebound phenomena. A interesting recent example can be found along the Gulf coast. Leveling in southern Mississippi indicates relative uplift landward of the Mississippi delta. This uplift can be interpreted as a "forebulge" caused by flow in a viscoelastic mantle driven by the sediment load being deposited in the delta (Jurkowski et. al., 1984). Interpretation of this uplift is complicated by subsidence effects caused by water withdrawal in the coastal plain, but the magnitude of motion (ca 3 mm/yr) may prove significant at the desired accuracy level of the NAVD.

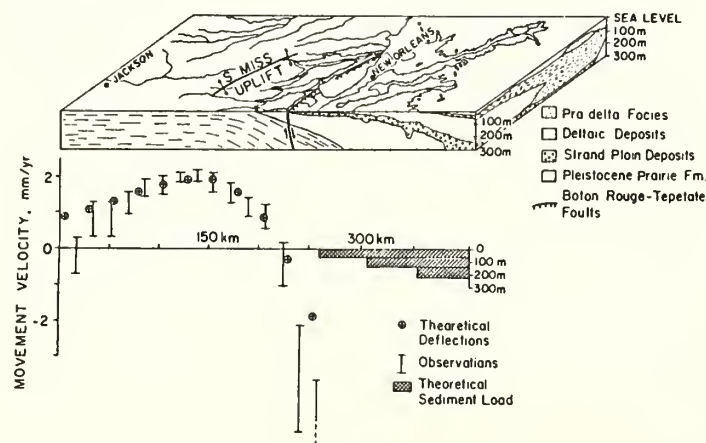


Figure 5. Crustal arching near the Mississippi Delta. This movement may be in response to sediment loading within the Delta. (Jurkowski et al., 1984)

EPEIROGENY

Much of the earth's tectonic activity is associated with orogeny, the severe deformations that are responsible for building the mountain systems of the continents. However, geology also records gentler warpings of the earth's surface, as exemplified by the broad sedimentary basins and arches of the North American interior. These subdued processes are sometimes referred to as epeirogeny. Though not as dramatic as earthquakes or volcanoes, the issue of epeirogenic motions is

quite relevant to the NAVD.

Evidence that epeirogenic movement may be significant can be found among releveling measurements in the continental interior. Maps of crustal motion for the U.S. and eastern Europe, for example, seem to show these areas undergoing relative uplift and subsidence at rates up to 0.5 cm/yr (Figure 6) If these motions are real, they may represent an important new tectonic process. The apparent uplift of the Appalachians in the eastern U.S., for example, suggests neotectonic reactivation of this ancient mountain belt, with serious implications for the seismicity in this area (e.g. Brown and Oliver, 1976).

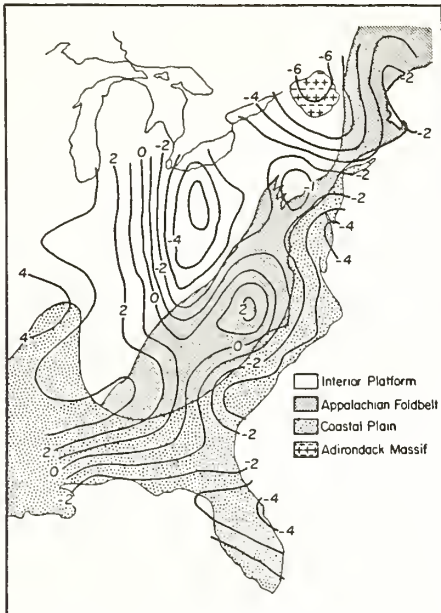


Figure 6. Map of apparent vertical crustal motion derived from releveling data in the eastern U.S. Whether patterns of motion, such as the uplift over the Appalachians, prove to be real or artifacts of systematic leveling error may have serious implications for defining the NAVD (Map courtesy of G. Jurkowski)

Interpretation of leveling from such areas is clouded, however, by suspicions that at least some of the indicated elevation changes may actually be artifacts of systematic leveling errors. The uplift over the Appalachians, for example, may prove to be due to elevation-correlated errors such as those due to atmospheric refraction or rod miscalibration. Already vertical motions along the east coast (Brown, 1978) are being reevaluated in light of new evidence of geomagnetic errors in leveling (e.g. Zilkoski, 1984).

MOVEMENT OR SYSTEMATIC ERROR?

As implied above, in some cases the problem of identifying vertical crustal motion merges with the problem of identifying, and removing, systematic leveling error. The recent controversy (e.g. Mark et al., 1981; Strange, 1981) over the reality of the Palmdale Bulge in southern California is but one of the more visible manifestations of this situation. Uncertainty as to the reality of vertical motions indicated by leveling in parts of the eastern U.S. is another. Because the issues of movement and systematic error are sometimes so intimately related, their discrimination may require both geodetic and geologic analysis.

An good example of how to deal with possible leveling error in a crustal movement investigation is provided by Larsen et al.'s (1985) reexamination of magma-induced uplift in New Mexico. The central uplift shown in Figure 4 is not in question; however leveling along a nearby survey line was found to be suspicious

(Figure 7). Leveling along this route between 1911 and 1959 seems to indicate relative uplift to the west. However, a new survey in 1981 shows exactly the opposite sense of motion between 1959 and 1981. Although it is not too unreasonable to expect some geological processes to be oscillatory, it stretches geological credulity to expect surveys carried out at three different times to coincidentally measure relative uplift and subsidence that is virtually identical in magnitude. That this flip-flop "motion" seems to correlate both with topography and with a change in survey instrumentation strongly suggests that rod error, not tectonic motion, is responsible. Larsen et al. (1985) go further and use this correlation to estimate an empirical correction which, when applied to the leveling surveys, results in a much more consistent and geologically "reasonable" picture of crustal motion in the area.

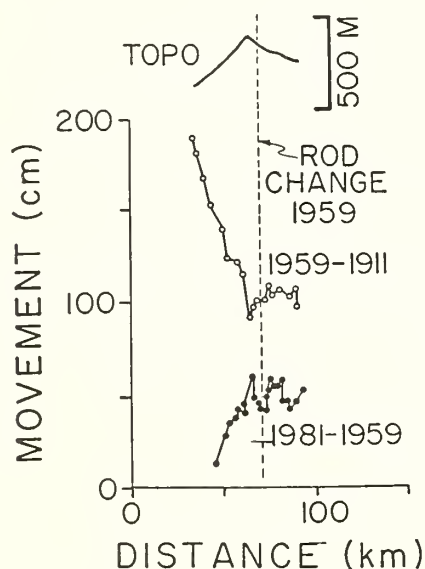


Figure 7. Comparison of elevation changes near Abo Pass, N.M., from levelings in 1911, 1959 and 1981. The equal but opposite magnitudes of the differences between these levelings, together with the strong topographic correlation when instrumentation was changed in the 1959 survey strongly indicates rod error, not crustal motion is being measured.

Because crustal motion considerations often make the most stringent demands on the accuracy of geodetic measurements, they can serve both to help identify possible systematic errors and evaluate the efficacy of new corrections to remove such errors. In this regard, even the relatively subtle "motions" indicated by leveling in many parts of North America may be important considerations in defining the NAVD. If real crustal movement is involved, the rates may or may not be large enough to impact the datum adjustment. However, if some of these "motions" prove to be artifacts of systematic error, the errors may easily exceed accuracy specifications for the NAVD. Thus for both geophysical and geodetic reasons, there is a clear need to resolve questions of systematic error, and the geologic perspective has a useful role to play in this process.

DISCUSSION

Geodetically significant vertical motions have been documented in association with a variety of tectonic processes in numerous parts of North America. Other areas may also be experiencing vertical motion but have not yet been detected due to a lack of repeated geodetic surveys. Though vertical motions may prove relatively commonplace, movements large enough to concern the definition of the NAVD may be restricted to a finite number of sites, such as areas of known

earthquake or magmatic activity. However, it is difficult to rule out significant vertical motions in other areas because of uncertainty as to whether releveling estimates of elevation change are due to ground motion or systematic error.

Proper treatment of vertical motions in the definition of the NAVD requires:

1) "Cleaning-up" historical leveling data with corrections for systematic errors, insofar as is possible.

2) Development and implementation of local, time-dependent network adjustment models based on mechanics of tectonic deformation.

and perhaps even

3) Selected reobservation at sites of known crustal instability to monitor the time behavior of significant motions.

Further into the future, space-based geodetic measurements will become an important factor in both datum definition and crustal motion observation. However, as these new technologies gain acceptance, it is important to remember that the conventional, historical measurements can never be replaced as far as crustal motion monitoring is concerned: they are our only link to what has gone on in the past.

Eventually only students of crustal motion will retain an interest in the present datum. All other applications will undoubtedly adopt whatever new and more accurate geodetic height estimates come along in the future. Yet, the datum established now, and in particular the measurements made to flesh out this network, will still be an important reference for estimating crustal motion in the future. Since the geodetic measurements will surely improve in the future, it is the accuracy of the present measurements which will ultimately limit the usefulness of any future crustal motion study.

ACKNOWLEDGMENTS

Supported by NASA Grant No. NAS5-27232. Contribution No. 14 of the Institute for the Study of the Continents.

REFERENCES

- Brown, L.D., 1978, Recent vertical crustal movement along the east coast of the United States, *Tectonophysics*, 44, 205-231.
- Brown, L.D., R.E. Reilinger, S.R. Holdahl, and E.I. Balazs, 1977, Postseismic crustal uplift near Anchorage, Alaska, *J. Geophys. Res.*, 82, 3369-3378.
- Castle, R.O., J.E. Estrem, and J.C. Savage, 1984, Uplift across Long Valley Caldera, California, *J. Geophys. Res.*, 89, 11507-11516.
- Clark, J.A., 1980, A numerical model of worldwide sea level changes on a viscoelastic earth, in *Earth Rheology, Isostasy, and Eustasy*, ed. by N.A. Morner, Wiley&Sons, N.Y., 525-534.
- Crittenden, M., Jr., 1963, New data on the isostatic deformation of Lake Bonneville, *U.S. Geo. Surv. Prof. Pap.* 454-E, 1-31.
- Dieterich, J.H., and R.W. Decker, 1975, Finite element modeling of surface deformation associated with volcanism, *J. Geophys. Res.*, 80, 4094-4102.
- Flint, R.F., 1971, *Glacial and Quaternary Geology*, John Wiley&Sons, N.Y., 892 pp.

- Holzer, T.L., 1979, Elastic expansion of the lithosphere caused by groundwater depletion, *J. Geophys. Res.*, 84, 4689-4698.
- Jurkowski, G., J. Ni., and L. Brown, 1984, Modern uparching of the Gulf Coastal Plain, *J. Geophys. Res.*, 89, 6247-6255.
- Larsen, S., R. Reilinger, and L. Brown, 1985, Evidence of ongoing crustal deformation related to magmatic activity near Socorro, N.M., *J. Geophys. Res.*, in press.
- Longwell, C.R., 1960, Interpretation of the leveling data, *U.S. Geol. Surv. Prof. Pap.* 295, 33-38.
- Mark, R.K., J.C. Tinsley III, E.B. Newman, T.D. Gilmore, and R.O. Castle, 1981, An assessment of the accuracy of the geodetic measurements that define the southern California uplift, *J. Geophys. Res.*, 86, 2783-2808.
- Nur, A., and G. Mavko, 1974, Post-seismic viscoelastic rebound, *Science*, 181, 204-206.
- Pelton, J.R., and R.B. Smith, 1982, Contemporary vertical surface displacements in Yellowstone National Park, *J. Geophys. Res.*, 87, 2745-2761.
- Plafker, G., 1969, Tectonics of the March 27, 1964, Alaska earthquake, *U.S. Geol. Surv., Prof. Pap.* 543-I, 1-74.
- Reilinger, R.E., L.D. Brown, J.E. Oliver, and J.E. York, 1979, Recent vertical crustal movements from leveling observations in the vicinity of the Rio Grande Rift, in *Rio Grande Rift: Tectonics and Magmatism*, ed. by R.E. Riecker, *Amer. Geophys. Union, Wash., D.C.*, 223-236.
- Reilinger, R., and J. Oliver, 1976, Modern uplift associated with a proposed magma body in the vicinity of Socorro, N.M., *Geology*, 4, 563-586.
- Reilinger, R. and L. Brown, 1981, Neotectonic deformation, near-surface movements and systematic errors in U.S. releveing measurements: implications for earthquake prediction, in, *Earthquake Prediction, An International Review*, ed. D.W. Simpson and P.G. Richards, *Amer. Geophys. Union, Wash., D.C.*, 422-440.
- Savage, J.C. and L.M. Hastie, 1966, Surface deformation associated with dip slip faulting, *J. Geophys. Res.*, 71, 4897-4904.
- Stein, R., and S.E. Barrientos, 1984, Planar fault slip associated with the 1983 Borah Peak, ID, earthquake, *EOS*, 45, 989.
- Strange, W.B., 1981, The impact of refraction correction on leveling interpretations in southern California, *J. Geophys. Res.*, 86, 2809-2824.
- Thatcher, W., 1981, Crustal deformation studies and earthquake prediction research, in *Earthquake Prediction, An International Review*, ed. by D.W. Simpson, P.G. Richards, *Amer. Geophys. Union, Wash., D.C.*, 394-410.
- Vanicek, P., and D. Nagy, 1980, The map of contemporary vertical crustal movements in Canada, *EOS*, 61, 145-147.
- Walcott, R.I., 1972, Late Quaternary vertical movements in eastern North America: quantitative evidence of glacio-isostatic rebound, *Rev. Geophys. Space Phys.*, 10, 849-884.
- York, J.E., and J.E. Oliver, 1976, Cretaceous and Cenozoic faulting in eastern North America, *Bull. Geol. Soc. Amer.*, 87, 1105-1114.
- Zilkoski, D.B., 1984, Geodetic leveling and mean sea level along the east coast of the United States, paper present at Chapman Conference on Vertical Crustal Motion, Harpers Ferry, Va., Oct. 22-26.

A TEMPORAL HOMOGENIZATION OF THE CANADIAN HEIGHT NETWORK

Galo Carrera
Survey Science
University of Toronto
Mississauga, Ontario
Canada L5L 1C6

Petr Vaníček
Surveying Engineering Department
University of New Brunswick
Fredericton, New Brunswick
Canada E3B 5A3

ABSTRACT. Two extended observation campaigns for the first order Canadian Height Network have been carried out: the first between 1900 and 1950, the second began in 1950 and still continues today. Heights have been referred to mean sea level determined at different times in five locations: Halifax, Yarmouth, Pointe au Père, Vancouver and Prince Rupert. In this study an algorithm for reducing levelled height differences as well as heights of tidal benchmarks to a selected epoch is shown. The results of applying this algorithm to the first order Canadian Height Network are presented and discussed.

INTRODUCTION

The idea of applying corrections to eliminate vertical crustal movement effects on height networks is not new. They were first applied in Finland (Kääriäinen, 1953, 1960; Korhonen, 1961) and were used since then in several other European countries (e.g., Ehrnsperger, 1979; Van Mierlo, 1983). On the American continent, although the need for these corrections has long been recognized, lack of information on vertical crustal movements (VCM) has often prevented their application. Our recent experiences, however, show that at certain locations in Atlantic Canada VCM are an important source of systematic errors (Merry and Vaníček, 1983; Carrera, 1984). This is not surprising in view of the considerable span of time over which levelling networks have been measured (e.g. Cannon, 1928, 1935; Lachapelle and Gareau, 1980).

Geodetic levelling observations and mean sea level determinations in Canada are scattered in time over the last one hundred years. First order levelling observations have been carried out in two extended campaigns. The first, usually referred to as the "old levelling", was made between 1900 and 1940, and the second, the

"new levelling", began in 1950 and still continues today. The annual mean sea level determinations used to establish a levelling datum for the 1928 adjustment were made for two Pacific and three Atlantic ports between 1897 and 1906. The corrections to these observations for the VCM undergone on the Canadian territory over this time provide the focus of this paper.

For the definition of terms and notation used herein the reader is referred to Vaníček and Krakiwsky (1982).

FORMULATION OF THE PROBLEM

The task of establishing a levelling network is analogous to the problem of determining the shape of a body deforming in time. This analogy is useful in that it describes the most general motion that a geodetic network can experience. This motion can be expressed as the sum of (Sommerfeld, 1950) three translations, three rotations and deformations. VCM are a particular case of the above general motion. They can be expressed as the sum of one translation and changes of height differences.

Both a rigid translation and changes of height differences induce temporal path dependence on an entire network. A rigid translation affects one type of observable: heights of tidal benchmarks. Changes in the other observable, height differences, affect all the levelled loops in a network. These two types of path dependent observables are also referred to as anholonomic of the first kind (Grafarend, 1979). Figure 1 shows a kinematic misclosure resulting from levelling two sections of a loop at two different epochs T_1 and T_2 .

METHOD

The systematic effect of VCM can be eliminated from a levelling network if all the observations are referred to a common epoch. This can be done, for example, through a kinematic adjustment. Such an adjustment can be formulated as a constant velocity model either in the observation space (e.g., Gale, 1970; Van Mierlo, 1983) or in the parameter space (e.g., Korhonen, 1961; Andersen and Remmer, 1982). This technique, however, poses a very stringent requirement, the entire network must be measured twice with the same design.

The Canadian levelling network does not meet the above requirement. Thus, the corrections developed in this study have to be based on an analytical representation of constant velocity VCM

developed by Vaníček and Nagy (1980).

If VCM are linear in time, the temporal transformation of heights of tidal benchmarks and levelled height differences from their original epochs of measurement T to a reference epoch T_o can be expressed as

$$H_i(T_o) = H_i(T) - \dot{U}_i (T - T_o) \quad (1)$$

and

$$\Delta H_{ij}(T_o) = \Delta H_{ij}(T) - (\dot{U}_j - \dot{U}_i) (T - T_o), \quad (2)$$

where \dot{U}_i and \dot{U}_j are uplift velocities at points P_i and P_j , respectively. It is of theoretical interest to note that when there is a single tidal benchmark in a network the second term in the right hand sides of eqns. (1) and (2) represent the corrections for a rigid translation and changes in height differences, respectively.

The uplift velocities in eqns. (1) and (2) are given in the general form

$$\dot{U}_i(X_i, Y_i) = \sum_n \sum_m C_{nm}(T) X_i^n Y_i^m, \quad (3)$$

where

$$X_i = X(\phi_i, \lambda_i) \quad \text{and} \quad Y_i = Y(\phi_i, \lambda_i).$$

By taking the uplift velocity given by eqn. (3), the correction needed to reduce a levelled height difference to the reference epoch is a function of the time elapsed between the observation and reference epochs, and the latitudes and longitudes of the end points of the levelled segment:

$$\begin{aligned} K_{ij}(X_i, Y_i, X_j, Y_j) &= - (\dot{U}_j - \dot{U}_i) (T - T_o) \\ &= - (T - T_o) \sum_n \sum_m C_{nm} (X_j^n Y_j^m - X_i^n Y_i^m) \end{aligned} \quad (4)$$

The variance of the correction is given by

$$s_k^2(X_i, Y_i, X_j, Y_j) = \underline{\Delta\Phi} \underline{C_c} \underline{\Delta\Phi}^T, \quad (5)$$

where $\underline{C_c}$ is the covariance matrix of the coefficients and $\underline{\Delta\Phi}$ is a vector formed by base function differences,

$$\delta\phi = (T - T_o) \sum_n \sum_m (X_j^n Y_j^m - X_i^n Y_i^m) \quad (6)$$

DATA

Data gathering for this study consisted in determining the location and field season dates (T) of observation of over 320 network links (Young, 1984). Every link was then subdivided in segments levelled in a single field season. As many as ten different segments were identified in one link but there are also links composed of only one segment. The next step involved the determination of the coordinates (ϕ, λ) of the end benchmarks of each segment. All the links investigated in this study belong to the "new levelling" since levelling data records prior to 1950 were not readily available.

The data set for the tidal benchmarks consisted of the dates (T) in which annual mean sea level was determined to serve as a geodetic datum in 1928: Halifax, 1895; Yarmouth, 1902; Pointe au Père, 1897; Vancouver, 1905; Prince Rupert, 1906. For the corrections of the tidal benchmark heights we decided to recompute linear trends ($L = -\dot{U}$) from sea level time series free from various meteorologic and oceanographic effects (Vaníček et al., 1985).

VCM information in Canada is scanty. All the investigations carried out so far have used a combination of sea level variation records, lake level variation records and results of repeated levellings of parts of levelling lines. The most complete selection of these data up to 1980 was used for the compilation of the Map of (linear) Recent Vertical Crustal Movements in Canada (Vaníček and Nagy, 1980). It is this map that was chosen in this investigation as a source of information on inland vertical motions. The map consists of three solutions for the coefficients of algebraic polynomials (of second, third and fourth degree) and their covariance matrices for nine areas covering Canada. However, following the recommendations by Vaníček and Nagy (1980), only the results from the third degree solution were kept.

RESULTS

The year 1962.0 was selected as the reference epoch to perform the temporal homogenization of the network. This epoch is close to the mean epoch of the data employed in the determination of the map of VCM.

Using eqn. (5) corrections were obtained for all the segments in each link. Corrections for links at the edges of the maps were eliminated since the VCM solution in these areas is not trustworthy. A significance test at the one sigma level (67%) was applied to the corrections. Only corrections for 58 network links out of the original 324, i.e., 18%, met the above two criteria. Figure 2 shows the distribution of these corrections in the individual areas. Figures 3 and 4 respectively, show the magnitude of the corrections and their ratio to their standard deviation.

Using equation (1) temporal corrections for tidal benchmarks at the five ports were determined. Table 1 shows a summary of these results.

CONCLUSIONS AND RECOMMENDATIONS

The largest contribution to the temporal homogenization of the entire network comes from the corrections to the tidal benchmark heights. This is not unexpected since the determination of annual mean sea level was carried out at the turn of the century. The tidal benchmark corrections indicate also the large distortions induced in the network in 1928 by using mean sea level determined at different epochs.

The most striking feature of this analysis is the small size of most of the temporal corrections for the levelled height differences in the network. Many of these corrections (82%) did not pass the statistical test at one sigma level because of the poor statistical reliability of the Map of VCM. Some strategies can be suggested to improve the accuracy of these corrections. One such improvement would be to revise the map of VCM. In its present form the displacement field depicted by the map must be understood as a broad picture of general trends of the actual VCM (Clague et al., 1982; Riddihough, 1982). The short spatial wavelength features as well as accelerated movements are not accounted for when the map is used to extract uplift velocities. A new map should include linear trends from sea level and lake level records from which meteorologic and oceanographic effects have been removed. An extended data base of relevelled segments should be sought (Holdahl, 1980). A joint effort by the U.S. and Canada (but preferably by all countries involved in the NAVD project) to obtain relevelled data would greatly enhance such a new solution.

information from different epochs. In Canada the "old" levelling data should be merged with the "new" levelling data with their respective accuracies. Only "old" height differences between end point of segments would have to be considered.

ACKNOWLEDGEMENTS.

The authors wish to acknowledge their appreciation for the helpful discussions held with Messrs. M. Craymer and P. Tetreault at the University of Toronto. The useful comments made by Dr. Robin Steeves, and Messrs. F. Young and R. Mazaachi from the Geodetic Survey of Canada on an earlier version of the manuscript are also gratefully acknowledged. This work is a result of research sponsored by the Department of Energy, Mines and Resources, Canada under contract number OST 8300053.

Table 1: Summary of tidal benchmark corrections and their standard deviations

° Site	Linear Trend (L) cm/century	Standard Deviation (s) cm/century	Correction cm	Standard Deviation cm
Halifax, N.S.	37.50	+ 0.86	-25.1	+ 0.6
Yarmouth, N.S.	33.80	+ 7.79	-20.3	+ 4.7
Pte. au Père, Que.	1.72	+ 1.40	-1.1	+ 0.9
Vancouver, B.C.	2.06	+ 1.13	-1.2	+ 0.6
Prince Rupert, B.C.	7.51	+ 1.60	-4.2	+ 0.9

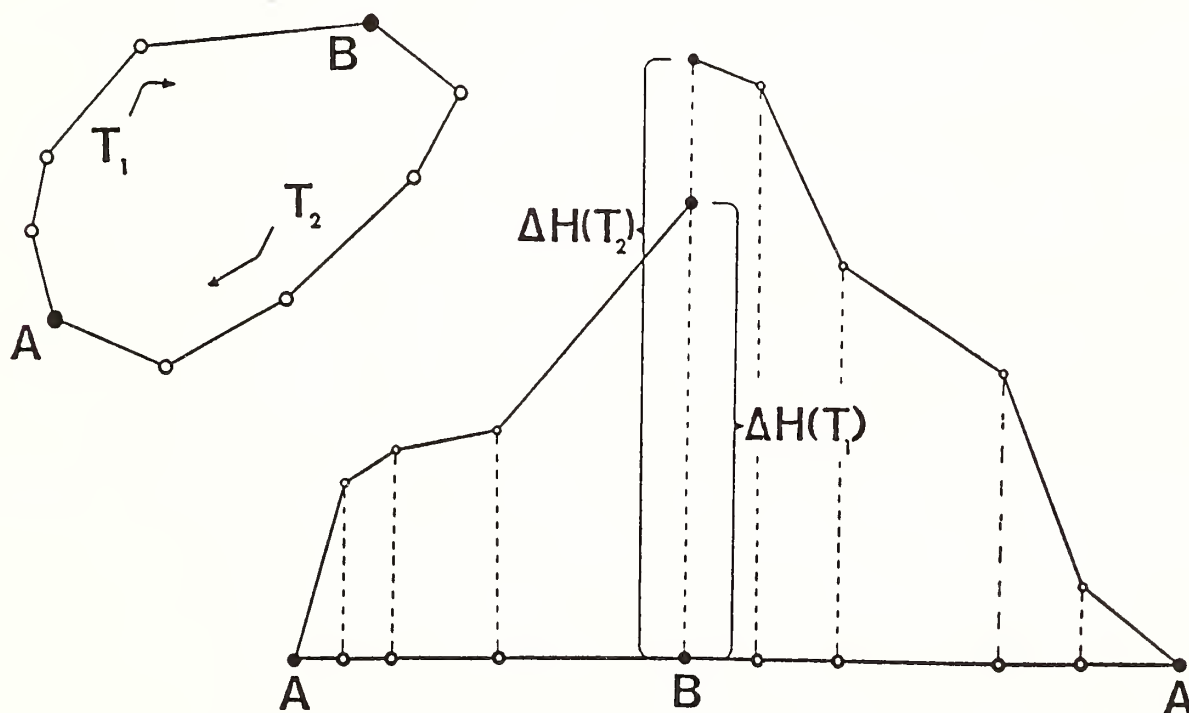


FIGURE 1:

LOOP LEVELLED AT TWO DIFFERENT EPOCHS
AND PLOT OF HEIGHT DIFFERENCES

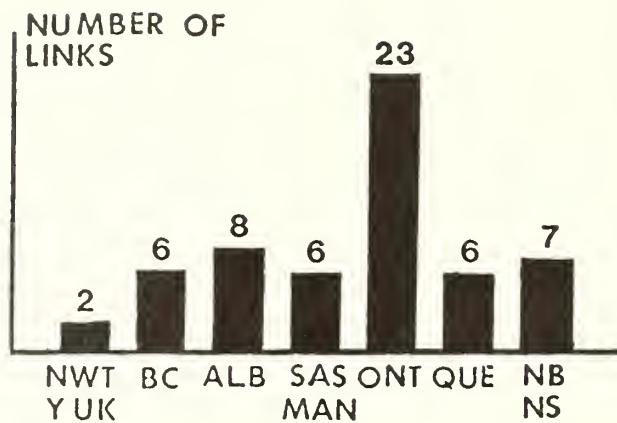


FIGURE 2: Geographic distribution of corrected links

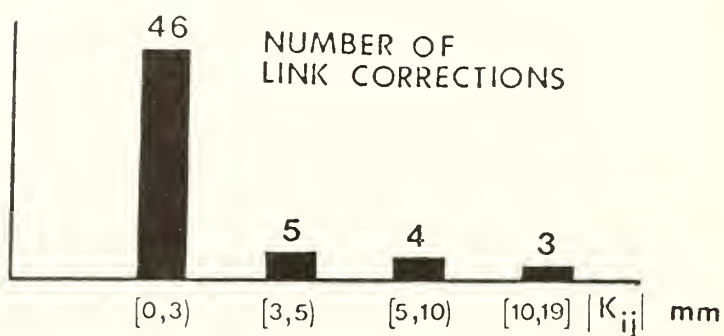


FIGURE 3: Absolute value of link corrections in mm

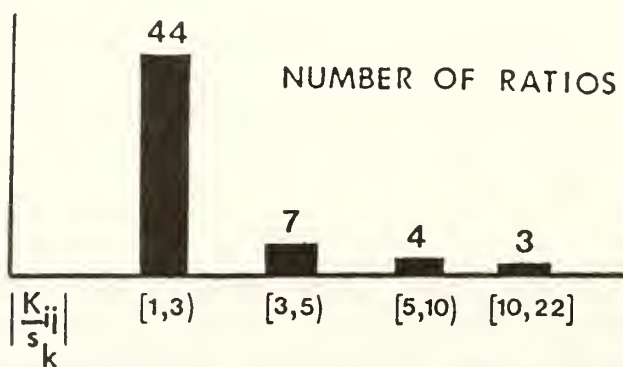


FIGURE 4: Ratio of the corrections to their standard deviations

REFERENCES

- Andersen, O.B. and O. Remmer (1982). Non-random effects in the Finnish levellings of high precision. Manuscripta Geodaetica, 7, 4, 353-373.
- Cannon, J.B. (1928). Adjustment of the precise level net of Canada. Geodetic Survey of Canada, Publication 28.
- Cannon, J.B. (1935). Recent adjustments of the precise level net of Canada. Geodetic Survey of Canada, Publication 56.
- Carrera, G. (1984). Heights on a deforming earth. University of New Brunswick Technical Report 107.
- Clague, J., J.R. Harper, R.J. Hebda and D.E. Howes (1982). Late Quaternary levels and crustal movements, coastal British Columbia. Can. J. Earth Sci., 19, 597-618.
- Ehrnsperger, W. (1979). Report on the adjustment of the United European Levelling Net (UELN-73). Presented at the IUGG 17th General Assembly.
- Grafarend, E.W. (1979). Space-Time geodesy. Boll. di Geod. e Sci. Affini, XXXVIII, 2, 551-589.
- Holdahl, S.R. (1980). Crustal movements and redefinition of heights. In Proceedings of the Second International Symposium on Problems Related to the Redefinition of North American Vertical Geodetic Networks (G. Lachapelle, ed.), Canadian Institute of Surveying, Ottawa, 567-578.
- Kääriäinen, E. (1953). On the recent uplift of the earth's crust in Finland. Publications of the Finnish Geodetic Institute, no. 42.
- Kääriäinen, E. (1960). Adjustment of the northern bloc in UELN and accuracy of the geopotential differences in it. Bulletin Geodesique, 55, 299-310.

- Korhonen, J. (1961). Adjustment of levellings in region of slow vertical movement. Ann. Acad. Sci. Fennicae, Ser. A III Geologica-Geographica, 61, 127-142.
- Lachapelle, G., and R. Gareau (1980). Status of vertical geodetic networks in Canada. In Proceedings of the Second International Symposium on Problems Related to the Redefinition of North American Vertical Geodetic Networks (G. Lachapelle, ed.), Canadian Institute of Surveying, Ottawa, 49-71.
- Merry, Ch. and P. Vaníček (1983). Investigation of local variations of sea-surface topography. Marine Geodesy, 7, 1-4, 101-126.
- Riddihough, R.P. (1982). Contemporary movements and tectonics on Canada's west coast: a discussion. Tectonophysics, 86, 319-341.
- Sommerfeld, A. (1950). Mechanics of Deformable Bodies. Lectures on Theoretical Physics, Vol. II Academic Press, New York, 396 pp.
- Vaníček, P. and E. Krakiwsky (1982). Geodesy: The Concepts. North Holland, Amsterdam, 691 pp.
- Vaníček P. and D. Nagy (1980). Report on the compilation of the map of vertical crustal movements in Canada. Earth Physics Branch, EMR, Open File 80-2.
- Vaníček P., G. Carrera and M. Craymer (1985). Corrections for systematic errors in the Canadian levelling networks. Surveys and Mapping Branch. Final Research Contract Report.
- Van Mierlo, J. (1983). On the reduction of levelling data to a common epoch. In Precise Levelling. Contributions to the Workshop on Precise Levelling. (Niemeier W. and H. Pelzer, eds.), Dummler, Bonn, 199-209.
- Young, F. (1984). Personal communication.

ROLE OF THE NORTH AMERICAN VERTICAL DATUM
FOR EARTHQUAKE RESEARCH AND PREDICTION: AN EXAMPLE FROM THE GREAT BASIN

Ross S. Stein
U.S. Geological Survey
Menlo Park, California 94025

ABSTRACT. The North American Vertical Datum (NAVD) provides a vital source of data for the study of deformation that precedes, accompanies, and follows large earthquakes. The unique attributes of the NAVD for earthquake investigations are the 150-km spacing of leveling lines in the network, which is dense enough to capture the deformation associated with many large earthquakes, and the close 1.5-km spacing of BM's along each line, which allows resolution of km-scale variations of fault slip and geometry. Geodetic elevation changes record the deformation associated with the recent $M=7.0$ 28 October 1983 Borah Peak, Idaho, earthquake on the Lost River fault. The crest of the Lost River Range rose 20 cm and adjacent Thousand Springs Valley subsided 100 cm, relative to reference points 45 km from the mainshock epicenter. The deformation was modeled by dislocations in an elastic half-space. Two meters of slip on a planar fault extending to a depth of 13 km provides the best fit to the geodetic data, and is consistent with seismic observations of the earthquake. The geodetic and geologic data permit a 5,000-10,000 year estimate for the earthquake repeat time, a value typical of the Basin and Range province of the western U.S. but much longer than repeat times observed at plate boundaries. Annual resurvey of leveling lines to monitor other active range-bounding normal faults in the Great Basin, such as the Wasatch fault zone near Salt Lake City, UT, will require leveling lines that extend at least 30 km normal to the fault zone, surveyed to a precision of about 30 mm.

INTRODUCTION

The North American Vertical Datum provides an invaluable baseline for investigation of earthquake mechanics, evaluation of earthquake hazards, and monitoring for earthquake prediction. Resurvey of leveling routes in the vicinity of large earthquakes enables precise measurement of the broadscale surface deformation caused by fault slip in the earth's crust. Such measurements are vital to improve our understanding of the subsurface structures on which earthquakes nucleate and propagate, and to monitor these structures in regions where the earthquake risk is high.

The 100-150 km spacing of the NAVD network arteries permits surface displacement associated with many large earthquakes to be measured in regions where no other instruments are located and where no other surveys were conducted before the earthquake. In addition, the typical 1.5-km spacing of bench marks (BM's) along the lines provides a spatial resolution that greatly exceeds that for horizontal geodetic control. Should the current standard of 1.5-km BM spacing give way to a less dense BM distribution once GPS surveys replace conventional geodetic leveling, a major loss of deformation data pertinent to the analysis of earthquake mechanics will result.

Vertical-elevation changes are most useful for tectonic analyses when other measurements accompany the releveing surveys. To distinguish tectonic deformation from sediment compaction, observations of elevation change deduced from resurvey of the vertical datum are most valuable when they are accompanied by repeat gravity measurements and water well hydrographs in sedimentary basins, which are commonly regions of groundwater-withdrawal induced subsidence (see

Holzer, this volume). Measurements of horizontal deformation obtained from resurvey of triangulation, astronomic azimuths, and trilateration form ancillary data sets that can improve resolution of the fault movements associated with earthquakes (see, for example, Jachens et al 1983).

Seismic and geodetic measures of the earthquake source furnish complementary records of the rupture process. The earthquake source measured from the radiation from seismic waves documents the initial phase of rupture that persists from seconds to minutes, whereas the source estimated from the ground surface displacements gives the final state of rupture after the passage of days to years. In general seismic or rapid fault slip is followed by time-decaying creep.

THE 1983 M=7.0 BORAH PEAK, IDAHO, EARTHQUAKE

Six large historical earthquakes have struck the Great Basin (Table 1); of these only the 1954 Fairview Peak, the 1959 Hebgen Lake the 1983 Borah Peak shocks have left a seismic and geodetic record that enables study of the subsurface fault slip. From this limited sample and from geologic observations, seismic hazards must be assessed in the Great Basin of the western U.S. The damage that can be inflicted by large earthquakes in this region depends, first,

Table 1: Large Historical Great Basin Earthquakes

Date	Location	Moment Magnitude
9 January 1872	Owens Valley, CA	7.8
2 October 1915	Pleasant Valley, NV	7.2
10 December 1954	Fairview Peak, NV	7.2
19 August 1959	Hebgen Lake, MT	7.3
28 October 1983	Borah Peak, ID	7.0

on the proximity of the active faults to population centers and critical facilities, and second, on the subsurface geometry of these faults. The 1983 Borah Peak earthquake (Fig. 1) provides a rare opportunity to study the depth and geometry of the fault rupture, and to estimate an earthquake repeat time.

DATA

The precision and spatial coverage of the geodetic data at Borah Peak equal or surpass all records of vertical-elevation changes associated with large earthquakes in regions of crustal extension. The leveling permit estimation of the fault geometry and slip independent of the seismic and geological data. The coseismic elevation changes were obtained by subtracting the relative heights of BM's surveyed after the earthquake in July 1984 from the heights of the same BM's surveyed before the earthquake in 1933/48. The coseismic period thus includes the 50 years preceding the earthquake and the 8 months after it, under the assumption that no man-induced subsidence took place during the period.

The leveling was conducted by the National Geodetic Survey. All data were corrected for level collimation, rod excess, rod thermal expansion, and atmospheric refraction. The observed rod temperatures were used for all surveys to compute rod expansion. The 1933 and 1948 surveys were corrected for refraction using REDUC4 after Holdahl (1981), in which temperature gradients are modeled as a function of time and location, whereas the 1984 observations were corrected following Kukkamaki (1938), using observed temperature differences made at every instrument setup.

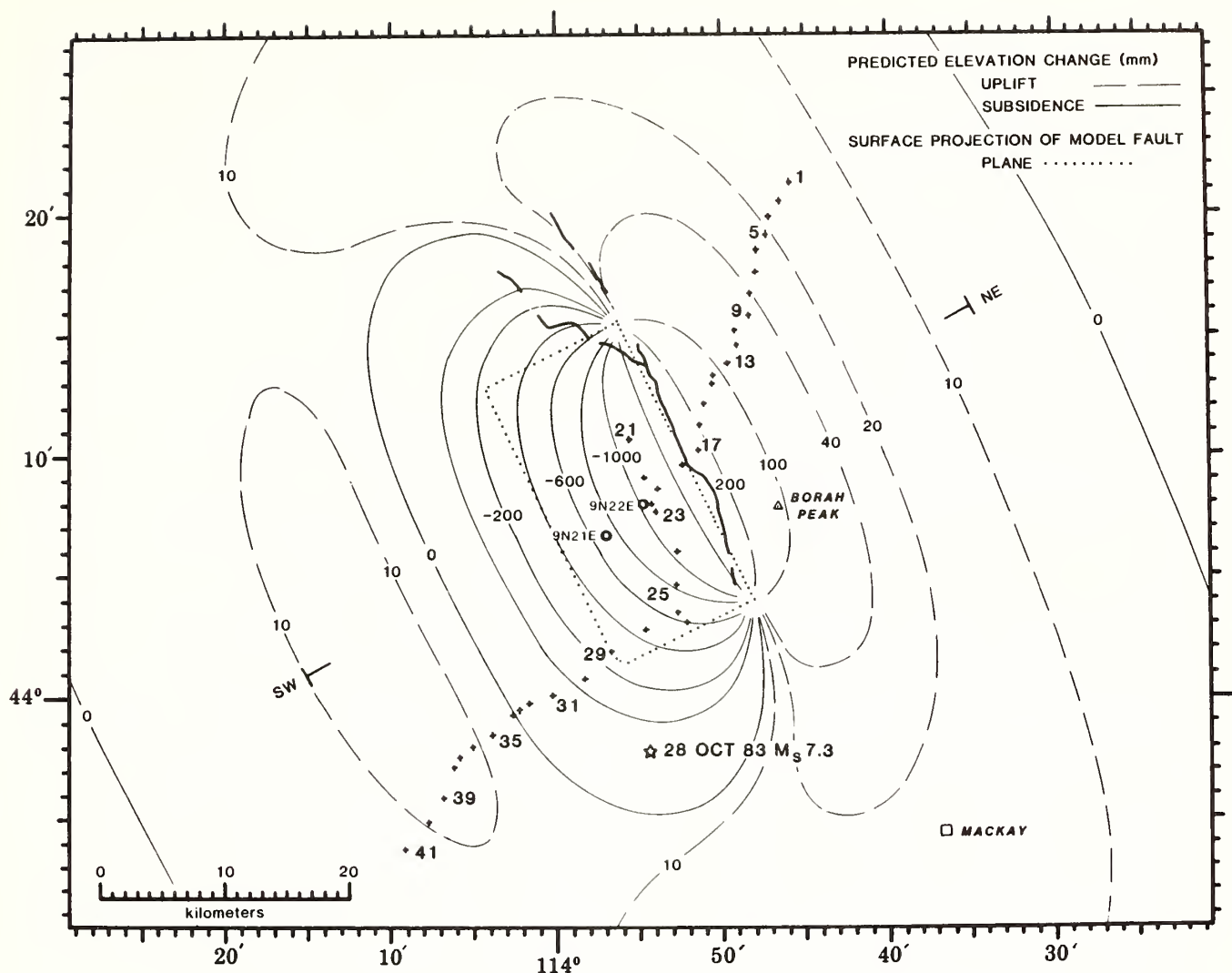


Figure 1a. Borah Peak earthquake site, showing BM's (crosses), observation wells (circles) in Thousand Springs Valley, the segment of the Lost River fault that sustained surface rupture in 1983 (heavy line), contours of predicted elevation change for the fault model (thin solid and dashed lines), and the surface projection of the model fault plane (dotted lines). The lower edge of the model fault plane is denoted by rounded corners on the model fault plane. The location of the Borah Peak main shock is shown by a star. The "T's" mark the azimuth of the projection for the profiles in Fig. 2.

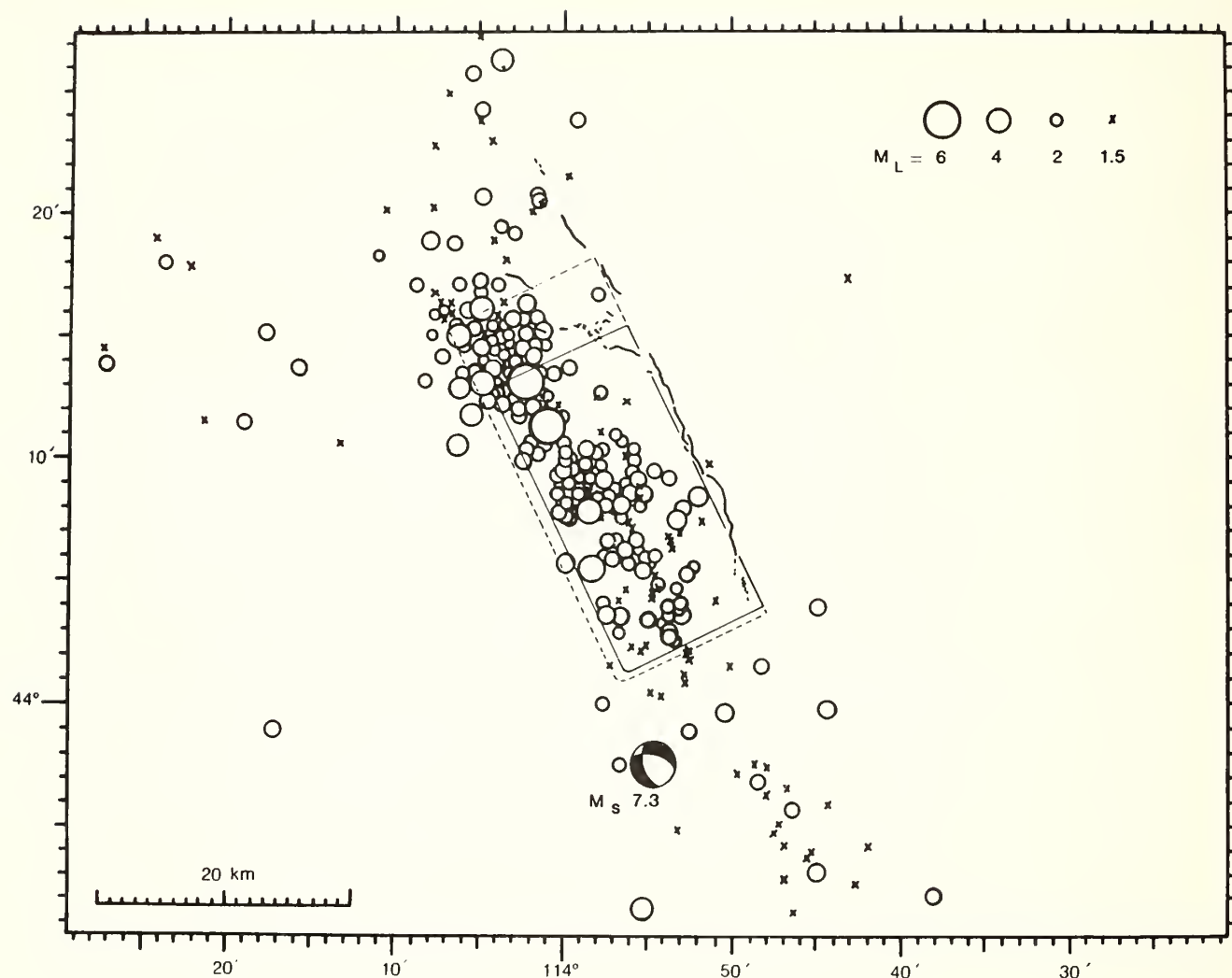


Figure 1b. Aftershocks recorded by a portable seismic array deployed between 10-29-83 and 11-19-83 are shown with the best-fit fault model (solid line) and the largest fault that can satisfy the leveling data, representing a 10 percent increase in model residuals over the best-fit fault (dashed line). Note that the main shock lies at or beyond the edge of the model fault, indicative that the earthquake focus was not the site of significant permanent fault slip, but rather where the rupture initiated.

Survey Errors

Potential sources of noise in the data include random and systematic surveying errors and nontectonic subsidence due to ground-water withdrawal. Estimated cumulative random error of the observed elevation changes nowhere exceeds 20 mm. Briefly, the mean difference for all (forward - backward) runnings of the sections must not differ significantly from zero, and the standard deviation of the difference, β , gives an indication of the random error per section, σ . In principle, $\sigma = \alpha L^{1/2}$, where α is a function of β (Bomford 1971). If β is Gaussian distributed and the survey is double-run with 1-km sections, $\alpha \approx 1/3\beta$. Because some of the 1984 survey was single-run using the procedure of Whalen and Balazs (1977), we set $\alpha = \beta$ (see Table 2). Thus the cumulative random error for the 70-km-long survey is $1.38\text{mm}L^{1/2} = 12\text{ mm}$. For the 1933 survey, $\beta = 1.83\text{mm}$, slightly larger than that for 1984. Because the 1948 leveling was single-run, β cannot be accurately assessed. We assume here that a value of $\alpha = 2.0\text{mm}$ provides a fair estimate of the combined 1933 and 1948 surveys. Taking the sum of the squares of the α 's, the cumulative error for the differenced preearthquake and postearthquake surveys becomes 20mm, about the size of the dots in Figure 2(top), and only about 2 percent of the coseismic signal.

Table 2: Leveling Specifications

NGS line	Survey period	Segment (BM's)	Single/Double Run	Order	Reruns (percent)	Rejection tolerance (mm)	β (mm)
L24832	6-7/84	22- 33	Single	1st	4.7	4.0	1.38
	6-7/84	1-22; 33-38	Double	1st	6.8	4.0	
L24812	11/83	16- 33	Double	1st	1.2	4.0	1.09
L12785	8/48	1- 23	Single	2nd	4.0	8.4	--
L951	10-11/33	22- 38	Double	1st	4.8	4.0	1.83

All surveys were examined for elevation-dependent error using the method of Stein (1981), and none were found. Inaccurate rod-calibration corrections, and under some circumstances, unmodeled refraction error, cause a dependence of elevation change on the elevation. In these cases, elevation change and elevation profiles tend to mimic or mirror each other, and thus disclose a systematic error unaccounted for by the random error estimates. If tilt and slope were correlated, this error could be identified and removed. Regression coefficients were calculated, but the fact that none of these coefficients depart significantly from zero indicates no systematic errors larger than the limits of detection, which is $20\text{ppm} \times$ the maximum topographic height difference (600m), or 12mm. Stein and Barrientos (1985a) plot tilt as a function of slope for this data and give the detailed statistics. Because the end points of the coseismic survey lie at nearly the same elevation, these BM's are essentially unaffected by slope-dependent errors.

Subsidence Errors

Hydrologic data demonstrate near-stasis of the water table during the coseismic period (1933-84), making subsidence due to fluid withdrawal unlikely. A reconnaissance water-resource survey of the valley (Stearns et al 1938, Plate 31) indicates that the water stood 3-6m below the ground during 1930-37 in Thousand Springs Valley in the vicinity of BM 22 (Fig. 1a). USGS observation well

9N22E-06CCA1, which was drilled about 150m west of BM 22 (Fig. 1a) in 1967, was observed in 1967/68, 1978, and 1983/84. The water table stayed 5.4 ± 0.9 m below the surface during 1967-84, indistinguishable from the 1930-37 level obtained by reconnaissance. USGS observation well 9N21E-14BBC1, located 4 km west of BM 23 (Fig. 1a), provides a continuous hydrograph during 1966-84. This well also shows a constant hydraulic head with only 1-m seasonal fluctuations (Whitehead 1985). The water table remained static because the alluvial aquifer beneath the leveling route has been recharged by water diversions from the Big Lost River since 1931.

The 1933 leveling and the 1948 leveling overlap at section 22-23 (Fig. 1a). We used the junction section to test for tilt during 1933-48. The 1933 and 1948 measurements of the height difference over the junction section differ by only 1.56 mm, less than the expected random error for either survey. The absence of measurable tilt during this 15-yr period in Thousand Springs Valley supplies a weak test of the assumption that deformation or subsidence preceding the earthquake was negligible.

EARTHQUAKE MODEL

We seek the simplest dislocation that can explain the observed elevation changes, subject to surveying errors and modeling simplifications. Fault slip was approximated by uniform displacement on a rectangular surface embedded in an elastic half-space, using the expressions of Mansinha and Smylie (1971). The half-space is a body with infinite depth and with a flat upper surface approximating the ground. Imposing a dislocation on a fault is equivalent to cutting the elastic body, displacing the two faces of the cut in equal and opposite directions parallel to the plane of the cut, and then bonding the faces back together. This will impose strains in the body and will deform its upper surface. The dimensions, orientation, and magnitude of the slip on the cut, or fault, are then matched to fit the deformation at the ground surface observed from releveling.

The leveling data can be simply explained by a planar fault rupture extending from a depth of 13.3 ± 1.2 km to the surface. Elevation changes at 94 percent of the BM's are satisfied with expected random and systematic errors (20 mm) by the coseismic model (Fig. 2). Contours of predicted elevation change for the model are shown in Fig. 1. The parameters describing the coseismic fault slip are: Slip = 2.05 ± 0.10 m; length = $23 \pm 8/-2$ km; dip (acute angle from the ground to the fault) = $47 \pm 2^\circ$; vertical depth = 13.3 ± 1.2 km. The geodetically measured seismic moment, M_0 (a measure of the earthquake size), is $2.6 \pm 0.4 \times 10^{19}$ Nm. Barrientos et al (1985) inverted the leveling data and obtained a similar result. Stein and Barrientos (1985b) tested for curved fault geometries and found the planar fault to be superior. The kinks in the model curve at BM's 22 and 26 in Figure 2 result from the azimuth change of the leveling route (Figure 1a). The misfitting BM 18 was not used in the modeling because it is a section corner and does not meet NGS standards for 1st Order survey marks, and could have been unstable.

The geodetic parameters accord well with the independently measured seismic parameters. Doser (1985) obtained $M_0 = 2.9 \times 10^{19}$ Nm, a focal depth of 16 ± 4 km, and a fault dip of $45-53^\circ$ (shown in Fig. 2), from teleseismic waveform modeling. The model is also consistent with the aftershock locations from Richins et al (1985), with the geodetically determined fault plane embedded within the aftershocks (Figures 1b and 2).

DISCUSSION

Coseismic Uplift of the Lost River Range

Leveling across the Lost River Range and Thousand Springs Valley permits tentative assignment of absolute elevation changes. The end point BM's give the same elevation within the measurement uncertainty, and they fall essentially outside of the region of modeled coseismic deformation. Absolute uplift of the ranges bounding an earthquake in a region of continental extension has never before been measured, because leveling was absent or ambiguous on the upthrown block (in this case, the NE side of the fault). Borah Peak, Idaho's highest point (Fig. 1a), probably lofted an additional 10-15 cm during the earthquake. An important advance in the ability to establish an absolute or global reference to leveling surveys will be possible once GPS surveys have been conducted throughout the NAVD. This will remove one degree of freedom in current earthquake modeling efforts, and enable a more thorough investigation of how regions like the Basin and Range that are under horizontal extension can locally uplift.

Earthquake Repeat Time from Geodetic and Geologic Data

An essential element of earthquake hazards assessment is the estimation of earthquake repeat times for fault segments. Although earthquakes do not repeat in a strictly periodic manner, earthquake recurrence is regular enough that an earthquake repeat time is one of the best indices of forecasting fault behavior. A mean fault slip of 2.05 ± 0.10 m was calculated for the 1983 Borah Peak earthquake from the leveling data, which also agrees well with the 1.5-2.5 m height of the surface rupture associated with the earthquake (Crone and Machette 1984). From fault excavations 0.5 km north of the leveling route, Schwartz and Crone (1985) found that one prehistoric event had taken place on the Lost River fault during the past 12,000-14,000 years, and this pre-1983 event also showed 2 m of surface slip. Thus the two events have slipped a total of 4 m in 14,000 yr, a rate of 0.3 mm/yr. From the total 3-km slip on the fault estimated by Scott et al (1985) for the past 4-7 million years, a similar slip rate emerges. Thus both the past 14,000 yr period and the past 4-7 million year period suggest a slip rate of 0.3 mm/yr and, if 2 m of slip per event is assumed, an earthquake repeat time of 5,000-10,000 yr.

Use of leveling surveys for earthquake prediction in the Great Basin

The base of an active fault (13 km at Borah Peak) is a plausible site for slippage before an earthquake. This is because the earth's crust attains its peak strength at a depth of about 10-15 km. Strength increases linearly with depth due to the load of the overlying rocks until a temperature is reached at which some of the rock constituents begin to fuse and melt; below this depth rocks deform by ductile flow or creep and earthquakes become rare (Sibson 1982). Detection of preseismic fault slip at a depth of 12-15 km is a much more challenging task than if premonitory slip were to take place close to the surface. To monitor slip at a depth of 12-15 km on a fault dipping 45° , geodetic surveys must extend from the fault trace for about 30 km on the downthrown (basin-side) block, and they must have sufficient precision to detect broad wavelength deformation (Fig. 3). A 4 by 4-km dislocation patch situated at the base of the fault would cause the ground to subside less than 20 mm per meter of fault slip. If the zone of preseismic slippage extended 35 km along strike (e.g., a 4 by 35-km strip beneath the entire Borah Peak rupture), then about 90 mm of subsidence per meter of buried slip would take place (Fig. 3). Because the

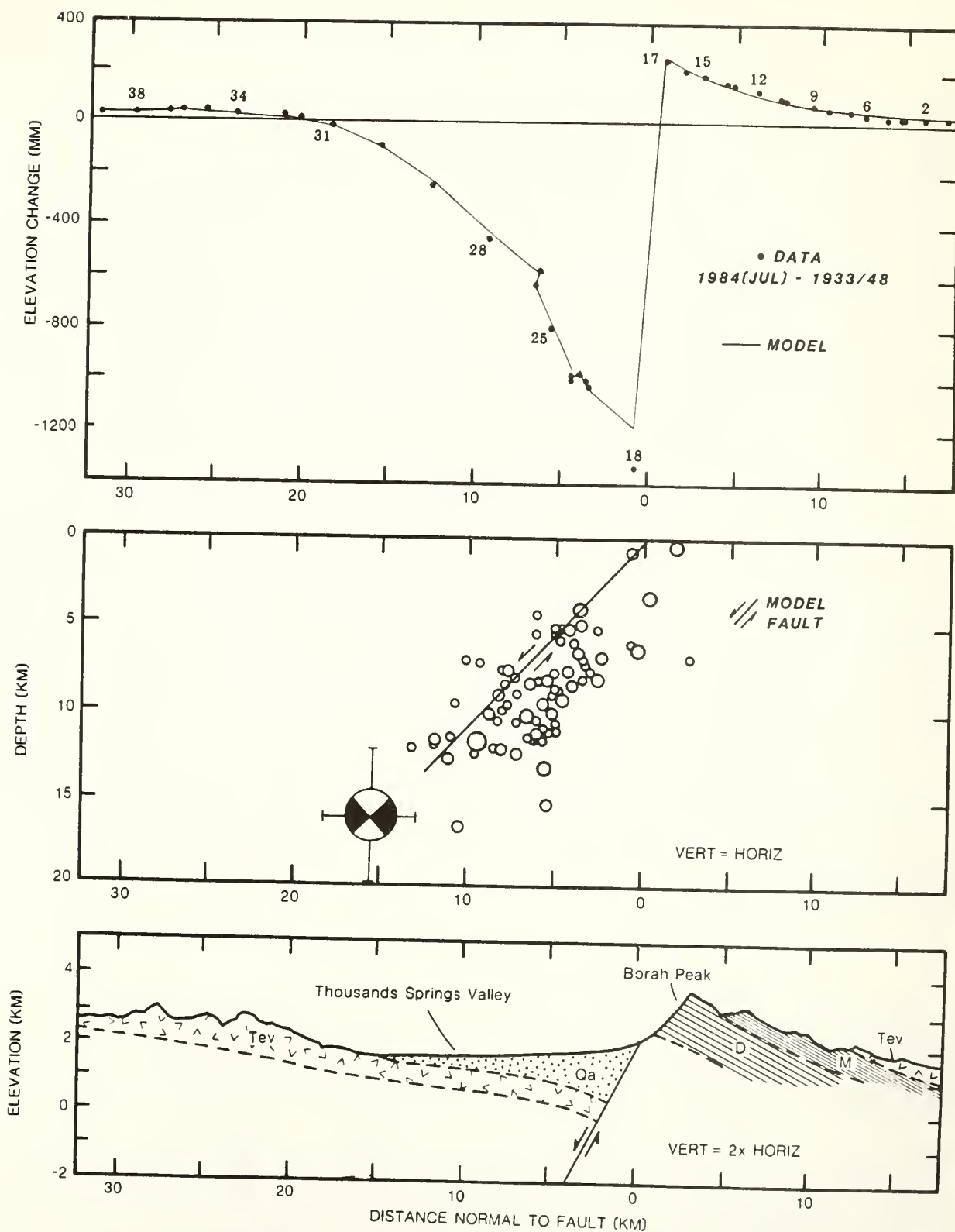


Figure 2. (Top) Observed and modeled coseismic elevation changes projected onto the azimuth shown in Fig.1a. (Middle) Depth cross-section of coseismic model fault with aftershocks and mainshock. (Bottom) Schematic geology of the basin and the Lost River Ranges.

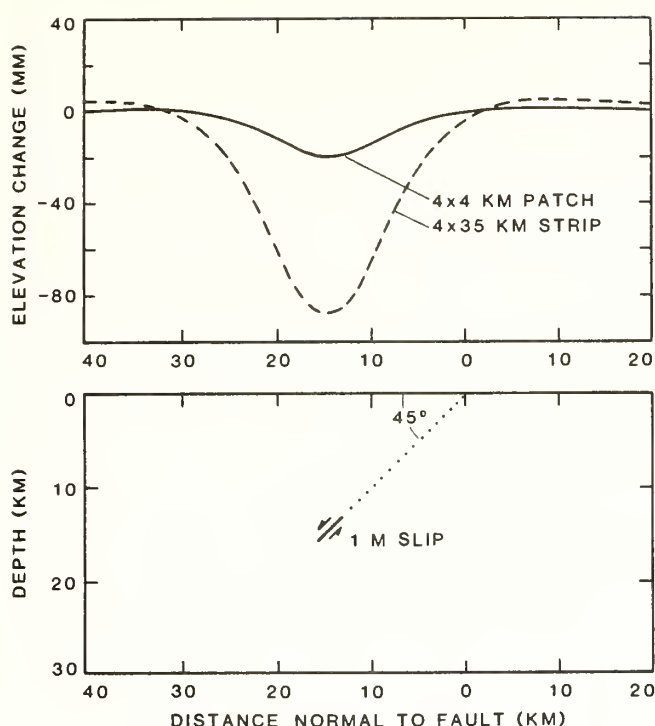


Figure 3. Surface deformation produced by hypothetical preseismic slippage at the base of the model fault, showing elevation change per meter of slip on a 4 by 4-km epicentral patch (solid line) and a 4-km-wide strip running the 35-km length of the coseismic fault (dashed). Detection of such broad wavelength deformation is compounded by the likelihood that the greatest subsidence will occur within the fault-bounded sedimentary basin.

greatest subsidence occurs within the basin, discrimination of tectonic deformation from ground-water-related subsidence may be very difficult. No such monitoring effort should be attempted without locating the leveling line near continuous recorder wells. Leveling that is restricted to within 10 km of the fault will in any event be insufficient to detect all but near-surface slip.

CONCLUSIONS

The North American Vertical Datum has become an essential element of earthquake investigations in the United States, and the role it plays will increase as vertical height measurement becomes less expensive and more accurate, and as our understanding of crustal deformation grows. One of the best records of coseismic elevation change ever measured for a large earthquake in a region of continental extension was used to determine the fault orientation, depth, and slip. Combining this information with geologic data allowed estimation of a 5,000-10,000 yr repeat time. Such a repeat time is probably typical of the Great Basin, but is much less than that at plate boundaries. The geodetically measured earthquake parameters are nearly equivalent to those measured seismically, indicative that most of the coseismic slip took place during the first 60 seconds of the mainshock, with negligible postseismic creep.

The heavily populated Wasatch fault zone in Utah shares many characteristics with the Lost River fault in Idaho. Efforts to detect premonitory elevation change and tilt caused by slip at the base of the Wasatch fault will be demanding and require precision leveling surveys that span the fault and the Salt Lake Basin for at least 30 km, or twice the probable depth of the fault.

ACKNOWLEDGEMENTS

I am indebted to the speed, skill, and tenacity of the NGS leveling crew headed by Curt Smith and guided by Bob Martine and Emery Balazs. I would also like to thank Tom Holzer for his review of this manuscript.

REFERENCES

- Barrientos, S., S.N. Ward, J.R. Gonzales-Ruiz, and R.S. Stein, 1985, Inversion for moment as a function of depth from geodetic observations and long period body waves of the 1983 Borah Peak, ID, earthquake, in Proc. Workshop XXVIII on the Borah Peak earthquake, U.S. Geol. Surv. Open-File Rep. 85-290, 485-518.
- Bomford, G., 1971, Geodesy, Oxford University Press, London, 226-280.
- Crone, A.J., and M.N. Machette, 1984, Surface faulting accompanying the Borah Peak earthquake, central Idaho, Geology, 12, 664-667.
- Doser, D.I., 1985, The 1983 Borah Peak, Idaho, and 1959 Hebgen Lake, Montana, earthquakes: Models for normal fault earthquakes in the Intermountain seismic belt, in Proc. Workshop XXVIII on the Borah Peak earthquake, U.S. Geol. Surv. Open-File Rep. 85-290, 368-384.
- Holdahl, S.R., 1981, A model of temperature stratification for correction of leveling refraction, Bull. Geodesique, 55, 231-249.
- Jachens, R.C., W. Thatcher, C.W. Roberts, and R.S. Stein, 1983, Correlation of changes in gravity, elevation, and strain in southern California, Science, 219, 1215-1217.
- Kukkamaki, T.J., 1938, Über die nivellitische refraction, Finn. Geod. Inst., 25.
- Mansinha, L., and D.E. Smylie, 1971, The displacement fields on inclined faults, Seismol. Soc. Am. Bull., 61, 1433-1440, 1971.
- Richins, W.D., R.B. Smith, C.J. Langer, J.E. Zollweg, J.T. King, and J.C. Pechmann, 1985, The 1983 Borah Peak, Idaho, earthquake: relationship of aftershocks to the mainshock, surface faulting, and regional tectonics, in Proc. Workshop XXVIII on the Borah Peak earthquake, U.S. Geol. Surv. Open-File Rep. 85-290, 285-310.
- Schwartz, D.P., and A.J. Crone, 1985, the 1983 Borah Peak earthquake: A calibration event for quantifying earthquake recurrence and fault behavior on Great Basin normal faults, in Proc. Workshop XXVIII on the Borah Peak earthquake, U.S. Geol. Surv. Open-File Rep. 85-290, 153-160.
- Scott, W.E., K.L. Pierce, and M.H. Hait, Jr., Quaternary tectonic setting of the 1983 Borah Peak earthquake, Central Idaho, in Proc. Workshop XXVIII on the Borah Peak earthquake, U.S. Geol. Surv. Open-File Rep. 85-290, 1-16.
- Sibson, R.H., 1982, Fault zone models, heat flow, and the depth distribution of earthquakes in the continental crust of the United States, Bull. Seismol. Soc. Am., 72, 151-163.
- Stearns, H.T., L. Crandall, and W. Steward, 1938, Geology and groundwater resources of the Snake River Plain in southeastern Idaho, U.S. Geol. Surv. Water Supply Pap. 774, 260 pp.
- Stein, R.S., Discrimination of tectonic displacement from slope-dependent errors in geodetic leveling from southern California, 1953-1979, in Simpson, D.W., and P.G. Richards, eds., Earthquake Prediction, An International Review: Maurice Ewing Ser., v.4, A.G.U., Washington, D.C.
- Stein, R.S., and S.E. Barrientos, 1985a, The 1983 Borah Peak, Idaho, earthquake: Geodetic evidence for deep rupture on a planar fault, in Proc. Workshop XXVIII on the Borah Peak earthquake, U.S. Geol. Surv. Open-File Rep. 85-290, 459-484.
- Stein, R.S., and S.E. Barrientos, 1985b, Planar high-angle normal-faulting in the Basin and Range: Geodetic analysis of the 1983 Borah Peak, Idaho, earthquake, J. Geophys. Res., in press.
- Whalen, C.T., and E. Balazs, Test results of First-Order Class III leveling, NOAA Tech. Rep. NOS 68 NGS 4, Rockville, MD, 1977.
- Whitehead, R.L., 1985, Hydrologic changes following the Idaho Borah Peak earthquake, in Proc. Workshop XXVIII on the Borah Peak earthquake, U.S. Geol. Surv. Open-File Rep. 85-290, 556-572.

Readjustment of Leveling Networks to Account for Vertical Coseismic Motions

Sandford R. Holdahl
National Geodetic Survey
Charting and Geodetic Services
National Ocean Service, NOAA
Rockville, Maryland 20852

ABSTRACT

In tectonically active regions of North America the geodesist is confronted with the problem of updating heights where the Earth's surface has been vertically deformed by an earthquake. Dislocation theory can be used as a basis for modeling coseismic elevation changes and be incorporated within a general least squares adjustment scheme to correct a network of old leveling measurements and heights that are within the deformed area. Releveling data and information obtained from seismologists about the general nature of the earthquake serve as input to the modeling process. Fundamental equations and considerations are presented in this paper to develop dislocation models of vertical coseismic motions. The reader is referred to a previous paper (Holdahl, 1985) wherein real data sets are analyzed and discussed. These examples show potential for the method when applied in other areas, even when the physical setting is made complex by ongoing subsidence. The primary benefit of modeling coseismic motion is to avoid the cost of releveling for some lines in a deformed region. Rough modeling prior to any resurveying helps to select the lines to relevel that are most critical to a successful final model. A good model for coseismic motion cannot restore geodetic levelings to their original reliability, but corrected heights may be used in applications not requiring accuracy better than 5-15 centimeters.

INTRODUCTION

Earthquakes larger than magnitude 5-6 can produce vertical deformations of the Earth's surface which are detectable by leveling measurements. Coseismic motions can exceed several meters for large earthquakes, but present a problem whenever the relative elevation changes exceed the normal accumulation of random and uncorrected systematic leveling errors.

Figure 1 shows the locations of earthquakes in the United States producing intensities greater than V. Concentrations of the smaller earthquakes undoubtedly produce vertical deformation. However, the impact on the North American Vertical Datum (NAVD) is not much different than aseismic secular tectonic motion. Such motion can be roughly modeled as occurring uniformly with time. The earthquakes with intensities of VIII or greater will instantly cause heights to change significantly out to distances of 10 to 300 km from the center of deformation. From figure 1 it can be readily seen that coseismic modeling will be a necessity in much of California, Alaska, Hawaii, western Nevada and Montana.

For the last two decades, researchers in Japan and the United States have been using the theory of dislocations to model the deformation produced by

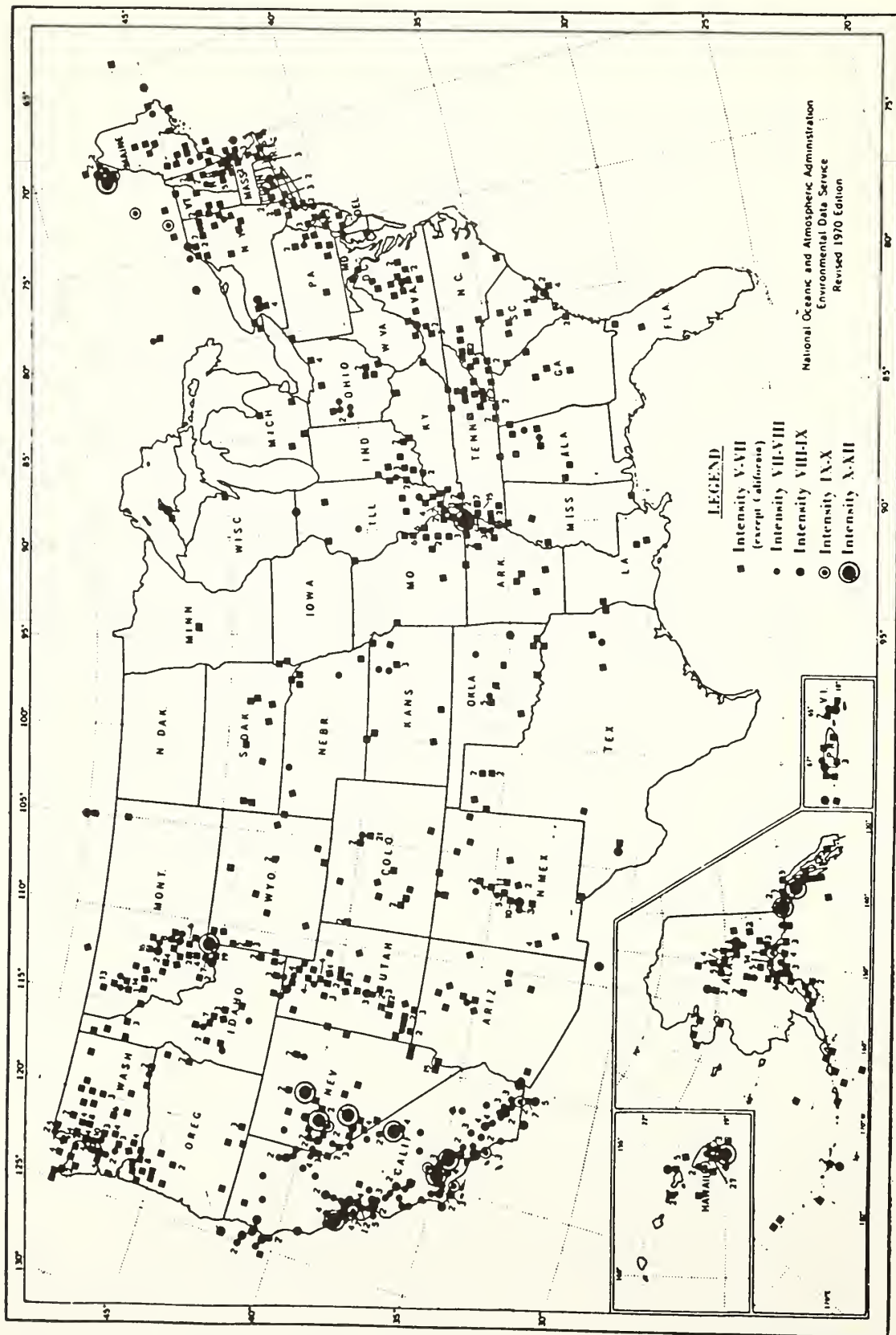


Figure 1 -- Earthquakes (intensity V and above) in the United States through 1970.

earthquakes (Kasahara, 1981). Recently the theory has been applied to adjustment of horizontal geodetic control networks in California, Hawaii, and Nevada in connection with project REDEAM (Snay et al, 1983). The latter efforts support the readjustment of the North American horizontal reference system.

The accuracy and geometry of leveling measurements are superior to horizontal measurement for modeling dip-slip motion on steeply dipping faults. For strike-slip faulting, the existence of a good postseismic horizontal resurvey may be sufficient to support modeling of vertical motion without extensive releveing. It is useful for the geodesist to become familiar with the variety of such circumstances and the associated terminology and concepts. Coseismic models derived from leveling measurements can improve adjustments of horizontal measurements, and the reverse is also true. The concepts described below will be applicable to studies of 3-dimensional surveys where vertical motion is significant.

MATHEMATICAL DEVELOPMENT

Adjustments of leveling networks may use the following mathematical expression to account for the secular rate of elevation change. The height, H_i , at time, t_i , of a geodetic station is given by

$$H_i = H_o + \dot{H}(t_i - t_o) \quad (1)$$

where H_o is the height of the station at t_o , a selected reference time. The change in height during the period $(t_i - t_o)$ is considered to have occurred uniformly at the rate of \dot{H} . \dot{H} is a velocity surface function that may be formulated in any number of ways. \dot{H} at a position (x,y) is calculated here using a method called multiquadric (MQ) analysis (Holdahl and Hardy, 1979):

$$\dot{H} = \sum_{j=1}^m r_j [(x-x_j)^2 + (y-y_j)^2]^{1/2} \quad (2)$$

The x_j , y_j are locations of MQ nodal points and the r_j values are unknown coefficients.

The model implied by eq. (1) is insufficient when the levelings within a network were accomplished both before and after a strong earthquake, Richter magnitude 6 or greater. The selected reference time, t_o , usually postdates any of the levelings; therefore a model for earthquake deformation is required to correct the pre-earthquake heights of those stations not reoccupied after the event. We thus augment eq. (1) with a term to describe coseismic deformation.

$$H_i = H_o + \dot{H}(t_i - t_o) + U \quad (3)$$

A dislocation model is used to describe the motion, U , that occurs during an earthquake. To implement dislocation theory we must have some knowledge about the nature of the earthquake. Figure 2 helps to explain the parameters which define the dislocation model and illustrates the fault-centered coordinate

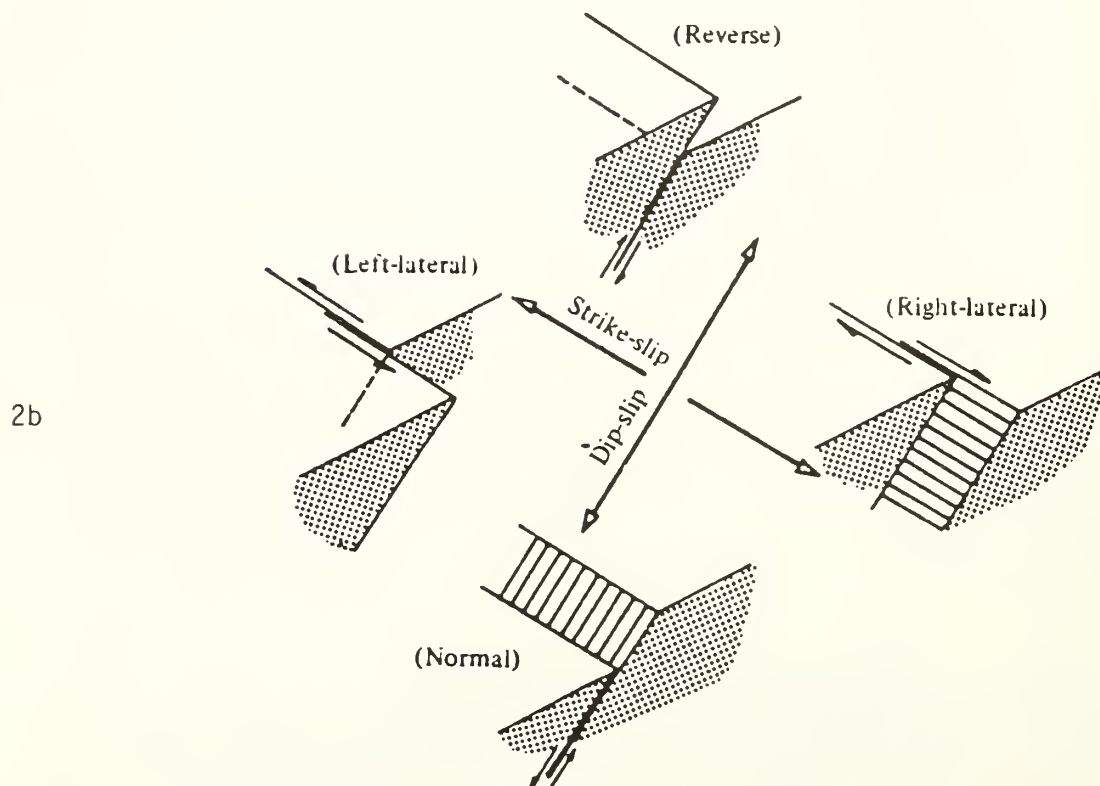
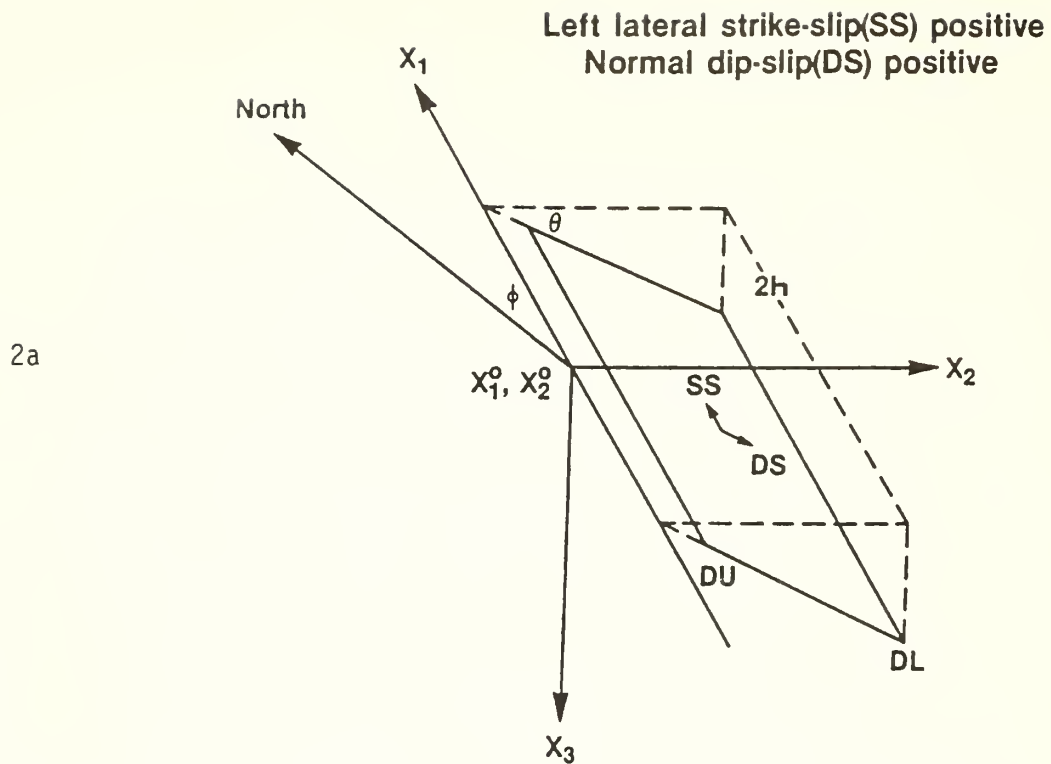


Figure 2 -- (a) Rectangular fault geometry. The coordinates x_1^0, x_2^0 give the origin of the fault-centered coordinate system;
(b) Various slip motions that are possible.

system. Slip is assumed to occur on a rectangular fault plane embedded in an isotropic elastic halfspace. The origin of the fault-centered coordinate system is at the midpoint of the fault trace obtained at the surface by projecting the fault plane along the dip angle. Dip, θ , is the angle of the fault plane with respect to the surface.

The azimuth of the fault trace, measured clockwise from north, is the fault strike (δ), and is the direction of the positive x_1 axis. The positive x_2 axis extends horizontally in the direction of dip. ¹Depth of the fault plane is measured along dip; DU is the upper depth, and DL is the lower depth. $W = DL - DU$ denotes the width of the ruptured fault plane, and h is the halflength.

Initial model parameters are estimated by geologists and seismologists. Seismologists analyze seismic waves from the earthquake to obtain fault-plane solutions which define quadrants of maximum compression and extension, from which strike and dip angle of the ruptured fault plane may be deduced. Seismologists also estimate earthquake magnitude, and record locations of aftershocks that help to define the halflength, width, dip, and depth of the slip surface. Geologists describe the physical structure of the crust underlying the deformed area, determine histories of previous earthquakes, and make field inspections of surface deformation to estimate strike and the directions and magnitude of slip that a successful dislocation model should corroborate.

We want to calculate the vertical surface displacements resulting from the earthquake. In the general case where secular motion is involved, the expression for a leveled height difference between two points at time t_i is

$$dH_{i,1-2} = H_{0,2} - H_{0,1} + (\dot{H}_2 - \dot{H}_1)(t_i - t_0) + U_2 - U_1 \quad (4)$$

The U term is only involved in the observation equation when

$$t_i < t_e < t_0 \quad \text{or} \quad t_0 < t_e < t_i \quad (5)$$

where t_e is the time of earthquake, and t_i is the time of observation.

For a single fault plane,

$$U = c_1 SS + c_2 DS \quad (6)$$

where SS is strike slip, and DS is dip slip (i.e., motion in the direction of dip). Formulas for c_1 and c_2 are given in the Appendix, and are functions of the assumed fault parameters that define the model. SS and DS are considered unknown, to be determined along with the heights, H_0 , for all or selected points in the level network.

Fault plane solutions and plots of aftershocks may suggest complex slip patterns involving more than one fault plane. For these complex cases, the coseismic deformation may be assumed to result from slip on two or more rectangular

planes. Equation (4) would then appear as

$$dH_{1,1-2} = H_{0,2} - H_{0,1} + (\dot{H}_2 - \dot{H}_1)(t_i - t_0) + \sum_{k=1}^n (U_{2,k} - U_{1,k}) \quad (7)$$

where n is the number of slipping fault planes. There will generally be two unknowns (strike slip and dip slip) for each fault plane, although the investigator might choose to eliminate one or both of the unknowns for a particular fault plane by forcing dip or strike slip to be consistent with a well accepted value. Multiple fault planes may be used to model several earthquakes at different times or be used to reflect complex motion associated with a single earthquake. However, it is advisable to keep the model as simple as possible.

The model must be realistic if we are to computationally update pre-earthquake levelings that did not contribute to the determination of the earthquake model. The proposed fault planes should have some physical justification and not exist just to improve the statistics used to evaluate fit.

The determination of the best fault parameters is a trial and error process. It is usually most efficient to extract the observations affected by the earthquake from the total data set and then find the fault parameters which produce the deformation surface that best fits this data subset. Working with the smaller data set is particularly helpful when the whole network is extensive or when other modeling problems outside the seismic deformation could bias the determination of the fault model. With less data, the computer can make quicker trial solutions as the various fault plane parameters are changed by small increments.

For regions where secular vertical motion can be assumed negligible, the trial and error process can be speeded up even more by deriving another form of observation from our subset of dH values. By comparing before and after dH values individually.

$$ddH = dH_{\text{after}} - dH_{\text{before}} \quad (8)$$

we obtain a new set of observations which allows us to efficiently compare the calculated and observed movements without using least squares to solve for heights at t_0 . Strike and dip slips, and the other fault parameters are specified in increments while seeking the best agreement between modeled and observed ddH values. Computer programs that perform this type of function are affectionately called "jiggle" programs and have been successfully used by Snay et al (1985) on horizontal data.

Constraints on the Solution

Analysis of horizontal measurements may benefit the modeling of vertical motions. Strike slip will usually be weakly determined from leveling data. A change of several meters in strike slip is difficult to sense if the postseismic leveling route is perpendicular to strike near the fault center. Leveling along the x_2 axis is ideal for determining dip slip, but is no help for resolving

strike slip. A poorly centered fault plane may give rise to unreasonably large estimates of strike slip. In leveling adjustments it is useful to constrain the unknown strike slip to within some maximum value, or prevent it from deviating far from a value obtained from analysis of other measurements, field inspection, or analysis of seismic waves.

The relationship between fault length and earthquake magnitude, M , is also useful,

$$\log L_m = 3.2 + 0.5M \quad (9)$$

where L_m is in centimeters (Kasahara, 1981). For earthquakes greater than magnitude 7.4, L is more easily determined because surface faulting almost always occurs.

The seismic moment of an earthquake, M_o , helps to place reasonable bounds on the solution. The seismic moment for a dislocation model is obtained using the formula

$$M_o = \mu \sum (s_i L_i W_i)$$

μ = rigidity modulus

s_i = total slip on the i -th fault plane

L_i = length of the i -th fault plane

W_i = width of the i -th fault plane (10)

The value of μ can be set to 3×10^{11} dyne/cm², a common value for rocks. M_o is well related to earthquake magnitude, M , by the expression (Hanks and Kanamori, 1979):

$$M_o = 10^{[1.5(M+10.7)]} \quad (11)$$

consequently the M_o derived from earthquake magnitude should agree within a factor of 2 with the M_o derived from the dislocation model. The length and width of the fault plane are therefore bounded somewhat.

APPLICATION TO THE LEVEL NETWORK

When only a subset of leveling lines in a deformed area has been releveled, we should attempt to restore the integrity of the lines that were not reobserved. Our dislocation model is the mechanism for this. After deriving the model from the subset of the data on releveled lines we can return to the total data set that covers the affected region and use our fault parameters and derived values for SS and DS to calculate the required correction to all observations.

In the preceding discussion the postseismic and preseismic leveling observations are given equal weight in determining the dislocation model. The misfit of the model is absorbed equally by the pre- and postearthquake levelings. This is objectionable in the final adjustment of the entire network because we consider the postearthquake observations as accurate indicators of surface heights after the earthquake. A more realistic method would be to adjust postearthquake levelings beforehand to fit stable points beyond the perimeter of the coseismic deformation. Then in determining the dislocation model, adjusted heights on postearthquake releveled lines could be held fixed, and all model misfit would be absorbed by the pre-earthquake levelings, thus yielding approximately the same dislocation model, but reducing the number of unknown heights, and giving more realistic error estimates for the corrections applied to pre-earthquake leveling data.

The adjustment of a large level network in a seismically active region such as California involves modeling all major coseismic motions since the level network was first constructed. There are 10-15 earthquakes which may have damaged the level network significantly during this period. After modeling the vertical motion for each earthquake separately it is then logical to adjust the entire network simultaneously involving all earthquakes. Points in the network that are far from any earthquake will undergo negligible coseismic height change. The radius of deformation for a magnitude 7 earthquake would be approximately 60 km, and would increase or decrease by a factor of approximately 10 for each integer change in earthquake magnitude. It is therefore unnecessary to evaluate the U-term of eq. (7) for points in the network which are obviously coseismically immobile. This will save computation time when the area adjusted is predominantly aseismic.

The most rigorous error propagation for height determination in a large seismic area is achieved by solving for all strike and dip slip values in the final adjustment. However, it is also reasonable to accept these values just as they come from previous adjustments of subnetworks, along with their standard errors and covariances. The error statistics can be used to calculate the variance of a coseismic correction term, and thus appropriately downweight affected observations.

Conclusions

Dislocation models can be a tool of the geodesist who must maintain networks of leveling in tectonically active regions. The modeling of vertical coseismic motion is surprisingly successful for most of the data sets reviewed by the author (Holdahl, 1985). Nevertheless, the ratio of model misfit to normal random leveling errors is large. Consequently, it would be unreasonable to expect dislocation models to restore damaged height relationships to their former precision. In contrast, the classical horizontal measurements have errors that are similar in magnitude to the dislocation model misfit; therefore postearthquake horizontal position relationships can be determined nearly as well as the original relationships.

The use of dislocation models with leveling data has several purposes:

1. The derived dislocation models refine our information about the nature of faulting and physics of the Earth's crust;
2. The model allows us to update heights on level lines that were not releveled after the earthquake, thus avoiding the cost of releveled; and
3. Rough modeling immediately after the earthquake will aid in planning postearthquake surveys so as to minimize expense of resurveying and maximize quality of the final model.

The reader should anticipate the beneficial impact of GPS measurements for modeling coseismic motion. A grid of Global Positioning System measurements would be nearly ideal for this work. Combinations of GPS and leveling will lead to reliable models. The geodesist should anticipate where earthquakes will occur, and economically establish the necessary grids before the earthquake.

ACKNOWLEDGMENT

The author greatly appreciates helpful discussions with Richard Snay, Edward L. Timmerman, and Michael W. Cline of the National Geodetic Survey. Robert H. Hanson and Anna Mary Miller wrote very useful graphics software. John H. Till assembled much of the leveling data, and Robert J. Harris wrote and coordinated software to access the NGS vertical control data base. Special thanks to Ross Stein for helpful comments and discussion.

REFERENCES

- Dunbar, William Scott, The determination of fault models from geodetic data, Ph.D. dissertation, Stanford University, 1977.
- Hanks, T. C., and H. Kanamori, A moment magnitude scale, J. Geophys. Res., 84 2348-2350, 1979.
- Holdahl, S. R., and R. L. Hardy, Solvability and multiquadric analysis as applied to investigations of vertical crustal movements, Tectonophysics, 52 (1979), 139-155.
- Holdahl, S. R., Readjustment of leveling networks to account for vertical coseismic motions; presented to International Symposium on Recent Crustal Movements, Maracaibo, Venezuela, to be published in Tectonophysics, 1985.
- Kasahara, K., Earthquake Mechanics, Cambridge University Press, London, 1981.
- Mansinha, L., and D. E. Smylie, The displacement fields of inclined faults, Bull. Seismol. Soc. Am., 61 1433-1440, 1971.

- Savage, J. C., and L. M. Hastie, Surface deformation associated with dip-slip faulting, J. Geophys. Res., 71, 4897-4904, 1966.
- Savage, J. C., and L. M. Hastie, A dislocation model for the Fairview Peak, Nevada, earthquake, Bull. Seismol. Soc. Am., vol. 59, no. 5, 1937-1948, 1969.
- Snay, R. A., M. W. Cline, and E. L. Timmerman, Dislocation models for the 1954 earthquake sequence in Nevada, U.S. Geological Survey Open-File Report, in press, 1985.
- Snay, R. A., M. W. Cline, and E. L. Timmerman, Regional deformation of the Earth model for the San Diego region, California J. Geophys. Res., vol. 88, No. B6, 5009-5024, June 10, 1983.
- Stein, R. S., Reverse slip on a buried fault during the 2 May 1983 Coalinga earthquake: Evidence from geodetic elevation changes, submitted to California Division of Mines and Geology, Coalinga volume, Sept., 1983.
- Stein, R. S., and S. E. Barrientos, The 1983 Borah Peak, Idaho, earthquakes: Geodetic evidence for deep rupture on a planar fault, Presented to U.S. Geological Survey workshop on Borah Peak Earthquake, 3-6 October, 1984.

Appendix

Equations to evaluate vertical displacements are given in indefinite integral form and must be evaluated at the four corners of the fault plane to obtain the result (Dunbar, 1977). For example,

$$c_i = f_i(h,DL) - F_i(h,DU) - f_i(-h,DL) + f_i(-h,DU), \quad i = 1 \text{ or } 2.$$

Recall

$$U = c_1 SS + c_2 DS$$

Expressions for f_1 and f_2 are given below.

First, the user must convert geodetic coordinates (ϕ, λ) into the fault-centered plane coordinates (x_1, x_2) .

$$dx = (\lambda - \lambda_0) R_e \cos(\phi)$$

$$dy = (\phi - \phi_0) R_e$$

$$x_1 = \cos(\delta) dy + \sin(\delta) dx$$

$$x_2 = \cos(\delta) dx - \sin(\delta) dy \quad x_3 = 0$$

ϕ_0, λ_0 are the geodetic coordinates of the fault center,

δ is the fault strike, and

$R_e = 6371000$ is the mean radius of the Earth.

The following auxiliary variables are introduced
(see Mansinha and Smylie, 1971):

$$r_2 = x_2 \sin \theta - x_3 \cos \theta \quad q_2 = x_2 \sin \theta + x_3 \cos \theta$$

$$r_3 = x_2 \cos \theta + x_3 \sin \theta \quad q_3 = -x_2 \cos \theta + x_3 \sin \theta$$

$$\begin{aligned} R^2 &= (x_1 - \xi_1)^2 + (x_2 - \xi_2)^2 + (x_3 - \xi_3)^2 \\ &= (x_1 - \xi_1)^2 + r_2^2 + (r_3 - \xi_0)^2 \end{aligned}$$

$$\begin{aligned} Q^2 &= (x_1 - \xi_1)^2 + (x_2 - \xi_2)^2 + (x_3 + \xi_3)^2 \\ &= (x_1 - \xi_1)^2 + q_2^2 + (q_3 - \xi_0)^2 \end{aligned}$$

$$k^2 = (x_1 - \xi_1)^2 + q_2^2$$

where

ξ_0 = DU or DL, and $\xi_1 = h$ or $-h$ depending on which corner
of the fault plane is being evaluated.

$$\xi_2 = \xi_0 \cos \theta \quad \xi_3 = \xi_0 \sin \theta$$

ν = Poisson's ratio = 0.25

$$\begin{aligned}
8\pi(1-\nu)f_1 &= (1-2\nu)\cos\theta \ln(R+r_3-\xi_0) + \frac{r_2 \sin\theta}{R} - \frac{r_2^2 \cos\theta}{R(R+r_3-\xi_0')} \\
&+ (1-2\nu)\cos\theta \ln(Q+q_3+\xi_0) + \sin\theta \frac{(3-8\nu)q_2 + 4\nu x_2 \sin\theta}{Q} \\
&- \frac{2(1-2\nu)x_2 x_3 \sin\theta + q_2 x_3 (1-2\sin^2\theta) + 4\nu x_2 q_3 \sin^2\theta + (3-8\nu)q_2 q_3 \sin\theta}{Q(Q+q_3+\xi_0)} \\
&+ 2q_2 x_3 \sin\theta \left\{ \frac{x_3+\xi_3 - q_3 \sin\theta}{Q^3} - q_2 q_3 \cos\theta \frac{(2Q+q_3+\xi_0)}{Q^3(Q+q_3+\xi_0)^2} \right\} \\
&- 4(1-\nu)(1-2\nu) \tan\theta \left\{ \ln(Q+x_3+\xi_3) - \sin\theta \ln(Q+q_3+\xi_0) \right\}
\end{aligned}$$

Note: As $\theta \rightarrow \pi/2$, $-\tan\theta \left\{ \right\} \rightarrow -\frac{x_2}{Q+x_3+\xi_3}$

$$\begin{aligned}
8\pi(1-\nu)f_2 &= (1-2\nu)\cos\theta\ln(R+x_1-\xi_1) + 2(1-\nu)\sin\theta \tan^{-1} \left\{ \frac{(x_1-\xi_1)(r_3-\xi_0)}{r_2 R} \right\} \\
&+ \frac{r_2(x_3-\xi_3)}{R(R+x_1-\xi_1)} - (1-2\nu)\cos\theta\ln(Q+x_1-\xi_1) - 2(1-\nu)\sin\theta \tan^{-1} \left\{ \frac{(x_1-\xi_1)(q_3+\xi_0)}{q_2 Q} \right\} \\
&- \frac{\xi_3(3-4\nu)q_2 - 4x_3\cos\theta + r_2x_3}{Q(Q+x_1-\xi_1)} + \frac{4(1-\nu)x_3(x_1-\xi_1)\sin\theta \cos\theta}{Q(Q+q_3+\xi_0)} \\
&- 2q_2x_3\xi_3(x_3+\xi_3) \frac{(2Q+x_1-\xi_1)}{Q^3(Q+x_1-\xi_1)^2} \\
&- 8(1-\nu)(1-2\nu)\sin\theta \tan^{-1} \left\{ \frac{(k-q_2\cos\theta)(Q-k) + k(q_3+\xi_0)\sin\theta}{(x_1-\xi_1)(q_3+\xi_0)\cos\theta} \right\}
\end{aligned}$$

No singularity as $\theta \rightarrow \pi/2$

THE EARTHQUAKE DEFORMATION CYCLE: IMPLICATIONS FOR THE
NORTH AMERICAN VERTICAL DATUM (NAVD)

Robert Reilinger*
Air Force Geophysics Laboratory
Hanscom Air Force Base, MA 01731

ABSTRACT. A particularly detailed set of releveled observations in the vicinity of an intraplate, thrust earthquake (M 7.4) in Argentina, indicate a cyclic pattern of deformation very similar to that reported previously for interplate earthquakes. This deformation cycle, which may be characteristic of many seismically active areas, consists of: 1) steady strain accumulation, possibly punctuated by strain reversals, 2) coseismic strain release, 3) a period of continued strain release due to after-slip (persisting for perhaps a year or so), 4) rapid postseismic strain accumulation which decreases exponentially and grades into steady strain accumulation. Permanent deformation results when strain accumulation is not exactly balanced by strain release. Vertical deformations associated with three earthquakes in the U.S. (1940, M7.1 Imperial Valley California; 1964, M8.4 Alaska; 1959, M7.5 Hebgen Lake, Montana) are used to demonstrate that: 1) significant vertical movements can occur in association with coseismic faulting in purely strike-slip environments, 2) large postseismic vertical movements can occur for strike-slip, thrust, and normal fault events, and 3) viscoelastic relaxation must be incorporated in models of earthquake related deformation.

INTRODUCTION

Observations of crustal movements (geodetic and geologic), primarily in the vicinity of large earthquakes along active plate margins, have revealed a cyclic pattern of deformation (e.g. Thatcher, 1984) which has a significant effect on the vertical datum. Recent analyses of geodetic measurements in the U.S. and abroad suggest that this deformation cycle (perhaps with some modifications) may apply to intraplate earthquakes as well as plate boundary events. This paper briefly reviews the observed earthquake deformation cycle (primarily vertical movements) placing particular emphasis on recent interpretations of deformation associated with a 1977 earthquake in Argentina. Examples are presented for deformation associated with three major earthquakes in North America. These earthquakes are characterized by three very different modes of deformation; a strike-slip event along the Pacific-North American plate boundary in S. California (M7.1, 1940 Imperial Valley), a major interplate thrust event in S. Alaska (M8.4, 1964 Alaska), and an intraplate normal fault event along the Intermountain Seismic Belt in southwestern Montana (M7.5, 1959 Hebgen Lake). The observations and interpretations presented here should help provide a basis for the development of quantitative procedures to incorporate earthquake related deformation in the determination and maintenance of the NAVD (Holdahl, 1985).

*Now at: Department of Earth, Atmospheric and Planetary Sciences, Earth Resource Lab, Massachusetts Institute of Technology, Cambridge, MA 02139

THE EARTHQUAKE DEFORMATION CYCLE

Figure 1a shows the idealized earthquake deformation cycle as recently summarized by Thatcher (1984) primarily on the basis of observations at convergent plate boundaries. The idealized cycle consists of interseismic strain accumulation leading to failure (coseismic). The essentially instantaneous coseismic deformation is followed by rapid postseismic recovery (i.e. opposite coseismic movements) which grades into steady state interseismic strain accumulation. Permanent deformation results when the postseismic and interseismic strain do not exactly balance the coseismic deformation. For the case shown in Figure 1a, permanent deformation is in the same sense as the coseismic deformation. The absence of a preseismic phase of deformation in the idealized cycle may reflect the lack of appropriate observations rather than evidence that anomalous (in relation to interseismic strain) preseismic movements do not occur.

A particularly detailed example of the earthquake deformation cycle, which is generally consistent with the idealized cycle shown in Figure 1a, exists for the 1977 Cauçete, Argentina earthquake. This event is unique in that multiple precise leveling surveys were conducted in the immediate epicentral area prior to the earthquake (Volponi et al, 1983). These pre-earthquake surveys, together with post-earthquake surveys conducted specifically to monitor earthquake deformation, provide information on vertical movements which occurred prior to, during and after the event (Volponi et al, 1983; Kadinsky-Cade et al, 1985; Reilinger and Kadinsky-Cade, 1985).

Figure 1b shows the time behavior of movements in the vicinity of the 1977 Cauçete, Argentina earthquake (solid circles). This time behavior, together with the spatial pattern of each phase of deformation, provides a basis for understanding fault behavior in this area. One possible interpretation, which is generally consistent with the idealized earthquake cycle, consists of the following sequence of events (Reilinger and Kadinsky-Cade, 1985). Deformation during the first preseismic period (1938 to 1967) results from slip on the eventual coseismic fault in the same sense as the 1977 coseismic slip. This slip may have been induced by the 1944 San Juan earthquake (M7.5) which occurred well west of the 1977 epicenter or may represent coseismic slip for a M6.5 earthquake in 1941 which occurred near the 1977 event. Deformation during the second preseismic period (1967 to 1976) is due to interseismic strain accumulation leading up to the large coseismic (1976 to 1978) fault slip. During the first postseismic period (1978 to 1980) movements result from after-slip (same direction as coseismic slip) on the coseismic fault, and movements for the second period (1980 to 1981) reflect the phase of rapid postseismic recovery, possibly due to viscoelastic relaxation in the asthenosphere. The permanent deformation (uplift \sim 1mm/yr) is determined independently from geological observations; namely 4 - 5 km of relief developed over 4 - 5 MY. This interpretation, while generally consistent with the earthquake deformation cycle shown in Figure 1a, suggest two possible modifications in this cycle. First, at least for this particular event, there is evidence for long term precursory deformation (between 40 years and 10 years before event), although no unusual deformation occurred during the 10 years immediately preceeding the event. Second, continued slip apparently occurred on the earthquake fault for at least one year following the earthquake. It is not known to what extent either of

OBSERVED EARTHQUAKE CYCLE (THATCHER, 1984)

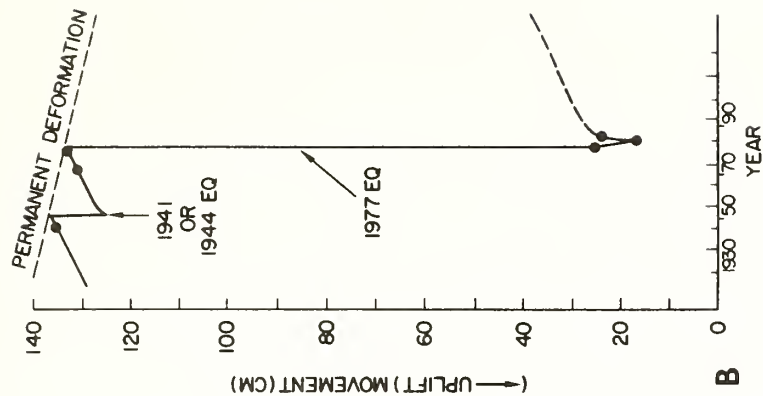
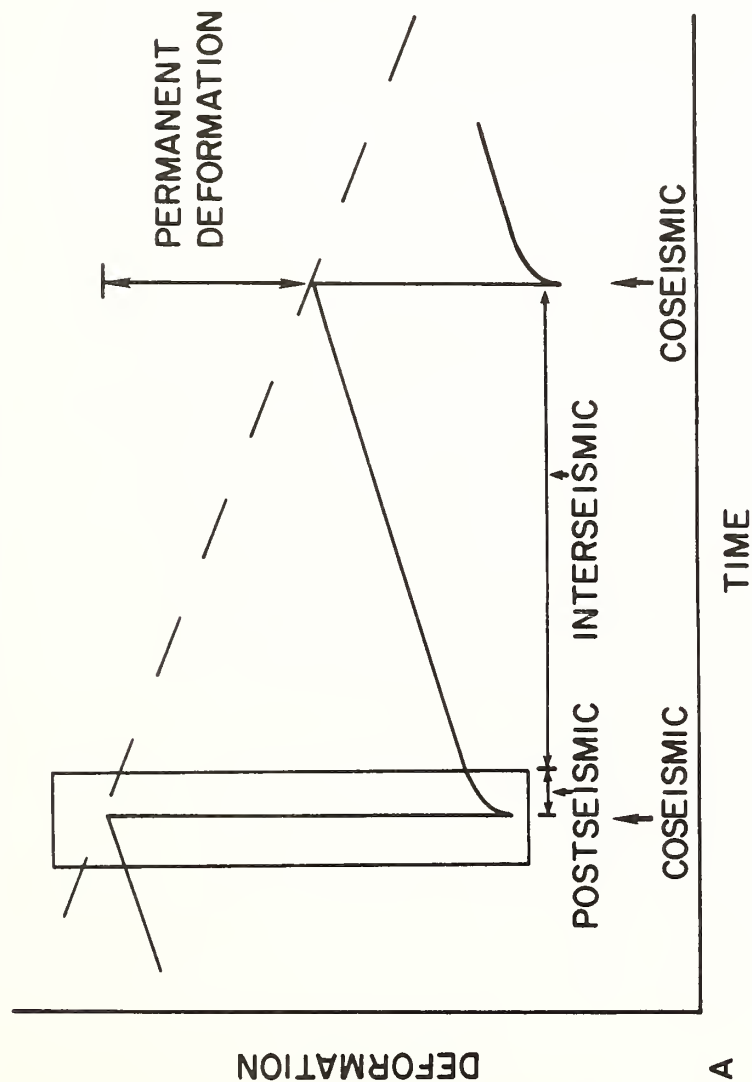


Figure 1: A) Idealized earthquake deformation cycle. Rectangle shows portion of cycle covered by observations in Figure 1B.

B) Relative movement versus time for benchmark near the epicenter of the 1977, Caucete, Argentina earthquake (from Reilinger and Kadinsky-Cade, 1985).

these modifications apply more generally, although significant after-slip has been suggested for a number of other events, for example the 1940 and 1979 Imperial Valley earthquakes (Reilinger, 1984; Sharp et al, 1982).

1940 IMPERIAL VALLEY EARTHQUAKE

The Imperial Valley of Southern California is a complex transition zone between crustal spreading in the Gulf of California to the south and right lateral transform motion along the San Andreas system to the north. Historically the Imperial Valley has been one of the most seismically active areas in the U.S. It is characterized by predominantly right stepping, right lateral en echelon faults presumably linked by zones of crustal spreading. The Imperial and Brawley faults, major elements of the system of faults that transect the Valley, experienced a significant earthquake (located on the Imperial fault) and associated surface faulting in 1940 (M7.1). Figure 2a (upper right) shows a schematic view of the Imperial and Brawley faults and the location of two leveling routes surveyed by first order leveling by the National Geodetic Survey (NGS) in 1931, 1941, and 1972 (more recent surveys have been conducted but are not presented here). Profiles of relative elevation change along these two routes for the coseismic period (1931 to 1941) and the postseismic period (1941 to 1972) are compared with two possible models for fault-related deformation in Figures 2a and 2b respectively (Reilinger, 1984). In both cases the models represent deformation of an elastic half-space due to a finite length, horizontal dislocation (pure strike-slip) on a vertical, rectangular fault (models from Chinnery, 1961). The major features of the coseismic model (Figure 2a) are large, shallow slip on the southern part of the Imperial fault (4.5m), lesser shallow slip on the northern part of the Imperial fault (1.5 m), and no slip on the Brawley fault. A somewhat improved fit is obtained by allowing a small amount of slip (0.5m) at depth along the entire length of the fault (presumably aseismic slip below the seismogenic zone). The primary features of the postseismic model (Figure 2b) are relatively large slip extending from near the surface to great depth (100 km) on the northern Imperial fault and the Brawley fault, no shallow slip on the southern Imperial fault, and lesser deep slip on the southern Imperial fault. Although these models appear somewhat complex, they suggest a rather simple scenario for coseismic and postseismic fault behavior. The earthquake caused large coseismic slip on the southern Imperial fault which transferred stress to the northern section of the Imperial fault and the Brawley fault. These stresses were subsequently released by aseismic slip to shallow depths on these fault segments during the postseismic period. This scenario is qualitatively consistent with observed coseismic offsets at the surface (Trifunac and Brune, 1970), geodetic estimates of horizontal deformation (Thatcher, 1979, Snay et al, 1982), and geophysical observations (fault creep, seismicity, surface faulting) of fault behavior (Reilinger, 1984).

Sauber et al. (1984) have investigated the contribution of viscoelastic relaxation to postseismic deformation for the 1940 Imperial Valley earthquake. They note that the reversal of the sense of movement during the postseismic period relative to the coseismic period along the east-west leveling route (Figures 2a, b) is qualitatively consistent with movements predicted by models of viscoelastic relaxation (e.g. Yang and Toksoz, 1981). Sauber et al. (1984) suggest that, while viscoelastic relaxation may account for some of the post-seismic deformation, additional mechanisms such as fault creep are required to match the observations.

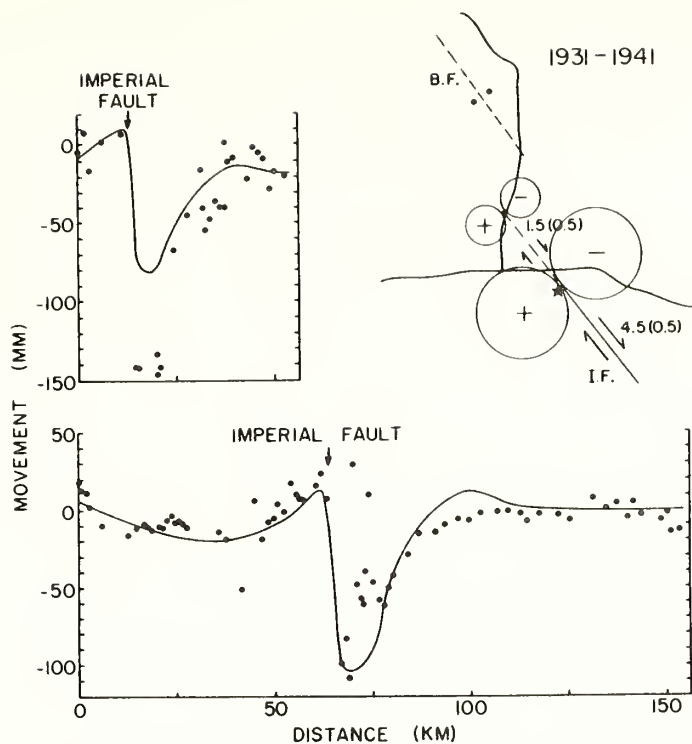


Figure 2A: (top right) Map view showing model of fault offsets for coseismic (1931 to 1941) vertical movements in Imperial Valley. Star indicates 1940 epicenter. Numbers indicate shallow (0 - 13km) slip; numbers in brackets slip at depth (13 - 100km). Comparison between observed (points) and theoretical vertical movements along north-south route (top left) and east-west route (bottom). I.F.- Imperial fault, B.F. - Brawley fault. (Reilinger, 1984).

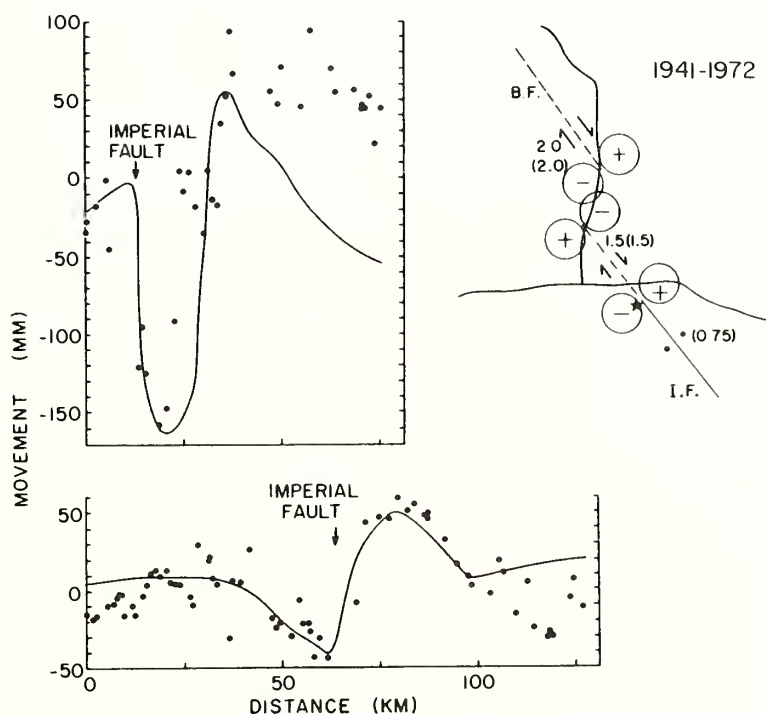


Figure 2B: Model of fault offsets for postseismic (1941 to 1972) vertical movements. Format as in Figure 2A.

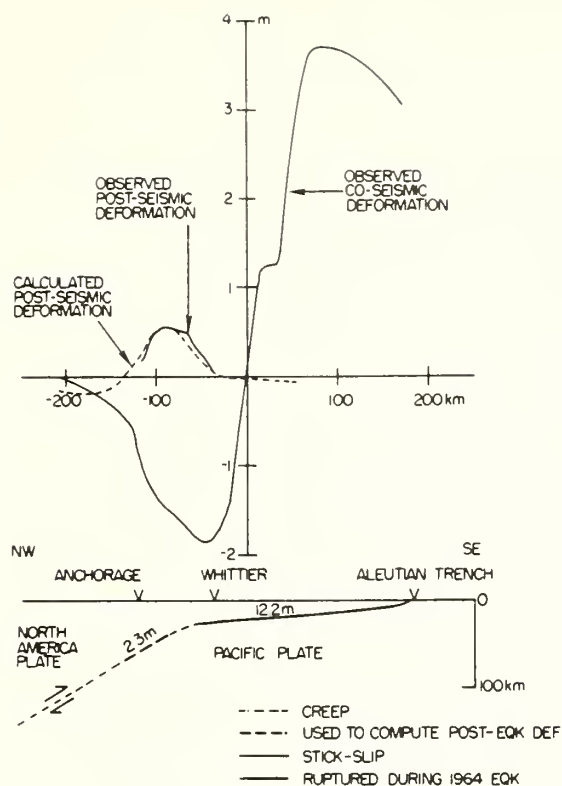


Figure 3A: Buried creep model for the observed postseismic deformation following the 1964, Alaska earthquake (from Brown et al., 1977).

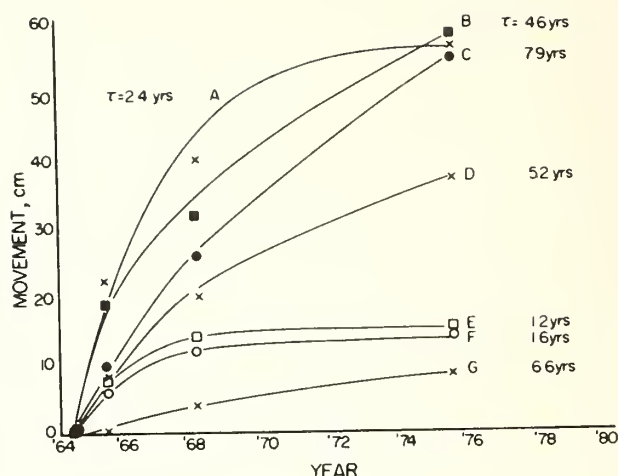


Figure 3B: Time behavior of observed postseismic uplift following 1964, Alaska earthquake. The fitted exponential functions, of form $Y=A(1-e^{-t/\tau})$ where Y is uplift, t is time, and A is a constant, are shown by solid lines (from Brown et al., 1977).

1964 ALASKA EARTHQUAKE

The 1964 (M8.4) Alaska earthquake occurred where the oceanic Pacific plate is being thrust under the North American plate at a rate of about 5 cm/yr. Surface displacements caused by the earthquake were well documented, affecting an area of at least 140,000 km² (e.g. Plafker, 1969). An interpreted profile (perpendicular to trench) of the observed coseismic deformation is shown in Figure 3a (Brown et al, 1977). This deformation was shown to be generally consistent with low-angle thrusting (12 m) on a fault approximately 600–800 km long, 200 km wide and dipping about 10° (Figure 3a). Analysis of the coseismic deformation associated with this event was instrumental in defining the subduction process and solidifying the plate tectonics hypothesis (e.g. Savage and Hastie, 1966, Hastie and Savage, 1970).

Following the 1964 earthquake the NGS conducted multiple leveling surveys (1964, 1965, 1968, 1975) specifically to monitor postseismic deformation along a route located in the zone of major coseismic subsidence. The elevation change profile derived from the 1964 and 1975 surveys is shown in Figure 3a and the time behavior of deformation in Figure 3b (Brown et al, 1977). These leveling data, in conjunction with tide gauge observations indicated exponentially decreasing uplift during the postseismic period in a region which had subsided 2 m during the earthquake. This uplift exceeded 0.5 m during the 10 years following the event.

Brown et al (1977) interpreted the postseismic uplift as resulting from after-slip down-dip of the coseismic fault (Figure 3a, bottom). More recently Wahr and Wyss (1980) suggested that the observed postseismic deformation following the Alaska event resulted from viscoelastic relaxation in the asthenosphere (a possibility also considered by Brown et al, 1977). Both of these mechanisms are generally consistent with the temporal and spatial character of the deformation.

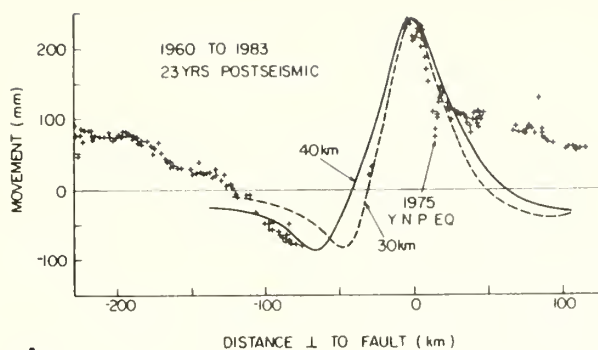
1959 HEBGEN LAKE EARTHQUAKE

The 1959, M7.5 Hebgen Lake earthquake occurred near the intersection of the Intermountain Seismic Belt and the Idaho Seismic Zone in southwestern Montana. The Intermountain Seismic Belt, a major zone of seismicity that extends from southern Utah northward through Montana, is characterized by east-west tensional stress and is generally coincident with a north trending zone of normal faults which have apparently been active since mid-Tertiary (Smith and Sbar, 1974). A sub-belt of the Intermountain Seismic Belt, the Idaho Seismic Zone, crosscuts the Intermountain Seismic Belt, extending approximately east-west from the Yellowstone area through central Idaho. The Idaho Seismic Zone is dominated by north-south tension (Trimble and Smith, 1975).

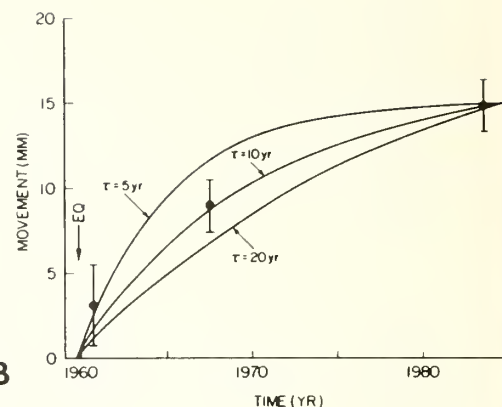
Myers and Hamilton (1964) and Savage and Hastie (1966) reported and interpreted coseismic deformation (geodetic and field observations) for the 1959 event. The observed deformation and seismic observations indicated that the earthquake was a normal fault event on a northwest-southeast striking, south dipping ($\sim 55^\circ$) fault. Coseismic subsidence reached a maximum of about 6.7m just south of the major surface break, requiring about 10 m of slip on the fault. In 1983 the NGS releveled a 440 km long route which tranversed the Hebgen Lake region, approximately normal to the earthquake fault, and which passed within about 25 km of the 1959 epicenter (Reilinger, 1985). This route was previously leveled in 1923 and 1960. Short segments of this route were surveyed in 1967 and 1975. The elevation change profile derived from the 1960 and 1983 surveys is shown along with two models of postseismic deformation in Figure 4a. All of the elevation change observations (including profiles derived from the 1923, 1960, 1967 and 1975 surveys) are consistent with a pattern of deformation consisting of uplift centered on the eastward projection of the coseismic fault and subsidence south of the fault (Reilinger et al, 1977; Reilinger, 1985). Relative movements for the postseismic period 1960 to 1983 reach 30 ± 2 cm and extend over a distance of at least 150 km.

Some indication of the time behavior of this deformation can be obtained by examining elevation changes between two benchmarks located about 40 km south of the earthquake epicenter. This is the only section of the route where sufficient information is available for this purpose (surveyed in 1923, 1960, 1967 and 1983). A plot of the movement between these marks versus time is shown in Figure 4b. The rate of vertical deformation appears to be decreasing exponentially with a characteristic decay time of about ten years.

The USGS has been conducting trilateration measurements to monitor horizontal strain in the Hebgen Lake region since 1973. Their observations indicate uniaxial extension normal to the Hebgen Lake fault at a rate of $0.28 \pm .02$ μ strain/yr (Savage, 1983). This is the largest strain rate observed anywhere in the conterminous U.S. outside of California and is comparable in magnitude to strains observed along the San Andreas fault.



A



B

Figure 4A: Comparison between observed (+) and theoretical vertical movements following the 1959 Hebgen Lake earthquake. 1975 Y.N.P. EQ shows vertical movements due to 1975 Yellowstone earthquake. Models represent postseismic viscoelastic relaxation for faulting of an elastic layer overlying a viscoelastic half-space. Two models for different thicknesses of elastic layer are shown. Models modified from Thatcher et al., 1980.

Figure 4B: Time behavior of deformation following the Hebgen Lake earthquake. Model curves as in Figure 3B.

One interpretation of the observed vertical movements for the period 1960 to 1983 is illustrated in Figure 4a. The models show the expected viscoelastic deformation following normal faulting of an elastic layer overlying a viscoelastic half-space (model modified from Thatcher et al., 1980). The thickness of the elastic layer (~ 30 – 40 km) and viscosity of the asthenosphere ($\sim 10^{20}$ Poise) are roughly consistent with estimates determined from isostatic rebound of Lake Bonneville which was located about 300 km south of the Hebgen Lake region. Postseismic viscoelastic relaxation may also account for the large horizontal strain rate. A particularly important aspect of the observed postseismic deformation in the Hebgen Lake area is that it is virtually impossible to fit with models of after-slip on the coseismic fault and/or down dip of the coseismic fault.

IMPLICATIONS FOR THE NAVD

The observations and interpretations described above have a number of implications for developing and maintaining the NAVD. Elevation changes in the Imperial Valley clearly indicate that spatially coherent vertical movements occur in association with pure strike-slip faulting. In addition, significant (> 20 cm) vertical movements apparently can occur aseismically during the postseismic period following major strike slip earthquakes. It seems likely that similar vertical movements have occurred in association with other strike-slip events but have gone undetected because of a lack of appropriate observations.

Deformations following each of the earthquakes described here clearly indicate that significant postseismic vertical movements occur for both interplate and intraplate events. The observed vertical movements following the Imperial Valley and Alaska earthquakes illustrate the inherent ambiguity in the interpretation of such postseismic deformation. Because of the large dimensions and shallow dips of the coseismic faults associated with subduction related earthquakes, it is very difficult to distinguish between creep mechanisms and viscoelastic relaxation (both have similar wavelengths). This ambiguity has been discussed in detail by Thatcher and Rundle (1984). This same ambiguity exists for strike-slip events such as the 1940 Imperial Valley earthquake (Sauber et al., 1984). On the other hand, the Hebgen Lake event clearly indicates that models of earthquake related deformation must include post-seismic viscoelastic relaxation. This has immediate implications for determining the affect of events such as the 1983, M7.3 Borah Peak, Idaho earthquake and the 1954, M7.1 Dixie Valley earthquake sequence on the NAVD (both of these events occurred in a similar tectonic setting as the Hebgen Lake earthquake).

Thatcher (1984), on the basis of observations in Japan, suggests that post-seismic deformation may be characterized by two timescales. The first, of about a year or less, apparently results from after-slip, and the second (which persists for 10's of years) reflects viscoelastic relaxation. This interpretation appears to be supported by the observations presented here.

While our understanding of the earthquake cycle is clearly incomplete, the observations and interpretations summarized here should help provide a physical basis for incorporating earthquake related deformation in the development and maintenance of the NAVD.

Acknowledgments. I am grateful to Shawn Larsen for a helpful review. The author was supported in part by the SCEE/Air Force Geophysics Scholar Program while engaged in the research reported here.

References

- Brown, L.D., R.E. Reilinger, S.R. Holdahl, and E.I. Balazs, 1977: Postseismic crustal uplift near Anchorage, Alaska, J. Geophys. Res., **82**, 3369-3378.
- Chinnery, M.A., 1961: The deformation of the ground around surface faults, Bull. Seismol. Soc. Am., **51**, 355-372.
- Hastie, L.M., and J.C. Savage, 1970: A dislocation model for the Alaska earthquake, Bull. Seismol. Soc. Amer., **60**, 1389-1392.
- Holdahl, S.R., 1985: Readjustment of leveling networks to account for vertical coseismic motions, Tectonophysics, submitted.
- Kadinsky-Cade, K., R. Reilinger, and B. Isacks, 1985: Surface deformation associated with the November 23, 1977 San Juan, Argentina earthquake sequence, J. Geophys. Res., submitted.
- Myers, W.F., and W. Hamilton, 1964: Deformation accompanying the Hebgen Lake earthquake of August 17, 1959, U.S. Geol. Surv. Pap. **435**, 55-98.
- Plafker, G., 1969: Tectonics of the March 27, 1964, Alaska earthquake, U.S. Geol. Surv. Prof. Pap., **543-I**, 1-74.
- Reilinger, R., 1984: Coseismic and postseismic vertical movements associated with the 1940 M7.1 Imperial Valley, California, earthquake, J. Geophys. Res., **89**, 4531-4537.

- Reilinger, R., 1985: Vertical movements associated with the 1959, M7.1 Hebgen Lake, Montana earthquake, U.S. Geol. Surv. Open-File Rep. 85-290, 519-530.
- Reilinger, R.E., G.P. Citron, and L.D. Brown, 1977: Recent vertical crustal movements from precise leveling data in southwestern Montana, western Yellowstone Park, and the Snake River plain, J. Geophys. Res., 82, 5349-5359.
- Reilinger, R., and K. Kadinsky-Cade, 1985: The earthquake deformation cycle in the Andean back-arc, western Argentina, J. Geophys. Res., submitted.
- Sauber, J., R. Reilinger and M.N. Toksoz, 1984: Postseismic viscoelastic relaxation associated with the 1940 Imperial Valley earthquake, EOS, Trans. Am. Geophys. Union, 65, 190.
- Savage, J.C., 1983: Strain accumulation in the western United States, Ann. Rev. Earth Planet. Sci., 11, 11-43.
- Savage, J.C., and L.M. Hastie, 1966: Surface deformation associated with dip-slip faulting, J. Geophys. Res., 71, 4897-4904.
- Sharp, R.V., et al, 1982: Surface faulting in the central Imperial Valley, U.S. Geol. Survey Prof. Pap., 1254, 119-143.
- Smith, R.B., and M.L. Sbar, 1974: Contemporary tectonics and seismicity of the western United States with emphasis on the Intermountain Seismic Belt, Geol. Soc. Amer. Bull., 85, 1205-1218.
- Snay, R.A., M.W. Cline, and E.L. Timmerman, 1982: Horizontal deformation in the Imperial Valley, California, between 1934 and 1980, J. Geophys. Res., 87, 3959-3968.
- Thatcher, W., 1979: Horizontal crustal deformation from historic geodetic measurements in Southern California, J. Geophys. Res., 84, 2351-2370.
- Thatcher, W., 1984: The earthquake deformation cycle, recurrence, and the time predictable model, J. Geophys. Res., 89, 5674-5680.
- Thatcher, W., T. Matsuda, T. Kato, and J. Rundle, 1980: Lithospheric loading by the 1896 Riku-u earthquake, northern Japan: Implications for plate flexure and asthenospheric rheology, J. Geophys. Res., 85, 6429-6435.
- Thatcher, W., and J.B. Rundle, 1984: A viscoelastic coupling model for the cyclic deformation due to periodically repeated earthquakes at subduction zones, J. Geophys. Res., 89, 7631-7640.
- Trifunac, M.D., and J.N. Brune, 1970: Complexity of energy release during the Imperial Valley, California, earthquake of 1940, Bull. Seismol. Soc. Amer., 60, 137-160.
- Trimble, A.B. and R.B. Smith, 1975: Seismicity and contemporary tectonics of the Hebgen Lake - Yellowstone Park region, J. Geophys. Res., 80, 773-741.
- Volponi, F., A. Robles, and J. Sisterna, 1983: Gravity variations in the epicentral zone of the Cauçete earthquake, November 23rd, 1977, Universitat Nacional de San Juan, Instituto Sismologico Zonda, 12 pp.
- Wahr, J., and M. Wyss, 1980: Interpretation of postseismic deformation with a viscoelastic relaxation model, J. Geophys. Res., 85, 6471-6477.
- Yang, M., and M.N. Toksoz, 1981: Time-dependent deformation and stress relaxation after strike-slip earthquakes, J. Geophys. Res., 86, 2889-2901.

MINIMIZING SYSTEMATIC ERRORS IN LEVELING

John H. Richards
Vertical Network Branch
National Geodetic Survey
Charting and Geodetic Services
National Ocean Service, NOAA
Rockville, Maryland 20852

ABSTRACT. When using leveling data to connect vertical control points, careful attention must be paid to the presence of systematic errors. This paper examines the systematic errors controlled by leveling procedures detailed in the 1984 Federal Geodetic Control Committee publication, Standards and Specifications for Geodetic Control Networks

INTRODUCTION

Analysis of high precision differential leveling is one of the fundamental tasks in the new adjustment of the North American Vertical Datum of 1988. The use of differential leveling in determining crustal motion, the validity of sea surface topography, and the estimation of geoid height differences with GPS is invaluable. But that use depends on understanding the systematic errors that plague differential leveling. Table 1a lists systematic error sources. The most practical approach to reducing systematic errors is to follow field observing procedures that minimize such errors. When observing procedures will not remove a particular systematic error, appropriate measurements of the error source must be taken so that a correction can be applied to the observation. Table 1b summarizes observation practices and corrections that can be applied to minimize known systematic errors. Table 1a is cross-referenced to table 1b for each procedure and/or correction that applies to a specific systematic error.

Some of the error sources could introduce more than 1 mm per km of error if proper procedures are not followed. Considering the large extent of some leveling projects, it is clear that using poor procedures in only one leveling project could be detrimental to any study of possible datum points. For that reason every possible effort is made to see that Federal Geodetic Control Committee (FGCC 1984) specifications are rigorously followed and the results meet the proper requirements for order/class before leveling data are accepted into the National Geodetic Vertical Network.

Table 1a.--Sources Of Systematic Error In Differential Leveling. (See Table 1b For Explanation Of Letters Used In Columns 2 And 3.)

<u>Systematic Errors</u>	<u>Observing Procedures</u>	<u>Corrections</u>
Rod verticality error	ABER	
scale error		AE
Thermal expansion of Invar strip		C
Rod Index error	AB	B
Movement of tripod during setup	GIJK	
Gradual movement of turning points (pins/plates) during setups	DGIJK	
Gradual movement of turning points between setups	DGI	
Collimation change with refocusing	HO	
Collimation fluctuations with temperature	MN	
Collimation	HMS	E
Oblique Horizon Error	LM	
Under- or overcompensation	LMS	
Refraction	CFH	D
Refraction change during setup	IJ	
Gravity anomalies		G
Diurnal Earth tides		F
Earth's magnetic field	P	H
NI 002 instrument parallax	Q	

Table 1b.--Observational Procedures and Corrections For Minimizing Known Systematic Errors. (The Identifying Letter Preceding Each Entry Is Also Used In Table 1a.)

Observation Procedures

- A: Leap frog rods between setups
- B: Use even number of setups
- C: Use minimum sight ground clearance, 0.5 m
- D: Use turning pins when they can be driven
- E: Use rod braces
- F: Limit sight length
- G: Reverse direction of running every other day
- H: Maintain closely balanced sight lengths
- I: Double run in opposite direction under different conditions
- J: Follow specified rod observing sequence
- K: Limit allowable reading check for setup
- L: Off level-relevel the instrument between scales
- M: Use leveling instruments with reversible compensator
- N: Use leveling instruments with fixed reticle
- O: Use leveling instruments that focus by displacement of mirrors
- P: Use instruments not influenced by the Earth's magnetic field
- Q: Refocus before every observation
- R: Check/adjust rod level bubbles weekly
- S: Check collimation and compensation

Corrections

- A: Apply rod correction from calibration against National Standard: based on several rod graduations
- B: Apply rod correction from calibration against National Standard: based on all rod graduations (detailed calibration)
- C: Apply rod correction for thermal expansion
- D: Use refraction (modeled or observed temperatures) correction
- E: Apply collimation correction
- F: Correct elevation difference for Earth tides
- G: Compute in geopotential height system
- H: Calibrate instruments for magnetic effect and apply correction

SYSTEMATIC ERRORS

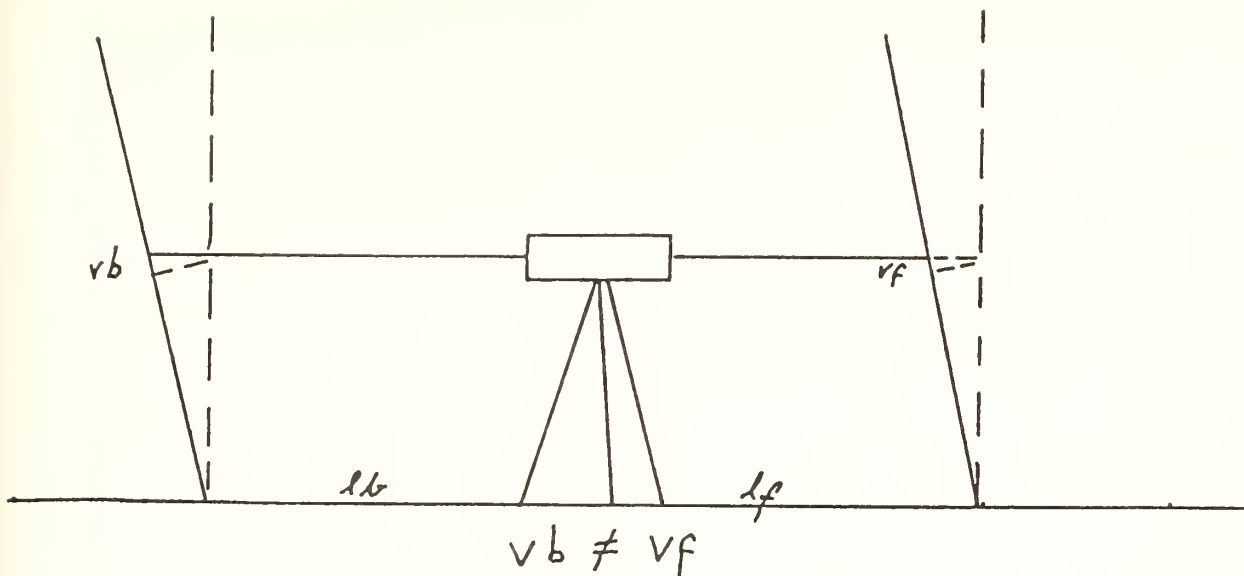
Rod verticality error occurs when a rod is not normal to the local equipotential surface. Due to errors in the level bubble on the rod and human error in leveling the rod, it may not be (and in fact seldom is) exactly vertical. Therefore, the observed scale reading is higher than it should be. (See fig. 1.) The first procedure is to check the rod bubble weekly or more often if misalignment is suspected. Although leap frogging the rods so that a rod used as the backsight in one setup is used as the foresight in the next setup nearly cancels the rod verticality error on level ground, leap frogging cannot remove the error between the two rods on sloping ground. The only way to avoid this problem is to use properly leveled rods. Braced rods minimize additional error due to rod movement while observing.

Rod scale error and thermal expansion of the Invar strip result from errors in the scribing of the graduations during manufacture, and the thermal expansion qualities of the Invar strip the graduations are scribed on, respectively. It is estimated that for a rod pair with length excess of 0.1 mm/m, a 2.0 mm error is introduced in a difference of elevation of 20 m. In addition, a difference in temperature of 10 degrees Celsius from the rod standardization temperature, with a coefficient of thermal expansion of 8×10^{-7} for the same difference in elevation, introduces an error of 0.16 mm (Balazs and Young 1982). The coefficient of thermal expansion for NGS rods varies between 8.6×10^{-7} and 36.2×10^{-7} , so careful determination of this variable is important. For instance, if the largest coefficient (36×10^{-7}) is used in the same section as given above, the error increases to 0.72 mm.

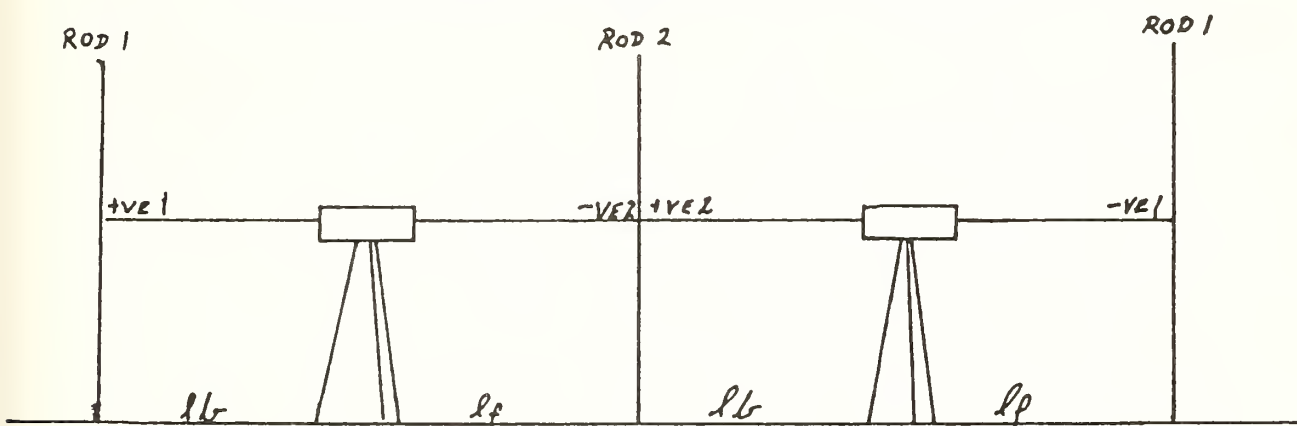
Prior to 1979 rods were calibrated by the National Bureau of Standards using an overlapping method whereby intervals from the base to the 0.2 m, 1.2 m, 2.2 m, and 3.2 m graduations were carefully compared against the National Standard of Length. For some rods this was repeated under different temperature conditions and a length excess, index error, and coefficient of thermal expansion were determined. This was used to correct observations for rod scale error and the effects of temperature change during the day. Since 1979 every graduation is calibrated with a laser interferometer and observed heights can be changed directly to calibrated values. Of course the coefficient of thermal expansion is still determined and a temperature correction applied.

For the older calibration procedure, although the rod index error is known, a correction is not required as long as the number of setups is even. Rod index error is nearly eliminated by leapfrogging. If the setups are not even, a correction is applied to the last setup. However if every graduation is calibrated, the rod index error is eliminated by conversion to a calibrated value and the number of setups does not have to be even. The rod verticality error in the last setup of an uneven number of setups will be so small as to not be worth the time needed for an extra setup (Balazs and Young 1982).

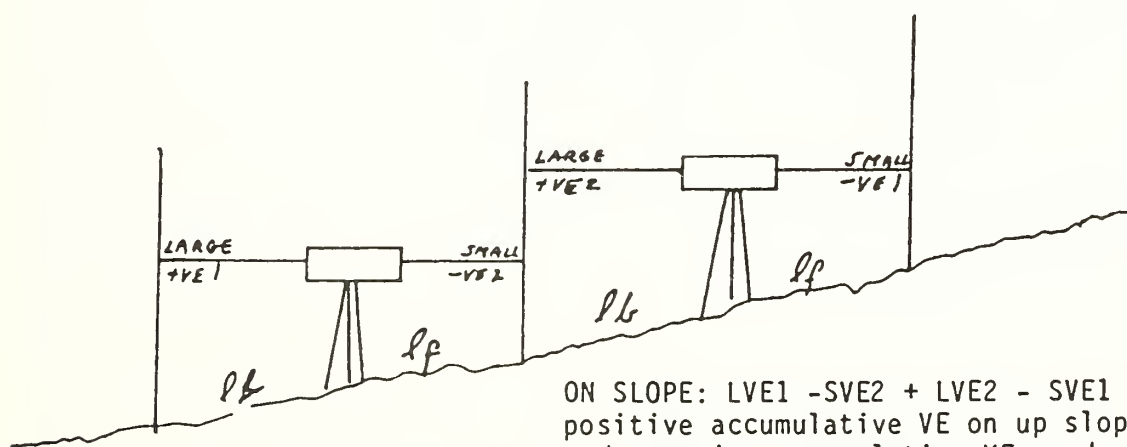
The vertical movement of a tripod during a setup can be 0.2 mm, for a



ERROR IS DEPENDENT ON HEIGHT OF ROD READING AND
DEGREE OF ERROR IN PLUMBING

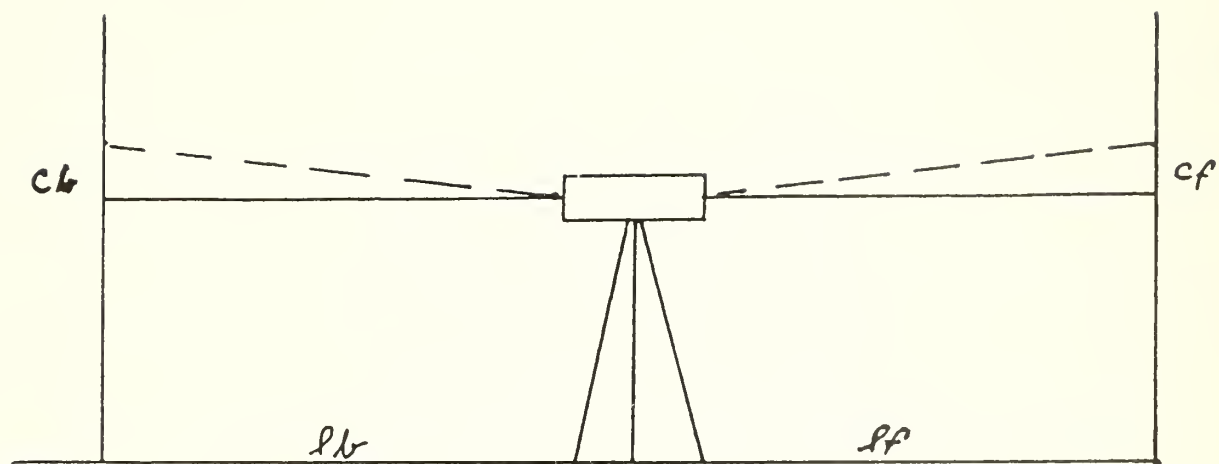


ON LEVEL TERRAIN: $VE1 - VE2 + VE2 - VE1 \approx 0$

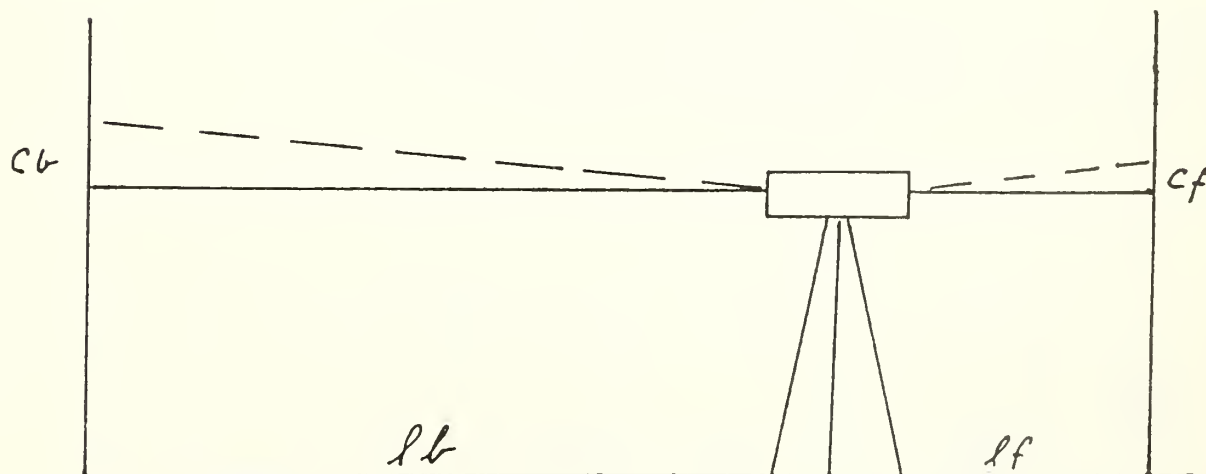


ON SLOPE: $LVE1 - SVE2 + LVE2 - SVE1 =$
positive accumulative VE on up slope
and negative accumulative VE on down slope

Figure 1.--Rod verticality error.



WHEN $l_b \approx l_f$ THEN $c_b \approx c_f$



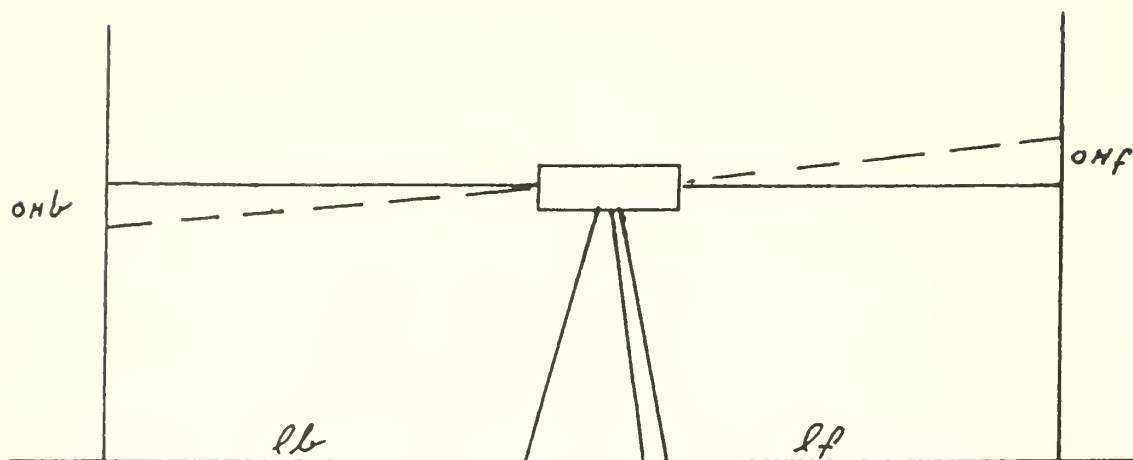
THE RESULT OF UNEQUAL SIGHT LENGTHS i.e. $l_b \neq l_f$

Figure 2.--Collimation error.

turning pin 0.2 mm, and for a turning plate 0.6 mm (Entin 1959). This accumulation of movement can be reduced only by following certain observation procedures. The use of turning plates should be limited to areas where a turning pin cannot be driven into the ground. By reversing the direction of leveling every other day, the effect of systematic movement is not accumulative in the line of leveling although some small effect does show up in individual elevations. When double running a section, the second running should be in the reverse direction and under different atmospheric conditions, such as forward running in the morning and backward running in the afternoon. Thus if a particular atmospheric condition causes movement, it will be apparent in the section closure and, if excessive, the section will be run again. Finally if the reading sequence of a double-scale set of rods is: (1) Backsight Low Scale (BLS), (2) Foresight Low Scale (FLS), (3) Foresight High Scale (FHS), (4) Backsight High Scale (BHS), any movement in the tripod or rods during the setup should be detected by the difference $((BLS - FLS) - (BHS - FHS))$. If the result is too large (0.40 mm for reversible compensator first-order, class I, or 0.25 mm for other instrument types and half-centimeter rods) the observations are reobserved. Index error would be too small for one setup to influence this error determination.

Collimation error is caused by the deviation of the line of sight from the horizontal position. (See fig. 2.) The collimation error of some instruments changes slightly when the instrument is refocused. Instruments that use displacement of mirrors to focus do not have this problem. For other instruments if the foresight and backsight are kept to equal length, the instrument need not be refocused when changing direction. Collimation changes due to temperature can be reduced by instruments that have the reticle engraved on the objective lens. When temperature changes occur, the reticle and objective lens change similarly, rather than separately as in other systems. However some influence on the compensator may occur (Karren 1964). If the instrument also has a reversible compensator, the effect of collimation error due to temperature is nearly removed. In fact, collimation error itself is usually very small for such an instrument. To reduce the error caused by collimation in other types of instruments, closely balanced sight lengths must be observed. Then collimation error in the backward direction will balance the collimation error in the forward direction because the error is proportional to the distance. (See fig. 2.) For small discrepancies in the balance of sight lengths, a correction can be applied using the known collimation error. This should be determined each day for most nonreversible compensator instruments and immediately if the instrument is severely jarred. In addition, the compensator on Nil instruments should be checked every 2 weeks or after any severe shock.

While collimation is in the same direction, up or down from horizontal, in the forward or backward sighting, the oblique horizon error is opposite and doubles the error. This depends on three factors: (1) the inclination of the telescope axis to the horizontal plane, (2) the position of the compensator in the telescope, and (3) the focal distance of the combined optics (Lucas 1982, Jones 1964). (See fig. 3.) If the following observing procedure using double-scale Invar rods is



IF $l_b \approx l_f$ THEN $|ohb| \approx |ohf|$ BUT
 (BACKSIGHT - ohb) - (FORESIGHT + ohf) =
 BACKSIGHT - FORESIGHT - $2oh$

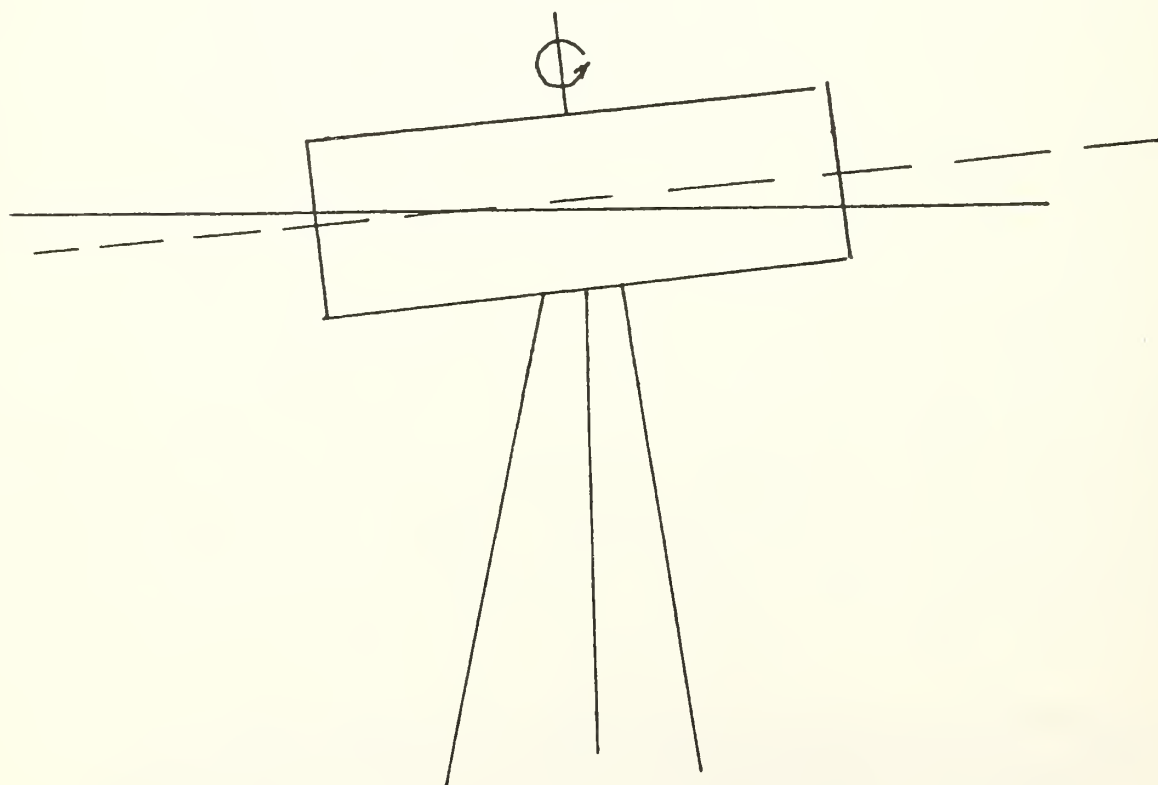


Figure 3.--Oblique horizon error.

followed, the oblique horizon error is reduced. The procedure of off-leveling and releveled the instrument, in effect, causes the error to be placed in each set of scale readings. First the low scale of the first rod is read. The instrument is turned and the low scale on the second rod is read. The instrument is off-leveled and releveled, reintroducing the oblique horizon error in the reverse direction. Now the high scale of the second rod is read and then the high scale of the first rod is read. The difference between the high and low scale readings for each rod now contains the same error and the means contain almost no error; i.e.,

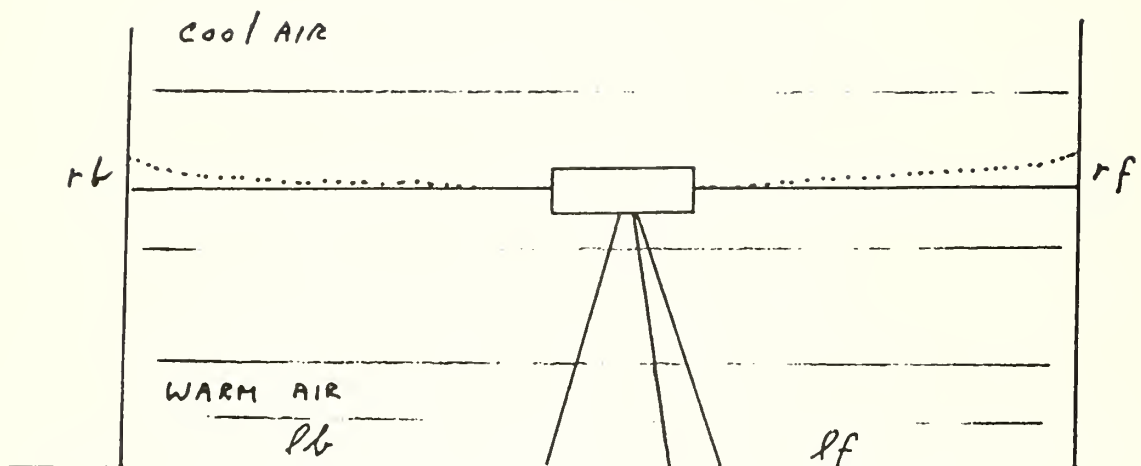
$$\begin{aligned} dH &= (BLS + \text{error} - (FLS - \text{error}) + BHS - \text{error} - (FHS + \text{error})) / 2 \\ &= (BLS - FLS + 2 * \text{error} + BHS - FHS - 2 * \text{error}) / 2 \\ &= (BLS - FLS + BHS - FHS) / 2 \end{aligned}$$

Insufficient data exist on the true magnitude of the oblique horizon error, but it is believed to be very small.

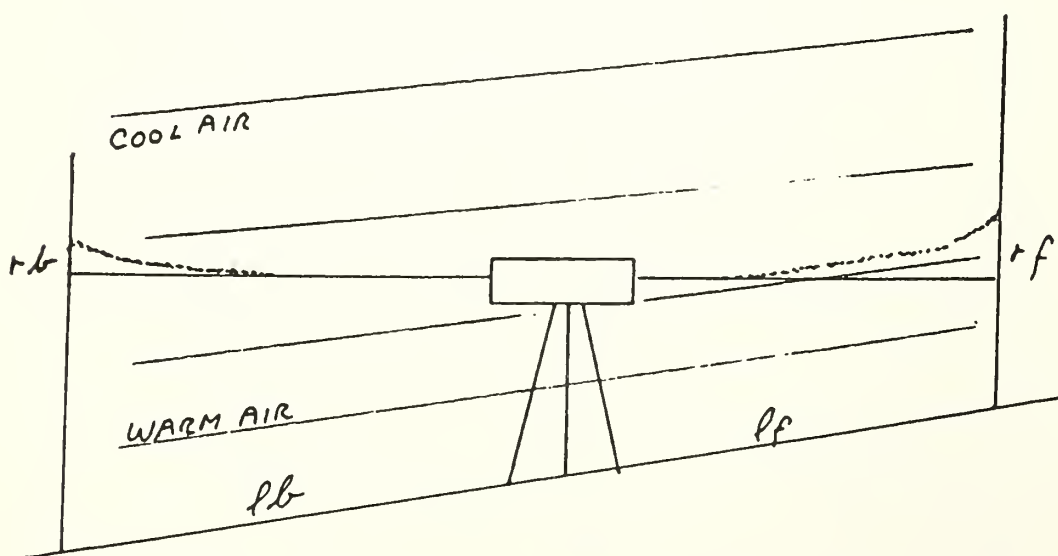
Under- or overcompensation is a product of friction in the compensator suspension or dampening system. It causes the compensator to fail to come to the exact position determined by gravity. This causes a tilting of the line of sight from true horizontal (Lucas 1982). If the compensator is not in the vertical axis when it is rotated, centrifugal force causes the compensator to swing out, and if the rotation is always in the same direction the compensator will always return to the same position from the same side. Therefore, if after leveling the instrument, the instrument is always rotated around its axis in the same direction, the error in the line of sight becomes the same in the foresight and backsight and, as with collimation, is nearly eliminated by keeping equal lengths of sight (Drodofsky 1957, Jones 1964). Instruments with reversible compensators minimize this error source automatically when the compensator is reversed between scale readings. If off-leveling, releveled is followed, the compensator should be reset and no turning of the scope is necessary (Jones 1964).

Refraction is an error introduced into leveling observations by temperature changes along the line of sight. Radiated heat causes the temperature gradient (the change in temperature with height) to vary greatest near the ground. By observing no lower than 0.5 m above the ground, temperature gradient is kept at a more stable level and extreme refraction error is avoided. Kukkamaki (1950) showed that refraction is proportional to the difference in elevation, temperature gradient, and the square of the sight length. Figure 4 shows how the effect of refraction is the same on a horizontal surface (assuming equal temperature gradients) in either sighting if the lengths of sight are kept equal. It also shows that shorter sight lengths reduce refraction error significantly.

This is one of the prime reasons why specifications for sight lengths are so stringent. Sight lengths for first-order, class I leveling are limited to 50 m (FGCC 1984). Temperatures at different heights should be recorded at the instrument to calculate the temperature gradient along the line of sight. Measurements made at approximately 0.3 m and 1.3 m above the ground are adequate to compute a correction where one



LEVEL TERRAIN: IF $lb \cong lf$ THEN $rb \cong rf$



ON A GRADE: IF $lb \cong lf$ THEN $rb \cong rf$ - correction

Figure 4.--Refraction error.

sighting in a setup is closer to the ground than the other (Holdahl 1982). For motorized leveling the temperatures are taken at higher elevations above the ground because of the height of the instrument.

Refraction change during setup is much like rod or instrument movement. Therefore the procedure of double-running in opposite directions under different conditions and reading the rods in the sequence (1)BLS, (2)FLS, (3)FHS, (4)BHS will either uncover excess change or remove some of its effect.

Systematic errors in heights caused by gravity anomalies can be corrected by gravity models. The model is based on a high density of gravity observations along leveling lines. Balazs and Young (1982) show that a change of 10 m in differences in elevation and 10 milligals change of gravity will cause a 0.1 mm error per km in leveling observations. In the new adjustment of the North American Vertical Datum (NAVD 88), the observed height differences will be converted to geopotential height differences. These will be used in the actual adjustment and then converted back to orthometric height differences.

Error caused by diurnal Earth tides are very small; however, they can be as much as 0.1 mm/km (Balazs and Young 1982). The error affects leveling lines running more in a north-south azimuth when aligned with the Sun and Moon. A correction is computed based on the position of the Sun and Moon and the azimuth of the observations.

Error due to the Earth's magnetic field can be overcome by the easiest of procedures. Do not use an instrument that has a magnetically sensitive compensator. However, where instruments with affected compensators have already been used, a procedure for calibrating the effect of the Earth's magnetic field on magnetic compensators has been developed (Whalen 1984). Currently corrections to the Zeiss NI1 and the Jenoptic NI 002 instruments are being carefully evaluated by NGS to see if these corrections significantly improve affected leveling lines. In the meantime all compensators, after calibration, have been replaced by non-magnetic compensators.

Study has shown that when the NI 002 is rotated, in addition to reversing the compensator, a small change occurs in the focus (Lehmuskoski 1982). This introduces a small systematic parallax that an observer might not detect. Because of the optical properties of the NI 002, refocusing does not affect the line of sight, and Jenoptic recommends refocusing the instrument after rotating and reversing the compensator.

Although this paper is primarily about systematic errors, it should be pointed out that random errors can also be controlled to some extent by proper observation techniques. Multiple micrometer readings will tend to average out short-period scintillation, an optical problem of light traveling through different densities of air. This causes the observed line of sight to fluctuate above and below the true line of sight. This scintillation should be as often negative as positive, and by meaning several micrometer readings, hopefully a more accurate reading is obtained.

Another random error, long period scintillation, occurs when the air temperature above the line of sight is greater than the temperature below. This is known as a positive temperature gradient. For best results, observations should not be made when this condition exists, since the line of sight is constantly, although slowly, moving in one direction with some small undulation.

CONCLUSION

By careful evaluation of known systematic errors and constant research into all possible variations in leveling results, differential leveling is reduced to the best possible source of height difference determination in the field of geodesy. With this knowledge, the current national vertical network and future levelings can be used for evaluation and determination of vertical datum points in the North American continent. It may be that one day differential leveling as a geodetic tool will be obsolete, but that will only come when a datum exists that can be fully accepted as representing the best possible fit to the geopotential surface. That cannot occur now without the use of differential leveling.

REFERENCES

- Balazs, E. I. and Young, G. M., 1982 : Corrections Applied By The National Geodetic Survey To Precise Leveling Observations: NOAA Technical Memorandum NOS NGS 34, National Geodetic Information Center, NOAA, Rockville, MD., 12 p.
- Drodofsky, M. 1957: Zeitschrift fur Vermessungswesen, pp. 430-434.
- Entin, I. I., 1959: Main Systematic Errors in Precise Levelling: Bulletin Geodesique, No. 52, pp. 37-45.
- Federal Geodetic Control Committee, 1984: Standards and Specifications for Geodetic Control Networks, National Geodetic Information Center, NOAA, Rockville, MD, 29 pp.
- Holdahl, S. R., 1982: The Correction for Leveling Refraction and its Impact on Definition of the North American Vertical Datum, presented to the 42nd Annual Convention of the ACSM-ASP, Denver, Colorado, March 14-20, 1982, 26 pp.
- Huther, G., 1973: The New Automatic Geodetic Level Ni002: Jena Review Special Issue Spring Fair Leipzig, pp. 56-80.
- Jones, P. B., 1964: An Investigation of Instrumental Sources of Error in Leveling of High Precision by Means of Automatic Levels: Survey Review, No. 132, pp. 276-286, No. 133, pp. 313-322, No. 134, pp. 346-354.
- Karren, R. J., 1964: Recent Studies of Leveling Instrumentation and

Procedures: Surveying and Mapping, XXIV, (3), pp. 383-397

Kukkamaki, T. J., 1950: Report on the Causes of Error Affecting Levelling: Bulletin Geodesique, No. 18, pp. 427-431.

Lehmuskoski, P., 1982: Systematic Error Resulting from Asymmetric Handling of a Zeiss NI002 automatic Levelling Instrument: Reports of The Finnish Geodetic Institute, 82:3, ISBN 951-711-080-4, ISSN 0355-1962, 16 p.

Lucas, J. R. 1982, Personal communication and unpublished notes on instrumental errors in automatic levels (Chief, Geometric Geodesy Section, Geodetic Research and Development Laboratory, National Geodetic Survey, NOAA).

Poetzschke, H., 1983: Variation of the Position of the Line of Sight in the NI 002 Leveling Instrument Due to Temperature Changes: NOAA Technical Memorandum NOS NGS 38, National Geodetic Information Center, NOAA, Rockville, MD.

Schomaker, C. M. and Berry, R. M., 1981: Geodetic Leveling: NOAA Manual NOS NGS 3, National Geodetic Information Center, NOAA, Rockville, MD, 209 p.

Whalen, C. T., 1984: Preliminary Test Results: Automatic Levels Affected by Magnetic Fields: ACSM Bulletin, No. 89, pp. 17,31.

Zilkoski, D. B., 1983: Justification of FGCC Vertical Control Specifications and Procedures: Technical Papers of The 43rd Annual Meeting ACSM, pp.128-143.

Mention of a commercial company or product does not constitute an endorsement by the National Oceanic and Atmospheric Administration. Use for publicity or advertising purposes of information from this publication concerning proprietary products or the tests of such products is not authorized.

REFRACTION BY REFLECTION : TEST RESULTS

P.V. Angus-Leppan *
School of Surveying
University of New South Wales
Kensington, Sydney
New South Wales, 2033
Australia

ABSTRACT. Refraction by reflection, a direct method of measuring refraction in levelling, has been described by Angus-Leppan (1983). The theory predicts that the refraction measured after reflection in a vertical mirror at the remote end of a line, is four times the single-path refraction along the line. The paper describes tests, carried out under varied conditions, which provide the first practical confirmation of the theory. Refraction was measured on a 50 m line by reflection and compared with refraction derived from a levelling technique. In one test, refraction was derived by four methods: from reflection, from levelling, from measured temperatures and from a meteorological estimation method. The reflection method gives a precision of ± 0.04 mm over this distance. Measurement of refraction by reflection has possible applications in high precision levelling and monitoring of structures. A variation using sloped sightlines has potential in the development of a new levelling system.

INTRODUCTION

Refraction is a significant error source in levelling, which can be minimized by keeping backsight and foresight lengths equal, and by shortening the length of sights. The magnitude of the refraction effect can be calculated from measured temperature gradients, but it is difficult to measure refraction directly. Refraction by reflection is a method of measuring directly the magnitude of refraction along a line.

The principle is shown in figure 1. Light travelling horizontally from an object A is bent by refraction on its way to B, where there is a vertical mirror. It is incident on the mirror at an angle α , so that it is reflected upwards, also at an angle α . After traversing the line AB, the ray has moved upwards by R , and after returning, it is $4R$ above its starting point A. This is not unexpected, as the ray has traversed twice the length of the line, and refraction propagates as the square of the distance.

* From March 1985 seconded to: World Bank/ADAB Land Titling Project
Department of Lands, Phra Phiphit Road, Bangkok 10200, Thailand.

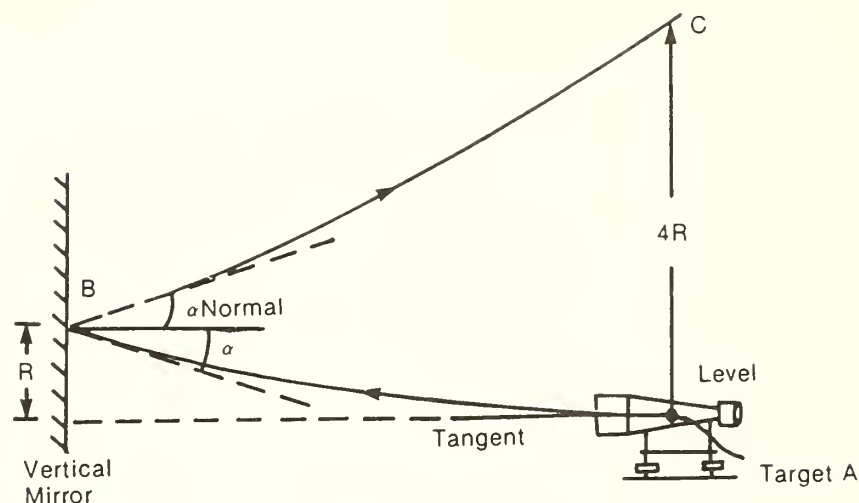


FIGURE 1. Principle of Refraction by reflection.

The concept of refraction by reflection was first introduced in 1983, and the feasibility of applying it in levelling, as well as some theoretical implications, have been investigated (Angus-Leppan 1983; 1985). The present paper describes the practical tests which have been carried out to test the principle that the refraction after reflection is four times the single-path refraction. The tests also provided some comparisons with refraction as deduced by other methods.

Refraction can be calculated from measured temperature gradients, and some geodetic levelling is corrected for refraction in this way. The additional temperature measurements are somewhat inconvenient in the field, and it is not possible to apply this method in the case of older levelling, where the necessary temperatures were not measured. A method of estimating the temperature gradients, based on micro-meteorological formulations, was developed to cover this case of historical levelling, (Holdahl 1978) and this method is being applied to the U.S. results in the NAVD adjustment.

It is theoretically possible also to measure refraction in levelling by dispersion, using light of two or more wavelengths, but the measurements would have to be extremely sensitive, as the angle measured in this method is a small fraction of the angle of refraction. It is doubtful whether the measurement could be carried out under field conditions. A further method, based on studies of light propagation in a turbulent medium, has been

proposed by Brunner (1978). The variance of the angle of arrival of the rays is used as a measure of the refraction. The theory of the method has been developed and confirmed with existing data, but instrumentation for the very precise measurement of the variation of the angle of arrival has still to be built. The reflection method has advantages over the others because it is a direct measure of the vertical refraction, and the quantity measured is four times the refraction.

TESTS

According to theory, the refraction after reflection should be four times the magnitude of the single-ray refraction. The tests were necessary to confirm whether this relationship holds in practice. The tests in the present report were carried out at the National Geodetic Survey's instrument and equipment laboratories at Corbin, Virginia.

The site was a 50-metre base between two firm bench marks, nearly level, over cropped grass. The principle of the tests was to measure refraction by a conventional method and by reflection. Level rods were placed on the bench marks, N and S, whose height difference was known accurately, and the refraction measured by placing a level at minimum focussing distance from one of the rods, N. A reading on rod N gave the height of the instrument, and the reading on the remote staff yielded the refraction, since the actual height was known.

Collimation error in the level would cause difficulties, so the level used was a Zeiss Jena N1002, which has the characteristic that the collimation effect is eliminated in the mean of readings with the compensator mirror in direct and reversed positions. This instrument has a compensator in the form of a near-vertical mirror: the small tilt is eliminated by the reversal of the mirror. To measure refraction by reflection, a vertical mirror is needed. The compensator of another N1002 was used near rod S. This was placed in the normal instrument casing, to avoid vibration from wind, but all other optical parts were removed. A target was necessary on the level near N, and this was in the form of a horizontal calibration line about one millimetre thick, on plates which were supported on either side of the level's telescope, and opposite the vertical axis so that its height would not be affected when the instrument was levelled. The height of the target was calibrated in the laboratory, over a short sightline on which refraction was negligible. This determined the micrometer reading for which refraction was zero.

The procedure was first to place the rods on their bench marks, guying them securely. They were not touched again during the test, as their height was required to remain constant to better than 0.1 mm. Next the targets were calibrated in the laboratory, and the height difference between the bench marks determined very carefully, first with four sightlines of 12.5 m, then with two of 25 m each. The level was then set up close to N, and the mirror set close to S. In order to make the reflection of the target

13 JAN 84
CORBIN VA.
DISTANCE 48m

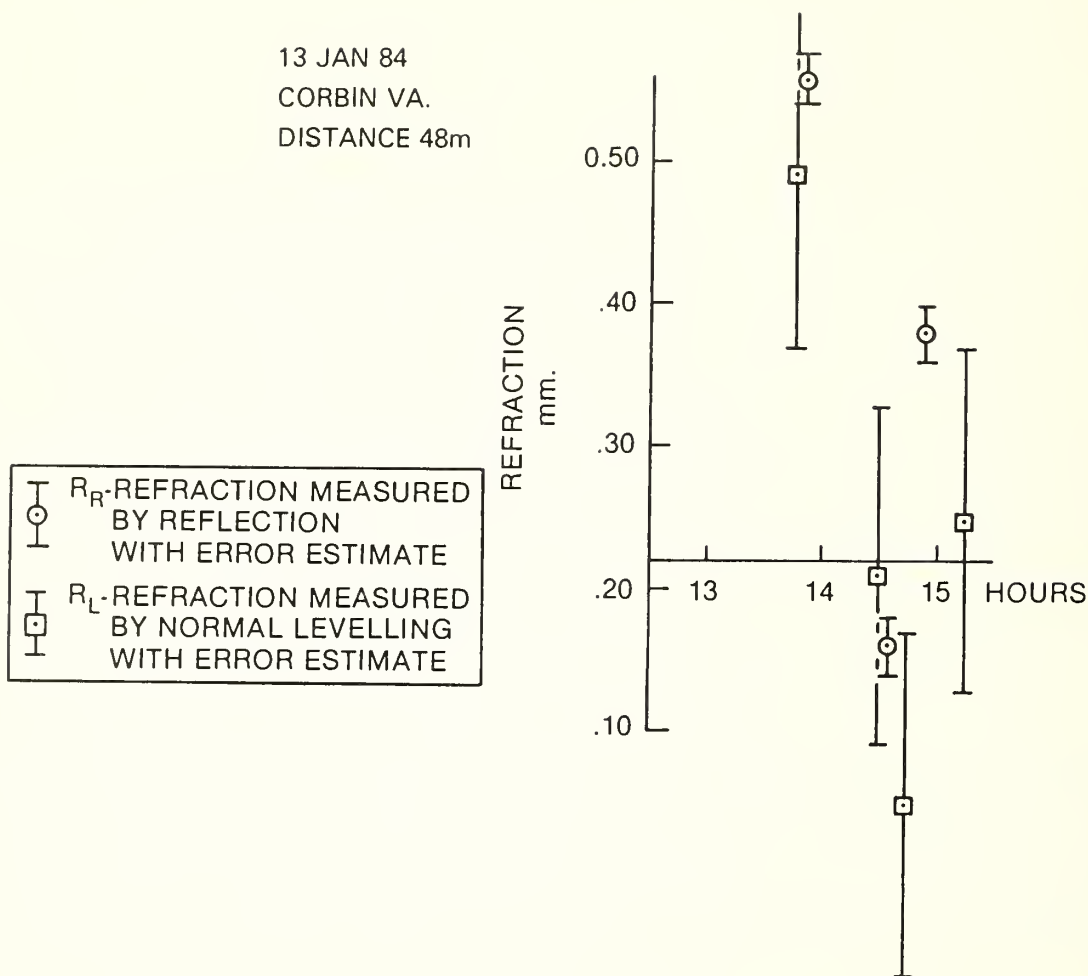


Figure 2. Refraction by reflection and by levelling - 13 Jan 1984.

visible, back at the level, the height and azimuth of the mirror had to be carefully adjusted.

Every hour, readings were taken of refraction from rod readings to N and S, and by reflection, from readings of the apparent height of the target. To avoid effects of any small lateral tilt of the level, readings were taken of the portions of the target on both sides of the telescope. Also, to eliminate errors, the level readings had to be taken with the level compensator in direct and reversed positions, while the mirror had also to be reversed.

Tests were carried out on three days: preliminary observations to test the feasibility on 13 January 1984 (figure 2), a full set of observations on 17 January 1984 (figure 3), and a full set with supplementary observations on 28 June 1984 (figures 4,5 and 6).

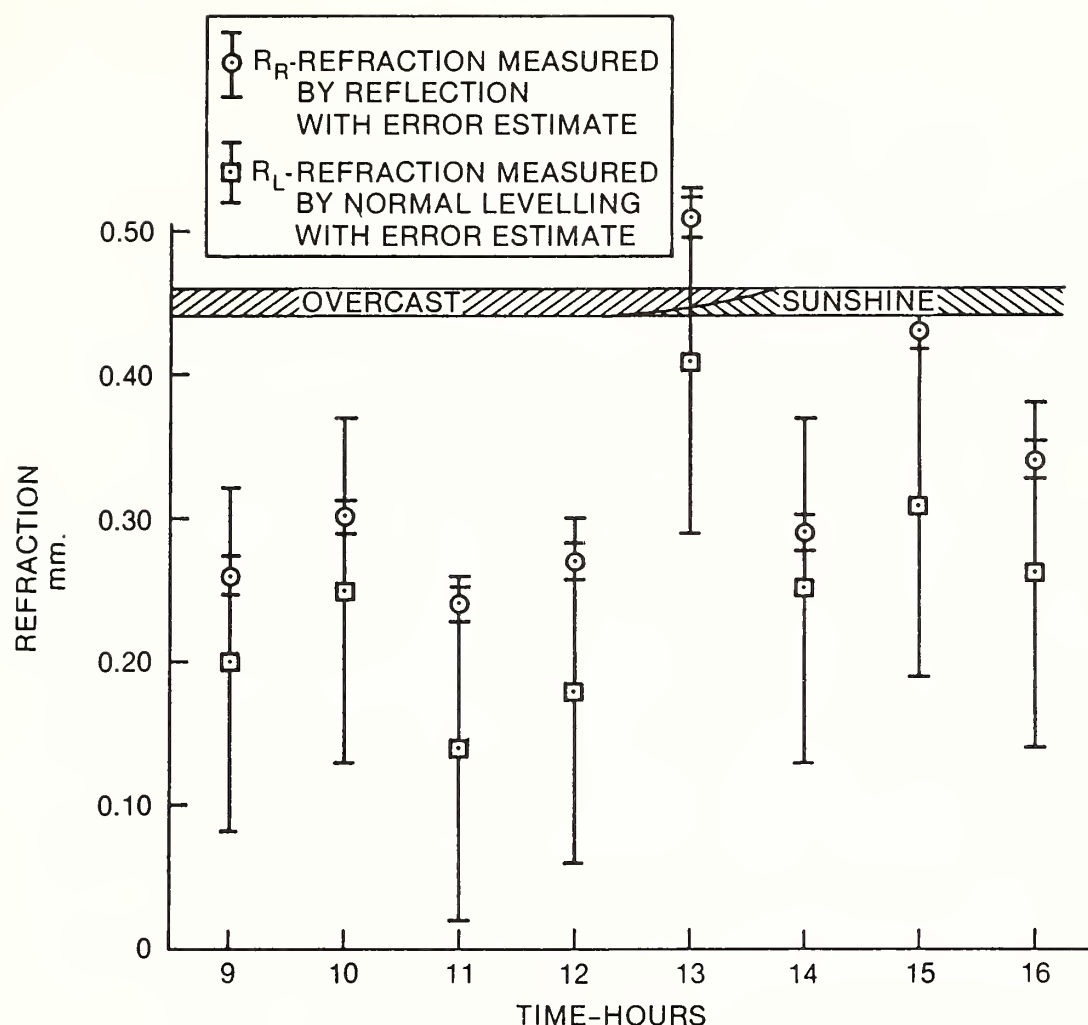


Figure 3. Refraction by reflection and by levelling - 17 Jan 1984.

In the last test, special precautions were taken to avoid any possibility of systematic error, as the earlier tests had shown that there might be a small bias. To ensure that the targets did not move with respect to the level, they were cemented on. Additional care was taken with the target calibration and the determination of the height difference. In order to ensure that the collimation effect was in fact eliminated, a third rod was placed halfway between the other two, its height was determined, and it was observed in each set of observations. Supplementary observations to obtain independent values of the refraction were made: temperatures were measured at three heights above the surface (0.73, 1.73 and 2.73 m), and records of cloud, wind and

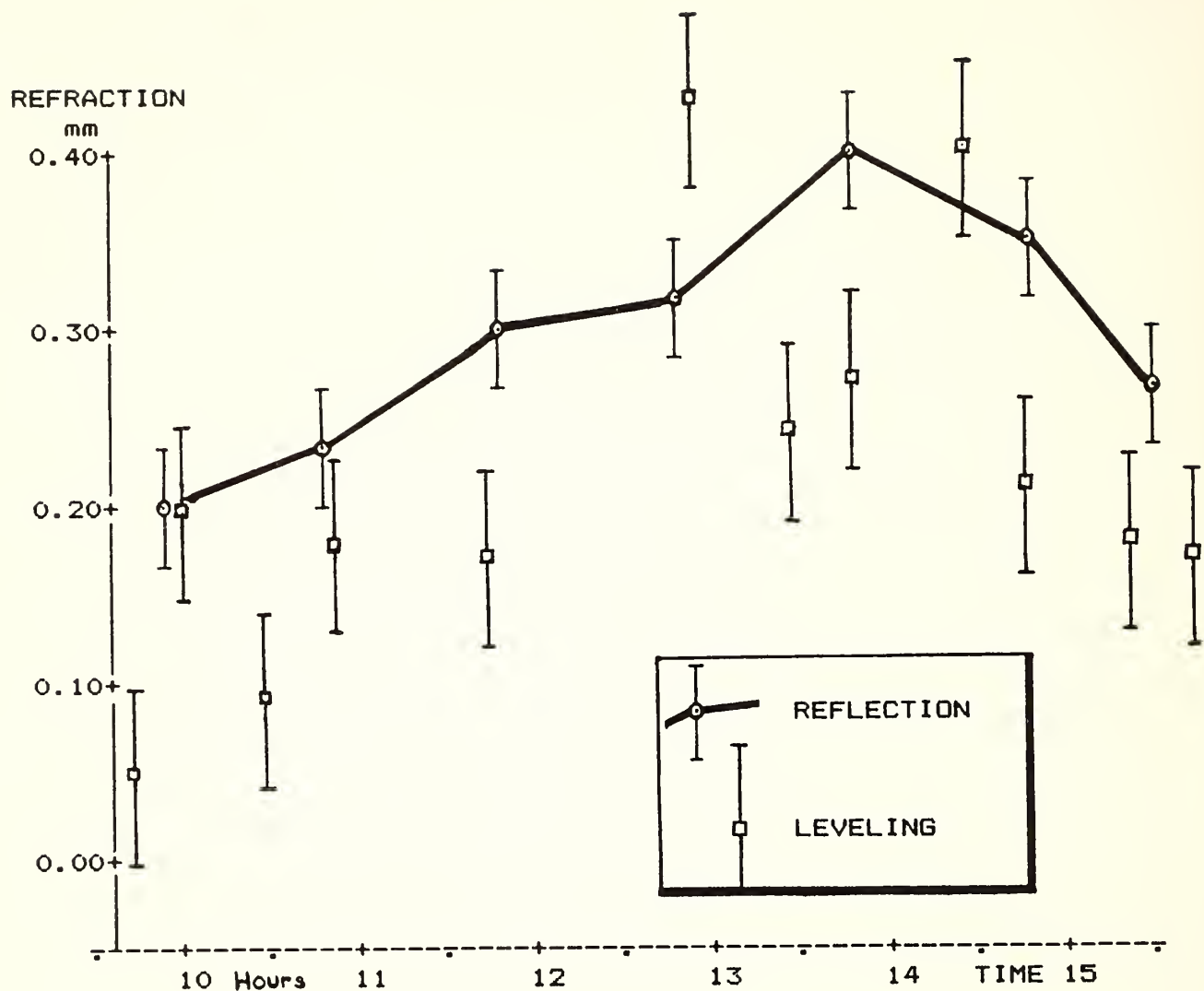


Figure 4. Comparison of refraction by reflection and by levelling.
28 June 1984.

surface moisture were recorded for the micro-meteorological method.

RESULTS

Figure 2 shows the first results, and the first practical confirmation of the refraction by reflection concept. Figure 3 shows the full set of observations, with a significant change of conditions, from overcast to clear sky. The two measures of refraction stay in substantial agreement through this change. There is a suggestion that the reflection method gives a higher result, by 0.08 mm, on average. This is a very small amount, less than the thickness of a sheet of paper, but nevertheless it was decided that because of this suggestion of possible systematic error, further precautions would be taken in the following test.

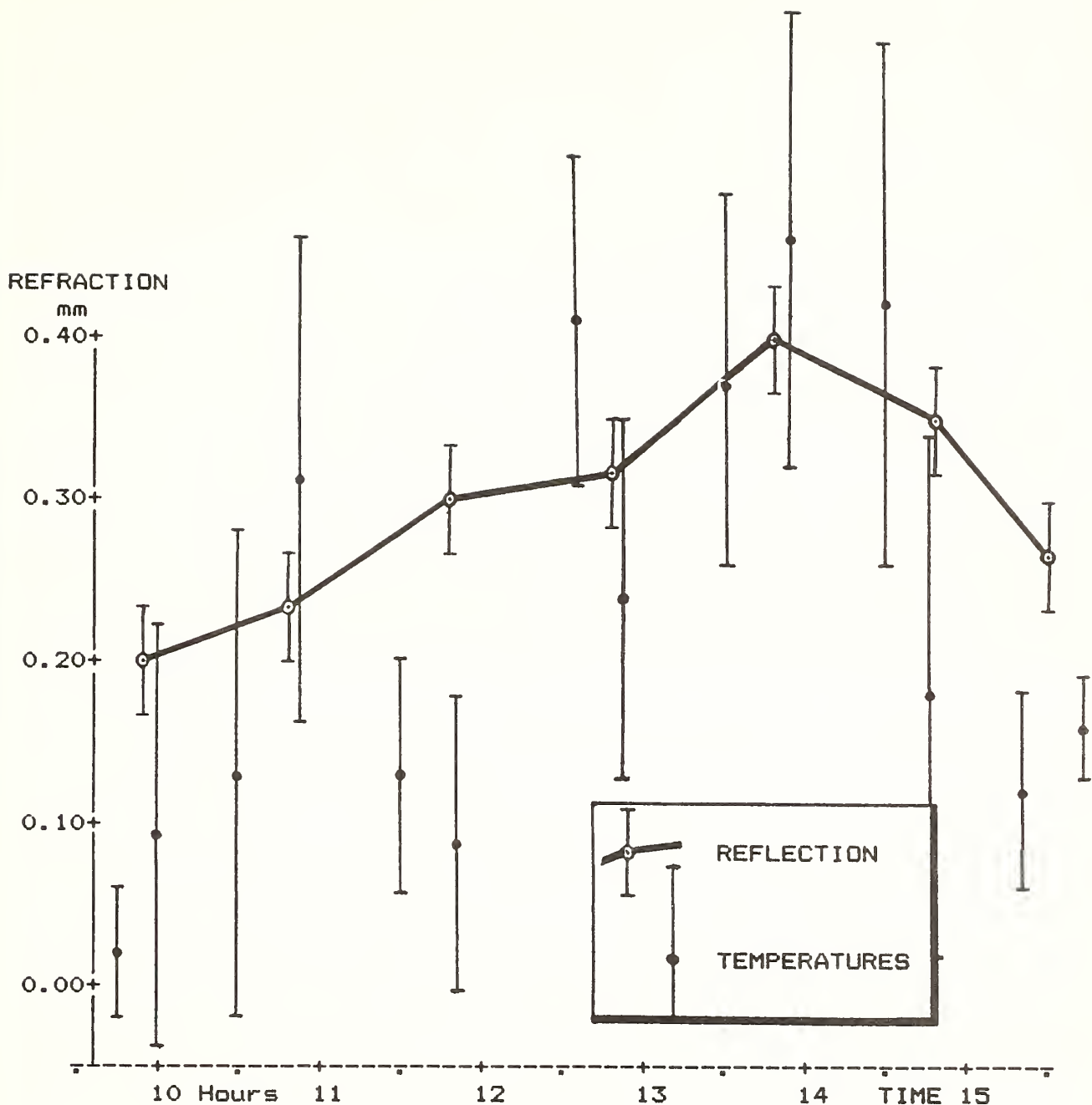


Figure 5. Comparison of refraction by reflection and by temperature gradients. 28 June 1984

The maximum values of refraction in the second test occurred, not when the sun was shining from cloudless skies, but during the transition from cloud to clear skies. There are two possible explanations, and probably they combined to produce the effect. The first is that with a partly cloudy sky, there is downward radiation from the clouds as well as from the sun, so that when the sun is unobscured, the total radiation is larger than from the sun alone. The second cause is that the surface was partly snow-covered, and as the sky cleared it radiated and reflected heat, causing a strong upward heat flow even though the actual

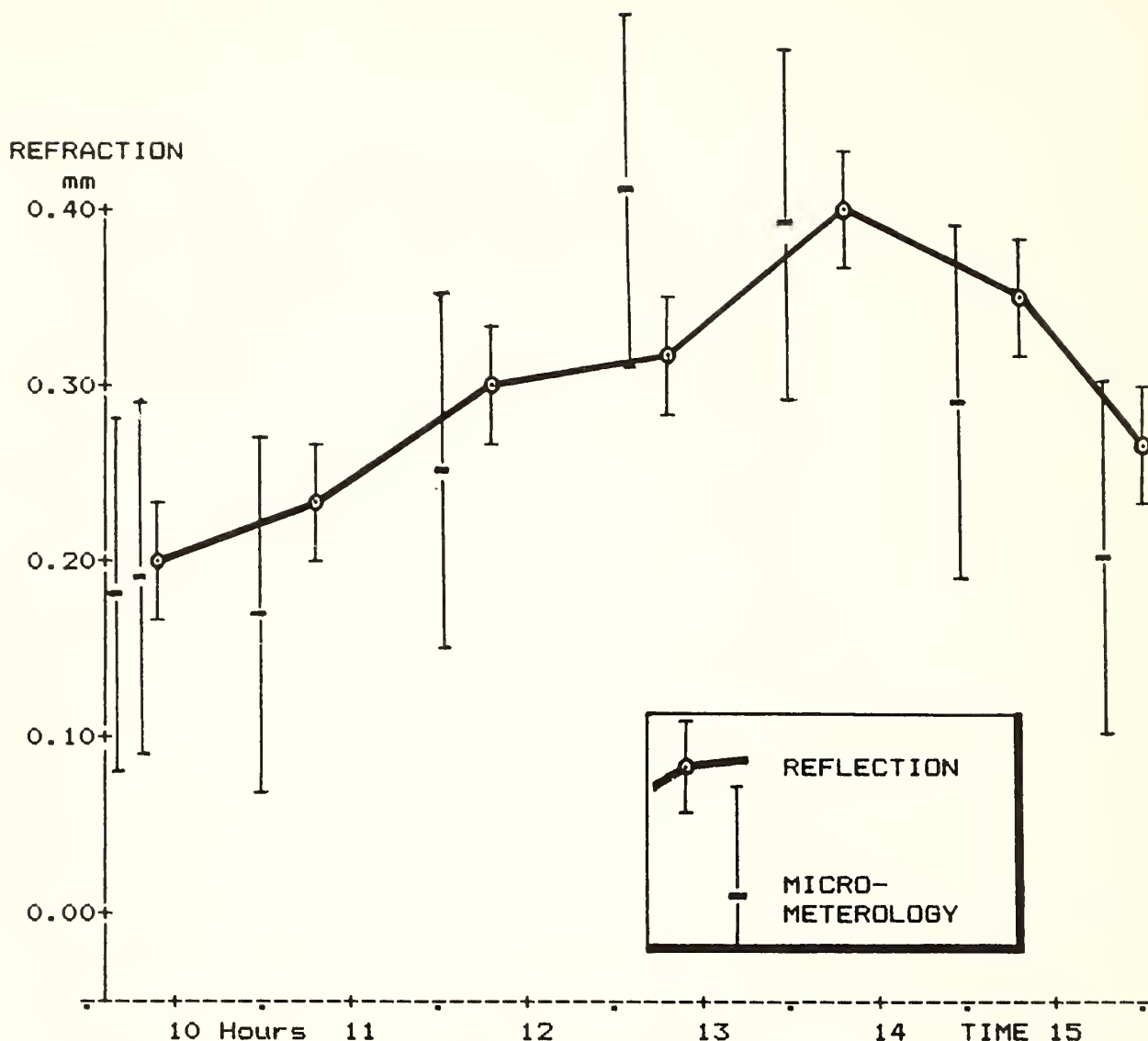


Figure 6. Comparison of refraction by reflection and by meteorological method. 28 June 1984.

temperatures remained low. When the sun came out, the snow began to melt, and the heat was absorbed as latent heat so that upward heat flow, as well as refraction, was reduced.

Figures 4, 5 and 6 show the results of the third day's test. On this day the sky was overcast, but the clouds were of variable thickness, and the wind was also variable. The result was a rapid variation in the radiation reaching the ground surface, and corresponding variations in refraction.

In Figure 4, the same measurements are shown as in the two previous figures. The error bars in these figures are based on the variance of the observations, but they have been increased to take into account other errors such as the calibration error and error in the determination of the height difference between rods. The comparison is good for most observations. During the day,

especially during the middle of the day, the refraction was changing very rapidly, and it was difficult to get consistent readings of the reflections of the target. Temperatures were also fluctuating rapidly and this is shown in Figure 5, which compares the measurements by reflection and by temperature gradients. The time variation could be the cause of some lack of agreement between the two curves. Refraction was calculated from temperature gradient using the formulae of the author (Angus-Leppan 1979; 1981)

Figure 6 shows the comparison between the reflection measurement and the refraction calculated using observed estimates of cloudiness, wind and soil moisture. The basis of this method is the formulation from micro-meteorological theory, of the forms of the temperature gradient, under the different regimes of atmospheric stability (Angus-Leppan and Brunner 1979). The observations are very simple, but the method gives remarkable agreement with the reflection method. One of the reasons for this is that both methods tend to smooth out the time fluctuations - the meteorological method because the observations are general, and the reflection method because there are many observations which necessarily spread over a finite time.

Overall the methods agree well with each other at the 0.1 mm level.

During the test it was not realized fully how rapidly the conditions were changing with time. It would be possible to take more careful and detailed 'met' observations. Under partly cloudy conditions, the intensity at one place on the surface varies with time. This is particularly so when there is wind and the cloud thickness is uneven, conditions which prevailed on the day of the test. It would be of value to take detailed visual observations, carefully timed, of the solar intensity, during such an experiment, to test whether there is good correlation with the temperature gradients. It is possible that the fluctuations of gradient are accounted for in some detail by the fluctuations in the solar radiation intensity. There may, however, be a time lag between the two.

APPLICATIONS

The applications of the reflection measurement of refraction fall into two categories: those using horizontal sights, and those with sloped sights. Taking first the horizontal case, the tests described above show one instrumental arrangement which determines height difference and refraction precisely. For a mobile system, the vertical mirror would be in housing which moved up and down the levelling rod, so that it could be clamped at the height of the horizontal sight from the level. The rod would have to be stabilized so that the compensator or mirror did not vibrate. The National Geodetic Survey has a suitable method of supporting the rod. It would then be possible to read the scale on the rod, as well as the refraction, from the readings to the reflection of the target on the level. One form of mirror would be a mercury pool

at the base of the rod, with a pentagonal prism sliding up and down the rod to the level of the line of sight.

The system would be applicable for precise engineering surveys where the environment often causes anomolous refraction. The ability to measure the refraction precisely would be useful. There are many cases where levels have to be monitored over long periods, where it would be worth setting up instruments for levelling plus refraction permanently.

Another set of applications comes from the use of sloped lines in precise height measurement. The specifications for levelling of high precision can be attained, if errors from all sources are carefully eliminated. The method has the disadvantage that both distance and vertical angle have to be measured very precisely. However there are now available electronic theodolites which measure angles precisely and automatically, and high precision EDM instruments. There has been a realization that geodetic levelling, a slow and expensive operation, should be replaced by a faster, modern measuring system. The U.S. National Geodetic Survey (NGS) has taken an initiative, under the aegis of the International Association of Geodesy, to develop such a system with international participation. The method of refraction by reflection may be part of the system.

In the NGS there are two developments along these lines. Precise height traversing has been tested, using Wild T2000 electronic theodolites and precise EDM, and special targets on the rods, or alternatively using targets attached to two theodolites, in a reciprocal sighting method (Whalen 1984). In the Charting and Geodetic Services, NOAA, investigations are in progress to develop an automated sighting method to eliminate the human observer in the levelling process (Huff 1984).

CONCLUSIONS

The method of refraction measurement by reflection appears to follow the predicted relationship, namely that it is four times the single-ray refraction. The method gives a precision of ± 0.04 mm, equivalent to less than 0.2 arcsecs, over the distance tested (50 m). There are several potential applications of the method, in precise levelling and in the development of new levelling systems.

ACKNOWLEDGEMENTS

Most of the work described was undertaken while the author was Visiting Senior Scientist, under the U.S. National Academy of Science, at the National Geodetic Survey. The encouragement given by many members of the NGS is acknowledged, and in particular the assistance in field observations by the staff at the Corbin laboratories of the NGS.

REFERENCES

- Angus-Leppan, P. V., 1979: Refraction in leveling - its variation with ground slope and meteorological conditions. Australian Journal of Geodesy, Photogrammetry and Surveying, No. 31, 27-41.
- Angus-Leppan, P. V., 1981: Refraction in levelling: extension to stable and neutral conditions. Proceedings of Second International Symposium on Problems Related to the Redefinition of North American Vertical Geodetic Networks, 677-690, Ottawa, Canadian Institute of Surveying.
- Angus-Leppan, P. V., 1983: Preliminary study for a new leveling system. Australian Journal of Geodesy, Photogrammetry and Surveying, No. 39, 69-81.
- Angus-Leppan, P. V., 1985: Theory of refraction by reflection and applications in leveling. (NOS - NGS Technical Report in preparation).
- Angus-Leppan, P. V. and Brunner, F. K., 1979: Atmospheric models for short range EDM. Canadian Surveyor.
- Brunner, F. K., 1978: Vertical refraction angle derived from variance of the angle-of-arrival fluctuations. Proceedings of the Symposium on Refractional Influences in Astrometry and Geodesy, 227-238, Amsterdam, Reidel.
- Holdahl, S. R., 1978: Removal of refraction errors in geodetic leveling. Proceedings of Symposium on Refractional Influences in Astrometry and Geodesy, Amsterdam, Reidel.
- Huff, L. C., 1984: A new rapid precision leveling system. EOS, No. 65, 45 (Abstract), American Geophysical Union.
- Whalen, C. T., 1984: Preliminary test results of precise trig-leveling with the Wild T2000-DI5 system. ACSM Bulletin, No. 93, 15-18.

REFRACTION AND DEFLECTION OF THE VERTICAL IN
TRIGONOMETRIC LEVELING

Vladimiro Achilli*, Paolo Baldi**, Marco Unguendoli***

* Istituto Nazionale di Geofisica, via Ruggero Bonghi 11/b,
00184 Roma, Italy.

** Dipartimento di Fisica, Settore di Geofisica,
Universita di Bologna, Viale Berti Pichat 8,
40127 Bologna, Italy.

*** Istituto di Topografia, Geodesia e Geofisica Mineraria,
Viale Risorgimento 2,
40125 Bologna, Italy.

ABSTRACT. The use of atmospheric models in the calculation of angles of refraction makes it possible to achieve considerable improvements in the results of trigonometric leveling. Furthermore, the use of mass models to calculate local components of the deflection of the vertical enables one to relate these measurements to a single reference surface. This paper provides a description of several examples of how these techniques are applied. The results confirm the possibility of using trigonometric leveling in specific applications, such as the setting up of three-dimensional networks and the checking of ground movements in areas undergoing rapid deformation.

INTRODUCTION

Over the last few years, the authors of this paper have been engaged in the study of ground movements in seismic and volcanic areas in Italy, and have made use of the whole range of modern geodetic techniques. In this kind of geodetic investigation, the technique of determination of height by triangulation, that is by means of zenith distances, has been used in order to reduce the distance measurements, to set up 3D networks in mountainous regions, and to link up spirit leveling lines separated by strips of sea or by areas that are hard to reach. It therefore became necessary to improve operating techniques as well as the methods used to correct measurements in such a way as to account for the effects of refraction and the deflection of the vertical.

An improvement in the results of trigonometric leveling justifies a much wider use of this technique. In some cases, trigonometric leveling may be combined with - or may even partially replace - spirit leveling, thus enabling a considerable reduction in costs, and, above all, making it possible to obtain much more rapid measurements between distant points. In this respect, we should mention experiments carried out in the Pozzuoli volcanic area (near Naples), in which bradyseism is occurring at a deformation rate in the order of several mm per day (Barbarella et al., 1983). In the seismic area of Ancona (Italy), measurements of height differences taken with coupled levels on control triangles are generally used in order to determine whether or not it is necessary to repeat spirit leveling measurements (more than 100 km over undulating terrain) (Baldi et al. 1977).

In the following, several examples are given of the ways in which trigonometric leveling may be used.

INSTRUMENTS

To carry out reciprocal and simultaneous trigonometric leveling between bench marks indicated by reinforced concrete pillars, pairs of theodolites (Wild T3 and DKM3) were used, as well as small size light targets. The latter could also be used during the daytime at distances of several kilometres, mounted directly on the theodolite telescope. To link up points that are at approximately the same height (less than 1.5 m), coupled levels (Zeiss) and light targets designed for long-distance collimation (5-6 km) were used. Atmospheric data (temperature, pressure, vapor pressure, and wind speed) were collected during the measurement period.

REFRACTION

As is well known, the degree of precision that trigonometric leveling can afford is limited by the effects of refraction. Essentially, there are two possible ways of reducing these effects. The first of these consists in two wavelength angular

refraction measurements, whereas the second approach uses complex atmospheric models of varying complexity, able to provide the refractive index variation with height. Since the first method, even though rather attractive, does not seem for the time being to be technically feasible (Williams and Kahmen, 1984; Prilepin and Medovikov, 1984), we have turned our attention to the extensive use of the second method.

In trigonometric leveling, difficulty in assessing the refraction coefficient is partly remedied by carrying out reciprocal and simultaneous observations, for which it is assumed that the refraction angles at the ends of the line are equal (fig.1)

$$h_A - h_B = D \left(1 + \frac{h_A + h_B}{R}\right) \tan \frac{1}{2} (Z_{AB} - Z_{BA} + \delta Z_{AB} - \delta Z_{BA}) \quad (1)$$

an assumption that may often however be far from correct.

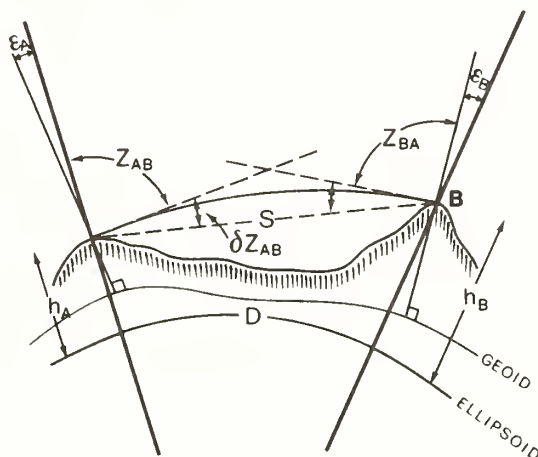


Fig.1 Scheme of trigonometric leveling.

The refraction angle at one end of the line of collimation may be expressed as follows (Moritz, 1967):

$$\delta Z_{AB} = \frac{10^{-6}}{S} \sin Z_{AB} \int_0^S \frac{dN}{dz} (S - x) dx \quad (2)$$

where Barrel and Sears (1938) have given refractivity N for the optical range of wave:

$$N = (n-1)10^6 = 0.2696 N \frac{P}{T} - 11.25 \frac{e}{T} \quad (3)$$

$$N_0 = 67.861 + \frac{31117.99}{146 - L^2} + \frac{269.43}{41 - L^4} ; \quad L = \frac{1}{\lambda} \quad (\lambda \text{ in } \mu\text{m}) \quad (4)$$

From the hydrostatic air equation:

$$\frac{dp}{dz} = 0.0342 \frac{p}{T} \quad (\text{mbar/m}) \quad (5)$$

we shall obtain:

$$\frac{dN}{dz} = -0.2696 N_0 \frac{p}{T^2} \left(0.0342 + \frac{dT}{dz} \right) + 11.25 \frac{e}{T^2} \frac{dT}{dz} + \frac{11.25}{T} \frac{de}{dz} \quad (6)$$

In the derivation of equation 6, the effect of the vapor pressure gradient, for wavelengths in the visible range, may be considered to be negligible (Brunner 1978). This assumption, however, is valid for heights above the ground of over 1 metre, as is generally the case with theodolite observations.

As may be seen from equation 6, the vertical temperature gradient is the overriding factor for the definition of the refractive index gradient, and hence for the refraction angle. In actual fact, rapid variations in temperature and in its gradient can occur with changes in height, especially in the first tens or hundreds of metres of the atmosphere. The different temperature values may be a result, not only of general weather conditions, but also of land morphology, the season of the year, the hour of the day, etc. Since atmospheric parameters cannot easily be measured along the line of sight, it becomes necessary to employ atmospheric models that represent real conditions.

As regards the evaluation of dT/dz , one can make use of the heat flux estimate, a parameter that can be deduced from the radiation budget equation. The use of this approach involves the determination of additional meteorological parameters such as net radiation, heat flux into and out of the ground, evaporation and wind speed (Angus Leppan and Webb, 1971; Brunner, 1978). Bearing in mind that the turbulent transfer of sensible heat H (heat flux) constitutes a component of the energy budget equation (Geiger, 1966), H can be expressed in the following form:

$$H = (S - B) - \lambda E \quad (7)$$

where S is net radiation, B is heat flux into and out of the ground, and λE is evaporation or condensation latent heat flux (λ is latent heat of this phase change). Parameters S , B and E can be measured directly (Brunner, 1978) or estimated on the basis of the climatic conditions observed, the structure of the terrain

and vegetation, wind speed, cloudiness, and sun height (Angus Leppan and Brunner, 1980).

Introducing potential temperature ϑ , defined as the temperature that an air mass would assume if it were carried adiabatically to the standard pressure (1000 mbar), the flux H may furthermore be expressed as a function of $d\vartheta/dz$. In the case of turbulent diffusion, one has:

$$H = -c_p K_H \frac{d\vartheta}{dz} \quad (8)$$

where c_p is the specific heat of air at constant pressure, air density and K_H represents the turbulent diffusion coefficient (Priestly, 1959). The value of K_H depends on height, on wind speed and on the kind of stable or unstable stratification (Brunner, 1978).

Air temperature variations are mainly due to the heating up and cooling down of the surface of the earth caused by solar radiation, turbulent eddies acting to promote heat diffusion. The degree of turbulence is strongly influenced by the temperature gradient. The relation between temperature gradients and potential temperature is expressed with a sufficient degree of precision by the expression:

$$\frac{d\vartheta}{dz} = \frac{dT}{dz} + \Gamma \quad (9)$$

where $\Gamma = -0.98^\circ\text{C}/100$ is the adiabatic lapse rate. When the potential temperature gradient $d\vartheta/dz=0$, i.e. when the potential temperature is constant with height, the temperature gradient is adiabatic, stability is neutral and air movements do not transfer heat. When $d\vartheta/dz > 0$, stratification is stable. This condition tends to have a stabilizing effect on movements of air masses and turbulence causes a downward heat transfer. When, lastly, $d\vartheta/dz < 0$, all air mass perturbations are accentuated by hydrostatic force, turbulence increases and there is an upward heat transfer. This kind of stratification is unstable and occurs when the surface of the earth is heated by solar radiation.

In general, three regions may be identified in the atmospheric layer close to the earth's surface, the physical behaviour of each of which is different. The boundaries of these regions are defined in relation to the Obukhov length L , which may be expressed by:

$$L = - \frac{\tilde{u}^3 c_p \rho \theta}{kgH} \quad (10)$$

where \tilde{u} is the so-called friction speed.

Schematically, disregarding the belt closest to the earth's surface on the grounds that it is extremely small ($z < 0.03L$), the gradients of may be defined as follows (Angus-Leppan 1979; Brunner 1984; Webb, 1984):

$$\begin{aligned}
 &\text{UNSTABLE CONDITION} \left\{ \begin{array}{ll} 0.03 |L| < z < |L| & \frac{d\theta}{dz} \approx - \left(\frac{H^2 T}{c_p^2 g \rho^2} \right)^{1/3} z^{-4/3} \\ |L| < z & \frac{d\theta}{dz} \approx 0 \end{array} \right. \\
 &\text{STABLE CONDITION} \left\{ \begin{array}{ll} z < L & \frac{d\theta}{dz} \approx - \frac{(1+z\alpha/L) H}{\rho c_p \tilde{u}_k} z^{-1} \\ L < z & \frac{d\theta}{dz} \approx - \frac{(1+\alpha)}{\rho c_p \tilde{u}_k} H z^{-1} \end{array} \right. \quad (11)
 \end{aligned}$$

where α is the Monin-Obukhov coefficient.

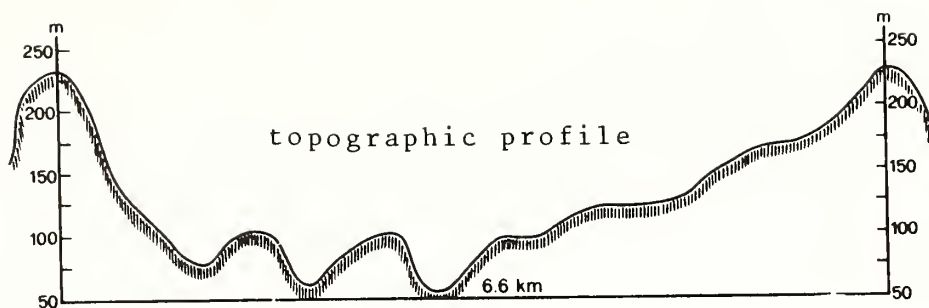
Further investigations into this subject as well as the effects linked to vapor pressure, etc. are described in detail by the authors mentioned.

Evaluating H by means of qualitative procedures (see Angus-Leppan and Brunner, 1980), it is possible to estimate the temperature and its gradient along the line of sight.

As an example of how the method may be applied, Tab. I sets out the results of 5 series of reciprocal and simultaneous measurements of zenithal angles relating to a link 6 km in length belonging to a triangle, taken in a variety of atmospheric conditions (Baldi and Achilli, 1985). The values measured have been corrected by the angle of refraction which was evaluated by a numerical integration of equation 2 for the various atmospheric conditions. The corrected values listed in Table I show that the deviations from the mean are much smaller than in the previous case. Furthermore, correcting the other two sides of the triangle in the same way, it should be pointed out that the mean value of the corrected determinations shows an appreciable improvement in the misclosure error.

DEFLECTION OF THE VERTICAL

In general, if we want to obtain the height difference relating to the ellipsoid, zenithal angles must first of all be corrected, while taking into account the deflection of the vertical.



Equipment	Height differences (cm)	Time (h)	Ground Temperature (°C)	δ''_a	δ''_b	Refraction correction (cm)	Corrected height difference (cm)	Mean of the observed values (cm)	Mean of the corrected values (cm)
Theodolite	822.9	13.0	30	-10.64	-8.61	- 3.19	819.7		
"	821.2	16.0	27	-10.64	-8.78	- 3.27	817.9		
"	812.0	20.0	25	-19.07	-22.03	4.65	816.7	816.0	819.0
"	810.9	2.0	20	-19.26	-25.84	10.33	821.2		
Double levels	813.2	21.0	13	-24.51	-28.43	6.16	819.4		

Table I Example of result of computation of refraction angles for reciprocal and simultaneous trigonometric leveling measurements.

Often, however, in particular applications, if the measurement area is small enough, the need to relate the measurements of the various links to one single surface, whether it be flat, spherical or ellipsoidal, may be satisfied, taking into account local anomalies in the deflection of the vertical only.

These anomalies are mainly due to the distortion of the gravity field caused by the distribution of the surrounding masses (morphology and density anomalies).

From local anomalies in the deflection of the vertical it is also possible to calculate, by means of numerical integration, the local anomalies of geoidal heights in order to refer the results of spirit leveling to a local reference system (see for example the problems connected with the construction of the plane of a large particle accelerator (Bell 1985, Mayoud 1985)).

In order to compute the local anomalies of the components of the deflection of the vertical using a mass model, we use a method previously described by Achilli and Baldi (1982). It consists in the evaluation of disturbing gravitational attraction exerted by the surrounding topography and by density anomalies. The data can be processed automatically by means of a subdivision of the area into regular grids and the use of specific subject maps illustrating the definition of the vertical dimension and the density of the elements. As has been clearly shown in the paper by Achilli and Baldi (1982), the error in the density of the structures appears to be negligible. On the other hand, errors in the evaluation of the average altimetric trend in the area close to the point at which the deflection of the vertical is calculated, influence the results considerably, and in these areas a smaller subdivision of the grid might well be introduced. The area is therefore represented by a set of parallelepipeds, the gravitational components of which can be calculated by means of the following formula:

$$T_{\xi}(P) = \sum_{i=1}^n t_{xi}(P) ; \quad T_{\eta}(P) = \sum_{i=1}^n t_{yi}(P) \quad (12)$$

where the summation, extended to all parallelepipeds, is

$$t_x(P) = \rho G \int_{x_1}^{x_2} \int_{y_1}^{y_2} \int_{z_1}^{z_2} \frac{x}{[(x-a)^2 + (y-b)^2 + (z-c)^2]^{3/2}} dx dy dz =$$

$$= \rho G f(z_1, z_2, y_1, y_2, x_1, x_2, a, b, c) \quad (13)$$

$$t_y(P) = \rho G f(x_1, x_2, z_1, z_2, y_1, y_2, a, b, c)$$

and where:

$$f(\xi_1, \xi_2, \eta_1, \eta_2, \zeta_1, \zeta_2, a, b, c) = \left| \left| \left| \begin{array}{c} \xi_2 \eta_2 \zeta_2 \\ E \ln(H+d) + H \ln(E+d) + Z \tan^{-1} \frac{Zd}{HE} \\ \xi_1 \eta_1 \zeta_1 \end{array} \right. \right| \right| \quad (14)$$

$$E = \xi - a; \quad H = \eta - b; \quad Z = \zeta - c; \quad d = (E^2 + H^2 + Z^2)^{1/2}$$

ρ = density; G = gravitational constant.

We finally obtain:

$$\xi = \arctan \frac{T_{\xi}}{g} ; \quad \eta = \arctan \frac{T_{\eta}}{g} \quad (15)$$

When the attraction of elements further away is calculated, an approximate form may be used, in which the total mass of the parallelepiped is assumed to be concentrated in the centre of the mass, thus reducing computing time considerably.

If the zenithal angles measured are corrected to take account of local anomalies in the deflection of the vertical:

$$\varepsilon_A = \xi_A^{\text{local}} \cos \alpha + \eta_A^{\text{local}} \sin \alpha \quad (16)$$

$$\varepsilon_A = \xi^{\text{local}} \cos \alpha + \eta^{\text{local}} \sin \alpha$$

they can in practice be referred to the normals of a smoothed surface which, at a first approximation, may be assumed to be the mean geoid of the area (fig.2).

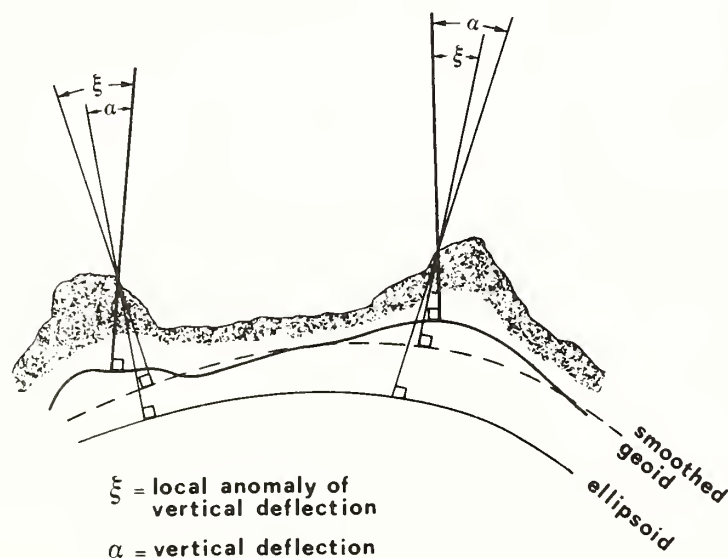


Fig. 2. Scheme of real deflection of vertical and of correction taking account of local geoid anomalies.

The smoothing effect is obvious in the example reported below, in which the deflections of the vertical measured by means of astronomical observations taken between points in a network measuring 10 x 10 km (Achilli et al., 1983) have been corrected to take account of the local effect calculated using the method described. The values corrected in this way are much more homogeneous (Table II).

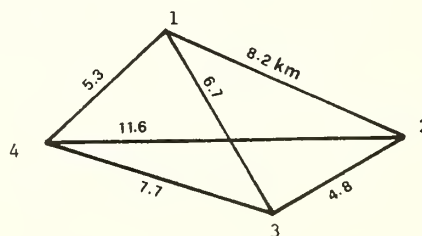
station	astronomic		topographic effect		corrected values	
	ξ	η	ξ^L	η^L	$\bar{\xi}$	$\bar{\eta}$
M. dei Corvi	4.4"	0.2"	2.0"	1.9"	2.4"	-1.7"
Montesicuro	3.3"	-0.5"	0.0"	0.5"	3.3"	-1.0"
Conero	5.7"	0.0"	3.0"	2.3"	2.7"	-2.3"
Ancona	3.9"	-2.3"	1.4"	0.3"	2.5"	-2.6"

Table II Components of the deflection of the vertical obtained using astronomic measurements, and corrected to take account of local effects.

NUMERICAL EXAMPLES

To apply the method, a test net has been introduced consisting of a quadrilateral with sides varying in length from 5 to 11.5 km and with maximum height differences of 400m, belonging to a larger net. A number of trigonometric leveling measurements on this quadrilateral have been taken, and particular attention has been paid to measurement working methods and to the collection of atmospheric data. The results, representing the average of three series of measurements taken under different atmospheric conditions, are given in Table III. This table shows that the closure errors of the various independent polygons improve markedly, following correction taking account of refraction and local anomaly components in the deflection of the vertical.

side	$h(m)$ measured	correction (m)
1-2	386.89	-0.01
1-3	54.57	0.
1-4	115.79	0.01
2-3	-332.41	0.06
2-4	-271.18	0.09
3-4	61.19	0.03



MISCLOSURE ERRORS

triangle	measured (m)	corrected (m)
1-2-3	-0.09	-0.04
1-3-4	0.03	-0.01
1-2-4	-0.08	-0.01

Table III Differences in height obtained by means of trigonometric leveling and correction to take account of refraction and local anomalies in the deflection of the vertical.

In the geodetic net set up in the Ancona seismic area (Baldi, 1977), as well as the distance measurements and the trigonometric leveling carried out in order to reduce the said measurements, spirit leveling was performed, linking up all the planimetric vertices. The heights of these vertices were therefore measured using a number of different methods. With a view to determining the efficiency of methods for the correction and reduction of trigonometric heights to the mean geoid, it was felt useful to compare them with height measurements obtained by means of spirit leveling. This kind of comparison is possible providing the two types of height measurement refer to the same surface, which, given the small size of the area (10 x 10 km), we can identify with the mean local geoid (smoothed geoid). To do this, the mass model method was used to calculate the trend of the local anomalies of the geoid at various heights. A substantial degree of parallelism in the surfaces thus obtained was noted (fig. 3). The height measurements obtained by means of spirit leveling were thus corrected.

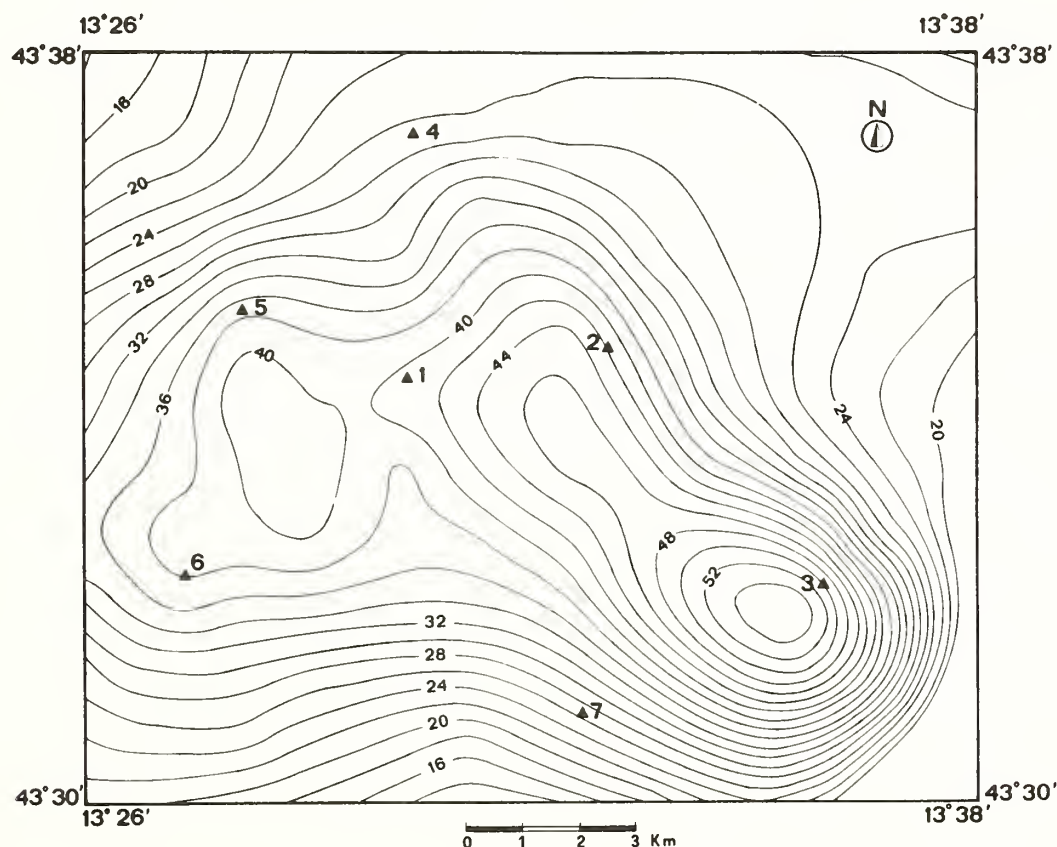


Fig. 3 Local anomalies of geoid in the Ancona area (mm).

The results, set out in Table IV, show that the corrections taking account of refraction and local anomalies of the vertical's deflection improve the congruence between the two height measurements, with maximum gaps of two centimetres.

TRIGONOMETRIC LEVELLING			SPIRIT LEVELLING
station	adjusted height (m)	corrected and adjusted height (m)	corrected (m)
1	195.83	195.83	195.83
2	238.23	238.19	238.18
3	582.77	582.74	582.75
4	121.57	121.55	121.55
5	251.14	251.12	251.13
6	311.61	311.65	311.67
7	250.40	250.41	250.39

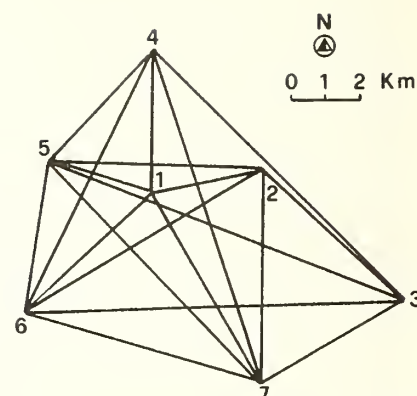


Table IV Comparison between height measurements obtained by means of trigonometric leveling and spirit leveling.

The results obtained through years of work confirm the usefulness of the approach adopted, which makes it possible to improve the results of trigonometric leveling.

ACKNOWLEDGEMENTS

This work was supported by Contract N. 84/01870/02, from the Italian National Research Council.

REFERENCES

- Achilli V., Baldi P. 1982: Computation of Local Anomalies of the Vertical's Deflection in Geodetic Networks. Survey Review vol. 26, 205, 327-335.
- Achilli V., Baldi P., Zerbini S. 1983. Astronomic Determination of Deflection of the Vertical. Survey Review vol. 27, 208, 75-80.
- Angus Leppan P.V., 1979. Use of meteorological measurements for computing refractive effects - A review. In: Refractive Influences in Astronomy and Geodesy. Tengstrom and Teleki (eds) Reidel, 165-178.
- Angus Leppan P.V., Brunner F.K., 1980. Atmospheric temperature models for short range EDM. Canadian Surveyor vol. 34, 2, 153-165.
- Angus Leppan P.V., Webb E.K. 1971. Turbulent heat transfer and atmospheric refraction. Paper presented at the XV General Assembly I.U.G.G., Moscow, Section 1, 15.
- Baldi P., Caputo M., Unguendoli M., Boschi E., 1977. Strain measurements in the Ancona area. Geophysics Journal, Roy. Astr. Soc., 51, 253-258.

- Baldi P., Achilli V., 1985. Atmospheric Models for Geodetic Measurements. Proceedings of the Conference: High Precision Geodetic measurements. Bologna 16-17 October 1984, 79-122, Bologna.
- Barbarella M., Folloni G., Gubellini A., Russo P., 1983. Risultati dei rilievi plano-altometrici attuati dal 1970 al 1981 per il controllo del bradisismo Flegreo. Publ. by Istituto di Topografia, Geodesia e Geofisica Mineraria, Bologna.
- Barrel M., Sears T., 1938. The refraction dispersion of air for the visible spectrum. Phil. Trans. Roy. Soc., Series A, 238.
- Bell B.A., 1985. A simulation of the gravity field around LEP. CERN-LEP-SU/85-1.
- Brunner F.K., 1978. Vertical refraction angle derived from variance of the angle-of-arrival fluctuation. Proc. Intern. Astronomical Union, Symposium No. 89, Uppsala.
- Brunner F.K., 1984. Modelling of Atmospheric Effects on terrestrial Geodetic Measurements. In: Geodetic Refraction. Springer-Verlag. Berlin, 143-162.
- Geiger R., 1966. The climate near the ground. Harvard University Press.
- Mayoud M., 1985. Applied geodesy for CERN accelerators - Part II. Proceedings of the Conference: High precision geodetic measurements. Bologna 16-17 October 1984, 239-283, Bologna.
- Moritz M., 1967. Application of the Conformal Theory of Refraction. Österreichische Zeitschrift für Vermessungswesen, Sonderband 25, 323-334.
- Priestly C.H.B., 1959. Turbulent transfer in the lower atmosphere. The University of Chicago Press.
- Prilepin M.T., Medovikov A.S., 1984. Effects of Atmospheric Turbulence on Geodetic Interference Measurements: Methods of its Reduction. In: Geodetic Refraction. Springer-Verlag. Berlin, 33-44.
- Webb E.K., 1984. Temperature and Humidity Structure in the Lower Atmosphere. In: Geodetic Refraction. Springer-Verlag. Berlin, 85-141.
- Williams D.C., Kahmen H., 1984. Two Wavelength Angular Refraction Measurements. In: Geodetic Refraction. Springer-Verlag. Berlin, 7-31.

A COMPARISON OF APPROACHES TO THE
LEVELLING REFRACTION PROBLEM

C. E. Calvert
Ordnance Survey of Great Britain
Romsey Road
Maybush
Southampton, U.K.

and
A. H. Dodson
Department of Civil Engineering
University of Nottingham
University Park
Nottingham, U. K.

ABSTRACT. Systematic errors due to refraction in levelling may be removed in one of three ways; the first is to use a field observation procedure which eliminates the error, the second is to determine additional measurements to enable the error to be found and the third is to model, if possible, the form of the error and to include it in the final adjustment.

The Ordnance Survey of Great Britain has recently carried out a series of tests to determine the best strategy to adopt with regard to refraction. Observing procedures which would minimise the effects had already been implemented yet an error still existed. Therefore either measuring refraction or modelling it had to be considered.

The two tests carried out were on a sloping base line and on a small levelling circuit. The results from the sloping base gave some evidence that Kukkamaki's and Mozzhukhin's formulae based on measured temperature profiles, produced better values than the raw, uncorrected data. On the other hand, on the test circuit the application of either correction produced answers which were not significantly different from the adjusted raw data. However, the use of a model parameter in the adjustment, based on Remmer's method, produced significantly better results.

The paper describes the tests carried out and discusses the results obtained, with particular regard to a choice of strategy for dealing with refraction errors in the levelling work of the Ordnance Survey.

INTRODUCTION

The Ordnance Survey has a requirement to maintain the national horizontal and vertical control archives of Great Britain. The last geodetic levelling network to be observed was undertaken thirty years ago although maintenance is continuous. A discrepancy between geodetic levelling and hydrodynamic levelling along the East coast of England may have been due to either a sea-surface slope or errors in levelling. Therefore not only the geodetic levelling network but also the methods used in its determination are due for reappraisal. Previous methods had sought to remove or minimize systematic errors, and refraction errors were considered insignificant if back and foresights were kept equal. Subsequent work by many researchers (eg Remmer, 1980 and Whalen, 1981) has shown this assumption to be wrong. The experiments described in this paper were conducted to study both the magnitude of refraction errors and the best method of their removal.

Two principles dictated the course of the work:-

- a) Variations in refraction should be seen to affect the quality of measurement of the height difference between two points
- b) Any field system designed to eliminate, or reduce, the refraction error must not detract the survey team from their primary duties of observation.

Test circuits to evaluate refraction corrections had previously been observed, but other sources of error masked any error due to refraction. However, they had confirmed that any test equipment had to be light and easily managed.

A static test observed between December 1981 and April 1982 was used to deduce both the magnitude of the refraction error and the effectiveness of the formulae due to Kukkamäki (1938), Garfinkel (1978) and Mozzhukhin (1976). All of these use observed temperatures to determine temperature gradients which, together with pressure measurements, are then used to derive corrections to the observed height difference.

Subsequent to carrying out the static test a small network was observed. This allowed testing of Remmer's (1980) method alongside the correction formulae already mentioned. More importantly, the observing conditions more closely resembled those of production levelling and any improvement detected in the test network could be translated to an expected improvement in the national network.

The various correction formulae are not quoted here in the interest of brevity. However, they may be found in the references given above.

STATIC TEST

Observations with a Zeiss Ni 002 were made to Zeiss geodetic levelling rods placed on bolts and supported by 3m tripods. Nineteen sets of observations were made, nine with balanced fore and backsights of 30 m and ten with imbalanced sights of 55 m (backsight) and 5m (foresight). Each set of observations consisted of sixteen determinations of the difference in height

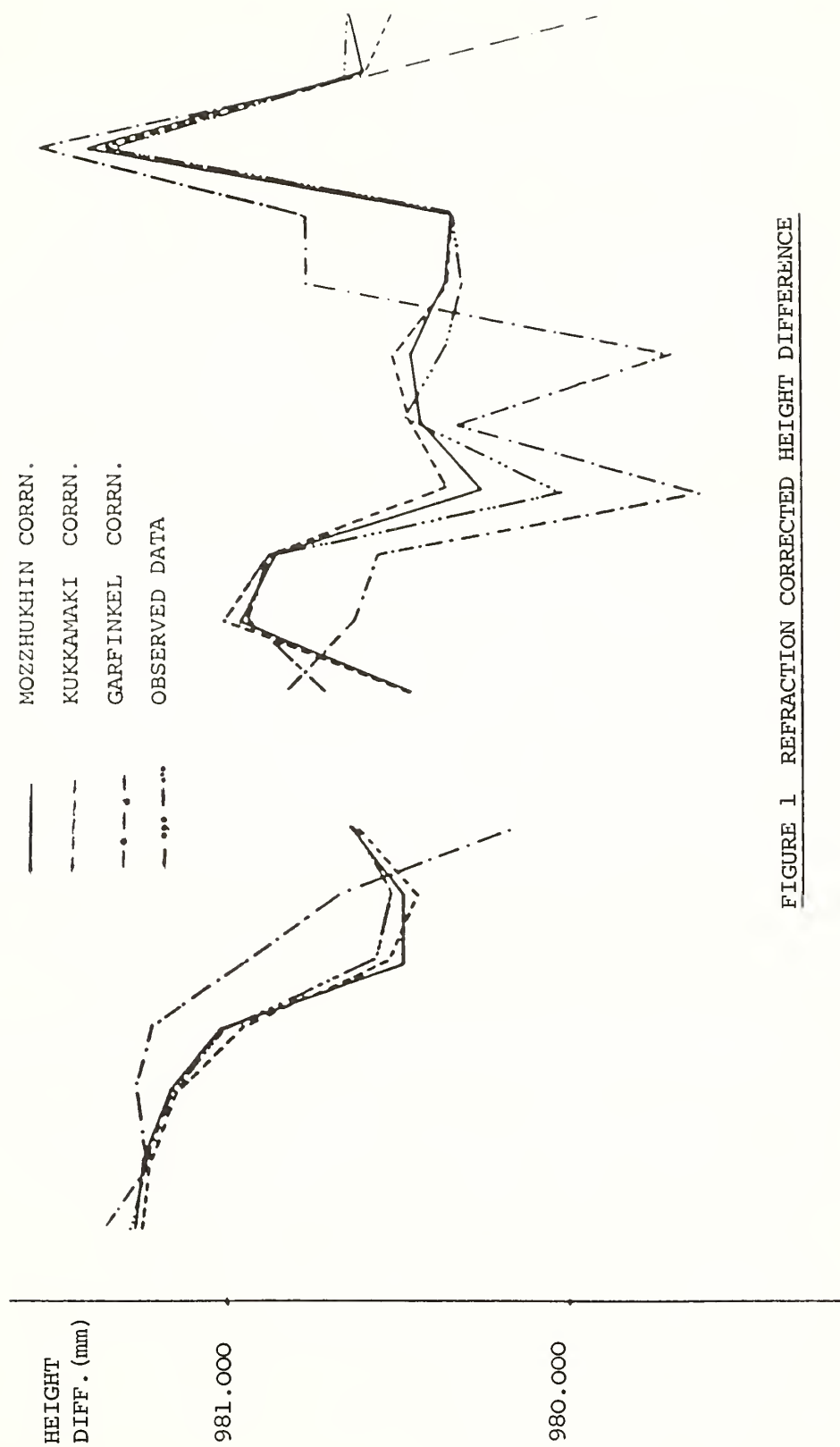


FIGURE 1 REFRACTION CORRECTED HEIGHT DIFFERENCE

Table 1 Static Test: Individual Set Results

Sets	Height Difference (ΔH)			
	Set Mean (mms)		Set s.e. (mms)	
	Max.	Min.	Max.	Min.
Balanced (sets 1-9)	981.275	980.487 (979.597)*	0.108 (0.247)*	0.033
Imbalanced Sets (10-19)	981.33.	980.269	0.097	0.043

Table 2 Static Test: Regression ΔH v ΔRI

Correction Applied	r^2
None	0.146
Kukkamäki corr ⁿ	0.126
Garfinkel corr ⁿ	0.088
Mozzhukhin corr ⁿ	0.027

Table 3 Static Test: Refraction Correction Results (all sets)

Correction Applied	Overall mean ΔH (mms)	s.e. of ΔH	s.e. of $\overline{\Delta H}$
None	980.733	0.352	0.083
Kukkamäki Corr ⁿ	980.736	0.348	0.082
Garfinkel Corr ⁿ	980.708	0.523	0.123
Mozzhukhin Corr ⁿ	980.752	0.368	0.087

*NOTE Set 8 was observed during a very rapid thaw of frozen ground. The very large standard deviation and low height differences obtained were assumed to be due to ground point instability during the thaw and this set has not been included in subsequent analysis.

together with associated meteorological readings. Each set took approximately one hour to complete. The maximum and minimum mean height difference determined from the balanced and imbalanced sets are given in Table 1 together with the maximum and minimum standard error of the sets.

The observations were corrected for staff calibration and the imbalanced sights for Earth curvature and collimation error. It is apparent from Table 1 that the large variation in mean height difference cannot be accounted for by random observational error alone.

The Kukkamäki, Garfinkel and Mozzhukhin corrections were applied to the observations. A regression analysis was then performed comparing the measured refractive index differences (between the values calculated for the fore and back staff points) and the corrected and uncorrected mean height differences. The resulting correlation coefficients (r) for the balanced sets are given in Table 2. These values are not very conclusive, however, the corrections (particularly the Mozzhukhin correction) have reduced the correlation between refractive index difference and mean difference of height. Similar results were obtained for the imbalanced observations.

The overall mean obtained by averaging the individual set mean values and the associated standard errors are given in Table 3. The difference between the means is very small and the individual pattern of the corrections (see Fig 1) show similar trends. However, the Garfinkel correction appears to be much larger than the others and has produced a wider spread of results, even more than that of the raw observations. The other two formulae have produced similar standard deviations (of approximately the same size as that of the uncorrected observations) although the Mozzhukhin correction does give a slightly higher mean value. In conclusion none of the corrections appear to eliminate the large variation in the set mean values, which if due to refraction, does not appear to be correctly modelled by any of the formulae used. Indeed, Garfinkel's formula appears to worsen the results. It was decided to test the other two formulae along with Remmer's approach on a levelling circuit.

TEST CIRCUIT

In order to evaluate the different approaches of Kukkamäki, Mozzhukhin and Remmer to the refraction problem a levelling circuit was established on Southampton Common. The circuit was premarked and each rod position nailed. Bench Marks were rivets in concrete blocks. The levelling was carried out in July using the same equipment that had been used for the static test. The maximum height difference between bench marks was approximately 25 m. The circuit is shown schematically in Figure 2, with the Junction Bench Marks (JBM) and the starting Bench Mark labelled.

The observed height differences are given in Table 4. It is immediately apparent that there is a systematic difference between the forward and back levelling, for which no obvious explanation presents itself. The circuit was levelled anticlockwise (arbitrarily) from Bench Mark 1, however, the split lines were levelled so that the forward levelling from 8 to 5 via 9 was uphill and the forward levelling from 6 to 3 via 9 was downhill. This has not however affected the sign of the forward-backward levelling difference.

Table 4 Test Circuit: Observed Height Differences

SERIAL	SPACE	FWD Δ HT (m)	BACK Δ HT (m)	FWD BACK (μ m)	MEAN Δ HT (m)
1	001-002	+ 1.54444	+ 1.54463	- 190	+ 1.544535
2	002-003	+ 4.71504	+ 4.71461	+ 430	+ 4.714825
3	003-004	+ 3.66954	+ 3.66828	+1260	+ 3.668910
4	004-005	+14.88787	+14.88643	+1440	+14.887150
5	005-006	- 8.99636	- 8.99723	+ 870	- 8.996795
6	006-007	- 6.56525	- 6.56534	+ 90	- 6.565295
7	007-008	- 3.22697	- 3.22767	+ 700	- 3.227320
8	008-001	- 6.02676	- 6.02704	+ 270	- 6.026900
9	009-009	+ 5.95198	+ 5.95169	+ 280	+ 5.951835
10	009-005	+12.83708	+12.83665	+ 430	+12.836865
11	006-009	- 3.83979	- 3.84037	+ 580	+ 3.840080
12	009-003	- 5.71926	- 5.71978	+ 520	- 5.719520

Table 5 Test Circuit: Loop Misclosures (mms)

LOOP	UNCORRECTED			KUKKAMAKI			MOZZHUKHIN			DIST (m)
	FWD.	BACK	MEAN	FWD.	BACK	MEAN	FWD.	BACK	MEAN	
35683	+1.55	-3.33	-0.89	+3.12	-3.46	-0.17	+4.14	-3.49	+0.32	2121
3983	0.00	+0.31	+0.16	-1.06	+0.42	-0.32	-1.10	+0.96	-0.07	1133
3953	-1.07	+1.72	+0.32	-0.08	+1.69	+0.80	-2.02	+1.60	-0.21	1363
5965	-1.65	+0.95	-0.35	-1.59	+1.00	-0.30	-1.14	+1.10	-0.02	1021
6986	+0.45	+0.95	+0.70	+0.87	+0.82	+0.84	-0.60	+0.67	+0.04	920
Mean			-0.01			+0.17			+0.01	
s.e.			± 0.62			± 0.60			± 0.20	

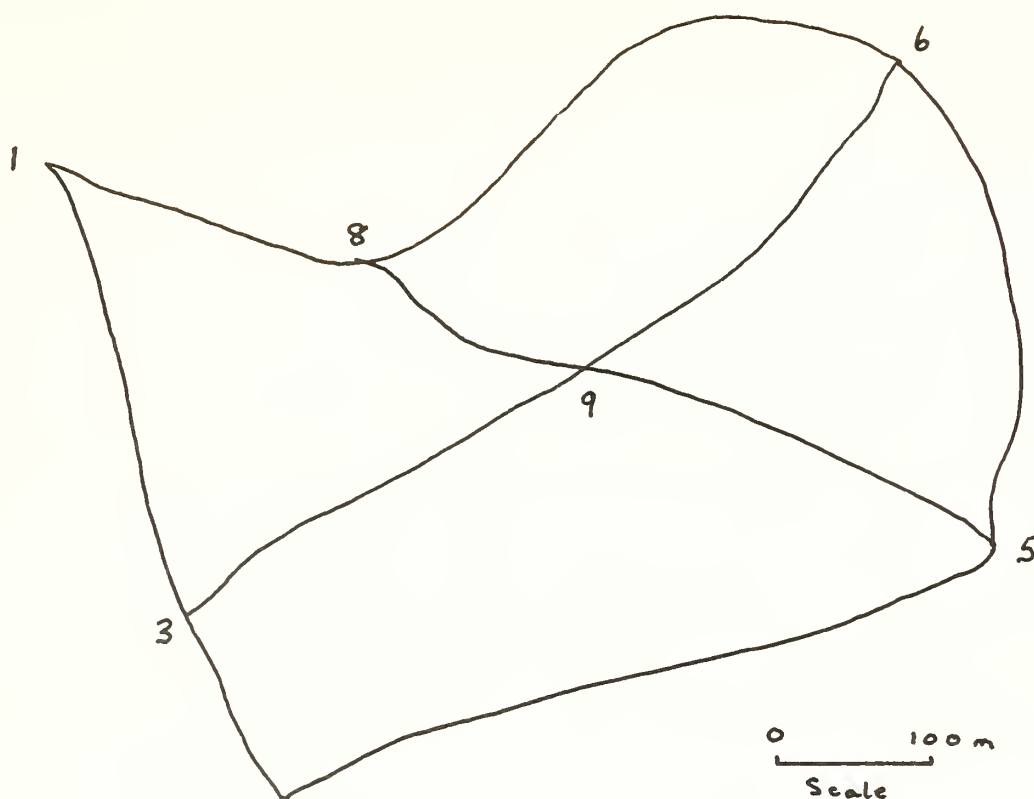


Figure 2 Test Circuit

Adjustments were carried out (using JBM 3 as an arbitrarily fixed datum) on the forward, backward and mean values for both the uncorrected and the refraction corrected observations. The loop misclosures before adjustment are given in Table 5 and the results of the adjustments including the adjustment variance, σ_0^2 are in Table 6.

The Mozzhukhin correction significantly reduces the mean loop misclosures (unlike the Kukkamäki correction) however, interestingly it generally increases the size of the forward and backward loop misclosures.

When considering the adjustment of the circuit as a whole the Mozzhukhin correction rather surprisingly produces less precise results than the uncorrected observations, whilst the Kukkamäki correction only improves the precision very slightly.

Turning to Remmer's approach of adjusting with an unknown refraction bias parameter, this was carried out using only the first order term of his proposed method (Remmer, 1980) due to lack of redundancy. The resulting JBM heights and standard errors, together with the adjustment variance are given in Table 7. It is apparent that Remmer's approach has produced a significantly smaller adjustment variance than the methods which apply a refraction correction based on the measured temperature profile.

Table 6 Test Circuit: Adjusted Height Values

JBM No.	FWD LEVELLING		BACK LEVELLING		MEAN LEVELLING		σ_o^2
	Ht (m)	s.e. (mm)	Ht (m)	s.e. (mm)	HT (m)	s.e. (mm)	
			UNCORRECTED				
3	100.00000	(JBM 3 was used as a fixed datum)					
5	118.55658	0.40	118.55605	0.68	118.55632	0.22	0.08
6	109.55973	0.42	109.55963	0.71	109.55968	0.23	
8	99.76750	0.38	99.76741	0.64	99.76746	0.21	
9	105.71954	0.34	105.71934	0.56	105.71944	0.19	
			" KUKKAMAKI				
3	100m	(JBM 3 used as a fixed datum)					
5	118.55676	0.41	118.55568	0.74	118.55622	0.22	0.06
6	109.55979	0.43	109.55955	0.77	109.55967	0.23	
8	99.76731	0.39	99.76746	0.69	99.76739	0.20	
9	105.71965	0.35	105.71949	0.62	105.71957	0.18	
			MOZZHUKHIN				
3	100m	(JBM 3 used as a fixed datum)					
5	118.55638	0.54	118.55632	0.68	118.55635	0.28	0.09
6	109.55950	0.57	109.55986	0.71	109.55968	0.30	
8	99.76717	0.51	99.76768	0.64	99.76742	0.27	
9	105.71932	0.46	105.71949	0.57	105.71941	0.24	

Table 7 Test Circuit: Bias Parameter Modelling

MEAN LEVELLING			
JBM No.	Ht (m)	s.e. (mm)	σ_o^2
3	100.00000	-	0.03
5	118.55598	0.21	
6	109.55917	0.19	
8	99.76682	0.17	
9	105.71879	0.16	

CONCLUSIONS

The results of the tests have been inconclusive. Although there are systematic effects present in the observations for both the static and the loop tests the application of refraction corrections using various established formulae does not significantly reduce these errors. The use of Remmer's approach of including a refraction bias parameter in an adjustment does significantly improve the adjustment variance. However the small number of redundant observations in the test network means that further evidence is required before it can be concluded that this parameter is accurately modelling refraction rather than other effects.

For this reason a new test network is being established in the Midlands area of England where there are greater elevation changes. This network is to be levelled at intervals under summer and winter conditions and the various approaches to refraction correction described in this paper will be further tested.

REFERENCES

- Garfinkel, B, 1978: "The theory of terrestrial refraction",
1st and 4th Quarterly Reports, Yale University.
- Kukkamäki, T J, 1939: "Formeln und tabellen zur berechnung der nivellitischen
refraktion", Veröff. Finnish Geodetic Institute No 27, Helsinki.
- Mozzhukhin, O A, 1976: "Systematic refraction effects on geometric levelling"
Geodesy, Mapping and Photogrammetry, Vol. 18, No 1.
- Remmer, O, 1980: "Refraction in levelling", Geodætisk Institut, København.
- Whalen, C T, 1981: "Results of levelling refraction tests by the NGS", NOAA Tech.
Mem. No 92.

FIELD TEST REPORT ON THE SYSTEMATIC EFFECT OF REFRACTION IN PRECISE LEVELLING

P. Heroux, W. Gale, F. Faucher
Geodetic Survey Division
Surveys and Mapping Branch
Energy, Mines and Resources, Canada
615 Booth Street
Ottawa, Ontario, K1A 0E9

ABSTRACT

The Canadian vertical network is to be re-adjusted on the proposed 1988 datum. In order to assess the importance of the systematic effect of atmospheric refraction in precise levelling and the efficiency of existing models in correcting for that effect, a refraction test was conducted during the summer of 1984 by the Primary Vertical Control Section of Geodetic Survey of Canada.

The field observation technique utilized two different sight lengths (approximately 45 and 22.5 metres) in order to obtain a direct measure of the systematic effect of refraction. The test site offered general slopes of 1% which were surveyed to accumulate a total distance of 34 kilometres. The average temperature difference between heights of 0.5 and 2.5 metres was -0.55 degrees Celsius. The total accumulated refraction error of 14 millimetres agreed with the value of refraction computed from Kukkamaki's equation using measured temperature gradients.

The results of this test served as a validation of instrumentation and of procedures used in collecting temperature data. They were also useful in evaluating the applicability of a temperature stratification prediction model to the Canadian environment.

INTRODUCTION

The Primary Vertical Control Section (PVCS) of Geodetic Survey of Canada has required all of its field crews to measure the vertical temperature gradient at each instrument setup in order to provide for the correction of precise levelling data for the systematic effect of refraction. The apparatus used consists of two probes (at elevations of .5 and 2.5 metres above the ground) attached to a staff connected to a digital meter. Analysis of the data collected in the past has indicated large fluctuations (up to 1 degree) of the vertical temperature gradient over short time intervals (a few minutes) when maximum sun and minimum wind conditions prevailed. This observation prompted PVCS to conduct further investigation into the behavior of its instrumentation as part of an ongoing study of the effect of refraction in Canadian levelling.

A field test was developed in order to measure directly the effect of refraction and thus obtain a true measure of the refraction error. The procedure involved the repeated measurement of several sections of a line using two different sight lengths, one being exactly double the other. Since the refraction error was known to be proportional to the square of the sight length, it was expected that the

differential effect of refraction would be reflected in the difference in elevation differences obtained from the two sight lengths. This value was compared to the computed value derived from measured temperature gradients entered into Kukkamaki's single-sight refraction equation. It was also compared to the computed value obtained from predicted temperature gradients used in Kukkamaki's equation. Each comparison was carried out in an attempt respectively to validate the apparatus presently used to measure the temperature gradients and to confirm the applicability of a temperature stratification prediction model to the Canadian environment. This measure of the true refraction error was also valuable in confirming the necessity of sampling the temperature gradient at every setup.

THEORY

Computation Of Refraction Error From Levelling Observations

The sight length is an important factor contributing to the systematic refraction error in levelling that can easily be controlled. By comparing elevation differences obtained on a section measured independently but under similar conditions with two different sight lengths, one would expect to isolate the differential refraction error existing between the sight lengths (assuming all other systematic errors are eliminated). This approach is used to obtain a measure of the refraction error, with one sight length double the length of the other.

Computation Of The Refraction Error Using Kukkamaki's Single-sight Equation With Measured Temperature Gradients

Another approach can be used to obtain the differential refraction error accumulated on a section. It consists of measuring the temperature gradient and then computing the refraction error for both sight lengths using Kukkamaki's single-sight equation. Kukkamaki's equation establishes the relation between temperature gradient and refraction error in the following way:

$$R_f = d \cot^2 E_f \frac{\Delta T}{Z_2^c - Z_1^c} \left[\frac{1}{c+1} Z_f^{c+1} - Z_0^c Z_f + \frac{c}{c+1} Z_0^{c+1} \right] \quad (1)$$

$$R_b = d \cot^2 E_b \frac{\Delta T}{Z_2^c - Z_1^c} \left[\frac{1}{c+1} Z_b^{c+1} - Z_0^c Z_b + \frac{c}{c+1} Z_0^{c+1} \right] \quad (2)$$

$$R = R_b - R_f \quad (3)$$

where: d : variation of air refraction per degree C (Kukkamaki 1939)

E_b, E_f : slope of the ground between the instrument and the rod on backsight and foresight

Z_2, Z_1 : temperature probe heights

ΔT : temperature difference between the probe heights Z_2 and Z_1

Z_b, Z_f : actual rod readings on backsight
and foresight

Z_0 : instrument height

c : coefficient of Kukkamaki's temperature
function, $t = a + bz^c$

By computing the refraction error on each setup for each sight length from the measured temperature gradients, it is possible to obtain the differential refraction error between sight lengths. This value can then be compared with the measured differential refraction.

Computation Of The Refraction Error Using Kukkamaki's Equation With Predicted Temperature Gradients

Using a model of temperature stratification that integrates observations of ambient temperature, sky cover and position with predicted solar radiation, it is possible to predict the vertical temperature gradient. In Canada, records of solar radiation are available for up to 58 weather stations located throughout the country. In order to determine the appropriate solar radiation value for a given levelling section, collocation is used to predict solar radiation from the known values of adjacent weather stations. The model also requires sky cover and wind conditions, azimuth and slope along the levelling line as well as the GMT time the section was observed. The latter serves to compute azimuth and elevation of the sun. All of these variables are recorded during the observation campaign or are computed afterwards and are used to predict the temperature gradient. Once the temperature gradient has been predicted, Kukkamaki's equation can be applied to calculate the refraction error on a setup basis for each sight length. This allows a direct comparison with the measured value.

METHODOLOGY

The site selected for the refraction test was a 5.7 kilometre stretch along highway 55, north of Sherbrooke, Quebec. The profile of the road presented gentle slopes with a grade of approximately one percent, allowing for long sight lengths of 50 metres, which was estimated to be the maximum usable sight length given an average vertical temperature gradient of 1 degree. With these anticipated conditions, it was predicted (using Kukkamaki's equation) that approximately one millimetre of differential refraction error between sight lengths would be accumulated for every kilometre of levelling. In order for the refraction error to accumulate in the same direction from section to section, the sections were assembled in such a way as to represent a continuous upward grade. Plans were to run 30 to 50 kilometres of levelling in order to obtain 30 to 50 millimetres of refraction error. A refraction error of this magnitude would be well outside the envelope formed by the propagation of random errors and would confirm decisively the existence of a systematic effect.

In order to ensure that the systematic effect being measured was indeed refraction, a procedure was followed to eliminate or minimize all other systematic errors. The instrument used was the Zeiss Jena NI-002 and independent elevation

differences for each compensator position were observed to eliminate any effect due to the inclination of the collimation line. In addition, to eliminate any propagation of the residual collimation error into elevation, the sight lengths were balanced within .2 metres on each setup. The systematic error that could have been introduced by the instability of the turning points was eliminated by installing permanent turning points (1.0 to 1.5 metre steel pins driven into the ground). The rods were calibrated at each graduation and each rod was read as many times on foresight as backsight on each section to eliminate any effect due to the difference in the zero offsets of the rods. The same instrument was used for levelling with both sight lengths, in order to cancel any error due to the magnetic field . To assure rod verticality and stability, braces were used.

The exact procedure followed on each set of three setups (2 short sight lengths and 1 long sight length) can be visualized using figure 1. On each set, referred to here as one dual independent setup, 3 rods were used and the instrument moved successively from position 1 to 3 measuring differences of elevation using respectively short sight length, long sight length and finally short sight length. The difference of elevation between rod positions 1 and 3 was thus determined independently using the two sight lengths. The rods were moved in such a way that the trailing rod became the centre rod on the following set and that each of the 3 rods was read as many times on backsight as on foresight for each section. Sections were accordingly divided into a multiple of 3 sets. Table 1 gives a summary of each section with regard to number of setups, average sight length and slope.

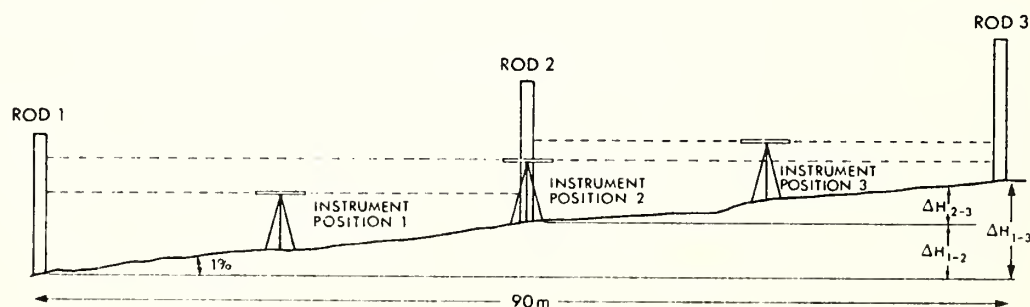


Figure 1.
The basic procedure for obtaining 2 independent elevation differences
(One dual independent setup)

RESULTS

The results were compiled section by section as reported on Tables 2 and 3. The runnings were assembled in chronological order into a continuous upward grade, to form a line 34 kilometres in length with a total elevation difference of 293 metres.

Since the refraction error was small in comparison to the random noise existing in the observations, it was difficult to detect at a section level the systematic effect that refraction had on the elevation differences. For this reason, the refraction error was accumulated over the total levelled distance. Three separate estimates of the refraction error and their accumulation were computed: the measured differential refraction error, the refraction error obtained from measured

Table 1
Site description: information associated with each section

Section From To	Number of setups		Average sight length (m.)		Slope (%)
	Long	Short	Long	Short	
84L036 84L006	6	12	42.2	21.1	1.5
84L006 84L007	12	24	44.9	22.4	0.7
84L007 84L008	9	18	47.3	23.6	-0.7
84L008 84L009	12	24	48.2	23.9	-1.1
84L009 84L010	12	24	44.0	22.0	-0.4
84L010 84L011	12	24	43.6	21.7	0.9

Table 2
Levelling results: information associated with individual runnings

From	To	Date	Time	Sun code	Wind code	Temperature gradient (Deg. C./2m.)	Distance (km.)	Elevation difference (m.)
84L006	84L007	22-06-84	11:07	2	0	-1.0	1.08	7.6
84L008	84L007	22-06-84	13:28	2	0	-1.2	0.85	6.4
84L009	84L008	22-06-84	15:25	2	1	-0.7	1.15	13.3
84L010	84L009	23-06-84	13:20	2	0	-1.5	1.06	4.5
84L010	84L011	25-06-84	08:55	0	0	0.0	1.04	9.9
84L010	84L011	26-06-84	09:12	1	0	-0.4	1.04	9.9
84L010	84L009	26-06-84	11:18	1	0	-0.3	1.08	4.5
84L009	84L008	26-06-84	14:49	1	0	-0.2	1.15	13.3
84L008	84L007	10-07-84	08:58	2	0	-0.5	0.85	6.4
84L006	84L007	10-07-84	10:05	2	0	-0.6	1.08	7.6
84L036	84L006	10-07-84	14:07	1	0	-0.2	0.50	7.8
84L036	84L006	10-07-84	14:46	2	0	-0.5	0.50	7.8
84L006	84L007	10-07-84	15:43	2	0	-0.5	1.08	7.6
84L008	84L007	25-07-84	11:24	2	1	-0.7	0.85	6.4
84L009	84L008	25-07-84	13:28	2	1	-0.7	1.15	13.3
84L010	84L009	25-07-84	14:52	1	1	-0.5	1.06	4.5
84L010	84L011	30-07-84	12:45	2	0	-0.6	1.04	9.9
84L010	84L011	30-07-84	14:00	2	1	-0.7	1.04	9.9
84L010	84L009	30-07-84	15:50	1	1	-0.5	1.06	4.5
84L006	84L007	31-07-84	12:51	2	1	-0.3	1.08	7.6
84L036	84L006	02-08-84	13:02	2	0	-0.5	0.50	7.8
84L036	84L006	02-08-84	13:41	1	0	-0.6	0.50	7.8
84L006	84L007	02-08-84	14:27	2	0	-0.6	1.08	7.6
84L009	84L008	02-08-84	15:47	2	0	-0.6	1.15	13.3
84L010	84L009	03-08-84	12:55	2	0	-0.6	1.06	4.5
84L010	84L011	03-08-84	14:08	2	0	-0.6	1.04	9.9
84L010	84L011	14-08-84	10:33	2	0	-0.5	1.04	9.9
84L010	84L009	14-08-84	14:31	2	0	-0.3	1.06	4.5
84L009	84L008	25-08-84	12:37	2	0	-0.6	1.15	13.3
84L036	84L006	27-08-84	14:08	2	0	-0.1	0.50	7.8
84L006	84L007	27-08-84	13:57	2	0	0.1	1.08	7.6
84L010	84L009	31-08-84	14:11	2	1	-0.8	1.06	4.5
84L010	84L011	07-09-84	14:30	1	0	-0.5	1.05	9.9
84L010	84L011	18-09-84	12:38	2	0	-0.6	1.04	9.9

84L010	84L009	18-09-84	13:48	2	1	-0.8	1.06	4.5
84L036	84L006	18-09-84	15:28	2	1	-0.5	0.50	7.8

Total distance: 34.61 kilometres
Elevation difference: 293.3 metres
Mean temperature gradient: -0.55 degrees celsius

Table 3
Differences between short and long sight length
refraction errors computed by 3 methods

From	To	Levelled	Sum	Kukkamaki (measured T)	Sum	Kukkamaki (predicted T)	Sum
		(mm.)	(mm.)	(mm.)	(mm.)	(mm.)	(mm.)
84L006	84L007	+0.15	+0.15	-0.59	-0.59	-0.63	-0.63
84L008	84L007	-1.40	-1.25	-0.82	-1.41	-0.59	-1.22
84L009	84L008	-4.05	-5.30	-1.18	-2.59	-1.39	-2.61
84L010	84L009	+1.05	-4.25	-0.42	-3.01	-0.34	-2.95
84L010	84L011	-0.33	-4.58	-0.31	-3.32	-0.43	-3.38
84L010	84L011	-0.80	-5.38	-0.39	-3.71	-1.18	-4.56
84L010	84L009	+0.25	-5.13	0.00	-3.71	-0.32	-4.88
84L009	84L008	-0.70	-5.83	-0.29	-4.00	-2.01	-6.89
84L008	84L007	+2.18	-3.65	-0.25	-4.25	-0.51	-7.40
84L006	84L007	+0.43	-3.22	-0.48	-4.73	-0.46	-7.86
84L036	84L006	-0.88	-4.10	-0.06	-4.79	-0.60	-8.46
84L036	84L006	+0.53	-3.57	-0.09	-4.88	-0.57	-9.03
84L006	84L007	+0.73	-2.84	-0.30	-5.18	-0.67	-9.70
84L008	84L007	-1.43	-4.27	-0.25	-5.43	-0.57	-10.27
84L009	84L008	-0.95	-5.22	-0.94	-6.37	-1.53	-11.80
84L010	84L009	+0.88	-4.34	-0.11	-6.48	-0.40	-12.20
84L010	84L011	-0.98	-5.32	-0.74	-7.27	-1.30	-13.50
84L010	84L011	-0.63	-5.95	-0.59	-7.81	-1.28	-14.78
84L010	84L009	-1.20	-7.15	-0.18	-7.99	-0.36	-15.14
84L006	84L007	+0.53	-6.62	-0.22	-8.21	-0.70	-15.84
84L036	84L006	+0.33	-6.29	-0.17	-8.38	-0.59	-16.43
84L036	84L006	-1.00	-7.29	-0.19	-8.57	-0.56	-16.99
84L006	84L007	+0.45	-6.84	-0.26	-8.83	-0.68	-17.67
84L009	84L008	-0.73	-7.57	-0.65	-9.48	-1.37	-19.04
84L010	84L009	-1.20	-8.77	-0.17	-9.65	-0.35	-19.39
84L010	84L011	-1.73	-10.50	-0.39	-10.04	-1.26	-20.65
84L010	84L011	-1.58	-12.08	-0.61	-10.65	-1.21	-21.86
84L010	84L009	+0.33	-11.75	-0.16	-10.81	-0.35	-22.21
84L009	84L008	-1.35	-13.10	-0.81	-11.62	-1.30	-23.51
84L036	84L006	+1.20	-11.90	-0.06	-11.68	-0.51	-24.02
84L006	84L007	+0.45	-11.45	+0.10	-11.58	-0.62	-24.64
84L010	84L009	-1.10	-12.55	-0.15	-11.73	-0.31	-24.95
84L010	84L011	+0.28	-12.27	-0.59	-12.32	-1.04	-25.99
84L010	84L011	+0.03	-12.24	-0.82	-13.14	-0.88	-26.87
84L010	84L009	-1.88	-14.12	-0.39	-13.53	-0.28	-27.15
84L036	84L006	+0.38	-13.74	-0.23	-13.76	-0.42	-27.57
Totals:			-13.74		-13.76		-27.57

temperature gradients and Kukkamaki's single-sight equation, and the refraction error derived from predicted temperature gradients using a temperature stratification model and Kukkamaki's single-sight equation. Figure 4 shows the results of the three methods.

PRECISION ANALYSIS

In order to validate the results obtained from the refraction test, a precision analysis was performed on the differences of elevation obtained from the levelling. This exercise was useful to determine if the systematic effect of refraction exceeded the envelope formed by the propagation of random errors as well as to assess the significance of the differences resulting from the comparison between the methods used to evaluate the refraction error.

The first step was to compute the standard error of an elevation difference for each sight length used. This was done by grouping all the setups that had sight lengths of 20 to 30 metres in one group and all the ones with sight lengths of 40 to 50 metres in another. The differences of elevation for small and large scale on each setup were compared in order to estimate the precision of the elevation difference resulting from each sight length. Histograms were also produced (figures 2 and 3) to show the distribution of the observations. Standard deviations of .17 and .29 millimetre were obtained for sight lengths of 20-30 and 40-50 metres respectively.

These estimates of precision for each setup were subsequently used in a random error propagation process to determine the total accumulation of random errors along the levelled line. The random error propagation formulas were the following:

$$S_{DDH}^2 = S_{DHL}^2 + 2 S_{DHS}^2 = (.29)^2 + 2 \times (.17)^2 = .14 \text{ mm.}^2 \quad (4)$$

where:

- S_{DDH} = Standard error on difference of difference of elevation (DDH) for one dual independent setup
- S_{DHL} = Standard error on difference of elevation for one long sight length setup
- S_{DHS} = Standard error on difference of elevation for one short sight length setup

The standard error of the total accumulated refraction error resulting from 387 dual independent setups (34.6 kilometres of levelling) was then equal to:

$$S_{DDH}^2(\text{total}) = 387 \times S_{DDH}^2(\text{setup}) = 387 \times .14 = 54.2 \text{ mm.}^2 \quad (5)$$

$$S_{DDH}(\text{total}) = 7.4 \text{ mm.}$$

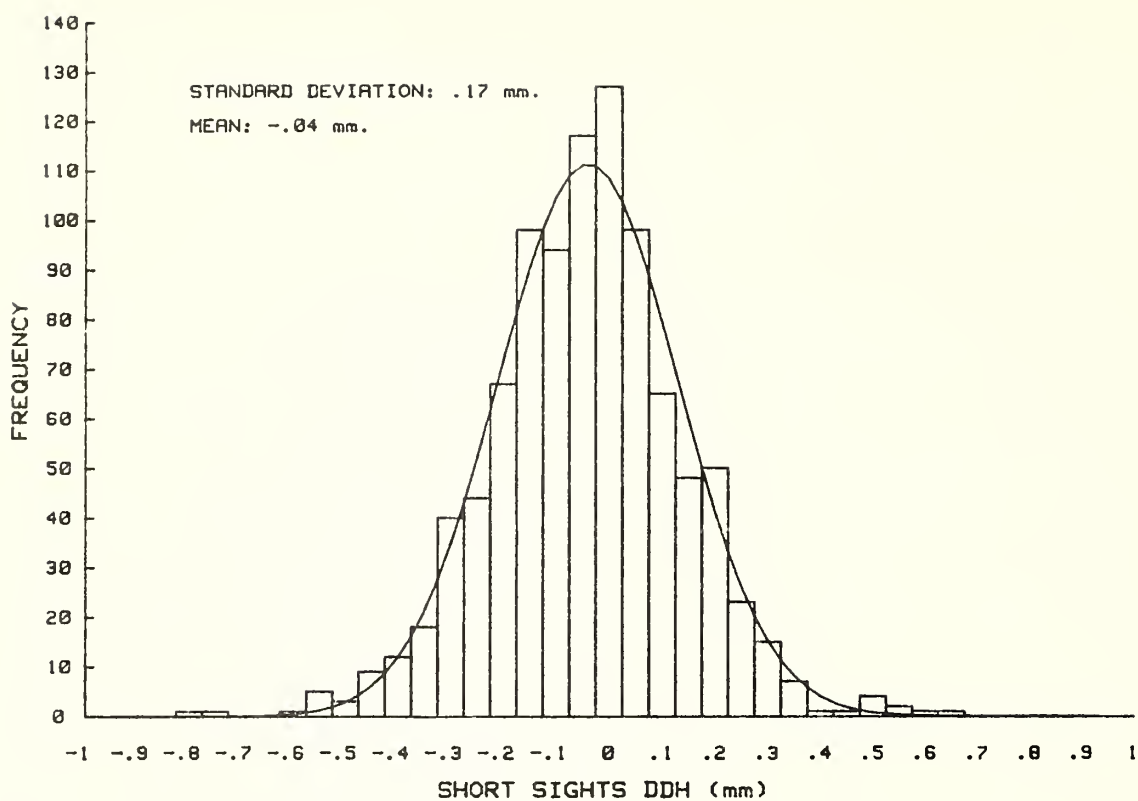


Figure 2.
Frequency distribution: DDH's between small and large scales
for short sight length setups

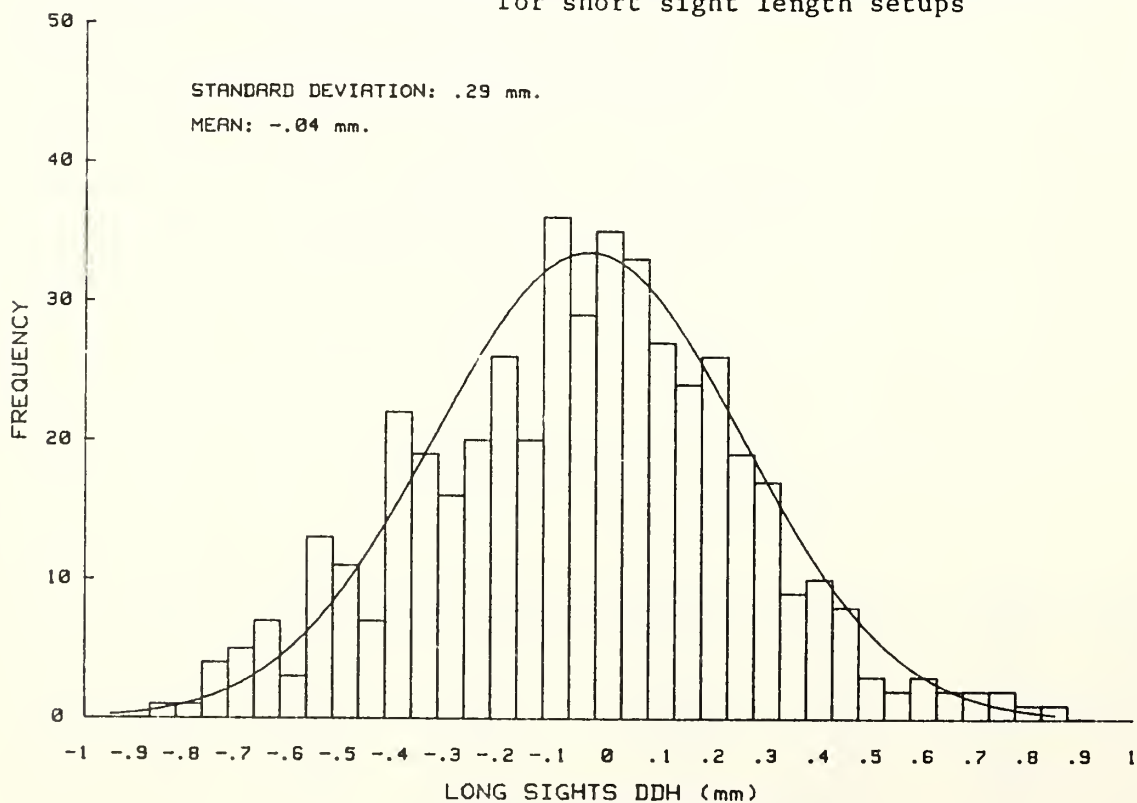


Figure 3.
Frequency distribution: DDH's between small and large scales
for long sight length setups

REFRACTION TEST - COMPARISON

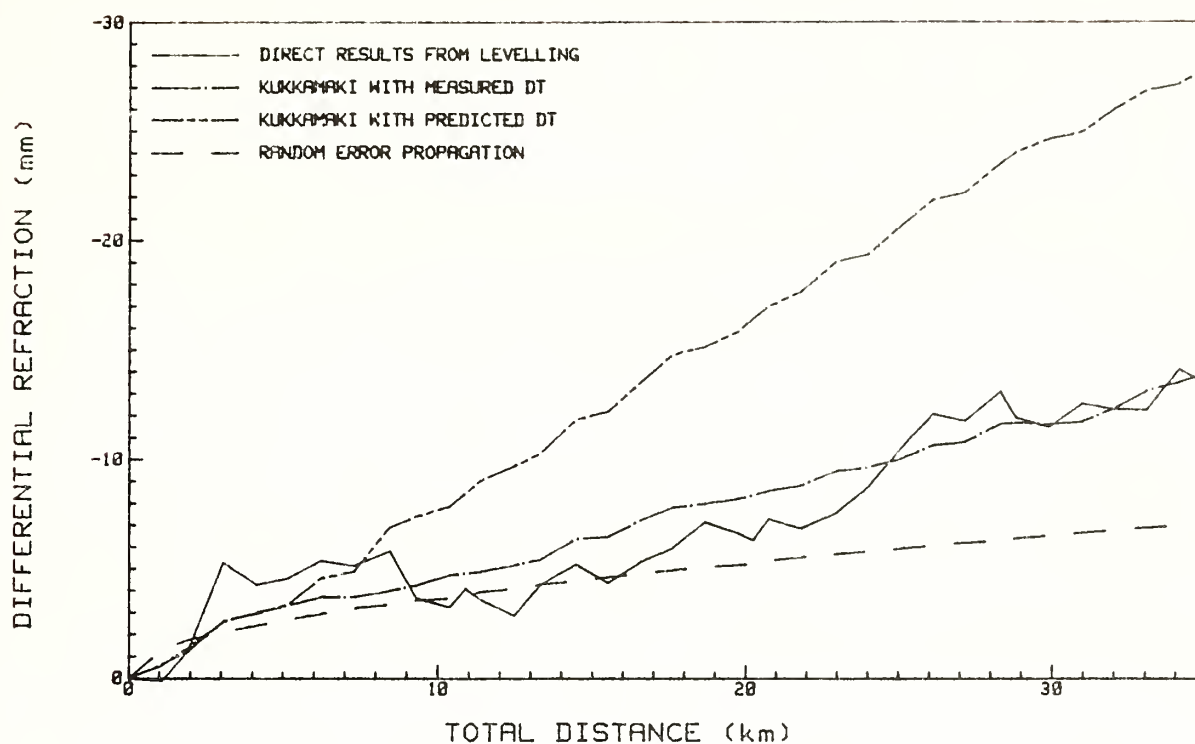


Figure 4.
Accumulated differences between short and
long sight length refraction errors using 3 methods

The propagation of random errors versus the accumulated measured differential refraction error are reported on figure 4. We can see that at a 68% confidence level, the systematic error due to refraction exceeds the envelope formed by the propagation of random errors.

If we use the estimate of the total standard error as a measure of the confidence we have in the differential refraction error determined directly from levelling, we can see that at a 68% confidence level, the refraction error computed using measured temperature gradients fell well within the confidence region of the levelling. The refraction error obtained using predicted temperature gradients did not agree with the levelled value at a 68% confidence level.

CONCLUSION AND DISCUSSION

The agreement obtained between levelled refraction error and Kukkamaki's equation using measured temperature gradients is a good indication that the apparatus presently used by PVCS to measure the temperature gradient is adequate. The significant difference existing with the predicted temperature gradients used in Kukkamaki's equation suggest that further investigation is required. The addition of certain parameters such as ground albedo and moisture are obvious improvements that could be made. The possibility of adapting Holdahl's surface fitting technique to the Canadian context or of using Holdahl's present model and adding meteorological data from Canadian weather stations could be considered.

Under conditions similar to the ones experienced in this test, the refraction error is of the order of 1 millimetre per kilometre of levelling for sight lengths of approximately 45 metres. Further analysis should be carried out using temperature data collected in the past to ensure that this data sample is representative of the Canadian environment.

BIBLIOGRAPHY

- Holdahl, S.R., 1982: A model of temperature stratification for correction of leveling refraction, Proceedings of the General Meeting of the IAG, Tokyo, 1982.
- Kukkamaki, T.J., 1939: Formulas and tables for computation of leveling refraction, Publication of Geodetic Institute, No. 27, Helsinki, Finland.
- Whalen, C.T., 1981: Results of leveling refraction test by National Geodetic Survey, NOAA Technical Report NOS 92 NGS 22.
- Whalen, C.T., Strange, W.E., 1983: The Saugus to Palmdale, California, leveling refraction test, NOAA Technical Report NOS 98 NGS 27.

THEORETICAL MODELS, PRACTICAL EXPERIMENTS
AND THE NUMERICAL EVALUTION OF
REFRACTION EFFECTS IN GEODETIC LEVELING

Rainer Heer
Wolfgang Niemeier

Geodätisches Institut
Universität Hannover
Nienburger Straße 1
3000 Hannover 1
Bundesrepublik Deutschland

ABSTRACT. In the first part of this paper theoretical comparisons of various models for leveling refraction are given and the precision of underlying meteorological parameters is discussed. Then some special instrumentation for the section wise determination of refraction effects is presented and first measuring results with this equipment are given. Finally the application of different refraction models on the leveling test loop Koblenz and the NGS test line Saugus-Palmdale, Cal., is discussed.

1. INTRODUCTION

Geometric leveling is one of the most precise geodetic leveling techniques; it is, however, extremely sensitive to systematic errors. As a great number of instrument setups and rod readings are required to get the desired observation - the raw height difference between two benchmarks - even small systematic errors within the individual readings may be of influence on the result. The elimination of systematic errors has therefore been among the main problems in precise leveling for a long time.

Besides the magnetic effects on automatic levels (e.g. Rumpf & Meurisch 1981, Beckers 1983) and the settlement of instrument and rods (e.g. Kukkamäki 1980, Lindstrot 1981) the leveling refraction effect is still of primary importance. Theoretical investigations for studying leveling refraction can be traced back to the last years of the 19th century. In general geodesists developed and applied refraction models in a very slow manner. Sometimes more than one decade was necessary to create and/or verify a new refraction formula. But within the last decade a remarkable number of refraction models was presented, based on different meteorological assumptions or descriptions on the physical behaviour of the lower atmosphere. A short description of some of the well-known refraction models is given in section 2.

For all models refraction correction have to be computed. For this computation additional data have to be measured or estimated parallel to the leveling observations. It can be shown (see section 3) that temperature information in different heights above grounds is the main factor for computing refraction correction and that all measured temperature differences should have a precision of about 0.02°K .

Besides the precision the representativity of temperature observations will be discussed in this paper. In principle, one can distinguish between different kinds of representativity:

- in time : one (mean) observation for each sight, set-up or section parallel to the leveling observations,
- in space : one (mean) observation for each sight, set-up or section parallel to the leveling observations,
- in height : 2 , 3 or more (e.g.5) temperature sensors to describe the meteorological conditions.

Short periodic fluctuations may have an influence on the set-up data, while the "mean" temperature field for a section may be considered to be too general for computing refraction corrections. From a practical point of view it's time consuming and expensive to carry out temperature observations for each set-up parallel to the leveling field operation, as the temperature sensors are relatively slow and additional staff handling the equipment would be required. The use of more than the till-now used number of 2 or 3 sensors allow a statistical treatment of the computed refraction correction. Here again a section - wise treatment with a registration over a longer period of time seems to be advantageous. All these aspects will be discussed for leveling data of the leveling test loop Koblenz and the line Saugus-Palmdale.

2. REFRACTION MODELLING

There are different principles to treat leveling refraction effects. Lucht (1971) and Fawaz (1981) tried to model refraction effects as correlations in the stochastic model of adjustment and Remmer (1980) applied a statistical method to estimate the refraction effect in network. The model discussed here belong to the class of deterministic or correction models, as here out of a set of physical parameters refraction corrections for the raw leveling observations are computed.

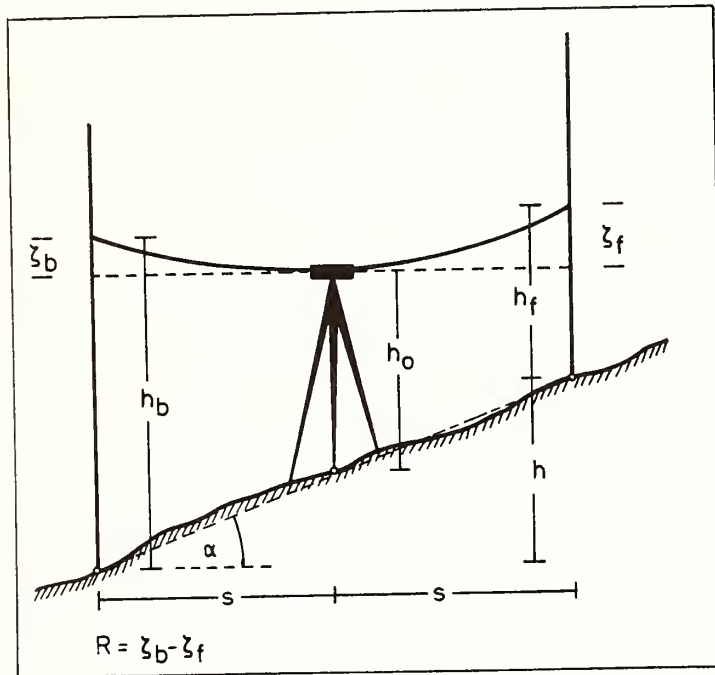
All models that are using this deterministic approach, can be divided into three main groups. The refraction correction can be computed by using

- i) directly measured temperature differences and a characteristic temperature-height-function (HUGERSHOFF, 1907, KUKKAMÁKI, 1938/39, REISSMANN, 1954, BÖHM, 1959, VISCOCIL, 1983, HEER, 1984) and additionally (GARFINKEL, 1979). The models are based on the assumption of isothermic surfaces parallel to the ground.
- ii) directly measured temperature differences and the temperature gradient dt/dz (BROCKS, 1948, FAWAZ, 1981, PELZER, 1982, MOZZUCHIN, 1977). The models are based on asymmetric ray curvature studies and the eikonal equation for the path of a light wave (MORITZ, 1967).
- iii) temperature measurements for calculating the gradient of the potential temperature. In this case the gradient is expressed in terms of meteorological and geometrical parameters, i.g. the azimuth of the level line and the sun, the zenith distance of the sun and the upward turbulent sensible heat flux (MONIN-OBUCHHOV, 1954, ANGUS-LEPPAN, 1979, HOHLDAHL, 1981)

The objective to apply numerous of these -standard - formulae for estimating the refraction effect is to show the range of the different models and to give an idea on the achievable reliability of refraction corrections.

2.1 REFRACTION MODELS WITH TEMPERATURE HEIGHT - FUNCTIONS

The basic assumption for the determination of the formulae in this section is the model of isothermic surfaces parallel to the ground, see Fig. 1.



The elementary sight deviation, resulting from different refractive indices from one isothermic layer to another as a function of change in temperature is derived on base of the law of Snellius.

The basic equation for computing refraction correction with different temperature-height-functions is derived from this model.

Kukkamäki (1938) and Reissmann (1954) found:

$$R = \cot^2 \alpha \cdot K \int_{h_o}^h \Delta t \cdot dh \quad (1)$$

where

- R : Refraction Correction
- h_o : height of the level
- h : staff reading
- Δt : temperature difference, expressed by characteristic temperature-height-functions
- dh : integration variable along the line of sight
- K : change in refractive index n for a change of 1° in temperature

The following table shows the different temperature-height-functions for defining the temperature variations near the ground with the corresponding authors.

Model No.	Function/Hypothesis	Author
1	$t=a+b\cdot h^2$	HUGERSHOFF, 1907
2	$t=a+b\cdot h+c\cdot h^2$	REISSMANN, 1954
3	$t=a+b\cdot h+c\cdot h^2+d\cdot h^3$	REISSMANN, 1954
4	$t=a+b\cdot h+c\cdot h^2+d\cdot h^3$	VISKOCYL, 1983
5	$t=a+b\cdot h+c\cdot h^2+d\cdot h^3$	BOEHM, 1959
6	$t=a+b\cdot h+c\cdot h^2+d\cdot h^3+e\cdot h^4$	REISSMANN, 1954
7	$t=a+b\cdot h^c$	KUKKAMAEMI, 1938
8	$t=a+b\cdot \exp(c\cdot h)$	HEER, 1984

TABLE 1: Different temperature-height-functions and corresponding authors

where

t : temperature
 a, b, c, d, e : parameters or coefficients of the functional models, varying with time
 h : height above the surface

Substituting in (1) and integrating leads to the following correction formulation for a single level setup, shown in table 2.

No.	Refraction Correction Formulae
1	$R = (s^2 \cdot K \cdot b \cdot dh) / 3$
2	$R = (s^2 \cdot K \cdot c \cdot dh) / 3$
3	$R = s^2 \cdot K \cdot [(c \cdot h_0) / 3 + d \cdot h_0] \cdot dh$
4	$R = (K \cdot s^2 \cdot dh \cdot [c + 3 \cdot d \cdot h_0]) / 2$
5	$R = (31 \cdot s^2 \cdot dh \cdot [c + 3 \cdot d \cdot h_0]) / 10^8$
6	$R = s^2 \cdot K \cdot (c / 3 + d \cdot h_0 + e \cdot [dh^2 / 20 + 2 \cdot h_0^2])$
7	$R = \cot^2 \alpha \cdot K \cdot b \cdot (1 / (c + 1) \cdot [hb^{c+1} - hf^{c+1}] - h_0^c \cdot dh)$
8	$R = \cot^2 \alpha \cdot K \cdot b \cdot (1 / c \cdot [\exp(c \cdot hb) - \exp(c \cdot hf)] - \exp(c \cdot h_0) \cdot dh)$

TABLE 2: Refraction corrections based on different temperature-height-functions (see table 1)

where s : sight length [m]
 dh : measured elevation difference
 h_f, h_b : staff readings - forward, backward -

In table 2 a lot of different refraction corrections are shown and it is easy to see that it is very difficult to approximate the temperature behaviour in this deterministic manners of "fixed" temperature height functions.

2.2 REFRACTIVE ERROR AS A FUNCTION OF THE VERTICAL TEMPERATURE GRADIENT

BROCKS found that the curvature of rays of light near the earth's surface, especially for a level setup is given by

$$\kappa = - \frac{\partial n}{\partial h} = \alpha_1 \frac{\partial P}{\partial h} - \alpha_2 \frac{\partial T}{\partial h} - \alpha_3 \frac{\partial e}{\partial h} \quad (2)$$

where

$\partial n / \partial h$: gradient of refractive
 $\partial P / \partial h$: gradient of air pressure
 $\partial e / \partial h$: gradient of vapor pressure
 $\partial T / \partial h$: gradient of air temperature

and neglecting the gradients of air and vapor pressure we have finally

$$\kappa = f \left(\frac{\partial T}{\partial h} \right) \cdot \alpha_2 \quad ; \quad \alpha_2 = -.98 \quad (3)$$

Modelling the temperature gradient $\partial T / \partial h$ (BROCKS, 1948)

by

$$\partial T / \partial h = a \cdot h^b \quad ; \quad a < 0, b < 0 \quad (4)$$

where

\hat{a} : temperature gradient for $h = 1m$
 h : height above the ground
 \hat{b} : parameter, constant, can be assumed as ~ -1

The value of \hat{a} depends on daily and yearly variations and is a function the zenith distance of the sun.

Based on the unified theory of geodetic refraction the path of a light wave was described by eiconal equations (Moritz, 1967)

$$R = \int_0^s \frac{dn}{dh} \cdot x \cdot dx \quad (5)$$

where n : refractive index
 x : lenght of the line of sight

Substituting dn/dh in terms of pressure and the given temperature gradient \hat{a} different refraction corrections formulations were given in Table 3 with corresponding authors.

No.	Refraction Correction Formulae/Author
9	$R = (-79.1264 * P * s^2 * \hat{a} * dh) / (T^2 * (hb + ho) * (hf + ho))$ MOZZUCHIN, 1977
10	$R = (.16 * s^3 * \hat{a} * \tan \alpha) / 10^6$ FAWAZ, 1981
11	$R = (.98 * \hat{a} * \cot^2 \alpha * G) / 10^6$ $G = [ho * \ln((1 + s * \tan \alpha / ho) / (1 - s * \tan \alpha / ho))] + s * \tan \alpha * \ln(1 - s^2 * \tan^2 \alpha / ho^2) - 2]$ PELZER, 1982
12	$R = (s^2 * 503 * P * ho^{(\hat{b}-1)} * \hat{a} * \hat{b} * dh * f_{II}) / (6 * r * T^2)$ $f_{II} = 1 + \sum 2 * (\hat{b}-1) \dots (\hat{b}-2 * n) * q^{(2 * n)} / (2 * n + 3)!$ $q = (hb - 1) / ho = (1 - hf) / ho$ BROCKS, 1948

where

P : air pressure [mbar]

T : temperature [$^{\circ}$ K]

\hat{a}, \hat{b} : parameters of
Brocks's Function

r : radius of the earth

TABLE 3: Refraction correction formulae for a single level setup by using the vertical temperature gradient \hat{a}

2.3 ANOTHER REFRACTION MODELLING

Additionally to chapter 2.1 another model for computing refraction corrections using directly measured temperatures was published in WHALEN, 1980 developed by GARFINKEL, 1978/1979.

No.	Refraction Correction Formulae/Author
13	$R = (-.00107 * P * s^2 * dt'' * dh) / (T * 6 * a^2)$ $dt'' = t_3 - 2 * t_2 + t_1$ GARFINKEL, 1978/79

2.4 TURBULENT TRANSFER MODELS

WEBB, 1968 demonstrated and showed geodesists that it might be practicable to compute temperature gradients in terms of other important meteorological parameters. His ideas are based on theories of atmospheric turbulence and heat balance in the lowest layers of the atmosphere.

Therefore it is necessary to distinguish two atmospheric conditions, unstable and stable, with an intermediate neutral state. When the surface is heated by radiation convection carries heat upwards in form of turbulent eddies of air. The atmosphere is being mixed and unstable, the temperature gradient is negative. This is the most typical case for the leveling situation and the relationship to temperature gradient has been found by

$$\frac{d\theta}{dh} \sim \frac{dT}{dh} = - \left\{ \frac{H^2 T}{(c_p \rho)^2 g} \right\}^{1/3} \cdot h^{-4/3} \quad (6)$$

where

$d\theta/dh$: gradient of the potential temperature

H : upward heat flux due to convection

C_p : specific heat at constant pressure
of the air

ρ : density of the air

g : acceleration due to gravity

In the height range of leveling the difference between actual and potential temperature gradient is negligible.

The upward heat flux H as one of the most significant meteorological parameters cannot be measured directly. The difficulty is to estimate H with an acceptable accuracy and reliability. Three possible ways can be given:

- i) Heat flux is a component of the energy at the ground surface.
The energy as a result of radiation effects reaching the surface must be balanced by the energy as a result of reflectivity.
The net radiation at the surface is given by

$$Q = (S_r + S_k + A_t) - (E_r + R_s + R_a) = V + H + B \quad (7)$$

where

Q : net radiation

S_r : direct sun's radiation

S_k : sky-radiation

A_t : atmospheric radiation

E_r : ground reflection

R_s : reflected sun and sky radiation

R_a : reflected atmospheric radiation
 $S_r + S_k - R_s$: short wave part
 $A_t - E_r - R_a$: long wave part
 $S_r + S_k$: global radiation
 V : latent heat in vaporisation of surface moisture
 B : heat conducted into the ground

so we have finally for the heat flux the equation

$$H = Q - V - B \quad (8)$$

- ii) Estimation of H in relation to its main parameters
(ANGUS - LEPPAN, 1979)

$$H = 450 \cdot C \cdot W \cdot \cos \zeta \quad (9)$$

where

C : factor for cloud cover
 W : factor for surface wetness
 ζ : sun's zenith distance

This model is best suitable for practical work, as no additional equipment is necessary. The crew leader has to estimate the parameters C and W and to store these factors in this manual. The precision of this rule of thumb for estimating H is low and - more dangerous - the estimates by the observer can be checked, i.e. there is no reliability.

- iii) Direct estimation by using measured temperatures in different heights.
From integration of equation (5) HOLDAHL, 1981 found the following expression.

$$t = t_0 + 3 \cdot \left\{ \frac{H^2 T}{(c_p \rho)^2 g} \right\}^{1/3} \cdot (h^{-1/3} - h_0^{-1/3}) \quad (10)$$

which can be easily transformed for computing the heat flux.

Following from equation (5) the last refraction correction formulation, developed by ANGUS-LEPPAN, 1979, for a single level setup was given.

No.	Refraction Correction Formulae
14	$R = (.0398 \cdot \cot^2 \alpha \cdot H^{(2/3)} \cdot (3 \cdot [h_b^{(2/3)} - h_f^{(2/3)}] - 2 \cdot h_o^{(-1/3)}))$

3. ON THE INNER PRECISION OF REFRACTION CORRECTIONS

3.1 Required precision for temperature measurements

In section 2 different models are presented to compute refraction corrections out of certain parameters, which describe the physical conditions in the lowest few meters of the atmosphere. In Janietz (1984) detailed studies are carried out on the error propagation within these models, i.e. on the dependency of these correction formulae on the accuracy of the underlying meteorological parameters and the leveling observations. It was found out that the influence of possible errors of e.g. air pressure, rod readings, height difference of temperature sensors or height of instrument are neglectable, compared with the influence of errors in the temperature measurements. It was shown that for the computation of significant refraction corrections the temperature measurements should have a precision σ_t of

$$\sigma_t < 0.02^\circ \text{ K} \quad (11)$$

This accuracy for temperature measurements can be achieved with the Advanced-Temperature-Measuring-System (ATMS), described in section 4.

3.2 EFFORT OF A MULTIPLE SENSOR SYSTEM

In usual temperature measuring systems only the minimum number of temperature sensors (2 or 3) are used, just to be able to compute the temperature functions required for the refraction correction formulae 1 - 14, as given in section 2.

Using more than three temperature sensors one gets a better insight into the temperature distribution of the lowest layer of the atmosphere. Further, it is now possible to compute the variance S_R^2 of any refraction correction by applying the usual law of error propagation

$$S_R^2 = s_0^2 \mathbf{F} \mathbf{Q}_{xx} \mathbf{F}^T \quad (12)$$

where

$$\begin{aligned} s_0^2 &: \text{variance of unit weight} \\ &\quad (\text{accuracy of temperature measurements at one point}) \\ \mathbf{F} &: \text{vector of partial derivatives} \\ \mathbf{Q}_{xx} &: \text{cofactor matrix of the unknown} \\ &\quad (\text{e.g. coefficients of the temperature height function,} \\ &\quad \text{temperature gradient, heat flux}) \end{aligned}$$

With known s_R the significance of a refraction correction R can be tested using the ratio R/s_R as test statistics and applying the well-known t-test. For all computations in section 4 this significance test was carried out. For the Test Loop Koblenz and the line Saugus-Palmdale the refraction corrections of each model turned out to be significant.

4. REALIZATION OF PRECISE TEMPERATURE MEASUREMENTS USING THE ADVANCE - TEMPERATURE - MEASURING - SYSTEM

As shown in chapter 3.1 before it is necessary to realize a accuracy of temperature measurements better than 0.02° K .

For studying the effectiveness of refraction corrections under reliability and accuracy aspects in consideration of the variations of meteorological parameter, especially in the temperature field, the Advanced - Temperature - Measuring - System

(ATMS) was created in (1981) and financed by the German Research Council (DFG) in 1983. In Figure 2, the components of this equipment are depicted.

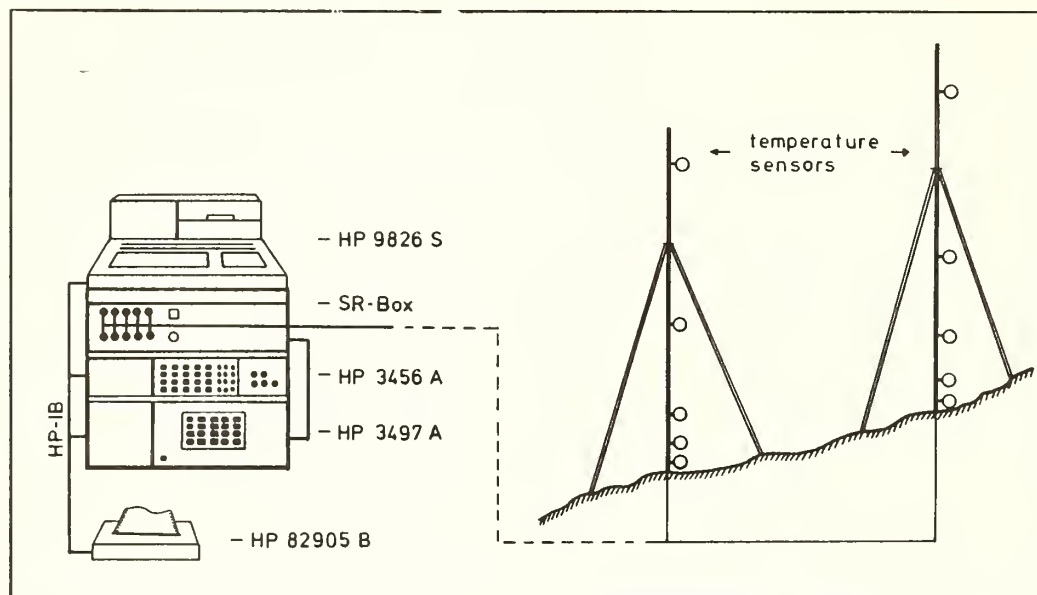


FIGURE 2: Components of the Advanced-Temperature-Measuring - System (ATMS) with an accuracy of better than 0.02°K

The different components are:

- HP 9826S : Desk-top computer with Floppy-Disc-Drive and a storage capacity of 1.6 M Byte. Programming languages are BASIC and PASCAL. Works like a controller in real-time processing.
- HP 82905B : matrix-printer for data-output and graphic sketches.
- HP 3456A : Fully guarded integrating voltmeter with 10ppm basic accuracy and $6\frac{1}{2}$ digits.
- HP 3497A : Data Acquisition / Control unit combines precision measurement capability with process monitoring and control functions. Resistance measurement compensation. These components are connected by HP-Interface bus for easy processing and standard input/output operations. This system is powered by 220 V.
- SR-Box : contains circuits for the power supply of the temperature sensors and a standard resistor (1000 ohm) of high precision (0.001 %) for compensating voltmeter effects.
- Temperature: ten air temperature-sensors mounted in different heights above
Sensors the ground are available for two stations. Each temperature sensor consisted of a 500 ohm RTD as a primary element and a 500 ohm standard resistor of high precision (0.01 %) for compensating outer effects, mounted within a tubular metal shield, which was mounted within a second tubular metal shield. The outer shield was polished for compensating radiation effects. A small fan was attached to each sensor for drawing air past the RTD.

Using adequately calibration functions for the RTD a temperature value was

computed. It is possible to realize numerous sampling rates for getting temperature values with an accuracy better than 0.01 K as an output from precise electronic measuring techniques.

This equipment allows very precise temperature observations, but it was not developed for mobile use, i.e. temperature measurements for each set-up. Extended testing was performed with more stationary use, i.e. by positioning the ATMS in a location characteristic for one (or more) section and measuring the temperature distribution during the whole observation period.

5. PRACTICAL APPLICATIONS OF MODERN TEMPERATURE MEASUREMENTS AND AVALUATION TECHNIQUES

5.1 Leveling Test Loop Koblenz

Since 1980 the lines of the German first order leveling network have been observed by the different surveying authorities of the Federal Republic of Germany. For the purpose of quantitative and qualitative studies of errors in leveling the Working Committee "Precise Leveling" decided to install a leveling Test Loop, which was to be observed before and after each yearly measuring period by each crew. The leveling Test Loop Koblenz is situated near the river Rhine in the Federal State Rhineland - Palatinate and depicted in Fig. 3.

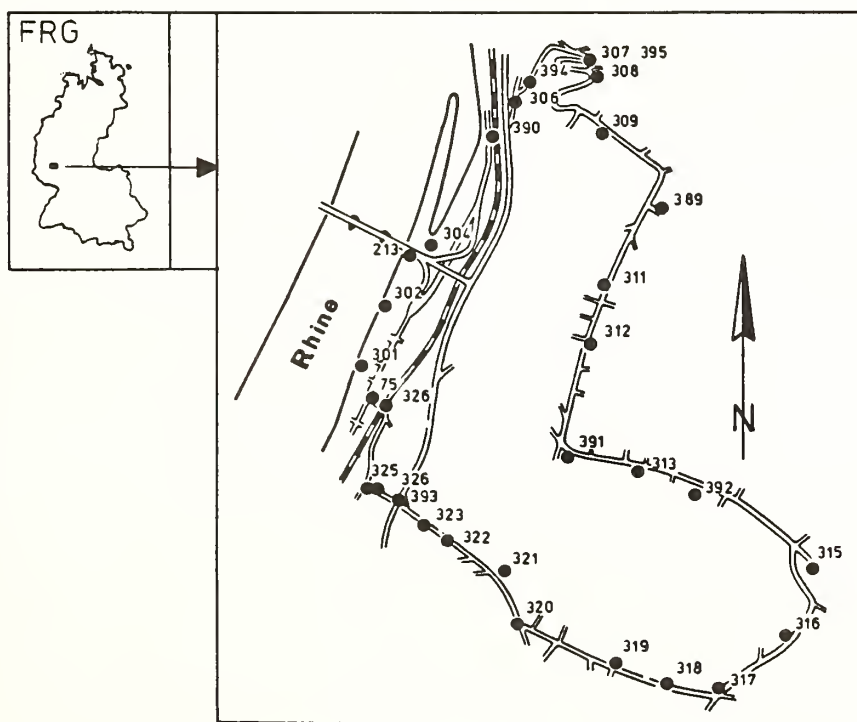
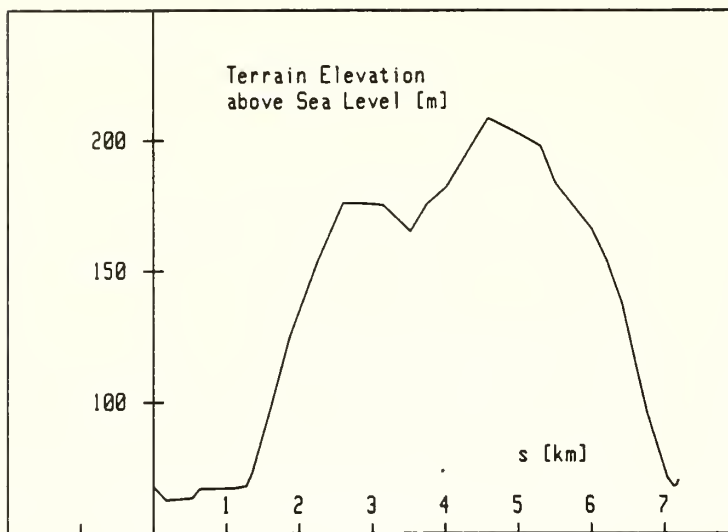


Figure 3: Leveling Test Loop Koblenz

The sketch below illustrates the ground profile of this loop. The height difference is about 146 m and the length of the loop is nearly 7.1 km with a maximum ground slope of 13 percent and a shortest sightline of 4 m. The loop consists of 31 sections. The rod stations are signed by fixed steel rivets in the ground for eliminating the rod movements.



Since 1978, fifty-five complete observations have been made. In Fig. 5 the differences from the mean values are depicted showing a bandwidth of nearly 8 mm from the lowest curve to the highest one. The source of this comparison is leveling data, rectified by rod calibration values and temperature corrections on account of the extension of the invar rod.

FIGURE 4: Ground Profile of the Leveling Test Loop

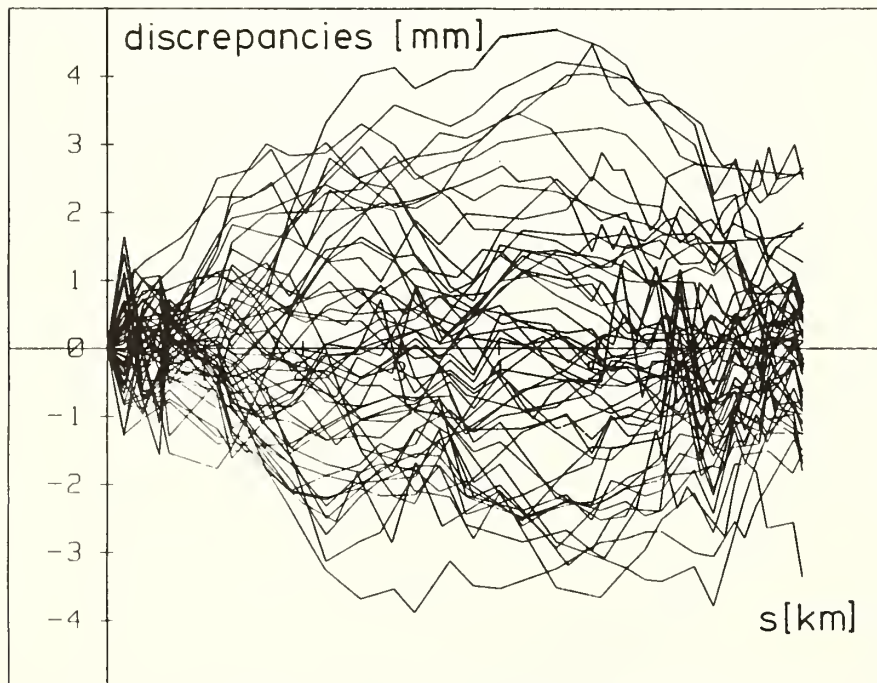


FIGURE 5: Leveling Discrepancies on the Leveling Test Loop

Noticing the high correlation between ground slope and these discrepancies it can be assumed that different refraction effects falsify the measuring results in a systematic way. The discrepancies cannot be explained by possible magnetic effects on the short N - S - sections within this loop. Further informations about this

problems are given in FREVEL, 1983 and HEER, 1983.

Detailed refraction studies were started at 1980 until now with different equipment for the determination of temperatures and other meteorological parameters. In 1983 we had the possibility to carry out precise temperature measurements with the ATMS - equipment as described in section 4. Additionally air pressure, cloud types, surface wetness, surface temperature and sun radiation were registered. The temperature station were changed every day. A typical situation of a measuring place is depicted in Fig. 6 below.

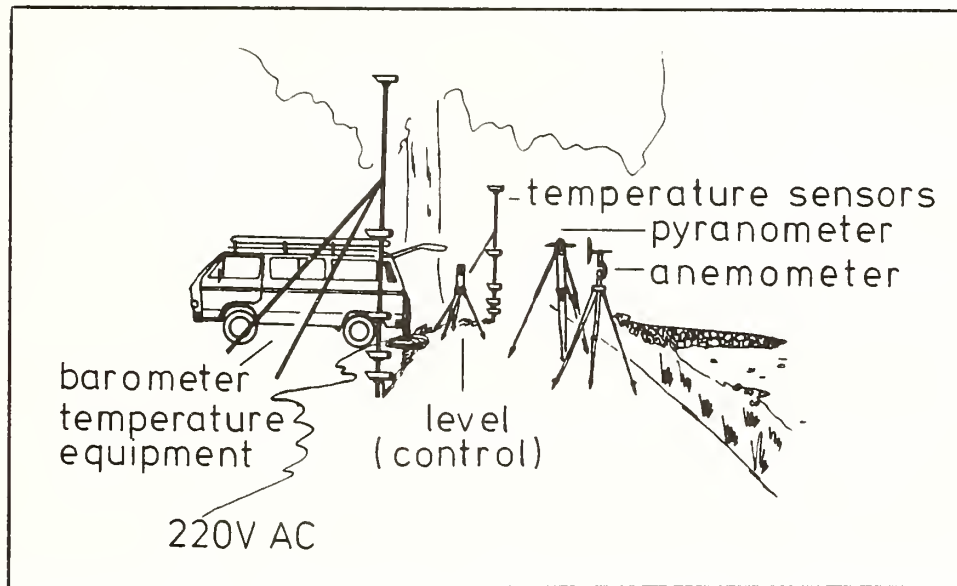


FIGURE 6: Temperature Measurements on the Leveling
Test Loop Koblenz (situation: near by point 301
at the river rhine)

The temperature measurements were used for computing the main parameters of the refraction models No 1 - 14, by using least-squares-techniques. Table 4 illustrates the values and corresponding standard deviations of the main parameters and its changes between two measuring periods on the Leveling Test Loop Koblenz.

No./Parameter	september	october	standard deviation	dimension
1-8 K	$-.993 \cdot 10^{-6}$	$-1.017 \cdot 10^{-6}$	$3 \cdot 10^{-9}$	$1/K_2$
1 b	$-.018$	$-.062$	$.013$	K/m_2
2 c	$.095$	$.202$	$.052$	K/m_2
3,4,5 c	$.810$	1.830	$.276$	K/m_3
d	$-.117$	$-.383$	$.046$	K/m_2
6 c	2.304	-----	-----	K/m_3
d	$-.816$	-----	-----	K/m_4
e	$.097$	-----	-----	K/m
7 b	$.369$	$.283$	so .004 K	K/m
c	-1.006	-1.363	-----	-----
8 b	2.871	2.409	so .004 K	K
c	-3.534	-3.490	-----	$1/m$
9,10,11 a	$-.268$	$-.290$	$.004$	K/m
12 a	$-.268$	$-.290$	$.004$	K/m
b	-1.518	$-.918$	$.038$	-----
13 dt"	$.196$	$.238$	$.007$	K
14 H	120.97	157.36	3.61	W/m^2

TABLE 4: Parameters of Refraction Correction Models
Dimension and Standard Deviation

The following Fig. 7 shows the approximated temperature-height-functions of one day (20-10-83).

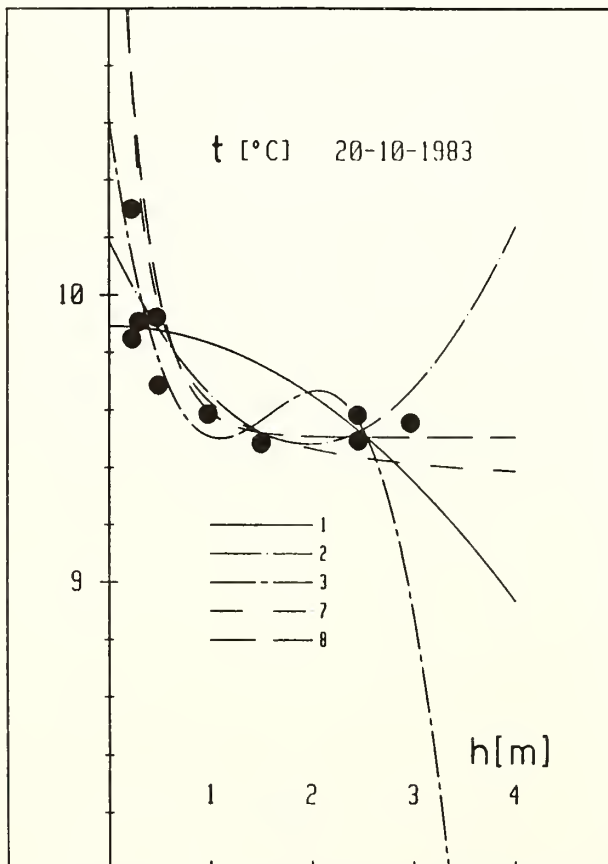


FIGURE 7: Daily temperature height functions
(20-10-83)

The corresponding variations of the temperature gradient and the daily variations of the estimated heat flux are shown in Fig 8.

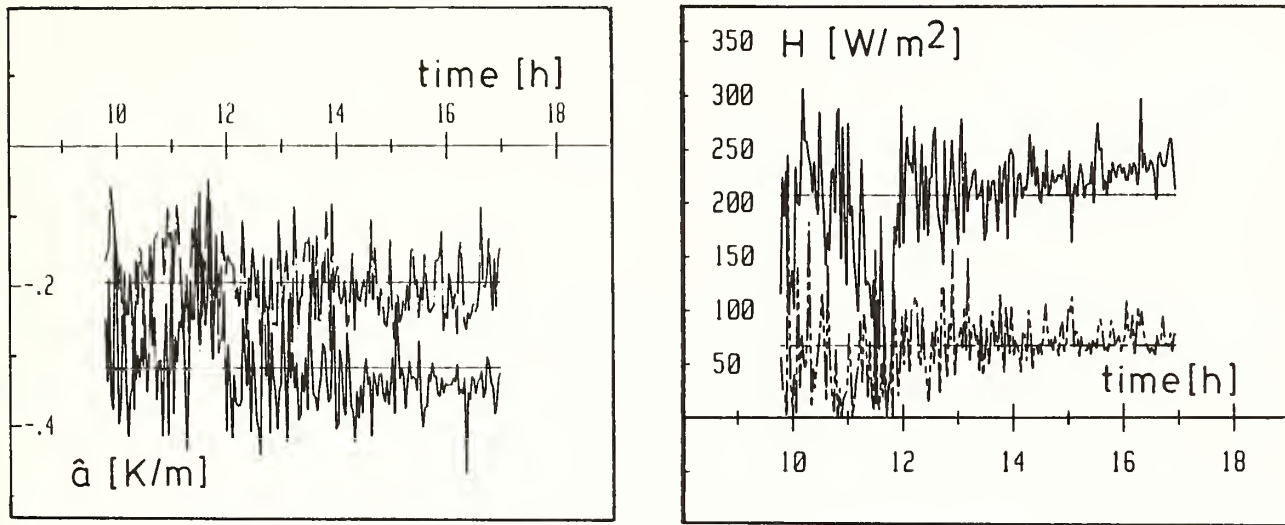


FIGURE 8: Daily variations of the temperature gradient and the heat flux on the Leveling Test Loop Koblenz (20-10-83)

The refraction modelling leads to typical so called "trend functions" of the different refraction corrections formulations of the level sections (not setups) as a systematic effect. These functions are depicted as summed-up values of the refraction corrections in Fig. 9.

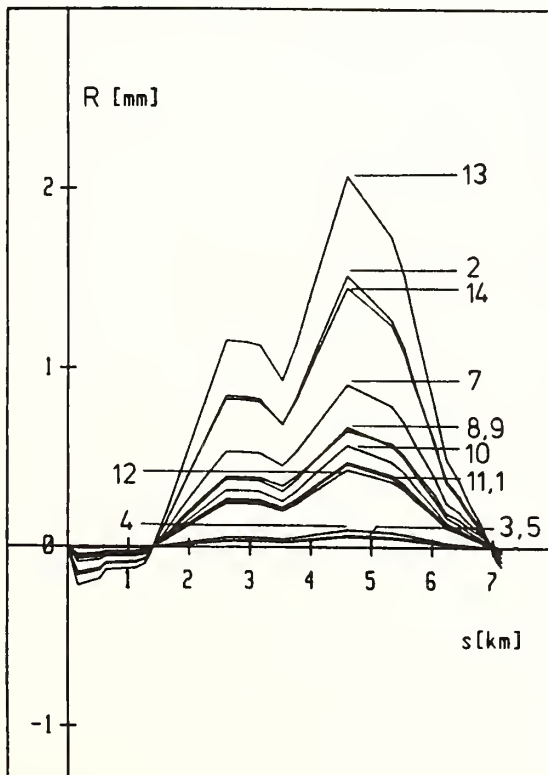


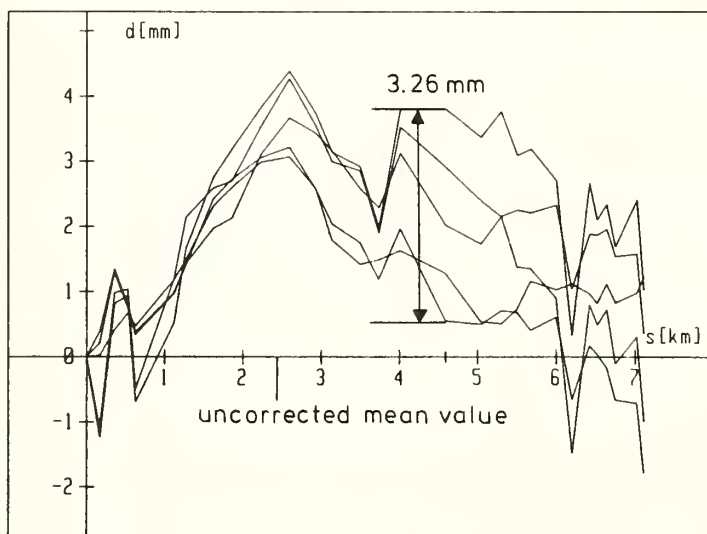
FIGURE 9: Summed-up Refraction Corrections (October 1983)

The maximum height changes appears at the highest point of the loop. These values of the two measuring periods are given in table 5

No.	1	2	3	4	5	6	7	8	9	10	11	12	13	14
september	.16	.82	2.17	3.25	2.03	.55	1.01	.94	.72	.59	.51	.62	1.32	1.48
october	.46	1.52	.06	.10	.06	---	.91	.65	.67	.57	.47	.43	2.07	1.45

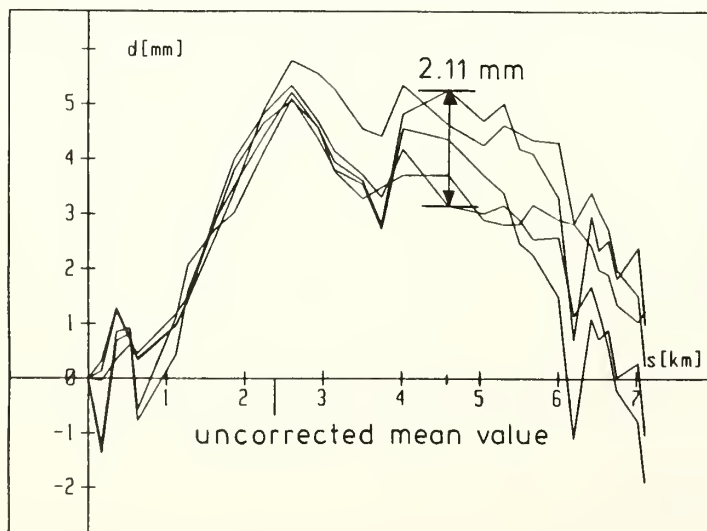
TABLE 5: Maximum Refraction Influence on the Leveling
Test Loop Koblenz in [mm] at point 315 (4,6 km)

In this case it is easy to see that there are great differences by modelling with fixed temperature height functions, especially with polynomials (degree > 2). Under the reliability point of view it seems to be impossible to approximate the complex temperature behaviour by these functions (Mod. 3,4,5,6), also seen in Fig. 7. The other values show in consideration to the Leveling Test Loop Koblenz typical differences based on the hypothesis in refraction modelling. The comparison of five corrected measurements (1980-1983) by Model No 14 (ANGUS-LEPPAN) leads to reduced discrepancies at the highest point. Fig. 10 illustrates this fact in a more adequate way.



uncorrected
elevation differences

FIGURE 10: Comparison of
Measurements
corrected by
Refraction
(Model No. 14
ANGUS-LEPPAN)



corrected
elevation differences

5.2 REFRACTION STUDIES ON THE SAUGUS TO PALMDALE SURVEY ROUTE

Because of the significant impact of the application of refraction corrections on the evaluation of crustal movement in southern California a refraction test had to be carried out along a leveling line that was essential to the interpretation of the proposed southern California uplift. The U.S. Geological Survey and the National Geodetic Survey (NGS) participated in a joint refraction test along the leveling route from Saugus to Palmdale. In addition to the standard leveling observations temperature measurements were carried out for each set-up with 3 sensors. The purpose of this test was:

- i) to determine the magnitude of the differences between heights determined using short- and long-sight distances along the same leveling route;
- ii) to test the ability of standard refraction models;
- iii) to test the ability of HOLDAHL'S temperature modelling

Further informations about these leveling refraction test is given in WHALEN, STRANGE, 1983.

Our objective was to study

- the discrepancies between all the different refraction models
- the differences between short- and long - sight levelings
- the differences between refraction corrections for each set-ups, as performed by the NGS, and refraction corrections for each section.

Before starting this comparison the situation of Saugus to Palmdale survey route and the terrain elevation above sea level should be given.

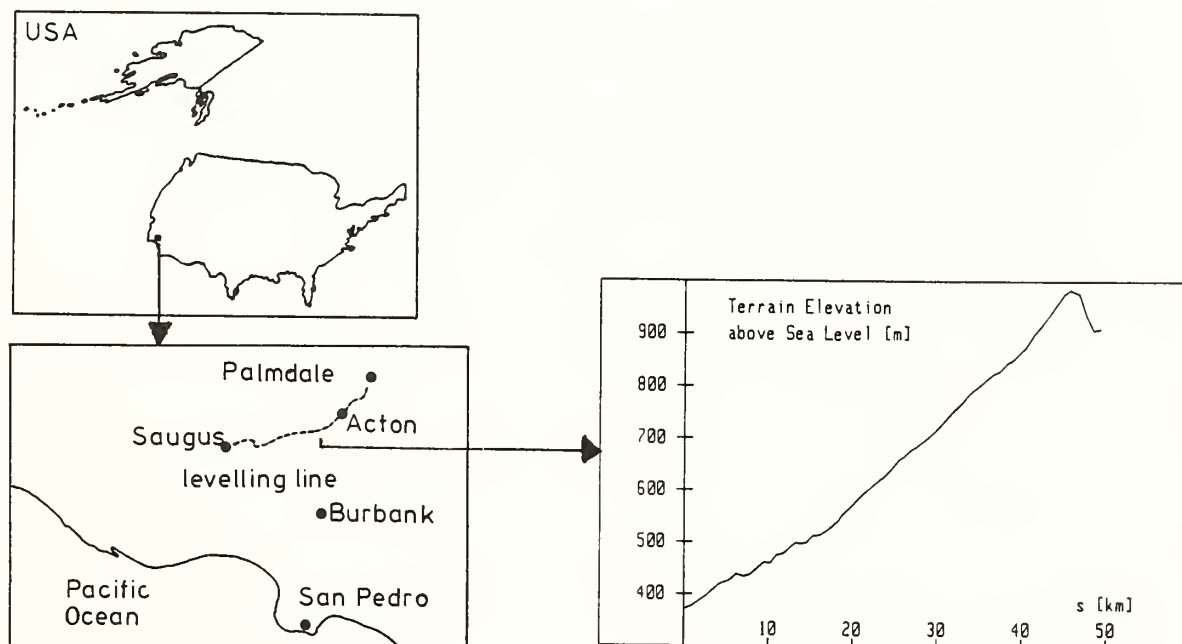


FIGURE 11: Saugus to Palmdale survey route
and terrain elevation above sea level

The setup corrections based on observed temperatures for each level setup are taken from WHALEN/STRANGE, 1983.

For our calculations we used the mean values of observed temperatures at the heights 0.5, 1.5 and 2.5 m for each section (level line) to compute the parameters of the available refraction models.

In Tab. 6 these parameters with the corresponding model No. are given

No./Parameter		Saugus-Palmdale	standard deviation	dimension
1,2,7,8	K	$-.841 \cdot 10^{-6}$	----	$1/K_2$
1	b	-.199	.007	K/m^2
2	c	.176	----	K/m^2
7	b	1.7361	----	K/m
	c	-.477	----	----
8	b	2.545	----	K
	c	-.668	----	$1/m$
9,10,11	a	-.840	.039	K/m
12	a	-.840	.039	K/m
	b	-.940	.041	----
13	dt"	.350	.052	K
14	H	509.6	27.3	W/m^2

TABLE 6: Parameters of Refraction Models
Saugus - Palmdale

The application of the refraction models leads to summarized refraction corrections for the short-sight and long-sight distances, depicted in Fig. 12.

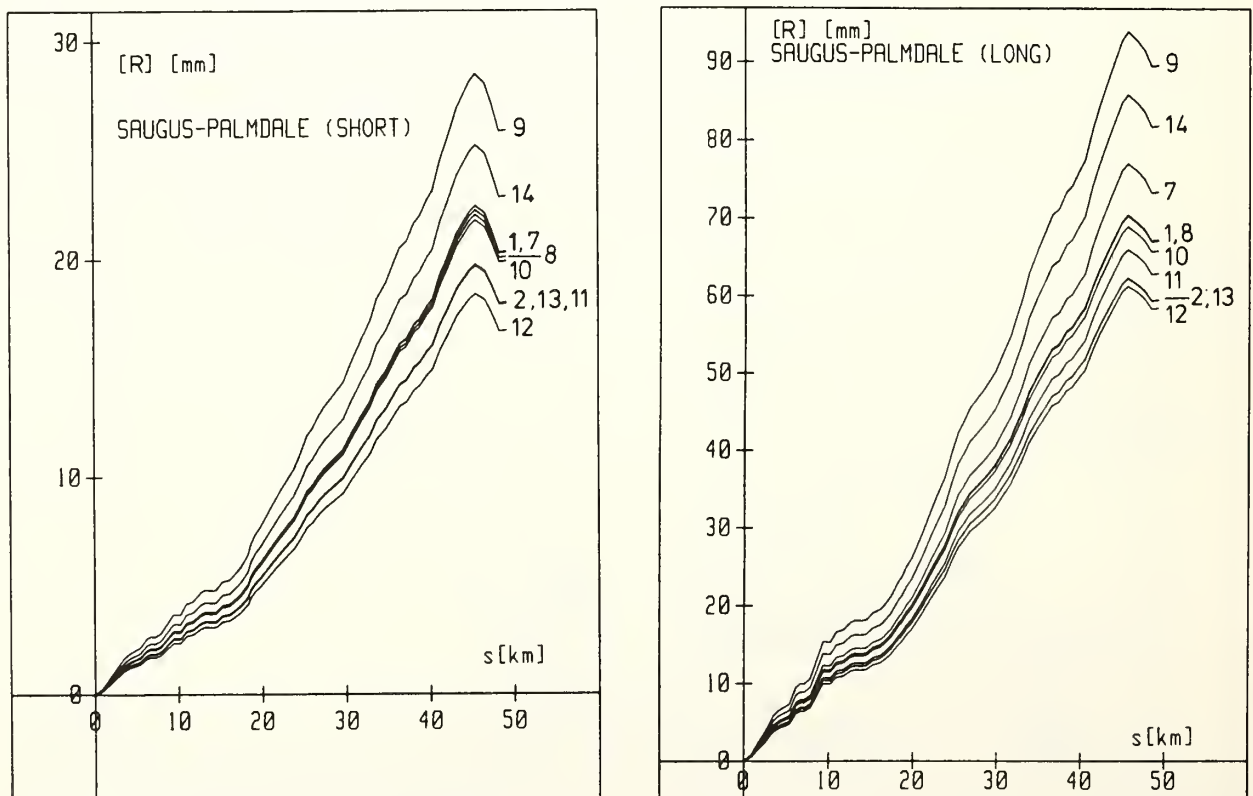


FIGURE 12: Summed-up Refraction Corrections for short (s)
and long (l) - sight distances

Additionally in Tab. 7 the maximum values at point 59 ($s = 45.48$ km) are given.

No.	1	2	7	8	9	10	11	12	13	14	Whalen/Strange
short	22.26	19.70	22.45	22.04	28.50	21.80	19.76	18.40	19.71	25.24	19.45
long	70.45	62.33	77.02	70.36	93.96	68.98	66.03	61.31	62.37	85.87	65.80
Δ	48.19	42.63	54.57	48.32	65.46	47.18	46.27	42.91	42.66	60.63	46.35

TABLE 7: Maximum values of Summed-up
Refraction Corrections of short (s) and long (l) - sight distances in [mm]

Finally the measured elevation differences were corrected. The summed up differences of the corrected and uncorrected elevations for short - and long sight length are presented in Fig. 13, additionally combined with the results taken from WHALEN, STRANGE, 1983.

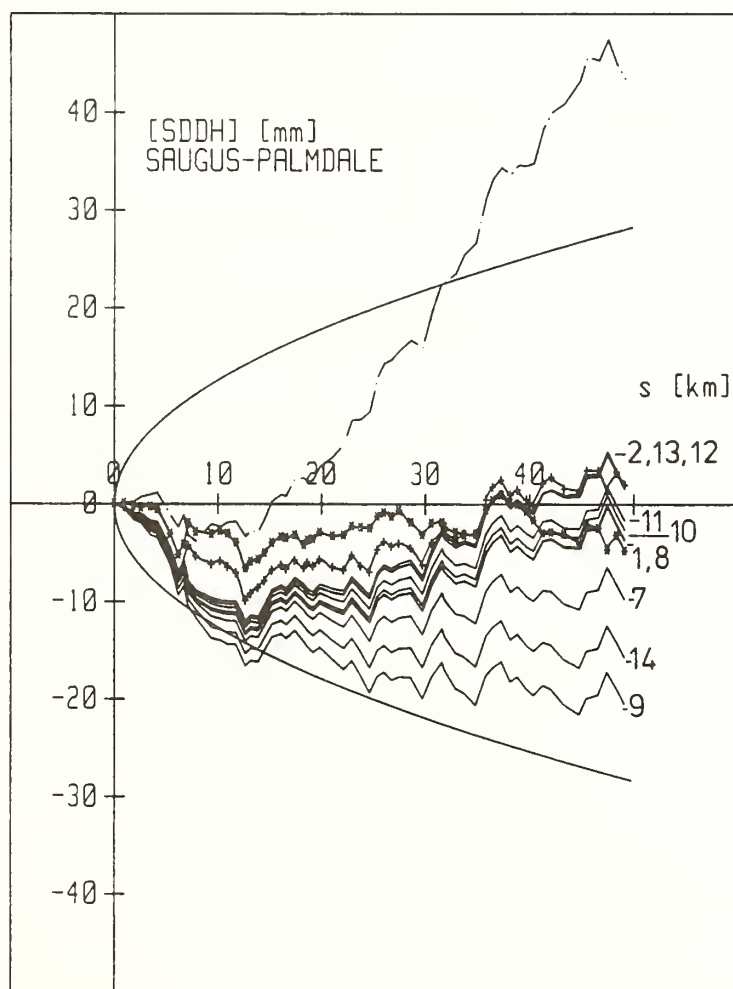


FIGURE 13: Effect of different
Refraction Corrections
Summed-up Elevation
Differences for each
section
(long-short)

(*) results from WHALEN/STRANGE
1983 -case one-

(+) results from WHALEN/STRANGE
1983 -case four-

It is easy to see that the application of refraction correction models randomize the differences between short- and long sight levelings. That means refraction does exist! The differing in all applications goes back to the functional and computing of parameters but shows that refraction correction models work ! Finally in Tab. 8 the estimation of standard deviations based on the differences of each section is given. The significance of the mean values is tested by well

known trivial statistical methods.

	SDDH	1	2	7	8	9	10	11	12	13	14
so	1.24	1.00	1.01	1.00	1.00	1.04	1.00	1.00	1.00	1.01	1.02
$so/\sqrt{2}$.88	.71	.71	.71	.71	.74	.71	.70	.71	.71	.72
$\hat{d}=[d]/n$.72	-.06	.03	-.16	-.06	-.34	-.04	-.03	-.03	.03	-.26
sd	.23	.18	.18	.18	.18	.19	.18	.18	.18	.18	.19
$\hat{t}=\hat{d}/sd$	3.18	-.32	.16	-.88	-.34	-1.79	-.24	-.15	.14	.16	-1.40

TABLE 8: Standard deviations of the
SAUGUS-PALMDALE Survey route

6. SUMMARY

Based on different meteorological models three group of model for refraction corrections exist; the main formulae are presented here.

These models require a precision of 0.02 K^0 for the observed temperatures and it is outlined here, that this precision can be achieved with an advanced multi-sensor temperature measuring system. Test observations with this equipment on the Leveling Test Loop Koblenz show the effectivity of the applied refraction models: the discrepancies between different observation periods can be reduced by applying an adequate refraction correction.

For the NGS test line Saugus-Palmdale it was pointed out, that a section wise treatment of refraction effects is sufficient or even more reliable than the computation of a correction for each individual set-up.

7. ACKNOWLEDGEMENTS

The authors thank the Surveying Authority of Rhineland-Palatinate for assistance and discussions and the NGS for sending data.

8. REFERENCES

- ANGUS-LEPPAN, P.V., 1979 : Refraction in Levelling - its Variation with Ground Slope and Meteorological Conditions. Australian Journal for Geodesy, Photogrammetry & Surveying, No. 31, p 27 - 41
- ANGUS-LEPPAN, P.V., 1984 : Refraction in Geodetic Levelling. In: Geodetic Refraction, F.K. Brunner (Ed.) Springer Verlag
- BECKERS, H., 1984 : Influence of Magnetism on Precise Levelling - Shown in the Rhineland-Palatine Part of the German First-Order Levelling Network. In: Pelzer/Niemeier (eds): Precise Levelling. Dümmler Verlag, Bonn

- BEST, A.C., 1935 : Transfer of Heat Momentum in the Lowest Layers of the Atmosphere. Meteorological Office, Geophysical Memoirs, No 65 (Eight Number, Volume VII)
- BROCKS, K., 1948 : Über den täglichen und jährlichen Gang der Temperatur in den unteren 300 m der Atmosphäre und ihren Zusammenhang mit der Konvektion. Berichte des Deutschen Wetterdienstes in der U.S.-Zone, Nr. 5
- FAWAZ, E., 1981 : Beurteilung von Nivellementsnetzen auf der Grundlage der Theorie der stochastischen Prozesse. Wiss. Arbeiten der Fachrichtung Vermessungswesen der Universität Hannover, Nr. 99.
- FREVEL, H., 1983 : Levelling Test Loop Koblenz - Results, Corrections and Remaining Problems. In: Precise Levelling, Pelzer, H. & Niemeier, W. (Eds), Dümmler Verlag, Bonn
- GARFINKEL, B., 1978/79 : Refraction Errors in Levelling - NGS Test Results. In: WHALEN, C.T. (1980), NAD-Symposium 1980, Ottawa, Canada, p 757 - 782
- HEER, R., 1983 : Application of Different Refraction Models on Measuring Results of the Levelling Test Loop Koblenz. In: Precise Levelling, Pelzer, H. & Niemeier, W. (Eds), Dümmler Verlag, Bonn
- HEER, R., 1984 : Refraktionsuntersuchungen auf der Nivellementsschleife Koblenz. Bericht zur 10.AG - Sitzung "Haupthöhennetz" 9.5.-11.5.1984 in Emden - unpublished -
- HOLDAHL, S.R., 1982 : The Correction for Levelling Refraction and its Impact on Definition of the North American Vertical Datum. Paper presented to the 1982 Annual Convention of the ASP, Denver, Colorado, March 9-15
- JANIETZ, U., 1984 : Theoretische und praktische Untersuchungen zur Leistungsfähigkeit unterschiedlicher Modelle für die Bestimmung der nivellitischen Refraktion. Diplomarbeit, Geodätisches Institut, - unpublished -
- KUKKAMÄKI, T.J., 1938 : Über die nivellitische Refraktion. Veröffentlichungen des Finnischen Geodätischen Institutes, Nr. 25, Helsinki
- KUKKAMÄKI, T.J., 1939 : Formeln und Tabellen zur Berechnung der nivellitischen Refraktion. Veröffentlichungen des Finnischen Geodätischen Institutes, Nr. 27, Helsinki
- KUKKAMÄKI, T.J., 1980 : Errors Effecting Levelling. NAD-Symposium, Ottawa, pp 1-10

- LINDSTROT, W., 1981 : Einsinkverhalten von Instrument und Latten. In: Niederschrift über die 25. Tagung des Arbeitskreises Präzisionsnivellement in Würzburg, 4.-6.11.1981, pp 21 - 27
- MONIN, A.S.
& OBUCHHOV, A.M., 1958 : Fundamentale Gesetzmäßigkeiten der turbulenten Vermischung in der bodennahen Schicht der Atmosphäre. In: Sammelband zur statistischen Theorie der Turbulenz, Hrsg.: GÖRING, H., Berlin, p 199 - 226
- MOZZUCHIN, O.A., 1977 : Die nivellitische Refraktion und die Methoden ihrer Berücksichtigung. Vermessungstechnik, 25. Jg., Heft 10, p 335 - 338
- PELZER, H., 1982 : Error Propagation in Levelling. Paper presented to International Symposium on Geodetic Networks and Computations of the IAG, DGK, Reihe B, No. 258, München
- REISSMANN, G., 1954 : Untersuchungen zur Ausschaltung des Einflusses der Vertikalrefraktion beim Präzisionsnivellement. Wiss. Berichte, Folge V, Vermessung, Heft 2, Berlin
- REMMER, O., 1980 : Role and Evaluation of Refraction for the Processing of Levelling Networks - An Analysis of the Second Precise Levelling of Finland and the Proper use of Kukkamämi's Correction. NAD-Symposium, Ottawa, Canada, p 623 - 646
- RUMPF, W.E.,
MEURISCH, H., 1981 : Systematische Änderung der Ziellinie eines Präzisionskompensatornivelliers - insbesondere des Zeiss Nil - durch magnetische Gleich- und Wechselfelder. XVI. FIG Kongreß, Montreux
- STRANGE, W.E., 1981 : The Impact of Refraction Correction on Levelling Interpretations in Southern California. Journal of Geophysical Research Vol. 86, No B4, pp 2809 - 2824
- WHALEN, C.T.,
& STRANGE, W.E., 1983 : The 1981 Saugus to Palmdale, California, Levelling Refraction Test. NOAA Technical Report NOS98, NGS27, Rockville, Md.
- WEBB, E.K., 1965 : Aerial Microclimate. Meteorological Monographs, Vol. 6, No 28, p 27 - 58

TURBULENCE EFFECTS ON A RAPID PRECISION LEVELING SYSTEM

Richard J. Lataitis,¹ Lloyd, C. Huff,² and Steven F. Clifford¹

¹Wave Propagation Laboratory
Environmental Research Laboratories, NOAA
Boulder, CO 80303

²Charting and Geodetic Services
National Ocean Service, NOAA
Rockville, MD 10852

ABSTRACT. A Rapid Precision Leveling System (RPLS) is proposed that consists of two tripod-mounted instruments, one at each end of a line-of-sight path, making synchronous measurements of the reciprocal zenith angles and slope distances. In this paper we evaluate the contribution of turbulence to uncertainties in the estimation of actual height differences between the two instruments. Assuming optical apertures of 15 cm, the RPLS is shown to be capable of first order leveling provided appropriate sight path lengths are chosen as dictated by the turbulence strength.

INTRODUCTION

A study is currently being conducted into the feasibility of constructing an essentially automated leveling system so configured as to yield very rapid and precise height difference measurements. The details of such a Rapid Precision Leveling System (RPLS) have been considered by Huff (1984). The RPLS concept is based on the EDM-trigonometric heighting technique (Rüeger and Brunner 1982) whereby height differences are calculated from the measured slope distances and zenith angles. The proposed RPLS consists of two tripod-mounted instruments, each capable of functioning as a transmitter and (or) receiver/reflector, located at opposite ends of a line-of-sight path (see Fig. 1). Each transmitter/receiver is assumed to be a common-optics system. The transmitter (A) projects an essentially collimated laser beam at a receiver (B) whose aperture is partially reflective thereby folding the path and allowing the RPLS to operate in two modes. The zenith angles required for the height difference calculation are Z_A and Z_B . The angle Z_A is the measured transmitter zenith angle. Neglecting the effects of turbulence, the angle Z_B , in the direct mode, is found from the sum of the measured receiver zenith angle Z_{BM} and the angle-of-arrival α_B of the direct beam wavenormal relative to the optical axis of the receiver at B. In principle, α_B is computed from $\alpha_B = d/f$, where d is the displacement of the direct beam focal spot from the optical axis of the receiver, and f is the receiver focal length. In the folded-path mode, the angle α_B is found from $\alpha_B = \alpha_A/2$, where α_A is the angle-of-arrival of the reflected beam at the receiver at A. (Note that, in Fig. 1, the separation between the direct and reflected paths has been greatly exaggerated, and that the receiver at A has been drawn above its actual position to more easily identify the relevant angles). We investigate the effect of turbulence on the ability of the RPLS to detect the angle-of-arrival α_A and α_B , and evaluate the contribution of turbulence to the height difference uncertainty for a 1 km traverse.

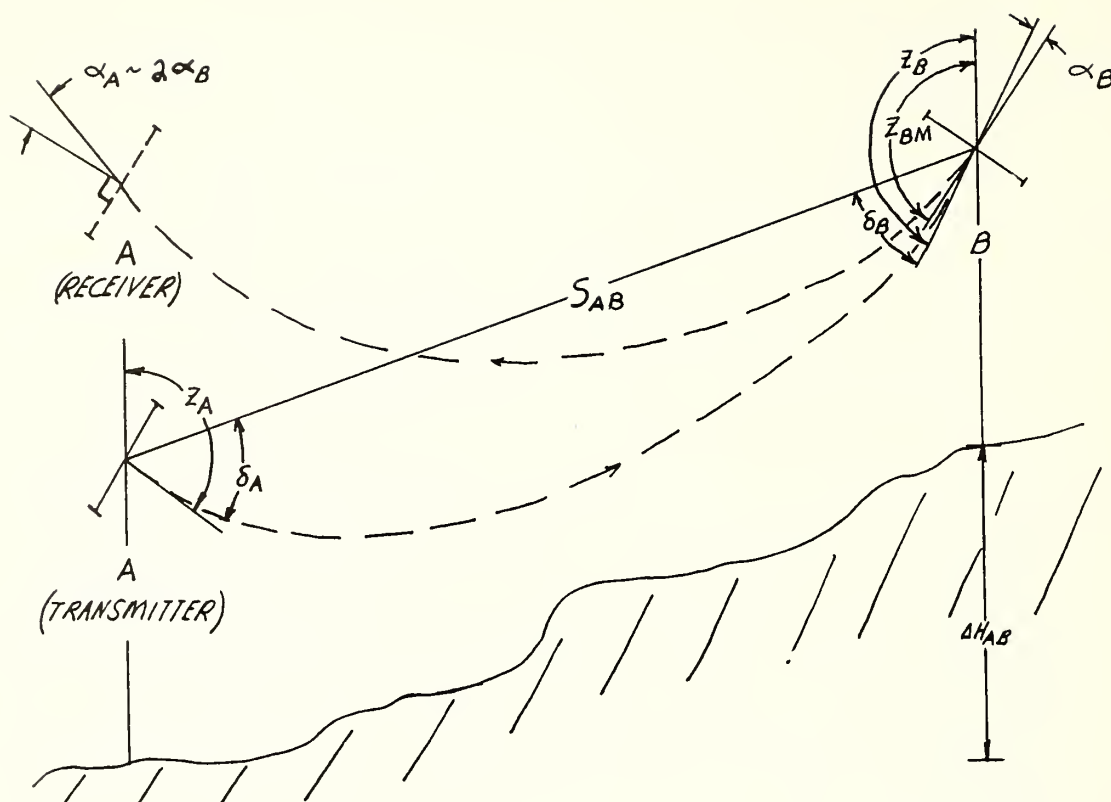


Figure 1. Operating principle of the RPLS.

RPLS RECIPROCAL EDM-HEIGHT TRAVERSING

Rüeger and Brunner (1982) (RB) give the following equation for the spheroidal height difference ΔH_{AB} used in reciprocal EDM-trigonometric heighting;

$$\Delta H_{AB} = \frac{1}{2} S_{AB} (\cos Z_A - \cos Z_B) - \frac{(S_{AB} \sin Z_A)^2}{4R} (k_A - k_B), \quad (1)$$

where $R \approx 6371$ km is the radius of the Earth, and the refraction coefficients k_A and k_B are related to the angles δ_A and δ_B through $k_{A,B} = \delta_{A,B}^2 2R / S_{AB} \sin Z_A$. A small term related to the deviation of the local zeniths from the true zeniths has been omitted, and we have assumed that the heights of the two instruments above the ground are equal. Neglecting any errors due to height transfers to and from bench-marks, and assuming the observations from leg to leg of the traverse are uncorrelated, the height difference variance of a height traverse of length L is given by RB as

$$\sigma_L^2 = \frac{L}{\ell} \cos^2 Z \sigma_S^2 + \frac{L\ell}{2} \sigma_Z^2 + \frac{L\ell^3}{16 R^2} (\Delta k)^2, \quad (2)$$

where $\Delta k = k_A - k_B$ has been treated as a random error, and equal horizontal distances $\ell = S_{AB} \sin Z_A$ and an average value, $\cos Z$, for all $\cos Z_A$ have been assumed. The variance of the distance and zenith angle measurements is represented by $\sigma_S^2 = \sigma_{Si}^2 + \sigma_{St}^2$ and $\sigma_Z^2 = \sigma_{Zi}^2 + \sigma_{Zt}^2$, where i and t describe the instrumental and turbulence-induced contributions respectively.

THE EFFECTS OF TURBULENCE

The RPLS works by measuring the off-axis displacement d of the receiver focal spot, from which the angle-of-arrival d/f is evaluated. In the absence of turbulence, the spot displacement is found by using an array of photodetectors to record the focal plane intensity distribution and by locating the position of its centroid relative to the optical axis. To understand how turbulence interferes with this measurement, we briefly discuss the effect of turbulence on a beam wave and the corresponding effect on the focal spot as it applies to the detection of the focal spot centroid. We assume that the turbulence is statistically homogeneous and isotropic, and that it can be described by the Kolmogorov spectrum. In addition, we require that the turbulence be sufficiently weak for the single-scatter theory to apply (Tatarski 1971).

We first consider the impact of the finite transverse extent of the beam. Turbulent fluctuations in the refractive index are produced primarily by refractive eddies advected by the mean wind. This gives rise to two finite beam effects (Yura 1973). A dancing or wander of the beam about its unperturbed position is produced by those eddies in the turbulent flow whose characteristic dimensions are larger than the beam diameter. A breathing or expansion of the beam about its instantaneous center of energy is caused by eddies that are smaller than the beam. In the plane of the receiver aperture, these effects manifest themselves as wander and expansion of the beam spot. Assuming equal transmitter and receiver diameters D , and a given beam divergence θ , the beam spot may, at times, only partially cover the receiver¹. This results in a distortion and reduction in intensity of the focal spot. For circular apertures, it can be shown that the focal spot distortion due to this turbulence induced misalignment does not influence the location of its centroid². In addition, the reduction in focal spot intensity due to beam wander and expansion is also of no consequence. Therefore, to evaluate the effects of turbulence, the finite transverse extent of the beam can be ignored and we can model the source as a plane wave.

In the plane of the receiver aperture, both the amplitude and phase of the wave fluctuate as a result of the intervening turbulence. The amplitude fluctuations produce a random pattern of light and dark patches across the receiver aperture which evolve in time (scintillation). The characteristic diameter of these patches

¹To effectively fold the path, it is important that the receiver intercept a significant portion of the beam. Under conditions of the largest expected path-integrated turbulence, the beam at the receiver may be displaced as much as a few centimeters. This requires that $D \gtrsim 10$ cm or that θ be sufficiently large to accommodate this effect.

²This is easily explained using the Fourier transform relationship between the field incident on the receiver aperture and the focal plane field (Goodman 1968).

is $\sqrt{\lambda S}$, where λ is the beam wavelength and S is the path length. As a result, the focal spot is distorted because of the irregular apodization of the aperture, and its intensity fluctuates because of the evolution of the scintillation pattern. Only the former factor affects the location of the focal spot centroid. However, if the aperture contains many of these patches ($D \gg \sqrt{\lambda S}$), the focal spot distortion is smoothed out (i.e., the aperture "averages" over the focal spot distortion produced by each irregular patch) and this effect can also be ignored. Larger apertures also minimize the effect of scintillation in the same manner. For the wavelengths and pathlength of interest, $\sqrt{\lambda S} \lesssim 2$ cm, indicating that apertures with $D \gtrsim 10$ cm are required.

The phase fluctuations across the receiver aperture have two effects on the focal spot. Turbulent eddies whose characteristic dimensions are larger than D produce similar size phase irregularities at the receiver, causing the focal spot to wander about its unperturbed position. Inhomogeneities whose size is smaller than D produce phase irregularities at the receiver smaller than the aperture; these tend to broaden the focal spot about its instantaneous center of energy. The characteristic time scale for fluctuations in the focal spot position is of order D/v , where v is the component of wind velocity across the path. Over time scales much shorter than this, the focal spot is broadened but constant in position.

The zenith angle Z_B required for the direct path height difference calculation is obtained from the sum of the measured receiver zenith angle Z_{BM} and the unperturbed angle-of-arrival α_B . In turbulence, α_B is found from the ensemble mean of the instantaneous angle-of-arrival α , where α is defined as the angle-of-arrival observed over times much shorter than D/v . An estimate for this ensemble mean can be obtained by forming a sampled mean from instantaneous samples of the focal plane intensity distribution. The corresponding variance in the zenith angle observation is (see Appendix)

$$\sigma_{Zt}^2 = \sigma_{ad}^2 \left(\frac{2N_o + 1}{N} \right), \quad (3)$$

where σ_{ad}^2 is the angle-of-arrival variance of the direct beam at the receiver at B , N_o is the correlation length of the samples, and N is the total number of samples. The folded path result can be obtained from Eq. (3) by replacing σ_{ad}^2 with $\sigma_{af}^2/4$, where σ_{af}^2 is the angle-of-arrival variance of the folded beam at the receiver at A . We estimate N_o as $SR \cdot \tau$, where $SR = N/T_s$ (T_s = total sampling time) is the sampling rate and $\tau = L_o/v$ is the turbulence correlation time. L_o is the outer scale of turbulence, defined as the largest isotropic eddy in the turbulent flow, and is usually estimated as the height h of the optical path above the ground.

To evaluate Eq. (3) numerically, we need to obtain an estimate for σ_{ad}^2 and σ_{af}^2 . The direct path angle-of-arrival variance is given by $\sigma_{ad}^2 = \langle (\Delta\phi(D) - \langle \Delta\phi(D) \rangle)^2 \rangle / (kD)^2$, where $\Delta\phi(D)$ is the phase difference across an aperture of diameter D , the angle brackets represent an ensemble average, and $k = 2\pi/\lambda$ (Fante 1975). For $\sqrt{\lambda S} \ll D < L_o$, the numerator is $2.92 k^2 S C_n^2 D^{5/3}$ so that $\sigma_{ad}^2 = 2.92 S C_n^2 D^{-1/3}$. The structure parameter C_n^2 is a measure of the turbulence

strength and can be related to the refractive index variance σ_n^2 through $C_n^2 \approx \sigma_n^2 6.5 L_o^{-2/3}$ (Clifford 1978). The folded path result can be obtained from this result by noting that if the phase perturbation produced by a single eddy over a one-way path is ϕ , then the phase perturbation produced by this eddy over a round trip path is 2ϕ . By replacing $\Delta\phi(D)$ by $2\Delta\phi(D)$ in the expression for σ_{ad}^2 we obtain $\sigma_{af}^2 = 4\sigma_{ad}^2$. This result is based on the assumption that the beam wave propagates through exactly the same turbulence on the forward and return trips. This requires that the angle-of-arrival at the reflector always be zero which is not the case because of turbulence-induced angle-of-arrival fluctuations. If the beam were to propagate through a completely different region of turbulence on the return path, the folded path result could be obtained by setting $S = 2S$ in the expression for σ_{ad}^2 which gives $\sigma_{af}^2 = 2\sigma_{ad}^2$. Therefore, we expect that $\sigma_{af}^2 = A\sigma_{ad}^2$, where $2 \leq A < 4$. By substituting σ_a^2 and $\sigma_{af}^2/4$ for σ_{ad}^2 in Eq. (3) we obtain σ_{Zt}^2 for the direct and folded path configuration respectively and note that σ_{Zt}^2 for the folded path is always less than that for the direct path. Neglecting any design considerations, it seems preferable to operate the RPLS in the folded rather than direct path mode.

To obtain an estimate for the turbulence induced variance in the sight path length S , we divide the total phase path for a round trip between the two instruments, namely $2kS \pm 2\sigma_\phi(S)$, where $\sigma_\phi(S)$ is the standard deviation of the plane wave phase fluctuations over the direct path, by $2k$ which gives $S \pm \sigma_\phi(S)/k$. The corresponding variance for a single sight path length measurement is $\sigma_\phi^2(S)/k^2$, where $\sigma_\phi^2(S) \sim k^2 C_n^2 L_o^{5/3} S$ (Lutomirski et al. 1973). Assuming one sample of the sight path length is recorded for each sample of the angle-of-arrival, we obtain $\sigma_{St}^2 = C_n^2 L_o^{5/3} S (2N_o + 1)/N$.

The turbulent contribution to the variance of a 1 km height traverse is obtained from Eq. (2):

$$\sigma_{1t}^2(m^2) = \frac{L\ell}{2} \sigma_{Zt}^2, \quad (4)$$

where all dimensioned quantities are in meters. We have neglected the contribution of the sight path length variance because it can be shown to be small relative to the other terms in Eq. (2). In Fig. 2 we plot σ_{1t} as a function of the sampling rate SR for $\ell = 200$ m, $\lambda = 0.6$ μ m, $C_n^2 = 10^{-13} \text{ m}^{-2/3}$, $D = 15$ cm, $\tau = h/v = 1$ s ($h = 2$ m, $v = 2$ m/s), and $T_S = 30$ s. The upper curve corresponds to the direct path case while the lower curve corresponds to the folded path case with $A = 2$. The correct result for the folded path lies between these two curves. Figure 2 indicates that σ_{1t} decreases as the sampling rate increases. For sufficiently low sampling rates, the samples are uncorrelated and σ_{1t} decreases as $1/\sqrt{N}$. For values of SR that yield a large number of samples in a time τ , the recorded time series is a quasi-continuous representation of the angle-of-arrival and the factor $(2N_o + 1)/N$ approaches its asymptotic value of $2\tau/T_S$, which is independent of the sampling

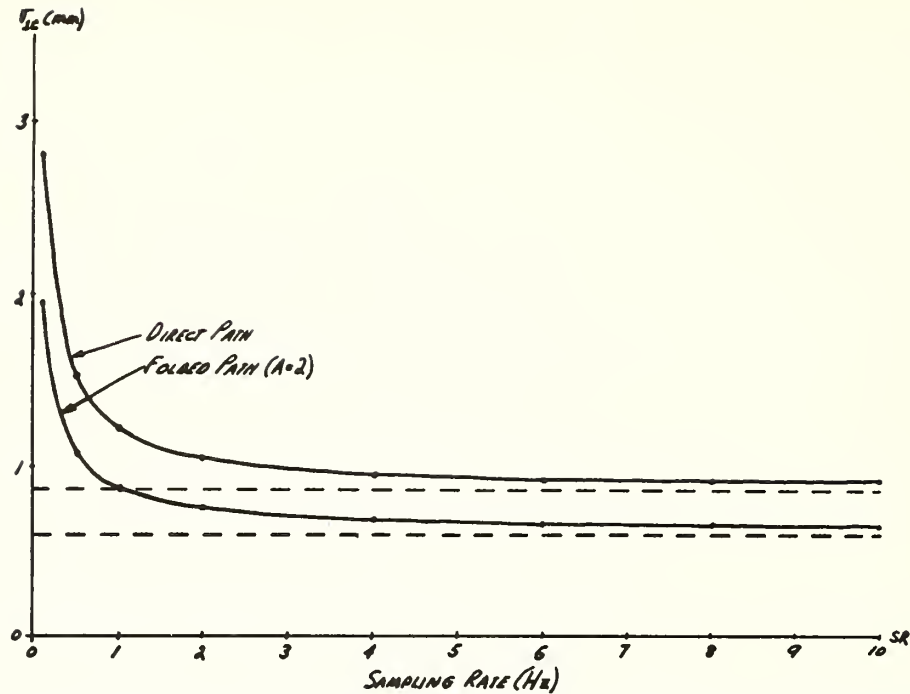


Figure 2. The turbulence-induced contribution to the standard deviation in the total height difference for a 1 km traverse as a function of the RPLS sampling rate SR. ($\ell = 200$ m, $\lambda = 0.6$ μ m, $C_n^2 = 10^{-13}$ m $^{-2/3}$, $D = 15$ cm, $\tau = 1$ s, $T_s = 30$ s).

rate. This produces the asymptotic behavior of the curve for high values of SR. For this particular example, there is no significant reduction in σ_{lt} for sampling rates above 2 Hz. In general, a reasonable sampling rate is one that yields approximately two samples in one turbulence correlation time (i.e., $SR \sim 2/\tau$). Assuming most leveling operations takes place in periods of light wind ($v < 10$ m/s ~ 22 mph), a value of $SR < 10$ hz is satisfactory. We also note that σ_{lt} decreases as the receiver diameter D increases. This is because as the size of the receiver aperture increases, an increasing amount of phase fluctuations in the plane of the receiver aperture have characteristic scales less than D producing more spreading and less wander of the focal plane spot, and reducing the angle-of-arrival variance. Because of this effect, and the aforementioned problems with the amplitude fluctuations, the largest practical aperture diameters will yield the best system performance, and $D \sim 15$ cm will satisfy both practical and operational considerations.

In Fig. 3, we plot σ_{lt} as a function of the horizontal component of the sight path (ℓ) over a 1 km height traverse for various levels of turbulence. We have chosen a receiver diameter of 15 cm, and a sampling rate of 2 Hz. All the other parameters are the same as in the previous figure. The solid lines correspond to the direct path result and the dashed lines correspond to the folded path configuration with $A = 2$. The correct result for the folded path lies between the solid and dashed line associated with each value of C_n^2 . RB give $\sigma_1 < 1.1$ mm as the criterion for first order leveling for a 1 km traverse. From Fig. 3 we see that higher levels of turbulence require shorter path lengths if first order standards are desired. For $C_n^2 < 10^{-13}$ m $^{-2/3}$, sight path lengths as long as 250 m are possible provided the instrumental and refractive uncertainties are sufficiently small. The allowable instrumental and refractive uncertainty σ_{ir} is found from $\sigma_{ir} = \sqrt{\sigma_1^2 - \sigma_{lt}^2}$. As an example, we consider the folded path configuration with ℓ

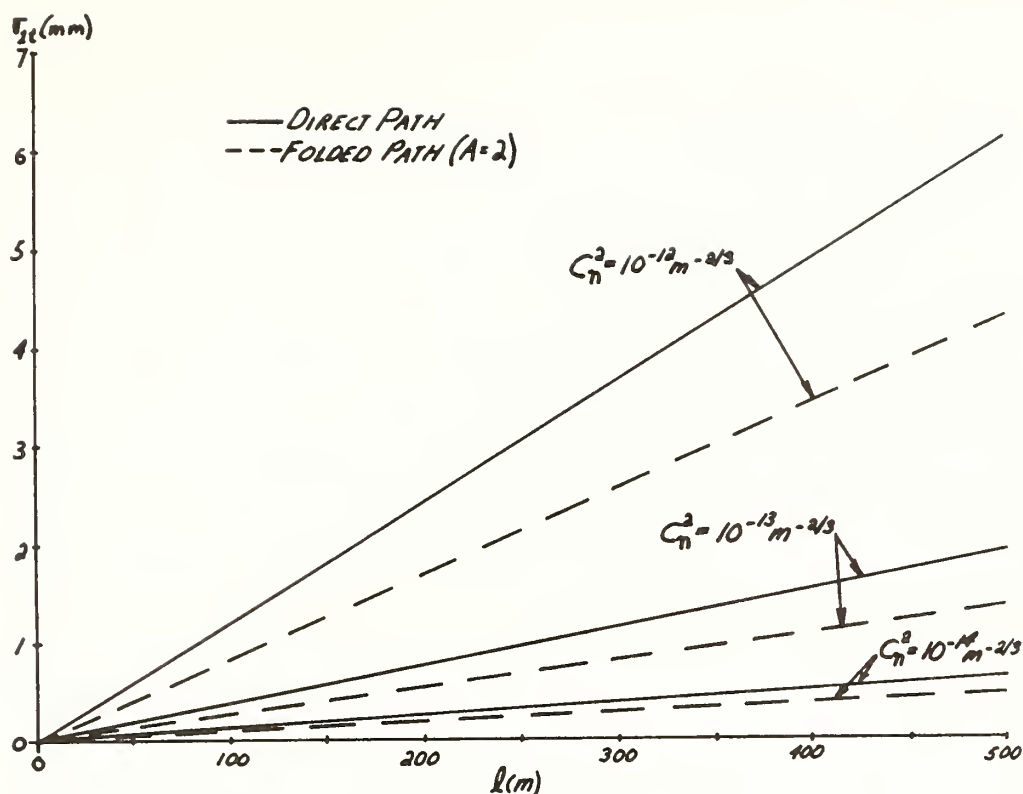


Figure 3. The turbulence-induced contribution to the standard deviation in the total height difference for a 1 km traverse as a function of the horizontal component of the sight path (l) for various turbulence strengths. ($\lambda = 0.6 \mu\text{m}$, $D = 15 \text{ cm}$, $\text{SR} = 2 \text{ Hz}$, $\tau = 1 \text{ s}$, and $T_s = 30 \text{ s}$).

$= 250 \text{ m}$ and $C_n^2 < 10^{-13} \text{ m}^{-2/3}$ for which $\sigma_{lt} \approx 0.9 \text{ mm}$. To meet first order leveling standards we must have $\sigma_{lr} < 0.63 \text{ mm}$. For C_n^2 values much larger than this, the maximum sight path length is limited to 100 m or less. $C_n^2 = 10^{-12} \text{ m}^{-2/3}$ is roughly the highest level of turbulence that would be encountered and corresponds to conditions that might be observed midday on a hot day. C_n^2 values of $10^{-13} \text{ m}^{-2/3}$ and less typically occur in the early morning and late afternoon hours when the air temperature approaches that of the ground (Lawrence 1976). To determine whether a certain sight path length will satisfy first order requirements, we need to know the turbulence strength at the time measurements are made. This information can be obtained from the variance of the sampled angle-of-arrival and can be used to determine the maximum sight path length for the next leg of the traverse.

CONCLUSIONS

Turbulence affects the performance of the RPLS primarily through angle-of-arrival fluctuations. We have shown that the RPLS is capable of performing first order leveling provided instrumental and refractive uncertainties are sufficiently small and appropriate path lengths are chosen. In the morning and late afternoon hours, turbulence levels generally do not exceed $C_n^2 = 10^{-13} \text{ m}^{-2/3}$ and the RPLS is capable of meeting first order standards for sight path lengths as long as 250 m.

During midday hours, when C_n^2 values may get as high as $10^{-12} \text{ m}^{-2/3}$, RPLS sight path lengths are limited to approximately 100 m.

The results presented here are also applicable to leveling operations where alignment between the instruments is achieved by observing a target through a transit telescope. Instead of the plane wave source approximation valid for the RPLS, a target of small transverse extent constitutes a point source producing a spherical wavefront which is subject to the same effects as those discussed here. The requirement of having sufficiently large sampling rates and long observation times translates to the need for observing the target for a sufficiently long period of time to adequately determine its mean position. The averaging in this case is performed by eye, and the accuracy to which the mean angle-of-arrival is determined depends to some extent on the skill of the observer. The diameter of the telescope has the same effect on the turbulence induced uncertainties as discussed earlier. Larger telescope apertures would yield target images that jitter less allowing for a more accurate determination of the mean angle-of-arrival. Thus, the turbulence contribution to the height difference uncertainty shown in Fig. 3 to some extent represents the uncertainty that would be expected for more conventional EDM-trigonometric leveling systems.

One final point concerns the capability of having both instruments function as transmitters. By calculating the height difference with one instrument active and then the other, for each leg of a traverse, we are able to reconstruct both a forward and backward sighting in a single traverse. The two values for the total height difference provide a check for the accuracy of the system and can be combined to yield an improved height difference estimate. We stress the figures presented here do not represent the absolute performance of the RPLS, but serve only to illustrate the effects of turbulence.

ACKNOWLEDGMENTS. The authors acknowledge the many valuable comments of Dr. James Churnside and Gerard Ochs of the Wave Propagation Laboratory.

REFERENCES

- Clifford, S. F., 1978, Laser Beam Propagation in the Atmosphere, p. 20, New York, Springer-Verlag.
- Fante, R. L., 1975, Electromagnetic beam propagation in turbulent media. Proc. IEEE, Vol. 63, No. 12, pp. 1669-1692.
- Goodman, J. W., 1968, Introduction to Fourier Optics, pg. 85, New York, McGraw-Hill.
- Huff, L. C., 1984, A new rapid precision leveling system, EOS Transaction, AGU, Vol. 65, No. 45, p. 857.
- Lawrence, R. S., 1976, A review of optical effects of the clear turbulent atmosphere, SPIE, Vol. 75, pp. 2-8.
- Lutomirski, R. F., Huschke, R. E., Meecham, W. C., and Yura, H. T., 1973, Degradation of laser systems by atmospheric turbulence, pp. 89-90, The Rand Corporation.

Rüeger, J. M., and Brunner, F. K., 1982, EDM-height traversing versus geodetic leveling, *The Canadian Surveyor*, Vol. 36, No. 1, pp. 69-87.

Tatarski, V. I., 1971, The Effects of the Turbulent Atmosphere on Wave Propagation, pp. 76 and 107, Springfield, National Technical Information Service.

Yura, H. T., 1973, Short-term average optical-beam spread in a turbulent medium, *J. Opt. Soc. Am.*, Vol. 63, No. 5, pp. 567-572.

APPENDIX

The zenith angle Z_B is defined through $Z_B = Z_{BM} + \langle \alpha \rangle$, where the angle brackets indicate an ensemble average. An estimate for Z_B is obtained by replacing $\langle \alpha \rangle$ with $\bar{\alpha}$, where the overbar indicates a sampled average over N samples. The resulting variance in the zenith angle observation is

$$\sigma_{Zt}^2 = \langle (\langle \alpha \rangle - \bar{\alpha})^2 \rangle = \langle \bar{\alpha}^2 \rangle - \langle \alpha \rangle^2 \quad (A1)$$

$$= \frac{1}{N^2} \sum_{i=1}^N \sum_{j=1}^N (\langle \alpha_i \alpha_j \rangle - \langle \alpha_i \rangle \langle \alpha_j \rangle) \quad (A2)$$

$$= \frac{\sigma_\alpha^2}{N^2} \sum_{i=1}^N \sum_{j=1}^N C(i, j) , \quad (A3)$$

where

$$C(i, j) = \frac{\langle \alpha_i \alpha_j \rangle - \langle \alpha_i \rangle \langle \alpha_j \rangle}{\sigma_\alpha^2} \quad (A4)$$

is the normalized covariance function of the sampled angle-of-arrival. Assuming $C(i, j) = C(|i-j|)$, the double sum in (A3) can be evaluated by writing the inner sum for $i=1$, $i=2$, etc., and recognizing a simple pattern that emerges. The result is

$$\sigma_{Zt}^2 = \frac{\sigma_\alpha^2}{N} \left[2 \sum_{u=1}^{N-1} \left(1 - \frac{u}{N} \right) C(u) + 1 \right] . \quad (A5)$$

Provided $N \gg 1$ and $C(u) \sim 0$ for some $u \ll N$, (A5) simplifies to

$$\sigma_{Zt}^2 = \frac{\sigma_\alpha^2}{N} \left[2 \sum_{u=1}^{N-1} C(u) - 1 \right] . \quad (A6)$$

The remaining sum is the correlation length N_o of the samples in units of samples, and

$$\sigma_{Zt}^2 = \sigma_\alpha^2 \left(\frac{2N_o + 1}{N} \right) , \quad 0 \leq N_o \ll N . \quad (A7)$$

ON η -VALUES IN LEVELLING REFRACTION

Ole Remmer
Geodetic Institute
Copenhagen
DK-2920 Denmark

ABSTRACT. Reviewing the recent work in the field of levelling refraction, it is pointed out that this refraction depends on the second derivative (of temperature as a function of height over ground) and not on the gradient or first derivative. Because the accumulated effect of refraction in a specific network may be described by just one parameter called η we may include the computation of the refraction in the adjustment procedures.

Based on reports from researches in this field the following η -values (and corresponding second derivatives) have been computed for different areas in the world:

	$\eta \text{ m}^{-2}$	$\frac{d^2 t}{dz^2}$ degree/m ²
Denmark	$-0.48 \cdot 10^{-7}$	0.31
United Kingdom	$-0.54 \cdot 10^{-7}$	0.35
Maryland	$-0.56 \cdot 10^{-7}$	0.36
California	$-0.55 \cdot 10^{-7}$	0.35
Finland	$-0.97 \cdot 10^{-7}$	0.62
Arizona	$-0.98 \cdot 10^{-7}$	0.63
Canada	$-1.02 \cdot 10^{-7}$	0.66

There thus seems to be two distinct groups of η -values, one belonging to an oceanic, the other to a continental climate.

1. ARGUMENTS FOR DEALING WITH REFRACTION IN LEVELLING

Scientific Arguments

An ever increasing accuracy is always pursued in the exact sciences. Without going into a deeper discussion on the general reasons for such a pursuit (and its limitations) we shall here give some concrete examples from geodesy and related sciences. Hopefully they will illustrate the above mentioned general idea.

A more accurate execution of a precise levelling will thus mean for example.

- a. A better determination of recent crustal movements and especially the determination of slower movements.

(Of obvious geophysical - geological interest).

- b. A better determination of the different mean sea levels of the tide gate mareographs for example the difference between the Mediterranean Sea, the Atlantic Ocean and the Baltic Sea.
(Of geodetic and oceanographic interest).
- c. A truer determination of sea-slopes.
(cf. the article in the Journal of Geophysical Research by Castle et al.[4] on the geodetic determination of the sea-slope along the coast of California).

Practical Arguments

For the practical application of a high precision levelling network it is of fundamental importance that a lay user may regard the heights in this network as error-free. It is evident that we get closer to this ideal state of a levelling network every time we get a better accuracy (that is every time our heights get a lower error, the term error here including both precision and reliability in Baarda's sense). On the other hand with new levelling measurements that are inherently more accurate than their older counterparts you will reach a certain prescribed level of accuracy quicker than before and thus be able to save money and manpower by making fewer (but as we said more accurate) measurements than you did before.

2. THE FUNDAMENTAL PARADOX OF LEVELLING

The purpose of precise levelling is to determine the height difference between two benchmarks. (As height difference I shall understand potential difference; every reader may however for the greater part of this paper use his own height definition instead of mine).

The actual execution of such a precise levelling, with precision levelling instruments, invar staves etc. rests upon two conditions:

- 1) The height difference between any two levelling points does not change with time.
- 2) Light follows a straight line.

Here 1) is the necessary condition for any sensible height difference definition while 2) is the sine qua non for any conventional levelling observation.

We thus see that these two conditions must be met in order to give the concept of a height difference meaning and to make this difference observable.

In reality however neither the points are stable nor the light linear!

(We might add that had we executed our levelling observations carelessly enough 1) and 2) would seemingly be true, the very precision of precise levelling however making impossible the survival of these illusions).

We can see that the negation of 1) and 2) produces errors which are independent of the levelling instruments or to put it in another way: obviously point movements and atmospheric refraction will prevail even should we get totally error-free instruments (including rods etc.)

Of course there are other instrument-independent errors than these two but secular movements and atmospheric refraction constitute by far the largest quantities in the error budget of precise levelling.

In the present paper however I shall concentrate on the effect of refraction and the possibility of letting the levelling observations themselves determine this effect.

3. THE DECISIVE PARAMETERS FOR LEVELLING REFRACTION

The fact that the temperature gradient appears in almost all formulae for levelling refraction should not make us forget that with a central position of the levelling instrument between the rods the total refraction effect from one levelling set up will always be the difference between such two gradients; these gradients being almost of the same size the difference will be very small and as we shall see this small difference will not surprisingly depend solely on the second derivative (or the gradient of the gradient if you like).

The most up to date treatment of the refraction in a single sighting is Brunner's in [2]. According to [2] p. 695 the refraction on a single stave is:

$$\langle r \rangle = 10^{-6} \left(\frac{N}{T} \right) \left[0.0122 S^2 + \int_0^S (S - \eta) \frac{\partial \langle \theta \rangle}{\partial z} (\eta) d\eta \right] \quad (1)$$

where $N = (n-1)10^{-6}$ (n refraction index) and $\partial \langle \theta \rangle / \partial z$ is the vertical gradient of the mean potential temperature $\langle \theta \rangle$, which may vary along the line of sight, η is the integration variable along the line of sight and S is the sight length. (We remark in passing that the main difference between Brunner's formula and Kukkamäki's formula is that whereas Kukkamäki presupposes that the isothermal surfaces are parallel to the ground Brunner does not and has thus formally a more general approach and subsequently formally a more general formula i.e. (1)).

We now make a Taylor expansion of $\partial \langle \theta \rangle / \partial z$ at the point $\eta = 0$:

$$\begin{aligned} \frac{\partial \langle \theta \rangle}{\partial z} (\eta) = & \left(\frac{\partial \langle \theta \rangle}{\partial z} \right)_{\eta=0} + \left(\frac{\partial^2 \langle \theta \rangle}{\partial z \partial \eta} \right)_{\eta=0} \eta \\ & + \frac{1}{2} \left(\frac{\partial^3 \langle \theta \rangle}{\partial z \partial \eta^2} \right)_{\eta=0} \eta^2 + \frac{1}{6} \left(\frac{\partial^4 \langle \theta \rangle}{\partial z \partial \eta^3} \right)_{\eta=0} \eta^3 + \dots \quad (2) \end{aligned}$$

By differentiation with respect to η we mean in the direction of the tangent \vec{n} to the curve of light (see Figure 1)

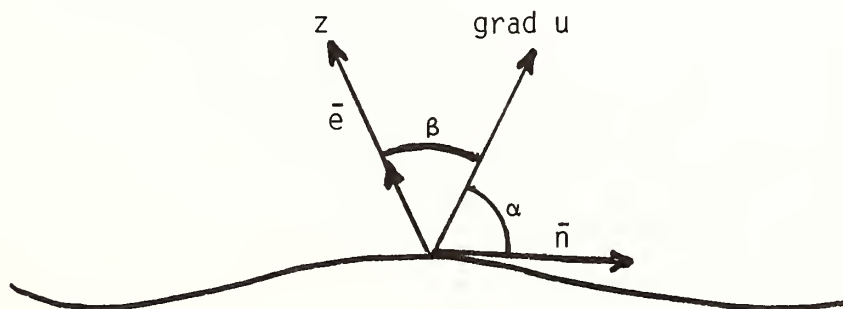


Figure 1

We write with easily understandable changes (2) into

$$\frac{\partial \langle \theta \rangle}{\partial z} (\eta) = D_1 + D_2 \eta + \frac{1}{2} D_3 \eta^2 + \frac{1}{6} D_4 \eta^3 + \dots \quad (3)$$

we obviously

$$\left. \begin{aligned} D_1 &= \left(\frac{\partial \langle \theta \rangle}{\partial z} \right)_0 \\ D_2 &= \left(\frac{\partial^2 \langle \theta \rangle}{\partial z \partial \eta} \right)_0 = \left(\frac{\partial}{\partial \eta} \frac{\partial \langle \theta \rangle}{\partial z} \right)_0 = \frac{\cos \alpha_1}{\cos \beta_1} \left(\frac{\partial}{\partial z} \frac{\partial \langle \theta \rangle}{\partial z} \right)_0 = \\ &\quad \frac{\cos \alpha_1}{\cos \beta_1} \left(\frac{\partial^2 \langle \theta \rangle}{\partial z^2} \right)_0 \\ D_3 &= \left(\frac{\partial^3 \langle \theta \rangle}{\partial z \partial \eta^2} \right)_0 = \frac{\partial}{\partial \eta} \frac{\partial}{\partial \eta} \frac{\partial \langle \theta \rangle}{\partial z} = \\ &\quad \sum_{i=1}^2 \frac{\cos \alpha_i}{\cos \beta_i} \left(\frac{\partial}{\partial z} \frac{\partial}{\partial z} \frac{\partial \langle \theta \rangle}{\partial z} \right)_0 = \sum_{i=1}^2 \frac{\cos \alpha_i}{\cos \beta_i} \left(\frac{\partial^3 \langle \theta \rangle}{\partial z^3} \right)_0 \\ D_4 &= \left(\frac{\partial^4 \langle \theta \rangle}{\partial z \partial \eta^3} \right)_0 = \left(\frac{\partial}{\partial \eta} \frac{\partial}{\partial \eta} \frac{\partial}{\partial \eta} \frac{\partial \langle \theta \rangle}{\partial z} \right)_0 = \\ &\quad \sum_{i=1}^3 \frac{\cos \alpha_i}{\cos \beta_i} \left(\frac{\partial}{\partial z} \frac{\partial}{\partial z} \frac{\partial}{\partial z} \frac{\partial \langle \theta \rangle}{\partial z} \right)_0 = \sum_{i=1}^3 \frac{\cos \alpha_i}{\cos \beta_i} \left(\frac{\partial^4 \langle \theta \rangle}{\partial z^4} \right)_0 \end{aligned} \right\} \quad (4)$$

where in (4) we have only used the fact that (see Figure 1)

$$\begin{aligned} \frac{\partial u}{\partial \eta} &= \text{grad } u \cdot \vec{n} = |\text{grad } u| \cos \alpha \\ \text{and} \\ \frac{\partial u}{\partial z} &= \text{grad } u \cdot \vec{e} = |\text{grad } u| \cos \beta \end{aligned} \quad \left\{ \begin{array}{l} (u \text{ some scalar function}) \\ \beta \neq \frac{\pi}{2} \end{array} \right.$$

We have obviously to presuppose that these derivatives from (3) exist; we remark that Brunner himself already presupposes the existence of D_1 ; in order for (1) to have a meaning with $\partial \langle \theta \rangle / \partial z$ substituted through (3) we may even allow (3) not to hold in a countable number of points.

Making the substitution of (3) into (1) we find the refraction error $\langle r \rangle_1$ on one stave

$$\begin{aligned}
\langle r \rangle_1 &= 10^{-6} \left(\frac{N}{T} \right) \left[0.0122 S^2 + \int_0^S (S-n) (D_1 + D_2 n + \frac{1}{2} D_3 n^2 + \frac{1}{6} D_6 n^3 + \dots) dn \right] = \\
&10^{-6} \left(\frac{N}{T} \right) \left[0.0122 S^2 + \int_0^S (D_1 S + (D_2 S - D_1) n + (\frac{1}{2} D_3 S - D_2) n^2 \right. \\
&+ (\frac{1}{6} D_4 S - \frac{1}{2} D_3) n^3 + \dots) dn \right] = \\
&10^{-6} \left(\frac{N}{T} \right) (0.0122 S^2 + [D_1 S n + \frac{1}{2} (D_2 S - D_1) n^2 + \frac{1}{3} (\frac{1}{2} D_3 S - D_2) n^3 \\
&+ \frac{1}{4} (\frac{1}{6} D_4 S - \frac{1}{2} D_3) n^4 + \dots]_0^S) = \\
&10^{-6} \left(\frac{N}{T} \right) (0.0122 S^2 + \frac{1}{2} D_1 S^2 + \frac{1}{6} D_2 S^3 + \frac{1}{24} D_3 S^4 + \dots) \quad (5)
\end{aligned}$$

This is, as already stated the error, $\langle r \rangle_1$, on one stave; the error on the other stave, $\langle r \rangle_2$, we get obviously through

$$\langle r \rangle_2 = 10^{-6} \left(\frac{N}{T} \right) \left[0.0122 S^2 + \int_0^S (S-n) \frac{\partial \langle \theta \rangle}{\partial z} (n) dn \right]$$

a computation similar to (5) we find

$$\langle r \rangle_2 = 10^{-6} \left(\frac{N}{T} \right) (0.0122 S^2 + \frac{1}{2} D_1 S^2 - \frac{1}{6} D_2 S^3 + \frac{1}{24} D_3 S^4 + \dots) \quad (6)$$

(We have here obviously presupposed that we have the same sight length, S , for both forward and backward sights).

The total Brunner correction for refraction is then

$$\underline{\langle r \rangle} = \langle r \rangle_1 - \langle r \rangle_2 = \underline{10^{-6} \left(\frac{N}{T} \right) \left(\frac{1}{3} \right) D_2 S^3 + \dots} \quad (7)$$

i.e. it is a clear second order effect! (plus maybe a term of fourth order). Even more important we see that it does not at all depend on the first derivative D_1 !

It should like to round off this study of Brunner's paper by showing that if you in (7) introduce the concept of parallelism between ground and isothermal surfaces you very quickly get Kukkamäki's formula.

In fact it is easy to see then that $\frac{\cos \alpha_1}{\cos \beta_1}$ from (4) is determined by

$$\frac{\cos \alpha_1}{\cos \beta_1} = \frac{\cos (\frac{\pi}{2} + \beta)_1}{\cos \beta_1} = \frac{\sin \beta_1}{\cos \beta_1} = \operatorname{tg} \beta_1 = \frac{\Delta z}{2S}$$

$$\begin{aligned} \langle r \rangle &= 10^{-6} \left(\frac{N}{T} \right) \left(\frac{1}{3} \frac{\cos \alpha_1}{\cos \beta_1} \left(\frac{\partial^2 \langle \theta \rangle}{\partial z^2} \right)_0 S^3 \dots \right) = \\ &10^{-6} \left(\frac{N}{T} \right) \left(\frac{1}{6} \right) \frac{\Delta z}{S} \left(\frac{\partial^2 \langle \theta \rangle}{\partial z^2} \right)_0 S^3 + \dots = \eta \Sigma S^2 \Delta z \\ &(\eta \text{ some parameter}) \end{aligned}$$

which of course is the well-known Kukkamäki formula.

The problem today is in other words simply to determine

$$D_2 = \left(\frac{d^2 t}{dz^2} \right)_0$$

(h height above ground, t temperature index zero meaning value at instrument height)

This is however more difficult than one might think off hand. We shall shortly describe the difficulties.

Calling the instrument height z_0 the simplest possible way for determining $\left(\frac{d^2 t}{dz^2} \right)_0$ would be to measure three temperatures t_1 , t_2 and t_3 in heights $z_0 - 1\text{m}$, z_0 and $z_0 + 1\text{m}$ above the ground. We should then have

$$\left(\frac{d^2 t}{dz^2} \right)_0 = (t_3 - t_2) - (t_2 - t_1) = t_3 - 2t_2 + t_1$$

Assuming that all three temperature measurements have the same standard deviation and that they are uncorrelated we get:

$$\sigma^2 \left\{ \left(\frac{d^2 t}{dz^2} \right)_0 \right\} = \sigma^2 + 4\sigma^2 + \sigma^2 = 6\sigma^2$$

We know that $\left(\frac{d^2 t}{dz^2} \right)_0$ has the magnitude of $\sim 0.3 \text{ degree/m}^2$ so that the standard error should not be greater than 0.15 degree/m^2 that is

$$\sigma^2 \left\{ \left(\frac{d^2 t}{dz^2} \right)_0 \right\} = 6\sigma^2 \leq (0.15)^2 \quad \text{or}$$

$$\sigma^2 \leq \frac{0.0225}{6} = 0.00375 \text{ degree}^2$$

and

$$\sigma \leq 0.061 \text{ degree}$$

i.e. you must be able to measure temperature with a standard deviation of $\frac{6}{100}$ degree Kelvin (under field conditions) while normally the claimed standard

deviation is 0.1 .

However even this figure may be much too optimistic according to a very recent thesis by R. Gottwald [5] from which I take the liberty of translating into english the following part of the conclusion (p. 139, line 13): "During this investigation it turned out that the values for the accuracies of air temperature measurements usually given in the literature as between 0.02 and 0.1 must be viewed as too optimistic and really only reflect the inner accuracy of the systems. Moreover, depending on the choice of sun cover and weather conditions one must expect systematic temperature errors larger than 1° . It was thus possible to prove that normal temperature sensors (such as thermistors) in principle are unsuitable for precise measurements of absolute air temperatures".

The other obvious method is to let the levelling measurements themselves monitor the refraction (as explained in greater detail in [10] and [11]). Our usual observation equation for levelling

$$l + v = \xi_i - \xi_{i-1}$$

then becomes instead

$$l + v = \xi_i - \xi_{i+1} + (\sum_{j=i}^n S_j^2, \Delta h_j) \eta \quad (8)$$

where n is the number of set-up's between two levelling points, S_j is the j 'th sight-distance, Δh_j is the j 'th height-difference and η is a common parameter to be determined along with the heights, ξ_j , in the adjustment.

There exists a very simple connection between η and the second derivative (see [10] p. 14):

$$\eta = \frac{1}{6} \left(\frac{dn}{dt} \right) \left(\frac{d^2 t}{dz^2} \right)_0 \quad (9)$$

where

$$\frac{dn}{dt} \sim -0.933 \cdot 10^{-6} \text{ degree}^{-1}$$

(n refractive index)

so that through we can very easily compute a mean value of the second derivative from our η -value.

On the basis of various reports from researchers in the field we are to day able to compute 7 η -values and corresponding second derivatives from different levellings (the reports on which the computation of the η -values is based are behind in brackets):

		η m^{-2}	$\left(\frac{d^2 t}{dz^2} \right)$ degree/ m^2
Denmark	[9]	$-0.48 \cdot 10^{-7}$	0.31
Maryland	[13]	$-0.56 \cdot 10^{-7}$	0.36
California	[12]	$-0.55 \cdot 10^{-7}$	0.35
United Kingdom	[3]	$-0.54 \cdot 10^{-7}$	0.35

Finland	[1]	$-0.97 \cdot 10^{-7}$	0.62
Arizona	[13]	$-0.98 \cdot 10^{-7}$	0.63
Canada	[8]	$-1.02 \cdot 10^{-7}$	0.66

Although we have only seven values they do seem to group themselves into two distinct groups. When looking at the places with respectively low and high η -values we see that it is tempting to say that we have one η -value around -10^{-7} m^{-2} when we are in a typical continental climate while the low η -value around $-0.5 \cdot 10^{-7} \text{ m}^{-2}$ is seen in near ocean areas.

For the measurements from California we have one independent estimate of $(\frac{d^2 t}{dz^2})_0$ namely from

$$(\frac{d^2 t}{dz^2})_0 = -0.46 - (-0.87) = 0.41 \text{ degree/m}^2$$

We remark that this value does not deviate significantly from the value above determined from the levelling observations themselves which was

$$(\frac{d^2 t}{dz^2})_0 = 0.35 \text{ degree/m}^2$$

the second derivative determined by temperature measurements having a standard deviation of 0.045 degree/m^2 .

References

- [1] Andersen, O. Bedsted (1982): Non-Random Effects in the Finnish Levelings of High Precision, Manuscripta Geodaetica. Vol. 7, pages 353-373.
- [2] Brunner, F. (1980): Systematic and random atmospheric refraction effects in geodetic Levelling. NAD SYMPOSIUM proceedings Ottawa.
- [3] Calvert, C. (1983): Personal Communication, 1983
- [4] Castle, R.O. and M. Elliot (1982): The Sea Slope Problem revised JGR. Vol. 87, No. 38, pages 6989-7024, August 10, 1982.
- [5] Gottwald, R. (1985): Zur Genauigkeitssteigerung und Erstellung eines automatisierten Datenflusses beim trigonometrischen Nivellement mit kurzen Zielweiten. D 82 (Diss. TH Aachen).
- [6] Kukkamäki, T.J., (1938): Über die Nivellitische Refraktion, Veröff. des Finn. Geodät. Inst. No. 25, Helsinki
- [7] Kukkamäki, T.J., (1939): Formeln und Tabellen zur Berechnung der Nivellitischen Refraktion. Veröff. des Finn. Geod. Inst. No. 27, Helsinki.
- [8] Lachapelle, G. and O. Remmer: The Solution of the Transcanadian Discrepancy, unpublished Manuscript.

- [9] Remmer, O., (1977): The Direct Experimental Detection of the
 Systematic Refraction Error of Precise Levelling, Geodætisk Inst.
 Medd. No. 52, København.
- [10] Remmer, O., (1980): Refraction in Levelling, Geodætisk Inst. Medd.
 No. 54, København.
- [11] Remmer, O., (1982): Modelling Errors in Geometric Levelling, Proceed-
 ings Survey Control Networks. Meeting of Study Group 5B, 7-9th
 July. Skrifterreihe, HSBW.
- [12] Stein, R.S., W. Thatcher, W.E. Strange, S.R. Holdahl and L.T. Whalen
 (1982): Field Test for the Accumulation of Differential Refraction
 in Southern California. Proceedings of the General Meeting of the
 IAG. Tokio.
- [13] Whalen. C.T., (1980) Refraction errors in Levelling - NGS test
 results; NAD SYMPOSIUM proceedings Ottawa.

EMPIRICAL DETERMINATION OF MAGNETIC CORRECTIONS
FOR N11 LEVEL INSTRUMENTS

by

William E. Strange
National Geodetic Survey, Charting and Geodetic Services
National Ocean Service, NOAA
Rockville, Maryland 20852

ABSTRACT. The magnetic error for a section surveyed with a N11 level instrument can be expressed as $dM = A C L$, where dM , C , and L respectively are the magnetic error, the horizontal component of the Earth's magnetic field in the direction of the leveling, and the length of the section. A is a constant with units of mm/km/Gauss, which is associated with a particular instrument and compensator. To correct N11 leveling the constant A must be determined. Compensators have been repeatedly changed in these instruments and are not always available for laboratory calibration.

An empirical approach was used to determine A by comparing N11 leveling data with Fischer leveling data along the same line. The validity of this approach is demonstrated by the ability of A values derived from one line to adequately correct leveling carried out using the same instrument and compensator on other lines. Also, where adequate records are available, changes in values of A for an instrument were found to correspond to replacement or repair of the compensator in the instrument. Significant differences were found between empirical and laboratory derived values of A .

INTRODUCTION

Beginning in the 1960's compensator instruments were introduced into leveling in order to reduce the time required to level the instrument prior to taking a reading. The compensators on most of these instruments employed some type of mirror suspended on invar wires. Three types of compensator instruments, the Ni2, Ni002, and Ni1 were extensively used by the National Geodetic Survey (NGS). Other types such as the MOM Ni A31 were used to a minor extent. Based on laboratory experiments, Rumpf and Meurisch (1981) reported errors were being introduced into the compensator levels by magnetic fields -- both the Earth's field and AC magnetic fields. This result has been verified by other investigators (Whalen 1984, 1985; Kukkamaki and Lehmuskaski, 1984) who have carried out additional laboratory determinations of magnetic effects on compensator levels.

The magnetic error has also been demonstrated by simultaneous leveling with compensator and spirit levels (Packard and MacNeil, 1983).

REASON FOR EMPIRICAL CORRECTIONS FOR N11 LEVELS

The laboratory calibrations of NGS compensator levels carried out by Whalen (1984) showed that the magnetic corrections for N11 levels were large and highly variable from instrument to instrument, i.e., from compensator to compensator. NGS records of instrument repair indicate that all of the N11 instruments used by NGS have had compensators replaced one or more times during their lifetime. Indeed, the larger part of NGS leveling using N11 instruments was carried out with compensators which have since been replaced and are not available for laboratory calibration. Thus laboratory calibrations are of limited value in correcting past geodetic data obtained with N11 instruments. It was decided to attempt to derive calibration factors for previous compensators by empirical methods. Also, although NGS had not used N11 levels since early 1980, calibration of these instruments was not begun until December 1983. Therefore, it was desirable to determine if magnetic calibration constants determined in 1983 and 1984 were valid for leveling prior to 1980, i.e., if calibrations were stable with time.

METHODS OF EMPIRICAL CALIBRATION

Laboratory calibration results showed that the magnetic correction for a bench mark to bench mark section of leveling using a N11 level can be written

$$dM = A C L \quad (1)$$

where

dM = magnetic error for the section in millimeters

$C = D \cos \phi$

D = horizontal component of Earth's magnetic field in Gauss

ϕ = azimuth of direction of leveling with respect to magnetic north

L = length of section in kilometers

A = compensator unique proportionality constant with units of mm/km/Gauss

The objective in calibration is to obtain an estimate of A .

Using eq. (1) the magnetic correction M_I summed over the first I sections of a level line, would be

$$M_I = A \sum_{i=1}^I C_i L_i. \quad (2)$$

Consider a line which has been leveled twice, once with a Nil level and once with a Fischer spirit level. Assume that the only error in either of the levelings is the magnetic error in the Nil instrument and that a magnetic correction has not been applied. Then

$$H_I = \sum_{i=1}^I [h_i(F) - h_i(N)] = M_I \quad (3)$$

where $h_i(F)$ = the height difference over section i using
Fischer leveling

$h_i(N)$ = the height difference over section i using
Nil leveling with no magnetic correction applied.

From eq. (2) and (3) one gets

$$A = \frac{\sum_{i=1}^I \{ [h_i(F) - h_i(N)] / C_i L_i \}}{\sum_{i=1}^I C_i L_i} = H_I / \bar{M}_I \quad (4)$$

where \bar{M}_I is the magnetic correction for a unit value of A (i.e., $A = 1$) for the first I sections of the level line and H_I is the difference between Nil and Fischer determinations of height difference over the first I sections of the level line D .

The assumption that there is no random or systematic error in either leveling other than magnetic error is clearly incorrect. However, if other systematic errors are small and random errors are no larger than indicated by formal statistics, and no crustal movement has taken place, one could get a close estimate of A by plotting H_I vs \bar{M}_I for all values of I from 1 to I_{\max} , the maximum number of sections in the line. The slope of the best fitting line through the points in the plot would then provide an estimate of A .

Because the leveling data had already been processed using an estimate of A (which we shall call A') it was more convenient to proceed slightly differently in practice and determine $\Delta A = A - A'$. To do this plots were made of H'_I vs \bar{M}'_I .

where

$$\begin{aligned}\bar{M}'_I &= A' \bar{M}_I \\ H'_I &= \sum_I [h_i(F) - h'_i(N)]\end{aligned}\quad (5)$$

and $h'_i(N)$ is the Nil height difference for section i computed after applying a magnetic correction computed with A' . Then A could be computed from

$$A = A' + \Delta A. \quad (6)$$

The accuracy of this empirical approach depends upon the nature and magnitude of other errors which are present. The largest problem will arise where other systematic errors mimic magnetic error. Therefore, every effort was made to use data where other systematic errors were minimized. To accomplish this, leveling from relatively flat areas was used in the analysis wherever possible to minimize the presence of errors due to refraction and rod calibration. Tectonically active areas were avoided. Care was taken to eliminate data where local subsidence due to groundwater withdrawal was occurring.

Since the value of A was expected to be different from compensator to compensator, it was important to determine from maintenance records if and when compensators were replaced or repaired. Although maintenance records were not complete a large amount of information was available which permitted the identification of times of most compensator replacements and repairs.

RESULTS

As examples of how empirical determinations of values for A were achieved two instruments will be discussed. These are Nil instruments numbered 90760 and 90823. Values obtained for A for the compensators associated with these instruments are summarized in Table 1. For instrument 90760 maintenance records indicated that the compensator had been changed twice, once on September 23, 1975, and again on March 26, 1979. Therefore, the observational data were used to derive three independent values of A , one for each compensator associated with instrument 90760. For the period prior to September 23, 1975, three level lines were examined: a September to November 1973, leveling from Rouses Point, N.Y. to Saratoga Springs, N.Y; a November 1973 to January 1974 leveling from Vicksburg to Greenville, Mississippi; and a September to December 1974 leveling from Charleston, South Carolina to Savannah, Georgia.

Table 1.--Magnetic calibration constants

Nil instr. No.	Time period of applicability	Calibration constant (A)	
		empirical value (mm/km/gauss)	laboratory value (mm/km/gauss)
90760	1972-9/23/75	-3.28	
	9/23/75 - 3/26/79	-8.74	
	3/26/79 - present	-4.48	-11.51
90823	1972 - 6/1/75	+2.39	
	6/1/75 - present(?)	-15.13	-6.37

Figure 1 gives a plot of \bar{M}_I' vs H_I' for the September/December 1974 leveling. Ignoring the points near Savannah that are affected by subsidence a straight line was fit visually to the data, giving a value for A of -3.28 mm/km/Gauss. Figure 2 indicates the result of applying a magnetic correction using A = -3.28 mm/km/Gauss to the New York level line. As can be seen there is a substantial improvement in the agreement between Fischer and Nil leveling using the empirical value of A derived from the September/December 1974 leveling. Similar improvements were found when the -3.28 mm/km/Gauss value was used to reduce the Vicksburg to Greenville leveling.

Figure 3 shows a plot of \bar{M}_I' vs H_I' for a survey from New Bern to Wilmington, North Carolina, carried out with instrument 90760 during the period August to October 1979. Figure 4 shows the result of using the A value derived from the New Bern to Wilmington level line to correct leveling carried out in April and May 1979. Figure 5 shows a plot of \bar{M}_I' vs H_I' for instrument 90823 along two level lines for the period prior to June 1975, when instrument 90823 was returned to the factory for service. At this time work may have been done on the compensator. As may be seen the results from two lines, one leveled in Wisconsin in August/October 1972 and one leveled in New York in September/November 1973, yield similar values for A.

CONCLUSIONS AND FUTURE DIRECTIONS

The results presented in Figures 2 through 5 indicate that: (a) estimates of the constant, A, required to provide magnetic corrections for Nil data can be estimated from comparisons of Nil and Fischer leveling, and (b) the value of A for a given compensator is stable and does not vary significantly with time.

Ni 1 #90760
 PLOT OF H'_I VS \bar{M}'_I

CHARLESTON, S.C. TO SAVANNAH, GA.
 SEPT/DEC 1974

$A' = -8.74 \text{ mm/km/Gauss}$

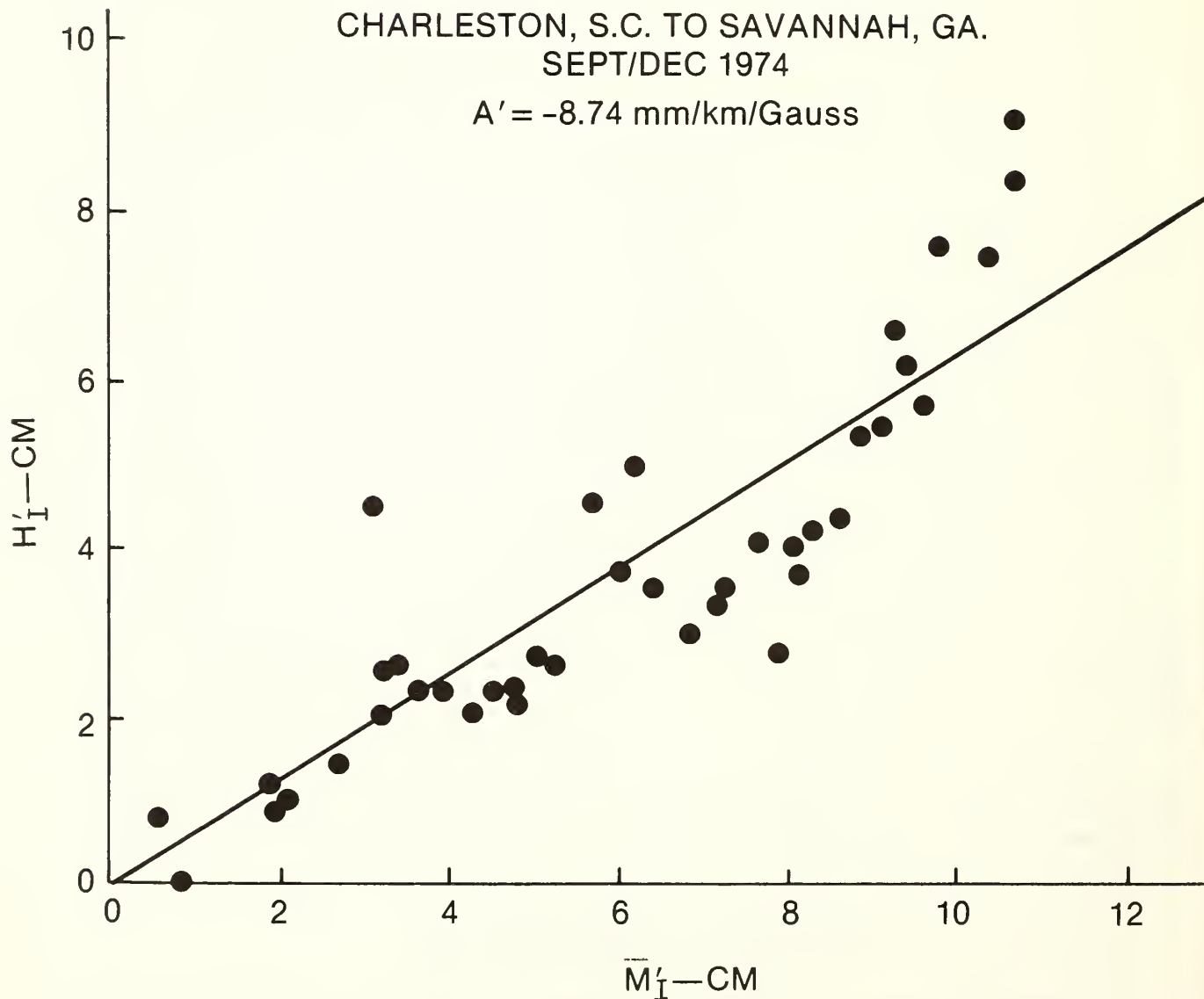


Figure 1

Ni 1 #90760

ROUSES POINT TO SARATOGA SPRINGS, NEW YORK
SEPTEMBER-NOVEMBER 1973

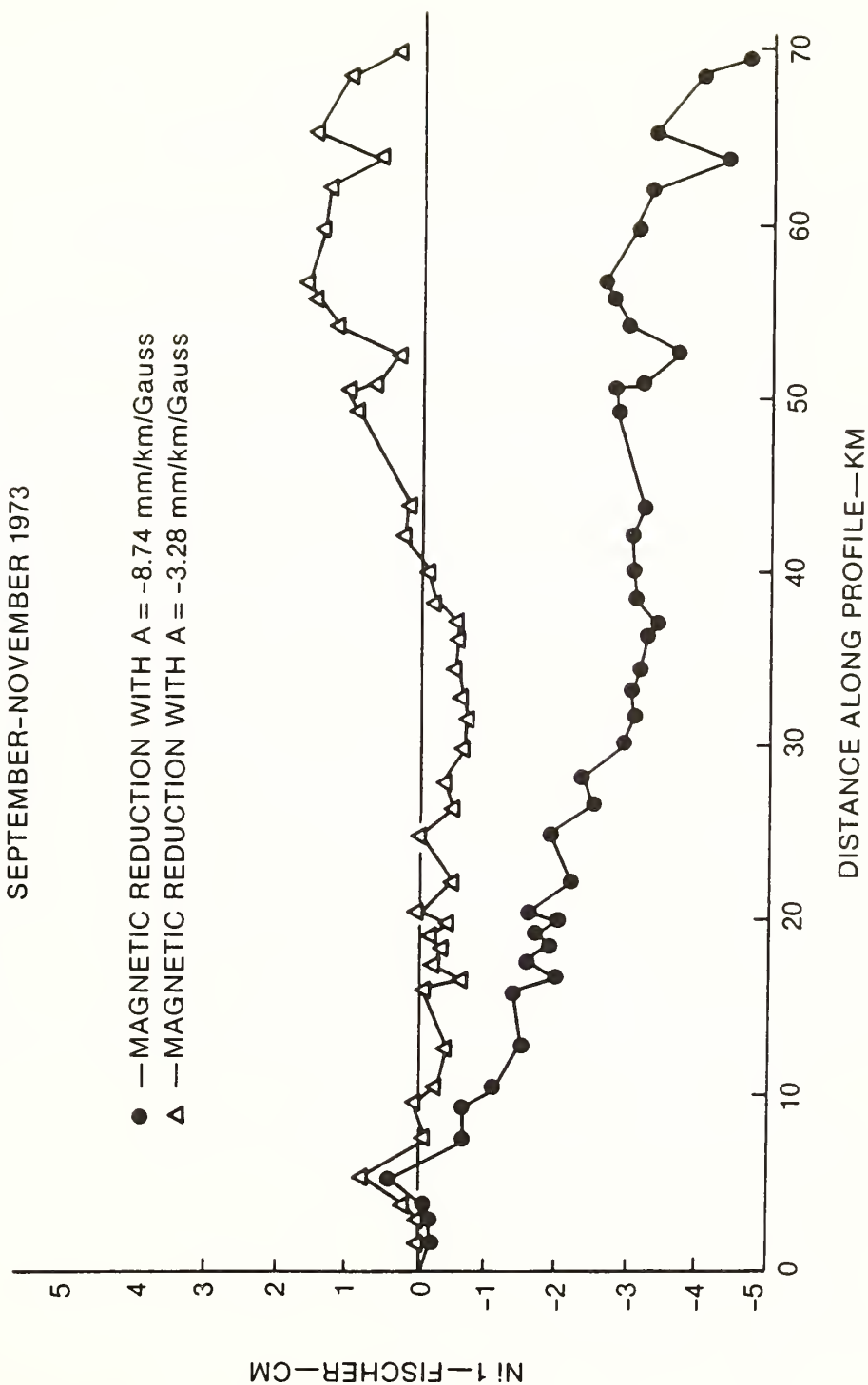


Figure 2

Ni 1 #90760
 PLOT OF H'_I VS \bar{M}'_I

NEW BERN TO WILMINGTON, N.C.
 AUG/OCT 1979

$A' = -11.51 \text{ mm/km/Gauss}$

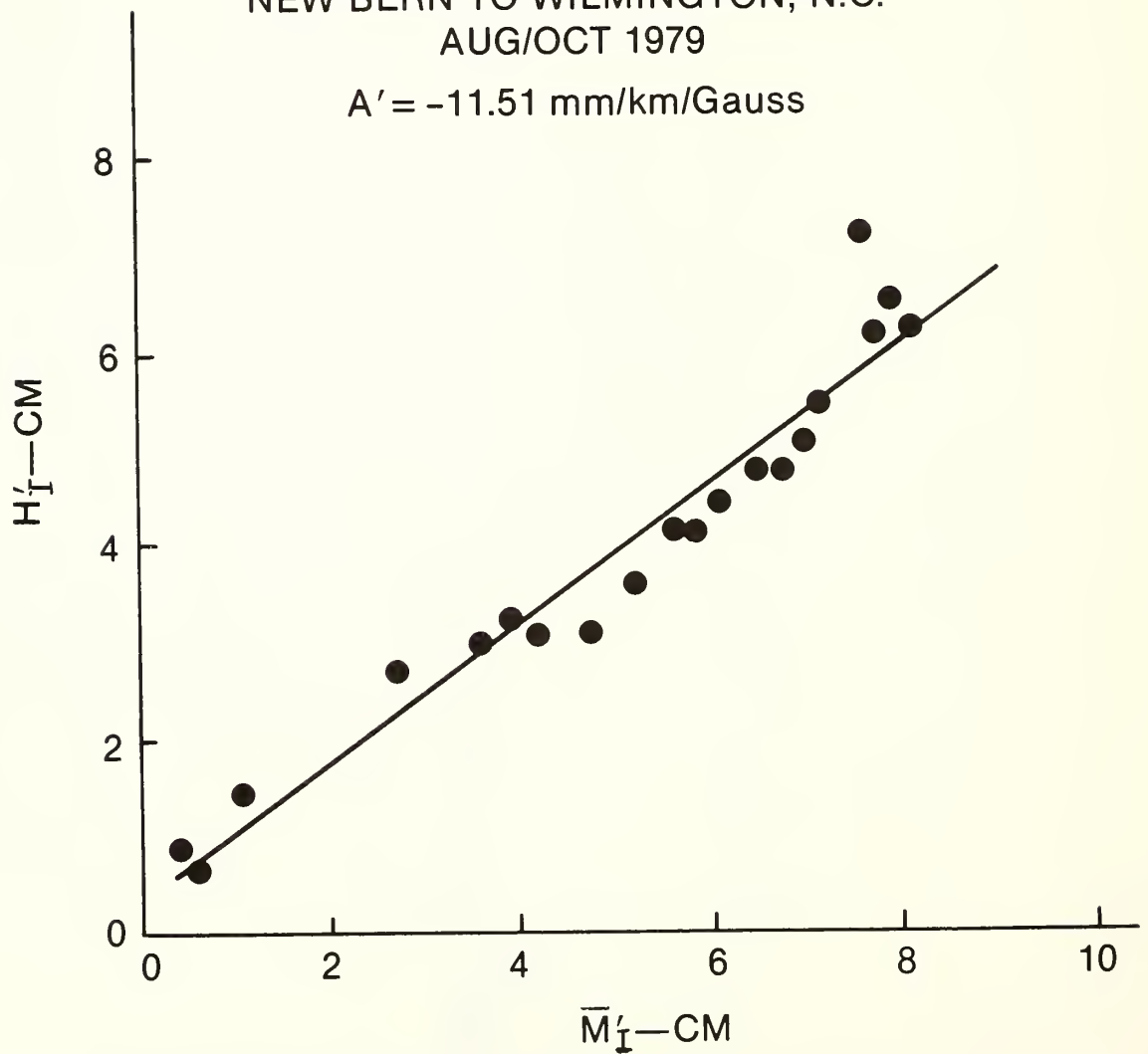


Figure 3

Ni 1 #90760

CHADBOURNE, N.C. TO CHARLESTON, S.C.
APRIL-MAY 1979

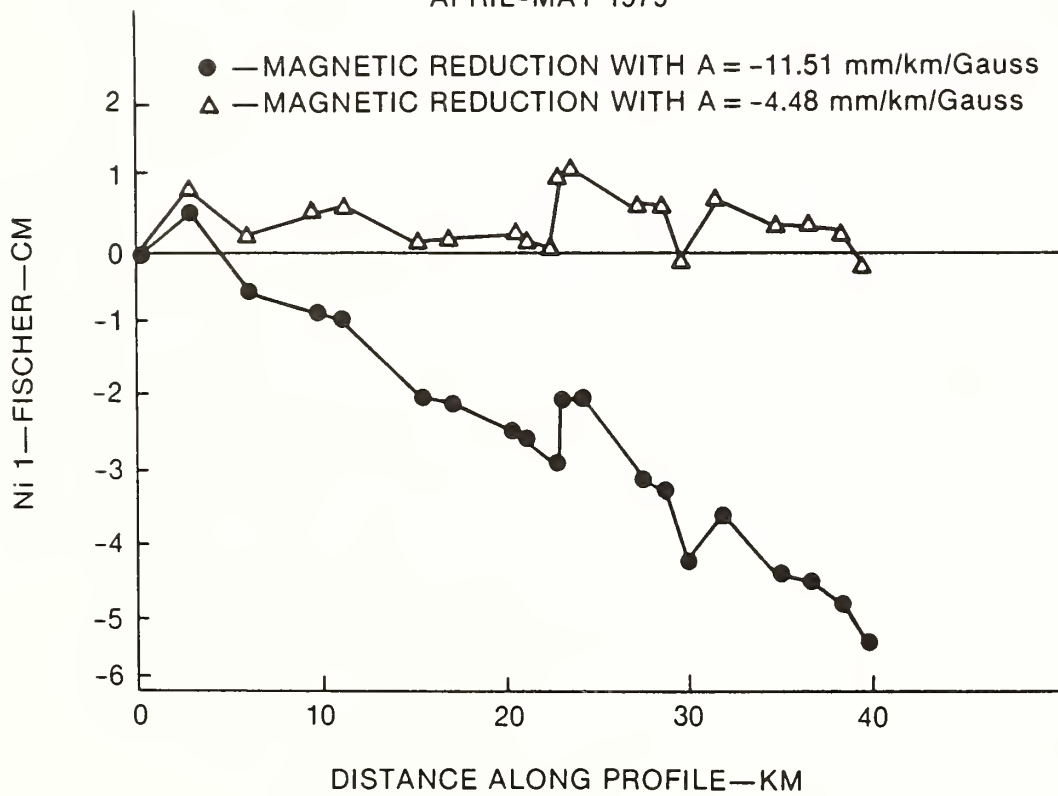


Figure 4

Ni 1 #90823
PLOT OF H'_I VS \bar{M}'_I

$A' = -6.37$ mm/km/Gauss

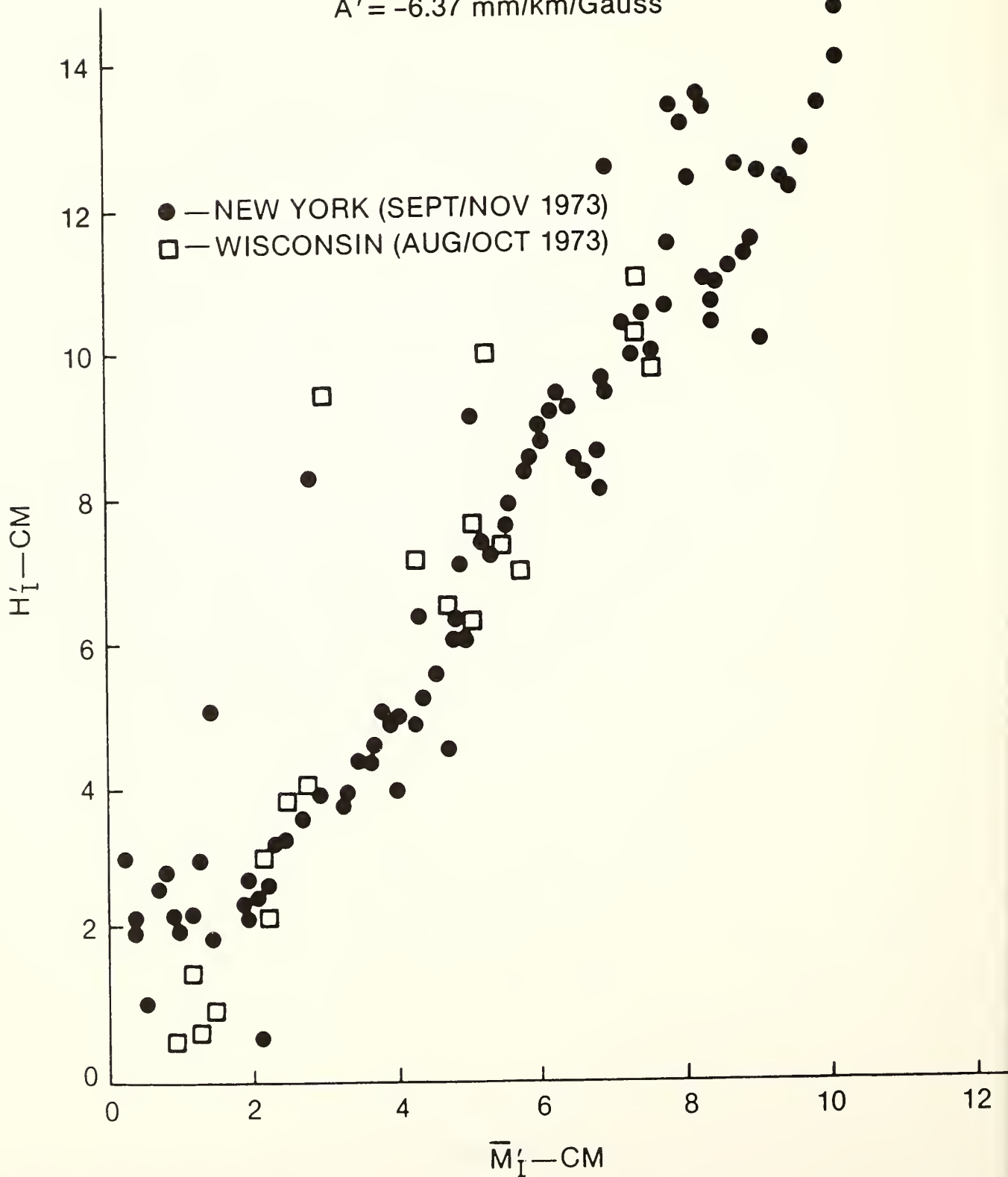


Figure 5

Obviously additional data must be analyzed to assure that the results obtained with this limited data set are generally applicable.

There are several points to be made concerning empirical derivation of A values. First, in computing the results reported here, the magnitude of the horizontal component of the magnetic field acting on a compensator was computed from a standard spherical harmonic representation of the Earth's magnetic field. This appears to have been an adequate representation for the lines examined, but it is important to note that this may not always be the case. For example, the magnetic field generated by a power transmission line running parallel to the survey route might be large enough to affect the results. Also, there are known to be very local variations in the Earth's magnetic field caused by highly magnetic rocks near the Earth's surface which are not modeled by the spherical harmonic approximation. Examples would be in the iron ranges of northern Wisconsin-northern Michigan and in volcanic areas such as Hawaii.

It should also be noted that empirically derived values of A do not always agree with those obtained by laboratory calibrations. This is indicated in Table 1. The reasons for this have not yet been determined. There are a number of possibilities: (1) errors in the empirical and/or laboratory calibrations, (2) unrecorded replacement or repairs of compensators during the 1980/1983 time laps between the last use of the instruments by NGS and the laboratory calibration, and (3) unidentified environmental effects.

Whatever the reason for the differences between empirical and laboratory calibrations it is clear that the 1983/84 laboratory calibrations will not always be successful in removing the magnetic error from data to which they are nominally applicable. For example, for instrument 90760 the empirically derived constant for the time period following the last known compensator change is found to produce much better agreement between Nil and Fisher levelings for three separate, geographically dispersed lines than does the laboratory derived constant. In this case the empirical constant is clearly the more accurate one.

Finally, the work reported here was an initial study to determine if useful magnetic corrections could be derived from an empirical approach. The results indicate that such an approach is possible. Derivation of final values of A from empirical analysis should be derived from some type of least squares adjustment. Such an adjustment would involve the total "suitable" leveling carried out with a given compensator. "Suitable" means that the Nil data used

and the data with which they are being compared are free of significant instrumental and environmental errors from other than magnetic sources as well as not contaminated by crustal movements. Two types of information are available for such an adjustment, differences of repeat leveling over the same line, as were used in this analysis, and values of loop closure using the Ni1 leveling.

REFERENCES

- Kukkamäki, T. J. and Lehmuskaski, P., 1984: Influence of the Earth magnetic field on Zeiss NI 002 levels, Reports of the Finnish Geodetic Institute, No. 84:1, Helsinki, Finland, 11 pp.
- Packard, R. F. and MacNeil, J. H., 1983: A direct comparison of spirit and compensator leveling, Geophysical Research Letters, Vol. 10, No. 9, p. 849-851.
- Rumpf, W. E., and Meurisch, H., 1981: Systematische Änderungen der Zeillinie eines Präzisions-kompensator-nivelliers -- insbesondere des Zeiss Ni 1 -- durch magnetische gleich- und wechselfelder. XVI International FIG Congress, Montreux, Switzerland.
- Whalen, C. T., 1985: Magnetic field effects on leveling instruments, submitted Jour. Geophys. Res.
- Whalen, C. T., 1984: Magnetic field effects on leveling instruments, (abst.), EOS, Trans. Amer. Geophys. Union,

ESTIMATION OF VARIANCE COMPONENTS IN LEVELING USING ITERATED ALMOST UNBIASED ESTIMATION

James R. Lucas
National Charting Research & Development Laboratory
Janice M. Bengston
David B. Zilkoski
National Geodetic Survey
Charting & Geodetic Services
National Ocean Service, NOAA
Rockville, MD 20852

ABSTRACT. The final adjustment of the North American Vertical Datum of 1988 (NAVD 88) project will combine sets of data acquired over more than half a century of changing instruments and procedures. It is essential that the weighting factors employed with these data be chosen with care. NGS has considered Minimum Norm Quadratic Unbiased Estimation (MINQUE) as a means of estimating the variance components in leveling data, but chose Iterated Almost Unbiased Estimation (IAUE) because of the ease with which it can be computed for sparse matrices. Results of using this technique in eight network adjustments are presented and analyzed, and plans for future investigations set forth.

INTRODUCTION

In recent years the geodetic community has become increasingly interested in methods of estimating variance components. This interest has been stimulated, in part, by a continually expanding need to merge into a single adjustment observations acquired by a variety of instrument systems. There is also a requirement for combining observation data acquired many years, or even decades, ago with modern observations in order to determine crustal motions. Since the technology employed in acquiring observations has been far less static than the quantities being observed, and the displacements are of about the same order of magnitude as observation errors, the weights assigned to these data must be chosen carefully. Estimation of components of variance from the observation data is one of the avenues being explored in an attempt to develop more realistic weighting factors for geodetic adjustments.

At the National Geodetic Survey (NGS), numerical investigations into variance component estimation were begun using MINQUE, as proposed by C. R. Rao (1971a). This method was tested in several different types of adjustments and found to produce estimates that were adequate. By numerical experiments, it was found that iterating MINQUE produces more reliable estimates. More importantly, if MINQUE produces negative estimates of one or more variance components, which it occasionally does, these estimates become positive after one or two iterations.

Prior to these numerical tests, a simpler estimation method had been derived by an NGS colleague, Allen J. Pope. This proved to be an independent derivation of AUE (Almost Unbiased Estimation) proposed by Horn et al. (1975), but Pope had the foresight to suggest that iterated AUE and iterated MINQUE should converge to the same set of estimates, though by different paths. His prediction was found to be correct and provided a more convenient estimation method for sparse matrix applications such as leveling.

In the final adjustment of the NAVD 88 project, different types of data will be combined into a single adjustment. Therefore, it is essential to impose a relative weighting scheme that is as nearly correct as possible. This implies that the a priori standard errors of each group of observation data must be estimated, a task which includes identifying the different groups of leveling observations and establishing and implementing a procedure to determine the appropriate a priori standard error to be used with each group.

Data sets (grouped according to instruments used and field procedures employed) have been identified, but may be modified after additional analysis. The data sets presently identified are described in this report. The Iterative Almost Unbiased Estimation (IAUE) technique has been implemented on an NGS minicomputer (HP-1000) and its application to leveling data is described in the next section.

THEORY

If a vertical network consists of a homogeneous set of observations, it fits the linear model

$$Y = AX + U\epsilon \quad (1)$$

where Y is an n -vector of observations, A is a known n by p matrix, X is a p -vector of unknown parameters, U is a known n by n matrix, and ϵ is an n -vector of random errors. If certain portions of the network were observed using different instruments or different observing procedures, it may be necessary to divide the observation data into homogeneous sets and write the model in the form

$$\begin{bmatrix} Y_1 \\ Y_2 \\ \vdots \\ Y_k \end{bmatrix} = \begin{bmatrix} A_1 \\ A_2 \\ \vdots \\ A_k \end{bmatrix} X + \begin{bmatrix} u_{11} & 0 & \dots & 0 \\ 0 & u_{22} & \dots & 0 \\ \vdots & \vdots & \ddots & \vdots \\ 0 & 0 & \dots & u_{kk} \end{bmatrix} \begin{bmatrix} \epsilon_1 \\ \epsilon_2 \\ \vdots \\ \epsilon_k \end{bmatrix} \quad (2)$$

Here, we have partitioned the matrix equation into k observation sets such that Y_i is an n_i -vector, A_i is an n_i by p submatrix, u_{ii} is a diagonal submatrix of dimension n_i , and ϵ_i is an n_i -vector of random

errors such that

$$\begin{aligned} E(\gamma_i) &= 0 \\ E(\gamma_i \gamma_i^T) &= \sigma_i^2 I \\ E(\gamma_i \gamma_j^T) &= 0 \quad (i \neq j) \end{aligned} \quad (3)$$

where E is the expected value operator and the σ_i^2 are unknown variance components.

From eq. (1), the expectation of Y is AX and its dispersion can be written

$$D(Y) = \sigma_1^2 V_1 + \sigma_2^2 V_2 + \dots + \sigma_k^2 V_k$$

where

$$V_i = U_i U_i^T \quad (4)$$

in which the U_i are obtained from partitioning U in the form

$$U = [U_1 \ U_2 \ \dots \ U_k].$$

Although the variances associated with the sets of random errors are considered to be unknown, some a priori estimate is always available.

Let α_i^2 be an a priori value for σ_i^2 from which we can form

$$H_i = \alpha_i^2 V_i \quad (5)$$

and a preliminary weight matrix

$$W = H^{-1}$$

in which

$$H = H_1 + H_2 + \dots + H_k.$$

Both the unknown parameters and the variance components can be estimated from the observation data. Standard least squares will provide an estimate

$$\begin{aligned} \hat{X} &= (A^T W A)^{-1} A^T W Y \\ &= N^{-1} A^T W Y \end{aligned} \quad (6)$$

for the parameters and there are a number of methods for estimating the σ_i^2 , most of which rely on some form of the matrix

$$R = W - W A N^{-1} A^T W. \quad (7)$$

Since $RA = 0$, $RY = RU\gamma$ and this matrix enables us to write k equations of the form

$$\begin{aligned} E(Y^T R V_i R Y) &= E(\gamma^T U^T R V_i R U \gamma) \\ &= \sigma_1^2 \text{tr}(R V_i R V_1) + \sigma_2^2 \text{tr}(R V_i R V_2) \\ &\quad + \dots + \sigma_k^2 \text{tr}(R V_i R V_k). \end{aligned} \quad (8)$$

Hence, we have the estimating system of equations

$$S \hat{\sigma} = q$$

where

$$S_{ij} = \text{tr}(R V_i R V_j) \quad (9)$$

$$q_i = Y^T R V_i R Y \quad (10)$$

and $\hat{\sigma}$ is a k -vector of estimates of the unknown variance components.

The MINQUE estimator was developed by Rao (1971a, 1971b, 1972) and it describes the various properties enforced in its derivation. Because MINQUE requires the trace of matrix products of the form shown in eq. (9), it appears that the full n by n matrix R is needed and, therefore, the full inverse of N . Since N can be very large and very sparse in vertical network adjustments, such a requirement would make variance component estimation impractical for large networks.

When this course of investigation began, it was believed that MINQUE did require the full inverse of N . It has since been learned, however, that MINQUE can be obtained from the full inverse of a relatively small submatrix of N involving only those parameters observed in two or more of the observation sets. This result will be employed in a future version of the estimating program, but its description is beyond the scope of this paper.

Another estimator can be developed directly from MINQUE by relaxing some of the requirements, such as the property of unbiasedness. If all a priori estimates were correct except for a single proportionality factor, i.e., $\sigma_i^2 = f \alpha_i^2$ for all i , then a slight modification of eq. (8) produces

$$\begin{aligned} E(Y^T R H_i R Y) &= f \alpha_i^2 [\text{tr}(R V_i R H_i) + \dots \\ &\quad + \text{tr}(R V_i R H_k)] \\ &= \sigma_i^2 \text{tr}(R V_i R H) \end{aligned} \quad (11)$$

The matrix product RH is an idempotent matrix. Therefore, $RHR = R$ and

$$\text{tr}(R V_i R H) = \text{tr}(V_i R H R) = \text{tr}(R V_i)$$

and eq. (11) produces a set of estimating equations of the form

$$\hat{\sigma}_i^2 = (Y^T R H_i R Y) / \text{tr}(R V_i) \quad (12)$$

proposed by Horn et al. (1975), called Almost Unbiased Estimator (AUE).

If the a priori estimates are proportional to the true estimates, it can be shown that AUE is unbiased, but this condition will seldom, if ever, be satisfied in practical applications. If the variance components were known to within a proportionality factor, we have the familiar problem of estimating a single variance factor, called the variance of unit weight. However, Horn et al. claim that the bias introduced by failure to meet the ideal conditions can be expected to be small. Hence, the appellation "almost unbiased."

Rather than assume a single f , it is sufficiently general to consider the a priori estimates to be related to the true variances by

$$\sigma_i^2 = f_i \sigma_i^2 \quad (13)$$

where f_i is an unknown variance factor. Substituting eq. (13) into a modified version of eq. (8), we have

$$\begin{aligned} E(Y^T R H_i R Y) &= \sigma_1^2 \text{tr}(R H_i R V_1) + \sigma_2^2 \text{tr}(R H_i R V_2) \\ &\quad + \dots + \sigma_k^2 \text{tr}(R H_i R V_k) \\ &= f_1 \text{tr}(R H_i R H_1) + f_2 \text{tr}(R H_i R H_2) \\ &\quad + \dots + f_k \text{tr}(R H_i R H_k) \end{aligned} \quad (14)$$

which provides a variation of MINQUE for estimating variance factors rather than the variance components.

Note that the variance factors will all approach unity as the a priori estimates approach the true variances. Using an iterative procedure, estimates of the variance factors are computed at each step and used to improve the estimates of the variance components going into the next iteration. Equation (14) can be rewritten in the form

$$\begin{aligned} E(Y^T R H_i R Y) &= \sum_{j=1}^k f_j \text{tr}(R H_i R H_j) + f_i \text{tr}(R H_i) \\ &\quad - f_i \sum_{j=1}^k \text{tr}(R H_i R H_j) \\ &= f_i \text{tr}(R H_i) + \sum_{j=1}^k (f_j - f_i) \text{tr}(R H_i R H_j) \end{aligned}$$

which separates the bias terms (in the summation) from the AUE for the variance factors. As the variance factors approach unity, the bias

terms vanish, and we have the estimating equation for iterated AUE expressed as

$$\hat{f}_i = (Y^T R H_i R Y) / \text{tr}(R H_i). \quad (15)$$

The estimating eq. (15) was employed in this study. It was derived independently at NGS, but it was later found to have been published by Forstner (1979a and 1979b). It has been shown (Schaffrin 1983) that this estimator converges to the same set of estimates as iterated MINQUE. It is less expensive to compute than iterated MINQUE, however, because it requires only the traces of products of R with the diagonal matrices H_i and these can be accumulated as scalar products, as will be shown.

For purposes of illustration, consider the matrix equation

$$\begin{bmatrix} -H & A \\ I & A^T \\ L & O \end{bmatrix} \begin{bmatrix} Z \\ X \end{bmatrix} = \begin{bmatrix} Y \\ I \\ O \end{bmatrix}.$$

The solution produces

$$X = N^{-1} A^T W Y,$$

the least squares estimate for the unknown parameters, and

$$Z = -W Y + W A X = -R Y,$$

the vector of weighted residuals.

The inverse of the coefficient matrix is found to be

$$\begin{bmatrix} -H & A \\ I & A^T \\ L & O \end{bmatrix}^{-1} = \begin{bmatrix} -R & W A N^{-1} \\ L N^{-1} A^T W & N^{-1} \end{bmatrix}$$

which provides a clue to a simple means of obtaining the trace of the matrix product involving R . If, after solution of the least squares normal equations and inversion of N , the observations are processed one at a time, elements of the weighted residual vector can be computed and the quadratic sum accumulated for the appropriate variance component. At the same time the diagonal element of R , corresponding to that observation, can be computed using a standard routine for sparse matrix inversion. The contribution to the appropriate $\text{tr}(R H_i)$ is then obtained from a single multiplication.

The only complication created by this variance component estimation technique is that iteration is now required. While estimation of the least squares parameters in a vertical network adjustment deals with a linear system of equations, the variance component estimation equations are nonlinear.

DATA SET SELECTION

In preparation for NAVD 88, circuits of leveling data (approximately 1 degree of latitude by 2 degrees of longitude) are being analyzed by performing minimally constrained adjustments on networks consisting of a few hundred stations in a procedure called block validation. All leveling observations which do not distort the primary net are included in these networks. Thus, boundary loops and intersecting interior lines may contain leveling of several epochs and accuracy classifications.

As a result, several questions have arisen. Should an accuracy classification of one epoch receive the same weight as the same accuracy classification of another epoch? Is the relative weighting scheme between accuracy classes accurate? Should the network geometry be considered in the relative weighting scheme?

In an attempt to answer these and other questions, NGS has programmed the IAUE algorithm to accept leveling data and compute estimates of variance components based on accuracy classification and epoch.

All leveling data were divided into eight epochs which were determined by major changes in leveling procedures and/or equipment as shown in table 1. Leveling was further separated into one of the seven different orders and classes. Thus a leveling line could be uniquely classified by order, class, and epoch.

Initial estimates of the variance components were based on order and class, ignoring the differences between epochs. These estimates were based on consideration of double-run levelings (Balazs 1985). A large number of forward and backward running differences were analyzed, and standard deviations to be applied to 1 kilometer sections of single-run leveling were estimated. The resulting values are given in table 2.

Input to the variance analysis program involved leveling data from block validation projects. Each network consisted of an outer primary loop, interior subnets connected to the primary loop, and any relevellings. Standard corrections to minimize systematic effects of temperature, rod scale, and other factors had been applied to all the data. The refraction correction was computed using Best's tables (Balazs and Young 1982). At the start of this study, Holdahl's temperature gradient model (Holdahl 1981) had not yet been incorporated into the data reduction program. Also, the influence of magnetic fields on compensator-type leveling instruments (Rumpf and Meurish 1981) had not yet been finalized, and therefore, no magnetic correction was applied. However, the networks had been subjected to thorough testing and blunders and outliers had been removed.

The study described in this report includes eight networks of which seven were in the northeastern United States and one in the southeast. Each network consists of at least 800 observations divided into at least four different categories of order, class, and epoch as displayed in table 3. Much of the leveling before 1915 had been removed

due to a large number of outliers between epochs, leaving little or no information on epochs 1 and 2.

Table 1.--Data epochs separated by significant changes in instrumentation or procedures

Data set identifier	Approximate dates	Significant change in instrumentation or procedure
1	before 1900	"Vienna" or "Stampfer" type instruments.
2	1900 - 1915	Introduction of the Fischer level.
3	1916 - 1956	Introduction of the C&GS Invar rod.
4	1957 - 1962	Reduction in maximum sight length from 150 to 75 meters and parties began "leap-frogging" rods.
5	1963 - 1970	Introduction of "parallel-plate micrometer" instruments and Kern double-scale Invar rods. Maximum sight length reduced from 75 to 50 m for first-order, class I; 60 m for first-order, class II and second-order, class I; and 70 m for second-order, class II. Maximum difference in length of forward and backward sights at each setup was reduced from 10 to 2 m for first-order, class I; 5 m for first-order, class II and second-order, class I. First-order also reduced from 10 to 4 m per section. Maximum section closure for micrometer method reduced to 3 mm/km.
6	1970 - 1975	Introduction of the Ni 1 compensator level. Introduction of the turning pin with cap. Increased use of 7 kg turning plate.
7	1976 - 1977	Introduction of the Ni002 reversible compensator. Use of new double-simultaneous method and automated recording system. Introduction of low- and high-scale checks.
8	1978 - present	Introduction of motorized leveling.

Table 2.--Estimated a priori standard error of observation

Order	Class	Standard Error mm/sqrt(km)
1	0	0.7
1	I	1.1
1	II	1.4
2	0	3.0
2	I	2.1
2	II	2.8
3	0	4.2

RESULTS

Tables 3 and 4 provide some interesting, and perhaps puzzling, information. First, all of the standard error estimates obtained from IAUE are larger than those obtained from analyses of forward and backward running differences. The pooled standard error estimates in first-order, class I are actually greater than the less precise first-order, class II in both epochs 5 and 6 (1961-1968 and 1969-1974). This could be an indication that some of the data are still contaminated by systematic errors that are not apparent until these data are combined with other data in a network analysis. As previously stated, not all of the corrections described by Balazs and Young (1982) had been applied to the data used in this study.

All data in the NGS vertical data base have now been processed using the latest corrections. These networks will be re-examined, and it is anticipated that the IAUE standard error estimates will be closer to the a priori due to the reduced influence of systematic errors.

The extent to which the estimated standard errors have been inflated by uncorrected systematic errors has yet to be determined. However, there were two sets of data from epoch 7 in which Zeiss Nil leveling instruments were used. It is well known that this compensator-type instrument is adversely affected by magnetic fields. The standard error estimated by IAUE for group 7 was 6.0175, which should decrease significantly after corrections for magnetic effects have been applied. It is interesting, and encouraging, to see that IAUE estimated so large a standard error for the data sample known to contain significant systematic error.

The design of the networks could be a reason for the large standard error estimates. Sixty-seven percent of all NGS leveling lines were observed following the procedures specified for second-order, class 0. Of these lines, 69 percent were leveled during epoch 3. The networks analyzed in this study were relatively small, and most groups did not consist of enough loop circuits to determine to what extent they were consistent within groups. This was not the case for second-order, class 0 levelings, however.

Table 3.--IAUE standard error estimates by project

Name of project	Epoch	Order	Class	Number of observations	Standard error	
					Estimated mm/sqrt(km)	a priori mm/sqrt(km)
L1BL161	3	1	2	800	4.8955	1.4
	3	2	0	2637	3.8616	3.0
	4	1	2	643	3.6452	1.4
	4	2	0	305	4.0875	3.0
	5	1	1	499	3.4062	1.1
	5	1	2	288	2.5237	1.4
	6	1	2	430	2.4193	1.4
	8	1	2	942	2.5022	1.4
S2RLNC	2	2	0	41	2.8727	3.0
	3	1	2	381	3.0681	1.4
	3	2	0	505	3.6682	3.0
	4	2	0	291	5.8190	3.0
	5	1	1	448	3.2272	1.1
	5	2	0	292	3.0733	3.0
	6	1	1	96	3.8406	1.1
	8	1	2	221	3.4087	1.4
S2RLWS	3	1	2	620	4.8719	1.4
	3	2	0	544	4.3131	3.0
	4	2	0	343	4.2253	3.0
	5	1	1	286	2.6956	1.1
	5	2	0	172	3.5252	3.0
	8	1	2	267	2.4673	1.4
J1ZNBK	3	1	2	384	3.6271	1.4
	3	2	0	926	3.5645	3.0
	4	2	0	298	6.2445	3.0
	5	1	1	289	3.8359	1.1
	5	2	0	270	3.6364	3.0
	8	1	2	333	1.9070	1.4
S2RC35	3	1	2	94	0.5222	1.4
	3	2	0	764	4.0339	3.0
	4	2	0	189	5.5347	3.0
	8	1	2	269	0.6023	1.4
S2RHAN	3	1	2	579	3.3573	1.4
	3	2	0	1250	4.1066	3.0
	4	1	2	94	3.2775	1.4
	4	2	0	565	3.8923	3.0
	5	1	2	68	2.6053	1.4
	5	2	0	261	4.8762	3.0
	6	1	1	152	3.8491	1.1
	8	1	2	375	3.2520	1.4
	3	1	2	48	2.1558	1.4
J1ZBRHL	3	2	0	504	4.6769	3.0
	6	2	0	83	4.4218	3.0
	8	1	2	119	2.2613	1.4
B3WNY3	3	1	2	482	4.4973	1.4
	3	2	0	947	3.6320	3.0
	5	1	2	163	2.0686	1.4
	7	1	1	85	6.0175	1.1
	8	1	2	96	2.4502	1.4

Table 3.--(continued)

Name of project	Epoch	Order	Class	Number of observations	Standard error	
					Estimated mm/sqrt(km)	a priori mm/sqrt(km)
B3WNY4	3	1	2	768	4.2771	1.4
	3	2	0	1553	3.6909	3.0
	5	1	2	90	2.5908	1.4
	7	1	1	41	6.1810	1.1
	8	1	2	498	2.2745	1.4
S2RPE34	3	1	2	19	2.2597	1.4
	3	2	0	851	2.3246	3.0
	4	2	0	162	5.3651	3.0
	5	1	1	400	1.2104	1.1
	5	2	0	184	8.8965	3.0
	6	2	1	151	3.3915	2.1
	8	1	2	170	2.4033	1.4

Table 4.--IAUE standard error estimates by data sets

Epoch	Order	Class	Number of obs.	Estimated standard error Pooled	a priori
2	2	0	41	2.8727	3.0
3	1	2	3388	4.1711	1.4
3	2	0	8077	3.9324	3.0
4	1	2	737	3.5986	1.4
4	2	0	1991	4.8529	3.0
5	1	1	1522	3.3166	1.1
5	1	2	519	2.3946	1.4
5	2	0	995	3.8322	3.0
6	1	1	248	3.8303	1.1
6	1	2	430	2.4193	1.4
6	2	0	83	4.4218	3.0
7	1	1	85	6.0175	1.1
8	1	2	2622	2.5086	1.4

During the last 50 years, much of the second-order, class 0 leveling was performed in support of topographic mapping activities. A 30 minute by 30 minute area usually consisted of many small second-order loops. These small circuits were leveled during one season and were internally consistent within the prescribed tolerances. Therefore, the sample networks analyzed in this study included many of these second-order, class 0 circuits, which were consistent with one another and may have dominated the data from other epochs, causing larger

standard error estimates. It is, however, encouraging that the IAUE estimates for second order, class 0 are close to their a priori estimates obtained from double-run leveling analysis. During the next phase of this analysis, larger networks consisting of fewer groups, but more circuits, will be used. This should help in obtaining more reliable standard error estimates.

Considering the small size of the sample, it appears that the relative weighting scheme requires further examination. Ideally, samples should contain an equal proportion of all accuracy classifications and epochs. However, second order, class 0 accounts for three times as much leveling as first order, class II, and together they make up 90 percent of all leveling. Furthermore, more than half the leveling was completed between 1916 and 1955 (epoch 3).

CONCLUSIONS

Results obtained so far from using IAUE to estimate standard errors for the various epochs, orders, and classes have to be regarded as inconclusive. The technique has been proven using simulated data, and it has performed well with some real data. It remains to be seen whether or not the available leveling data contain sufficient information, after all known systematic errors have been removed, to provide estimates that are characteristic of a particular group.

Now that all data have been adequately corrected, these networks will be analyzed further, and it is hoped that more consistent results will be obtained. As block validation progresses to other areas, it will be possible to test the hypothesis that the IAUE estimates will begin to cluster about mean values for each valid group.

REFERENCES

- Balazs, E. and G. Young, 1982: Corrections applied by the National Geodetic Survey to precise leveling observations. NOAA Technical Memorandum NOS NGS-34, National Geodetic Information Center, NOAA, Rockville, MD.
- Balazs, E., 1985: Personal communication.
- Forstner, W., 1979a: Konvergenzbeschleunigung bei der posteriori varianzschätzung, Zeitschrift für Vermessungswesen, 97, 166-172.
- Forstner, W., 1979b: Ein verfahren zur schätzung von varianz- und kovarianz komponenten, Allgemeine Vermessungsnachrichten, 85, 264-269.
- Holdahl, S. R. 1981: A model of temperature stratification for correction of leveling refraction, Bulletin Geodesique, 55, 231-249.
- Horn, S. D., R. A. Horn, and D. B. Duncan, 1975: Estimating heteroscedastic variances in linear models, Journal of the American Statistical Association, 70, 380-385.

- Rao, C. R. 1972: Estimation of Variance and covariance components in linear models, Journal of the American Statistical Association, 67, 112-115.
- Rao, C. R ., 1971a: Estimation of variance and covariance components--MINQUE theory, Journal of Multivariate Analysis, 1, 257-275.
- Rao, C. R., 1971b: Minimum variance quadratic unbiased estimation of variance components, Journal of Multivariate Analysis, 1, 445-456.
- Rumpf W. E., and H. Meurish, 1981: Systematische aunderungen der ziellinie eines prazisions kompensator-nivelliers--insbesondere des Zeiss Ni 1 -- durch magnetische gleich - und wechselfelder. XVI International FIG Congress, Montreaux, Switzerland.
- Schaffrin, B., 1983: Varianz-kovarianz-komponenten-schatzung bei der Ausgleichung heterogener Wiederholungsmessungen, Publ. DGK C-282, Munich, German Democratic Republic.

ASSESSMENT OF LEVELLING MEASUREMENTS
USING THE THEORY OF MINQE

Yong-qi Chen*
Adam Chrzanowski
Department of Surveying Engineering
University of New Brunswick
P.O. Box 4400
Fredericton, N.B.
Canada
E3B 5A3

ABSTRACT: The determination of observation weights and of error models in levelling networks is a current problem. The method of Minimum Norm Quadratic Estimation (MINQE) is proposed for the determination of the error model. Different possible models of error structure of levelling measurements are estimated from the adjustment of a network or from the forward-backward discrepancies of levelling lines using the iterated MINQE. An appropriate model of error structure can be obtained after comparing the estimated parameters in the models with their standard deviations. As an example, a first-order levelling network has been analysed. The results demonstrate the usefulness of the method.

INTRODUCTION

The problem of evaluating levelling errors has concerned geodesists for decades, not only for proper weighting of the observations in the adjustment of vertical networks but also for a better understanding of the behaviour of the accumulation of errors in levelling. In 1912, the International Association of Geodesy adopted Lallemand's formula [Bomford, 1980], in which the levelling error was represented by a random part proportional to the square root of the length of a levelling line and a systematic part accumulating linearly with the length. Later, Vignal [Bomford, 1980] modified Lallemand's formula by considering the systematic error as liable to change after certain distance intervals, such as some tens of kilometres. In 1948, a collection of formulae designed to provide a systematic method for the evaluation of levelling was accepted by the Association. However, these formulae are not prevalent in the practice of network adjustment. Instead, a weight inversely proportional to the length of a levelling line is used in many countries (e.g., Kok et al. [1980]; Skaggs [1980]). This is also suggested in a new proposal [Remmer, 1984] on redefinition of the error parameters for levelling networks. There are two possible reasons for this. One is due to the existence of some shortcomings in these formulae, especially relating to the empirical nature of certain parameters. The other is, as pointed out by Bomford [1980], the adoption of these formulae for the weighting of levelling lines implies some correlation between the errors of adjacent lines, which is difficult to formulate. Some scientists have questioned this weighting scheme. Among others, Lucht [1972], Steinberg [1978], and Vanicek and Grafarend [1980], have considered the correlation of individual height differences between consecutive segments along a levelling line, which has led to the so-called "power law" of error propagation. Based on the same idea, Anderson and Blais [1980] mentioned their consideration of a fully populated variance-covariance matrix for a levelling network. In addition, Mecherski [1981] and Bou [1983] have found that the accuracy of a levelling line also depends on the

* On leave from the Wuhan Technical University of Surveying and Mapping, Wuhan, People's Republic of China.

height difference.

Regarding these developments, the problem in the realization and testing of different suggestions and considerations still remains to be solved. It is the authors' opinion that the error structure model for a levelling network should be established from the analysis of the survey data rather than from some assumptions or definitions. In connection with this, a systematic method should be developed.

The concept of the estimation of variance-covariance components can be extended a little further to fit this purpose. In surveying engineering, some special applications of the methods of variance-covariance component estimation can be found in Sjöberg [1980], Grafarend and Kleusberg [1980], Koch [1981], and Chen [1983]. However, due to the complexity of the error behaviour in levelling, no attempt has been made to apply it to the assessment of levelling measurements.

In this paper the authors propose to use the theory of Minimum Norm Quadratic Estimation (MINQE), a method of the estimation of variance-covariance components, to evaluate levelling measurements. First, the basic theory is summarized, followed by considerations of its application in levelling. Finally, an example of the evaluation of a first-order network is given.

SUMMARY OF THE MINQE THEORY

Consider the linear Gauss-Markoff model $(\underline{l}, A\underline{x}, \Sigma)$ with \underline{l} as an n -vector of observations, A as the design matrix of $n \times u$ dimensions, and \underline{x} as a u -vector of unknown parameters such that the expectation values $E\{\underline{l}\} = A\underline{x}$ and the dispersion matrix $D\{\underline{l}\} = \Sigma$, which has the structure

$$\Sigma = \sum_{i=1}^m \theta_i T_i, \quad (1)$$

where $\theta_1, \dots, \theta_m$ are the unknown variance-covariance components to be estimated, and T_1, \dots, T_m are given matrices. A quadratic function $\underline{l}^T M \underline{l}$ is said to be a Minimum Norm Quadratic Estimator with unbiasedness and invariance in a translation of \underline{l} by $A\underline{x}$ of $p_1 \theta_1 + \dots + p_m \theta_m$ (a linear function of θ_i), denoted by MINQE(U, I), if the quadratic matrix M is determined from (Rao and Mitra, 1971):

$$\left. \begin{array}{l} \text{Tr}\{M\Sigma(\underline{\theta}_0)M\Sigma(\underline{\theta}_0)\} \text{ is minimum} \\ \text{subject to } MA=0, \text{Tr}\{MT_i\} = p_i, \forall i \end{array} \right\} \quad (2)$$

where $\Sigma(\underline{\theta}_0) = \sum_{i=1}^m \theta_i^{(0)} \cdot T_i$ with $\theta_i^{(0)}$ as a priori value of θ_i . From the solution of equation (2), one obtained the estimated variance-covariance components as:

$$\underline{\hat{\theta}} = (\hat{\theta}_1, \dots, \hat{\theta}_m)^T = S^{-1} \underline{q}, \quad (3)$$

where the (i,j) th element of matrix S is

$$S_{ij} = \text{Tr}\{R(\underline{\theta}_0) T_i R(\underline{\theta}_0) T_j\}, \quad (3a)$$

and the i th component of vector \underline{q} is

$$q_i = \underline{l}^T R(\underline{\theta}_0) T_i R(\underline{\theta}_0) \underline{l}, \quad (3b)$$

and

$$R(\underline{\theta}_0) = \Sigma(\underline{\theta}_0)^{-1} (I - A(A^T \Sigma(\underline{\theta}_0)^{-1} A)^{-1} A^T \Sigma(\underline{\theta}_0)^{-1}) \quad (3c)$$

with I being the identity matrix.

It is clear from equation (2) that the MINQE(U,I) so obtained are locally best estimates. Thus, numerical iterations are performed to ensure uniformly best estimates. Let the estimators from equation (3), denoted by $\hat{\underline{\theta}}_1$, be chosen as the approximate values of $\underline{\theta}$. When the MINQE(U,I) is recomputed, the estimators from the second iteration are:

$$\hat{\underline{\theta}}_2 = (S(\hat{\underline{\theta}}_1))^{-1} \underline{q}(\hat{\underline{\theta}}_1) \quad (4)$$

If the process is continued and the solution for $\underline{\theta}$ converges, the limiting values will satisfy the equation

$$(S(\underline{\theta}))\underline{\theta} = \underline{q}(\underline{\theta}) \quad (5)$$

The solution of equation (5) is defined as IMINQE(U,I), the iterated MINQE(U,I).

There are other methods to estimate variance-covariance components in statistics, e.g., the method based on the analysis of variances [Searle, 1971], and the method of maximum likelihood estimation [Harvill, 1977]. Compared with the others, the MINQE seems to be as fundamental as the least-squares method of estimation, where no assumption about the distribution of observations is made. This becomes important if levelling measurements are considered as following a truncated distribution due to some tolerances in specifications. However, if they are assumed to be normally distributed, the MINQE(U,I) will be identical with the best invariant quadratic unbiased estimation (BIQUE) [Lamotte, 1973], and both the method of marginal maximum likelihood estimation and the method of maximum likelihood estimation are special cases of the MINQE [Rao, 1979]. The former is equal to IMINQE(U,I) and the latter is the same as IMINQE(I), i.e., the iterated MINQE without the unbiasedness condition of $\text{Tr}\{MT_i\} = p_i, \forall i$, in equation (2).

APPLICATION OF THE MINQE THEORY IN THE ASSESSMENT OF LEVELLING MEASUREMENTS

The accuracy of precise levelling depends on personal, instrumental, topographical and atmospherical influences. Its sources of error have been discussed in many publications (e.g., Bomford [1980]; Kukkamäki [1980]). For a specific levelling operation, the variance of a levelling line i can be generally considered as a function of its length ℓ_i and height difference h_i :

$$\sigma_i^2 = f(\ell_i, h_i) \quad (6)$$

Equation (6) may be approximated by a simple polynomial:

$$\sigma_i^2 = \alpha \ell_i + \beta \ell_i^2 + \gamma |h_i| + \delta h_i^2 \quad (7)$$

or some other, non-linear functions could be employed. Because of some similarities in topographic or in atmospheric or in both conditions in the area covered by a levelling network, correlation among the levelling lines, especially neighbouring lines, may exist. The covariance of the levelling lines i and j is expressed as

$$\sigma_{ij} = \sigma_i \cdot \sigma_j \cdot \rho_{ij} \quad (8)$$

where ρ_{ij} is the correlation coefficient. The correlation coefficient ρ is related to a correlation function. Different families of correlation functions can be postulated, for instance, the Gaussian function

$$\rho(a; d) = a d^2, \quad (9)$$

or Hirvonen's function

$$\rho(c; d) = 1/(1 + \frac{d^2}{c^2}), \quad (10)$$

or a polynomial function

$$\rho(b_i; d) = \sum_i b_i d^i, \quad (11)$$

where d is the distance between the midpoints of two levelling lines, and a, b_i, c are parameters. If only the correlation between the neighbouring lines is considered and a constant correlation coefficient is used, equation (8) becomes:

$$\sigma_{ij} = \sigma_i \cdot \sigma_j \cdot \rho. \quad (12)$$

The parameters involved in the variance and covariance can be estimated from the real data using the IMINQE(U,I) method given in the previous section. Several possible models of error structure for a levelling network can be constructed. The significance of the estimated parameters are tested by comparing them with their standard deviations. If some estimated parameters are small against their standard deviations, it can be reasoned that either the corresponding error components may not exist or the given sample is not large enough to obtain reliable estimators. Then, the postulated model of error structure is consequently modified.

Under the normality assumption that $\underline{l} \sim N(\underline{Ax}, \Sigma)$, the covariance of two quadratic functions $\underline{l}^T \underline{M}_1 \underline{l}$ and $\underline{l}^T \underline{M}_2 \underline{l}$ is computable from [Rao and Mitra, 1971]:

$$\text{cov}\{\underline{l}^T \underline{M}_1 \underline{l}, \underline{l}^T \underline{M}_2 \underline{l}\} = 4\underline{x}^T \underline{A}^T \underline{M}_1 \Sigma \underline{M}_2 \underline{Ax} + 2\text{Tr}\{\underline{M}_1 \Sigma \underline{M}_2 \Sigma\} \quad (13)$$

Applying equation (13) to equation (5), one obtains:

$$\begin{aligned} \text{cov}\{q_i(\underline{\theta}), q_j(\underline{\theta})\} &= \text{cov}\{\underline{l}^T \underline{R}(\underline{\theta}) \underline{T}_i \underline{R}(\underline{\theta}) \underline{l}, \underline{l}^T \underline{R}(\underline{\theta}) \underline{T}_j \underline{R}(\underline{\theta}) \underline{l}\} \\ &= 2\text{Tr}\{\underline{R}(\underline{\theta}) \underline{T}_i \underline{R}(\underline{\theta}) \Sigma \underline{R}(\underline{\theta}) \underline{T}_j \underline{R}(\underline{\theta}) \Sigma\} \\ &= 2S_{ij} \end{aligned}$$

Thus, the dispersion matrix of $\hat{\underline{\theta}}$ is

$$D\{\hat{\underline{\theta}}\} = 2(S(\hat{\underline{\theta}}))^{-1} \quad (14)$$

The computation of the MINQE as it is defined by equation (3) involves the inversion of $\Sigma(\underline{\theta}_{-k}) = \sum_{i=1}^m \theta_i^{(k)} \cdot \underline{T}_i$, an n th order matrix, and of $(\underline{A}^T \Sigma(\underline{\theta}_{-k})^{-1} \underline{A})$, a u th order matrix. But, the computation efforts can be considerably reduced if the method of condition adjustment is applied. Let

$$\underline{B}\underline{v} + \underline{w} = 0 \quad (15)$$

be the condition equations of a levelling network, where \underline{B} is the configuration matrix of $r \times n$ dimensions, \underline{v} is the vector of residuals, and \underline{w} is the vector of misclosures. Then, the expressions for S_{ij} and q_i in equation (3) are derived in Chen [1983] as:

$$S_{ij} = \text{Tr}\{B^T T_i B^T (B \Sigma(\theta_0) B^T)^{-1} B^T T_j B^T (B \Sigma(\theta_0) B^T)^{-1}\} \quad (3a')$$

$$q_i = \underline{w}^T (B \Sigma(\theta_0) B^T)^{-1} B^T T_i B^T (B \Sigma(\theta_0) B^T)^{-1} \underline{w}, \quad (3b')$$

where $\Sigma(\theta_0)$ and T_i have been defined previously.

Precise levelling is usually performed in two opposite directions and under different meteorological conditions to reduce the various systematic sources of error. The mean values of the height differences from the forward and backward runs are used in the adjustment. Since the mean values and the forward-backward discrepancies generally do not contain the same error information [Entin, 1959; Strange, 1980], the error structure model for weighting the observations should be estimated from the adjustment of networks. On the other hand, one may be interested in investigating the differences between the error structure model estimated from the adjustment of a network and that estimated from the discrepancies. In such a case, the error structure model of levelling measurements is obtained from the discrepancies in the following way.

Let Δ_k ($k=1, \dots, n$) be the discrepancies between the two runs of levelling line k and let us postulate, for instance,

$$\sigma_k^2 = \alpha \ell_k^2 + \beta \ell_k^2 + \delta h_k^2 \quad (16)$$

as the error structure model. Using formulae (3a') and (3b'), one obtains

$$\left. \begin{aligned} S_{ij} &= \sum_{k=1}^n t_{ik} \cdot t_{jk} / (\sigma_k^{(o)})^4, \quad (i, j=1, 2, 3) \\ q_i &= \frac{1}{4} \sum_{k=1}^n t_{ik} \cdot \Delta_k^2 / (\sigma_k^{(o)})^4, \quad (i=1, 2, 3) \end{aligned} \right\} \quad (17)$$

where $t_{1k} = \ell_k$, $t_{2k} = \ell_k^2$, $t_{3k} = h_k^2$, and $(\sigma_k^{(o)})^2$ is the approximate value of the variance of levelling line k , which is calculated from the error model (16) with the a priori values of $\alpha^{(o)}$, $\beta^{(o)}$, and $\delta^{(o)}$. It is interesting to note that the equations (17) correspond to the normal equations of the following least-squares fitting:

$$\frac{1}{4} \Delta_k^2 + r_k = \alpha \ell_k^2 + \beta \ell_k^2 + \delta h_k^2, \quad (k=1, \dots, n) \quad (18)$$

where r_k is the residual after the fitting. The weight of the "observation" Δ_k^2 is inversely proportional to the variance of Δ_k^2 , i.e.,

$$V\left\{\frac{1}{4} \Delta_k^2\right\} = 2\sigma_k^4. \quad (19)$$

EXAMPLE AND DISCUSSION

Figure 1 shows a first-order levelling network in West Germany, which consists of six subnetworks, 339 levelling lines, and 114 circuits, surveyed in different periods of time. The data is obtained from Heller [1955]. Some basic information on the network is summarized in Table 1.

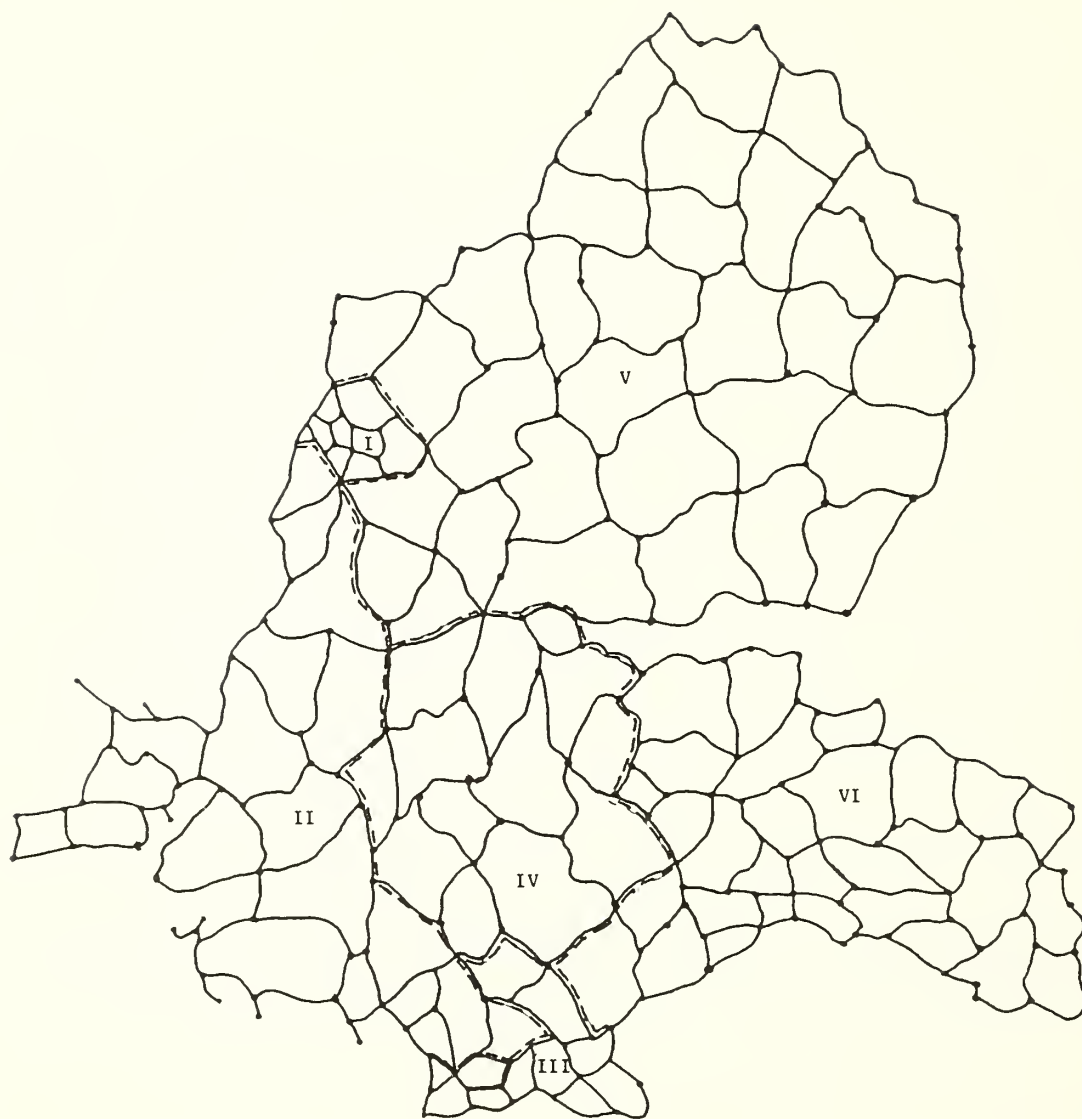


Figure 1: A first order levelling network (not to scale)

TABLE 1

Basic information on the levelling network.

Subnetworks	Number of Levelling Lines	Number of Circuits	The total Length (km)	Period of Survey
I	32	11	679	1912 - 1921
II	68	19	4052	1912 - 1926
III	30	11	967	1935
IV	42	13	2445	1936 - 1938
V	91	31	6525	1939 - 1942
VI	76	29	1899	

In the assessment of the measurements, the subnetworks were adjusted separately to avoid the influence of possible vertical crustal movements over the period of thirty years, but the error structure models were estimated from all the data to ensure enough redundancies. Several possible models were attempted using the method of the IMINQE(U,I) and the results are presented in Table 2. Comparing the estimated parameters with their standard deviations, one can clearly see that model 3 is the most appropriate. This model indicates that the random error of the levelling lines is $0.43 \text{ mm/km}^{1/2}$ and the non-random error is 0.054 mm/km . The term of non-random error comes from Wassef [1974] to include unmodelled systematic errors and other causes of internal correlations. Height differences do not play a significant role in the accuracy of this particular network.

TABLE 2

The variance components and their standard deviations
estimated from the subnetworks.

	Error structure models	α	β	γ	δ
1	$\sigma_i^2 = \alpha l_i + \beta l_i^2 + \gamma h_i + \delta h_i^2$	0.17(0.09)	0.0031(0.0016)	-1.93(32)	1.05(4.5)
2	$\sigma_i^2 = \alpha l_i + \beta l_i^2 + \delta h_i^2$	0.16(0.10)	0.0029(0.0017)		0.67(0.96)
3	$\sigma_i^2 = \alpha l_i + \beta l_i^2$	0.18(0.10)	0.0029(0.0017)		
4	$\sigma_i^2 = \alpha l_i + \delta h_i^2$	0.35(0.06)			0.69(1.0)

Notes: Standard deviations of the variance components are in parentheses; line lengths in kilometres; height differences in 100 metres.

Error structure models were also estimated from the forward-backward discrepancies. The discrepancies of 206 levelling lines which are in subnetworks I, II, III, VI were available from Heller [1955]. The results are given in Table 3.

TABLE 3

The variance components and their standard deviations estimated from the discrepancies.

	Error structure models	α	β	γ	δ
1	$\sigma_i^2 = \alpha l_i + \beta l_i^2 + \delta h_i^2$	0.098(0.028)	0.0023(0.0008)		-0.08(0.17)
2	$\sigma_i^2 = \alpha l_i + \beta l_i^2$	0.095(0.028)	0.0024(0.0008)		
3	$\sigma_i^2 = \alpha l_i + \delta h_i^2$	0.202(0.020)			-0.13(0.14)

It is clear that model 2 is the most appropriate. In this model, the random error is $0.31 \text{ mm/km}^{1/2}$ and the non-random error is 0.048 mm/km . The same model was estimated from the adjustment of the subnetworks I, II, III, and VI. The estimated components are

$$\alpha = 0.198 \text{ mm}^2/\text{km}$$

$$\beta = 0.0029 \text{ mm}^2/\text{km}^2$$

Three problems concerning the above results are discussed below.

(1) Consideration of the height differences between the two terminal points of levelling lines in modelling may be incomplete if a large change in the elevations within levelling lines is present. Due to the lack of detailed information on individual lines, an investigation of this possible factor could not be made.

(2) Unmodelled systematic errors and internal correlation may not necessarily produce an error which is linear with the length of a levelling line. However, the most appropriate models obtained from the adjustment of the subnetworks and from the discrepancies will approximate the actual situations in the best possible way. Higher order polynomial can also be used to model the error. In this case, negative components should be allowed. For example, an error model of the third-order polynomial was estimated from the discrepancies resulting in:

$$\sigma_i^2 = 0.068 l_i + 0.004 l_i^2 - 1.7 \times 10^{-5} l_i^3$$

For a comparison, the standard deviations of levelling lines calculated from this model and from model 2 in Table 3 are listed in Table 4. It is clearly shown that

TABLE 4

Standard deviations of levelling lines evaluated from the two models

distance (km)	10	20	30	40	50	60	70	80	90	100
Models										
$\sigma_i^2=0.068l_i + 0.004l_i^2 - 1.7\times10^{-5}l_i^3$	1.0	1.7	2.3	2.8	3.4	3.8	4.4	4.7	5.1	5.5
$\sigma_i^2=0.095l_i + 0.0024l_i^2$	1.1	1.7	2.2	2.8	3.3	3.8	4.4	4.8	5.3	5.8

Note: the standard deviations are in mm.

the differences are not apparent.

(3) Compared with the values estimated from the subnetworks I, II, III, and VI, the random error obtained from the discrepancies is significantly reduced but the non-random error remains compatible. This result seems difficult to interpret because one usually expects that the random errors would remain compatible while the non-random errors would be different. Regarding the error behaviour in the discrepancies and in the mean values, there have been different opinions and results among researchers. Remmer [1984] considered that the error calculated from discrepancies of two runs would be a random error and the mean value might contain systematic error. Strange [1980] found that the discrepancies systematically accumulated with distance, but the mean values gave very nearly the correct values. Other authors (e.g., Chiarini and Piepi [1974], Vanicek and Craymer [1984]) have also found some systematic trends in the discrepancies.

If all the levelling lines in a network are more or less uniform in length, the two error components of α and β cannot be well determined. In this case, use of the inverses of the lengths of the levelling lines for weighting is justified, provided that the height differences of levelling lines have been proved to be an insignificant factor.

The six subnetworks were adjusted using two different weighting schemes: one using the established error structure model, and the other using the inverses of the lengths of the levelling lines. The differences in the residuals were not excessive. Out of a total of 339 levelling lines, 14 lines exceeded 1 mm and the maximum difference was 3.5 mm. The reason for this was due to the uniformity of the lengths of the levelling lines in the subnetworks, which was reflected by the correlation coefficient of -0.8 between the estimated components α and β .

The correlation among the levelling lines was also studied using the method of the IMINQE(U,I). In the first investigation, Hirvonen's correlation function (10) was used. The error structure model is:

$$\sigma_i^2 = \alpha l_i + \beta l_i^2$$

and

$$\sigma_{ij} = \sigma_i \sigma_j / (1 + \frac{d_{ij}^2}{c^2})$$

where c is the correlation length. The distance d_{ij} between the midpoints of levelling lines i and j was measured from the figures given in Heller [1955], where only approximate scale was provided. The components of α , β , and c were estimated. Because of non-linearity with respect to component c , linearization and iteration procedures were required. The results were obtained from the subnetworks II, IV, V, and VI, and are presented in Table 5.

TABLE 5

Estimated variance and covariance components with their standard deviations.

Models	α	β	c (km)	ρ
$\sigma_{ij} = \sigma_i \sigma_j / (1 + \frac{d_{ij}^2}{c^2})$	0.29(0.2)	0.0021(0.0026)	9(10.0)	
$\sigma_{ij} = \sigma_i \cdot \sigma_j \cdot \rho$	0.20(0.1)	0.0030(0.0017)		0.021(0.1)

In another investigation, only the correlation between the neighbouring lines was considered. The covariance of the neighbouring lines i and j is

$$\sigma_{ij} = \sigma_i \cdot \sigma_j \cdot \rho$$

The values of α , β , and ρ were estimated from six subnetworks and are listed in Table 5.

It can be concluded from Table 5 that no significant correlation exists in this network. The question may arise why the significant non-random error has been found in the levelling lines without any significant correlation between them. One could try to answer this question by assuming, for instance, that the levelling lines had been surveyed by different survey crews, or the lines from junction points had been measured at different times. The real reason might be impossible to determine. However, the most important output of the analysis has been to find the facts contained in the real data.

CONCLUDING REMARKS

For nation-wide and continent-wide levelling networks, it is worth evaluating the measurements in detail not only for weighting purposes at the adjustment stage but also for a better understanding of the nature of error accumulation. The MINQE theory of estimation of the variance-covariance components provides an optimal and straightforward method for estimation of different possible models of error structure. An appropriate model of error structure for a levelling network can be established after comparing the estimated quantities with their standard deviations. The example shows that the proposed method to evaluate levelling measurements seems to work well, though it is not claimed that a complete analysis of this particular network has been made.

Since the method is of a statistical nature, a sufficient number of redundancies are required to obtain reliably estimated quantities. Further research on its application to national networks with more detailed information should be conducted.

ACKNOWLEDGEMENT

This work was supported by the Natural Science and Engineering Research Council of Canada.

REFERENCES

- Anderson, E.G. and J.A.R. Blais, 1980: "Weight estimation in geodetic levelling." Proceedings of the Second International Symposium on Problems Related to the Redefinition of North American Vertical Geodetic Networks, Ottawa, May, p. 453 (abstract only).
- Bomford, G., 1980: Geodesy. 4th Ed., Oxford University Press, London.
- Bou, Z.P., 1983: "On the accuracy and weighting of the first order levelling." Journal of Wuhan Technical University of Surveying and Mapping, No. 2, pp.1-15, Wuhan, People's Republic of China.
- Chen, Y.Q., 1983 : "Analysis of deformation surveys--A generalized method." Department of Surveying Engineering Technical Report No. 94, University of New Brunswick, Fredericton, N.B., Canada.

- Chiarini, A. and L. Pieri, 1971: "Statistical analysis of discrepancies in high precision levelling." Bulletin Geodesique, pp. 5-27.
- Entin, I.I., 1959: "Main systematic errors in precise levelling." Bulletin Geodesique, No. 52, pp. 37-45.
- Grafarend, E. and A. Kleusberg, 1980: Expectation and variance component estimation of multivariate gyrotheodolite observations I." Allgemeine Vermessungs-Nachrichten, 87, pp. 129-137, Herbert Wichmann Verlag, Karlsruhe.
- Harvill, D.A., 1977: "Maximum likelihood approaches to variance component estimation and to related problems." Journal of American Statistics Association, 72, pp. 330-340.
- Heller, E., 1955: "Entwicklung und Genauigkeit des neuen deutschen Haupthöhennetzes." Deutsche Geodätische Kommission, Reihe B, Heft Nr. 17.
- Koch, K.R., 1981: "Varianz und Kovarianzkomponentenschätzung für Streckenmessungen auf Eichlinien." Allgemeine Vermessungs-Nachrichten, Heft 4, pp. 125-132, Herbert Wichmann Verlag, Karlsruhe.
- Kok, J.J., W. Ehrnsperger and H. Rietveld, 1980: "The 1979 adjustment of the United European Levelling Network (UELN) and its analysis of precision and reliability." Proceedings of the Second International Symposium on Problems Related to the Redefinition of North American Vertical Geodetic Networks, Ottawa, May, pp. 455-483.
- Kukkamäki, T.J., 1980: "Errors affecting levelling." Proceedings of the Second International Symposium on Problems Related to the Redefinition of North American Vertical Geodetic Networks, Ottawa, May, pp. 1-10.
- Lamotte, L.R., 1973: "Quadratic estimation of variance components." Biometrics, 29, pp. 311-330.
- Lucht, H., 1972: "Korrelation im Präzisionsnivellement." Wissenschaftliche Arbeiten der Institutes für Geodäsie und Photogrammetrie und Kartographie, Nr. 48, Technische Universität Hannover.
- Mecherski, I.N., 1981: "On the accuracy of the first order levelling in mountainous area." Geodesy and Kartography, No. 3, Moscow (in Russian).
- Rao, C.R. and S.K. Mitra, 1971: Generalized Inverse of Matrices and its Applications. John Wiley & Sons, Inc., Toronto.
- Rao, C.R., 1979: "MINQE theory and its relation to ML and MML estimation of variance components." Sankhya, Vol. 41, Series B, pp. 138-153.
- Remmer, O., 1984: "Error parameters for levelling networks." Meddelelse No. 56, Geodetic Institute, Copenhagen.
- Searle, S.R., 1971: "Topic in variance component estimation." Biometrics, 27, pp. 1-76.
- Sjöberg, L., 1980: "Maximum likelihood estimation of covariances and weighted mean with application to repeated EDM-observations." Zeitschrift für Vermessungswesen, Heft. 10, pp. 484-490, Verlag Konrad Wittwer, Stuttgart.

- Skaggs, H., 1980: "Status of vertical geodetic data at the Defense Mapping Agency Hydrographic/Topographic Center for Mexico and Central America." Proceedings of the Second International Symposium on Problems Related to the Redefinition of North American Vertical Geodetic Networks, Ottawa, May, pp. 39-48.
- Steinberg, J., 1978: "Zur Fehlertheorie des Nivellements höchster Genauigkeit.: Arbeiten aus dem Vermessungs und Kartenwesen der DDR, Band 40.
- Strange, W.E., 1980: "The effect of systematic errors on geodynamic analysis." Proceedings of the Second International Symposium on Problems Related to the Redefinition of North American Vertical Geodetic Networks, Ottawa, May, pp. 705-727.
- Vanicek, P. and E.P. Grafarend, 1980: "On the weight estimation in levelling." NOAA Technical Report NOS 86 NGS 17, Rockville, MD, U.S.A.
- Vanicek, P. and M. Craymer, 1983: "Autocorrelation functions in the search for systematic errors in levelling." Manuscripta Geodaetica.
- Wassef, A.M., 1974: "On the search for reliable criteria of the accuracy of precise levelling based on statistical considerations of the discrepancies." Bulletin Geodesique, No. 112, pp. 149-163.

MODULATED NORMAL DISTRIBUTION STUDY
AND ITS POSSIBLE APPLICATION
TO LEVELLING ERRORS

Rachid Mazaachi
Geodetic Survey Division
Surveys and Mapping Branch
Energy, Mines and Resources
615 Booth Street Ottawa
Ontario K1A-0E9 Canada

ABSTRACT. From the beginning of time, as we remember, geodesists, in their analysis of repeated observations and observation errors, have considered these populations as normally distributed. In fact, a considerable majority of large samples are leptokurtic, that is to say, in the central part the observed points are clearly above the representative curve, while on both wings they are correspondingly below this curve. For this reason, a history of the normal distribution is briefly described in order to highlight the assumptions that form the base of Hagen's theory (1837)[3].

An attempt is made to expand these Hagen's Assumptions in order to introduce the modulated normal distribution of type I and type II. A brief description of the theories of these two probability density functions is developed.

A good example of leptokurtic tendency is given and analyzed, as gravimetric observations. An application of the modulated normal distribution of type I is made to levelling observations where the considered variate is the actual discrepancy between forward and backward runnings.

Finally, recommendations are made relating to the possible application of the modulated normal distribution to the levelling observations.

1. HAGEN'S ASSUMPTIONS AND NORMAL DISTRIBUTION

In order to introduce the normal distribution concept, we have to consider the Hagen's Assumptions (1837)[3] which constitute the foundation of his theory. From the point of view of this report, it is preferable to subdivide his single sentence into four components.

a- each measurement is, in Hagen's words, disturbed by an "infinite" number of causes of errors. In fact, it is necessary, in order to make an analytical use of such a hypothesis, to assume first that this number is finite but extremely large. This number will be designated by the symbol k .

b- each cause of errors produces an error which can be either positive or negative. This error will be termed "elementary error".

c- all elementary errors have the same absolute value. This value will be designated by the symbol $\epsilon/2$ ($\epsilon > 0$). Thus, an elementary error can be equal to $+\epsilon/2$ or $-\epsilon/2$. The quantity ϵ is first considered as finite but extremely small. There is obviously a relationship between the magnitude of k and ϵ .

d- the probability p that an elementary error will be positive is equal to the probability q that it will be negative. They are constants and equal to

$$p = q = 1/2 \quad (1.1)$$

The first variate we shall consider is denoted by X and is defined as the number of positive elementary errors. If Y is the number of negative errors, so that $Y=k-X$, the probability P_X that in a set of k events the number of pluses (i.e. of positive elementary errors) would be equal to X is

$$P_X = \frac{k! p^X q^Y}{X! Y!} \quad (1.2)$$

P_X passes through one single maximum P_M , where M is the first moment ω_1 with respect to the origin ($X=0$) which is

$$\omega_1 = M = \bar{X} = k/2 \quad (1.3)$$

The second central moment m_2 is expressed by

$$m_2 = k/4 \quad (1.4)$$

Many important properties of the binomial variate are evidenced by the introduction of the centered form. The new variate V is defined by the equation

$$V = X - kp \quad (1.5)$$

and the expression for P_V is then :

$$P_V = \frac{k!}{((k/2)+V)!((k/2)-V)!} (1/2)^k \quad (1.6)$$

A method based on differentiation procedures is applied to this formula and after several algebraic transformations we find

$$P_V = f(V) = \frac{1}{\sqrt{\pi(k/2)}} e^{-2V^2/k} \quad (1.7)$$

The total resulting error H , which is termed "Hagen's variate", is given by

$$H = \epsilon V = x \quad (1.8)$$

The first moment μ with respect to the origin (theoretical mean) and the second

central moment σ^2 (variance) are expressed by

$$\mu = \bar{H} = 0 \quad \sigma^2 = k\epsilon^2/4 \quad (1.9)$$

Using 1.8 and 1.9, 1.7 leads to:

$$f(x) = (1/\sigma\sqrt{2\pi}) e^{-x^2/2\sigma^2} \quad (1.10)$$

very well known formula of the probability density function of a normal distribution. This expression was published for the first time by de Moivre in his famous "Approximatio" (1732) [5] and later rediscovered by Adrian (1808) [1] and Gauss (1809) [2].

We see that it follows from Hagen's Assumptions that a random error x is distributed normally with a mean $\mu=0$, a standard deviation σ and a probability density function given respectively by (1.9) and (1.10)

2. MODULATED NORMAL DISTRIBUTION OF TYPE I

We notice that in Hagen's theory we assume the elementary error can take only two values, either $+\epsilon/2$ or $-\epsilon/2$. The basic new assumption, which will be added, is that the elementary error can also be equal to zero. It must, however, be stressed that the probabilities p (of $+\epsilon/2$), q (of $-\epsilon/2$) and r (of 0) cannot all be constant as this would lead to a trinomial variate which is extremely close to normality. To have a useful experimental applicability, we consider that p, q, r are not all constant. The analysis proceeds then as follows.

Thus k is subdivided into two parts,

$$k = n + z \quad (2.1)$$

n designating the number of non-zero errors ($\pm \epsilon/2$) and z the number of zero errors. From the standpoint of a physicist, the most natural assumption is that n can range between zero and k , in other words that an observation is not necessarily disturbed by all k error producing causes.

In order to give the additional assumption an analytical expression, we shall admit that there is a function $\phi(n)$ such that the differential

$$\phi(n)dn \quad (2.2)$$

will indicate the probability that n will fall into the interval $(n, n+dn)$. All those errors x which correspond to a given n , according to (1.9), are distributed normally with the variance

$$\sigma_n^2 = n\epsilon^2/4 \quad (2.3)$$

The compound probability that, simultaneously, n will fall into $(n, n+dn)$ and x

into $(x, x+dx)$, is given, considering (1.10), by the product

$$\phi(n)dn \cdot \frac{1}{\sigma \sqrt{2\pi}} e^{-x^2/2\sigma^2} dx \quad (2.4)$$

The total probability dP_X that x will fall into $(x, x+dx)$ whatever, the value of n , is

$$dP_X = \frac{2dx}{\epsilon \sqrt{2\pi}} \int_0^k e^{-2x^2/n\epsilon^2} \frac{\phi(n)}{\sqrt{n}} dn \quad (2.5)$$

To progress beyond this point, it is necessary to suggest an analytical expression for $\phi(n)$. This constitutes a new experimental and statistical question which can be approached only pragmatically, i.e. through a working hypothesis, the validity of which could be tested in practical applications. Such a hypothesis is, for example, that $\phi(n)$ is of the form

$$\phi(n) = An^a, \quad A \text{ and } a \text{ constants} \quad (2.6)$$

so that 2.5 become

$$dP_X = \frac{2(a+1)dx}{\epsilon k^{a+1} \sqrt{2\pi}} \int_0^k e^{-2x^2/n\epsilon^2} n^{a-1/2} dn \quad (2.7)$$

We obtain as the second central moment τ^2 (variance)

$$\tau^2 = \frac{a+1}{a+2} \cdot \frac{k\epsilon^2}{4} \quad (2.8)$$

P. McLane (1967) [4] has shown that it is valid to reverse the order of integrations in obtaining this equation.

The change of variable

$$t = n/k \quad (2.9)$$

and the elimination of the factor $(k\epsilon^2)$ in (2.7) yields the final expression of the probability density function

$$f(a, x) = \frac{(a+1) \sqrt{a+1}}{\tau \sqrt{2\pi} \sqrt{a+2}} \int_0^1 e^{-\frac{x^2}{2\tau^2} \frac{(a+1)}{(a+2)} \frac{1}{t}} t^{a-1/2} dt \quad (2.10)$$

A distribution which has such a pdf is said to be a modulated normal distribution of type I. The fact that n is variable is termed "modulation", $\phi(n)$ is the "modulating function" and a the "modulator".

Depending of the value of modulator a , the distribution is said equi-normal if $a=0$, radico-normal if $a=1/2$, lineo-normal if $a=1$ and quadri-normal if $a=2$.

All the representative curves $f(a,x)$ are leptokurtic with respect to the normal curve ($a=\infty$), that is to say in the central part these curves are clearly above the normal curve while on both wings they are correspondingly below this curve, as illustrated in figure 1.

The index of leptokurtosis $\omega(a)$ is defined as the ratio of the central ordinate $f(a,0)$ to the central ordinate of that normal curve in which the variance σ^2 is equal to the variance τ^2 of the modulated normal curve. This ratio is equal to

$$\omega(a) = \frac{2a+2}{2a+1} \sqrt{\frac{a+1}{a+2}} \quad (2.11)$$

The normal curve $f(\infty, x)$ is thus the extreme and "flatest" member of a family of modulated normal curve because (2.11) approaches unity as a tends towards infinity and as indicated in figure 1.

3. MODULATED NORMAL DISTRIBUTION OF TYPE II

In the modulation process as envisaged until now, the number of non-zero errors has been assumed to range between 0 and a certain number k . The physical interpretation of this assumption was quite clear and satisfying. From a purely theoretical point of view, there is no objection to envisage also the assumption that n can be larger than k , i.e. that it can range between a certain k and infinity. The distribution thus defined is termed the modulated normal distribution of type II.

This type of modulation has been examined only recently (Romanowski and Isaacs (1972) [8]). It is based upon the modulation function

$$\phi(n) = \frac{B}{n^b} = \frac{b-1}{n^b} k^{b-1} \quad (3.1)$$

which leads to the variance

$$\tau^2 = \frac{b-1}{b-2} - \frac{\epsilon^2 k}{4} \quad (3.2)$$

which indicates that τ^2 is finite only under the condition $b > 2$

The calculations leading to the expression of the probability density function $f(a,x)$ of the type II modulated normal distribution are similar to those of type I. The function $f(b,x)$ is

$$f(b,x) = \frac{(b-1)/b-1}{\tau\sqrt{2\pi}/b-2} \int_1^\infty e^{-\frac{x^2}{2\tau^2}} \cdot \frac{b-1}{b-2} \cdot \frac{1}{t} t^{-(b-1/2)} dt \quad (3.3)$$

and the index of leptokurtosis is

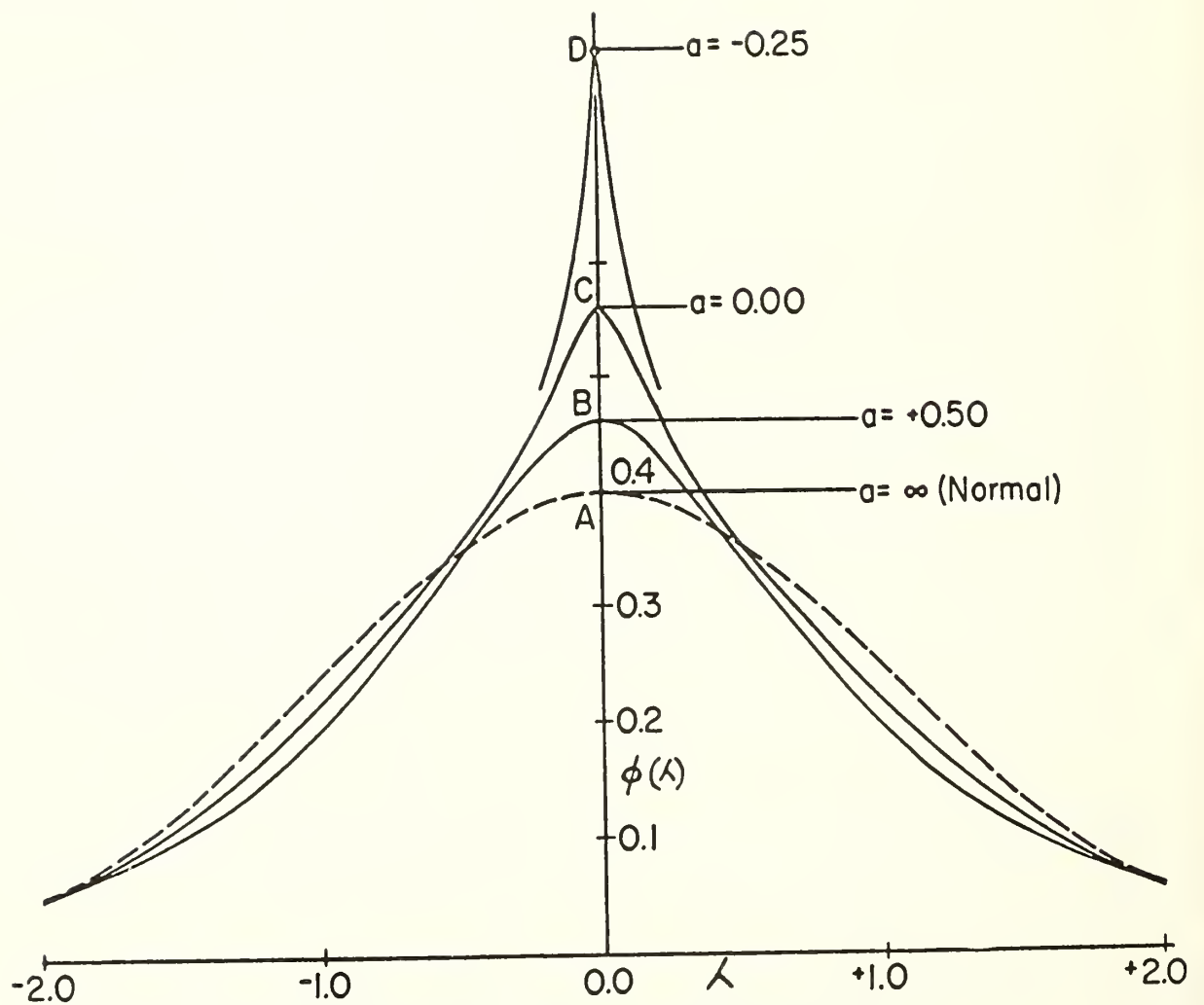


FIGURE 1 : Representative Curves of Normal and Type I

Modulated Normal Distributions (Romanowsky 1970 (6))

$$\omega(b) = \frac{2b-2}{2b-1} \sqrt{\frac{b-1}{b-2}} \quad (3.4)$$

The numerical solution of the equation $\omega(a) = \omega(b)$ presents no difficulty and establishes the correspondence between the value of a and b lead to the same central ordinate. For instance

$$\begin{aligned} a &= 1.00 \dots\dots\dots b = 3.342 \\ a &= 0.50 \dots\dots\dots b = 2.848 \\ a &= -0.49 \dots\dots\dots b = 2.001 \end{aligned}$$

The curves of type II, illustrated in figure 2, have broader shoulders, their tops are always rounded, which is a good feature. All moments of orders higher than 2 are infinite.

It is difficult to foresee the role type II will play in the theory of errors. Perhaps it will simply play the role of a formal analytical extension of type I. It is too early to make a plausible prediction as, perhaps, other types of modulation functions may be suggested and explored in the future.

4. STATISTICAL ANALYSIS METHOD

In the next two sections two examples of observation errors will be given and analyzed as gravimetric and levelling observation errors. For this reason we explain in this part the procedure which will be followed in the statistical analysis of these two samples of repeated observations.

We consider a sample of n "results" $m_i (i=1, \dots, N)$ obtained by repeating N times the measurement of a fixed quantity. The arithmetic mean \bar{m} and the standard deviation σ_m of this sample are

$$\bar{m} = \frac{1}{N} \sum_{i=1}^N m_i \quad \sigma_m^2 = \frac{1}{N-1} \sum_{i=1}^N (m_i - \bar{m})^2 \quad (4.1)$$

The deviation of each individual observation m_i from the mean \bar{m} , termed "residual", is denoted by the symbol v_i

$$v_i = m_i - \bar{m} \quad (4.2)$$

This sample of residuals v_i are classified by means of intervals of equal size

$$\Delta v = \alpha \sigma_m \quad (4.3)$$

where $\alpha(\%)$ is a fraction of the standard deviation σ_m . The classes are numbered with a rank J and the one which extends from $(-\Delta v/2)$ to $(\Delta v/2)$ is given the rank $J=0$. The lower limit and the upper limit of the interval J are respectively $(2J-1)\Delta v/2$ and $(2J+1)\Delta v/2$.

Because we consider only the residuals which are greater than $-4\sigma_m$ and less than $+4\sigma_m$ (at 99.99% confidence level) the number of classes is then $N_{CL} = 8\sigma_m / \Delta v$.

In practice, numerical calculations are greatly simplified if the rank J is taken as the variable. This is equivalent to changing the unit in which the

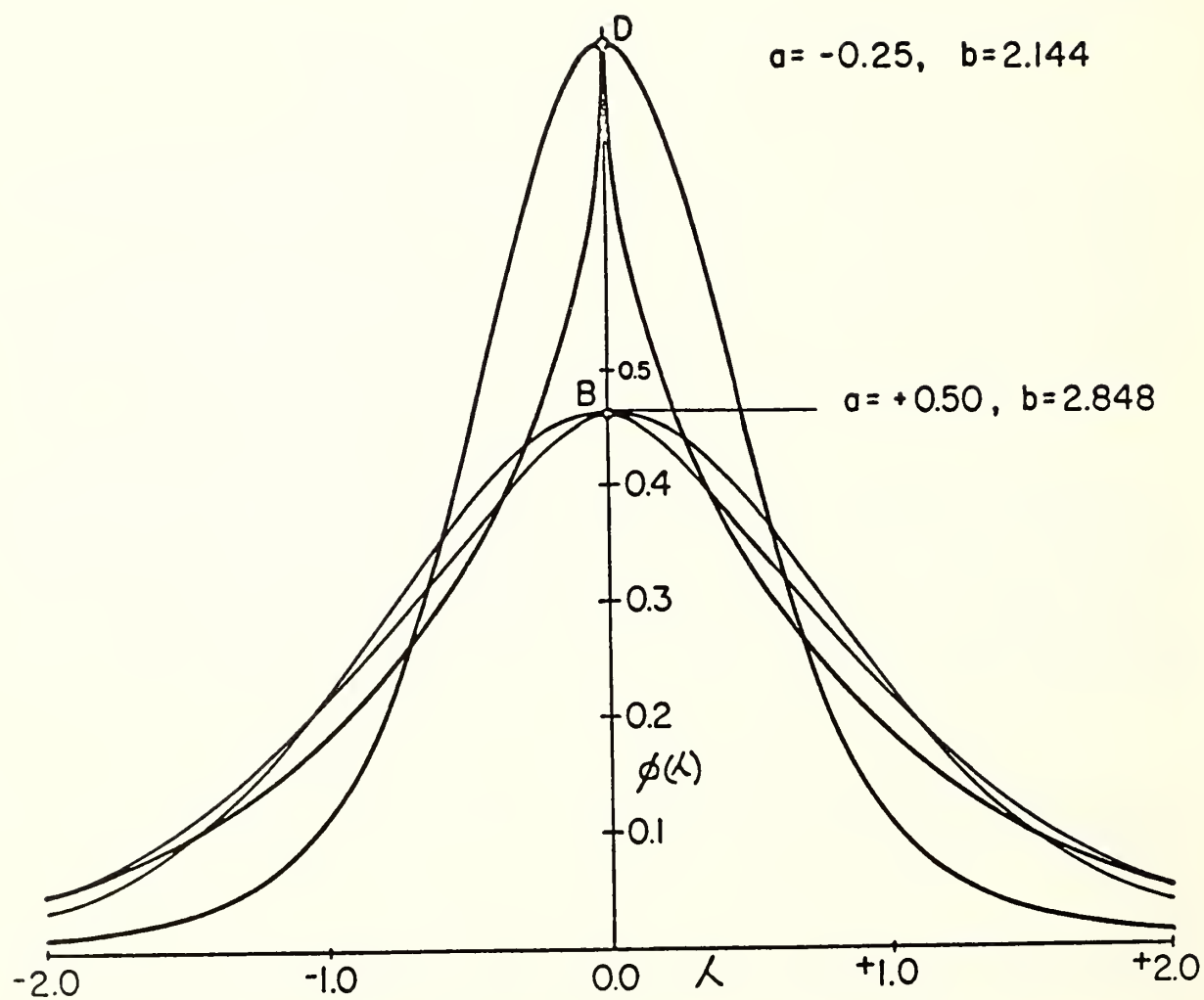


FIGURE 2 : Representative Curves of Type I and Type II

Modulated Normal Distributions (Romanowsky 1970 (6))

quantities v_i are evaluated. The new unit is taken as equal to the size Δv of an interval. While the observed frequency of the J-th class is denoted by F_J then the mean \bar{J} and the variance s^2 of the new variate J are

$$\bar{J} = \sum F_J J/N \quad s^2 = \sum F_J (J - \bar{J})^2 / (n-1) \quad (4.4)$$

The expected frequency f_J of the J-th class, in accordance with the given probability density function (normal or modulated normal), is equal to

$$f_J = N f(J) \Delta J = N f(J) \quad (4.5)$$

since $\Delta J = 1$. By introducing the symbol λ_J to designate the standardized value of J,

$$\lambda_J = (J - \bar{J})/s \quad (4.6)$$

we get

$$f_J = (N/s) f(\lambda_J) \quad (4.7)$$

In the case of the normal distribution, by using (1.10),

$$f(\lambda_J) = (1/\sqrt{2\pi}) e^{-\lambda_J^2/2} \quad (4.8)$$

and for the type I modulated normal distribution, by considering (2.10)

$$f(a, \lambda_J) = \frac{(a+1)\sqrt{a+1}}{\sqrt{2\pi}\sqrt{a+2}} \int_0^1 e^{-\frac{\lambda_J^2(a+1)}{2(a+2)}} \cdot \frac{1}{t} t^{a-1/2} dt \quad (4.9)$$

Finally, in order to perform the test of goodness of fit, the calculation of chi-square yields

$$\chi^2 = \sum (F_J - f_J)^2 / f_J \quad (4.10)$$

The theoretical Chi-square is obtained by considering the degree of freedom equal to the number of classes minus 2 and at 95% confidence level.

5. GRAVIMETRIC OBSERVATIONS ERRORS

This sample, supplied by Gravity and Geodynamics Division of Earth Physics Branch (Canada), consists of 25352 residuals that are outcome of gravity observations distributed over an offshore area close to Newfoundland.

An observation is constituted by the measurement of the difference between the acceleration g_i and g_j in two stations i and j.

Each measurement requires that a certain number of corrections be applied to the instrument's reading as non-linearity of spring's action, the changes of temperature and of atmospheric pressure, the influence of mechanical vibrations, etc ... A comparison between station i and j, after all the corrections had been applied, leads to the following equation

$$g_i - g_j = K(R_i - R_j) \quad (5.1)$$

where R_i and R_j are the indications of the gravimeter and K is the constant of proportionality between the arbitrary units in which R_i and R_j are expressed and the gravity units.

The statistical analysis is summarized in table 1 and representative curves of the distribution are drawn in figures 3 and 4.

6. LEVELLING OBSERVATION ERRORS

In order to participate in the readjustment of the north american vertical network, Geodetic Survey of Canada is automating the Canadian levelling network on the basis of section runnings. The samples are collections of discrepancies Δ_i between elevation differences F_i of the forward direction running and B_i of the backward direction running normalized i.e divided by the square root of the smallest distance L of the given section runnings as

$$\Delta_i = (F_i + B_i)/\sqrt{L} \quad (6.1)$$

Levelling is limited by systematic errors such as: rod graduation irregularities, rod expansion, index error, collimation error, magnetic effect, refraction effect, tide effect, crustal movement, etc ... All have to be modelled and the appropriate corrections must be applied to the observed elevation differences before analyzing these discrepancies samples. In this report we consider only the raw data. A more deep study and exhaustive research will be investigated in the future.

To build more homogeneous samples we divide the country into three areas: eastern, central and western Canada. We consider two other samples, the first being constituted by the observations made in the province of Ontario and the second one by the observations made in the whole country using the level instrument NI 1 from the year 1972 to 1979.

The statistical analysis of these five samples are summarized in tables 2 to 6 and the representative curves of the correspondent distributions are drawn in figures 5 to 14.

TABLE 1: NEWFOUNDLAND OFFSHORE GRAVIMETRIC OBSERVATIONS

NUMBER OF OBSERVATIONS : 25352
 MEAN : .00000
 STANDARD DEVIATION : .69290
 FRACTION OF THE STANDARD DEVIATION : .20

LENGTH OF THE CLASS : .13444
 UPPER LIMIT(GIVEN AS INPUT TO 440STGMA1) : -3.39520
 LOWER LIMIT(GIVEN AS INPUT TO 440STGMA1) : 3.39520
 NUMBER OF CLASSES : 49
 MODULATOR : 1.00

CLASS NUMBER	LOWER LIMIT	UPPER LIMIT	CLASS MIDDLE	CLASS RANK	OBSERVED FREQUENCY (F)	STANDARDIZED CLASS RANK	NORMAL EXPECTED FREQUENCY (FN)	NORMAL EXPECTED FREQUENCY (F(N))	(F-FN)*2	(F-FN)*2
									FN	F(N)
1	-3.39520	-3.25663	-3.32592	-24	10.0	-4.97	.0	.0	10923.0	0
2	-3.25663	-3.11805	-3.18734	-23	9.0	-4.74	.0	.0	3155.0	0
3	-3.11805	-2.97947	-3.04876	-22	7.0	-4.51	.0	.0	710.6	0
4	-2.97947	-2.84089	-2.91018	-21	14.0	-4.34	.0	.0	1853.3	574.1
5	-2.84089	-2.70231	-2.77160	-20	14.0	-4.17	.0	1.4	443.3	94.7
6	-2.70231	-2.56373	-2.63302	-19	17.0	-3.92	1.0	2.7	265.8	77.4
7	-2.56373	-2.42515	-2.49444	-18	22.0	-3.71	2.0	5.3	144.2	40.7
8	-2.42515	-2.28657	-2.35586	-17	34.0	-3.40	5.0	9.4	215.4	71.2
9	-2.28657	-2.14799	-2.21728	-16	37.0	-3.23	9.0	16.5	82.2	24.7
10	-2.14799	-2.00941	-2.07970	-15	55.0	-3.04	14.0	27.4	74.7	22.7
11	-2.00941	-1.87083	-1.94012	-14	50.0	-2.88	34.0	44.4	20.1	4.5
12	-1.87083	-1.73225	-1.80154	-13	64.0	-2.67	61.0	72.4	.9	.5
13	-1.73225	-1.59367	-1.66296	-12	100.0	-2.45	104.0	114.7	.1	2.1
14	-1.59367	-1.45509	-1.52438	-11	132.0	-2.25	169.0	174.2	4.2	11.1
15	-1.45509	-1.31651	-1.38580	-10	178.0	-2.04	265.0	261.4	28.7	26.7
16	-1.31651	-1.17793	-1.24722	-9	276.0	-1.83	394.0	377.7	17.2	27.4
17	-1.17793	-1.03935	-1.10864	-8	357.0	-1.62	474.0	430.7	79.4	56.8
18	-1.03935	-.90077	-.97006	-7	524.0	-1.41	741.0	717.7	43.2	44.3
19	-.90077	-.76219	-.83148	-6	699.0	-1.20	1074.0	944.2	104.0	64.6
20	-.76219	-.62361	-.69290	-5	909.0	-.99	1294.0	1215.2	115.0	77.2
21	-.62361	-.48503	-.55432	-4	1344.0	-.74	1554.0	1409.7	25.9	15.1
22	-.48503	-.34645	-.41574	-3	1720.0	-.57	1707.0	1404.2	3.3	4.2
23	-.34645	-.20787	-.27716	-2	2364.0	-.35	1942.0	1207.0	74.6	41.4
24	-.20787	-.06929	-.13858	-1	2744.0	-.15	2092.0	1254.4	205.7	104.4
25	-.06929	.06929	.00000	0	3477.0	.05	2114.0	1293.4	479.0	403.1
26	.06929	.20787	.13858	1	2457.0	.26	2044.0	1214.7	43.3	74.7
27	.20787	.34645	.27716	2	1953.0	.47	1592.0	1040.1	1.9	.1
28	.34645	.48503	.41574	3	1576.0	.44	1477.0	1045.4	6.0	3.4
29	.48503	.62361	.55432	4	1102.0	.49	1422.0	1055.2	71.9	44.4
30	.62361	.76219	.69290	5	820.0	1.10	1154.0	1070.4	96.7	44.4
31	.76219	.90077	.83148	6	567.0	1.31	997.0	919.4	121.1	77.7
32	.90077	1.03935	.97006	7	437.0	1.52	667.0	674.1	79.1	44.2
33	1.03935	1.17793	1.10864	8	294.0	1.73	474.0	444.0	49.4	42.4
34	1.17793	1.31651	1.24722	9	203.0	1.94	323.0	311.1	44.7	34.7
35	1.31651	1.45509	1.38580	10	167.0	2.15	211.0	210.9	9.1	10.3
36	1.45509	1.59367	1.52438	11	110.0	2.35	131.0	141.2	3.5	7.1
37	1.59367	1.73225	1.66296	12	91.0	2.57	79.0	91.4	2.0	.0
38	1.73225	1.87083	1.80154	13	73.0	2.74	49.0	57.4	17.6	4.0
39	1.87083	2.00941	1.94012	14	53.0	2.99	24.0	35.0	32.9	9.2
40	2.00941	2.14799	2.07870	15	37.0	3.19	13.0	21.2	45.3	11.7
41	2.14799	2.28657	2.21728	16	33.0	3.40	4.0	12.2	100.3	33.4
42	2.28657	2.42515	2.35586	17	27.0	3.61	3.0	4.0	144.7	54.4
43	2.42515	2.56373	2.49444	18	20.0	3.82	1.0	1.0	243.0	71.4
44	2.56373	2.70231	2.63302	19	21.0	4.03	1.0	2.1	464.9	167.9
45	2.70231	2.84089	2.77160	20	14.0	4.24	.0	1.1	1197.4	270.1
46	2.84089	2.97947	2.91018	21	11.0	4.44	.0	.5	1122.1	204.5
47	2.97947	3.11805	3.04876	22	10.0	4.64	.0	.7	2433.7	0
48	3.11805	3.25663	3.18734	23	4.0	4.87	.0	.0	1653.0	0
49	3.25663	3.39520	3.32592	24	4.0	5.09	.0	.0	12042.9	0

AVERAGE OF THE CLASS RANKS : -.263
 VARIANCE OF THE CLASS RANKS : 22.823
 STANDARD DEVIATION OF THE CLASS RANKS : 4.777
 DEGREE OF FREEDOM : 47

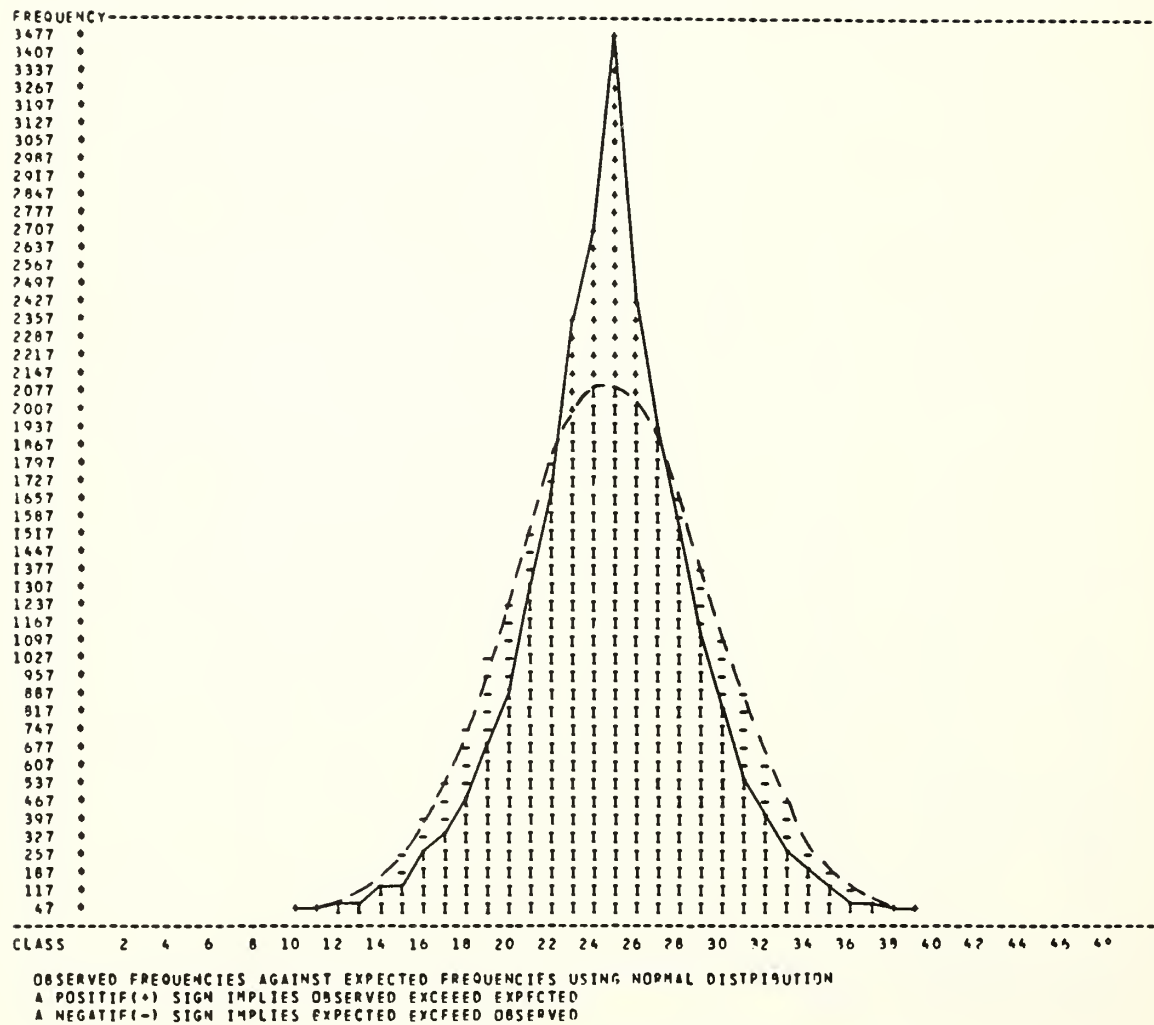


FIGURE 3: NEWFOUNDLAND OFFSHORE GRAVIMETRIC OBSERVATIONS

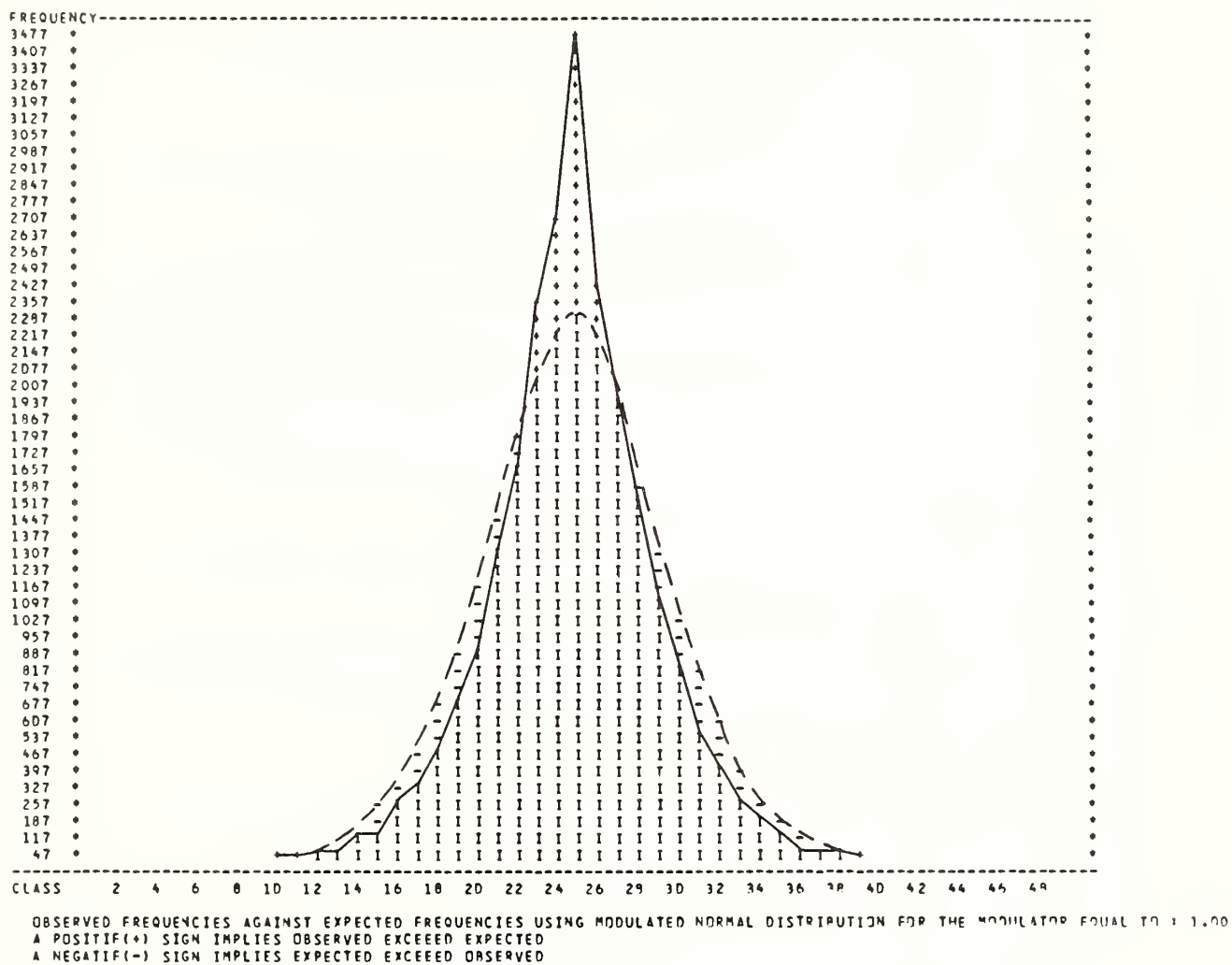


FIGURE 4. NEWFOUNDLAND OFFSHORE GRAVIMETRIC OBSERVATIONS

TABLE 2: PROJECT OF THE WHOLE AREA : EASTERN

NUMBER OF OBSERVATIONS : 8898
 MEAN : .00008
 STANDARD DEVIATION : .00281
 FRACTION OF THE STANDARD DEVIATION : .20

LENGTH OF THE CLASS : .00096
 UPPER LIMIT GIVEN AS INPUT OR +4SIGMA : -.01126
 LOWER LIMIT GIVEN AS INPUT OR -4SIGMA : .01126
 NUMBER OF CLASSES : 41
 MODULATOR : .25

CLASS NUMBER	LOWER LIMIT	UPPER LIMIT	CLASS MIDDLE	CLASS RANK	OBSERVED FREQUENCY (F)	STANDARDIZED CLASS RANK	NORMAL EXPECTED FREQUENCY (FN)	IMPROVED NORMAL EXPECTED FREQUENCY (F-FN)	(F-FN) ²	(F-FN) ³
1	-.01126	-.01098	-.01112	-20	.0	-4.20	.0	1.7	.1	.7
2	-.01098	-.01041	-.01069	-19	3.0	-3.99	.0	1.5	28.4	1.5
3	-.01041	-.00985	-.01013	-18	5.0	-3.78	1.0	2.4	32.6	2.6
4	-.00985	-.00929	-.00957	-17	12.0	-3.57	1.0	4.1	89.4	15.3
5	-.00929	-.00872	-.00901	-16	6.0	-3.36	3.0	6.7	4.2	.1
6	-.00872	-.00816	-.00844	-15	12.0	-3.15	5.0	10.6	6.7	.2
7	-.00816	-.00760	-.00788	-14	21.0	-2.94	10.0	16.7	12.3	1.1
8	-.00760	-.00704	-.00732	-13	16.0	-2.73	18.0	23.6	.0	2.3
9	-.00704	-.00647	-.00675	-12	36.0	-2.52	31.0	38.5	.7	.2
10	-.00647	-.00591	-.00619	-11	49.0	-2.31	52.0	56.7	.1	1.0
11	-.00591	-.00535	-.00563	-10	61.0	-2.10	82.0	81.6	5.4	5.2
12	-.00535	-.00478	-.00507	-9	83.0	-1.89	125.0	119.2	14.0	9.0
13	-.00478	-.00422	-.00450	-8	141.0	-1.68	181.0	159.2	9.0	2.1
14	-.00422	-.00366	-.00394	-7	220.0	-1.47	252.0	218.7	4.1	.1
15	-.00366	-.00310	-.00338	-6	298.0	-1.26	336.0	286.3	4.2	.5
16	-.00310	-.00253	-.00281	-5	369.0	-1.05	428.0	372.3	3.5	.7
17	-.00253	-.00197	-.00225	-4	464.0	-.84	521.0	473.8	6.3	.2
18	-.00197	-.00141	-.00169	-3	619.0	-.63	608.0	589.0	.2	1.5
19	-.00141	-.00084	-.00113	-2	718.0	-.42	679.0	713.8	.4	.0
20	-.00084	-.00028	-.00056	-1	872.0	-.21	725.0	831.6	29.8	2.0
21	-.00028	.00028	.00000	0	906.0	.00	741.0	920.8	36.6	2.2
22	.00028	.00084	.00056	1	804.0	.21	725.0	837.2	8.6	1.3
23	.00084	.00141	.00113	2	719.0	.42	679.0	713.8	2.4	.0
24	.00141	.00197	.00169	3	583.0	.63	608.0	589.0	1.0	.1
25	.00197	.00253	.00225	4	444.0	.84	521.0	473.8	11.5	1.9
26	.00253	.00310	.00281	5	365.0	1.05	428.0	372.3	9.2	.1
27	.00310	.00366	.00338	6	269.0	1.26	336.0	286.3	13.3	1.1
28	.00366	.00422	.00394	7	191.0	1.47	252.0	218.7	14.9	2.8
29	.00422	.00478	.00450	8	144.0	1.68	181.0	159.2	7.7	1.5
30	.00478	.00535	.00507	9	109.0	1.89	125.0	119.2	2.0	.3
31	.00535	.00591	.00563	10	76.0	2.10	82.0	81.6	.5	.4
32	.00591	.00647	.00619	11	57.0	2.31	52.0	56.7	.5	.0
33	.00647	.00704	.00675	12	42.0	2.52	31.0	38.5	3.7	.3
34	.00704	.00760	.00732	13	28.0	2.73	18.0	23.6	5.5	.2
35	.00760	.00816	.00788	14	27.0	2.94	10.0	16.7	29.2	6.3
36	.00816	.00872	.00844	15	11.0	3.15	5.0	10.6	6.3	.0
37	.00872	.00929	.00901	16	11.0	3.36	3.0	6.7	26.2	2.8
38	.00929	.00985	.00957	17	6.0	3.57	1.0	4.1	17.3	.9
39	.00985	.01041	.01013	18	7.0	3.78	1.0	2.4	68.8	6.7
40	.01041	.01098	.01069	19	2.0	3.99	.0	1.5	11.4	.2
41	.01098	.01126	.01112	20	.0	4.19	.0	.7	.1	.7

AVERAGE OF THE CLASS RANKS : .001
 VARIANCE OF THE CLASS RANKS : 22.731
 STANDARD DEVIATION OF THE CLASS RANKS : 4.768
 DEGREE OF FREEDOM : 39

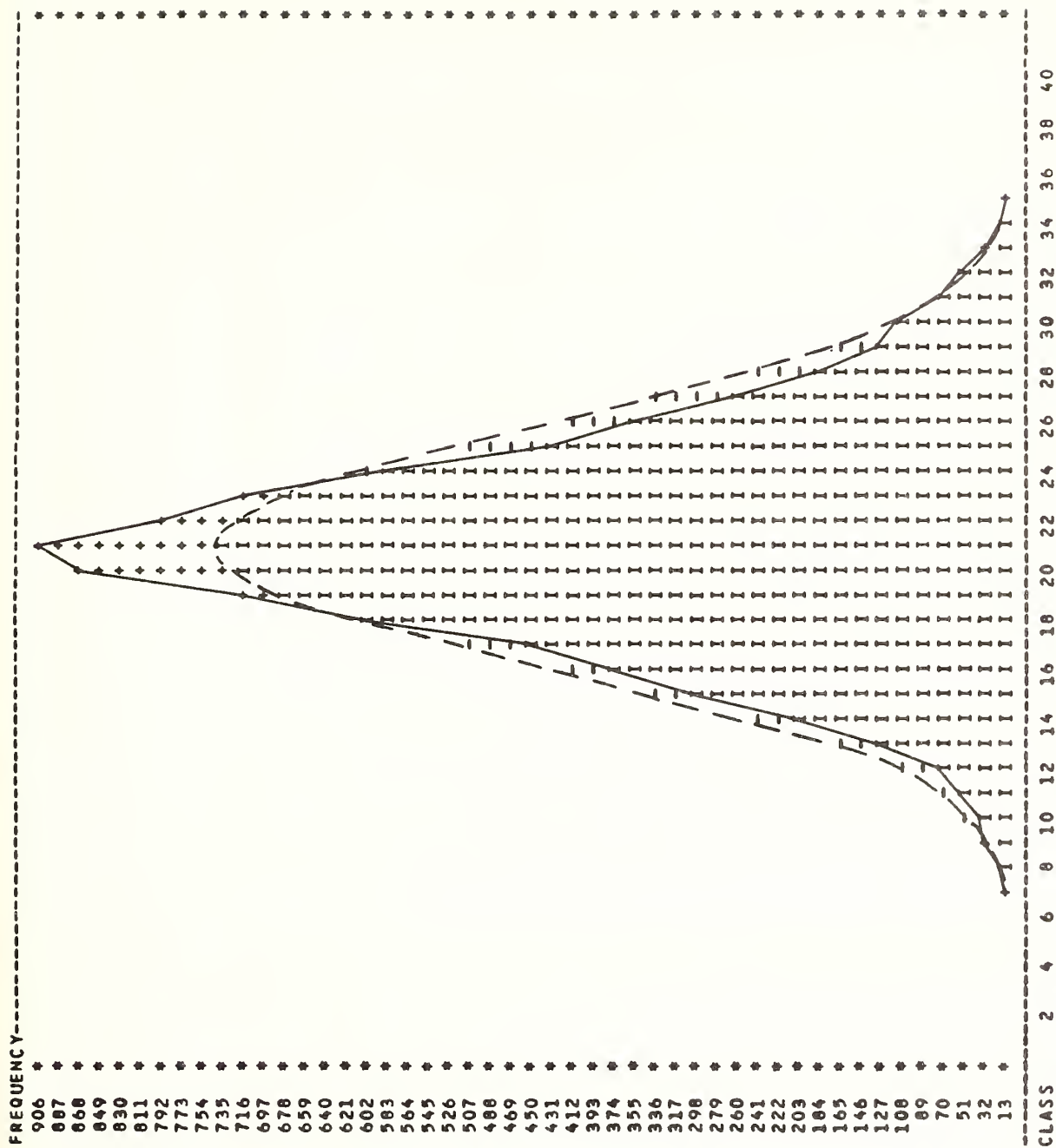
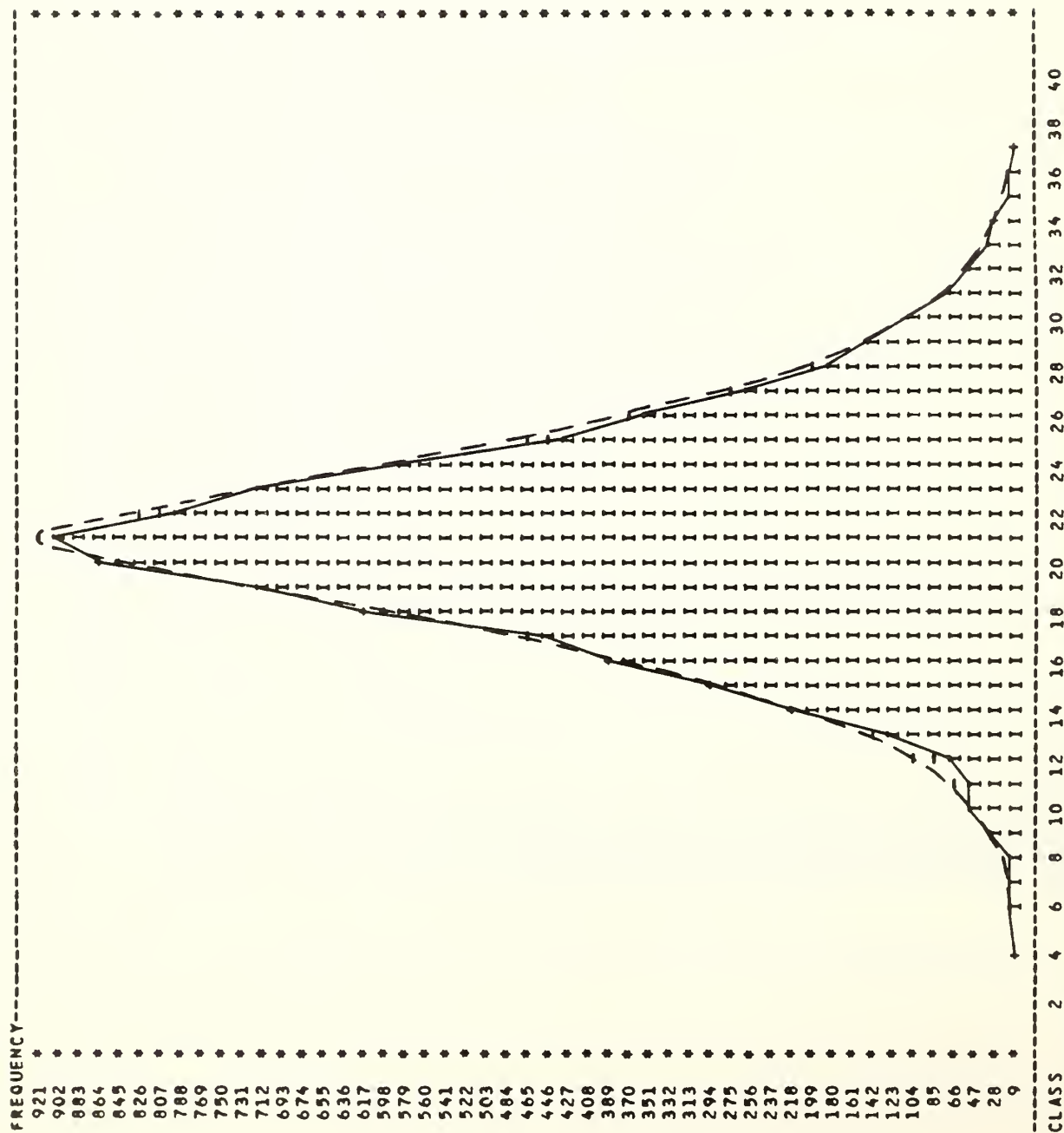


FIGURE 5: EASTERN AREA



OBSERVED FREQUENCIES AGAINST EXPECTED FREQUENCIES USING MODULATED NORMAL DISTRIBUTION FOR THE MODULATOR EQUAL TO : .25
 A POSITIVE(+) SIGN IMPLIES OBSERVED EXCEED EXPECTED
 A NEGATIVE(-) SIGN IMPLIES EXPECTED EXCEED OBSERVED

FIGURE 6: EASTERN AREA

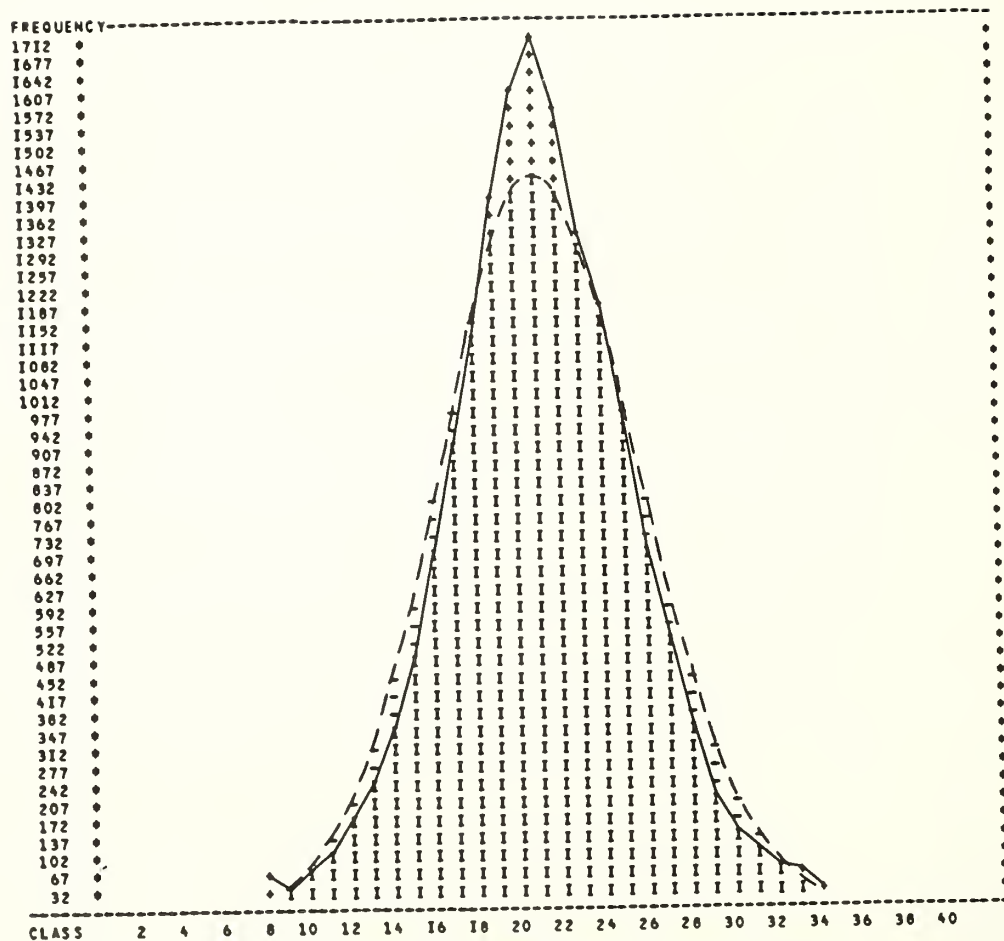
TABLE 3: PROJECT OF THE WHOLE AREA : CENTRAL

NUMBER OF OBSERVATIONS : 16759
 MEAN : .00009
 STANDARD DEVIATION : .00284
 FRACTION OF THE STANDARD DEVIATION : .20

LENGTH OF THE CLASS : .00057
 UPPER LIMIT(GIVEN AS INPUT OR $\pm 4 \cdot \text{SIGMA}$) : -.01136
 LOWER LIMIT(GIVEN AS INPUT OR $-4 \cdot \text{SIGMA}$) : .01136
 NUMBER OF CLASSES : 41
 MODULATOR : .50

CLASS NUMBER	LOWER LIMIT	UPPER LIMIT	CLASS MIDDLE	CLASS RANK	OBSERVED FREQUENCY (F)	NORMAL FREQUENCY (FN)	STANDARDIZED NORMAL FREQUENCY (FNM)	MOD. NORMAL (F-FNM) * 2	(F-FNM) * 2 FM
1	-.01136	-.01108	-.01122	-20	2.0	-.434	0	29.4	2.2
2	-.01108	-.01091	-.01099	-19	7.0	-4.12	0	149.3	21.2
3	-.01091	-.00994	-.01023	-18	9.0	-3.90	1.0	149.3	21.2
4	-.00994	-.00937	-.00966	-17	13.0	-3.68	2.0	109.5	19.3
5	-.00937	-.00861	-.00909	-16	13.0	-3.47	4.0	23.2	2.1
6	-.00861	-.00824	-.00852	-15	15.0	-3.25	7.0	8.7	0
7	-.00824	-.00767	-.00795	-14	30.0	-3.03	15.0	14.5	0
8	-.00767	-.00710	-.00739	-13	68.0	-2.82	27.0	39.2	1.3
9	-.00710	-.00653	-.00682	-12	50.0	-2.60	49.0	60.4	21.1
10	-.00653	-.00597	-.00625	-11	86.0	-2.38	84.0	61.0	2.0
11	-.00597	-.00540	-.00568	-10	114.0	-2.17	138.0	94.1	0
12	-.00540	-.00483	-.00511	-9	183.0	-1.95	216.0	141.3	7
13	-.00483	-.00426	-.00454	-8	253.0	-1.73	322.0	203.8	4.3
14	-.00426	-.00369	-.00398	-7	331.0	-1.52	458.0	291.3	5.1
15	-.00369	-.00312	-.00341	-6	517.0	-1.30	622.0	405.7	14.9
16	-.00312	-.00256	-.00284	-5	701.0	-1.08	805.0	543.4	25.1
17	-.00256	-.00199	-.00227	-4	909.0	-.87	995.0	718.5	17.7
18	-.00199	-.00142	-.00170	-3	1125.0	-.65	1173.0	923.4	13.5
19	-.00142	-.00085	-.00114	-2	1401.0	-.43	1319.0	1139.5	7.4
20	-.00085	-.00028	-.00057	-1	1634.0	-.22	1415.0	1371.6	2.0
21	-.00028	0	0	0	1712.0	0	1415.0	1371.6	5.1
22	0	0	0	1	1599.0	.00	1449.0	1683.7	33.7
23	0	0	0	2	1361.0	.22	1416.0	1378.0	47.7
24	0	0	0	3	1199.0	.43	1319.0	1371.6	23.8
25	0	0	0	4	975.0	.65	1173.0	1139.5	1.3
26	0	0	0	5	712.0	.87	995.0	923.4	6
27	0	0	0	6	518.0	1.08	806.0	718.5	4
28	0	0	0	7	348.0	1.30	622.0	543.4	10.9
29	0	0	0	8	218.0	1.52	458.0	405.7	11.4
30	0	0	0	9	171.0	1.73	322.0	291.3	26.6
31	0	0	0	10	111.0	1.95	216.0	203.8	33.8
32	0	0	0	11	78.0	2.17	138.0	141.3	9.5
33	0	0	0	12	44.0	2.38	84.0	94.1	5.4
34	0	0	0	13	27.0	2.60	49.0	61.0	2.7
35	0	0	0	14	30.0	3.03	27.0	39.2	4.2
36	0	0	0	15	25.0	3.25	15.0	24.3	10.1
37	0	0	0	16	13.0	3.47	7.0	14.5	16.5
38	0	0	0	17	8.0	3.68	4.0	8.7	42.4
39	0	0	0	18	10.0	3.90	2.0	5.1	23.2
40	0	0	0	19	3.0	4.12	1.0	2.9	24.8
41	0	0	0	20	2.0	4.33	0	1.9	120.0
								24.2	17.3
								29.3	2.2

AVERAGE OF THE CLASS RANKS : .001
 VARIANCE OF THE CLASS RANKS : 21.286
 STANDARD DEVIATION OF THE CLASS RANKS : 4.614
 DEGREE OF FREEDOM : 39



OBSERVED FREQUENCIES AGAINST EXPECTED FREQUENCIES USING NORMAL DISTRIBUTION
 A POSITIVE(+) SIGN IMPLIES OBSERVED EXCEEDS EXPECTED
 A NEGATIVE(-) SIGN IMPLIES EXPECTED EXCEEDS OBSERVED

FIGURE 7: CENTRAL AREA

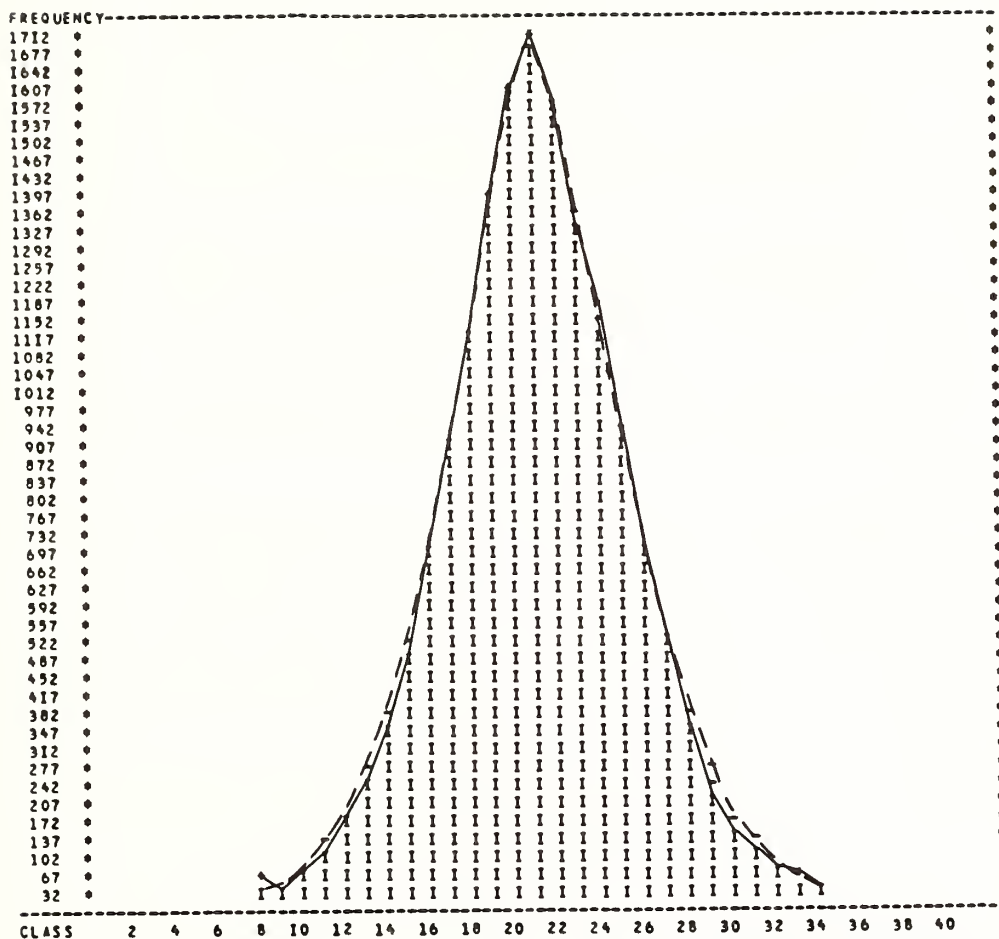


FIGURE 8: CENTRAL AREA

TABLE 4. PROJECT OF THE WHOLE AREA - WESTERN

CLASS NUMBER	LOWER LIMIT	UPPER LIMIT	CLASS MIDDLE	CLASS RANK	OBSERVED FREQUENCY (F)	STANDARDIZED CLASS RANK	NORMAL		IMD.		(F-FM) **2		(F-FM) **2	
							EXPECTED FREQUENCY (FM)	EXPECTED FREQUENCY (FM)	EXPECTED FREQUENCY (FM)	EXPECTED FREQUENCY (FM)	FM	FM	FM	FM
1	-.01085	-.01038	-.01072	-20	6.0	-4.13	.0	1.5	111.2	11.2	13.8			
2	-.01038	-.01004	-.01031	-19	8.0	-3.92	1.0	2.6	79.8	11.3	11.3			
3	-.01004	-.00950	-.00977	-18	10.0	-3.72	1.0	4.8	49.0	5.6	5.6			
4	-.00950	-.00895	-.00923	-17	16.0	-3.51	3.0	8.1	53.1	7.6	7.6			
5	-.00895	-.00841	-.00868	-16	18.0	-3.30	6.0	13.3	21.6	1.7	1.7			
6	-.00841	-.00787	-.00814	-15	33.0	-3.10	12.0	21.4	35.3	6.3	6.3			
7	-.00787	-.00733	-.00760	-14	29.0	-2.89	23.0	34.3	1.7	.8				
8	-.00733	-.00678	-.00705	-13	55.0	-2.68	40.0	52.4	5.3	.1				
9	-.00678	-.00624	-.00651	-12	75.0	-2.48	69.0	60.1	.6	.3				
10	-.00624	-.00570	-.00597	-11	103.0	-2.27	112.0	119.7	.8	2.3				
11	-.00570	-.00516	-.00543	-10	135.0	-2.06	176.0	171.4	9.4	7.7				
12	-.00516	-.00461	-.00488	-9	205.0	-1.86	263.0	244.5	12.9	6.4				
13	-.00461	-.00407	-.00434	-8	293.0	-1.65	378.0	340.1	19.2	6.5				
14	-.00407	-.00353	-.00380	-7	465.0	-1.44	521.0	456.1	6.0	.2				
15	-.00353	-.00298	-.00326	-6	595.0	-1.24	697.0	605.7	12.2	.2				
16	-.00298	-.00244	-.00271	-5	746.0	-1.03	868.0	784.4	17.1	1.9				
17	-.00244	-.00190	-.00217	-4	1032.0	-.82	1251.0	979.4	.3	2.8				
18	-.00190	-.00136	-.00163	-3	1223.0	-.62	1355.0	1201.8	.0	.4				
19	-.00136	-.00081	-.00109	-2	1441.0	-.41	1453.0	1425.6	5.4	.2				
20	-.00081	-.00027	-.00054	-1	1639.0	-.20	1473.0	1612.1	26.5	.5				
21	-.00027	-.00000	-.00000	0	1682.0	.00	1473.0	1711.8	29.5	.5				
22	-.00000	.00000	.00000	1	1520.0	.21	1441.0	1604.3	4.3	4.4				
23	.00000	.00081	.00109	2	1527.0	.42	1350.0	1415.2	23.1	8.8				
24	.00081	.00136	.00163	3	1208.0	.62	1213.0	1190.7	.0	.3				
25	.00136	.00190	.00217	4	810.0	.83	1043.0	954.1	.3	3.3				
26	.00190	.00244	.00271	5	586.0	1.04	860.0	775.6	2.9	1.5				
27	.00244	.00298	.00326	6	422.0	1.24	680.0	597.9	18.3	1.5				
28	.00298	.00353	.00380	7	273.0	1.45	514.0	449.5	16.6	1.7				
29	.00353	.00407	.00434	8	195.0	1.66	373.0	335.0	38.7	20.1				
30	.00407	.00461	.00488	9	122.0	1.86	259.0	240.4	16.0	8.6				
31	.00461	.00516	.00543	10	108.0	2.07	173.0	168.4	14.9	12.8				
32	.00516	.00570	.00597	11	79.0	2.28	110.0	117.4	.0	.8				
33	.00570	.00624	.00651	12	68.0	2.48	67.0	78.7	2.0	.0				
34	.00624	.00678	.00705	13	39.0	2.69	39.0	51.3	20.6	5.4				
35	.00678	.00733	.00760	14	23.0	2.90	22.0	33.6	12.8	.9				
36	.00733	.00787	.00814	15	11.0	3.10	12.0	21.1	10.3	.2				
37	.00787	.00841	.00868	16	6.0	3.31	6.0	12.9	31.2	3.9				
38	.00841	.00895	.00923	17	3.0	3.52	3.0	7.8	20.9	1.4				
39	.00895	.00950	.00977	18	13.0	3.72	1.0	4.4	93.1	16.6				
40	.00950	.01004	.01031	19	5.0	3.93	1.0	2.6	234.2	42.0				
41	.01004	.01058	.01072	20		4.14	.0	1.5	78.6	8.4				

AVERAGE OF THE CLASS RANKS : -.020
 VARIANCE OF THE CLASS RANKS : 23.417
 STANDARD DEVIATION OF THE CLASS RANKS : 4.839
 DEGREE OF FREEDOM : 39

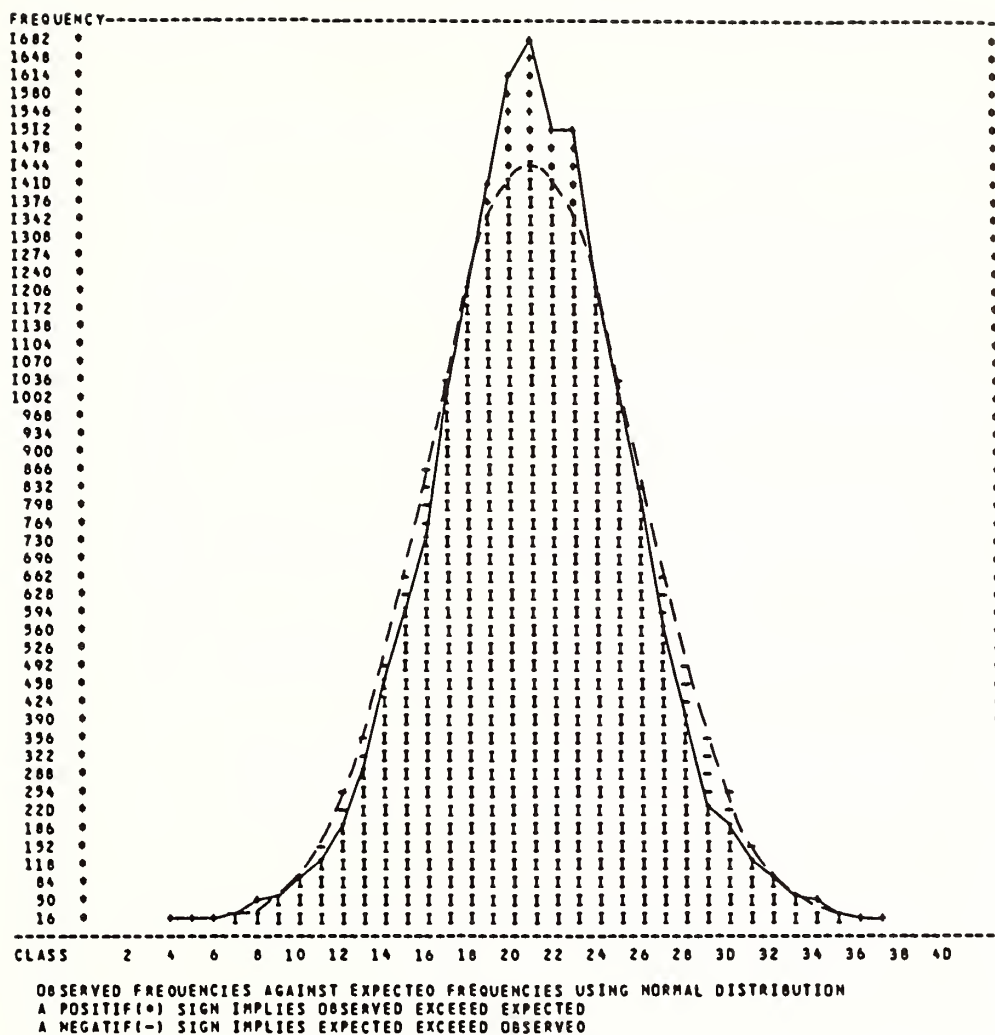
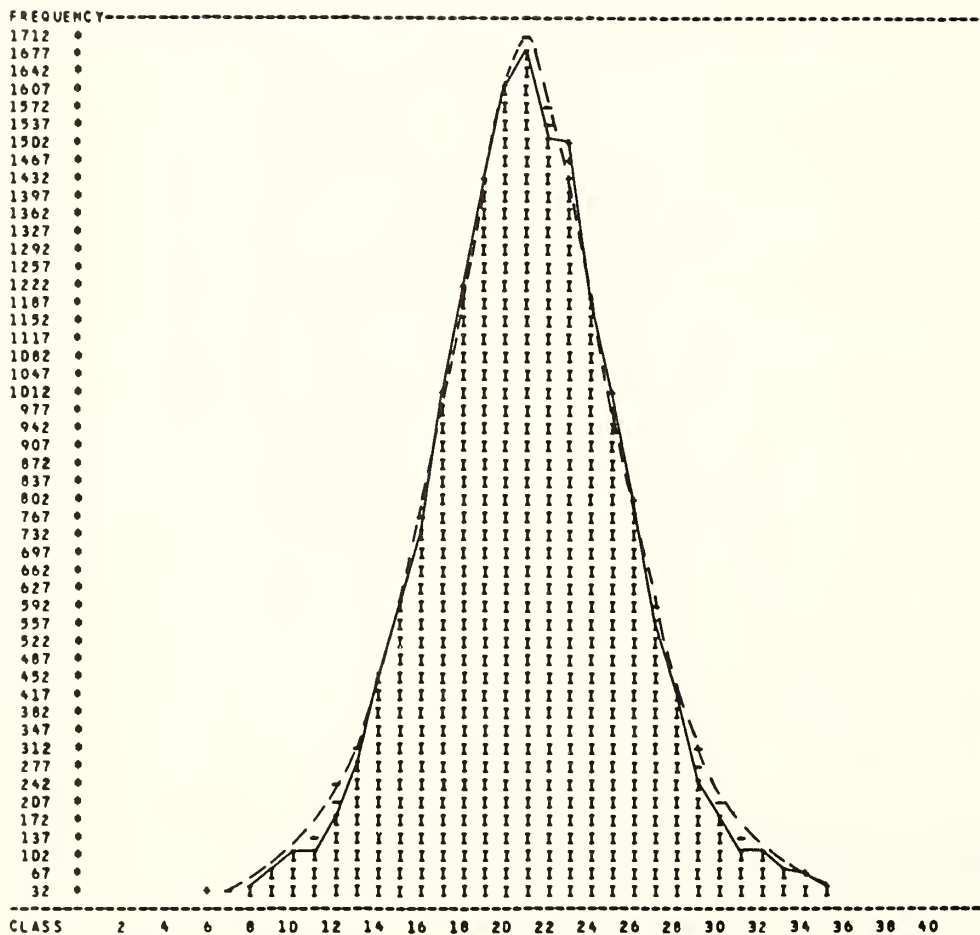


FIGURE 9: WESTERN AREA



OBSERVED FREQUENCIES AGAINST EXPECTED FREQUENCIES USING MODULATED NORMAL DISTRIBUTION FOR THE MODULATOR EQUAL TO 1 .50
 A POSITIF(+) SIGN IMPLIES OBSERVED EXCEEDS EXPECTED
 A NEGATIF(-) SIGN IMPLIES EXPECTED EXCEEDS OBSERVED

FIGURE 10: WESTERN AREA

TABLE 5: PROJECT OF THE WHOLE AREA + CANADA WITH INSTRUMENT NO + 000779 AND YEAR FROM + 72 TO + 79

NUMBER OF OBSERVATIONS + 1647
 MEAN + -.00007
 STANDARD DEVIATION + .00234
 FRACTION OF THE STANDARD DEVIATION + .20
 LENGTH OF THE CLASS + .00047
 UPPER LIMIT GIVEN AS INPUT OR +4(SIGNAL) + -.00935
 LOWER LIMIT GIVEN AS INPUT OR -4(SIGNAL) + .00935
 NUMBER OF CLASSES + 39
 MODULATOR + .50

CLASS NUMBER	LOWER LIMIT	UPPER LIMIT	CLASS MIDDLE	CLASS RANK	OBSERVED FREQUENCY (F)	STANDARDIZED CLASS RANK	NORMAL EXPECTED FREQUENCY (FN)	MOD. NORMAL EXPECTED FREQUENCY (FMN)	(F-FN)*2	(F-FMN)*2
1	-.00935	-.00865	-.00900	-19	3.0	-4.24	.0	.1	48.3	75.6
2	-.00865	-.00815	-.00841	-18	2.0	-4.02	.0	.2	83.5	14.3
3	-.00815	-.00771	-.00795	-17	.0	-3.80	.0	.4	.1	.4
4	-.00771	-.00725	-.00748	-16	1.0	-3.57	.0	.7	2.3	.2
5	-.00725	-.00678	-.00701	-15	1.0	-3.35	1.0	1.2	.4	.0
6	-.00678	-.00631	-.00654	-14	3.0	-3.12	1.0	2.0	3.2	.5
7	-.00631	-.00584	-.00608	-13	1.0	-2.90	2.0	3.3	.6	1.6
8	-.00584	-.00538	-.00561	-12	7.0	-2.68	4.0	5.3	2.1	.5
9	-.00538	-.00491	-.00514	-11	9.0	-2.45	7.0	8.3	.4	.1
10	-.00491	-.00444	-.00467	-10	9.0	-2.23	12.0	12.6	.8	1.0
11	-.00444	-.00397	-.00421	-9	15.0	-2.01	20.0	19.0	1.1	.8
12	-.00397	-.00351	-.00374	-8	20.0	-1.78	30.0	27.3	3.3	1.9
13	-.00351	-.00304	-.00327	-7	30.0	-1.56	43.0	38.2	4.2	1.8
14	-.00304	-.00257	-.00280	-6	49.0	-1.34	60.0	52.9	2.0	.3
15	-.00257	-.00210	-.00234	-5	55.0	-1.11	79.0	70.2	7.3	3.3
16	-.00210	-.00164	-.00187	-4	106.0	-.89	99.0	91.6	.5	.0
17	-.00164	-.00117	-.00140	-3	115.0	-.67	118.0	114.4	.1	.0
18	-.00117	-.00070	-.00093	-2	134.0	-.44	133.0	137.9	.0	1.1
19	-.00070	-.00023	-.00047	-1	175.0	-.22	143.0	159.9	7.0	1.4
20	-.00023	.00000	.00000	0	167.0	.00	147.0	170.6	2.8	1.1
21	.00000	.00070	.00047	1	175.0	.23	143.0	159.1	7.1	1.6
22	.00070	.00117	.00093	2	141.0	.45	133.0	136.9	.5	.1
23	.00117	.00164	.00140	3	127.0	.67	117.0	113.3	.9	1.7
24	.00164	.00210	.00187	4	84.0	.90	98.0	90.6	2.0	.5
25	.00210	.00257	.00234	5	62.0	1.12	78.0	69.3	3.4	.8
26	.00257	.00304	.00280	6	53.0	1.34	56.0	52.2	.7	.0
27	.00304	.00351	.00327	7	31.0	1.57	43.0	38.2	3.3	1.4
28	.00351	.00397	.00374	8	16.0	1.79	29.0	26.8	6.2	4.4
29	.00397	.00444	.00421	9	8.0	2.02	19.0	18.6	6.6	6.1
30	.00444	.00491	.00467	10	9.0	2.24	12.0	12.6	.7	1.0
31	.00491	.00538	.00514	11	6.0	2.46	7.0	6.2	.2	.6
32	.00538	.00584	.00561	12	4.0	2.69	4.0	3.2	.0	.3
33	.00584	.00631	.00608	13	5.0	2.91	2.0	3.3	3.8	.9
34	.00631	.00678	.00654	14	4.0	3.13	1.0	2.0	7.8	2.2
35	.00678	.00725	.00701	15	3.0	3.36	1.0	1.2	11.6	2.8
36	.00725	.00771	.00748	16	3.0	3.58	.0	.7	31.4	8.2
37	.00771	.00818	.00795	17	2.0	3.80	.0	.4	33.7	7.2
38	.00818	.00865	.00841	18	.0	4.03	.0	.2	.0	.2
39	.00865	.00935	.00900	19	2.0	4.25	.0	.1	223.6	32.3

AVERAGE OF THE CLASS RANKS + -.018
 VARIANCE OF THE CLASS RANKS + 20.025
 STANDARD DEVIATION OF THE CLASS RANKS + 4.475
 DEGREE OF FREEDOM + 37

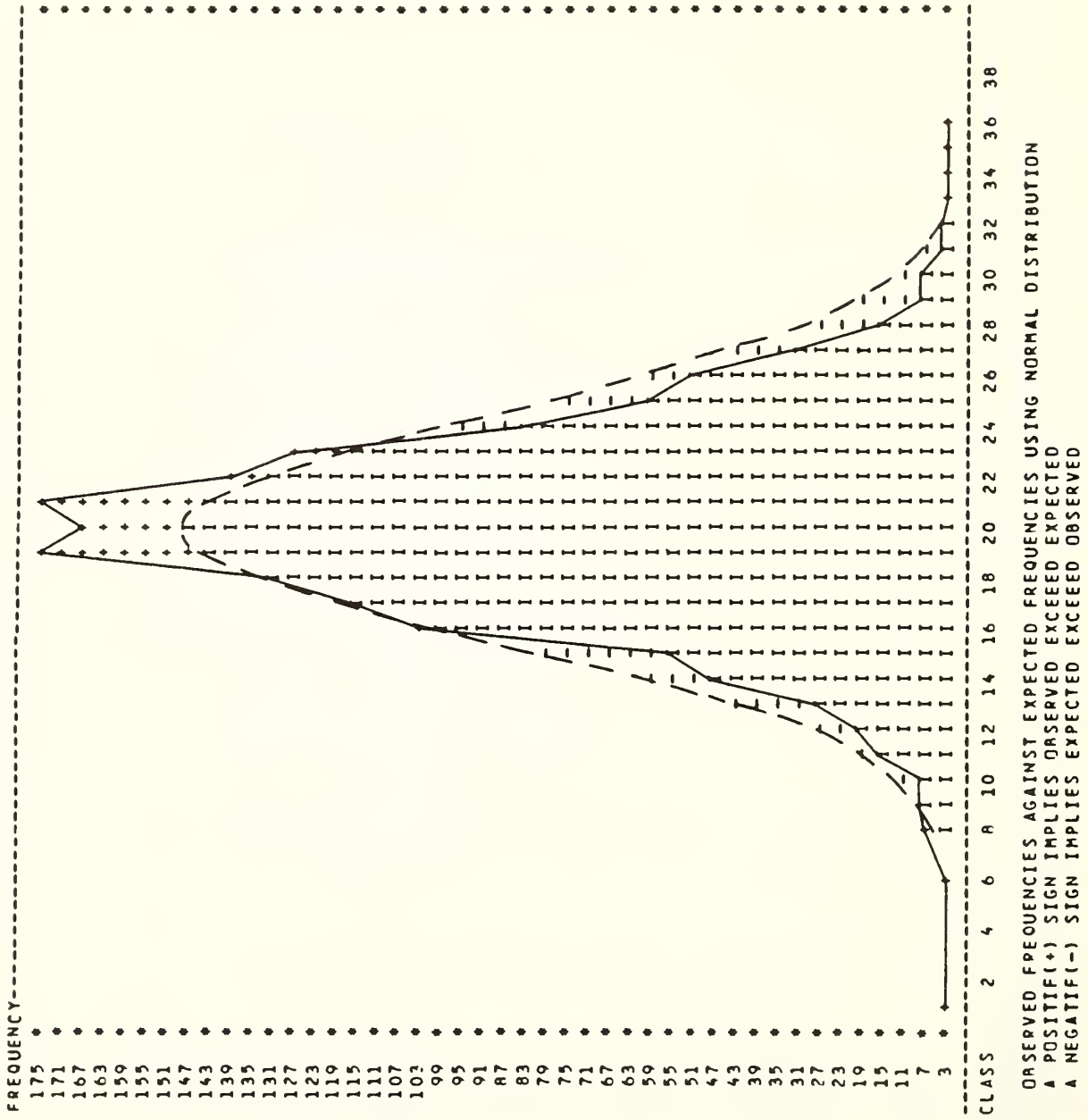
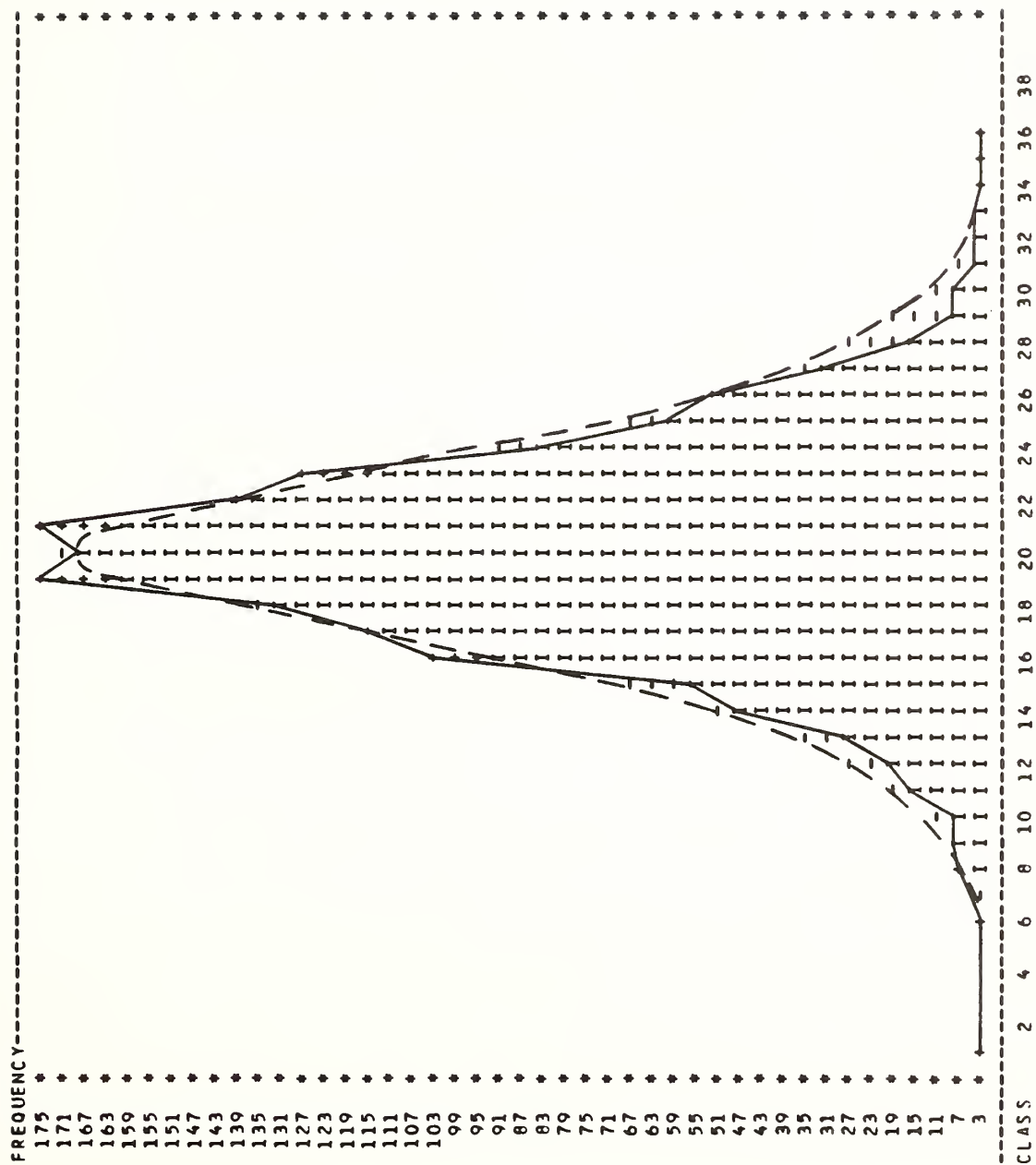


FIGURE 11: CANADA, INSTR: 90779, YEARS: 1972 to 1979



OBSERVED FREQUENCIES AGAINST EXPECTED FREQUENCIES USING MODULATED NORMAL DISTRIBUTION FOR THE MODULATOR EQUAL TO : .50
 A POSITIVE(+) SIGN IMPLIES OBSERVED EXCEEDS EXPECTED
 A NEGATIVE(-) SIGN IMPLIES EXPECTED EXCEEDS OBSERVED

FIGURE 12: CANADA, INSTR: 90779, YEARS: 1972 to 1979

TABLE 6: PROJECT OF A GIVEN PROVINCE - ONTARIO

NUMBER OF OBSERVATIONS : 13654
 MEAN : .00002
 STANDARD DEVIATION : .00292
 FRACTION OF THE STANDARD DEVIATION : .20

LENGTH OF THE CLASS : .00058
 UPPER LIMIT(GIVEN AS INPUT OR $+4\sigma$ SIGMA) : -.01160
 LOWER LIMIT(GIVEN AS INPUT OR -4σ SIGMA) : .01160
 NUMBER OF CLASSES : 41
 MODULATOR : .25

CLASS NUMBER	LOWER LIMIT	UPPER LIMIT	CLASS MIDDLE	CLASS RANK	OBSERVED FREQUENCY (F)	STANDARDIZED CLASS RANK	NORMAL EXPECTED FREQUENCY (FN)	100% NORMAL EXPECTED FREQUENCY (FNM)	(F-FNM)*2	(F-FNM)*2
1	-.01158	-.01139	-.01153	-20	2.0	-4.38	.0	.9	44.9	1.4
2	-.01139	-.01080	-.01110	-19	5.0	-4.16	.0	1.5	110.1	6.2
3	-.01080	-.01072	-.01051	-18	9.0	-3.94	1.0	2.7	142.6	14.8
4	-.01072	-.00964	-.00993	-17	10.0	-3.72	1.0	4.5	86.6	6.8
5	-.00964	-.00905	-.00934	-16	10.0	-3.50	3.0	7.5	21.3	1.9
6	-.00905	-.00847	-.00876	-15	17.0	-3.28	5.0	12.6	24.7	1.6
7	-.00847	-.00788	-.00818	-14	16.0	-3.07	11.0	20.3	2.4	.9
8	-.00788	-.00730	-.00759	-13	55.0	-2.85	21.0	32.3	56.4	16.0
9	-.00730	-.00672	-.00701	-12	50.0	-2.63	38.0	50.2	3.9	.8
10	-.00672	-.00613	-.00642	-11	68.0	-2.41	66.0	75.9	.1	.1
11	-.00613	-.00555	-.00584	-10	92.0	-2.19	109.0	112.4	2.5	3.7
12	-.00555	-.00496	-.00526	-9	158.0	-1.97	171.0	160.2	1.0	.0
13	-.00496	-.00438	-.00467	-8	190.0	-1.75	257.0	226.9	17.6	6.0
14	-.00438	-.00380	-.00409	-7	280.0	-1.53	369.0	314.5	21.3	3.8
15	-.00380	-.00321	-.00350	-6	404.0	-1.31	503.0	426.0	19.7	1.1
16	-.00321	-.00263	-.00292	-5	571.0	-1.09	655.0	563.9	10.9	.1
17	-.00263	-.00204	-.00234	-4	700.0	-.88	913.0	729.5	13.7	1.2
18	-.00204	-.00146	-.00175	-3	933.0	-.66	962.0	920.2	.8	.2
19	-.00146	-.00088	-.00117	-2	1139.0	-.44	1084.0	1129.2	2.8	.1
20	-.00088	-.00029	-.00058	-1	1329.0	-.22	1193.0	1336.2	23.2	1.1
21	-.00029	.00000	.00000	0	1454.0	.00	1193.0	1461.7	57.2	.5
22	.00000	.00000	.00000	1	1320.0	.22	1164.0	1338.2	20.8	.2
23	.00000	.00000	.00000	2	1123.0	.44	1083.0	1129.2	1.4	.0
24	.00000	.00000	.00000	3	1001.0	.66	961.0	920.2	1.7	7.1
25	.00000	.00000	.00000	4	782.0	.88	812.0	729.5	.5	5.4
26	.00000	.00000	.00000	5	562.0	1.10	655.0	563.9	13.1	.0
27	.00000	.00000	.00000	6	432.0	1.31	503.0	426.0	10.0	.1
28	.00000	.00000	.00000	7	275.0	1.53	368.0	314.5	23.6	5.0
29	.00000	.00000	.00000	8	177.0	1.75	257.0	226.9	24.9	11.0
30	.00000	.00000	.00000	9	130.0	1.97	171.0	160.2	9.8	5.7
31	.00000	.00000	.00000	10	94.0	2.19	108.0	110.6	1.9	2.5
32	.00000	.00000	.00000	11	63.0	2.41	66.0	75.9	.1	2.2
33	.00000	.00000	.00000	12	52.0	2.63	38.0	50.2	5.4	.1
34	.00000	.00000	.00000	13	37.0	2.85	21.0	32.3	12.8	.7
35	.00000	.00000	.00000	14	25.0	3.07	11.0	20.3	18.5	1.1
36	.00000	.00000	.00000	15	14.0	3.28	5.0	12.6	13.6	.2
37	.00000	.00000	.00000	16	9.0	3.50	3.0	7.5	16.0	.3
38	.00000	.00000	.00000	17	10.0	3.72	1.0	4.5	66.8	6.8
39	.00000	.00000	.00000	18	5.0	3.94	1.0	2.7	40.1	2.0
40	.00000	.00000	.00000	19	3.0	4.16	.0	1.5	37.5	1.5
41	.00000	.00000	.00000	20	2.0	4.38	.0	.9	45.1	1.4

AVERAGE OF THE CLASS RANKS : -.002
 VARIANCE OF THE CLASS RANKS : 20.858
 STANDARD DEVIATION OF THE CLASS RANKS : 4.567
 DEGREE OF FREEDOM : 39

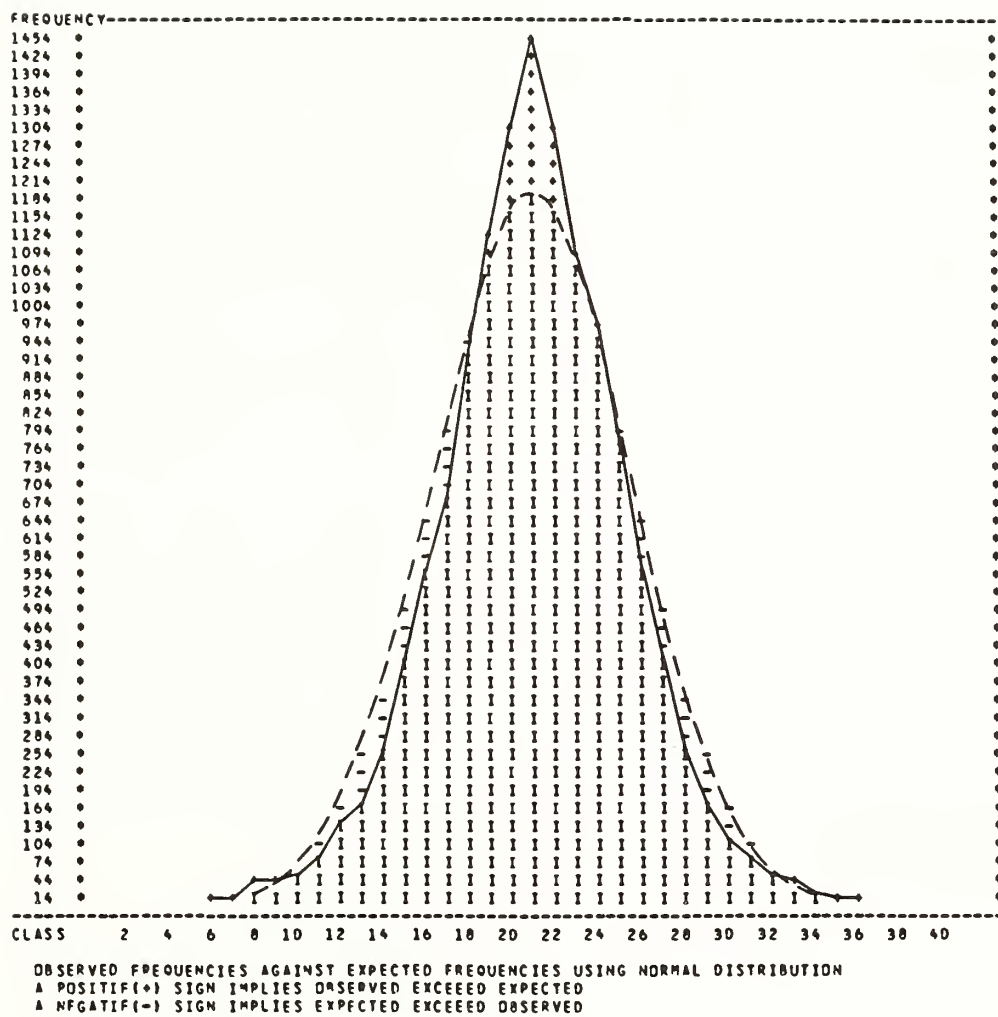


FIGURE 13: ONTARIO

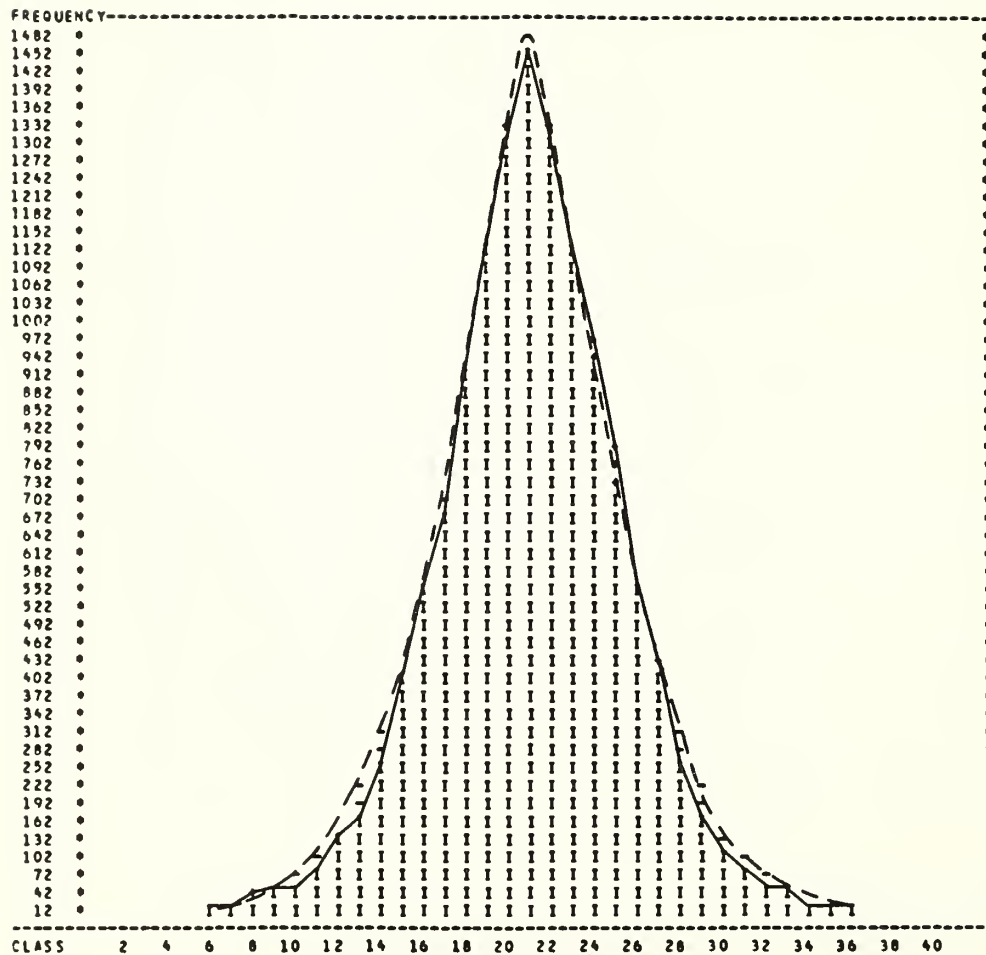


FIGURE 14: ONTARIO

7. RECOMMENDATIONS AND CONCLUSIONS

By analyzing the histograms relating to the levelling observations (section 6) we notice a significant leptokurtic tendency. Is this leptokurtosis due to the modulation? That is the first question we have to ask. Modulation is an attempt to interpret the leptokurtosis, at least in certain cases and type. It may not be universal. Modulation exists because of leptokurtosis and not vice-versa.

In our case, it is very difficult to make conclusions. As mentioned before, the samples of levelling discrepancies have not been reduced by any systematic error corrections. The data processed here is not rigorously homogeneous. We tried to minimize this weakness by grouping them into the same area, the same period of time or by the same instrument, etc... A set of measurements is said to be homogeneous if it is made in similar conditions, in the same period of time and by the same observer. It may also mean that the operation had not been disturbed by a major accident, such as breaking the instrument level.

In the other hand, leptokurtosis could be due to some other physical phenomenon, perhaps, also to some sort of "principle" which may not necessarily be perceptible by our common sense. This other phenomenon could be a "mixture". The mixture of two samples (populations N_1 and N_2 of different standard deviations σ_1 and σ_2) is obtained by simply joining into one single sample the populations of the two components. The mixture is, therefore, represented by a sample of size $(N_1 + N_2)$. Then if our samples are a mixture of two normal populations then it is obvious that there is no homogeneity. However, if there is no experimental reason to think that, but if it is nevertheless clearly leptokurtic, then the sample may belong to the category of modulated normal distributions. This aspect of the problem will be investigated in another research.

Finally, modulation is apparent only in large samples of observational errors: thousand is the lowest limit if reliable conclusions are expected. Whether modulation is capable of solving certain difficult problems in such operations as levelling, has not yet been answered. All those institutions which fabricate large amounts of repeated observations should be presently aware of the existence of leptokurtosis and, perhaps, of modulation.

REFERENCES

ADRAIN, R. (1808), The Analyst, No. IV, p. 93-109.

GAUSS, F. (1809) "Theoria motus corporum coelestium", In English: Dover Publ. Second Book, third section, p.249-273 (1963).

HAGEN, G.H.L. (1837) "Grundzuge der Wahrscheinlichkeitsrechnung", Berlin. 2nd Edition 1867.

MCLANE, P.G. (1967), Bulletin Geodesique, No. 83, p. 9.

MOIVRE, A. (1732) "Approximatio ad Summam Terminorum Binomii $a+b^n$ in Seriem expansi", "A Source Book in Mathematics", Smith, D.E., Dover, New York, Vol. 2 p. 566-575.

ROMANOWSKI, M. (1979) "Random Errors in Observations and the influence of Modulation on their Distribution", Ed. Konrad Wittwer Verlag

ROMANOWSKI, M. (1985), "Personal Communications".

ROMANOWSKI, M. and ISAACS, L. (1972), Bulletin Geodesiques, No. 104, p. 195.

THE DETERMINATION OF EARTH TIDAL PARAMETERS THROUGH GEOMETRIC LEVELLING

Ole Remmer
Geodetic Institute
Copenhagen
DK-2920 Denmark

ABSTRACT. Instead of applying the so-called astronomical (i.e. really = model tidal) correction to geometric observations, amplitude coefficients and phase shifts for the various waves may in principle be determined through the levelling observations themselves. Simple signal to noise computations show that M_2 can be determined with a precise levelling line of roughly 2000 km's length.

An analysis of a real (Danish) levelling line gave the surprising amplitude factor

$$\gamma_0 = 4.2$$

that is about 6 times the normal γ -values. This is interpreted as a result of so-called indirect effects due to ocean loading.

The fact that these effects only affect levelling lines close to the coast make them (and a high γ_0) a likely candidate to explain the difference between geodetic and oceanographic determination of Mean Sea Level along the Atlantic coast of the USA.

A project which will analyze the levelling lines in the Eastern United States close to the Atlantic Ocean is planned in cooperation with NGS.

1.

INTRODUCTION

The fact that the plumb line deviates from some zero-position has, within precise levelling, been recognized some forty years (see [2]).

And since all levelling instruments measure with respect to this plumb line this has given rise to Jensen's well-known formulae which are normally called Astronomical Correction but which more correctly should be called (earth-) tidal correction, t_c , to levelling.

There is however, (as with every other correction) a fundamental ambiguity in applying the tidal correction in levelling. Let the tidal correction be called t_c , then t_c will equal some sum of theoretical tidal constituents:

$$t_c = \sum_{i=1}^n R_i \cos \phi_{it} \quad (1)$$

where R_i and ϕ_{it} are the amplitude and phases of the theoretical earth tide (i.e. some model tide).

In Jensen's application then this correction was applied so to say on "the left-hand side" of the observation equation of precise levelling:

$$z - tc + v = x_i - x_{i-1} + (\sum s^2 \Delta z) n \quad (2)$$

Here n is a parameter which determines the refraction ($\sum s^2 \Delta z$ is a known coefficient, see [6] and [7] for details), while x_i and x_{i-1} are the height of the points P_i and P_{i-1} in some suitable vertical system while z is the measured height difference between P_i and P_{i-1} and v the residual. In (2) we suppose as already said that we know (or can compute accurately enough) tc (and $\sum s^2 \Delta z$ but that is another story), while x_i , x_{i-1} and n are parameters which are determined by a Least Squares Adjustment.

The fact that some of colleagues actually measure tc (or other functions of earth tide) has of course made those of us working with levelling aware that model computations were just not good enough.

As Melchior [3] has already suggested some years ago this problem could be (in principle) solved by having a tilt-meter accompanying the levelling instrument throughout the levelling campagne.

Although one must agree with Melchior's suggestion there are certain formidable practical difficulties (there simply does not exist as far as the author is informed, a tiltmeter which can be moved every 5 minutes or less and measuring in between).

Therefore we shall suggest another solution which may be formulated the following way: Let the levelling observations themselves monitor the earth tides.

This we may also say even simpler namely: move tc in (2) from the left-hand side to the right-hand side!

2. THE NEW OBSERVATION EQUATION IN GEOMETRIC LEVELLING WHEN EARTH TIDES ARE TAKEN INTO ACCOUNT.

In geometric levelling we usually measure the same height-difference twice, one forward and one reverse, that is we have between two benchmarks P_i and P_{i-1} two height-differences:

z_{if} observed at time t_f

z_{ir} observed at time t_r

For each of these we can write down (2) (with tc moved to the right-hand side of the equation):

$$z_{i_f} + v_f = x_i - x_{i-1} + (\sum s^2 \Delta z)_n + tc_{t_f} \quad (3)$$

$$z_{i_r} + v_r = x_i - x_{i-1} + (\sum s^2 \Delta z)_n + tc_{t_r} \quad (4)$$

Subtracting (4) from (3) we get

$$\Delta z_i + v_i = tc_{t_f} - tc_{t_r} \quad (5)$$

And calling $\Delta tc = tc_{t_f} - tc_{t_r}$

we get from (5):

$$\Delta z_i + v_i = \Delta tc \quad (6)$$

Now we don't write Δtc according to (1), when we perform measurements to monitor earth tides.

Instead we write (inspired by Chojnicki [1]).

$$tc = \sum_{i=1}^h R_i \gamma_i \cos(\varphi_{it} + \Delta\varphi_i) \quad (7)$$

so that (6) becomes

$$\Delta z_i + v_i = \sum_{i=1}^h R_i \gamma_i \cos(\varphi_{it} + \Delta\varphi_i) \quad (8)$$

(8) is then our new observation equation for determining earth tidal parameters through geometric levelling.

In (8) R_i and φ_{it} are still the theoretical values of amplitude and phase while γ_i is the amplitude coefficient and $\Delta\varphi_i$ is the phase shift both being in principle different for each tidal constituent.

Through (8) we can by a Least Squares Adjustment find

$$\Delta\varphi_1, \Delta\varphi_2, \dots, \Delta\varphi_h \quad \text{and} \quad \gamma_1, \dots, \gamma_h.$$

This is of course in reality only possible if

$$\sum_{i=1}^h R_i \gamma_i \cos(\varphi_{it} + \Delta\varphi_i)$$

regarded as signal can be seen through the noise of our levelling observations Δz_i .

We shall discuss this problem in our next section.

3. SIGNAL TO NOISE CONSIDERATIONS WHEN MONITORING EARTH TIDES WITH GEOMETRIC LEVELLING.

In Melchior's first book [3] on earth tides (p.291) he mentions that the deviations of the vertical have an amplitude of 0".04. From the context it seems really that it is the distance from "top to bottom" on the registration paper, so that the amplitude of the vertical deviations may be put to

$$\sim 0".02$$

This is then the signal which we shall try to convert into a linear displacement of the levelled height difference over the distance of 1km. In radians 0".02 is of course

$$\frac{0.02}{3600} \frac{\pi}{180} \text{ radians}$$

For a distance of 1km this corresponds to a vertical displacement of

$$\frac{0.02}{3600} \frac{\pi}{180} 10^3 \text{ m}$$

And in mm we find that the vertical displacements is

$$s = \frac{0.02}{3600} \frac{\pi}{180} 10^3 10^3 \text{ mm} = 0.1 \text{ mm/km}$$

Then is then our signal.

Let us now look on the noise in our height-difference-difference Δz_i . In a good precise levelling the standard error of the height-difference-difference will be (see [5])

$$\sigma\{\Delta z_i\} = \sigma\{z_{i_f} - z_{i_r}\} = 0.6 \text{ mm}/\sqrt{\text{km}}$$

For a levelling line of Lkm's length we have correspondingly that the signal is

$$s(L) = L \times 0.1 \text{ mm}$$

while the standard error is

$$\sigma(L) = \sqrt{L} \times 0.6 \text{ mm}$$

In order to have conventional significance we must have $s(L) > 1.96 \sigma(L)$ i.e.

$$L \times 0.1 > 1.96 \times \sqrt{L} \times 0.6 \quad \text{or}$$

$$\sqrt{L} > \frac{1.96 \times 0.6}{0.1} \quad \text{that is}$$

$$\sqrt{L} > 11.76 \quad \text{and finally}$$

$$\underline{L > 138.3 \text{ km}}$$

That is for a levelling network which comprises more than 140 km double-measured levelling we should be able to compute tidal parameters from the levelling observations themselves.

However, after 140 km we are just able to "see" the total tidal signal. Let us now try to find out how large a levelling network we need in order to see the five principal waves K_1 , O_1 , N_2 , M_2 , and S_2 :

We have (Melchior [3] p.76-77) that the amplitudes for these five waves in locations assumed to be lying between latitude 40° and 70° are:

	East-West	Mean	$\times 0.7$
K_1	0".005-0".008	0".0065	0".0046
O_1	0".0035-0".005	0".0047	0".00329
N_2	0".002-0".001	0".0015	0".00105
M_2	0".012-0".005	0".0085	0".0060
S_2	0".005-0".0025	0".0038	0".00266
North-South			
K_1	-0".004-0".005	0".00225	0".0016
O_1	-0".002-0".004	0".0015	0".0010
N_2	0".001-0".001	0".001	0".0007
M_2	0".007-0".005	0".006	0".0042
S_2	0".003-0".002	0".0025	0".00175

And supposing (which is completely realistic) that the levelling lines are evenly distributed in Azimuth we may as amplitude for a levelling line take the mean of the amplitudes of the East-West and North-South components respectively, giving the following mean amplitudes for our principal waves which we then convert into mm/km according to our prior deliberations:

$$\begin{aligned}
 K_1 & 0".0031 \sim \frac{0.031}{0.02} \times 0.1 = 0.0155 \text{ mm/km} \\
 O_1 & 0".0021 \sim \frac{0.0021}{0.02} \times 0.1 = 0.0105 \text{ mm/km} \\
 N_2 & 0".0009 \sim \frac{0.0009}{0.02} \times 0.1 = 0.0045 \text{ mm/km} \\
 M_2 & 0".0051 \sim \frac{0.0051}{0.02} \times 0.1 = 0.0255 \text{ mm/km}
 \end{aligned}$$

$$S_2 \quad 0.0022 \sim \frac{0.0022}{0.02} \times 0.1 = 0.0110 \text{ mm/km}$$

We now make for each wave in decreasing order of magnitude the same computation as we did before for the total tidal signal. That is we ask when the signal of this particular wave rises above the noise of our levelling observations.

We find

$$\begin{aligned} M_2: \quad L \times 0.0255 &> 1.96\sqrt{L} \times 0.6 \\ \sqrt{L} &> 46 \\ L &> 2116 \text{ km} \end{aligned}$$

i.e. after roughly 2000 km's precise levelling we should be able to see the largest wave M_2 .

Corresponding we find

$$\begin{aligned} \text{for } K_1: \quad L &> 5776 \text{ km} \\ \text{for } O_1 \text{ and } S_2: \quad L &> 12544 \text{ km} \\ \text{for } N_2: \quad L &> 68121 \text{ km} \end{aligned}$$

Looking on the last number of 68.000 km by which we should be able to discriminate the five principal tidal waves K_1 , O_1 , N_2 , M_2 , and S_2 , we observe that the first order levelling network of the USA comprises a sufficient number of km levelling lines. That is even should our estimates of the accuracy of the American lines be too optimistic by a factor of 2, we should still be able to compute γ - and $\Delta\phi$ -values for K_1 , O_1 , N_2 , M_2 , and S_2 for the continental United States. Furthermore these tidal parameters will of course be integrated over the whole continent and we should thus most emphatically get rid of "local" effects which otherwise plague tilt measurements.

4. AN EXAMPLE FROM THE SECOND PRECISE LEVELLING OF DENMARK

As we have said above we can not for shorter distances of levelling networks hope to see the different waves of the tidal signal but we should fairly soon be able to see the total tidal signal.

$$\text{Putting in (8) } \Delta\phi_1 = \Delta\phi_2 = \dots \Delta\phi_n = 0$$

and $\gamma_0 = \gamma_1 = \dots = \gamma_n$ we may rewrite (8)

$$\Delta z_j + v_j = \gamma_0 \sum_i^h R_i \cos \varphi_{it} \quad (9)$$

and calling the model tidal signal $\Delta t c_0$ we get:

$$\Delta tc_0 = \sum_i^h R_i \cos \varphi_{it} \quad (10)$$

Combining (9) and (10) we find

$$\Delta z_j + v_j = \gamma_0 \Delta tc_0 \quad (11)$$

It is this equation (11) which has been used in a primitive regression analysis of 100 Danish height-difference-differences. As Δtc_0 has been Jensen's old so-called "astronomical" (i.e. real = tidal) corrections, not multiplied by 0.7.

The question that was asked was very simply: can we see the tidal signal in these few levelling observations? The result was somewhat surprising:

We found for increasing levelling distance L:

L km	γ_0 dimension- less	$s\{\gamma_0\}$ dimension- less	degree of freedom	level of significance %
5	5.54	3.87	17	92
10	6.38	2.83	28	98
15	5.34	3.10	34	95
20	4.68	3.06	41	93
25	5.19	2.98	48	96
30	4.38	2.81	59	93
35	4.78	2.41	73	97
40	4.83	2.34	82	98
45	4.21	2.16	95	97
47	4.23	2.14	99	97

Table 1

We can see several things. First from L = 35 and onward we are beyond the conventional significance level (95%), but we also note that the tidal signal really is there already from the 5km-level and this is of course surprising.

We also see that γ_0 is much larger than 1! That means that we are in a situation with so-called indirect effects (see Melchior [3] pp. 189-201) We note that the final γ_0 -value from our little analysis is

$$\gamma_0 = 4.23$$

In Melchior [3] p.196 is mentioned a $\gamma_0 \sim 5$ so that we seem to have stumbled accidentally into a situation with very large indirect effects too in this small analysis.

It is interesting to compare our findings with those of Zschau [9].

Although no number is given for the size of the indirect effects in N-S direction ([9] p. 581) Zschau's remarks seem to indicate that he has found indirect effects in the North-South direction which are in the same order of magnitude as given by our γ_0 above.

The interest thing is that practically all the levelling observations in our little analysis above lie in the North-South direction very close to the east coast of Jutland going 47km north from the city of Fredericia, i.e. they are lying in the same distance from both the North Sea and the Baltic as are Zschau's borehole tiltmeters. And we seem to be able to reproduce Zschau's effect in the N-S direction over a much longer distance (i.e. 47km).

To us this indicates that the reason for these large indirect effect in Denmark and Schleswig-Holstein in the N-S direction still represent an open question.

5.

FURTHER RESEARCH

The small analysis above seems to indicate that we have tidal signals in near-coastal areas which have for greater amplitudes than the model tidal signals. From earth tide literature this is really not surprising.

As is well-known a systematically increasing difference exists between the mean sea level of Atlantic coast tide gauges determined by geodetic levelling and by oceanographic data respectively.

A likely candidate to explain this systematic difference between geodetic and oceanographic data would be a systematic error in the geodetic observations. The "astronomical" correction (i.e. = tidal correction) to levelling has a systematic tendency in the North-South direction (because we always measure during daytime and the sun will in the mean be standing south of us).

If now our model tidal correction only takes away a fraction of the real signal in near-coastal areas, then of course the remainder of this tidal signal would produce a systematic error exactly in the North-South direction, and it would thus be a most promising candidate for the explanation of the difference between geodetic and oceanographic data.

In consequence of this an analysis of the most coast-near levelling lines of the eastern United States along the ideas scetched in this paper is planned in cooperation with the NGS.

We hope to be able to publish the results of this analysis in the near future.

References

- [1] Chojnicki, T.: Ein Verfahren zur Erdgezeiten Analyse in Anlehnung an das Prinzip der kleinsten Quadrate Mitt. aus den Inst. f. Theor. Geod. Bonn 1973.
- [2] Jensen, H.: Formulas for the Astronomical Correction to the Precise Levelling. Geod. Inst. Medd. No. 23, København 1949.
- [3] Melchior, P.: The Earth Tides. Oxford 1966
- [4] Melchior, P.: The Tides of the Planet Earth. Oxford 1978.
- [5] Remmer, O.: Levelling Errors in Statu Nascendi. Geod. Inst. Medd. No. 51, København 1975.
- [6] Remmer, O.: The Direct Experimental Detection of the Systematic Refraction Error of Precise Levelling. Geod. Inst. Medd. No. 52, København 1977.
- [7] Remmer, O.: Refraction in Levelling. Geod. Inst. Medd. No. 54. København 1980.
- [8] Simonsen, O.: Report on the Astronomical Correction in The New Danish Precise Level Network. Bull. Geod. No. 18. 1950
- [9] Zschau, J.: Tidal Sea Local Tilt of the Crust, and its Application for the study of Crustal and Upper Mantle Structure. Geophys. J.R. Astr. Soc. (1976) pp. 577-593.

AN INVESTIGATION OF SYSTEMATIC ERRORS IN CANADIAN LEVELLING LINES

Michael R. Craymer and Petr Vaníček
Survey Science
University of Toronto
Mississauga, Ontario, L5L 1C6

ABSTRACT

Analyses of 15 lines selected randomly from the first order Canadian levelling network have revealed the presence of systematic errors. Effects of turning point settlement, rod miscalibration, refraction, crustal motion and an as yet unexplained effect correlated with section heights have been recognized. An attempt to model these effects was made. The most common and dominant effect detected is turning point settlement. Interestingly, the refraction effect is relatively small, however, the lack of sufficient auxiliary data limited the effectiveness of the modelling of this effect. It is also interesting that all of the detected effects behave differently according to the characteristics of the individual lines, thus requiring each line to be examined on an individual basis. Classification of the individual lines has not shown so far any conspicuous relation between levelling circumstances and kinds of systematic effects present.

INTRODUCTION

This investigation of systematic effects present in Canadian first order levelling lines is based on the application of the data series analysis and multiple linear regression techniques proposed by Vaníček and Craymer (1983a;b) and Craymer (1985). The subject of our analyses is the discrepancy between the forward and backward runnings of each section. Letting dH_F and dH_B represent the section height differences (of opposite sign) for the forward and backward runnings, respectively, the discrepancy d is given by

$$d = dH_F + dH_B . \quad (1)$$

The basic hypothesis upon which this analysis is founded is that the existence of systematic effects in levelling observations introduces trends or autocorrelations or both among the discrepancies. Denoting the true value of dH by dH^* and its error by e , we have

$$d = (dH^* + e)_F + (dH^* + e)_B = e_F + e_B . \quad (2)$$

Any deviation of the expected value of this quantity from zero would imply the presence of systematic error(s) in the observations.

METHOD

The analyses consist of two parts: discrepancy series analysis and multiple linear regression analysis. We use the former to identify the various effects present in the discrepancies and the latter to obtain quantitative estimates of the individual effects.

Series analysis involves the construction of a series of discrepancies ordered with respect to any argument representing a specific systematic effect or condition under which the levelling was performed. The presence of a systematic effect will introduce trends or autocorrelations into the discrepancy series. In our investigation, we estimate and remove the bias and linear trend from the series and subsequently compute the least squares spectrum (Vaniček, 1971; Wells and Vaniček, 1978) of the residual series. From the least squares spectrum we then compute the autocorrelation function for this series using a cosine transform of the spectrum (Vaniček and Craymer, 1983a). The presence of systematic effects is primarily revealed through the existence of a statistically significant linear trend while significant spectral frequencies and autocorrelations reflect both the deviation of the actual trend from a linear one as well as the presence of other systematic effects.

Multiple linear regression is used to model simultaneously the presence of more than one systematic effect in the discrepancies. We employ a model of the form (Craymer, 1984)

$$\underline{d} = \underline{B}\underline{c} + \underline{e} , \quad (3)$$

where \underline{d} is a vector of n observed discrepancies, \underline{c} is a vector of u coefficients (i.e., linear trends) to be estimated, \underline{e} is a vector of residuals to be minimized and \underline{B} is an $n \times u$ Vandermonde matrix containing the values of the arguments as its columns. Here, we do not provide for bias estimation (in which case there would be an extra column of 1's in \underline{B}) because we have no physical explanation for its existence.

Assuming the discrepancies to be equally weighted and the arguments to be statistically independent, minimization of the sum of weighted squares of the residuals (quadratic norm) leads to the well known "least squares" estimates for the coefficients

$$\underline{c} = (\underline{B}^T \underline{B})^{-1} \underline{B}^T \underline{d} \quad (4)$$

with its estimated covariance matrix given by

$$\underline{C}_c = s_o^2 (\underline{B}^T \underline{B})^{-1} , \quad (5)$$

where the variance factor is

$$s_o^2 = (\underline{B}^T \underline{c} - \underline{d})^T (\underline{B}^T \underline{c} - \underline{d}) / (n-u) . \quad (6)$$

The best fitting regression model is selected by comparing the results of all models using various combinations of different kinds of arguments. In order to reduce the number of models to be analysed, we employ a backward, stepwise approach (Neter and Wasserman, 1974, p.386). That is, all arguments potentially present are included in the initial model and the one with the least statistically significant coefficient is eliminated from the model. This is repeated in a stepwise fashion

until all remaining coefficients are statistically significant (i.e., statistically different from zero).

In our analyses we prefer to use the critical uncertainty level (probability that the coefficient is not zero) for determining statistical significance. In this case, the larger the critical uncertainty level the greater the probability that the coefficient is different from zero. For these tests, the Fisher F statistic is used (cf. Srivastava and Carter, 1983, p.41). Throughout this paper, quantities are considered statistically significant if their uncertainty level is equal to or greater than 90%.

A number of other criteria are also used to assess the applicability of the models. These include: the critical uncertainty level for the hypothesis that all coefficients are simultaneously equal to zero; the coefficient of determination R (percentage of sum of squares explained by the model); the estimated standard deviation s_v of model residuals; the estimated, normalized standard deviation s_{1km} for a line of 1km length; the sum of residuals $\sum v$ and its corresponding uncertainty level; the frequency of partial sums of residuals $\sum v_i$ falling within the limits of random, uncorrelated error propagation; defined by

$$s(L_i) = s_{1km} L_i^{1/2}, \quad (7)$$

where L_i is the partial accumulated section length up to the i-th section.

DATA

The data used in this analysis were obtained in a computed readable format from the NAVD section of the Geodetic Survey of Canada. A more or less random selection of 15 lines was made from the available database. These lines covered a wide variety of areas, epochs and conditions: five lines from British Columbia levelled in 1959, 1960 and 1966; two lines from Manitoba and two lines from northern Ontario levelled in 1979; four lines from Nova Scotia levelled in 1975; two lines from southern Ontario levelled in 1981. Table 1 summarizes the characteristics of these lines.

In general, the data included for each section: starting/ending benchmark numbers; starting/ending times; starting/ending air temperatures; number of setups; length of running; observed (uncorrected) height difference; direction of running. The kinds of auxiliary data available (notably temperature measurements and starting/ending times of runnings) varied among the lines. Furthermore, the number of setups in each running were not listed for some sections and these were omitted from the analyses.

MODELS FOR SYSTEMATIC EFFECTS

In order to apply the data series and regression techniques, arguments representing various known systematic effects were derived from linear models characterizing these effects. Models for the average effects of differential refraction, turning point settlement, rod miscalibration and crustal motion have been developed. These models will only be briefly discussed here. Vaníček et al. (1985) provide a more detailed development.

The effect d_i of an argument a_i on the discrepancy may be written in a linear form

as:

$$d_i = c_i a_i \quad (8)$$

where c_i is the coefficient to be estimated. The arguments and coefficients for the effects of refraction (a_R, c_R), turning point settlement (a_{TP}, c_{TP}), rod scale miscalibration (a_s, c_s) and crustal motion (a_c, c_c) are defined by (Vaníček et al., 1985)

$$a_R = dH [(S/2n)_F^2 - (S/2n)_B^2] \quad c_R = dt A \quad (9)$$

$$a_{TP} = n_F + n_B - 2 \quad c_{TP} = \text{settlement effect on } d \quad (10)$$

$$a_s = dH \quad c_s = s_F - s_B \quad (11)$$

$$a_c = dT \quad c_c = dv \quad (12)$$

Here, A is the coefficient in Kukkamaki's (1939) balanced sight refraction equation, dH is the average section height difference, dt is the average temperature difference at heights 0.5m and 2.5m above ground, dT is the time elapsed between the forward and backward runnings, dv is the difference in the rate of movement of the end benchmarks of a section, n is the number of setups in a section running, s is the average scale error for the rod pair in a section running and S is the total length of a running.

Expected values for some of the above coefficients have been derived by Vaníček et al. (1985). These are: $c_R = 3 \times 10^{-5}$ to -19×10^{-5} mm/m³; $c_{TP} = 0.02$ to 0.05 mm/turning point; $c_s = 10$ to 100 ppm. It must be re-iterated that these models describe only the average effects.

In addition to the above described arguments we also use the height H of the end benchmarks of a section, the section length S , the accumulated section length L , the average slope dH/dS of the section and, where available, the difference dt in the average air temperatures of the runnings. Note that the magnetic effect is not included since it cancels in the discrepancy (Vaníček et al., 1985).

RESULTS

The results of our analyses contain an enormous amount of information. Vaníček et al. (1985) report our initial attempts to interpret them. Here, we shall only summarize the general observations and conclusions from these analyses and, as an example, present the results of our analyses of line A12N10.75.

Figure 1 displays the accumulated observed discrepancy for line A12N10.75. The steady accumulation of the discrepancies exceeds the values expected for random uncorrelated error propagation thereby implying (statistically) that systematic effect(s) may be present. The series analysis (Table 2) detects the presence of statistically significant trends (at the 90% uncertainty level) for the series ordered with respect to arguments a_s , H , and L . Note that the effects of settlement (a_{TP}) and refraction (a_R) are close to being statistically significant.

Furthermore, there is also a statistically significant bias in this series for which

we have no explanation at present.

Subsequent multiple linear regression analyses (Table 3) are performed on the discrepancies initially using the arguments for all of the known systematic effects (a_R , a_{TP} , a_s) as well as those found significant in the discrepancy series analysis (H , L). The backward, stepwise approach selects as the best fitting model the one containing the arguments for rod and instrument settlement (a_{TP}), rod miscalibration (a_s) and an , as yet, not understood effect depending on the section height (H). The estimated coefficients for settlement (0.011 mm/turning point) and rod miscalibration (19 ppm) agree well with their expected values. In addition, the residual discrepancies behave in a manner consistent with random uncorrelated error propagation (Figure 1). The residual discrepancies now accumulate to only -7.8 mm as compared with the original 30.5 mm and is not statistically different from zero.

In general, the 15 lines selected display a wide variety of systematic effects depending on the arguments for the known effects (i.e., refraction, rod and instrument settlement, rod miscalibration and crustal motion) and also on arguments for which we have, as yet, no explanation (i.e., section height (H), difference in length of runnings (dS), difference in average air temperature of runnings (dt), difference in elapsed time of runnings (dET) and difference in number of setups in runnings (dNS)). The last two (dET and dNS) are each present in only one line. A comparison of the occurrences of the presence of these effects with line characteristics is given in Table 4. However, no firm conclusions should be drawn from this table because of the small number of lines sampled.

The most notable feature of the analyses was that all of the systematic effects behave differently according to the characteristics of the individual lines. Thus, all lines should be examined individually for the presence of the various systematic effects.

One of the most surprising results of this analysis is that refraction does not appear to be as dominant as many investigators would believe. In fact, the effect on the accumulated discrepancies is relatively small in comparison with the other effects. The estimate of the effect varies in sign in a range from -24.5×10^{-5} to 11.3×10^{-5} mm/m³. However, the lack of proper temperature measurements limits any discussion of the significance of these results.

On the other hand, the effect of turning point settlement on the discrepancies is extremely important and seems to contribute the most to the total accumulated discrepancy. The estimates of the effect vary from 0.01 to 0.03 mm/turning point for all but one line (where rebound appears to occur at -0.01 mm/turning point). This agrees remarkably well with their expected values. However, it should be remembered that the effect will in practice cancel in the mean section height difference as long as the number of setups in forward and backward runnings are approximately balanced.

Another of the effects seen to be present in a few of the lines was the rod miscalibration effect dependent on the section elevation difference dH . The estimates of this effect (± 15 ppm) are within the theoretical limits of the accuracy of the calibration method.

CONCLUSIONS

The hereby described attempts to diagnose and model systematic effects have revealed some interesting points. The most important revelation seems to be the fact that the refraction effect is not any more significant than rod and instrument settlement and rod miscalibration effects. A similar observation had been made in the Swiss Federal Office of Topography (Schneider, Personal communication, 1981). There does not seem, however, to be much uniformity in the investigated lines; it appears to us that each line has to be treated individually. Not all errors could be modelled because of the limitation in the availability of auxiliary data. The possible dependence of individual systematic errors on terrain and other line characteristics should be further investigated.

Finally, judging from the sparse sample of the 15 analysed lines it appears that Remmer and Lachapelle (1981) may have been well justified in asserting that the 2m Trans-Canada levelling discrepancy is due to rod settlement and residual refraction.

ACKNOWLEDGEMENTS

This investigation was funded by the Geodetic Survey of Canada (research contract no. OST 83-00053). We thank Dr. R.R. Steeves of the Geodetic Survey of Canada, Mr. G.H. Carrera of the University of Toronto and Dr. R.O. Castle of the U.S. Geological Survey for many useful comments and suggestions during the course of this study. The data used in this analysis was kindly provided by Messrs. F. Young and R. Mazaachi of the Geodetic Survey of Canada.

REFERENCES

- Craymer, M.R., 1984: Data series analysis and systematic effects in levelling. Technical Report No. 3, Survey Science, University of Toronto, Mississauga, Ontario.
- Kukkamaki, T.J., 1939: Formeln und tabellen zur berechnung der nivellischen refraktion, Publication No. 27, Finnish Geodetic Institute, Helsinki.
- Neter, J. and W. Wasserman, 1974: Applied Linear Statistical Models, Richard D. Irwin, Inc., Homewood, Illinois.
- Remmer, O. and G. Lachapelle, 1981: The solution of the Trans-Canada discrepancy, Draft Manuscript, Geodetic Survey of Canada, Surveys and Mapping Branch, Dept. of Energy, Mines and Resources, Ottawa.
- Srivastava, M.S. and E.M. Carter, 1983: An Introduction to Applied Multivariate Statistics, North-Holland, New York.
- Vaniček, P., 1971: Further development and properties of the spectral analysis by least squares, Astrophysics and Space Science, Vol.12, pp.10-33.
- Vaniček, P. and M.R. Craymer, 1983a: Autocorrelation functions as a diagnostic tool in levelling, in H. Pelzer and W. Niemeier (Eds.), Precise Levelling: 38 Contributions to the Workshop on Precise Levelling, Hannover, F.R.G., 16-18

March 1983, Dummler Verlag, Bonn.

Vaníček, P. and M.R. Craymer, 1983b: Autocorrelation functions in the search for systematic errors in levelling. Manuscripta Geodaetica, Vol.8, pp.132-341.

Vaníček, P. and E.J. Krakiwsky, 1982: Geodesy: The Concepts, North-Holland, Amsterdam.

Vaníček, P., G.H. Carrera and M.R. Craymer, 1985: Corrections for systematic errors in the Canadian levelling network, Final Report, DSS Contract No. DST 83-00053, Geodetic Survey of Canada, Surveys and Mapping Branch, Dept. of Energy, Mines and Resources, Ottawa.

Wells, D. and P. Vaníček, 1978: Least squares spectral analysis, Technical Report No. BI-R-78-8, Bedford Institute of Oceanography, Dartmouth, N.S.

TABLE 1: Levelling lines selected for analysis

GSC Line Numbers					
	F55C15.66	A261C55.59A	A281C59.59	D108C22.60	D171C34.60A
Location (from-to)	Matsqui to Tranquille, 8.C.	Lumby to Needles, 8.C.	Kelowna to Summerland, B.C.	New Denver to Slocan, B.C.	Nelson to Kelway, 8.C.
Year levelled	1966	1959	1959	1960	1960
Terrain	mountainous	mountainous	uniform	uniform	uniform
No. of sections	478	100	57	51	70
Line length (km)	391	108	61.4	46.8	67
Ave. elevation (m)	251	842	454	645	744
Total elev diff (m)	341	-31	354	-0.3	246

GSC Line Numbers					
	A1N75.75	A12N10.75	A2N75.75	A3N75.75	A1N79.79
Location (from-to)	Annapolis Royal to New Germany, N.S.	Antigonish to Mulgrave, N.S.	Mulgrave to Guysborough, N.S.	Newport to Maitland, N.S.	Brandon to Peace Garden, Man.
Year levelled	1975	1975	1975	1975	1979
Terrain	undulating	uniform/coastal	undulating/coastal	undulating	uniform
No. of sections	157	106	346	142	64
Line length (km)	114	69	239	93	103
Ave. elevation (m)	172	16	6	35	498
Total elev diff (m)	44	-68	-36	23	301

GSC Line Numbers					
	A225M50.79	A247U53.79	A32U13.79	F279U58.818	F8U71.81
Location (from-to)	Gretna to Winnipeg, Man.	Kenora to Manitou Rapids, Ont.	Rainy River to Fort Frances, Ont.	Brights Grove to Goderich, Ont.	Eagle to Cedar Springs, Ont.
Year levelled	1979	1979	1979	1981	1981
Terrain	flat	flat	flat	flat/shore	flat/shore
No. of sections	76	85	75	214	63
Line length (km)	123	140	95	163	53
Ave. elevation (m)	238	339	346	201	204
Total elev diff (m)	-7	-22	28	78	4

TABLE 2: Results of discrepancy series analysis of GSC line A12N10.75.

A12N10.75			A12N10.75		
a(s) (m)	St.Dev.V (mm) Bias (mm) Trend (ppm) LSS peaks ACF(CT) - dist ACF(CT) - shape ACF(DE) - dist ACF(DE) - shape	1.44 0.25 (93%) 16 (87%) many small peaks 2.997 wavy 6.774	dt (C)	St.Dev.V (mm) Bias (mm) Trend (mm/C) LSS peaks ACF(CT) - dist ACF(CT) - shape ACF(DE) - dist ACF(DE) - shape	1.45 0.25 (92%) 1.178
H (m)	St.Dev.V (mm) Bias (mm) Trend (ppm) LSS peaks ACF(CT) - dist ACF(CT) - shape ACF(DE) - dist ACF(DE) - shape	1.43 0.25 (93%) -7 (91%) several small peaks 5.395 wavy 20.23	a(c) (yr)	St.Dev.V (mm) Bias (mm) Trend (mm/yr) LSS peaks ACF(CT) - dist ACF(CT) - shape ACF(DE) - dist ACF(DE) - shape	1.45 0.25 (92%) many small peaks 0.001 correlation 0.016
S (km)	St.Dev.V (mm) Bias (mm) Trend (mm/km) LSS peaks ACF(CT) - dist ACF(CT) - shape ACF(DE) - dist ACF(DE) - shape	1.44 0.25 (92%) 0.486 (78%) 0.179 slight neg. trend 0.138 exp. trend	a(TP) (turn. pt)	St.Dev.V (mm) Bias (mm) Trend (mm/tp) LSS peaks ACF(CT) - dist ACF(CT) - shape ACF(DE) - dist ACF(DE) - shape	1.44 0.25 (93%) 0.024 (86%) several sml peaks 1.790 wavy
L (km)	St.Dev.V (mm) Bias (mm) Trend (mm/km) LSS peaks ACF(CT) - dist ACF(CT) - shape ACF(DE) - dist ACF(DE) - shape	1.45 0.25 (92%) -0.001 (92%) few small peaks 10.50 long per. trend 12.60 neg. trend	a(R) (mE3)	St.Dev.V (mm) Bias (mm) Trend (mm/mE3) LSS peaks ACF(CT) - dist ACF(CT) - shape ACF(DE) - dist ACF(DE) - shape	1.44 0.25 (93%) -3.136x10E-5 (79%) few small peaks 1.468x10E5 periodic 1.321x10E6

Notes: Uncertainty levels for bias=0 and trend=0 are included in brackets following the estimated value.
No entries indicates no significant results.

TABLE 3: Results of multiple linear regression analysis for GSC line A12N10.75.

	Model 1	Model 2	Model 3
a(s) = dH (m)			
est. (ppm)	14	17	19
Uncert. est = 0	78%	88%	94%
Effect (mm)	-0.934	-1.162	-1.323
H (m)			
est. (ppm)	-12	-8	-8
Uncert. est = 0	99%	97%	97%
Effect (mm)	7.301	4.694	4.620
L (km)			
est. (mm/km)	-0.011		
Uncert. est = 0	94%		
Effect (mm)	-39.825		
a(TP) (turning pt.)			
est. (mm/tp)	0.045	0.024	0.024
Uncert. est = 0	100%	100%	100%
Effect (mm)	66.279	34.916	34.939
a(R) (mE3)			
est. (mm/mE3)	-3.323x10E-5	-2.044x10E-5	
Uncert. est = 0	77%	78%	
Effect (mm)	0.104	0.064	
Uncert of model = 0	99%	96%	98%
% of SST0 Explained by the model	13.554%	7.487%	7.018%
St.Dev. V (mm) (St.dev.D = 1.46 mm)	1.394	1.412	1.409
St.Dev. V (1km) (mm) (sd.dev.D (1km) = 2.104 mm)	1.999	2.084	2.084
Sum V (mm) (Sum D = 30.460 mm)	0.195	- 8.052	-7.777
Uncert Sum V = 0	1%	36%	35%
Freq of Sum V < s(L) (Freq of Sum D < s(L) = 16%)	100%	98%	100%
Correlations	-0.34 = r(dH,dR) -0.27 = r(dH,dTh) 0.56 = r(H,L) -0.44 = r(H,TP) -0.79 = r(L,TP) -0.33 = r(dR,dTP)	-0.19 = r(dH,H) 0.28 = (dH,dTh)	-0.21 = r(dH,H)

Notes: Uncert. model = 0 means the uncertainty that all parameters are simultaneously zero.
See text for explanation of of other table entries.

TABLE 4: Comparison of statistically significant effects
(90% uncertainty level) with line characteristics

Attribute	Significant Regression Arguments								
	a(s)	H	dS	dt	dET	a(c)	a(TP)	a(R)	dNS
Total Stations with Effect	4	2	4	3	1	2	7	3	1
Terrain:									
flat	0	0	1	2	1	0	0	1	0
uniform slope	1	1	1	1	0	2	4	1	0
undulating	0	1	1	0	0	0	2	0	1
mountainous	3	0	0	0	0	0	1	1	0
Location:									
B.C.	3	0	1	0	0	1	2	1	0
Man.	0	0	0	0	0	0	0	0	0
N.Ont.	0	0	2	1	1	0	0	0	0
S.Ont.	0	0	0	2	0	1	2	2	0
N.S.	1	2	1	0	0	0	3	0	1
Line Direction									
north-south	2	1	2	1	0	1	4	2	0
east-west	2	1	2	2	1	1	4	1	1
No. Setups / Section:									
odd	4	2	2	0	0	1	3	1	1
even	0	0	2	3	1	1	1	2	0
Frequency of Sum D within $\pm s(L)$									
< 68%	3	1	1	1	0	0	5	1	0
> 68%	1	0	3	2	1	2	2	2	1
Date of Levelling									
< 1978	4	2	2	0	0	1	5	2	1
> 1978	0	0	2	3	1	1	2	1	0

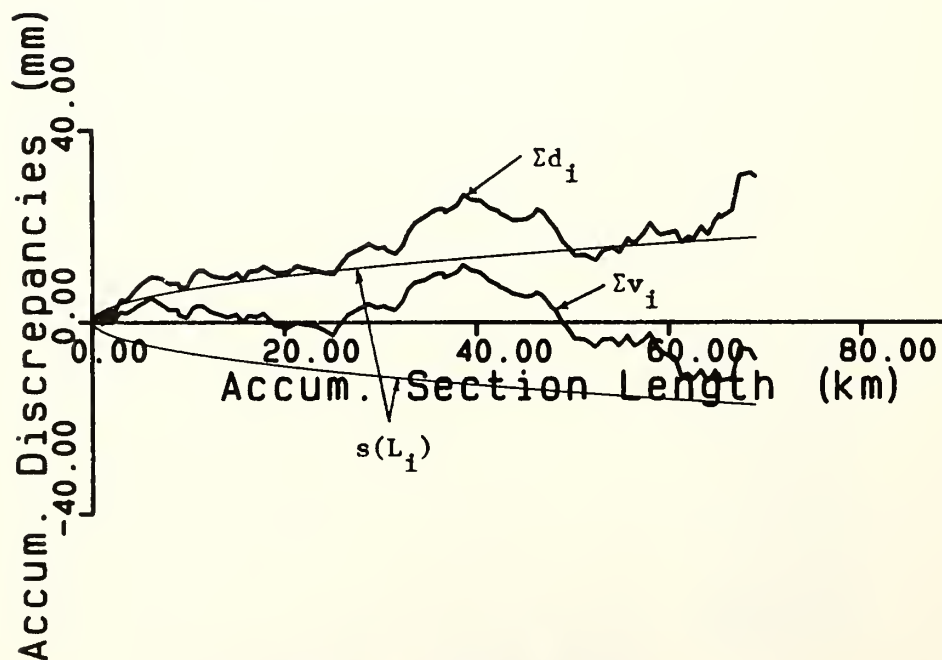


FIGURE 1: Accumulated discrepancies for GSC line A12N10.75.

ACCUMULATION OF THE CHOLESKY SQUARE ROOT IN HELMERT BLOCKING

D. R. Junkins and R. R. Steeves
Geodetic Survey of Canada
Surveys and Mapping Branch
615 Booth Street
Ottawa, Ontario, Canada K1A 0E9

ABSTRACT. The Helmert blocking method [Wolf, 1978] can be used to advantage in the upcoming readjustment of the North American vertical networks. Combining this method with the Cholesky computational method, [e.g. Jennings, 1977] provides a very efficient method for the solution of large systems of linear equations. A by-product of this approach is a "partial" Cholesky square root for each Helmert block. This paper demonstrates that the Cholesky square root for the entire system of normal equations can be "accumulated" through the Helmert block adjustment, even though various re-orderings of the unknown parameters are necessary throughout the computations. The entire Cholesky root can then be used to compute the inverse of the normal equation coefficient matrix, which is needed for post-adjustment statistical analyses.

1. INTRODUCTION

The effort to readjust the North American vertical networks will require the solution of a system of linear equations involving several thousand unknowns. By grouping the associated observations into sets, or "blocks", of a manageable size, the solution of the system is facilitated. This is the approach used in the Helmert blocking method. The rigorous solution of the very large system of equations is accomplished in a way which requires the treatment, at any one time and/or agency, of a relatively small system of equations. The treatment of these smaller systems of equations is further simplified with the application of the Cholesky computational method.

Not only is the solution of the very large system of equations of interest for the readjustment, but also the inverse of the normal equation coefficient matrix is needed for post adjustment statistical analyses and statements of precision. As is well known, the Cholesky method also facilitates the inversion of this matrix, since the inverse of the normal equation coefficient matrix can be computed directly from the Cholesky square root. However, during the Helmert blocking process only Cholesky square roots for the smaller sub-systems of equations are generated. Can these smaller square roots be used to build up, part by part, the square root for the entire system? If so, a substantial saving in computational costs can be made. It turns out that this is indeed possible even when it is necessary to re-order the unknowns at certain stages during the Helmert blocking process. The objective of this paper is to show how this accumulation of the entire Cholesky square root is possible.

2. BLOCKING OF OBSERVATIONS AND NORMAL EQUATIONS

The Helmert blocking process subdivides the solution of large systems of equations by separating the observations into groups or "blocks". Our notation will be such that any subscripted matrix or vector will be a sub-matrix or partition of it's non-subscripted parent. Suppose we have a set of observations L , with associated covariance matrix C_L , which are related to a vector x of unknown parameters by the design matrix A , so that

$Ax=L=v$. Now suppose that we divide L into two blocks L_1 and L_2 , that are statistically independent, i.e. with no off-diagonal covariance terms in C_L between observations of separate blocks. The normal equations then become

$$(A_1^T P_1 A_1 + A_2^T P_2 A_2)x = (A_1^T P_1 f_1 + A_2^T P_2 f_2), \quad (2.1)$$

where f_1 and f_2 are the misclosure vectors corresponding to L_1 and L_2 respectively [Vanicek & Krakiwsky, 1982].

Now, suppose we divide the vector x of unknown parameters into three partitions: x_1 , x_2 , and x_3 . Partition x_1 contains the unknown parameters for which all observations are contained in block 1. Similarly, x_2 contains those parameters for which all observations are contained in block 2. Partition x_3 contains all unknown parameters for which some observations are contained in both blocks 1 and 2. Thus, we call vectors x_1 and x_2 the interior parameters for blocks 1 and 2 respectively, and vector x_3 contains the junction parameters, since they are common to the two blocks.

Expanding equation (2.1) in terms of the partitioned x vector gives

$$(A_{11}^T P_1 A_{11})x_1 + (A_{11}^T P_1 A_{13})x_3 = A_{11}^T P_1 f_1, \quad (2.2)$$

$$(A_{22}^T P_2 A_{22})x_2 + (A_{22}^T P_2 A_{23})x_3 = A_{22}^T P_2 f_2, \quad (2.3)$$

and,

$$\begin{aligned} (A_{13}^T P_1 A_{11})x_1 + (A_{23}^T P_2 A_{22})x_2 + (A_{13}^T P_1 A_{13} + A_{23}^T P_2 A_{23})x_3 \\ = A_{13}^T P_1 f_1 + A_{23}^T P_2 f_2. \end{aligned} \quad (2.4)$$

Equation (2.4) can be separated into the sum of the following two expressions:

$$(A_{13}^T P_1 A_{11})x_1 + (A_{13}^T P_1 A_{13})x_3 = A_{13}^T P_1 f_1 \quad \text{and}, \quad (2.5a)$$

$$(A_{23}^T P_2 A_{22})x_2 + (A_{23}^T P_2 A_{23})x_3 = A_{23}^T P_2 f_2. \quad (2.5b)$$

Equations (2.2) and (2.5a) can thus be formed independently using the block 1 observations L_1 , as can equations (2.3) and (2.5b) from the block 2 observations L_2 . Neither equations (2.2) nor (2.3) includes terms involving the observations from the other block, but the contributions from both blocks must be included before equation (2.4) is complete. Figure 1 shows this process diagrammatically.

This method of accumulating normal equations can easily be extended to any number of blocks contributing to a single junction block. Similarly, junction block normal equations can be added together to form a larger system. For each contributing junction block, the interior and junction parameters are identified, and the normal equations partitioned appropriately. The junction portion is then added to the new junction block formed at the next level. This process may be repeated to form as many levels of blocking as necessary to handle the entire system. Figure 2 shows an example of such a system. The area above the elementary block interior parameter coefficients is entirely empty (see Figure 2, Level 1). It is this sparseness of the overall normal equation coefficient matrix that allows us to form the blocks. The coefficients of the elementary block junction parameters (Level 2) are further subdivided into interior and junction parameter coefficients for higher level blocks (Levels 3 and 4) that lie on the upward path of the block combination strategy.

3. ELIMINATION OF PARAMETERS

Using the notation introduced in Figure 1, the normal equation contribution from the k^{th} block to the junction block can be written in the following form.

$$N_{ii}x_i + N_{ij}x_j = b_i \text{ and,} \quad (3.1)$$

$$N_{ij}^T x_i + N_{jj}x_j = b_j, \quad (3.2)$$

where x_i is the vector of interior parameters for the block, and x_j is the vector of junction parameters. We can conclude from the development of section 2 that N_{ii} is non-singular, provided that the overall system is non-singular, and that N_{jj} will generally be singular.

Rearranging equation (3.1), making use of the non-singularity of N_{ii} , gives

$$x_i = N_{ii}^{-1}(b_i - N_{ij}x_j). \quad (3.3)$$

and substituting equation (3.3) into (3.2) gives

$$N_{ij}^T N_{ii}^{-1}(b_i - N_{ij}x_j) + N_{jj}x_j = b_j. \quad (3.4)$$

Rearranging, we get

$$(N_{jj} - N_{ij}^T N_{ii}^{-1} N_{ij})x_j = b_j - N_{ij}^T N_{ii}^{-1} b_i. \quad (3.5)$$

We have thus "reduced" the block normal equations (3.1) and (3.2), to a set of normal equations (3.5), by eliminating the interior parameters x_i . We therefore call equation (3.5) the reduced normal equations, which are expressed in terms of the junction parameters x_j . This process takes place for each block, and the reduced normal equations for x_j from each block are combined by straightforward matrix addition into a single complete expression for x_j :

$$N_{jj}^* x_j = b_j^*, \quad (3.6)$$

$$N_{jj}^* = \sum_{k=1}^n (N_{jj} - N_{ij}^T N_{ii}^{-1} N_{ij})_k \text{ and,}$$

$$b_j^* = \sum_{k=1}^n (b_j - N_{ij}^T N_{ii}^{-1} b_i)_k.$$

After solving system (3.6) for x_j , the interior parameters x_i may be solved, for each block, by substitution into equation (3.3).

4. CHOLESKY COMPUTATIONAL METHOD

a) Cholesky Decomposition

The symmetric, positive definite matrix of normal equation coefficients N may be decomposed into the product of two triangular matrices, one lower and one upper (L and U , respectively), such that

$$N = LU, \quad (4.1)$$

where $L = U^T$.

The matrix U (or its transpose L) is known as the Cholesky square root of the normal equations N . It can be computed using a well known algorithm [Jennings, 1977], the details of which will not be given here.

b) Solution of Parameters

The normal equations $Nx = b$, can thus be written in terms of the Cholesky square root as

$$LUx = b, \text{ or} \quad (4.2)$$

$$Ux = L^{-1}b. \quad (4.3)$$

The solution of the normal equations (4.2) consists of two steps. We first define the forward solution vector d as the right hand side of equation (4.3), i.e. $d = L^{-1}b$, which by rearranging can be written as

$$Ld = b. \quad (4.4)$$

This is a system of equations in d which is easily solved by a "forward substitution" process, since L is triangular. Once we have computed d , it can be used as the right hand side of equation (4.3) giving

$$Ux = d, \quad (4.5)$$

which can be solved by a simple "backward substitution" process since U is triangular. Note that the solution of $Nx = b$ has been performed without requiring the inversion of N ; this results in a substantial saving in computational expense.

c) Inverse of Normal Equation Coefficient Matrix

The inverse of the normal equation coefficient matrix for the overall system of equations is needed, at least in part, for the error analysis of the adjustment. We show below that the (entire) Cholesky square root of the system can be used to compute this inverse. We show later how the Cholesky square root for the entire system can be built up from results of the separate treatment of each Helmert block.

Since $N = U^T U$ (see equation (4.1)), we have

$$N^{-1} = (U^T U)^{-1} = U^{-1} (U^{-1})^T. \quad (4.6)$$

By setting $S = U^{-1}$, we have, by definition,

$$US = I, \quad (4.7)$$

where I is the identity matrix. Again we see that, since U and S are both triangular, we can compute S easily from equation (4.7). The inverse of N is then given by

$$N^{-1} = SS^T. \quad (4.8)$$

5. HELMERT BLOCKING USING THE CHOLESKY COMPUTATIONAL METHOD

Expanding the normal equation coefficient matrix of equations (3.1) and (3.2) in terms of a similarly partitioned Cholesky square root of that matrix gives

$$N_{ii} = L_{ii} U_{ii}, \quad (5.1)$$

$$N_{ij} = L_{ii} U_{ij}, \quad (5.2)$$

$$N_{ij}^T = L_{ji} U_{ii}, \text{ and} \quad (5.3)$$

$$N_{jj} = L_{ji}U_{ij} + L_{jj}U_{jj}. \quad (5.4)$$

The Cholesky root partition $[U_{ii} \ U_{ij}]$ is computed by the standard decomposition algorithm, by halting the process before entering N_{jj} . This is the partial Cholesky root for the eliminated interior parameters of the block.

By substituting these results into the left hand side of equation (3.4), we get

$$N_{jj} - N_{ij}^T N_{ii}^{-1} N_{ij} = N_{jj} - L_{ji}U_{ij}. \quad (5.5)$$

Note at this point that substituting (5.4) into (5.5) gives the following interesting relationship:

$$N_{jj} - N_{ij}^T N_{ii}^{-1} N_{ij} = L_{jj}U_{jj}. \quad (5.6)$$

Put simply, this means that the further solution for x_j can be treated as a separate problem, and the Cholesky square root of the reduced normal equations is identical to the lower partition of the full Cholesky root. Since N_{jj} is generally singular for an individual block, this root exists only after all contributions from other blocks have been added.

Substitution of equations (5.1) and (5.3) into the right hand side of equation (3.5) gives

$$b_j - N_{ij}^T N_{ii}^{-1} b_i = b_j - L_{ji}L_{ii}^{-1} b_i.$$

To further simplify this, we make use of the forward solution vector, d , and the relationship $Ld = b$. We have

$$L_{ii}d_i = b_i, \text{ and} \quad (5.7)$$

$$L_{ji}d_i + L_{jj}d_j = b_j. \quad (5.8)$$

The partial forward solution vector, d_i , can be calculated directly. Substituting the relationship $L_{ii}d_i = b_i$ into the above gives

$$b_j - N_{ij}N_{ii}^{-1}b_i = b_j - L_{ji}L_{ii}^{-1}L_{ii}d_i = b_j - L_{ji}d_i. \quad (5.9)$$

Thus, the simplified form of the reduced normal equations is

$$(N_{jj} - L_{ji}U_{ij})x_j = b_j - L_{ji}d_i. \quad (5.10)$$

These reduced normal equations may now be combined with those from other blocks, and the solution for x_j computed by the Cholesky method. To compute the back solution for the eliminated parameters, we substitute the expression for the forward solution vector, d , into the relationship $Ux = d$. That is

$$U_{ii}x_i + U_{ij}x_j = d_i, \text{ and} \quad (5.11)$$

$$U_{jj}x_j = d_j. \quad (5.12)$$

Then, with x_j and d_i having already been computed, x_i is solved for by back substitution into the expression

$$U_{ii}x_i + U_{ij}x_j = d_i. \quad (5.12)$$

The complete Cholesky square root for the block is formed by combining the partial Cholesky square root for the eliminated parameters with the Cholesky square root for the junction parameters. This entire process is depicted in Figure 3. Figure 4 shows the form of the complete Cholesky square root for a two block system, along with the short-hand notation for the block combination and solution process.

6. RE-ORDERING THE UNKNOWN PARAMETERS

During the solution of the junction block parameters, it is obviously desirable to re-order the junction block normal equations in order to minimize the non-zero profile of the normal equations. Also, it is generally certain that the reduced normal equations from the various blocks will have been formed with different orderings of the junction block parameters x_j . Thus, a re-ordering is required when combining the reduced normal equations. How does this affect the partial Cholesky square root?

For the system of normal equations $Nx = b$, suppose that we wish to re-order the vector x into the vector y such that $y = Rx$. Then R can be shown to be an identity matrix with its rows re-ordered in the same way as are the elements of x . This Jacobian, R , is orthogonal, so that $R^T = R^{-1}$. The re-ordering of the observation equations $Ax - L = v$ (which gave rise to the system of normal equations), gives

$$(AR^T)Rx - L = v. \quad (6.1)$$

The corresponding re-ordered normal equations are then

$$(RNR^T)Rx = Rb. \quad (6.2)$$

This demonstrates that the ordering of the unknown parameters in the vector x is arbitrary, and that the normal equations can be re-ordered, even after they have been formed, which is useful for minimizing the non-zero profile of the normal equations. Considering the Cholesky square root, we have

$$RNR^T = (RL)(UR^T) = L^*U^*. \quad (6.3)$$

Note that pre-multiplying by R interchanges rows, and post-multiplying by R^T interchanges columns. Thus, any such operation will generally yield a matrix that is no longer triangular, and therefore general re-ordering of the Cholesky square root may not meaningfully take place after it's computation. There is, however, an exception which is very useful in the Helmert blocking process.

Partitioning the second factor of equation (6.3) with respect to the interior and junction parameters gives

$$U_{ii}^* = U_{ii}R_{ii}^T + U_{ij}R_{ji}^T, \quad (6.4)$$

$$U_{ij}^* = U_{ii}R_{ij}^T + U_{ij}R_{jj}^T, \quad (6.5)$$

$$U_{ji}^* = U_{jj}R_{ji}^T, \quad (6.6)$$

$$U_{jj}^* = U_{jj}R_{jj}^T. \quad (6.7)$$

Since there is no external information for the interior parameters x_i , we have no requirement for re-ordering them. This means that R_{ii} is the identity matrix, and thus R_{ij} and R_{ji} are zero matrices. The partial Cholesky square root $[U_{ii} \ U_{ij}]$ has already been computed during the elimination process, but the Cholesky root for the junction parameters will not be computed until after their normal equation partition has been re-ordered. Re-writing equations (6.4) to (6.7) with this information yields

$$U_{ii}^* = U_{ii}, \quad (6.8)$$

$$U_{ij}^* = U_{ij}R_{jj}^T, \quad (6.9)$$

$$U_{ji}^* = 0, \quad (6.10)$$

$$U_{jj}^* = U_{jj}R_{jj}^T. \quad (6.11)$$

We see from this that, since U_{ii} is unaffected, and U_{jj}^* is computed after re-ordering of the corresponding normal equation partition, we still have an upper triangular form. We need to show that $U_{ij}^* = U_{ij}R_{jj}^T$ is a legitimate operation on the previously computed partial root. Expanding equation (6.3) further shows that

$$N_{ij}R_{jj}^T = U_{ii}^T U_{ij}^*. \quad (6.12)$$

Recalling that $N_{ij} = U_{ii}^T U_{ij}$, from equation (5.2), then

$$U_{ii}^T U_{ij}R_{jj}^T = U_{ii}^T U_{ij}^*,$$

and pre-multiplying both sides by $(U_{ii}^T)^{-1}$, since U_{ii} is non-singular, yields

$$U_{ij}R_{jj}^T = U_{ij}^*, \quad (6.13)$$

as required.

Thus, the previously computed partial Cholesky square root may indeed be used provided that the further re-ordering of the junction parameters x_j by R_{jj} is taken into account, so that the partial root becomes

$$[U_{ii} \ U_{ij}R_{jj}^T]. \quad (6.14)$$

We saw from equation (6.2) that the vector of constant terms from the normal equations requires re-ordering also. But what about the forward solution vector d ? Recall from equations (4.4) and (4.5) that $d = Ux = L^{-1}b$. Introducing the re-ordering Jacobian, R , and recalling that $R^T = R^{-1}$, we get

$$d = (UR^T)Rx = (RL)^{-1}Rb. \quad (6.15)$$

Thus d is independent of the ordering of the unknown parameters.

7. THE CHOLESKY ROOT FOR A HELMERT BLOCKING SYSTEM

In the development presented in the previous section, we used the simple example of a system of two elementary blocks. We assumed that we could add their reduced normal equations together directly to form the junction block normal equations after a simple reordering of the junction parameters. In the more general case, there will be a difference not only in the ordering of parameters between the reduced normal equations being combined, but there will also be some junction block parameters not contained in all contributing blocks. This situation is shown diagrammatically in Figure 5.

The theoretical approach (as opposed to practical implementation) to managing this disparity involves augmenting the junction parameter vector of each individual block to include all other parameters of the complete junction block. The corresponding normal equation coefficient matrix (of the reduced normal equations) is similarly (but again theoretically) extended to include zero coefficients for these extra parameters, as shown in Figure 6. The temporary singularity of this matrix is not a problem, since contributions to these coefficients will come from other blocks - at this or some higher level - before any solution or inversion is attempted.

The situation is now the same as in our previous discussion, and a reordering matrix can be defined to make each individual reduced normal equation ordering identical to the

junction block ordering. We can also generalize the notation of the reordering matrix R_{jj} to be $R_{p,q}$, which reorders the augmented junction parameter vector of contributing block p into the order of the parameter vector of junction block q .

Recall also from the example in Figure 2, that further subdivision and re-ordering of the elementary block junction parameters will take place as each junction block has its interior parameters eliminated. This takes place as we work our way up the blocking strategy. However, full knowledge of these details is not available when the lower level elimination takes place. Thus, the normal equation coefficients and the partial Cholesky root computed during elimination have all of their junction parameter coefficients in a single group. The separation comes about by the successive re-ordering of each junction block.

Consider block 1 in Figure 2 as an example. Its junction parameters are contained as interior parameters in blocks 9, 11, and 13. Thus, its normal equations contribution eventually becomes

$$[N^*]_1 = R_{11,13} R_{9,11} R_{1,9} [N]_1 R_{1,9}^T R_{9,11}^T R_{11,13}^T. \quad (7.1)$$

From equations (6.3) and (6.14), we can see that the partial Cholesky root can be re-ordered. It becomes

$$[U_{1,1} \ U_{1,9} \ U_{1,11} \ U_{1,13}] \quad (7.2)$$

Thus, each partial Cholesky root computed during the elimination process can be saved and re-ordered. The combination of all such roots yields a complete Cholesky root for the entire system, as shown in Figure 7. Its block profile is identical to that of the original normal equations. This root may then be used to compute the inverse of the normal equation coefficient matrix for use in post adjustment statistical analyses.

8. CONCLUSIONS

We have shown that, during a Helmert block adjustment using the Cholesky computational method, a general re-ordering of the partial Cholesky roots is not possible. But the specific re-ordering necessary in order that the accumulated components of the Cholesky root can be used to form the entire root, is indeed possible and very useful.

The computer implementation of the method will use "pointer vectors" which can be re-ordered; the storage locations of the actual Cholesky root components will not change throughout the adjustment process. Therefore, re-ordering matrices are not actually used in the computations.

We propose to employ the methods outlined in this paper in the upcoming readjustment computations after thorough testing of their computer implementation has been carried out.

9. REFERENCES

- Jennings, A. (1977) Matrix computations for Engineers and Scientists. John Wiley and Sons, pp. 107 ff.
- Vaníček, P. and E. J. Krakiwsky (1982) Geodesy: The Concepts. North Holland Publishing Company, p. 206.
- Wolf, H. (1978) The Helmert Block Method - Its Origin and Development. Proceedings of the Second International Symposium on Problems Related to the Redefinition of the North American Geodetic Networks, pp. 319-326.

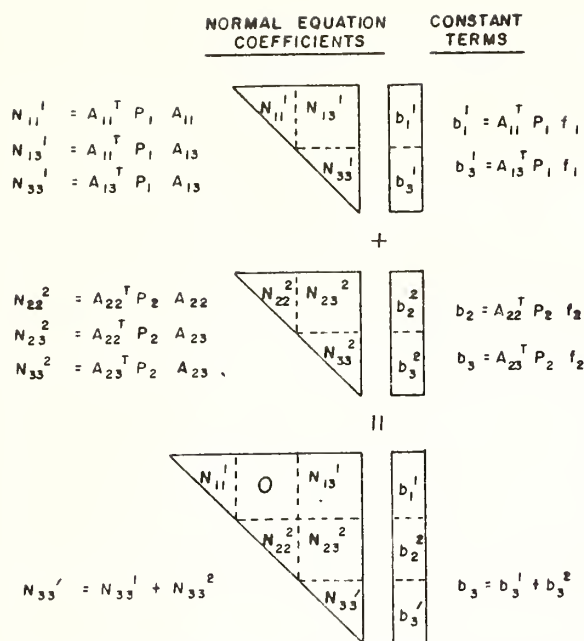


Figure 1

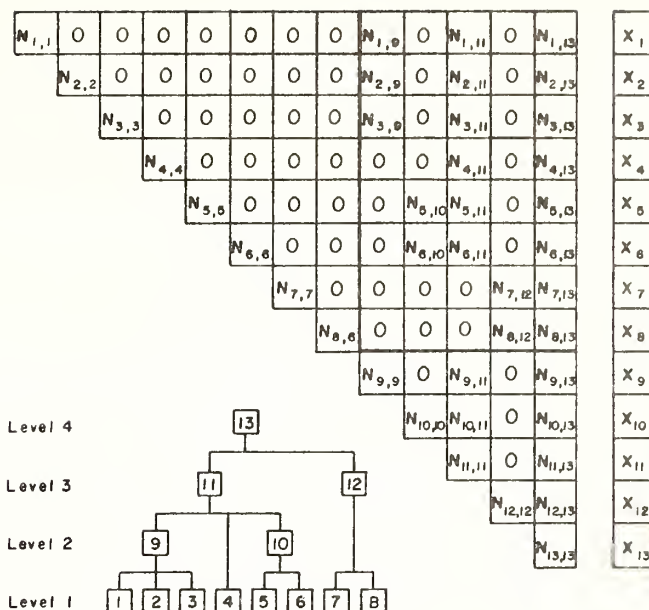


Figure 2

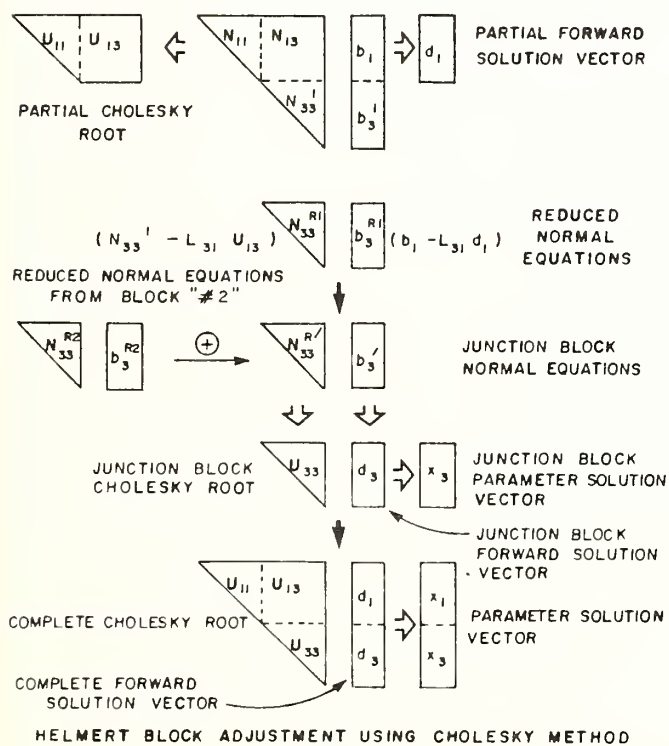
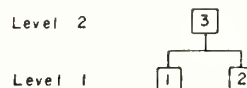


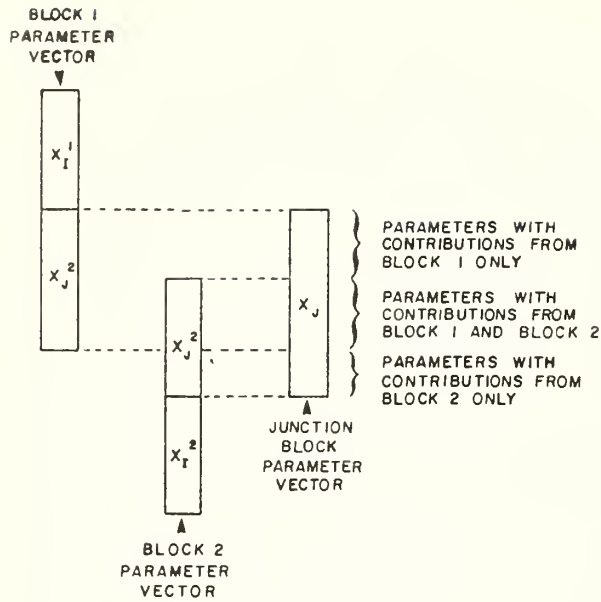
Figure 3

CORRESPONDING BLOCK ADJUSTMENT TREE



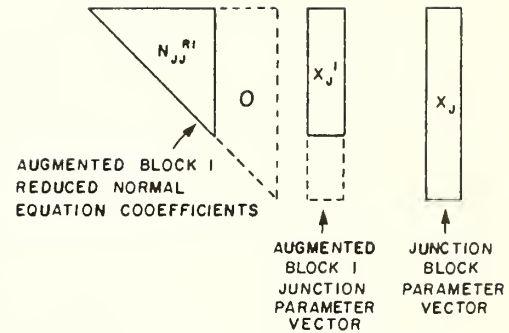
FORM OF CHOLESKY ROOT FOR COMPLETE SYSTEM OF TWO BLOCKS AND TWO LEVELS

Figure 4



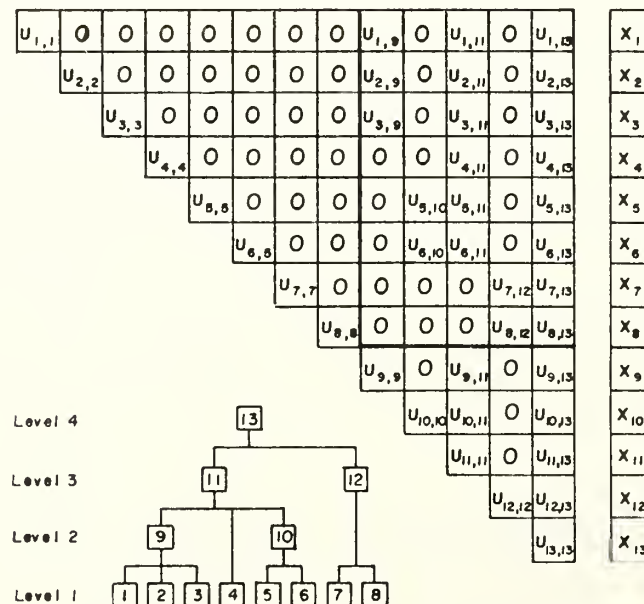
DISPARITY BETWEEN JUNCTION PARAMETER VECTORS
OF REDUCED NORMAL EQUATIONS CONTRIBUTING TO A
JUNCTION BLOCK

Figure 5



AUGMENTING THE REDUCED NORMAL EQUATIONS FOR
COMPATIBILITY WITH JUNCTION BLOCK PARAMETERS

Figure 6



COMPLETE CHOLESKY ROOT FOR AN EIGHT - BLOCK
FOUR - LEVEL ADJUSTMENT

Figure 7

A SUMMARY OF SURVEY CONDITIONS ENCOUNTERED BY NGS

Lloyd C. Huff

Office of Charting and Geodetic Services
National Oceanic and Atmospheric Administration
Rockville, MD 20852

ABSTRACT. Temperature gradients, sight lengths and height differences, encountered at setups on over 25,000 sections representing modern first order leveling performed by NGS, have been analyzed. These analyses were part of an engineering study associated with the design, development and testing of a Rapid Precision Leveling System (RPLS). The statistical distribution of sight lengths, stratified by temperature gradient and height difference, are presented. In these presentations, one can easily discern the effects of both NGS survey policy and survey practice. The distribution of section lengths between bench marks on lines in the U.S. National Geodetic Vertical Network is discussed. The monument separation distribution is shown to be dominated by two most frequent lengths, one around 1600 m and the other less than 50 m. The frequency of occurrence for the former is about half of that for the latter. The monument separation distribution is shown to have a marked effect on the predicted survey production rates for the RPLS. An analysis of temperature measurements from successive setups confirms that the variability in temperature measured at 0.3 m above the ground significantly exceeds the variability in temperatures measured at 1.3 m. Furthermore based on the differences in gradients at successive setups one is led to the conclusion that on sight lengths which the RPLS must use in order to achieve high production rates, directional differences in refraction may be a significant contributor to random leveling errors.

INTRODUCTION

Given an instrumentation suite intended for vertical leveling one proceeds to devise survey methods which will optimize the quality of the results and maximize productivity, subject to constraints imposed by the physical working environment. This has surely been the experience of the National Geodetic Survey as it has made several upgrades in instrumentation from the Fisher Spirit Level, to the Jenoptik NI002 which is currently being employed in the NGS motorized leveling operations. With our improved understanding and appreciation for the mechanisms thru which mean refraction and thermal turbulence can negatively impact survey operations, it is only reasonable that prior to designing new

instrumentation one must be mindful of the anticipated working environments. With an eye toward using the history of past NGS surveys as a prologue to further conditions, I have conducted an investigation into the physical environmental conditions under which NGS has conducted post 1974 first order leveling. It was hoped the study would specifically illustrate how thermal turbulence and steep terrain were impacting the operation of present instrumentation by causing sight distances to be shortened. Before presenting details from that study, I must say that the study was limited because it was found that NGS survey operations were often dominated by practices and policies instead of by environmental factors. However, I should be quick to point out that those practices and policies have themselves evolved to allow high quality standards to be met with the present instrumentation suite which is prone to systematic and random errors whose root causes are generally the operating environment.

DISCUSSION

The NGS has considerable experience with measuring air temperature for use in determining corrections for refraction. Air temperatures are measured with a resolution of 0.1°F using two thermistor probes located at 0.3 and 1.3 m above the ground. The probes are shielded from direct insolation heating and aspirated by small fan motors which draw air horizontally. The nature of the survey operation and the temperature sampling is such that successive temperature measurements along a section are separated in time on the order of minutes and in space on the order of a hundred meters.

A summary of the upper (1.3m) and lower (0.3m) temperature data from numerous sections indicated that the variance of the latter is 1.34°C^2 while the variance of the former is only 0.75°C^2 . This significant difference in variance makes sense when one considers that insolation heats the surface of the ground and then an upward flux of temperature warms the overlying air mass. Further above the surface, the air temperature is less controlled by the thermal characteristics of the local underlying surfaces and short term fluctuations of insolation. Generally air temperature becomes more uniform and thermal turbulence decreases as the level above the ground increases.

Employing the same set of upper and lower temperature data to evaluate the gradient, one determines that the variance in thermal gradient along those same sections was $0.53^{\circ}\text{C}^2/\text{m}^2$. Consequently one finds that 75% of the variance in temperatures along the sections is common mode between the two measurement levels. This high value of common mode variance is probably why NGS can successfully correct for refraction by using the average of the gradients observed at each instrument station on a section to compute the refraction correction for that section (Holdahl 1981).

These temperature data were also combined in various ways to compute the variances contained in the difference between temperature gradients observed on various setup separations. Table 1 presents the results of this analysis. With this analysis it is not possible to distinguish temporal factors in thermal gradients from spatial factors in thermal gradients. The values of 0.3 and 0.5 suggested by Brunner (1974) for the differences in refraction coefficients between foresights and backsights associated respectively with simultaneous reciprocal and (nonsimultaneous) reciprocal zenith distance observations would indicate that approximately one-third of the variance in temperature gradients is of spatial origin and two-thirds is of temporal origin. One can, however, clearly see that the common mode is high and that the random component is large compared to the effect of the data having been sampled with a 0.1°F ($5/90^{\circ}\text{C}$) resolution.

Table 1

Separation in setup	Variance in difference of gradient ($^{\circ}\text{C}/\text{m}$) ²
1	0.26
2	0.31
3	0.32
4	0.34
5	0.35

We understand that refraction can displace a line of sight and that the displacement is proportional to the magnitude of the refractive gradient and to the square of the sight length. Therefore refractive errors tend to be magnified on long sight lengths. When thermal gradients become large one is also likely to encounter thermal turbulence which results in image dance and imprecise rod readings. A bivariate analysis of observed temperature gradients and setup length was constructed to determine if it could be shown that the sight distances were regularly being shortened in order that the quality of survey could be maintained as thermal gradients increased and the potential for observing errors consequently increased. Figure 1 presents the bivariate distribution of temperature gradient and setup length. Temperature gradient was computed by subtracting the upper level temperature measurement from the lower level temperature measurement. Looking first at the solid curves, one can determine the 10, 50, and 90 cumulative percentiles of setup lengths which were employed under conditions of various temperature gradients. For example, of all

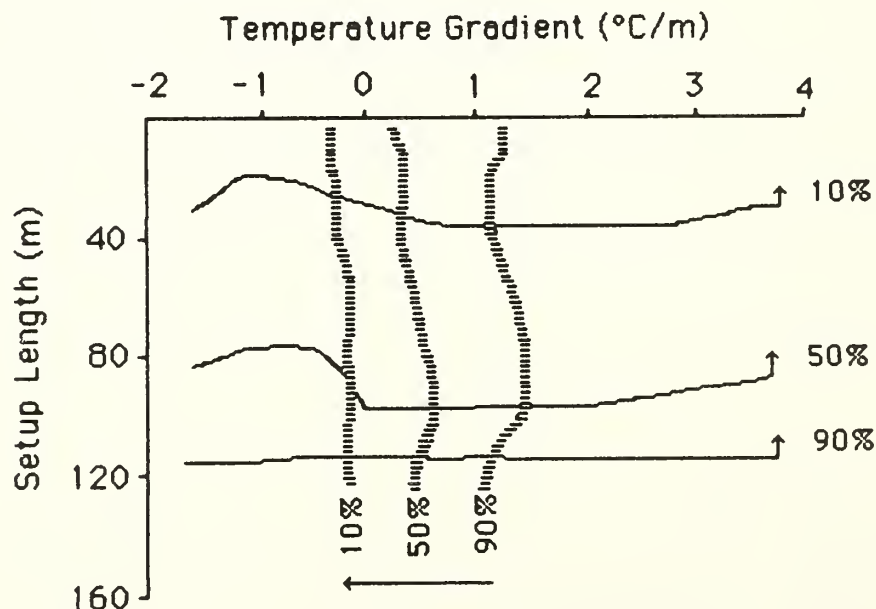


Figure 1. Bivariate Distributions of Temperature Gradient and Setup Length

the cases when the thermal gradient was $1^{\circ}\text{C}/\text{m}$, 10% of the setup lengths were 40m or less, 50% of the setup lengths were 100m or less and 90% of the setup lengths were less than 120m. Using the dashed lines in a similar manner, one can determine the cumulative percentiles of the temperature gradients which were present when any given setup length was employed. The cumulative percentiles of setup lengths (solid line) is greatly skewed as a result of the 50 and 60 meter limitations on allowable sight distances for first order class I and class II, respectively. It would appear that when the temperature gradient exceeds $2^{\circ}\text{C}/\text{m}$ that there is a tendency to reduce the setup distance. This was likely in response to image dance (a result of thermal turbulence) causing difficulty in obtaining precise rod readings. The location of the 90% dashed line however indicates that this problem is serious less than ten percent of the time. The knee in the 50% solid curve which occurs at 0°C gradient is quite pronounced. This knee along with the bulge in the 10% solid curve was probably in response to long period shimmer (which occurs in a neutral or stable atmosphere) causing difficulty in obtaining precise rod readings. This implies that some of the NGS observations made under negative temperature gradients may have been significantly and unpredictably affected by unnoticed long period shimmer. Sufficient winds may allow precise surveying to still be carried out under conditions of negative temperature gradient but such operations are ill advised. It is also possible that some of the near zero temperature gradients were associated with intermittences in the normal turbulent field, where "thermal chimneys" allow rapid upward movement of large volumes of heated air.

Thermal conditions are but one of the reasons most often cited for short sight lengths and low production rates. Slope of the local terrain can also certainly have a negative impact. Especially so, when one considers the fixed lengths of rods and a restriction against sight lines which come within 0.5m of the ground. At this symposium, J-M. Becker of the National Land Survey of Sweden has reported that by increasing the levelling staff employed in their fully motorized levelling technique to a length of 3.5 m and restricting sight lines to greater than 0.7 m above the ground, productivity was significantly increased and the effects of refraction and shimmer were almost totally eliminated.

One might expect to see a notable signature in the bivariate analysis of observed delta h's and setup lengths illustrated in Figure 2. In this figure the solid curves are the cumulative percentiles of setup lengths for the various delta h's and the dashed curves are the cumulative percentiles of delta h for the

various setup lengths. Here one notes that the 10% and 50% solid curves generally decreased with increasing Δh , as does the 90% solid curve once it moves back from the mandated maximum of 120m. In the dashed curves one sees an possible artifact of NGS policies and practices. The tendency for the 10% dashed curve to peak at 30m, quite likely results from the requirement to have a even number of setups per section. The peak in the 50% dashed curve probably expresses a genuine slope limitation in combination with the even setup requirement. The majority of the 90% dashed curve is potentially limited by rod length.

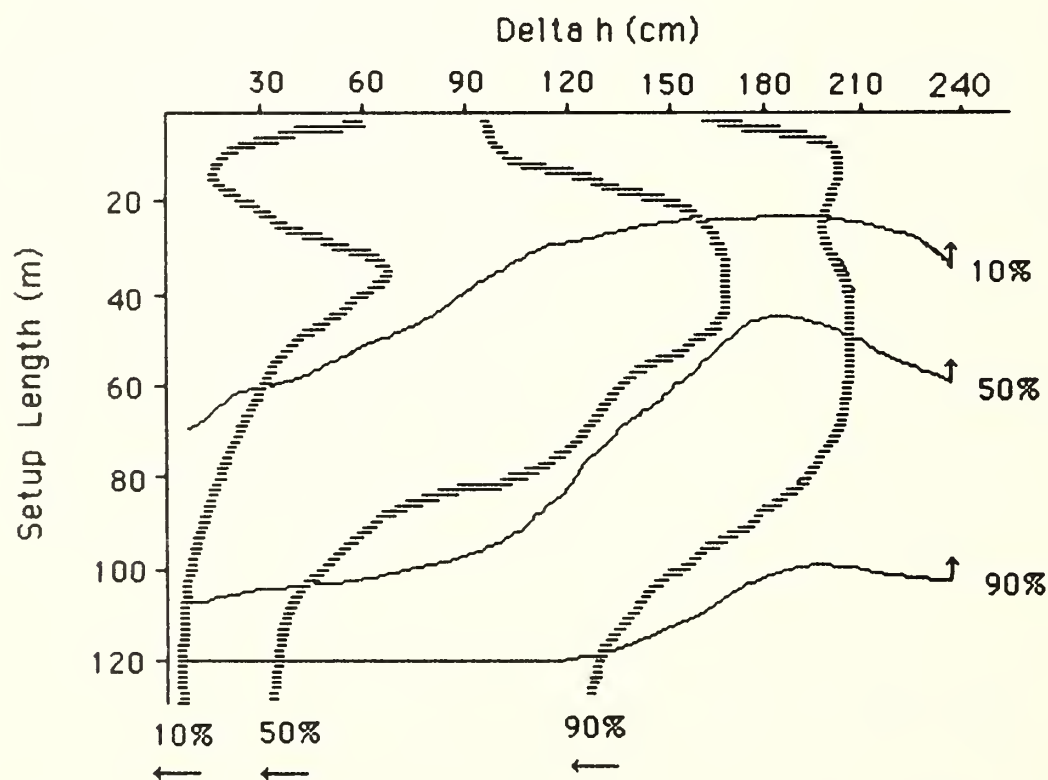


Figure 2. Bivariate Distributions of Observed Δh and Setup Length

The Rapid Precision Leveling System (RPLS) is intended to increase surveying productivity. In part this is to be achieved by increasing sight lengths. Increasing sight length can itself be broken into two separate problems. First to be sure that the RPLS error budget is compatible with high order leveling. Most of the potential factors contributing to the RPLS error budget increase with sight length. The second part of the problem is to be sure that long expanses of clear unobstructed space are present between monuments. This is most often

couched as if only the rise and fall of the terrain need be considered. There are however, also curves in the roadways to be considered, but more importantly, "How widely separated are the monuments?". Monument separation, as such, is not a part of the NGS data base, but section lengths can be determined by summing the stadia distances of all observations between monuments. Figure 3 illustrates the percent density of NGS section lengths which occur in a 50 meter interval centered around lengths from 0.025 to 2.5 km. The median section length is about 1 km, but by far the most densely populated intervals are near zero. This heavy concentration is composed of some short spurs, clusters around tide or water level stations and triangulation stations, but is almost totally dominated by monuments whose original purpose was to document and preserve horizontal position. Nevertheless, these "horizontal" monuments have become part of the vertical network and consistent with present NGS policies and practices, will be maintained as part of the vertical network.

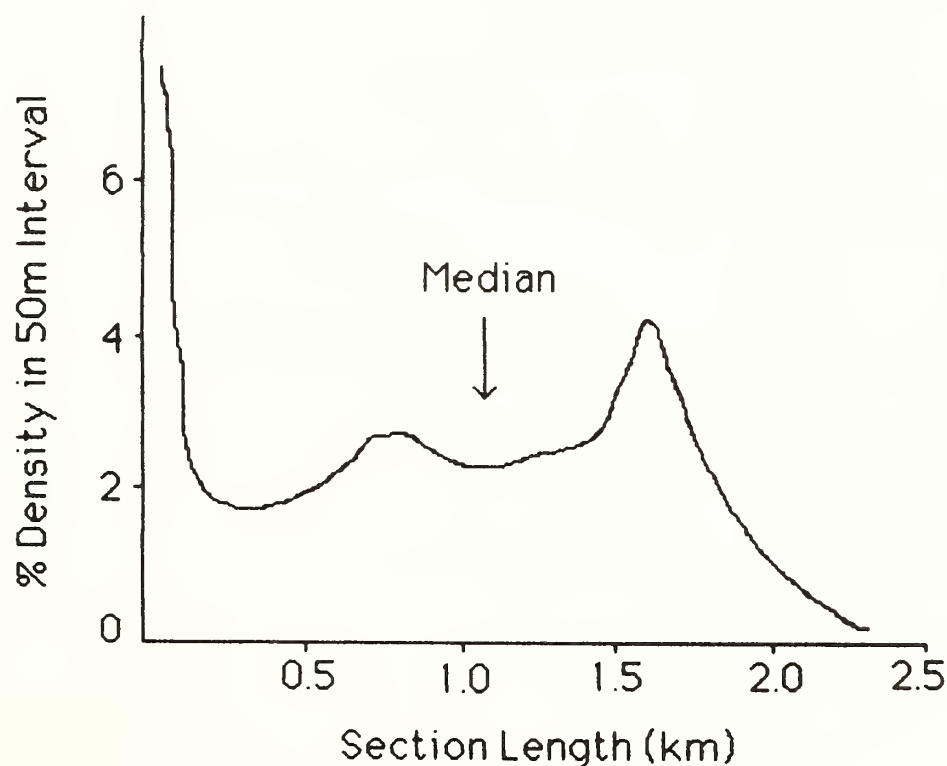


Figure 3. Density Function for Monument Separation

A productivity model for the RPLS has been developed which takes into consideration vehicle speed, measurement time for running the level line, measurement time for getting on/off a bench mark and sight length. If all monuments were at a uniform separation of 1.6 km. then the productivity in kilometers per surveyor hour would approach an upper limit independent of sight length. This is illustrated in Figure 4 with an assumed vehicle speed of 12 km/hr. The upper limit is approached as time becomes principally devoted to moving the vehicle forward. In the case of a three vehicle operation the upper limit of productivity is reached more rapidly than in the case of a two vehicle operation. If however the RPLS productivity model uses the actual section lengths between monuments, then the RPLS production on a 6-hour working day would drop by two to four kilometers per day.

Under typical NGS survey conditions a He-Ne 632 nm laser beam propagating under various thermal gradients would be displaced from its initial elevation. Figure 5, with its family of curves for different temperature gradients, is not

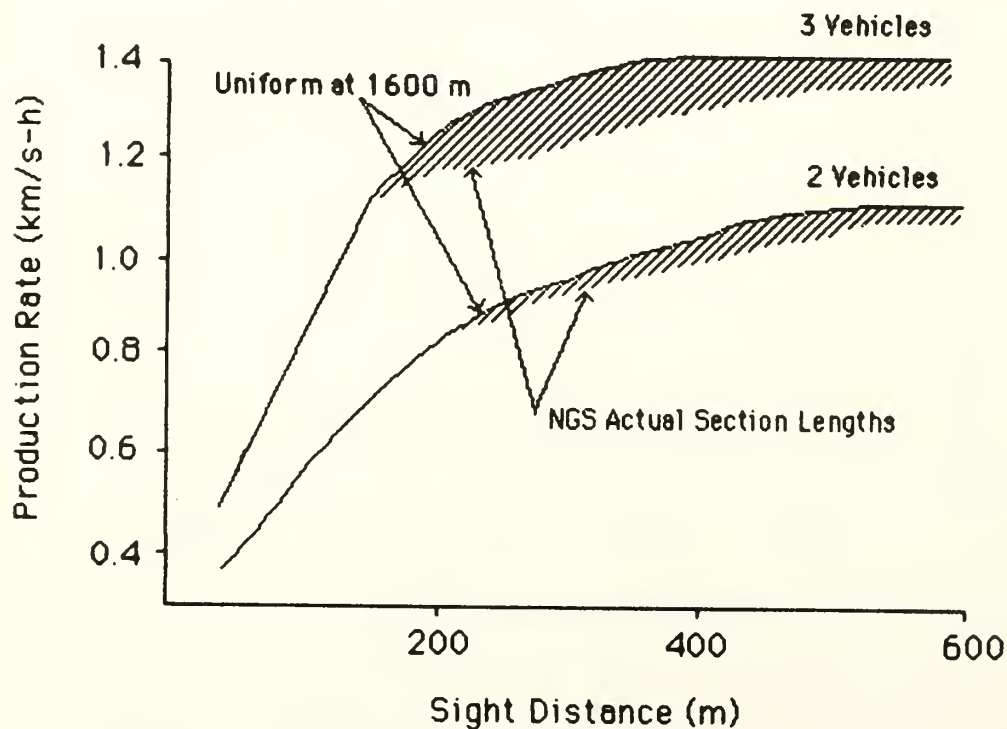


Figure 4. Rapid Precision Leveling System Productivity

new but is presented to serve as a backdrop to point up possible impacts of non-uniform temperature gradients along the sight line. The median temperature gradient encountered by NGS is $0.75\text{ }^{\circ}\text{C/m}$. Due to the typical shape of mean temperature profiles in the first few meters above the surface and the fact that the probes used to obtain these NGS temperature data are at heights of 0.3 and 1.3 m, the variance in gradients at 2.5 m, where the RPLS might work, could be reduced to only three-eighths of those listed in Table 1 and the median gradient could be reduced to $0.5\text{ }^{\circ}\text{C/m}$. Considering $0.3\text{ }^{\circ}\text{C/m}$ to represent the typical difference in thermal gradients at the two ends of a sight line whose length might be 100 to 300 meters, one might get a handle on the potential impact of non-uniform thermal gradients. One can not be sure of the manner in which the gradient behaved between data points, but the worse case would probably be if the gradient changed as a step function close to one end of the sight line. At 250 meters, in this worse case, the sight line from one end might be displaced by 5

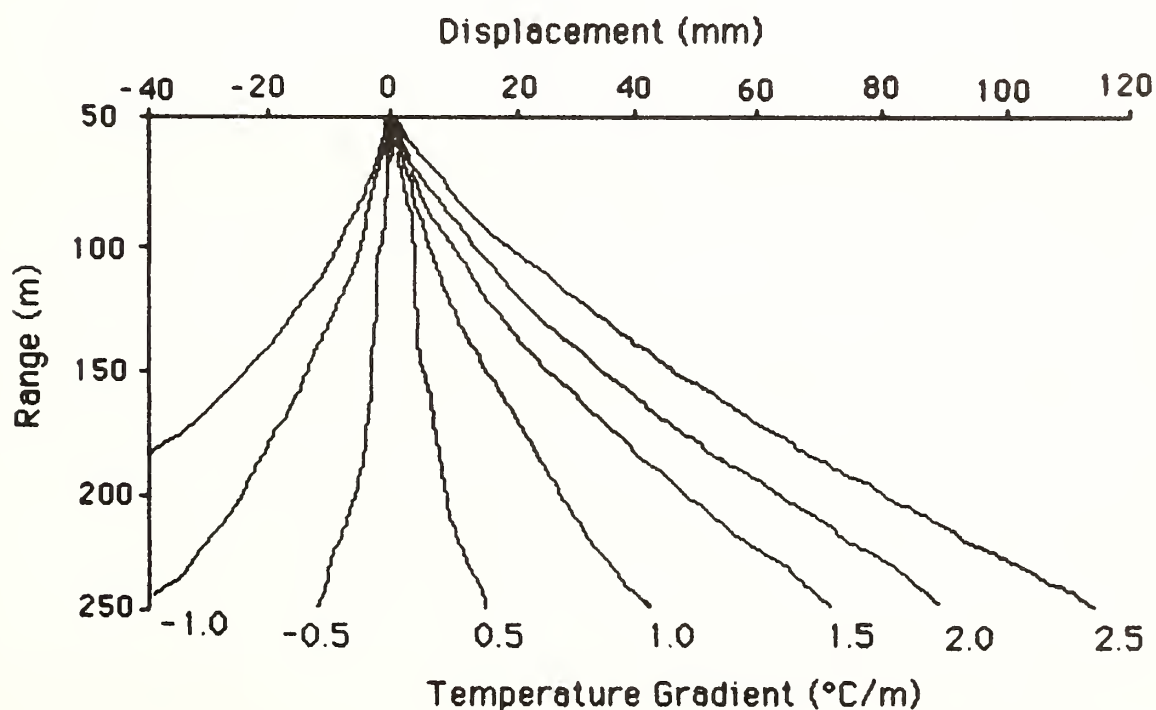


Figure 5. Sight Line Displacement Due to Refraction

or 30 mm depending on which end of the sight line the step function in gradient has occurred. Uncertainty of this magnitude would prevent simultaneous reciprocal observations from being first order.

SUMMARY

In the start of this paper it was indicated that one must be mindful of the physical working environment when designing a new instrumentation suite because once new instrumentation exists the only freedom one is likely to have is to adapt its use to the environment. The material presented in this paper indicates that some existing NGS survey methods might not allow even the present instrumentation to be utilized for production rates as large as might be achieved and still meet the standards for high order work. This study of NGS physical environmental conditions has shown that large simultaneous differences in temperatures and temperature gradients can exist between local points whose separations are comparable to the sight lengths which the RPLS must employ to achieve greater productivity. Therefore, this fact must be considered when designing the RPLS or other new instrumentation.

REFERENCES

- Brunner, F. K. - Trigonometisches Nivellement - Geometrisches Nivellement, Oester. Zeitschrift fur Vermessungswesen, Vol. 62, p. 49-60. 1974
- Holdahl, S. R. - A Model of Temperature Stratification for Correction of Levelling Refraction: NOAA Technical Memorandum NOS NGS 31. 1981

ADVANCED TECHNOLOGY FOR A NEW PRECISE LEVELLING ROD

Harald Schlemmer
Geodetic Institute
University of Karlsruhe
Englerstrasse 7
D-7500 Karlsruhe
WEST GERMANY

ABSTRACT. A new precise levelling rod has been developed. To avoid systematic effects in levelling caused by inexact graduation of the invar tape, a new technique to produce precise graduations has been installed. While the invar tape is moved to the desired position using a laser interferometer and a control device the graduation line is marked by using a pulsed gas laser with high energy in a very short time. The calibration demonstrates the excellent precision of the new graduation. The line corrections are better than ± 5 microns for the total graduation. A further advantage of the new technique is the fact that any line distance and any contour of line is possible. In addition, a new rod frame was designed. The cross-section of the aluminium-frame is selected to minimize the sag of the rod, and the spring tension is reduced to minimize the influence of temperature-produced extension of the frame on the invar tape.

INTRODUCTION

To prevent systematic errors in precise levelling caused by the rod, the surveying engineer has to calibrate the graduation of the rod because the scale of the levelling net results from graduation of the invar tape. The author has shown that it is rarely sufficient to determine the "average" or "mean rod metre". Instead, line corrections of every graduation line - relative to the zero point of the rod - ought to be determined and used to correct the measured values (SCHLEMMER 1975). Thus new comparators with modern measuring equipment for the calibration of levelling rods were developed. The calibration is now carried out automatically with the aid of a photoelectric microscope and a laser-interferometer. By the new procedure of calibration it was not only possible to determine the position of every individual line, but also for the first time we got an information about the quality of a graduation. On the other hand we obtained indirectly a reference to the manufacturing methods of the invar tapes.

THE EXISTING MANUFACTURING METHODS

The results of the calibration of many rods (more than 100) from different manufacturing firms indicate that there are two various techniques to produce the graduations:

The stencil technique

The invar tape is fastened to the bottom end and pulled with a spring on the upper end with the same energy as later in the frame. The graduation is added to the invar tape, which is furnished with a light first coat of paint, with the aid of a invar stencil. After the stencil is placed on top of the tape, black paint is sprayed for marking the graduation. Stencils of different length are used. If a 3m long stencil is used, scale corrections amount to about $\pm 20 \dots 30$ microns and their distributions are not random. Some manufacturers apply a 1m or 0.5m long stencil. In such graduations discontinuities growing up to 80 microns occur at the points where the stencil coincides. The problems concerning these discontinuities are pointed out in (SCHLEMMER 1978). A further problem of this technique is caused by cleaning the stencil from residual paint being necessary again and again. Caused by the cleaning the position of the lines of the stencil - and simultaneously the scale corrections of the graduation - vary.

The profile milling technique

The lines of the graduation are produced using a milling machine. A white plastic coating on the invar tape is milled off, until the black first coat of painting appears. The feed of such a milling machine is in general 1 metre. This means the tape must be clamped three times. The spindle has a distinct error over the feed of 1 metre. This periodical error of the spindle will be reproduced in the graduation. Therefore we must expect maximum errors of the lines of ± 50 microns. Moreover, the milling technique needs a thick white plastic coating on the invar tape, causing great problems connected with the thermal coefficient of expansion of the rod.

THE NEW TECHNIQUE

To determine line corrections of every graduation line and, if necessary, to correct the measured values requires more time and effort compared with the determination of the mean rod metre. Of course, time and effort can be reduced by using modern calibration equipments in the laboratory and microcomputers for data collection in the field, but the risk of errors or confusions remains. It was already during the development of the new laser interference comparator for the calibration when the idea arised: if we are able to measure the position of every line with such a high accuracy, why not produce the lines by this technique. The problem of this technique is not the determination of the position of the line - the laser interferometer measures very precise values - but marking the line onto the invar tape. Two alternative techniques for marking the graduation are imaginable:

- the static technique
- the dynamic technique

The static technique

The invar tape on which the lines are to be marked is moved to the desired position by the aid of the laser interferometer equipment using a control device. There it is stopped and the line of the graduation is marked with the conventional spray painting or milling technique. It will be however,

very difficult to stop and to hold the complete graduation including the shunting installation with the required accuracy of ≤ 1 micron. Furthermore, the operating time to produce a complete graduation with this technique will be very long, so that this alternative is inapplicable.

The dynamic technique

The invar tape is moved with a constant velocity and the movement is controlled by the interferometer. When the required position is reached, the line is marked immediately without stopping the tape and the shunting installation. If the tape is moved with a velocity of 5 mm/s and an accuracy of ≤ 1 micron is aimed at the process, the marking must be finished within 0.2 ms. That is why the conventional techniques to mark the lines by spray painting or milling are not practicable. The problem is solved by using a high energy pulsed gas laser to mark the lines in a very short time (≤ 1 microsecond). The gas laser is composed of the laser unit, the beam steering module, the mask holder module and the focusing module. The process of marking a line is accomplished by a single pulse of energy from the laser. The desired contour of the line is figured in a pattern which is fixed in the mask holder module. The burst of the infrared energy from the laser is transmitted through the mask, forming the required image. This image is then reduced in size by projecting through an objective onto the surface of the invar tape. The invar tape is lacquered with a black subsurface and a light (white or yellow) coat of lacquer. The burst of energy from the laser removes the coated surface, exposing the contrasting black subsurface. The Figure 1 shows a general view and a block diagram of the equipment. The invar tape on which the graduation is to be marked is moved on a shunting installation with constant velocity. The motion is measured

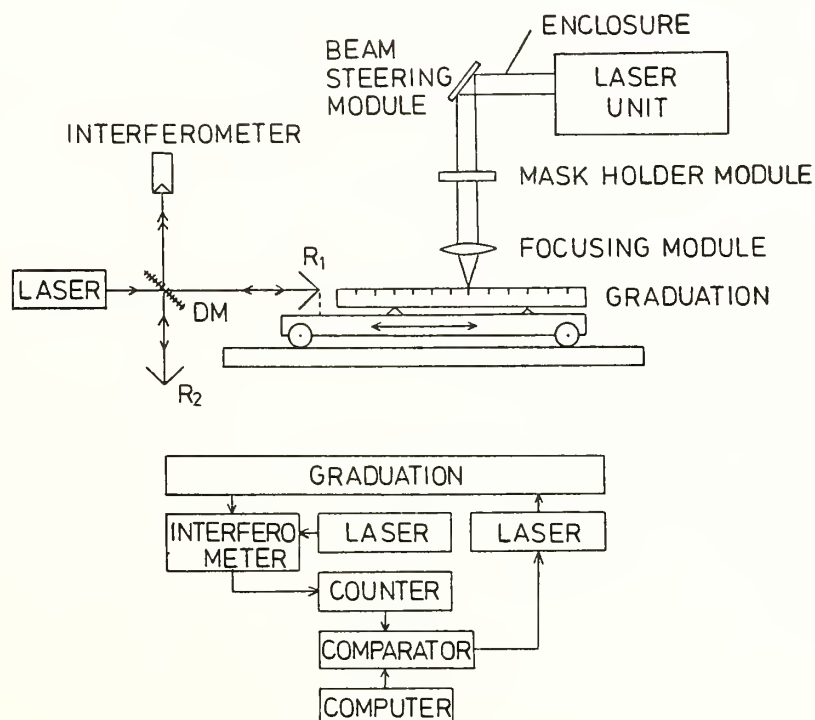


FIGURE 1: General view and block diagram of the equipment

by an interferometer and represented in the counter. The computer precalculates the position of the next line and the comparator compares continuously the information coming from the interferometer, i.e. the instantaneous position of the invar tape, and the information from the computer, i.e. the required position of the next line. If both informations are equal, the comparator generates a trigger input for the gas laser, and the line is marked immediately. The computer precalculates once more the position of the next line and the procedure is repeated until the whole graduation is burned up automatically.

I	-----	I
I		I
I	RESULTS OF CALIBRATION	I
I		I
I	levelling rod : Nestle&Fischer,Dornstetten(FRG)	I
I	standard of length: Hewlett Packard HP 5526A	I
I	microscope : photoelectric (KA)	I
I	supporting points : 2 (Bessel points)	I
I	temperature : 21.5 C	I
I		I
I	-----	I
I	line error line error line error	I
I	m mm m mm m mm	I
I	-----	I
I	0.00 0.000 1.00 0.003 2.00 -0.001	I
I	0.05 0.003 1.05 0.001 2.05 -0.000	I
I	0.10 -0.002 1.10 -0.002 2.10 0.003	I
I	0.15 -0.000 1.15 -0.001 2.15 0.001	I
I	0.20 0.001 1.20 0.005 2.20 0.003	I
I	0.25 0.002 1.25 0.003 2.25 0.000	I
I	0.30 -0.002 1.30 -0.001 2.30 -0.001	I
I	0.35 -0.001 1.35 -0.003 2.35 -0.002	I
I	0.40 -0.004 1.40 0.003 2.40 -0.001	I
I	0.45 0.002 1.45 0.004 2.45 0.002	I
I	0.50 0.000 1.50 0.001 2.50 0.001	I
I	0.55 0.001 1.55 0.003 2.55 0.004	I
I	0.60 0.003 1.60 0.001 2.60 0.001	I
I	0.65 0.002 1.65 -0.004 2.65 0.003	I
I	0.70 0.004 1.70 -0.000 2.70 0.001	I
I	0.75 0.002 1.75 0.000 2.75 -0.002	I
I	0.80 -0.001 1.80 -0.002 2.80 0.004	I
I	0.85 0.002 1.85 0.000 2.85 0.000	I
I	0.90 -0.003 1.90 0.003 2.90 0.002	I
I	0.95 -0.001 1.95 0.004 2.95 -0.003	I
I	-----	I
I		I
I	mean rod metre : 1 m + 0.001 mm	I
I	mean line correction : +-0.003 mm	I
I	coefficient of expansion : + 1.1 ppm/°C	I
I		I
I	-----	I

Table 1: Results of Calibration

Table 1 shows the result of a calibration of the graduation produced by the new technique. The calibration was carried out using a laser interferometer and a photoelectric microscope. The line corrections are within the limits of ± 5 microns for the 3 m long graduation. If we take into account that the standard error of the calibration is about $\pm 2...3$ microns, the maximum error in placing the graduation lines according to the new method is approximately ± 3 microns. This means an excellent quality of the new graduation. Also the microscopic inspection of the lines (sharpness of edge and contrast) shows a very good result. The quality of the shape of lines is much better compared to spray painted or milled lines.

A further advantage of the new technique is that any line separation (2.54 mm, 5 mm, 5.08 mm, 10 mm ...) can be produced. Furthermore, the production of nearly any contour of line is possible too. This is easily done by exchanging the mask in the gas laser's course of beam. Every user is able to find out the best contour for his range of application and after constructing a corresponding pattern for the mask, the manufactory produces the optional graduation.

Finally, it will not be necessary to calibrate this new graduation line by line. The surveying engineer only has to check the scale of the invar rods. Line corrections of every graduation line may be completely disregarded in the interpretation of the measuring results.

THE ROD FRAME

Gottwald and Witte (GOTTWALD, WITTE 1983) demonstrated that, in horizontal position, the frames of the levelling rods and with them the invar tape sag considerably. They measured different amounts of sag or deformations of the invar tape (from 0.5 mm up to 4 mm), which depend on the type of the rod and the way it is supported. Furthermore, they show that the large amount of sag can influence the calibration results of levelling rods in horizontal position.

To avoid this sag or deformation of the frame and the invar tape, the manufacturer designed a new rod frame. The material of the frame is not any longer wood but aluminium. This material prevents the influence of the humidity on the rod, which was a great problem concerning the wooden frames. The cross-section of the new aluminium-frame is specially selected to minimize the sag of the rod. Further, the invar tape is no longer supported in fixed points in the frame but it is guided in a groove reaching from top to bottom of the rod. To check the alignment of the new rod in horizontal position, a measuring device using the autocollimation was installed. The device consists of an autocollimating telescope ($f = 200$ mm) and an autocollimation surface mirror. The mirror is moved over the invar tape of the rod and the angular difference between the collimator axis and the normal of the mirror are measured continuously observing the image of the illuminated measuring mark in the focal plane of the autocollimator. The resolving power of the measuring device determining the sag of invar tape is about 5 microns. Table 2 shows results for the sag of invar tape for different supporting points.

supporting points m	sag mm		
	bottom	center	top
0.2 2.9	0.00	-0.15	0.05
0.6 2.3 (Bessel points)	-0.05	0.10	0.00
1.1 1.9	-0.10	0.15	-0.05

Table 2 Sag of the invar tape for different supporting points of the frame

THE THERMAL EXPANSION COEFFICIENT

Because of the great thermal expansion coefficient of the rod frame material (22.5 ppm/°C) we have to take precautions that temperature-produced extension of the frame is not transmitted to the invar tape. The spring tension is reduced from 100 N to 10 N to minimize this effect.

To know the thermal expansion coefficient with sufficient accuracy, the new rod had been investigated in an environmental chamber over the temperature range from -20°C up to +40°C. The standard of length was a laser interferometer and the horizontal spotting was executed with an optical microscope. The result of repeated determinations of real rod expansion was:

$$\beta = +1.1 \text{ ppm/}^\circ\text{C} \pm 0.2 \text{ ppm/}^\circ\text{C}$$

The coefficient β characterizes the expansion not only of the invar tape but of the rod as a whole. In order to correct levelling measurements we need to know the coefficient β and the real temperature of the invar tape in the field (ZIPPELT 1983).

REFERENCES

- SCHLEMMER, H. (1975): Laser-Interferometer zur Prüfung von Präzisionsnivellierlatten, Deutsche Geodätische Kommission, Reihe C Heft Nr. 210, München.
- SCHLEMMER, H. (1983): A new technique to produce precise graduations on invar tape, Precise Levelling, Dümmler-Verlag Bonn, pp 119 - 125.
- SCHLEMMER, H. (1978): Untersuchungen zu Teilungsfehlern von Invarband-Nivellierlatten, Allgemeine Vermessungs-Nachrichten, Vol. 86, pp 193 - 198.
- GOTTWALD, R.; WITTE, B. (1983): A microcomputer-controlled comparator for visual and photoelectric calibration of levelling rods, Precise Levelling, Dümmler-Verlag Bonn, pp 127 - 140.
- ZIPPELT, K. (1983): Measurements of level rod's temperature and effects on precise levelling, Precise Levelling, Dümmler-Verlag Bonn, pp 165 - 177.

LIST OF REGISTERED PARTICIPANTS

VLADIMIRO ACHILLI
ISTITUTO NAZIONALE DI GEOFISICA
C/O DIPARTIMENTO DI FISICA
VIA RUGGERO BONGHI 116
ROMA, ITALY 00184

GABRIEL ALVAREZ
DGG-INEGI
SAN ANTONIO ABAD 124
MEXICO CITY, MEXICO 06820

ELEANOR Z. ANDREE
NATIONAL GEODETIC SURVEY
N/CG1X7
NOS, NOAA
ROCKVILLE, MD 20852

PETER V. ANGUS-LEPPAN
DEPARTMENT OF LANDS - THAILAND
PHRA PHIPHIT ROAD
BANGKOK 10200 THAILAND

JAMES L. ANNIS
NATIONAL GEODETIC SURVEY
11400 ROCKVILLE PIKE - RM 622
ROCKVILLE, MD 20852

ANTHONY P. ATKINSON
ORDNANCE SURVEY
ROMSEY ROAD
SOUTHAMPTON
UNITED KINGDOM SO9 4DH

YOSHIO BABA
GEOGRAPHICAL SURVEY INSTITUTE
KITAZATO-1, YATABE-MACHI,
TSUKUBA-GUN, IBARAKI-KEN
JAPAN 305

GEORGE BABBAGE
GEODETIC SURVEY OF CANADA
615 BOOTH STREET
OTTAWA, ONTARIO, CANADA K2G 1V2

EMERY I. BALAZS
NATIONAL GEODETIC SURVEY
N/CG132
6001 EXECUTIVE BLVD.
ROCKVILLE, MD 20852

PAOLO BALDI
DEPT. DI FISICA
UNIVERSITY OF BOLOGNA
VLE PICHAT 8*
BOLOGNA, ITALY 40100

D. CRAIG BARNES
ALBERTA BUREAU OF SURVEYING
AND MAPPING
4949 94B AVENUE
EDMONTON, ALBERTA
CANADA T6B 2T5

JEAN-MARIE BECKER
IAG
NATIONAL LAND SURVEY OF SWEDEN
LANTMATERIGATAN 7
GAVLE, SWEDEN

JANICE M. BENGSTON
NATIONAL GEODETIC SURVEY
N/CG133
NOS, NOAA
11400 ROCKVILLE PIKE
ROCKVILLE, MD 20852

JOHN D. BOSSLER
CHARTING AND GEODETIC
SERVICES, N/CG
NOAA
ROCKVILLE, MD 20852

CLAUDE BOUCHER
INSTITUTE GEOGRAPHIQUE NATIONAL
2, AVENUE PASTEUR
ST-MANDE, FRANCE 94160

THOMAS K. BRAY
U.S. GEOLOGICAL SURVEY
NATIONAL MAPPING DIVISION
BOX 25046, M.S. 509
DENVER FEDERAL CENTER
DENVER, CO 80225

LARRY BROWN
INSTOC
3114 SNEE HALL CORNELL UNIV.
ITHACA, NY 14853

DR. FRITZ K. BRUNNER
WILD HEERBRUGG, INC.
CH-9435
HEERBRUGG, SWITZERLAND

HUBERT J. BUTEAU
DEFENSE MAPPING AGENCY
DMAHTC/BUILDING 833
F.E. WARREN AFB
WYOMING 82005

LAWRENCE E. BUTLER
NATIONAL GEODETIC SURVEY
6001 EXECUTIVE BLVD.
N/CG133
NOS, NOAA
ROCKVILLE, MD 20852

HUGH N. CADDESS
DMA IAGS TDS
BLDG 144
FORT SAM HOUSTON, TX 78234

GALO CARRERA
UNIVERSITY OF TORONTO
SURVEY SCIENCE
MISSISSAUGA, ONTARIO
CANADA L5L 1C6

MARTHA CARRERA (SPOUSE)
UNIVERSITY OF TORONTO
SURVEY SCIENCE
MISSISSAUGA, ONTARIO
CANADA L5L1C6

DAVID E. CARTWRIGHT
INST. OF OCEANOGRAPHIC SCIENCES
BIDSTON OBSERVATORY
BIRKENHEAD, MERSEYSIDE
UNITED KINGDOM L43 7RA

CHARLES W. CHALLSTROM
CHARTING AND GEODETIC
SERVICES, N/CGX2
NOS, NOAA
ROCKVILLE, MD 20852

MAURICE CHAMPAGNE
ENERGIE ET RESSOURCES, QUEBEC
1995 BOUL. CHAREST
QUEBEC, CANADA G1N 4H9

WILLIAM H. CHAPMAN
U.S. GEOLOGICAL SURVEY
3802 HOWARD STREET
ANNANDALE, VA 22003

YONGQI CHEN
DEPT. OF SURVEYING ENGINEERING
UNIVERSITY OF NEW BRUNSWICK
FREDERICTON, NEW BRUNSWICK
CANADA E3B 5A3

BERNARD H. CHOVITZ
U.S. DEPARTMENT OF COMMERCE/NOAA
NATIONAL GEODETIC SURVEY, N/CG1X2
6001 EXECUTIVE BLVD.
ROCKVILLE, MD 20852

JACQUELINE CHOVITZ (SPOUSE)
U.S. DEPARTMENT OF COMMERCE/NOAA
NATIONAL GEODETIC SURVEY, N/CG1X2
6001 EXECUTIVE BLVD.
ROCKVILLE, MD 20852

ADAM CHRZANOWSKI
DEPT. OF SURVEYING ENGINEERING
UNIV. OF NEW BRUNSWICK
FREDERICTON, N.B.
CANADA E3B 5A3

OSCAR L. COLOMBO
EG&G (W.A.S.C.I.)
5000 PHILADELPHIA WAY - SUITE J
LANHAM, MD 20706

MICHAEL R. CRAYMER
UNIVERSITY OF TORONTO
SURVEY SCIENCE - ERINDALE CAMPUS
MISSISSAUGA ROAD
MISSISSAUGA, ONTARIO
CANADA M2R 3T2

MICHAEL W. DAY
NATIONAL GEODETIC SURVEY
NOAA
ROCKVILLE, MD 20852

HEINER DENKER
INSTITUT FUR ERDMESSUNG
NEINBURGER STRASSE 6
3000 HANNOVER
FEDERAL REPUBLIC OF GERMANY

ALAN H. DODSON
NOTTINGHAM UNIVERSITY
CIVIL ENGINEERING DEPARTMENT
UNIVERSITY PARK
NOTTINGHAM
UNITED KINGDOM N97 2RD

FRANCOIS FAUCHER
ENERGY, MINES & RESOURCES CANADA
GEODETIC SURVEY
615 BOOTH STREET
OTTAWA, ONTARIO, CANADA K1A 0E9

CHARLES J. FINLEY
NASA HQ CODE EEG
600 INDEPENDENCE AVE., S.W.
WASHINGTON, D.C. 20546

WILLIAM O. FISK
VERMONT TRANSPORTATION AGENCY
SURVEY
133 STATE STREET
MONTPELIER, VT

STEPHEN J. FRAKES
NATIONAL GEODETIC SURVEY - NOAA
N/CG125
11400 ROCKVILLE PIKE
ROCKVILLE, MD 20852

WALTER L. GALE
GEODETIC SURVEY OF CANADA
615 BOOTH ST.
OTTAWA, ONTARIO, CANADA K1A 0E9

RENE M. GAREAU
GEODETIC SURVEY, CANADA
ENERGY, MINES & RESOURCES
615 BOOTH STREET
OTTAWA, ONTARIO, CANADA K1A 0E9

JOHN G. GERGEN
NATIONAL GEODETIC SURVEY
N/CG15
NOAA
ROCKVILLE, MD 20852

RENE GONZALEZ
INSTITUTO GEOGRAFICO MILITAR
AV LAS AMERICAS 5-76 Z-13
GUATEMALA, GUATEMALA

ERICH GUBLER
FEDERAL OFFICE OF TOPOGRAPHY
GEODETIC DEPARTMENT
SEFTIGENSTRASSE 264
CH-3084 WABERN, SWITZERLAND

TONG KIAT GUOY
HYDROGRAPHIC DEPT. (RMN)
DEPT. OF NAVY, MINISTRY OF DEF.
JALAN PADANG TENBAK
KUALA LUMPUR 15-03, MALAYSIA

D. P. HAJELA
THE OHIO STATE UNIVERSITY
GEODETIC SCIENCE
1958 NEIL AVENUE
COLUMBUS, OH 43210

JOHN HANNAH
DEPARTMENT OF LAND AND SURVEY
PRIVATE BAG
WELLINGTON, NEW ZEALAND

BJORN GEIRR HARSSON
NORGES GEOGRAFISKE OPPMALING
GEODESY
N-3500 HONEFOSS
NORWAY

GUNTER W. HEIN
INSTIT. OF ASTRO. & PHY. GEODESY
UNIVERSITY FAF MUNICH
WERNER-HEISENBERG-WEG 39
D-8014 NEUBIBERG
FEDERAL REPUBLIC OF GERMANY

ROBERT H. HANSON
NATIONAL GEODETIC SURVEY
N/CG1X6
NOS, NOAA
ROCKVILLE, MD 20852

EDWARD H. HERBRECHTSMEIER
NATIONAL GEODETIC SURVEY, N/CG15
ROCKVILLE, MD 20852

SANDFORD R. HOLDAHL
NATIONAL GEODETIC SURVEY
N/CG113

NOAA
ROCKVILLE, MD 20852

THOMAS L. HOLZER
U.S. GEOLOGICAL SURVEY
MS 977
345 MIDDLEFIELD ROAD
MENLO PARK, CA 94025

JAMES HOOBLER
NOAA-NGS-CGS
ROCKVILLE, MD 20852

LLOYD C. HUFF
NOAA N/CGX3
6001 EXECUTIVE BLVD.
ROCKVILLE, MD 20852

ANDRE JAEGLER, SGNM
INSTITUT GEOGRAPHIQUE NATIONAL
GEODESIE-NIVELLEHENT
2 RUE PASTEUR
SAINT-MANDE, FRANCE 94160

ANDREW C. JONES
SOUTH AUSTRALIAN DEPT. OF LANDS
P.O. BOX 1047, GPO ADELAIDE
ADELAIDE, S. AUSTRALIA
AUSTRALIA 5001

WILLIAM J. JONES
U.S. GEOLOGICAL SURVEY
11109 PINION CT.
GAITHERSBURG, MD

HERIBERT KAHMEN
GEODETIC INSTITUTE
UNIVERSITY OF HANNOVER
NIENBURGER STR. 7
D3000 HANNOVER 7
FEDERAL REPUBLIC OF GERMANY

WILLIAM M. KAULA
CHIEF, NATIONAL GEODETIC SURVEY
N/CG1 NOS/NOAA
6001 EXECUTIVE BLVD.
ROCKVILLE, MD 20852

RAINER H. KELM
DEUTSCHES GEOD. FORSCH INST. I
MARSTALLPL. 8
8000 MUNICH
FEDERAL REPUBLIC OF GERMANY

JOHN G. KIRK
GEODYNAMICS CORPORATION
BLDG. D
5290 OVERPASS ROAD
SANTA BARBARA, CA 93111

W. J. KORNACKI
SURVEYING ENG. - UNIV OF N.B.
BOX 4400 HEAD HALL
FREDERICTON, NEW BRUNSWICK
CANADA E3B 5A3

M. KUMAR
DMA
6500 BROOKES LANE
WASHINGTON, DC 20315

RICHARD J. LATATIS
NOAA ERL WPL
325 BROADWAY
BOULDER, CO

RODNEY J. LEE
NATIONAL GEODETIC SURVEY
N/CG132
NOS, NOAA
ROCKVILLE, MD 20852

DAVID J. LEHMAN
INTERAMERICAN GEODETIC SURVEY
DRAWER K
APO MIAMI 34004

WOLFGANG LINDLOHR
UNIVERSITY OF STUTTGART
DEPT. OF GEODETIC SCIENCE
KEPLERSTRASSE 11
D-7000 STUTTGART 1
FEDERAL REPUBLIC OF GERMANY

HARRY A. LIPPINCOTT
NOAA N/OMA124
6001 EXECUTIVE BLVD.
ROCKVILLE, MD 20852

JOHN D. LOVE
NATIONAL GEODETIC SURVEY
N/CG171
NOS, NOAA
ROCKVILLE, MD 20852

JAMES R. LUCAS
NOAA/NOS
6001 EXECUTIVE BLVD.
ROCKVILLE, MD 20852

MICHEL M' KASSER
I.G.N.
2 AV. PASTEUR
ST. MANDE, FRANCE 94160

ANDRE MAINVILLE
GEODETIC SURVEY OF CANADA
7039 TREEBOURNE DRIVE
REYNOLDSBURG, OH 43068

JAMES I. MARLOWE, PH.D.
DEWBERRY & DAVIS
WATER RESOURCES/ENVIRON. ENG.
8401 ARLINGTON BOULEVARD
FAIRFAX, VA 22031

RACHID MAZAACHI
NAVD PROJECT
GEODETIC SURVEY OF CANADA
615 BOOTH STREET
OTTAWA, ONTARIO, CANADA J9H 5J8

MATTHEW B. MILLER
FEMA
500 C STREET, SW
WASHINGTON, DC 20472

GILBERT J. MITCHELL
NATIONAL GEODETIC SURVEY
N/CG1X10
NOAA
ROCKVILLE, MD 20852

RICHARD J. MITCHELL
L. A. COUNTY ENG.-RET.
255 PORTOFINO WAY
REDONDO BEACH, CA

GARRETT R. MOORE
DEFENSE MAPPING SCHOOL
DEPARTMENT OF SURVEY
FT. BELVOIR, VA 22060-5828

PEGGY MORRISH
NATIONAL GEODETIC SURVEY
N/CG174
NOS, NOAA
ROCKVILLE, MD 20852

RICHARD B. MUMMA
U.S. GEOLOGICAL SURVEY-NMD
1400 INDEPENDENCE ROAD
ROLLA, MO

PAUL E. NEEDHAM
U.S. GEOLOGICAL SURVEY
NATIONAL MAPPING DIVISION, MS-525
12201 SUNRISE VALLEY DRIVE
RESTON, VA 22092

KENNETH NELSON
DMAAC/GDGB
3200 SOUTH BROADWAY
ST. LOUIS, MO 63118

WOLFGANG NIEMEIER
GEODETIC INSTITUTE
UNIVERSITY OF HANNOVER
NIENBURGER STR. 1
HANNOVER, WEST GERMANY 3000

RANDLE W. OLSEN
U.S. GEOLOGICAL SURVEY
NATIONAL MAPPING DIVISION
510 NATIONAL CENTER
RESTON, VA 22092

KAREN RAMSEY
LA. GEOLOGICAL SURVEY
UNIVERSITY STATION BOX G
BATON ROUGE, LA 70893

RICHARD RAPP
OHIO STATE GEODETIC SCIENCE
1958 NEIL AVENUE
COLUMBUS, OH 43210

CHRISTOPHER H. REED
VERMONT DOT
AERIAL ENG/DESIGN
133 STATE STREET
MONTPELIER, VT 05602

SAMUEL M. REESE
NATIONAL GEODETIC SURVEY
6001 EXECUTIVE BLVD.
N/CG133
NOS, NOAA
ROCKVILLE, MD 20852

ROBERT REILINGER
AIRFORCE GEOPHYSICS LAB
AFGL/LWH
HANSCOM AFB, MA 01731

OLE REMMER
STATSGEOAET
GEODETIC INSTITUTE
GAMLEHAVE ALLE 22
CHARLOTTENLUND, DENMARK

JOHN H. RICHARDS
NATIONAL GEODETIC SURVEY
N/CG133
NOS, NOAA
ROCKVILLE, MD 20871

GRAEME JAMES RUSH
DEPT. OF MAPPING & SURVEYING
P.O. BOX 234 NORTH QUAY
BRISBANE, QUEENSLAND
AUSTRALIA 4000

PAUL H. SALAMONOWICZ
U.S. GEOLOGICAL SURVEY
NATIONAL MAPPING DIVISION
MS 521 NATIONAL CENTER
RESTON, VA 22092

RAFAEL N. SANCHEZ
UNIVERSITE LAVAL
GEODETIC SCIENCE
823 MOREAU
STE-FOY, QUEBEC
CANADA G1V 3B5

HARALD SCHLEMMER
UNIVERSITY OF KARLSRUHE
GEODETIC INSTITUT
ENGLERSTRASSE 7
KARLSRUHE, BW D-7500
FEDERAL REPUBLIC OF GERMANY

JOSEPH W. SIRY
NASA GODDARD SPACE FLIGHT CTR
GREENBELT, MD 20016

LARS E. SJOEBERG
GEODESY
THE ROYAL INSTITUTE OF TECHNOLOGY
STOCKHOLM, SWEDEN S-100 44

RICHARD A. SNAY
NATIONAL GEODETIC SURVEY
N/CG113
NOS, NOAA
ROCKVILLE, MD 20852

ING SOEBAGIO
PT GEOBECONSURVEYS
JL.MARTAPURA 9
JAKARTA, INDONESIA

GRACE C. SOLLERS
NATIONAL GEODETIC SURVEY
N/CG17X2
NOS, NOAA
ROCKVILLE, MD 20852

JOHN F. SPENCER
NATIONAL GEODETIC SURVEY
N/CG17
NOS, NOAA
ROCKVILLE, MD 20852

LOWELL STARR
ASST. DIVISION CHIEF FOR RESEARCH
NATIONAL MAPPING DIVISION - USGS
519 NATIONAL CENTER
RESTON, VA 22092

ROBIN R. STEEVES
EMR CANADA
GEODETIC SURVEY DIVISION
615 BOOTH STREET
OTTAWA, ONTARIO, CANADA K1A 0E9

ROSS S. STEIN
U.S. GEOLOGICAL SURVEY
BRANCH OF TECTONOPHYSICS
345 MIDDLEFIELD ROAD, MS977
MENLO PARK, CA 94025

ARTHUR STOLZ
UNIV. OF NEW SOUTH WALES - SURVEY
P.O. BOX 1
KENSINGTON, NEW SOUTH WALES
AUSTRALIA 2033

WILLIAM E. STRANGE
NATIONAL GEODETIC SURVEY
6001 EXECUTIVE BLVD.
ROCKVILLE, MD 25414

BRIAN J. TAIT
DEPARTMENT OF FISHERIES AND
OCEANS
615 BOOTH STREET
OTTAWA, ONTARIO, CANADA K1A 0E6

PIERRE TETREAU
UNIVERSITY OF TORONTO
SURVEY SCIENCE
3349 MISSISSAUGA RD. #73
MISSISSAUGA, ONTARIO
CANADA L5L 1J7

LOUIS G. THORSEN
DMA IAGS
BLD 144
FORT SAM HOUSTON, TX 78234

ULRIKE TILK
UNIVERSITY OF HANNOVER
GEODETIC INSTITUTE
NIEBURGER STR. 1
HANNOVER, WEST GERMANY 3000

JOHN H. TILL
NATIONAL GEODETIC SURVEY - NOAA
425 CHRISTOPHER AVE. APT. 23
GAITHERSBURG, MD

RAFAEL SOSA TORRES
DGG-INEGI
SAN ANTONIO ABAD 124 PB
MEXICO DF, MEXICO 06820

MARCO UNGUENDOLI
UNIVERSITY OF BOLOGNA
VIALE RISORGIMENTO 2
BOLOGNA, ITALY 40100

✓
PETR VANICEK
UNIV. OF NEW BRUNSWICK
UNB, DEPT. OF SURVEYING ENG.
P.O. BOX 4400
FREDERICTON, NEW BRUNSWICK
CANADA E3B 5A3

JOHN F. WAANANEN
U.S. GEOLOGICAL SURVEY
NATIONAL MAPPING DIVISION
NATIONAL CENTER 510
RESTON, VA 22092

WILLIAM W. WALLACE
NATIONAL GEODETIC SURVEY
N/CG17
NOS, NOAA
ROCKVILLE, MD 20852

R. BRUCE WARD
NATIONAL GEODETIC SURVEY - NOAA
NOAA
ROCKVILLE, MD 20852

ATTALLAH M. WASSEF
UNIVERSITY OF TORONTO
77 QUEBEC AVENUE #1136
TORONTO, ONTARIO
CANADA M6P 2T4

JACK A. WEIGHTMAN
BRITOL PLC (EXPLORATION DIV.)
150 SAINT VINCENT STREET
GLASGOW, SCOTLAND G2 5LJ

EGON J. WETZKER
DMAAC
3211 SOUTH BROADWAY
ST. LOUIS, MO 63118

CHARLES T. WHALEN
NOAA/N/CG1
ROCKVILLE, MD 20852

FRED W. YOUNG
NAVD PROJECT
GEODETIC SURVEY OF CANADA
615 BOOTH STREET
OTTAWA, ONTARIO, CANADA K1A 0E9

GARY M. YOUNG
NATIONAL GEODETIC SURVEY
N/CG13
NOS, NOAA
ROCKVILLE, MD 20852

DAVID B. ZILKOSKI
NATIONAL GEODETIC SURVEY
N/CG13
NOS, NOAA
ROCKVILLE, MD 20852

*U.S. GOVERNMENT PRINTING OFFICE: 1985-461-135:36617

PENN STATE UNIVERSITY LIBRARIES



A000070941326